



THA 2017

*International Conference on
"Water Management and climate Change
Towards Asia's Water-Energy-Food Nexus"*

*25-27 January 2017
Bangkok, Thailand*



CONTENTS

PREFACE	i
ORGANIZATION COMMITTEES	ii
CONFERENCES ORGANIZING INSTITUTE	v
AIMS AND SCOPE	vii
PROGRAMME	ix
OPENING SPEECH	xviii
CONGRATULATION SPEECH	xx
OPENING REMARKS	xxiv
Session A Climate Change and Uncertainty in Hydrology and Meteorology	
TA02 Probabilistic Flood Forecasting Using Ensemble Numerical Weather Prediction Rainfalls During The 2011 Largest Flood Event In Japan	2
TA03 River Discharge and Reservoir Operation Assessment under a Changing Climate at the Sirikit Reservoir	8
TA04 Determination of Extreme Design Waves under Climate Change in the Gulf of Thailand	15
TA05 Analysis of Farmers' Choice of Adaptations to Climate Change at Nong Sua District, Rangsit Canal, Thailand.....	22
TA06 Change of the Probability Distribution of Annual Maximum River Discharge Derived from the d4PDF datasets at the Indochinese Peninsula.....	31
TA09 Comparison of the Spatial Rainfall in Khun Dan Prakan Chon Reservoir by Spatial Interpolation Techniques.....	32
TA11 Assessment of Satellite Rainfall Estimates as A Pre-Analysis for Water Environment Analytical Tools: A Case Study for Tonle Sap Lake in Cambodia	38
TA14 Climate change and landslide risk assessment in Uttaradit province	39
TA15 Assessment of an Urban Drainage System in Phnom Penh Using Storm Water Management Model.....	40
TA16 Development of Design Storm Pattern with Climate Change in Monsoon Asia.....	46
TA17 Correlation Analysis Between Tsengwen-Wushantou Reservoirs Operation and Environmental Factors.....	52

CONTENTS (con't)

TA18	Spatial heterogeneity and trans-boundary pollution: A case study on the 3S River Basin.....	57
TA21	Change of water budget between 1960's and 2000's at the seasonal tropical forest in Northern Thailand.....	64
TA22	Stochastic Simulation and Frequency Analysis of the Concurrent Occurrences of Multisite Extreme Rainfalls.....	68
TA23	Climate Extremes, People's Perception and Adaptation in Lower Songkhram River Basin, Thailand.....	70
TA26	Assessment of Water Resources During the 21st Century in Northern Thailand with Focus on Ping River Basin.....	77

Session B Participatory Management for Water and Irrigation Project

Invited Papers

B	Principles And Methods For Pim In Action Is The Japan's Model Exceptional?.....	87
---	---	----

Papers

TB01	Water-Food Nexus: Water Use Efficiency in Central Asia.....	89
TB02	Improving Crop Water Use with the use of Efficient Irrigation Technologies and Coconut Mulch Husk: A study on long-bean production.....	93
TB04	Participatory Water Management in the Specific Locale of Sub-watershed: Negotiation Process and Institutionalization.....	97
TB05	Water Quality Profiles And The Reservoir Utilization With Special References To Jatiluhur, Cirata And Saguling Reservoirs.....	103
TB06	Proposal of a reservoir management method based on the observed accumulated areal mean rainfall for the Sirikit reservoir in the Chao Phraya River basin, Thailand.....	107

Session C Emerging Technologies in Water Management and Environment Towards Nexus (WEF)

Invited Papers

C01	Water-Energy-Food Nexus: The Roadmap In Korea.....	114
C02	Smart Urban Water Systems – In Practice.....	115

Papers

TC01	Achieving Sustainable Resources Security through the Water-Energy-Food Nexus.....	116
------	---	-----

CONTENTS (con't)

TC03	Characteristics of CH ₄ Flux from Paddy Field Adopting the Intermittent Irrigation Technique during the Winter-Spring and Summer-Autumn Seasons in the Red River Delta, Vietnam.....	122
TC07	Water Energy Carbon Nexus in Urban Water Supply System of Kathmandu Valley	129
TC08	Satellite Based Sub-Daily Downscaling Of Gauged Rainfall For Flood Analysis Via Fully Distributed Hydrological Model.....	135
TC09	A Case Study on Industrial Mis management of Tanneries in Hazaribagh: Water Pollution and Chromium Poisoning in Dhaka, Bangladesh.....	141
TC10	Quantifying climate change impact on rice production in Northeast of Thailand: a critical review through water footprint concept.....	148

Session D Disaster Management / Groundwater Management

Invited Papers

D01	Japan's Policies and Technical Works for Flood Damage Reduction under Climate Change.....	154
D02	Prediction of extreme floods and risk curve development under a changing climate.....	158

Papers

TD01	Groundwater balance and river interaction analysis in Pleistocene aquifer of the Saigon River basin, South of Vietnam by stable isotope analysis and groundwater modeling.....	164
TD02	Estimation of river conductance values along Saigon River, Vietnam.....	170
TD03	Estimation of Hydrological Parameter Distribution by Geostatistical methods in the Upper Central Plain, Thailand.....	176
TD04	Mechanism of land subsidence due to groundwater production.....	181
TD05	Flow budget of groundwater system and conjunctive use pattern under climate change in Upper Central Plain, Thailand.....	186
TD06	Flood Mapping along the Lower Mekong River in Cambodia.....	192
TD08	Drought Risk Assessment of Irrigation Project Areas in a River Basin	193
TD09	Assessment of rainfall-runoff models for streamflow predictions in the Nam Song River basin	199
TD10	An Assessment of Salt water Intrusion in Cebu City Aquifers	205
TD12	Flood Risk Maps and Its Applications	212

CONTENTS (con't)

TD16	Analysis of Rainfall Induced Landslide Dam Geometries and Failures	218
TD19	Iron oxide coated activated carbons for arsenate adsorption from groundwater	224
TD20	SWAT and MODFLOW Modeling of Spatio-Temporal Runoff and Groundwater Recharge Distribution	230
TD21	Groundwater Vulnerability and Risk Assessment in Thailand using GIS-Based Modified DRASTIC Approach.....	237
TD22	Potential Impact and Risk Assessments of Future Climate Conditions on Salinisation in Central Huai Luang River Basin, Northeast, Thailand	247
TD23	Impact of decreasing percentage of imperviousness area with flooding in urban area at Sukhumvit, Bangkok, Thailand.....	253
TD24	Land Cover/Use Scenario Building and its Impact on Flooding inside the Iligan River Basin.....	259
TD26	Input-Output Analysis of Water Deficits in Nan River Basin, Thailand	265
Reviewers		272
Supporter		273
Sponsors		273

Preface

In the 2017 conference under the theme of “Water management and climate change towards Asia” Water-Energy-Food Nexus.

We have discussed about climate change and uncertainty in hydrology and meteorology, participatory management for water irrigation project, emerging technologies in water management and environment, and ground water management.

Eight guest speakers from Malaysia, Vietnam, Korea, Japan, Denmark and USA. 69 papers on 4 sub-themes. 18 papers on climate change, 6 papers on participatory irrigation management, 11 papers on emerging technologies in water resources and 22 papers on disaster management and ground water. Also, there are 12 papers on groundwater under changing world.

The first sub-theme, climate change, hydrology and meteorology, covers the range of climatic and rainfall change including climate change adaptation. In hydrology, the coverage is wide from hydrology and meteorology such as storm prediction, river flow, sedimentation and drainage. Research papers about the impact of climate change are such as flooding, ocean wave, reservoir management and water quality.

The second theme on PIM or participatory irrigation management covers the experience in Thailand and Japan and water use efficiency for crop and water-food nexus.

The third theme on emerging technologies in water management and environment covers many issues of water energy and food nexus. The technologies on urban water supply, irrigation technology, water quality management, downscale for rainfall prediction and water footprint.

The last theme is about disaster management and groundwater. It covers the issues about policy on disaster management, assessment of extreme events including flood and drought, groundwater modeling, assessment of changing groundwater under climate changing, groundwater sustainable yield estimation and land use change.

In conclusion, this conference gives opportunities for researches and people who are interested in climate change and water- energy-food nexus to gain knowledge and share ideas about this topic. Information and knowledge that are contributed from this conference can be further studied and used for sustainable development goal (SDG).

Assoc.Dr. Bancha Kwanyuen
Editor of Proceeding THA 2017

Organization committees

Advisory Committees:

- | | | |
|----|--|---|
| 1 | Prof. Dr. Bundhit Eua-arporn | Chulalongkorn University |
| 2 | Assoc. Prof. Dr. Chongrak Watcharinrat | Kasetsart University |
| 3 | Prof. Dr. Worsak Kanok-Nukulchai | Asian Institute of Technology |
| 4 | Mr. Sanchai Ketwonrachai | Director General of Royal Irrigation Department |
| 5 | Mr. Worasart Apaipong | Director General of Department of Water Resources |
| 6 | Mr. Suphot Towichakchaikun | Director General of Department of Groundwater Resources |
| 7 | Dr. Poramete Vimolsiri | Secretary General of Office of National Economic and Social Development Board |
| 8 | Dr. Subin Pinkayan | President of Thai Hydrologist Association |
| 9 | Prof. Suthipun Jitpimolmard, M.D. | Director General of Thailand Research Fund |
| 10 | Mr. Li He | Food and Agriculture Organization of the United Nations (FAO) |
| 11 | Prof. Dr. Toshio Koike | ICARM, Japan |
| 12 | Prof. Dr. Yasuto TACHIKAWA | Kyoto University, Japan |
| 13 | Prof. Tsugihiko WATANABE | President of PAWEES, Japan |
| 14 | Prof. Wei Cheng Lo | NCKU, Taiwan |
| 15 | Prof. Kwansue Jung | KWRA, Korea |
| 16 | Dr. Ramasamy Jayakumar | UNESCO-IHP |

Organizing Chair:

- | | | |
|---|--|--------------------------|
| 1 | Assoc. Prof. Dr. Supot Teachavorasinskun | Chulalongkorn University |
|---|--|--------------------------|

Organizing Co-Chair:

- | | | |
|---|-----------------------------------|---|
| 2 | Assoc. Prof. Dr. Banha Kwanyuen | Dean of Engineering Faculty, Kasetsart University |
| 3 | Assoc. Prof. Dr. Chanatip Pharino | Thailand Research Fund |

International Scientific Committees:

- | | | |
|---|---------------------------------|---------------------------------|
| 1 | Assoc. Prof. Dr. Banha Kwanyuen | Kasetsart University |
| 2 | Dr. Yutaka Matsuno | PAWEES, Kinki University, Japan |

3	Prof. Dr. SAYAMA Takahiro	ICHARM, Public Works Research Institute, Japan
4	Dr. Kimihito Nakamura	Kyoto University, Kyoto, Japan
5	Dr. Andrew Whitaker	Niigata University, Niigata, Japan
6	Dr. Shinji Fukuda	Tokyo University of Agriculture and Technology, Japan
7	Dr. Takanori Nagano	Kobe University, Hyogo, Japan
8	Assoc. Prof., Dr. Kenji Tanaka	Department of Civil and Earth Resources Eng., Kyoto University, Japan
9	Prof. Koike Toshio	ICHARM, Japan
10	Dr. Hirodata Matsuki	Director of International Affairs Office, River Planning Division, Water and Disaster Management
11	Prof. K.S. Cheng	National Taiwan University, Taiwan
12	Dr. WT Feng	National Taiwan University, Taiwan
13	Prof. Jian-Ping Suen	NCKU, Taiwan
14	Dr. Meng-Hsuan Wu	NCKU, Taiwan
15	Dr. Byung Man Choi	K-water Institute, Korea
16	Prof. Kwansue Jung	Chungnam National University, Korea
17	Prof. Hyunuk An	Chungnam National University, Korea
18	Prof. Tae-woong Kim	Hanyang University, Korea
19	Prof. Juheon Lee	Joongbu University, Korea
20	Prof. Giha Lee	Kyongpook National University, Korea
21	Prof. Chang-lae Jang,	Korea National University of Transport, Korea
22	Dr. Yeonsu Kim	K-water, Korea
23	Dr. Wansik Yu	International Water Resources Research Institute, Korea
24	Dr. Ole Mark	DHI, Denmark
25	Assoc. Prof. Dr. Sucharit Koontanakulvong	Chulalongkorn University
26	Asst. Prof. Dr. Aksara Putthividhya	Chulalongkorn University
27	Asst. Prof. Dr. Anurak Sriariyawat	Chulalongkorn University
28	Assoc. Prof. Dr. Tuantan Kitpaisalsakul	Chulalongkorn University

- | | | |
|----|---------------------------------|---|
| 29 | Dr. Piyatida Ruangrassamee | Chulalongkorn University |
| 30 | Dr. Pongsak Suttinon | Chulalongkorn University |
| 31 | Dr. Yutthana Talaluxmana | Kasetsart University |
| 32 | Assoc.Prof. Dr. Shrestha Sangam | Asian Institute of Technology |
| 33 | Asst.Prof. Dr. Nguyen Hoang Duc | Asian Institute of Technology |
| 34 | Assoc.Prof.Dr. Avishek Datta | Asian Institute of Technology |
| 35 | Asst.Prof.Dr. Sarawut Ninsawat | Asian Institute of Technology |
| 36 | Assoc. Prof. Amnat Chidthaisong | King Mongkut's University of Technology Thonburi, TRF |
| 37 | Dr. Oranuj Lophensi | Department of Groundwater Resources, Thailand |

Working Committees:

- | | | |
|---|---|---|
| 1 | Assoc.Prof.Dr. Sucharit Koontanakulvong | Chulalongkorn University |
| 2 | Dr. Supattra Visessri | Chulalongkorn University |
| 3 | Dr.Jutithep Vongphet | Kasetsart University |
| 4 | Assoc. Prof. Amnat Chidthaisong | King Mongkut's University of Technology Thonburi, TRF |
| 5 | Mr. Somkiat Kitsuwanakul | Thai Hydrologist Association |

Website and Information System :

- | | | |
|---|---------------------------|------------------------------|
| 1 | Miss Mada Iaumsupanimit | Chulalongkorn University |
| 2 | Miss Daunpen Punayangkool | Chulalongkorn University |
| 3 | Miss Napaporn Noppakhun | Chulalongkorn University |
| 4 | Miss Marayart Petcharat | Thai Hydrologist Association |

Conference Organizing Institutes:



100th Anniversary Chulalongkorn University

**Chulalongkorn University (CU),
Thailand**



**Faculty of Engineering at
Kamphaengsaen,
Kasetsart University (KU),
Thailand**



**Asian Institute of Technology,
Thailand**



**Royal Irrigation Department (RID),
Thailand**



**General of Department of Water
Resources (DWR),
Thailand**



**Department of Groundwater Resources,
Thailand**



**National Economic and Social
Development Board,
Thailand**



**Thai Hydrologist Association,
Thailand**



**Thailand Research Fund,
Thailand**

AIMS AND SCOPE

The objective is to provide a platform for researchers, scientists, practitioners, and policy makers to share and present new advances, research findings, perspectives, and experiences in Disaster, Irrigation and Water Management towards W-E-F Nexus. Special attentions will be given to developing certain skills or competence, or general upgrading of performance ability for climate change adaptation, participatory water management disaster and environmental management, and sustainable development in irrigation and drainage in the monsoon Asia. The conference will bring together leading researchers, engineers, scientists, and officials in the domain of interest from around the world

The conference will bring together leading researchers, engineers, scientists, and officials in the domain of interest from around the world topics of the conference are:

- A. Climate Change and Uncertainty in Hydrology and Meteorology**
- B. Participatory Management for Water and Irrigation Project**
- C. Emerging Technologies in Water Management and Environment Towards W-E-F Nexus**
- D. Disaster Management/ Groundwater Management**

The presentation contents can be highlighted as follows:

Session A Climate Change and Uncertainty in Hydrology and Meteorology

The session started with the research results of downscaling research based on the Multi-Model Simulations of SEACLID/CORDEX Southeast Asia. The climate change data had been utilized to study impact on weather prediction, design wave, river discharge, landslide risk, reservoir operation. The studies on satellite rainfall estimate, extreme rainfall, urban flood, spatial heterogeneity and trans-boundary pollution were presented and lastly, the change of water budget in the seasonal tropical forest was presented for discussion.

Session B Participatory Management for Water and Irrigation Project

The session started with question on principles and methods of PIM in Action from Japanese experiences. The study on improving crop water use with efficient irrigation technologies was presented and discussed with the negotiation process and institutionalization in the participatory water management. The water use efficiency is discussed with the Water-Food Nexus approach.

Session C Emerging Technologies in Water Management and Environment Towards W-E-F Nexus

WEF Nexus in practices were introduced to achieve sustainable resources security with proposed indicators under a DPSIR framework. New concept on Water Footprint for quantifying impact on rice production was reviewed and criticized. Lastly the concept of smart urban water systems – in practice was introduced for discussion.

Session D Disaster Management/ Groundwater Management

The session started with the introduction of policies and technical works on river management for disaster risk reduction under climate change and the research on extreme flood frequency analysis and risk curve development under a changing climate was also presented. The assessment of the climate change impacts of groundwater abstraction was presented with various studies on groundwater parameter estimation under various situations. The discussion evaluation of near-real-time satellite-based rainfalls and research on Input-Output analysis of water deficits were presented for discussion.

Publication Opportunities

Journal Publication

Selected manuscripts from THA2017 proceedings will be recommended to be published in the Engineering Journal (EJ) : International Journal ISSN 0125-8281 (indexed with ESCI (Web of Science), Scopus, IET Inspec, Index Copernicus, DOAJ, and TCI: <http://www.engj.org>.)

Conference Proceedings

The full papers after correction will be published in the Conference Proceedings.

(Some selected/related full papers will also be published in book titled “Water and Disaster Management and Climate Change with NEXUS approach in Monsoon Asia” after peer review.)

Programs of conference

1st day THA 2017 International Conference (Wednesday- 25 January 2017)

Venue: Le Concorde Ballroom, 2nd floor

08.00		Registration	
Opening Session			
09.00	Exhibition	Report Speech:	Prof. Dr. Bundhit Eua-arporn President of Chulalongkorn University
09.10		Introduction Speech:	Dr. Gwang-Jo Kim Director, UNESCO Asia and Pacific Regional Bureau for Education (UNESCO Bangkok)
09.20		Congratulation Speech:	Mr. Vongthe pArthakaivalvatee Deputy Secretary-General of ASEAN Socio-Cultural Community Department ASEAN Secretariat
09.30		Opening Remarks:	Prof. Emeritus Khunying Suchada Kiranandana Chairman of the University Council
09.40		Group Photo	
		Tour for Exhibition on Green and Smart Technology for Water Management and Press conference	
10.10		Coffee Break	
Scope Session			
10.30	Exhibition	Keynote Speakers I The water-food-energy nexus: future challenges and opportunities in Asia	Ms. Louise Whiting Regional Office for Asia and the Pacific Food and Agriculture Organization of the United Nations (FAO)
11.00		Keynote Speakers II Water Planning Strategies under SDG and WEF Nexus (tentative)	Dr. Poramete Vimolsiri Secretary General of Office of National Economic and Social Development Board, Thailand
11.30		Keynote Speakers III Water management under climate change and WEF approach (tentative)	Dr. Gwang- Jo Kim Director, UNESCO Asia and Pacific Regional Bureau for Education UNESCO Bangkok
12.00		Lunch Break	

DAY 1 (Wednesday- 25 January 2017) THA 2017 Plenary session presentation

Scope	Plenary session presentation Venue: Salon A		Plenary session presentation Venue: Salon B		Plenary session presentation Venue: Krisana	
Chair	Assoc. Prof. Dr. EkasitKositsakulchai		Dr. Sangam Shrestha		Dr. Patama Singhruck	
Briefing	Dr. Saisunee Budhakooncharoen		Ass.Prof.Dr. Uma Seeboonruang			
13.00		Invited A: Projected changes in mean precipitation, temperature and extremes over Southeast Asia region based on the multi-model simulations of SEACLID/CORDEX Southeast Asia Prof. FredolinTangang, PhD, School of Environmental and Natural Resource Sciences, Malaysia		Invited C: Water-Energy-Food Nexus: the roadmap in Korea Dr. Byung Man Choi Project manager of Water-Energy-Food Nexus in Korea, Former Head of K-water Institute, Korea		Invited D: Japan's Rivers Policies and Technical Works for Disaster Risk Reduction under climate change Mr. Takafumi Nakui, International Affairs Office, River Planning Division, Water and Disaster Management Bureau, Ministry of Land, Infrastructure, Transport and Tourism(MLIT), Japan
13.30	TA016	Development of Design Storm Pattern with Climate Change in Monsoon Asia Dr. Sutat Weesakul, Hydro and Agro Informatics Institute, Thailand	TB001	Water-Food Nexus: Water Use Efficiency in Central Asia Dr. Younghun Jung, K-water, Korea	TD020	SWAT and MODFLOW Modeling of Spatio-Temporal Runoff and Groundwater Recharge Distribution Dr. AKSARA Putthividhya, Chulalongkorn University, Thailand
13.55	TA002	Probabilistic Flood Forecasting using Ensemble Numerical Weather Prediction rainfalls during the 2011 Largest Flood Event in Japan Dr. Wansik YU, Chungnam National University, Korea	TA017	Correlation Analysis Between Tsengwen-Wushantou Reservoirs Operation and Environmental Factors Yi-Lung YehSheng, National Pingtung University of Science and Technology, Taiwan	TD001	Groundwater balance and river interaction analysis in Pleistocene aquifer of the Saigon River basin, South of Vietnam by stable isotope analysis and groundwater modeling Mr. Tran Thanh Long, Chulalongkorn University, Thailand
14.20	TA024	Land Cover/Use Scenario Building and its Impact on Flooding inside the Iligan River Basin Mr. ALAN MILANO, MSU- Iligan, Institute of Technology, Philippines	TC016	The Roles of virtual water for assessing the impacts of food security and global food trade on Water-Energy-Food Nexus Dr. Sang-Hyun Lee, Texas A&M, USA	TD003	Estimation of Hydrological Parameter Distribution by Geostatistical methods in the Upper Central Plain, Thailand Ms.Pwint Phyu Aye, Chulalongkorn University, Thailand

14.45		Coffee Break (15 Minute)				
DAY 1 (Wednesday- 25 January 2017) THA 2017 Plenary session presentation (cont.)						
15.00	TD025	Evaluation of Near-Real-Time Satellite-based Rainfalls over Thailand Mr. Teerawat Ram-Indra, Chulalongkorn University, Thailand	TC001	Achieving Sustainable Resource Security through the Water-Energy-Food Nexus Dr. Eul Rae Lee, K-water ,Korea	TD021	Groundwater Vulnerability and Risk Assessment in Thailand using GIS-Based Modified DRASTIC Approach Dr. AKSARA Putthividhya, Chulalongkorn University, Thailand
15.25	TB002	Improving Crop Water Use with The use of Efficient Irrigation Technologies and Coconut Mulch Husk: A study on long-bean production. Mr. Iep., National University of Lao,Lao	TC007	Water Energy Carbon Nexus in Urban Water Supply System of Kathmandu Valley Mimansha Joshi, AIT, Nepal	TD005	Flow budget of groundwater system and conjunctive use pattern under climate change in Upper Central Plain, Thailand Mr. ChokchaiSuthidhummajit, Chulalongkorn University, Thailand
15.50	TB005	Water Quality Profiles And The Reservoir Utilization With Special References To Jatiluhur, Cirata And Saguling Reservoirs Dr. Luki Subehi, Indonesian Institute of Sciences, Indonesie	TA018	Spatial heterogeneity and trans-boundary pollution: A case study on the 3S River Basin Mr. Manish Shrestha, AIT, Thailand	TD010	An Assessment of Saltwater Intrusion in Cebu City Aquifers Mr. Nelson Stephen L. Ventura, De La Salle University, Philippines
16.15	TA026	Assessment of Water Resources During the 21st Century in Northern Thailand with Focus on Ping River Basin Miss. Srisunee Wuthiwongyothin , Thailand	TC013	Developing food-energy-water (FEW) nexus indicators with DPSIR framework: Experience from Taiwan Shang-Lien Lo, National Taiwan University,Taiwan	TD026	Input-Output Analysis of Water Deficits in Nan River Basin, Thailand Mr. Pavisorn Chuenchum Chulalongkorn University, Thailand
18.00		Reception Dinner (For registration participant) Venue: Le Lotus 1				

1st day ASEAN FORUM PROGRAMME (Wednesday- 25 January 2017)

Venue: Jamjuree Room, 2nd floor

16.00 -13.00	Session 1: Planning presentation Objectives: To present national water management status, to share strategies to deal with the issue of climate change and WEF Nexus and propose research/training needs. (15 minutes each)
13.00	Opening speech Mr. Saroj Srisai Assistant Director/ Head of Environment Division Sustainable Development Directorate ASEAN Socio-Cultural Community Department
13.15	Thailand Country Report 1 Dr. Somkiat Prajamwong Deputy Director General for Engineering Royal Irrigation Department, Thailand
13.30	Myanmar Country Report Ms. Htay Htay Than Department of Meteorology and Hydrology, Ministry of Transportation, Myanmar
13.45	Lao PDR Country Report Dr. Mayphou Mahachalearn Department of Meteorology and Hydrology Ministry of Natural Resources and Environment, Lao PDR
14.00	Vietnam Country Report Dr. Le Minh Nhat Head of the Climate Change Adaptation Department of Meteorology, Hydrology and Climate Change
14.15	Cambodia Country Report HE Pohn Sachak Director General Technical Affairs of Ministry of Water Resources and Meteorology of Cambodia
14.30	Coffee Break
14.45	Thailand Country Report 2 Mr. Worasart Apaipong Director-General Department of Water Resources, Thailand
15.00	Indonesia Country Report Assoc. Prof. Dr. Zainal Arifin Deputy Chairman of Earth Sciences of Indonesian Institute of Sciences/ Chairman of Indonesia National Committee of UNESCO-IHP
15.15	Philippines Country Report Dr. Seville D. David Jr. Executive Director, National Water Resources Board Philippines
15.30	Malaysia Country Report Datuk Mohd Adnan Mohd Nor Academy Science of Malaysia (ASM), Malaysia
15.45	Thailand Country Report3 Mr.Suphot Tovichakchaikul Director-General Department of Groundwater Resources, Thailand
18.00	Reception Dinner

DAY 2 (Thursday- 26 January 2017) THA 2017 Plenary session presentation

Scope		Plenary session presentation Venue: Salon A		Plenary session presentation Venue: Salon B		Plenary session presentation Venue: Krisana	
Chair		Dr. Duc H. Nguyen		Dr. Sompop Sucharit		Assoc. Prof. Chaiyuth Sukhsri, CU	
Briefing		Dr. Saisunee Budhakooncharoen				Dr. Praphawadee Otarawanna	
09.00	Exhibition		Invited C: Smart Urban Water systems – in practice Mr. Sten Lindberg, DHI, Denmark		Invited B: Principles and Methods for PIM in Action -Is the Japan’s model exceptional? Dr. Masayoshi Satoh, Prof. Emeritus, University of Tsukuba, Japan		Invited D: Extreme flood frequency analysis and risk curve development under a changing climate Prof. Dr. Yasuto Tachikawa, Kyoto University, Japan
09.30		TC008	Satellite based sub-daily downscaling of daily gauged rainfall for flood analysis via fully distributed hydrological model Mr. Pallav Kumar Shrestha, AIT, Nepal	TB004	Participatory Water Management in the Specific Locale of Sub-watershed: Negotiation Process and Institutionalization. Mr. Man Purotaganon, Thai Water Partnership, Thailand		Invited D: Assessment of the impacts of groundwater abstraction and climate change on groundwater resources in Mekong Delta, Viet Nam Mr. Nguyen Tien Tung, Division of Water Resources Planning and Investigation for the South of Vietnam, Vietnam.
09.55		TC003	Characteristics of CH4 flux from paddy field adopting the intermitted irrigation technique During the winter-spring and summer-autumn seasons in the Red River Delta, Vietnam Mr. Fumiya Inagaki, Kyoto University, Japan	TA004	Determination of Extreme Design Waves under Climate Change in the Gulf of Thailand Dr. Sutat Weesakul, Hydro and Agro Informatics Institute, Thailand		Invited D: The PhEDEX Model: Anomalous (nonlocal) solute transport in groundwater modeled by keeping track of age of sorbate Prof Dr. Tim Ginn Ph.D., Civil and Environmental Engineering, WSU, 2016- Present
10.20		TC009	A Case Study on Industrial Mismanagement of Tanneries in Hazaribagh: Water Pollution and Chromium Poisoning in Dhaka, Bangladesh Mrs. Nilay Kumar Sarker, AIT, Thailand	TB006	Proposal of a reservoir management method based on the observed accumulated areal mean rainfall for the Sirikit reservoir in the Chao Phraya River basin, Thailand Dr. Kentaro Dotani, Toyama Prefectural University, Japan	TD 009	Assessment of rainfall-run off models for stream flow and flood predictions in the Nam Song River Basin Mr. Bounhome Kimmany Chulalongkorn University, Thailand
10.45		Coffee Break (15 Minute)					
11.00	TA022	Stochastic Simulation and Frequency Analysis of the Concurrent Occurrences of Multisite Extreme Rainfalls Prof. Ke-Sheng Cheng, National Taiwan University, Taiwan	TA005	Analysis of Farmers’ Choice of Adaptations to Climate Change at NongSua District, Rangsit Canal, Thailand Dr. Sutat Weesakul, Hydro and Agro Informatics Institute, Thailand	under Changing	The Possibility of Using Solute Age to Evaluate the Effectiveness of Riverbank Filtration (RBF) Dr. Warangkana Larbkich, System Plan and Policy Analyst, Practitioner Level	

DAY 2 (Thursday- 26 January 2017) THA 2017 Plenary session presentation (cont.)

11.25	TA011	Assessment of Satellite Rainfall Estimates as a Pre-Analysis for Water Environment Analytical Tools: A Case Study for Tonle Sap Lake in Cambodia Arun. Chan. Phoern, Institute of Technology of Cambodia, Cambodia	TC014	Effect of water management on growth of malabar chestnut Dr. Yung-Liang Peng, National Taiwan University, Taiwan		Simulation and optimization methodologies to estimate groundwater sustainable yield in the Central Chi River Basin, Northeast Thailand Dr. Tussanee Nettasana, Geologist, Senior Professional Level
11.50	TD012	Flood Risk Maps and Its Applications Prof. Ming Daw SU, National Taiwan University, Taiwan	TD006	Flood Modelling in Lower Mekong River in Cambodia Dr. Sarann Ly, Institute of Technology of Cambodia, Cambodia.		Roles of Groundwater in the FED Triangle Water Resources Management Model in Thailand. Mr. Chaipom Siripornpibul, Former Inspector of Ministry of Natural Resources and Environment
12.00	Lunch Break					
Chair	Dr. Avishek Datta		Prof. Tawatchai Tingsan chali		Asst. Prof. Dr. Aksara Putthividhya	
Briefing	Dr. Saisunee Budhagooncharoen		Assoc. Prof. Dr. Tuantan Kitpaisalsakul		Dr. Warangkana Larbkich	
13.00	TA023	Climate Extremes, People's Perception and Adaptation in Lower Songkhram River Basin, Thailand, Miss. Pisinee Bariboon, AIT, Thailand	TD023	Impact of decreasing percentage of imperviousness area with flooding in urban area at Sukhumvit, Bangkok, Thailand. Mr. Detchphol Chitwatksir, Valaya Alongkom Rajabhat University under the Royal Patronage, Thailand	Ground Water under Changing Word	Assessing and Characterizing the Efficacy of the Constructed Wetland for Treating Pollutants in Landfill Leachate Miss Chadapom Busarakum, Geologist
13.25	TC010	Quantifying climate change impact on rice production in Northeast of Thailand: a critical review through water footprint concept Miss. Ranju Chapagain, AIT, Thailand	TA006	Change of the Probability Distribution of Annual Maximum River Discharges derived from the d4PDF datasets at the Indochinese Peninsula Mr. Patinya Hanittinan, Kyoto University, Japan		Application of the Precipitation-Runoff Modeling System (PRMS) to the Investigation of the Effects of Land-use Changes on the Runoff Coefficient in the Prachinburi River Basin, Thailand Dr. Phatcharasak Arlai
13.50	TA003	River Discharge and Reservoir Operation Assessment under a Changing Climate at the Sirikit Reservoir Mr. Donpapob Manee, Kyoto University, Japan	TA014	Climate change and landslide risk assessment in Uttaradit Province Miss Shotiros Protong, Department of Water Resources, Thailand		Hydrological Assessment Using Stable Isotope Fingerprinting Technique In The Upper Chao Phraya River Basin Asst. Prof. Dr. Aksara Putthividhya
14.15	TA009	Comparison of the spatial rainfall in Khun Dan Prakan Chon Reservoir by spatial interpolation techniques. Mr. Peerapong Rattanaburi RID, Thailand	TD019	Iron oxide coated activated carbons for arsenate adsorption from groundwater Miss. Manavanh MUONGPAK, Chulalongkorn University, Thailand		The Study on Groundwater Quality and Quantity Fluctuation near the Coastal Area Due To Climate Change, Thailand Dr. Praphawadee Otarawanna, Geologist, Professional Level

14.40		TA008	Effect of Land Cover Change to Annual Sedimentation in Nan Basin, Thailand Dr. Kwanchai Pakoksung, Kochi University of Technology, Japan	TD002	Estimation of river conductance values along Saigon River, Vietnam Mr. Tuan Pham Van Chulalongkorn University,Thailand		Assessment of Climate Change on Groundwater Vulnerability to Drought of Areas in Eastern Thailand Asst. Prof. Dr. Uma Seeboonruang
DAY 2 (Thursday- 26 January 2017) THA 2017 Plenary session presentation (cont.)							
15.05					Coffee Break (15 Minute)		
15.20		TA015	Assessment of an Urban Drainage System in Phnom Penh Using Storm Water Management Model Mr. Sokchhay Heng, Institute of Technology of Cambodia, Cambodia	TD004	Mechanism of land subsidence due to groundwater production. Mr. P.,Phong prayoon, non-affiliated,Thailand		Impact of Climate and Land Use Changes on Surface Water and Groundwater Potential in Huai Sai bat Watershed, NE, Thailand Dr. Phayom Saraphirom
15.45		TA021	Change of water budget between 1960's and 2000's at the seasonal tropical forest in Northern Thailand Dr. Katsushige Shiraki, Tokyo University of Agriculture and Technology, Japan	TD022	Potential Impact and Risk Assessments of Future Climate Conditions on Salinisation in Central Huai Luang River Basin, Northeast, Thailand Miss. Kewaree Pholkem , Khon Kaen University , Thailand		Hydrogeochemical Features of Karst in the Western Thailand Mr. Mahippong Worakul, Geologist, Senior Professional Level
16.10		TD016	Analysis of Rainfall Induced Landslide Dam Geometries and Failures (Poster) Prof. KWANSUE JUNG, Chungnam National University, South Korea, Korea	TD008	Drought Risk Assessment of Irrigation Project Areas in a River Basin Prof. Tawatchai Tingsanchali, AIT , Thailand		Developing Policy Recommendations for the Water, Energy, and Food Security of Thailand (Assoc. Prof. Dr. Lampang Manmat)

2nd day ASEAN FORUM PROGRAMME (Thursday- 26 January 2017)

Venue: Jamjuree Room

-09.00 1200.	Session 2: Academic presentation Objective: To update research status and results on water management under climate change environment and future research/training plan
09.00	Presentation on Cambodia research Dr. Sarann Ly Head Department of Rural Engineering Institut de Technologie du Cambodge (ITC), Cambodia
09.20	Presentation on Vietnam research Assoc. Prof. Dr. Hoang Minh Tuyen Vice Director of IMHEN, Vietnam
09.40	Presentation on Malaysia research Ir Mohd Zaki Mat Amin National Hydraulic Research Institute of Malaysia (NAHRIM) Director of Research Centre for Water Resources
10.00	Presentation on Lao PDR research Mr. Saykham Sithavong Deputy Head of Irrigation Department Faculty of Water Resource, NUOL
10.20	Presentation on Thailand research 1 Dr. Piyatida Ruangrassamee Department of Water Resources Engineering Faculty of Engineering, Chulalongkorn University, Thailand
10.40	Coffee Break
11.00	Presentation on Indonesia research Dr. Fauzan Ali Director of Research Centre for Limnology/Secretary of Indonesian National Committee of UNESCO-IHP
11.20	Presentation on Philippines research Prof. Alan E. Milano Civil Engineering Department MSU-Iligan Institute of Technology, Philippines
11.40	Presentation on Thailand research 2 Dr. Pongsak Suttinon Department of Water Resources Engineering Faculty of Engineering, Chulalongkorn University, Thailand
12.00	Summary of the session
12.10	Lunch
- 13.00 16.00	Session 3.2: Technical Training (more details in separate training programme) Objective: To provide hands-on training and perform satellite bias correction for hydrological applications Introduction of satellite-based rainfall product and bias correction. Bias correction workshop for drought analysis. Coordinated by Dr. Piyatida Ruangrassamee Department of Water Resources Engineering Faculty of Engineering, Chulalongkorn University, Thailand
- 16.10 16.30	Closing Ceremony (Joint closing ceremony for the THA2017 and ASEAN Forum)
18.00	Farewell Party Dinner (For foreign and invited guests)

2nd day ASEAN FORUM PROGRAMME (Thursday- 26 January 2017)

Venue: Sakthong Room

- 13.00	Session 3.1: ASEAN Roundtable
16.00	Objective: To present existing collaborative activities and discuss future collaborative activities/proposals on research/education
13.00	Sharing climate change projection data for impact assessment studies in ASEAN region Prof. Dr. Yasuto Tachikawa Department of Civil and Earth Resources Engineering, Graduate School of Engineering Kyoto University, Japan
13.15	Progressive Drought Monitoring and Risk Assessment Using SPI - Experiences of Taiwan Prof. K S Cheng National Taiwan University, Taiwan
13.30	Present and Future collaboration Prof. Dr. Kwansue Jung KWRA, Korea
13.45	Present and Future collaboration of International Organizations Dr. Ramasamy Jayakumar UNESCO, Bangkok.
14.00	“Recent Development of Precipitation Climate Dataset for Monitoring Hydroclimate Extremes.” Prof. Dr. Kuolin Hsu Center for Hydrometeorology and Remote Sensing, University of California - Irvine, UCIrvine
14.15	Present and Future collaboration Assoc. Prof. Dr. Chanathip Pharino Deputy Director Public Well-Being Division Thailand Research Fund
14.30	Coffee Break
14.45	Research/training possibility of Philippines Prof. Alan E. Milano
14.55	Research/training possibility of Indonesia Assoc. Prof. Dr. Zainal Arifin
15.05	Research/training possibility of Lao PDR Mr. Saykham Sithavong
15.15	Research/training possibility of Malaysia Ir Mohd Zaki Mat Amin
15.25	Research/training possibility of Vietnam Assoc. Prof. Dr. Hoang Minh Tuyen
15.35	Research/training possibility of Cambodia Dr. Sarann Ly
15.45	Discussion on research/training/education of future research proposals (i.e. satellite application and WEF Nexus)
16.00	Conclusions
- 16.10	Closing Ceremony (Joint closing ceremony for the THA2017 and ASEAN Forum)
16.30	
18.00	Farewell Party Dinner (For foreign and invited guests)

Opening Speech

Prof. Dr. Bundhit Eua-arporn

President of Chulalongkorn University

Dear Prof. Emeritus Khunying Suchada Kiranandana, the Chairman of the University Council; ASEAN secretariat delegate; the Director UNESCO Asia and Pacific Regional Bureau for Education; the chairman of the THA 2017 International Conference on Water Management and Climate Change Towards Asia's Water-Energy-Food Nexus; Regional Water Management Officer, FAO Regional Office for Asia and the Pacific; Secretary-General, Office of the National Economic and Social Development Board (NESDB), Thailand, management from water institutions, faculties from universities in ASEAN and in neighboring region and all honorable guests.

I, Prof. Dr. Bundhit Eua-arporn, the President of Chulalongkorn University would like to report on the background of the THA2017 International Conference as follows:

There has been the higher frequency of water disasters and water shortage in Asian region including Thailand over recent years. Each country has attempted to deal with the problems using various means depending on physical characteristics, economic and social conditions in the area. To address water-related problems at an international level, the dimensions of economy, society and environment must be taken into account together at the same time. Moreover, the dimensions of water, food and energy must also be considered as they are interconnected. Recently, the issue of climate change and WEF Nexus has become a crucial factor which needs to be integrated into planning to achieve sustainability. A forum for exchange knowledge, information and experience in planning is therefore important.

The THA International Conference was first initiated in 2015 under the theme of Climate Change and Water & Environment Management in Monsoon Area. The THA 2015 international conference was successful according to the main objective of serving as the public assembly. There were three keynote speakers, 268 Thai participants, 83 foreign participants from 15 countries. The ASEAN Academic network was formally formed. A hands-on technical training about "Satellite-based Rainfall (PERSIANN) for Planning and Management for Natural Disasters in Monsoon Asia" was conducted.

This year, 2017, Chulalongkorn University will celebrate its 100th anniversary of founding, we, in association with 8 national and 16 international collaborative agencies organize the THA 2017 International Conference on Water Management and Climate Change Towards Asia's Water-Energy-Food (WEF) Nexus during January 25-27, 2017. This conference serves as a public forum for researchers, scientists, practitioners and policy makers to present their research findings, share knowledge, experience and perspective, update new progress of relevance to the issue of disaster, irrigation and water management. The conference pays particular attention to developing the skills and ability to address the problems of climate change and WEF Nexus.

The conference consists mainly of five parts including oral presentation, poster exhibition, special training, and study tour. The presentations are categorized into four main themes including 1) Climate Change and Uncertainty in Hydrology and Meteorology, 2) Participatory Management for Water and Irrigation Project, 3) Emerging Technologies in Water Management and Environment Towards W-E-F Nexus, 4) Disaster Management/ Groundwater Management.

The THA 2017 International Conference is running in parallel to the workshop on ASEAN Academic Networking. This is to provide an opportunity for the management and Thai scholars to exchange knowledge and experience and prepare for the establishment of the ASEAN Academic Network which aims to promote collaboration in research and education in ASEAN that can be extended to other countries in the future.

The THA 2017 International Conference is therefore:

- 1) gathering scholars and combining the knowledge of climate and water and disaster management together to be able to identify the problem in a holistic manner through the view of planners, practitioners and academic researchers
- 2) gathering the management at DG level from ASEAN countries and Thailand to exchange perspectives on planning, addressing water problems and to propose key areas of future collaborative research to cope with global climate change and WEF Nexus issues especially in ASEAN region
- 3) providing an opportunity to meet distinguished scholars coming from ASEAN and international to exchange research concept and research findings as well as to seek for collaborative support for the establishment of the ASEAN Academic Network from countries outside ASEAN in the future.

The THA 2017 International Conference has received kind cooperation from a number of international organization for example, UNESCO; DHI, Denmark; ICHARM Japan; PAWEES, Japan; Kyoto University, Japan, National Taiwan University; Chungnam National University, Korea; K-Water, Korea; NCKU, Taiwan; and University of California – Irvine.

I hope that all participants of the THA 2017 International Conference will gain more knowledge and innovations regarding climate change, water and environmental resources management, water disaster management, new technology and operation of basin organization from the presentations given by scholars and experts from several countries in different regions of the world. This is believed to lead to the creation of a network for academic and professional research as well as cordial collaboration in this region.

Now it is good timing, I would like to open the THA 2017 International Conference and hope that the conference will proceed smoothly towards the objectives set.

Congratulation Speech

Dr. Gwang-Jo Kim

Director, UNESCO Asia and Pacific Regional Bureau for Education (UNESCO Bangkok)

Prof. Emeritus Khunying Suchada Kiranandana, Chairman of University Council

Prof. Bundhit Eua-arporn, President of Chulalongkorn University

Distinguished Guests,

Ladies and Gentleman,

It is my pleasure to join you for the opening of the 2017 Thailand Hydrologists Association International Conference. I'm pleased to note that that this international conference is being jointly organised by Chulalongkorn University, as part of its centenary celebration.

The Taoist Chuang-Tzu once said, "Water is the blood of the Earth, and flows through its muscles and veins."

And, indeed, it is the desire to keep that lifeblood strong – to ensure its flow sustains us now and for generations to come – that brings us here today. We are here to discuss issues of critical importance to the survival of our countries, this region and our planet – specifically the impacts of climate change and other pressing challenges on Asia's water-energy-food nexus.

Before we discuss the other sectors of this nexus, let's focus first on water. Freshwater is central to all aspects of life – from economic development to human health and sustainability and it cuts across all of UNESCO's fields of competence. Water – and the lack of it – is not simply an issue for innovative technology and science to address. The implications are far broader. It is about social equity and justice. It is about gender equality. It is about lasting peace and sustainable development.

Freshwater has been a priority for UNESCO since the Millennium Summit and the Millennium Development Goals, which focused in part on improving access to clean drinking water and basic sanitation. We worked towards those aims and have now refocused and renewed our efforts around the 2030 Agenda for Sustainable Development and specifically Goal 6: Ensure availability and sustainable management of water and sanitation for all. We pursue this important goal in concert with what we might call the UNESCO Water Family, comprising:

- our flagship International Hydrological Programme;
- the network of 26 water-related centres under UNESCO's auspices;
- the World Water Assessment Programme, the flagship UN-Water programme that brings together 30 UN agencies and produces the now-yearly World Water Development Reports;
- and the 39 water-related UNESCO Chairs and UNITWIN network, including the latest one at Chulalongkorn University on Water, Disaster Management and Climate Change.

The stakes are high. Freshwater is limited, unevenly distributed, poorly managed and under severe pressure.

Billions of people remain vulnerable to water scarcity, deterioration of water quality and water-related disasters, such as floods and droughts.

Water security is essential to sustainable development and vital to building inclusive, peaceful societies. This is UNESCO's position, and it is reflected in the strategic plan developed for the 8th Phase of the International Hydrological Programme on Water Security, which responds to local, regional, and global challenges.

This plan highlights six knowledge areas – water-related disasters, groundwater, water scarcity and water quality, water for human settlements, ecohydrology, and water education – each of which is critical for water security.

Ladies and Gentlemen,

The water-energy-food nexus, the main theme of this conference, offers a way of looking at our modern resource challenges that reframes these issues to emphasize their interconnectedness. It is a holistic concept and one that, if properly understood, can help societies around the world deliver on the SDGs.

The nexus is a forward-thinking way to identify pathways to a sustainable future. Water is essential to the nexus and it plays a primary role in climate change. The impacts of climate change are typically expressed through the water cycle, leading to undesirable outcomes, ranging from flooding to crop failure to climate migration.

Geopolitical tensions have the potential to pose grave threats to water security, although at present there are more examples of water scarcity leading to cooperation rather than conflict.

The close links between the different sectors of the water-energy-food nexus are also apparent – hydropower dams, for example, manage both water supply and generate electricity. The nexus indicates that a holistic approach is essential to a deeper understanding of the challenges ahead.

The need for an integrated and participatory approach focused on the water-energy-food nexus is essential to achieving the SDGs.

Policy-makers who want to address the water-energy-food nexus in a forward-looking and effective manner tend to approach these issues in a horizontal manner, with a mandate to develop a broader cross-cutting vision.

Ladies and Gentlemen,

Our efforts to expand our knowledge in these crucial areas and deepen and localize our focus takes a major step forward today. UNESCO and Chulalongkorn University would like to take this opportunity to launch the UNESCO Chair in Water, Disaster Management and Climate Change, which we have agreed to establish at Chulalongkorn University's Faculty of Engineering.

On behalf of UNESCO, I would like to congratulate Prof. Bundhit Eua-arporn, President of Chulalongkorn University, on the establishment of the new UNESCO Chair.

Prior to the establishment of the UNESCO Chair Programme in 1992, our organization ran a fellowship programme, and while it did facilitate technology transfer from developed to developing countries, some weaknesses were apparent. For example, the direct beneficiaries were few in number; costs were high and there was a risk of a brain-drain occurring.

Developing countries pointed out these weaknesses, which led to the establishment of the UNESCO Chair Programme. Under this unique programme, eminent specialists and professors are appointed UNESCO Chair at universities or institutions of higher education in developing countries. This approach means that more people can benefit from their shared expertise, and the risk of a brain drain is significantly lessened.

The UNESCO Chairs and UNITWIN Networks serve as think tanks and bridge-builders between academia, civil society and local communities as well as between research and policy-making.

They have proven useful in informing policy decisions, establishing new teaching initiatives, spurring innovation through research and enriching existing university programmes, while promoting cultural diversity.

In areas suffering from a dearth of expertise, these Chairs and Networks have become touchstones of excellence and innovation at the regional and sub-regional levels. They have also strengthened North-South-South cooperation.

This programme has attracted significant interest from developing countries, universities and donors. The UNESCO Chair Programme currently involves over 700 institutions in 128 countries.

The current UNESCO Chair on Water, Disaster Management and Climate Change hosted by Chulalongkorn University realizes the importance of collaboration on water and disaster management among ASEAN countries. To that end, UNESCO partnered with Chulalongkorn University to organize the first workshop on ASEAN Academic Networking in Water, Disaster Management and Climate Change in 2014 and the 2nd technical workshop in 2015. These initiatives brought academics from ASEAN countries together to promote and support collaborative research, discuss new technologies as well as share methods of preparation, warning and adaptation related to water and disaster management and climate change. This UNESCO Chair will serve as a platform for disseminating and sharing knowledge of water and disaster management and climate change in achieving related SDGs.

Under the auspices of the UNESCO Chair, Chulalongkorn formed the ASEAN Academic Network, inviting faculty members and researchers from ASEAN Universities and policymakers to share knowledge and experiences at the regional level. Joint research to address water-related disaster threats faced by several ASEAN member states – such as floods, droughts, and landslides – can improve the efficiency of resource utilization due to pooled resources. Such a collaboration can mean tremendous savings for countries thanks to reduced redundancies in infrastructure investment, technology and personnel. Technology transfer costs will also be reduced due to economies of scale across ASEAN countries.

Parallel to this conference, UNESCO and the UNESCO Chair are jointly organising the ASEAN Technical Workshop on the Satellite-based Rainfall Adjustment and Drought Monitoring System under UNESCO-IHP-GWADI, a global initiative with University of California, Irvine.

Experts from the Center for Hydrometeorology & Remote Sensing (CHRS), at the University of California Irvine, will provide hands-on training to experts from ASEAN on the use of PERSIANN – Precipitation Estimation from Remotely Sensed Information using Artificial Neural Networks. This system, which was developed at the University of California, Irvine's Center for Hydrometeorology & Remote Sensing (CHRS), is used to monitor and estimate precipitation through satellites, and is a contribution to the UNESCO-IHP-GWADI initiative.

The workshop brings together academics, scientists, policy-makers and researchers to share information and learn about the potential benefits of satellite-based rainfall applications in their countries.

Going forward, UNESCO expects the UNESCO Chair at Chulalongkorn to play an important role in facilitating technical knowledge dissemination within ASEAN as well as to enhance north-south partnerships in technology transfer.

The Chinese philosopher Lao Tzu once said: "The highest form of goodness is like water. Water knows how to benefit all things without striving with them." The partnerships that we aim to foster and strengthen here and the knowledge we share aspire to this ideal – to protecting and preserving water's life-giving benefits.

I wish the UNESCO Chair great success in advancing this mission and I hope you all a fruitful discussion over the next three days on the critical issues before you.

Thank you.

Opening Remarks

Prof. Emeritus Khunying Suchada Kiranandana

Chairman of the University Council

Distinguished delegates, ladies and gentlemen, it is my great pleasure to welcome you all to the THA 2017 International Conference on Water Management and Climate Change Towards Asia's Water-Energy-Food Nexus and the ASEAN Academic workshop which are organised by Chulalongkorn University, in association with 8 national and 16 international collaborative agencies. This event provides a forum for water planners and water professionals in academia coming from a number of countries including Thailand, other ASEAN countries, countries in ASIA, and USA to present academic findings, exchange knowledge and experience in water and disaster management to increase preparedness and capability to cope with climate change and Water-Energy-Food Nexus issues which are likely to be more intense. I have a great honour to attend the THA International Conference and the ASEAN Workshop today. I would like to take this opportunity to provide you information and philosophy of water management in Thailand that are applied to the royal projects. This could probably be of beneficial to encouraging collaboration on water, disaster management and climate change within the ASEAN region which could be extended to other regions in the foreseeing future.

Thailand has adopted the Philosophy of Sufficiency Economy into developing the 8th-10th (1997-2011) Economic and Social Development Plans. The Philosophy of Sufficiency Economy has been adapted to be used at various scales ranging from household, community and national as a whole. It has been well proved to increase resilience to a rapid change in climate between 2012 to 2016. The Philosophy of Sufficiency Economy in combination with knowledge, science, technology innovation and creativity are critical components to attain sustainable development and stability.

The philosophy of water resources management initiated by the late King Bhumibol Adulyadej focuses on the development for solving water problems in the country by considering infrastructure and management simultaneously. Also, His Majesty King Bhumibol attempted to address the problems of agriculture and soil. Examples of the royal projects area project for improving soil acidity (Klang Din), new theory agriculture and organic farming. His Majesty King Bhumibol established a cooperative system, Sufficiency Economy and Suwannachart retail shop for the development of community. To improve education and literacy of Thai residents, His Majesty King Bhumibol established an education centre demonstrating how to deal with the problems of forest, soil and water. Distance learning is also used to disseminate knowledge to rural areas to increase the resistance and resilience of the local residents to various kinds of risks including land slide, flood and drought and to solve the problem of poverty directly at the community level.

The royal projects are undertaken based on the philosophy of His Majesty King Bhumibol covering three dimensions of conceptual principle, framework and technology.

Conceptual principle refers to self-reliance, comprehensive thinking and integrating, using natural means as solutions to natural problems. Everything has its own value and no waste. Solutions to the problems must be designed to comply with the surrounding context of the area and lead to

sustainability. Also, there must not be unfavourable effects on other people. Solutions must be turned into actions for real demonstration.

Framework means the use of information, work diagram, mind map, integration of information and work diagram into actual site where the problem occurs, network of operation, experiment, monitoring, evaluation and extension of the results.

Technology includes handheld transceiver, computer, internet, GIS map, GPS, data from satellite, radar and tele-gauges. Appropriate technologies for specific site must be selected.

Examples of the royal projects that have been implemented are: the Rainmaking Project to expedite rainfall in the desired areas; the monitoring of storm data for the use of reservoir management; the application of satellite data for flood monitoring; using natural pond for waste water treatment such as the LaemPhakBia Project

Each royal project has adopted and applied the philosophy of Sufficiency Economy initiated by His Majesty King Bhumibol into resources management leading to sustainable development and improved shelter from future climate change.

I sincerely hope that water management under the philosophy of Sufficiency Economy initiated by His Majesty King Bhumibol as mentioned above will be beneficial to you as it provides information for discussion session on preparedness for climate change. Also it encourages further academic collaboration within the region which can subsequently be extended to other regions.

Now it is good timing to open our International Conference and ASEAN Workshop. I wish that the International conference and ASEAN Workshop proceed smoothly and achieve the desired objectives.

Session A

Climate Change and Uncertainty in Hydrology and Meteorology

Probabilistic Flood Forecasting using Ensemble Numerical Weather Prediction rainfalls during the 2011 Largest Flood Event in Japan

Wansik YU^{1,a,*}, Kwansue JUNG^{2,b}

Abstract In early September, 2011, local heavy rainfalls due to season’s 12th typhoon, “Talas” caused large flooding and enormous landslide disasters over the Kinki, Chugoku, Shikoku, and Tokai regions in Japan. It also caused unprecedented human damages, resulting in 78 dead and 16 missing persons. In these types of extreme events, it is essential to be able to provide as much advance warning as possible. This advance warning requires both quantitative precipitation forecasting (QPF) and quantitative flood forecasting (QFF). Ensemble flood forecasting driven by ensemble NWP rainfall provides additional information to the deterministic flood forecast in the short forecast range (1~2days). Therefore, in this study, we assessed the ensemble NWP rainfall with 2km horizontal resolution and 30hr forecast time whether it can produce suitable rainfall or not during typhoon “TALAS”, 2011. We also assessed the ensemble flood forecast based on ensemble NWP rainfall for hydrological application. It can be concluded from the study that ensemble NWP rainfall could improve the forecast accuracy compared with deterministic forecast in terms of quantitative precipitation forecast. Ensemble flood forecast driven by ensemble rainfall forecasts also could produce comparable results in comparison of observed data, even the maximum peak discharge value among ensemble was underestimated. For the improvement of this underestimation, we tried to utilize the spatial shift of NWP rainfall fields. Later, we also need to examine a variety of case studies of typhoon event in order to assess the performance of ensemble flood forecasts.

Keywords *Typhoon Talas, Ensemble NWP rainfall, Ensemble Hydrological Forecasting*

Wansik YU
PhD, International Water Resources Research Institute
Chungnam National University, Daejeon, South Korea.
yuwansik@gmail.com

Kwansue Jung
Professor, Department of Civil Engineering
Chungnam National University, Daejeon, South Korea.
ksjung@cnu.ac.kr

Introduction

Flood forecasting is an important technique to reduce damages from flood disasters. As the accuracy of weather forecasts has steadily improved with advances in numerical weather prediction (NWP) techniques over the years with increasing computing power, it is now possible to generate high-resolution rainfall forecasts at the catchment scale and to integrate quantitative precipitation forecasting (QPF) into flood forecasting systems with extended forecast lead time (Demeritt *et al.*, 2007; Cuo *et al.*, 2011). At the same time, one of the rinsing scientific research themes in the flood forecasting area is the development of ensemble prediction systems (EPS). Several authors have been utilized and investigated the EPS, and they found that ensembles increase forecast accuracy and allow for skillful predictions at longer lead times (Buizza *et al.*, 1999; Gouweleeuw *et al.*, 2005; Roulin and Vannitsem, 2005; Palmer and Buizza, 2007; Roulin, 2007; Xuan *et al.*, 2009).

However, in many cases, the potential of forecasting with EPS is described alongside cautious approaches regarding a considerable variability and uncertainty, which would have to be reduced in the future. First, the time/space scale of the hydrological model is still much finer than that of the meteorological model, although limited-area predictions was used directly into flood forecast in large catchments (>10,000km²) in few cases (Cloke and Pappenberger, 2009). Schaake *et al.* (2004) analyzed the statistical properties of the prediction outcomes from the US National Centers for Environmental Prediction (NCEP) during 1997 and 1999 over the continental US. They found that ensemble forecasts were biased in many cases and the ensemble spread was insufficient to capture the forecast error distribution. Ebert *et al.* (2007) also stated that QPF quality needs to be improved to provide reliable hydrologic prediction, and errors in QPF location, timing, and intensity hampered the direct application of QPF from the NWP into hydrologic prediction. They also found that displacement of the forecasting rainband was the dominant error source in QPF in most cases, which means that the intensity and shape of the forecasted storm cell may be correct but the location of the storm cell is wrong. As a result, it has caused the under-dispersion of ensemble spread (i.e. not enough

spread, and thus under-representation of uncertainty). In order to use EPS properly into flood forecasting systems on a small catchment scale, above mentioned meteorological characteristics (e.g. spatial shift, and rather coarse resolution yet) should be considered carefully.

Given the current issue with ensemble forecast methods, the aims of this research is (1) to evaluate the applicability of current ensemble NWP rainfall into the flood forecasting of the catchment scale in Japan, (2) to identify the forecast error and the ensemble spread and their time evolution with the forecast lead time, and (3) to examine the spatial shift of ensemble rainfall fields to correct the displacement of the spatial position and to improve the flood forecast accuracy. For these objectives, we used the latest ensemble rainfall forecast with 30h forecast time and a horizontal resolution of 2km, which was experimentally announced by the JMA, Japan during the typhoon in 2011. The typhoon event brought severe flood disasters in the Shingu river basin of Kii peninsula and this study evaluate the applicability of the latest NWP forecast scheme of the JMA in a viewpoint of the hydrologic forecasting. Normalized root mean square error (RMSE) and log ratio bias were utilized as error indexes to assess the performance of the ensemble forecasting.

Data, Methodology and Study Area

Meteorological Input data

The latest forecast model was developed and implemented by Meteorological Research Institute (MRI) of Japan Meteorological Agency (JMA), Japan for rainfall prediction with extended lead time using nonhydrostatic model (Saito *et al.*, 2007). These studies are composed of 11 members (1 unperturbed and 10 perturbed members), with a horizontal resolution of 10

km and 2 km, and the latter nested inside the former with a 6-hour lag. Both the 10 km and 2 km resolution systems used the JMA Non-hydrostatic Model (NHM) as the forecast model. Whereas the 10 km resolution forecast adopted the cloud microphysical process and Kain-Fritsch convective scheme, the 2 km resolution forecast did not use a convective scheme because of its cloud resolving resolutions. One forecast, the “control run,” is forecast with a non-perturbed analysis and is similar to the Meso-Scale Model (MSM) of JMA from the viewpoints of initial and lateral boundary conditions. At first, the ensemble prediction with a horizontal resolution of 10km was performed up to 36h forecast time at 9pm JST, and its downscale forecast with a horizontal resolution of 2km was performed up to 30h forecast at 3am JST. In this study, the ensemble surface precipitation (Psrf) from 2km downscaled NWP data was utilized as input data into a hydrologic model, and the control run forecast was regarded as deterministic forecast to evaluate the efficiency of the ensemble flood forecasting.

A distributed hydrologic model

We used a distributed hydrologic model based on “Object-oriented Hydrological Modelling System (OHMyoS)” (Takasao *et al.*, 1996). A digital elevation mode with 250 m resolution is used to calculate the flow direction and to delineate a sub-catchment for each river segment. One dimensional kinematic wave method for subsurface and surface flow simulation, which was enhanced by Tachikawa *et al.* (2004), is applied to each grid-cell. Fig. 1(a) is a schematic of spatial flow movement in this model. The rainfall over all hillslope elements flows one-dimensionally into the river nodes and then routes to the catchment outlet.

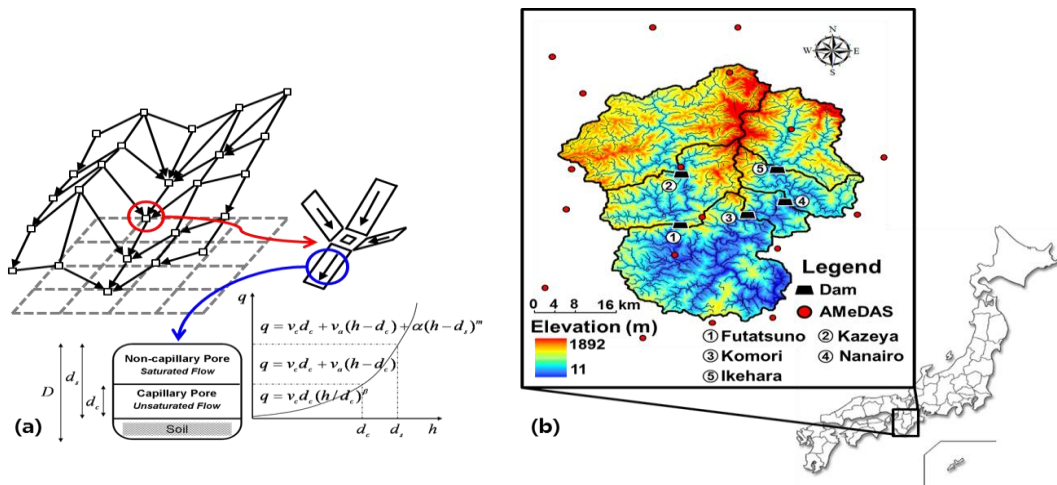


Fig.1 1. (a) Spatial flow movement and stage–discharge relationship of flow process in the hillslope elements (b) Study area within Kii peninsula in Japan

$$q = \begin{cases} v_c d_c (h/d_c)^\beta, & 0 \leq h \leq d_c \\ v_c d_c + v_a (h - d_c), & d_c \leq h \leq d_s \\ v_c d_c + v_a (h - d_c) + \alpha (h - d_s)^m, & d_s \leq h \end{cases} \quad (1)$$

$$\frac{\partial h}{\partial t} + \frac{\partial q}{\partial x} = r(x, t) \quad (2)$$

The discharge per unit width q [m^2/s] is calculated by Eq. (1), combined with the continuity equation, Eq. (2), where t is the time (s), x is space (m), $r(t)$ is the rainfall intensity (mm/h), $v_c = k_c i$ (m/s), $v_a = k_a i$ (m/s), $k_c = k_a / \beta$ (m/s), $\alpha = \sqrt{i} / n$ ($\text{m}^{1/3}/\text{s}$), $m=5/3$, i is the slope gradient, k_c (m/s) is the hydraulic conductivity of the capillary soil layer, k_a (m/s) is the hydraulic conductivity of the non-capillary soil layer, n ($\text{m}^{1/3}/\text{s}$) is the roughness coefficient, and d_c and d_s are soil depth in the capillary and non-capillary pore, respectively.

Target Area

In this study, we selected the Shingu River basin as the study area to assess the flood forecast applicability utilizing the ensemble NWP rainfall because Typhoon ‘Talas’ caused enormous flooding and landslide disasters in the Shingu River Basin. Shingu River Basin is located in the Kii peninsula of the Kinki region, Japan and covers an area of $2,360 \text{ km}^2$ (Fig. 1(b)). The topography of the basin is characterized by a mountainous upstream in the north and a flatter plain in the south. The elevation in the basin is in the ranges from 11 to 1892 m, with an average of about 644 m. The

five dams Futatsuno, Kazeya, Komori, Nanairo, and Ikehara are located upstream.

Results and discussion

Ensemble flood forecasting

We focused two sub-catchments, which are Futatsuno and Nanairo dam catchments (Nos. 1 and 4 of Fig. 1(b)) located in the Shingu River basin to assess the performance of ensemble flood forecast driven by NWP rainfall. The analysis was performed in rising limb and peak discharge periods separately because these two periods are most important phase of the real-time flood forecasting. Two additional dams, Kazeya and Ikehara (Nos. 2 and 5 of Fig. 1(b)), are located in the upstream of the Futatsuno and Nanairo dam catchments, respectively. Here, observed outflow from the Kazeya dam and Ikehara dam were directly utilized as the upper boundary conditions to the subject dam basins to focus on only the Futatsuno and Nanairo catchments.

Fig. 2 shows the results of the 30h ensemble flood forecast over the Futatsuno and Nanairo dams in the rising limb (Top) and the peak discharge period (Bottom) during Typhoon ‘Talas’ event. As shown the rising limbs period of Futatsuno dam catchment, both the control run and the ensemble forecast produced a suitable discharge up to 18h lead time, but were under-predicted compared with the true value from 18 to 30h lead times caused by the underestimation of the rainfall forecast (it is not shown in this paper, refer to Yu *et al.* (2013) for details of the predicted rainfall result). In the forecast period of peak discharge, on which we focused in this study, the control run forecast was typically lower than the observed discharge caused by spatial shift of predicted rainfall field from the correct spatial

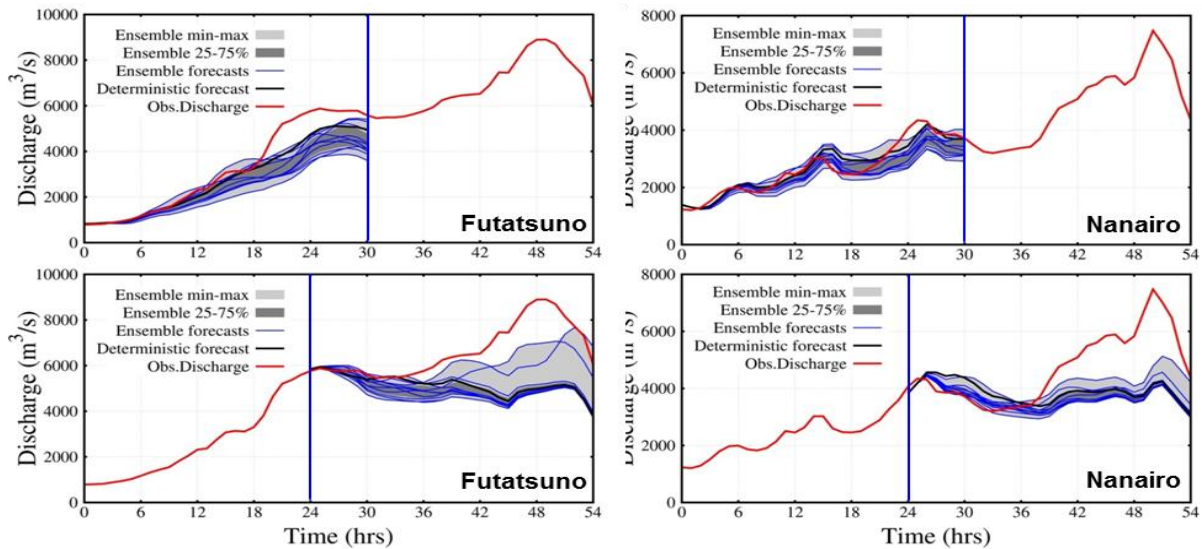


Fig.2 30h ensemble forecasts (top: on 2 September 2011 at 03:00 JST - time 0 in the figure, bottom: on 3 September 2011 at 03:00 JST - time 24 in the figure, left: Futatsuno dam - 356.1 km^2 , right: Nanairo dam - 182.1 km^2)

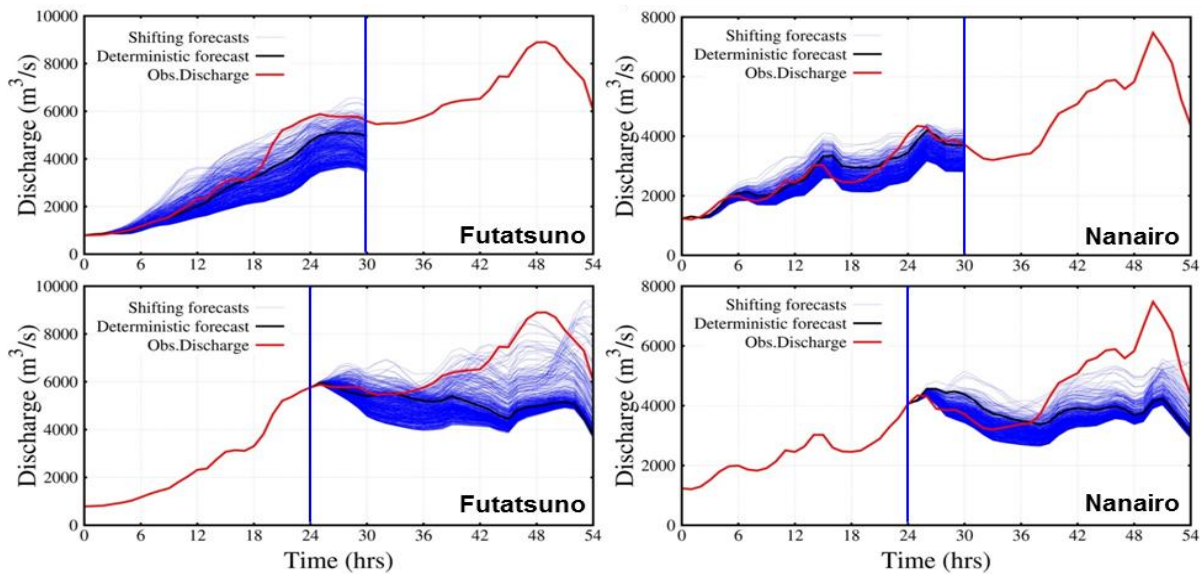


Fig.3 Same as Fig. 2, but with the spatial shift of ensemble rainfall field.

position. The most ensemble members were also under-predicted than the observed discharge, but a few ensemble members exceeded the deterministic control run forecast, and were close to the true value. In the rising limbs period of Nanairo dam catchment, the deterministic forecast provided the suitable prediction compared with the ensemble forecasts and the true value, and ensemble spread could cover the uncertainty of the deterministic forecast. In the forecast term of peak discharge, both the deterministic and the ensemble forecasts were under-predicted than the true value as the same reason in Futatsuno dam catchment. However, we could confirm that (1) the ensemble forecasts produced better results as compared with deterministic forecast, and (2) the ensemble forecasts have the potential to overcome the insufficiency of the deterministic forecast in terms of QPF.

Accuracy improvement of flood forecast using spatial shift of rainfall field

We examined the spatial shift of ensemble rainfall fields considering the displacement from the correct spatial position to improve the flood forecast skill. Fig.4 shows a schematic of spatial shift scheme using ensemble NWP rainfall fields. For the spatial shift with ensemble NWP rainfall fields from the original position, the transposed catchment mask (100 km × 100 km) moved into the original forecast domain with a maximum distance in the x and y directions of each at about 40 km with 5 km interval and in 8 directions from the right side rotating in a counter-clockwise direction with 45° intervals in order to produce additional ensemble information. We finally constructed additional 715 transposed ensemble domains (existing 11 ensemble

members × 8 distances × 8 directions + 11 original locations of established ensemble members). And then we compared error indexes, which are the normalized root mean square error (RMSE) and the log ratio bias, to assess the performance of the spatial shift method. For the spatial shift of ensemble rainfall fields, the catchment mask moved within the forecast domain with a maximum distance in x and y direction of about 80km with 5km interval.

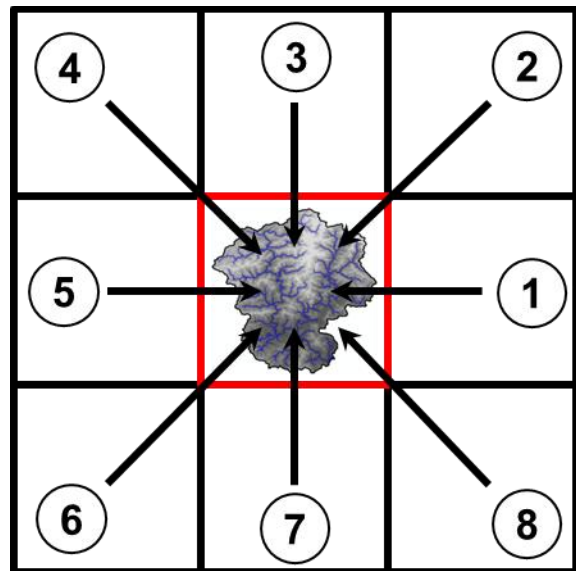


Fig.4 A schematic diagram representing the of spatial shift of ensemble NWP rainfall fields

Fig.5 shows the results of the 30h ensemble flood forecast over the Futatsuno and Nanairo dams in the rising limb and the peak discharge period using the spatial shift of ensemble rainfall fields. As shown the

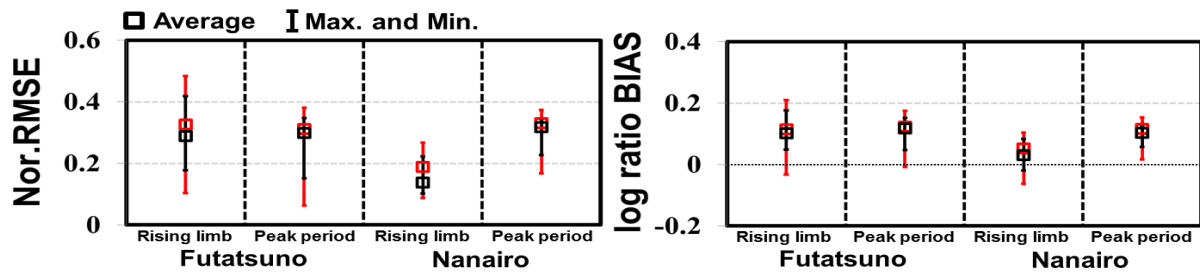


Fig.5 Verification results of discharge with normalized RMSE and log ratio bias for rising limb and peak period. Red and black color mean original and spatial shift ensemble forecast results, respectively.

rising limbs period of Futatsuno dam catchment, the accuracy of the under-predicted area was improved and ensemble members by the spatial shift could capture the forecast error. Also, in the peak discharge period, ensemble members were close to the observed discharge in the peak period. In case of Nanairo dam catchment, it was also improved in the rising limb and the peak discharge period although it was underestimated in the peak discharge period.

To evaluate the accuracy improvement of the flood forecast, we calculated two error indexes (Fig. 4). The first is the normalized root mean square error (RMSE), which is normalized by the mean value of the observations during the each forecast period (30h). The second is the log ratio bias, which a relative error and provides information about the total amount of rainfall. A log ratio bias value of zero indicates a perfect forecast; positive and negative values indicate underestimated and overestimated forecasts, respectively. From the index of normalized RMSE and log ratio bias, we could know that the flood forecast using the spatial shift of ensemble rainfall fields provided the suitable results compared with the original flood forecast. However, in the flood forecast using spatial shift of ensemble rainfall fields, they have a lot of noise coming from original ensemble members. Therefore, it should be investigated the shift location and ensemble member, which have the highest efficiency criteria in future work.

Concluding Remarks

The findings from EPS projects and case studies (hindcasts) evaluating ensemble flood forecasting clearly showed great potential for using EPS to increase flood early warning time, but equally emphasized the need for further research on the interpretation of ensemble outputs, sufficient events for statistical analysis, especially pre/post-processing (i.e., some kind of correction) of the raw ensemble outputs. This study assessed the applicability of flood forecast using ensemble NWP rainfall and a distributed hydrologic model on the Shingu river basin during Typhoon ‘Talas’ event. The latest ensemble rainfall forecast with 30h

forecast time and a horizontal resolution of 2km was utilized to provide the input data into the hydrologic model.

It can be concluded from the study that the ensemble forecasts produced better results as compared with deterministic forecast, and the ensemble forecasts have the potential to overcome the insufficiency of the deterministic forecast in terms of QPF, although peak discharge value was underestimated, and the flood forecast using the spatial shift of ensemble rainfall fields produced the appropriate result compared with the original one. However, in the spatial shift result, they have a lot of errors came from original ensemble members. Therefore, it should be examined the shift location and ensemble member, which have the best efficiency criteria.

Acknowledgement

This research was supported by a grant (16AWMP-B079625-03) from Water Management Research Program funded by Ministry of Land, Infrastructure and Transport of Korean government.

References

- Cuo, L., Pagano, T., and Wang, Q. (2011), A Review of quantitative precipitation forecasts and their use in short- to medium-range streamflow forecasting, *Journal of hydrometeorology*, 12, 713-728.
- Demeritt, D., Cloke, H., Pappenberger, F., Thielen, J., Bartholmes, J., and Ramos, M. (2007), Ensemble predictions and perceptions of risk, uncertainty, and error in flood forecasting, *Environ. Hazards*, 7, 115-127.
- Xuan, Y., Cluckie, I., and Wang, Y. (2009), Uncertainty analysis of hydrological ensemble forecasts in a distributed model utilizing short-range rainfall prediction, *Hydrol. Earth Syst. Sci.*, 13, 293-303.
- Buizza, R., Miller, M., and Palmer, T. (1999), Stochastic representation of model uncertainties in the ECMWF Ensemble Prediction System, *Quart. J. Roy. Meteor. Soc.*, 125, 2887-2908.



- Palmer, T. and Buizza, R. (2007), Fifteenth anniversary of EPS, ECMWF Newsletter 114 (Winter 07/08), 14.
- Roulin, E. (2007), Skill and relative economic value of medium-range hydrological ensemble predictions, *Hydrology and Earth System Sciences*, 11(2), 725–737.
- Roulin, E. and Vannitsem, S. (2005). Skill of medium-range hydrological ensemble predictions, *Journal of Hydrometeorology*, 6(5), 729–744.
- Gouweleeuw, B., Thielen, J., Franchello, G., de Roo, A. and Buizza, R. (2005), Flood forecasting using medium-range probabilistic weather prediction, *Hydrology and Earth System Sciences*, 9(4), 365–380.
- Cloke, H. and Pappenberger, F. (2009) Ensemble flood forecasting: A review, *J. of Hydrology*, 375, 613–626
- Schaake, J., Perica, S., Mullusky, M., Demargne, J., Welles, E. and Wu. L. (2004), Pre-processing of atmospheric forcing for ensemble runoff prediction, *Proceedings of the 84th AMS Annual Meeting*.
- Ebert, E. and McBride, J. (2000), Verification of precipitation in weather systems: Determination of systematic errors. *Journal of Hydrology*, 239, 179–202.
- Saito, K., Ishida J., Aranami K., Hara T., Segawa T., Narita M., and Honda Y. (2007), Nonhydrostatic atmospheric models and operational development at JMA, *J. Meteor. Soc. Japan*, 85B, 271–304.
- Takasao, T., Shiiba, M., and Ichikawa, Y. (1996), A runoff simulation with structural hydrological modeling system, *JHHE*, 14(2), 47-55.
- Tachikawa, Y., Nagatani. G., and Takara, K. (2004), Development of stage discharge relationship equation incorporating saturated unsaturated flow mechanism, *Ann. J. Hydraul. Eng, JSCE*, 48, 7–12 (in Japanese)
- Yu, W., Nakakita, E., and Yamaguchi, K. (2013), Assessment of probabilistic flood Forecasting using ensemble NWP rainfall with 30hr forecast time during typhoon events. *Advances in River Engineering, JSCE*, 19, 235-240.

River Discharge and Reservoir Operation Assessment under a Changing Climate at the Sirikit Reservoir

MANEE Donpapob^{a,*}, TACHIKAWA Yasuto^{2,b}, ICHIKAWA Yutaka^{3,c} and YOROZU Kazuaki^{4,d}

Abstract The large scale reservoir plays an important role in modern water resources management by regulating the water to address severe flood and drought problems. Therefore, the proper planning of water resource availability based on uncertainty climate change impact is very necessary. The objective of this study is to evaluate the changes of water storage and outflow based on present and past operation with the different future reservoir inflow data by using Atmospheric General Circulation model (MRI-AGCM3.2S) forcing data which is jointly developed by Meteorological Research Institute of Japan and Japan Meteorological Agency. For each 20-km grid cell, the surface runoff generation of MRI-AGCM3.2S was used to simulated river discharge at the Sirikit reservoir by a distributed flow routing model (1K-FRM) based on the kinematic wave theory. In this study, distribution mapping methods are applied to raw daily river discharge simulated data for remove systematic bias between model and observed data. After bias correction to daily discharge achievement, the future corrected reservoir inflow of different scenarios were given to reservoir operation model algorithms and using the Artificial Neural network (ANN) for calculation the future release flow and reservoir storage based on remain the downstream water requirement and amount of water losses in this reservoir same as present climate condition. The evaluation of future reservoir operation based on present rule curve will show the necessary decision way to revise or improve current operation to adapt to probably water resources availability.

Keywords *Artificial Neural Network, Flow Routing Model, Atmospheric General Circulation Model, Bias Correction*

MANEE Donpapob
Department of Civil and Earth Resources Engineering
Kyoto University
Kyoto, Japan
manee.donpapob.85v@kyoto-u.jp

TACHIKAWA Yasuto
tachikawa@hywr.kuciv.kyoto-u.ac.jp

ICHIKAWA Yutaka
icichikawa@hywr.kuciv.kyoto-u.ac.jp

YOROZU Kazuaki
yorozu@hywr.kuciv.kyoto-u.ac.jp

Introduction

Water is indispensable for all forms of life and is needed, in large quantities, in almost all human activities. According to the 2013 Intergovernmental Panel on Climate Change (IPCC), the global water cycle will change, with increases in disparity between wet and dry regions, as well as wet and dry seasons, with some regional exceptions. Water resources is an increasingly limited and highly essential resource for many countries where agriculture is the main income of the economy corresponding with ensures the well-being of the people. The proper planning of water resource availability based on uncertainty climate change impact is very necessary; because, the projection of hydrologic inflow data can support and help government stakeholder and reservoir operator to adapt their decision making to release the water subjected to the rule or constraint in advance and be consisted of the sustainable development plan in future. The large scale reservoir plays an important role in modern water resources management by regulating the water to address severe flood and drought problems. It is the effective tool to store water when severe flood occurs for mitigation of the huge loss, damage of lives and economics. Not only the excess water resource problem, but the inadequate water supply in Thailand also experienced the extreme drought. Therefore, to investigate the current reservoir operation is an important and interested finding to respond to future climate change for water management effectively and cope with future flood event as well. Therefore, the proper planning of water resource availability based on uncertainty climate change impact is very necessary. The objective of this study is to evaluate the changes of water storage and outflow based on present and past operation with the different future reservoir inflow data by using Atmospheric General Circulation model (MRI-AGCM3.2S).

Study area

The Sirikit reservoir with coverage catchment area of 13,130 km² is located of the midstream of Nan River basin in Thailand as shown in **Fig.1**. The upstream of the Sirikit reservoir is a mountainous area which is not affected by major flow regulations or any other direct human activities impacts.

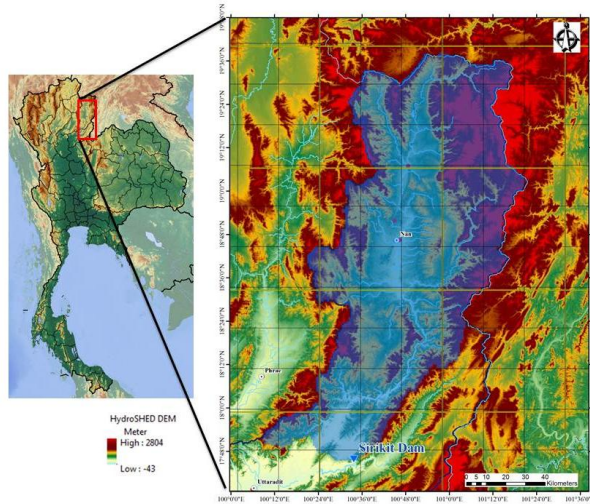


Fig.1 Map showing the study area, reservoir location and spatial 20 km x 20 km square grid of MRI-AGCM3.2S.

The continuous time series data of observed inflow into the reservoir is available for the period of 1974-2013 (40 years). Its climate is tropical with distinctly clear dry and wet seasons. The seasons are defined as follows: the dry season starts from November until April and the wet season starts from May until October.

Methodology

The overall of this research can be divided into river discharge prediction part and reservoir operation assessment part for present and future climate scenarios. To estimate river flow for water resource assessment, the hydrological model is widely represented the interaction between hydrologic cycle element such as precipitation, soil Moisture, river flow and evapotranspiration. Several impacts of climate change studies with distributed hydrological model were conducted at the Chao Phraya River Basin in Thailand (Wichakul et al., 2015; Hunukumbura and Tachikawa, 2012). In this study, the 1K-FRM distributed flow routing model was chosen to handle input spatial data such as gridded rainfall; therefore, this model can applicable to access reservoir inflow under a changing climate as well. 1K-FRM is originated development in Hydrology and Water Resources Research Laboratory at Department of Civil and Earth Resources Engineering, Kyoto University. 1K-FRM is a distributed flow routing model based on kinematic wave flow approximation. The kinematic wave model is conduct to all rectangular elements gridded to link the water to downstream associate with the derived catchment model. Basically, the selecting of Digital Elevation Model (DEM) data used in catchment model is HydroSHEDS (Hydrological data and maps based on SHuttle Elevation Derivatives at multiple Scales) provides hydrographic information in a comprehensive and consistent format for both local and global-scale applications (Lehner, 2006). 1K-FRM used 30 arc-second resolutions (approximately 1 kilometer at

near equator area) as a catchment model. The flow direction is defined into 8 directions which assigns flow depends on the different elevation with in a direction of steepest downward slope as illustrated in Fig. 2. The basic kinematic wave equation for each rectangular slope elements is

$$\frac{\partial A}{\partial t} + \frac{\partial Q}{\partial x} = q_L(x, t) \quad (1)$$

where t denotetime; A is the cross-sectional area; Q is discharge; and $q_L(x, t)$ is the lateral inflow per unit length of each slope element. Another equation used to solve above equation is the relationship of Manning type of the discharge and a rectangular cross-section area of each cell as follows:

$$Q = \alpha A^m, \alpha = \frac{\sqrt{i_0}}{n} \left(\frac{1}{B} \right)^{m-1}, m = \frac{5}{3} \quad (2)$$

where i_0 is slope gradient; n is the Manning's roughness coefficient; and B is the width of the flow. There are two main parameters inside 1K-FRM model which consist of the Manning's roughness coefficient for the slope unit n_s and Manning's roughness coefficient for the river channel unit cell n_r . In this study, the parameter of $n_s = 0.03 \text{ m}^{-1/3} \text{ s}$ and $n_r = 0.1 \text{ m}^{-1/3} \text{ s}$ were used for the suitable values.

General circulation models (GCMs) have been commonly used in climate change impact studies. The several studies of application to use GCMs in Chao Phraya River Basin and surrounding River Basin were conducted. For instance, Hunukumbura and Tachikawa (2012) utilized the runoff projected by MRIAGCM3.1S, which showed the increasing of extreme discharge at the upper part of Chao Phraya River Basin and the decreasing of monthly discharge in October at the Pasak River basin. Kure and Tebakari (2012) showed the increased tendency of the mean annual river discharge and annual maximum daily flow at the NakhonSawan station located at the downstream of the four major rivers in the in upper Chao Phraya River Basin using the precipitation and temperature projected by MRI-AGCM3.1S and MRI-AGCM3.2S. Champathong et al. (2013) assessed the uncertainty of river flow projections using the outputs of MRIAGCM3.1S and MRI-AGCM3.1H. Kitpaisalsakui et al. (2016) also used MRI GCM data to assesses the impact of climate change on reservoir operation in Central Plain Basin of Thailand.

The GCM outputs used for this research were gridded runoff generation data from MRI-AGCM 3.2S (Mizuta et al., 2012), where 'S' refers to super-high resolution developed by Japan Meteorological Agency (JMA) and the Meteorological Research Institute (MRI). The AGCMs grids covering the Sirikit reservoir study area were total of 88 grids (8 columns and 11 rows) with the spatial resolution 0.1875 degree (approximately 20 km), located between the latitude of 17 degrees 42 minutes and 19 degrees 35 minutes north and the longitude of 100 degrees 7 minutes and 101 degrees 26 minutes east. To obtain the high resolution of climatic forcing data is to used downscaling technic by an atmospheric general circulation model (Kitoh et al.,

2015). The high-resolution that is obtain the observed or projected sea surface temperature (SST) as boundary condition. This type of mechanism simulations, which uses the observed present day inter-annually varying SST plus ensemble mean future SST changes obtained by CMIP-class models, can minimize the effects of climate model bias. Based on the SST data of 28 CMIP5 model, the different SST spatial patterns are analyzed by a cluster analysis of these 28 CMIP5 model. After that, the 28 CMIP5 model classified into 3 clusters from 8, 14 and 6 models of cluster 1, cluster 2 and cluster 3, respectively.

That model has a horizontal resolution of triangular truncation 959 (TL959) and a vertical resolution of 64 levels (top at 0.01 hPa) to transform grid uses 1920* 960 grid cells with corresponding to approximately a 20 km grid interval. The 20-km mesh MRI-AGCM3.2 was employed in each 25-year time-slice experiment for the present-day climate (1979-2003) and late 21st century climate (2075-2099) scenarios with the Representative Concentration Pathway (RCP) 8.5 that refers to the final radiative forcing achieved by the year 2100 around 8.5 watts per square meter (W/m^2). Moreover, the cluster analysis also analyzed the ensemble SST to classify the characteristic pattern of SST into three groups as following 1) cluster 1: Uniform warming in the tropics zone pattern or in the both hemispheres, 2) Cluster 2: Larger warming over the central equatorial Pacific (so-called El Nino-like pattern) and 3) Cluster 3: Larger warming in the north Indian Ocean and north-west Pacific pattern. Therefore, the future climate projection was combined of different SST (4 future SSTs) to assess the uncertainty of future water availability. However, for 20 km grid output data provide a new cumulus convection scheme (Yoshimura et al, 2015), called the “Yoshimura scheme” only. For each 20-km grid cell, the various hydrological components of MRI-AGCM 3.2S such as precipitation, evaporation, transpiration and surface runoff generation were calculated through the land surface scheme as shown in Fig 2. The runoff generation of MRI-AGCM3.2S was used to simulated river discharge at the Sirikit reservoir by a distributed flow routing model (1K-FRM) based on the kinematic wave theory (Tachikawa and Tanaka, 2013). All period of simulation has been performed at a spatial resolution of 1 km and temporal resolution of one day. For the verification data, the observed time series of daily inflow was obtained from the Electricity Generating Authority of Thailand (EGAT).

A recent bias correction method based on a relationship of cumulative distributions (CDFs) of the GCMs and observation data has been commonly used for hydrologic simulations and climate change studies. The distribution mapping technique adjusts all particles of the cumulative distribution function (CDF) of projected data with GCM outputs by using the CDF of observation and construct a transfer function to convert the projected data using GCMs to corrected data.

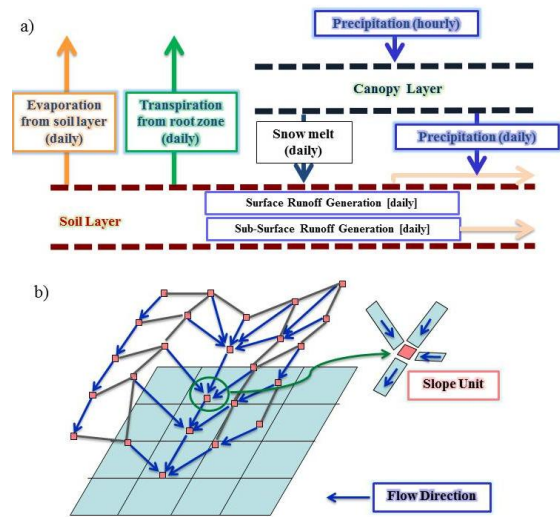


Fig.2 The framework diagram river discharge simulation.

a) Land surface generation data of MRI-AGCM3.2S fed into river discharge simulation in a grid. b) Schematic drawing of a catchment and flow routing model using HydroSHEDS DEM.

All bias correction methods of quantile mapping have to initiate by 1) sorting long-term observation and simulation river discharge data to create CDFs for each calendar month (Jan-Dec); 2) correcting bias in the frequency and intensity distribution on each different method; and 3) rearranging corrected data back to the original time series.

The classical distribution quantile mapping (eQM) is expressed by setting the pair with the same non-exceedance probability as follow

$$Q^* = F_{obs,C}^{-1}(F_{raw,C}(Q_{raw,C})) \quad (3)$$

where Q^* is the corrected river discharge value, $Q_{raw,C}$ is the raw original river discharge value and stands for the inverse function of CDFs of the observed daily discharge, and accordingly $F_{raw,C}$ as the CDFs of the projected river discharge using MRI-AGCM3.2S. However, for the application of eQM method to the future climate condition, if we assume that the transfer function is stable and follows the same current climate condition. Li et al. (2010) proposed the eQM with the difference of CDFs or referred to as equidistant CDF matching (EDCDF_m) to calculate by adding the difference between CDFs of GCM and observation river discharge during future climate condition as following equation:

$$Q^* = Q_{raw,P} + [F_{obs,C}^{-1}(F_{raw,P}(Q_{raw,P})) - F_{raw,C}^{-1}(F_{raw,P}(Q_{raw,P}))] \quad (4)$$

where, $Q_{raw,P}$ is the original river discharge value for the future projection period. The $F_{obs,C}^{-1}$ and $F_{raw,C}^{-1}$ stand

for the inverse function of CDFs of the observations and raw GCMs during present climate period, respectively.

Moreover, The gamma distribution with shape parameter β and scale parameter α is defined as:

$$f(x) = x^{\alpha-1} \cdot \frac{1}{\beta^\alpha \cdot \Gamma(\alpha)} \cdot e^{-\frac{x}{\beta}}; x, \alpha, \beta > 0 \quad (5)$$

where Γ is the gamma function. In this study, the shape and scale parameter were fitted with observation and GCMs projection on each calendar month. The gQM method is a parametric correction method which can be expressed as:

$$Q_c^* = F_Y^{-1}(F_Y(Q_{raw,C} | \alpha_{raw,C}, \beta_{raw,C}) | \alpha_{obs,C}, \beta_{obs,C}) \quad (6)$$

$$Q_p^* = F_Y^{-1}(F_Y(Q_{raw,P} | \alpha_{raw,C}, \beta_{raw,C}) | \alpha_{obs,C}, \beta_{obs,C}) \quad (7)$$

Maneet al. (2016) found the equidistant CDF matching (EDCDFm) and the empirical with gamma distribution quantile mapping (gQM) methods showed the good overall performance and applicable to potentially changed climate condition in term of less bias of water balance and proper for adjusted peak river discharge.

For reservoir operation assessment part aims to estimate the future water storage and to evaluate the tendency of excess water use (flood risk) and insufficient water use (drought risk) by given the bias-corrected river discharge based on the methodology of previous section. The Flowchart of reservoir simulation procedure for calculated future reservoir outflow and storage is shown as **Fig. 3**. Kim et.al (2009) investigated the adaptability of current dam operation rules under climate change condition to a dam in the upper part of Tokyo, Japan based on AGCM20 input data. The Artificial Neural Network (ANN) is selected to learn the past reservoir operation and transferred to the machine learning. The relationship of storage and reservoirs inflow is important to give through covariates (also known as input variables) and response variables (also known as output variables) is represented as release flow of reservoir. The ANN consists of the neurons are organized in layers, which are usually fully connected by synapses. A synapse can only connect to subsequent layers. The input layer consists of all covariates in separate neurons and the output layer consists of the response variables.

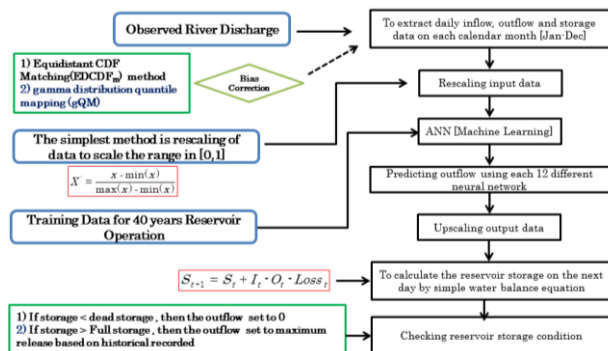


Fig.3 Flowchart of reservoir simulation for future reservoir outflow and storage.

The layers in between input and output layers are referred to as hidden layers, as they are not directly observable. Input layer and hidden layers include a constant neuron relating to intercept synapses. The number of hidden layers and numbers of nodes in each hidden layer are usually determined by a trial-and-error procedure (Govindaraju, R. S., 2000); therefore, the output of a node in a layer is only a dependent on the inputs it receives from previous layers and the corresponding weight.

This neural network models the relationship between the two covariates (inflow and water storage) and the response variable outflow. There are twelve neural networks which are constructed by separating reservoir operation data (reservoir inflow, outflow and water storage) into on different each calendar month. For the future outflow estimation, the analysis was calculated by bias-corrected inflow as an input to reservoir and setting the daily loss in the reservoir based on 40 years historical reservoir operation. Lastly, the general water balance equation was used to calculate the future reservoir storage as

$$S_{t+1} = S_t + I_t - O_t - Loss_t \quad (8)$$

where t stands for the month, S_{t+1} stands for next day reservoir storage, S_t is current reservoir storage, I_t is daily inflow to reservoir, O_t is the daily outflow that is acquired from different model structure of ANN and $Loss_t$ is total daily losses from reservoir. In this study, the losses from reservoir were calculated by the different water storage from general water balance equation and the observed water storage. According to the various the future river discharge projection was conducted before given to reservoir operation model, the initial reservoir storage setting is also important to control reservoir storage at the initial condition, So the initial reservoir storage condition is defined into three different level as follow, normal condition (at 8,250 MCM), upper rule curve condition on January, 1st (at 9,494 MCM) and lower rule curve condition on January, 1st (at 6,405 MCM).

Results and discussion

The results of average daily reservoir inflow of bias-corrected river discharge at Sirikit dam during present climate (1979-2003) were summarizes in the flow duration curve plot for comparison the characteristic of high and low flow between reservoir inflow observation and both bias-corrected river discharge as shown in **Fig4**.

Table 1 Summary of ensemble simulation name for future experiment.

Bias Correction Method	Empirical distribution quantile mapping	Gamma distribution quantile mapping
Future SST setting		
Ensemble Mean SST	Mean_EDCDF	Mean_gQM
Cluster1 SST	C1_EDCDF	C1_gQM
Cluster2 SST	C2_EDCDF	C2_gQM
Cluster3 SST	C3_EDCDF	C3_gQM

For the changes in river discharge through Sirikit reservoir under a changing climate. The majority cases of the future annual reservoir inflow are higher than present observed Sirikit reservoir except the c1_gQM and c2_gQM. The amount of water resources availability in the future climate experiment showed that the reservoir inflow with SST of c3 pattern reproduce a highest value. However, after applying bias-corrected reservoir inflow data can cause the contrast of low flow occur in the case of reservoir inflow with SST of c2 pattern as shown in **Fig.5** and **Fig.6**.

Comparison release flow simulation and observation during 1974-2013

The output of reservoir operation based on the Artificial Neural Network (ANN) have been evaluate by compared with the observed outflow from 1974-2013.

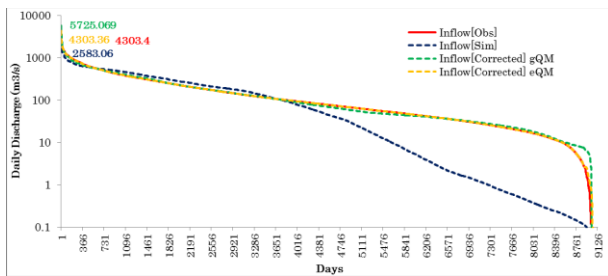


Fig.4 The total-flow duration curve between observation, raw simulation and bias-corrected river discharge at Sirikit dam during present climate (1979-2003).

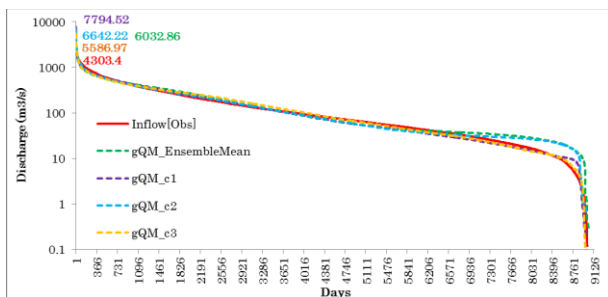


Fig.5 The total-flow duration curve between observation, raw simulation and bias-corrected river discharge (gQM method) at Sirikit dam during future climate (2075-2099).

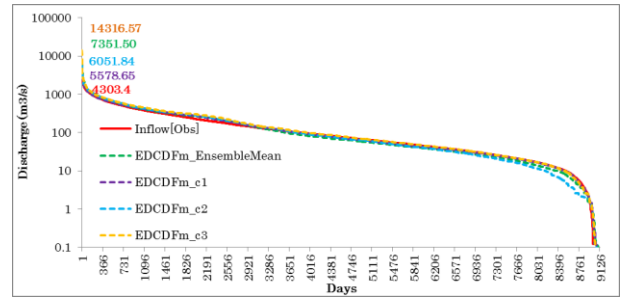


Fig.6 The total-flow duration curve between observation, raw simulation and bias-corrected river discharge (EDCDF_m method) at Sirikit dam during future climate (2075-2099).

The best simulated results of average monthly outflow and water storage showed a good performance and reasonable to utilized for the future release flow assessment under the impacts of climate change. **Fig.7** showed that the average outflow simulation performed well with the small difference between average outflow and water storage. However, the amount of outflow in particular month found some error for monthly outflow analysis as shown in **Fig.8**.

Lastly, the future reservoir storage and outflow simulation under different scenarios showed that in percentage of changes in **Table 2** for water storage and **Table 3** for water release of different reservoir inflow projection data. The limitation of this projection is to assume the same rate of downstream water requirement and reservoir loss during present climate condition. According to the **Table 2**, the tendency of future storage might be decreasing of all scenarios with bias-corrected gQM cases of reservoir inflow projection data.

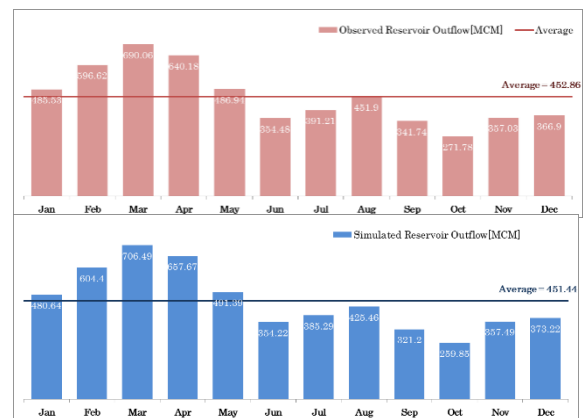


Fig.7 The average monthly observed and simulated outflow during 1974-2013.

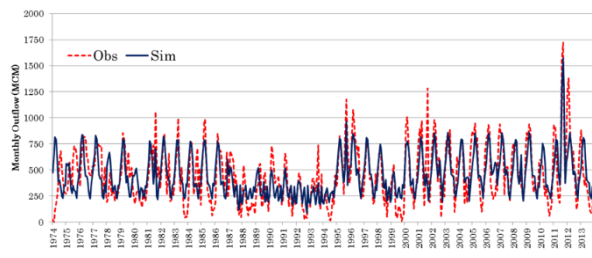


Fig.8 Comparison of monthly outflow observation and simulation by ANN

Furthermore, the future storage water storage of bias-corrected Mean_EQCDFm and c1_EQCDFm showed the decreasing water storage from January until July and increasing water storage from August until December. For c2_EQCDFm and c3_EQCDFm cases showed the increasing water storage trend throughout the year. The overall water release flow results showed the reasonable and matching with the relationship of water storage. For instance, the tendency of future water release might be decreasing of all scenarios with bias-corrected gQM cases.

Table 2 The percentage of water storage changes on each different reservoir inflow projection data.

Scenarios	Initial Storage	Jan	Feb	Mar	Apr	May	Jun	Jul	Aug	Sep	Oct	Nov	Dec
Observed	normal	6,742	6,406	5,900	5,316	4,847	4,675	4,780	5,466	6,406	6,918	6,301	6,776
EDCDFm_EnsembleMean	Upper	2.26	0.36	-0.68	-0.87	-0.28	-0.40	2.14	2.79	4.47	6.57	6.36	5.21
	Normal	0.28	-1.69	-3.02	-3.77	-3.80	-4.16	-1.43	0.15	2.83	5.24	5.10	3.93
	Lower	-1.39	-3.33	-4.64	-5.33	-5.22	-5.43	-2.58	-0.76	2.14	4.68	4.55	3.33
EDCDFm_c1	Upper	-0.15	-2.17	-3.32	-3.88	-4.22	-3.79	0.15	3.29	3.07	2.28	2.63	1.73
	Normal	-0.95	-3.01	-4.42	-5.02	-4.43	-6.11	-1.92	1.99	2.53	2.19	2.58	1.68
	Lower	-2.21	-4.39	-5.75	-7.00	-7.75	-7.32	-3.05	1.15	2.14	1.95	2.38	1.48
EDCDFm_c2	Upper	8.04	7.10	6.28	6.52	7.32	7.45	10.36	9.37	11.13	13.12	13.03	13.22
	Normal	6.25	4.33	3.17	2.91	3.24	3.50	6.52	6.37	8.91	11.21	12.02	11.54
	Lower	4.41	2.52	1.38	1.22	1.73	1.99	5.32	5.41	8.11	10.48	11.29	10.45
EDCDFm_c3	Upper	12.35	10.61	9.70	9.15	8.68	9.11	14.15	16.10	15.31	15.36	15.86	15.35
	Normal	10.47	8.60	7.27	6.14	5.09	5.30	10.69	13.80	13.51	14.21	14.70	14.18
	Lower	8.76	6.84	5.54	4.48	3.73	4.23	9.74	13.05	12.94	13.71	14.19	13.67
gQM_EnsembleMean	Upper	-3.15	-5.05	-6.10	-6.01	-4.79	-3.33	-1.93	-2.06	-1.09	0.39	0.13	-0.82
	Normal	-5.88	-7.91	-9.33	-9.85	-9.22	-8.50	-6.22	-5.33	-3.44	-1.68	-1.91	-2.87
	Lower	-8.00	-10.02	-11.42	-11.82	-11.04	-10.21	-7.76	-6.60	-4.47	-2.62	-2.83	-3.87
gQM_c1	Upper	-2.42	-4.24	-5.16	-5.18	-4.89	-3.53	-2.01	-1.39	-0.56	-0.43	-0.40	-1.05
	Normal	-3.21	-5.05	-6.27	-6.83	-7.02	-5.82	-4.15	-2.84	-1.14	-0.55	-0.46	-1.11
	Lower	-4.62	-6.51	-7.80	-8.39	-8.51	-7.19	-5.39	-3.81	-1.77	-0.95	-0.80	-1.45
gQM_c2	Upper	-3.95	-5.83	-7.29	-7.31	-7.23	-6.51	-4.71	-4.89	-2.21	-0.79	-0.71	-1.22
	Normal	-6.93	-8.88	-10.53	-11.06	-11.21	-10.60	-8.29	-7.77	-4.50	-2.84	-2.75	-3.38
	Lower	-8.39	-10.25	-11.93	-12.40	-12.45	-11.64	-9.26	-8.57	-5.16	-3.46	-3.39	-3.90
gQM_c3	Upper	1.13	-1.08	-2.51	-3.36	-3.77	-3.15	0.55	1.37	1.76	3.54	3.80	3.04
	Normal	-1.33	-3.65	-5.45	-6.85	-7.74	-7.19	-3.16	-1.42	-0.15	1.86	2.12	1.31
	Lower	-2.86	-5.10	-6.91	-8.27	-9.07	-8.40	-4.23	-2.34	-0.90	1.19	1.45	0.71

Table 3 The percentage of water release changes on each reservoir inflow projection data.

Scenario	Initial Storage	Jan	Feb	Mar	Apr	May	Jun	Jul	Aug	Sep	Oct	Nov	Dec	DrySeason	WetSeason	Annual
Observed	normal	486	497	490	480	487	484	481	482	474	472	467	467	418	2,288	5,214
EDCDFm_EnsembleMean	Upper	0.77	-0.27	-0.73	-0.94	-0.96	-1.12	-1.17	-1.42	-2.10	-3.08	-3.28	-3.19	-1.19	-7.80	-2.65
	Normal	-0.70	-4.14	-1.25	-1.25	-2.30	-2.38	0.10	-2.50	-14.93	-31.23	-10.95	-1.47	-0.35	4.59	1.74
	Lower	-2.17	-5.36	-2.93	-3.33	-3.37	-3.39	-1.05	-3.62	-12.42	-30.92	-11.04	-0.51	-1.48	2.92	0.38
EDCDFm_c1	Upper	-2.21	-4.17	-4.58	-2.96	-2.29	-3.05	-3.21	9.51	6.23	-1.51	-1.66	2.30	-3.20	1.11	1.38
	Normal	-2.00	-4.34	-0.70	0.79	-0.87	-4.11	-7.94	1.40	-5.09	-5.07	-1.67	2.34	-1.59	-3.25	-2.29
	Lower	-3.96	-4.83	-1.42	0.77	-2.24	-5.14	-8.49	-1.31	-9.94	-8.57	-2.17	2.95	-2.25	-5.50	-3.64
EDCDFm_c2	Upper	-0.40	-7.20	-1.69	-1.21	-2.55	4.92	4.88	15.40	20.90	6.21	2.82	1.51	1.52	0.50	2.73
	Normal	-1.09	-8.17	0.56	-0.53	-1.19	1.49	2.19	8.65	20.50	5.85	2.86	2.05	-1.14	5.80	1.80
	Lower	-3.27	-9.29	-1.40	-3.41	-4.30	-0.63	1.24	8.01	20.44	5.82	2.89	3.55	-2.53	4.51	0.44
EDCDFm_c3	Upper	5.01	2.38	5.80	9.33	9.77	7.74	16.12	32.71	44.66	19.66	0.32	1.13	4.58	21.41	11.60
	Normal	5.07	2.84	9.41	10.79	13.28	5.44	11.22	22.72	36.42	19.57	0.24	0.28	5.66	17.76	10.78
	Lower	6.46	1.96	7.52	8.13	8.12	2.48	10.50	21.30	35.50	19.89	0.26	0.25	4.68	15.88	9.42
gQM_EnsembleMean	Upper	-3.74	-4.05	-4.53	-5.56	-11.00	-8.90	-1.76	-2.71	-10.73	-3.17	-0.27	-2.89	-4.91	-5.24	-5.65
	Normal	-4.04	-4.10	-4.55	-6.39	-9.76	-7.97	-4.59	-13.68	-13.69	-4.34	-0.25	-4.36	-4.26	-2.29	-5.97
	Lower	-5.73	-5.34	-6.90	-9.63	-11.94	-9.91	-6.16	-14.29	-14.50	-9.28	-1.95	-5.65	-5.65	-3.61	-7.32
gQM_c1	Upper	-6.85	-5.10	-9.90	-11.73	-11.77	-8.51	-4.73	1.71	-3.07	-2.72	-0.18	-11.74	-8.06	-5.05	-6.75
	Normal	-7.15	-5.07	-6.14	-8.77	-9.62	-9.10	-7.12	-6.60	-15.69	-6.85	-0.18	-11.78	-6.61	-9.11	-7.67
	Lower	-7.59	-5.37	-6.94	-10.20	-11.85	-10.52	-8.30	-8.59	-21.05	-9.15	-0.20	-12.05	-7.25	-11.45	-9.02
gQM_c2	Upper	-11.98	-1.84	-7.53	-9.33	-4.99	-10.41	-4.88	-10.47	-20.35	-9.07	-0.96	-13.52	-7.61	-5.53	-8.14
	Normal	-11.50	-4.04	-6.16	-8.24	-6.00	-12.28	-10.79	-13.16	-22.79	-8.41	-0.95	-13.21	-7.44	-11.97	-9.36
	Lower	-11.43	-4.27	-7.63	-11.00	-8.58	-14.52	-11.19	-13.24	-22.98	-7.64	-1.10	-13.63	-9.11	-12.91	-10.71
gQM_c3	Upper	0.36	1.36	-1.53	-1.70	-6.80	-2.24	-11.40	-7.13	-15.55	-12.53	0.26	-7.28	-1.19	-8.92	-4.46
	Normal	0.23	0.89	1.23	-0.20	-6.41	-5.94	-15.15	-15.71	-19.38	-12.62	0.30	-7.37	-0.29	-12.18	-5.38
	Lower	-2.97	0.05	-0.94	-2.25	-8.22	-7.04	-15.72	-16.26	-19.61	-12.91	0.14	-9.48	-2.01	-13.17	-6.73

Conclusions

The tendency of future reservoir inflow after applying both the empirical distribution quantile mapping with difference between cumulative distribution functions (CDFs) of GCM and observation river discharge (eQM) and the empirical with gamma distribution quantile

mapping (gQM) provides higher than present climate condition at Sirikit Reservoir.

Finally, the future reservoir storage and outflow simulation under different scenarios showed the tendency of future storage might be decreasing of all scenarios with bias-corrected gQM cases of reservoir inflow projection data. On the other hand, the scenarios with bias-corrected eQM cases of reservoir inflow projection data presented the increase storage due to high reservoir inflow on wet season as similarly with the water storage trend analysis.(Maneet.al, 2015). The results indicated that, The SK dam seems to reduce the release flow due to decreasing bias-corrected gQM reservoir inflow. The overall water inflow and storage results showed the reasonable and matching with previous studies (Kitpaisalsakuiet.al, 2016).

Acknowledgement

We acknowledge Japan Meteorological Agency (JMA) and the Meteorological Research Institute (MRI) for providing General circulation model (GCM) data and also sincere thanks to The Electricity Generating Authority of Thailand (EGAT) for observed reservoir inflow information.

References

Changphong, A., Komori, D., Kiguchi, M., Sukhannaphan, T., Oki, T., &Nakaegawa, T. (n.d.). Future projection of mean river discharge climatology for the Chao Phraya River basin. *Hydrological Research Letters*, 7(2), 36-41.

Govindaraju, R. S. (2000). Artificial neural networks in hydrology. I: Preliminary concepts. *Journal of Hydrologic Engineering*, 5(2), 115-123.

Hunukumbura, P. B., &Tachikawa, Y. (2012). River discharge projection under climate change in the Chao Phraya River Basin, Thailand, using the MRI-GCM3.1S dataset. *Journal of the Meteorological Society of Japan*, 90A, 137-150.

IPCC. (2013). *Climate Change 2013: The Physical Science Basis. Contribution of Working Group I to the Fifth Assessment Report of the Intergovernmental.* Cambridge, United Kingdom and New York, NY, USA: Cambridge University Press.

Kim, S., Tachikawa, Y., Nakakita, E., & Takara, K. (2009). Reconsideration of reservoir operations under climate change: case study with Yagisawa Dam, Japan. *Annual Journal of Hydraulic Engineering, JSCE*, 53, 597-611.

Kitoh, A., & Endo, H. (2016). Changes in precipitation extremes projected by a 20-km mesh global atmospheric model. *Weather and Climate Extremes*, 11, 41-52.

Kitpaisalsakui, T., Koontanakulvong, S., &Chaowiwat, W. (2016). Impact of Climate Change on Reservoir Operation in Central Plain Basin of Thailand. *Journal of Thai Interdisciplinary Research*, 11(2), 13-19.

Kure, S., &Tebakari, T. (2012). Hydrological impact of regional climate change in the Chao Phraya River Basin, Thailand. *Hydrological Research Letters*, 6(0), 53-58.

Lehner, B., Verdin, K., & Jarvis, A. (2006). *HydroSHEDS technical documentation, version 1.0.* World Wildlife Fund US, 1-27.

Li, H., Sheffield, J., & Wood, E. F. (2010). Bias correction of monthly precipitation and temperature fields from



- Intergovernmental Panel on Climate Change AR4 models using equidistant quantile matching. *Journal of Geophysical Research: Atmospheres*, 115 (D10), 1-20.
- Manee, D., Tachikawa, Y., & Yoroze, K. (2015). Analysis of hydrologic variable changes related to large scale reservoir operation in Thailand. *Journal of Japan Society of Civil Engineers, Ser. B1 (Hydraulic Engineering)*, 71(4), 61-66.
- Manee, D., Tachikawa, Y., Ichikawa, Y., & Yoroze, K. (2016). Evaluation of Bias Correction Methods for Future River Discharge Projection. *Global environment engineering research*, 24, 7-12.
- Mizuta, R. Y., Matsueda, M., Endo, H., Ose, T., & Kusunoki, S. (2012). Climate Simulations Using MRI-AGCM3.2 with 20-km Grid. *Journal of the Meteorological Society of Japan, Ser. II*, 90A, 233-258.
- Tachikawa, Y., & Tanaka, T. (n.d.). 1K-FRM. Retrieved June 23, 2016, from Hydrology and Water Resources Research Laboratory Webpage: <http://hywr.kuciv.kyoto-u.ac.jp/products/1K-DHM/1K-DHM.html>
- Wichakul, S., Tachikawa, Y., Shiiba, M., & Yoroze, K. (2015). River discharge assessment under a changing climate in the Chao Phraya River, Thailand by using MRI-AGCM3.2S. *Hydrological Research Letters*, 9(4), 84-89.

Determination of Extreme Design Waves under Climate Change in the Gulf of Thailand

Nguyen Thi Hien^{1,a}, Sutat Weesakul^{2,b*}, Rosh Ranasinghe^{3,c} Johan Reynolds^{3,d}
Chatlada Sriumpoldech^{1,e} and Weerasinghe L.K.K^{1,f}

Abstract A number of studies showed that wave climate have been effected spatially from climate change in a global scale. Present study analyzes the extreme wave characteristics in a regional scale covering the Gulf of Thailand (GoT) and extended to Cambodia, Vietnam and Malaysia. Climate data from present days to future are NCEP, ECHAM 5 and GFDL CM2.1 under A2 scenario with 20 years' time window. There are six wave parameters have been computed and evaluated i.e. storm duration, storm frequency, mean intensity of significant wave height of 1% highest wave, wave height at 99th percentile, wave directions and design wave height. The designed wave height corresponding to 2 to 100 years return period was calculated based on Generalized Extreme Value Distribution, in serving structures design. Mike 21 SW is used as an analysis tool for wave generation and their propagation. Model calibration and validation are conducted with good results. It is found that the general trend of design wave height increase at every locations from near future to far future climate, especially the locations in Vietnam and Malaysia. The designed significant wave height results indicate an increase trend less than 3% for stations in the upper gulf and 17% over all stations in the lower gulf. Outside GoT, it is remarkably increase to 33%. This is because the upper gulf planform is confined while the lower gulf configuration is in the open sea area which is more exposed to tropical monsoon from South China Sea. Two GCMs perform comparable results of wave height and wave direction. The average intensity of extreme events is getting higher from 1 to 4 storms per year to 2 to 5 storms per year at most in the far future. Also, the mean storm duration becomes longer from 10 hours to 14 hours in the future at half of locations. Wave directions have locally changed. The trend of wave direction is slightly shifted to Northeast in the far future with less number of waves from west direction. Climate change has influenced to wave parameters from the lower gulf of Thailand extended to Malaysia. Increment of design significant wave heights under future extreme climate in regional scale to present waves are provided with 20 and 50 years return periods which can be used to examine the robustness of coastal infrastructures further.

Keywords *Extreme wave, Design wave, Gulf of Thailand, Climate change*

¹Graduate Student Asian Institute of Technology (AIT)
Thailand

²Hydro and Agro Informatics Institute (HAI) and Asian Institute of Technology (AIT)
Thailand

³Department of Water Engineering
UNESCO-IHE
The Netherlands

^a hiennguyen.fhwr@gmail.com

^b sutat@haii.or.th

^c R.Ranasinghe@unesco-ihe.org

^d j.reyns@unesco-ihe.org

^e mink.chatlada@gmail.com

^f kanchana_eng@yahoo.com

Introduction

Climate change is causing stochastic climate parameters from temperature, rainfall, sunlight to wind, wave and currents. The coastal areas, as a result, are becoming a critical environment under extreme climate change context and have been experienced higher chance of extreme waves recently. Grabemann and Weisse, (2008) showed the extreme wave heights was projected to increase in large parts in the southern and eastern North Sea by about 0.25 to 0.35 m (5–8% of present values) towards the end of the twenty first century due to the global warming. Future ocean wave climate in comparison with present one based on the GCM from MRI-JMA with A1B scenario and Global Wave model was computed by Mori et al (2010) using SWAN (Simulating Waves Nearshore). It showed that both extreme and annual average wave heights changed from present to future climate. They increased at both middle latitudes and in Antarctic Ocean with decrease at the equator. Kaushalya (2011) and Sriumpoldech (2012) studied offshore and nearshore wave variability due to future climate in the lower gulf of Thailand. Annual significant wave height will increase 0.037 to 0.059 m. while that in

northeast monsoon season will increase 0.10 to 0.14 m. The mean wave direction was projected to change anti-clockwise direction by 11 degree from the present direction (111.3 degree from north).

Analysis of wind-wave climate on the south-east Australia was carried out by Hemer et al (2012) using Wave Watch III and SWAN. Three global climate model run with CSIRO MK3.5, GFDLcm2.0 and GFDLcm2.1 Cubic conformal atmospheric model (CCAM), under A2 and B1 were used. The projected mean annual significant wave height was less than 0.2 m, associated with a decrease in storm energy in the region. Wang et al (2014) computed global ocean wave heights using 20 CMIP5 (Coupled Model Inter-comparison Project Phase 5). It shows significant wave height increases in the tropics especially in the eastern tropical Pacific and in Southern Hemisphere high latitudes, south of 45 degree. The occurrence frequency of the present –day 1 in 10 year extreme wave height is likely to double or triple in several coastal regions. These wave height increases are primarily driven by increased sea level pressure and increased surface wind energy. Increased annual maximum wave height in the Gulf of Thailand in year 2080-2099 to year 1989-1999 can be 0.15 to 0.30 m under RCP8.5 scenario. The safety of coastal and deep water platforms are required to be examined with the future extreme waves. Coastal erosion should be investigated which is effected from variation of sediment transport from wave direction and wave height change. Slott et al (2006) showed that shift of coastline shape were expected on a complex-shaped coastline in US Southeast, Gulf coastlines and the northwest Alaska coast.

Research finding shows that the variability of future waves climate in global scale have been changed. There are few studies related to regional scale for future wave. These topics should be prepared and studied because results can be used for further research to investigate the effect of climate change to wave and beach/structure interactions in the nearshore area. The objectives of present study are to analysis spatially and temporally of wave characteristics under climate change driven in the Gulf of Thailand and its vicinity and to analyze the extreme waves including design wave height in regional scale.

Methodology

Data Collection

Climate data in present days is taken from NCEP and future-data are taken from ECHAM 5 and GFDL CM2.1 under A2 scenario with 20 years' time window. Those two GCMs are selected considering their appropriate spatial resolution (0.5°) and short interval time of wind field (6 hours) for computing

wind-driven wave. The present condition is defined using data from 1981 to 2000, the near future is from 2041 to 2060 and the far future is from 2081 to 2100. The bathymetry data from General Bathymetric Chart of the Oceans (GEBCO) with one arc minute grid resolution is used as model input. Table 1

Data type	Period	Sources	Description
Bathymetry	2014	GEBCO	Grid data sets of 30 arc-second resolution and Thai Nautical Charts
Shoreline	2015	NOAA	GSHHS version 2.2.2
Wind field	1981 – 2000	CCAM	ECHAM 5 and GFDL CM2.1 for A2 scenario, 6 hourly, 0.5°
	2041 – 2060	CSIRO	
	2081 – 2100	NCEP	
Buoy wave data	1985 - 2006	NRCT	Wave parameters: H_{m0} , T_{m0}

summarizes data collection.

Table Summary of data and descriptions.

Model Set up and Locations

In the present study, the response of the wave climate to CCAMs derived surface wind is investigated using a MIKE 21 numerical spectral wave model. Mainly, the mesh and bathymetry, wind field, boundary conditions and bottom friction are important in setting up the model.

A flexible mesh over the domain 98° - 120° E and 2° S- 25° N is implemented using MIKE zero mesh generator tool. Computational area is extended up to the end of South China Sea to avoid the boundary effect to the wave modeling in Gulf of Thailand. The fine resolution is set nearshore area and a coarse resolution was set for remain area (maximum area is less than 0.5°). Fig. 1 shows the flexible mesh with bathymetry over the computational domain. It is consisting the 2,370 number of elements and 1,479 number of node points.

There are six locations with two locations in the Upper Gulf, two locations at Vietnam and Cambodia, one position at Botru, Songkhil and one from Malaysia as can be seen in Fig. 1 and Table 2. Those locations are in intermediate and deep water. In order to use results as representatives at shoreline orientation, distances between locations are set to be equal.

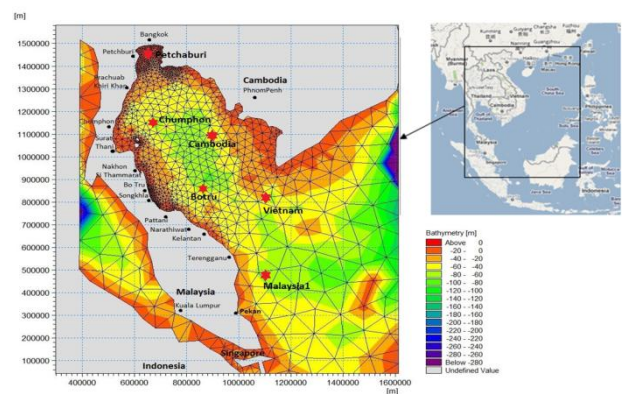


Fig.1 Computational domain for modelling and locations for wave analysis

Table 2 Water depth at six interested locations along the GoT

No	Area Name	Depth (m)	Remarks
1	Petchaburi	25	Upper Gulf
2	Chumphon	65	Upper Gulf
3	Botru, Songkhla	72	West Coastline
4	Malaysia	80	Lower Gulf
5	Cambodia	60	East Coastline
6	Vietnam	70	Lower Gulf

Analysis of Extreme Waves

An extreme event is defined as the all data between an up-crossing and a down-crossing of threshold wave height as shown in Fig.2. The 99th percentile wave height (H_{99th}) value is traditionally used as a threshold (Grabemann and Weisse, 2008). Three extreme event characteristics will be extracted are storm intensity which is defined as the different between the threshold value (H_{99th}) and maximum significant wave height ($H_{s,max}$), storm duration and storm frequency which is the count of events (N) divided by the length of model time slice (20 years in the present study). In addition, the 99th percentile wave direction and the 1% highest wave height can be extracted from statistical analysis of computed present, near future and far future waves. Therefore there are totally six extreme waves parameters. The designed wave height corresponding to 2 to 100 years return period was calculated based on Generalized Extreme Value Distribution (GEV), in serving structures design.

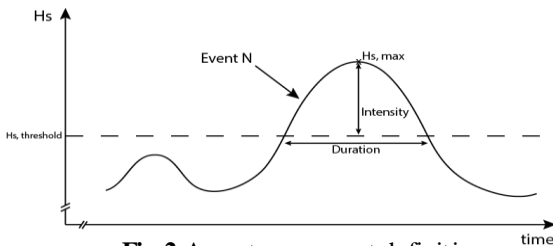


Fig.2 An extreme event definition

Results and Discussion

Model Calibration and Validation

Model modification is calibrated with the buoy wave data using wind forcing NCEP/CFSR. Oceanographic buoy locations are show in Fig.3.

Wind forcing is applied in temporally (6-hourly) and spatially uniform ($0.5^\circ \times 0.5^\circ$) over the computational domain. There are three processes in wave modelling, which are typically for the dissipation due to white-capping, bottom friction and wave breaking in shallow water. Bottom friction

model parameters are available in terms of friction coefficient, friction factor, Nikuradse roughness, k_s (m), and sand grain size, D_{50} (m). Model calibration of this present study calibrated bottom friction parameter using Nikuradse roughness, k_s . The last two model parameters are wave breaking in shallow water, Gamma (γ) and Alpha (α). The present work is focused in intermediate and deep water wave as shown in six locations. Then the process of dissipation due to white-capping with two white-capping parameters, $Cdis$ and $DELTA_{dis}$ (δ) with the tunable range from 1.0 to 5.0 and 0 to 1.0, respectively will be used for calibration as shown in Eq. (1).

The source function of can be expressed as

$$S_{ds}(f, \theta) = -C_{ds} \left(\frac{\hat{\alpha}}{\hat{\alpha}_{PM}} \right)^m \left\{ (1-\delta) \frac{k}{\bar{k}} + \delta \left(\frac{k}{\bar{k}} \right)^2 \right\} \bar{\sigma} E(f, \theta) \quad (1)$$

Where, $\bar{\sigma}$ is the mean relative angular frequency, \bar{k} is the mean wave number, $\hat{\alpha}$ is the overall steepness of the wave field and $\hat{\alpha}_{PM}$ is the value of $\hat{\alpha}$ for the Pierson Moskowitz spectrum.

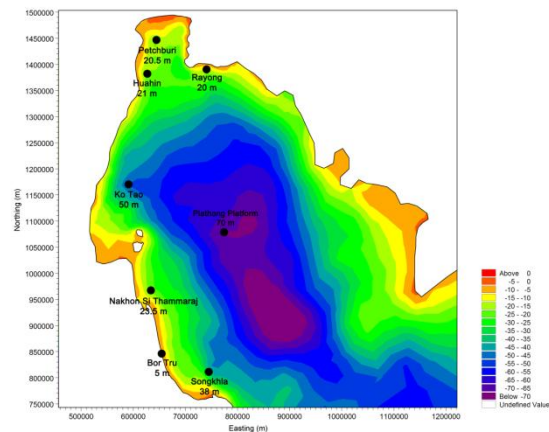


Fig.3 Depth and Oceanographic buoy stations on the bathymetry model modification (Sriumpoldech 2012)

Calibrating model parameters is conducted by adjusting model default value used in MIKE 21 SW until the observed and simulated significant wave height and wave period obtained minimum in errors. The $Cdis$ parameter, modified by Komen et al. (1994) produces significantly change to significant wave height and slightly change to wave period. Increased in $Cdis$ constant, significant wave height and wave period is decreased. $DELTA_{dis}$ parameter produces a bit of change or almost no effect to significant wave height but produces significantly change to wave period. The more $DELTA_{dis}$ is increased, the more wave period is increased. Calibrating $Cdis$ and $DELTA_{dis}$ is done at Songkhla buoy during the calibration period started from 1st November – 31st December, 1993. The model modification is using $Cdis$ equal to 1.0 same as the model default value and

DELTA_{dis} equal to 1.0 for the source function of the dissipation due to white capping. Nikuradse roughness, k_s is important in term of energy dissipation due to the bottom friction. Waves approaching to shallow water are significantly influenced by the bottom friction more than in deep water. Bottom roughness produces slightly change for both wave height and wave period. Increased in k_s , significant wave height and wave period is decreased. Calibrating k_s parameter is done at Nakhon Si Thammarat buoy during the calibration period started from 1st December, 1997 – 20th February, 1998. Nikuradse roughness is 0.04 m. Variation of simulated significant wave height, H_{m0} and wave period, T_{m0} by calibrated model parameters, C_{dis} , *DELTA_{dis}*, k_s are shown in Figs.4,5 and 6 respectively.

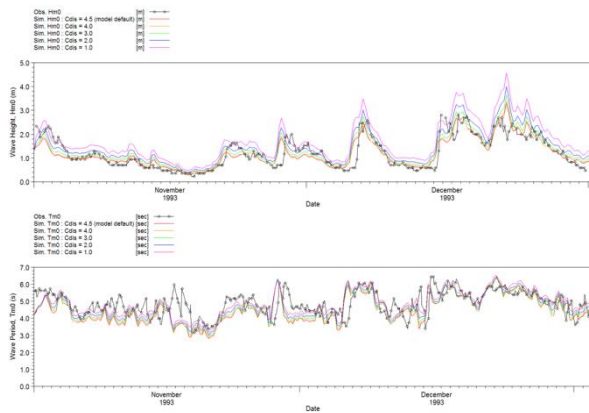


Fig.4 Variation of significant wave height, H_{m0} and wave period, T_{m0} at Songkhla buoy by calibrating C_{dis} , white-capping parameters

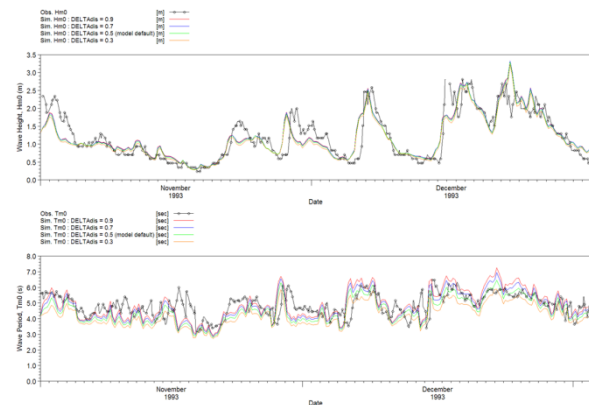


Fig.5 Variation of significant wave height, H_{m0} and wave period, T_{m0} at Songkhla buoy by calibrating *DELTA_{dis}*, white-capping parameters

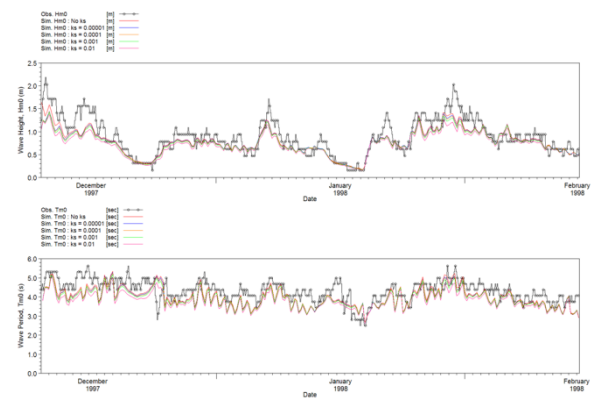


Fig.6 Variation of significant wave height, H_{m0} and wave period, T_{m0} at Nakhon Si Thammarat buoy by calibrating Nikuradse roughness, k_s , bottom friction parameters

Present and Projected Wave Climate

Stations along at the GoT

The wave roses at Chumporn, Petchaburi and Cambodia for present and far future for ECHAM5 are shown in the Fig. 7. Dominate wave direction at Chumporn at present and far future is the same i.e. near-northeast direction. Shoreline at Chumporn is in north-south orientation then the predominant longshore sediment transport direction does not alter but its magnitude can be changed with wave height square. Located in the Upper Gulf, Petchaburi predominant wave direction is same for present and far future, i.e. southeast with increased percentage of occurrences. It is noticed that there are more number of 0.3 to 0.6 m wave height in northeast direction while number of wave height in west direction are reduced. Wave roses at Cambodia shows clearly the same pattern of changing wave directions. Number of high waves between 1.8 to 2.4 m increase in northeast direction and southeast direction for 0.6 to 1.8 m as well. Waves propagate from west direction are reduced.

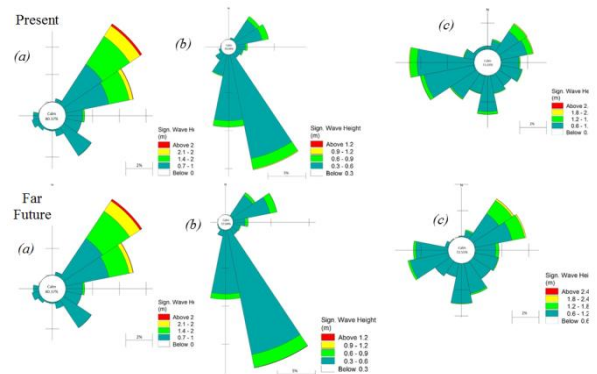


Fig.7 Wave rose diagrams at (a) Chumphon (b) Petchaburi & (c) Cambodia for present and far future using ECHAM5

Bo Tru (Songkhla) in Lower Gulf of Thailand

The wave rose at Botru deep water locations can well demonstrate the coming wave direction from present to far future time slices. It is quite similar pattern in the upper gulf wave direction change i.e. reduced waves in east direction and increase waves in northeast and near south directions. However, this trend is slightly shifted to northeast in the near and far future. In addition, there is less noticeable east coming wave in far future as can be seen in Fig.8. Similar results of coming wave directions are found with the simulations from GFDL CM2.1 model in the far future.

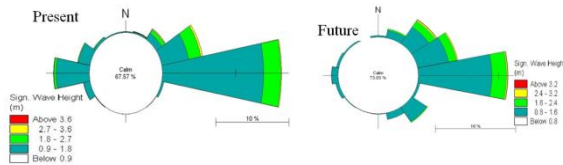


Fig.8 Wave rose diagram at Botru(Songkhla) from present to far future

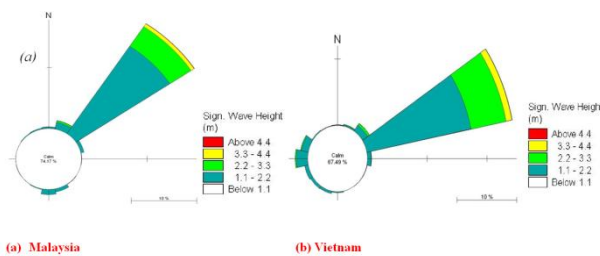


Fig.9 Wave rose diagram at stations at (a) Malaysia and (b) Vietnam in present climate

The model results are in Fig. 9 and 10 for present and future conditions. They show coming wave from the North direction (average 40°) toward Malaysia, but in Northeast direction (average 66°) toward Vietnam station. These two directions dominate at two locations from present to far future. The standard deviation of wave direction at Vietnam and Malaysia are very small in the future with less than 6° in both GCMs. Numbers of waves from west direction are reduced.

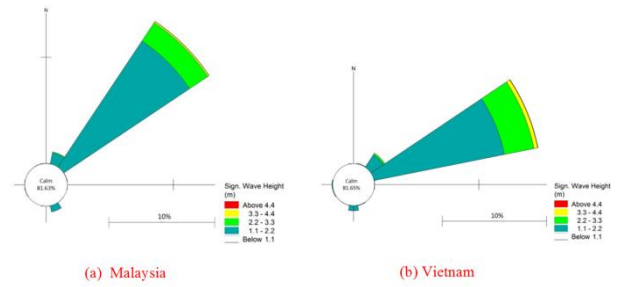


Fig.10 Wave rose diagram at stations at (a) Malaysia and (b) Vietnam in far future climate

Extreme Wave Analysis

Highest wave characteristics

This section shows results of Mean 99th wave height, Mean 1% highest significant wave height and mean wave direction as summarized in Tables 3,4 and 5. Two GCM, ECHAM 5 and GFDL have similar trend and provide similar results. Mean 99th wave heights are slightly increasing except Petchaburi which seems to be constant. Mean 1% highest significant wave height are increasing as well except Petchaburi and Cambodia. It means that number of extreme waves increases especially at Malaysia and Vietnam for near and future climate. Mean wave directions are the same values with small fluctuation except Cambodia which mean wave direction has changed from west to northeast and continue for further future.

Storm Intensity

Results of mean storm intensity, storm duration and storm frequency are in Tables 4 and 5 for present and future climate. Storm intensities do not change at Petchaburi, Chumphon and Cambodia. Stations at Bo Tru (Songkhla), Malaysia and Vietnam show slightly increase storm intensities for ECHAM 5. Storm durations do not alter for future at Petchaburi and Chumphon. Starting from Cambodia, it shows longer storm duration from 9 to 13 hours. Bo Tru shows longer storm duration from 10,12 and 14 hours for present, near future and far future respectively and similarly for Vietnam. All stations show small change for storm frequency from present to near future but it is clearly increase from near future to far future. It increases from 1 to 4 storms per year to 2 to 5 storms per year. Bo Tru (Songkhla) shows the highest increment from 2.5 to 4.5 storms per year.

Table 3 Mean 99th percentile wave height at 6 locations throughout the years, Unit: (m)

Station	NCEP 1981-2000	ECHAM 1981-2000	GFDL 1981-2000	ECHAM 2041-2060	GFDL 2041-2060	ECHAM 2081-2100	GFDL 2081-2100
Station Petchaburi	0.86	0.74	0.75	0.73	0.70	0.72	0.73
Station Chumphon	2.16	1.92	1.97	2.07	1.91	2.23	2.14
Station Cambodia	2.28	1.49	1.46	1.46	1.42	1.54	1.51
Station Botru	2.51	1.81	1.81	1.84	1.74	2.17	2.17
Station Malaysia	3.07	2.40	2.21	2.28	2.08	2.57	2.47
Station Vietnam	3.34	2.55	2.43	2.49	2.32	2.91	2.62

Table 4 Mean 1% highest significant wave height of 6 locations, Unit: (m)

Station name	NCEP	ECHAM	GFDL	ECHAM	GFDL	ECHAM	GFDL
	1981-2000	1981-2000	1981-2000	2041-2060	2041-2060	2081-2100	2081-2100
Station Petchaburi	1.02	0.83	0.87	0.82	0.77	0.80	0.84
Station Chumphon	2.48	2.24	2.32	2.42	2.24	2.56	2.45
Station Cambodia	2.63	1.72	1.68	1.75	1.64	1.73	1.72
Station Botru	2.85	2.15	2.15	2.28	2.05	2.47	2.47
Station Malaysia	3.55	2.71	2.62	2.76	2.40	2.99	2.85
Station Vietnam	3.75	2.97	2.91	3.08	2.67	3.31	2.99

Table 5 Mean wave direction at 6 locations from present to future climate, Unit: ($^{\circ}$)

Station name	NCEP	ECHAM	GFDL	ECHAM	GFDL	ECHAM	GFDL
	1981-2000	1981-2000	1981-2000	2041-2060	2041-2060	2081-2100	2081-2100
Station Petchaburi	164.23	123.42	154.17	107.01	120.91	121.44	129.13
Station Chumphon	39.27	51.49	49.79	49.38	49.28	51.26	48.43
Station Cambodia	274.96	15.29	49.09	45.65	31.85	55.47	43.48
Station Botru	64.80	78.29	68.57	63.94	65.50	64.36	64.36
Station Malaysia	41.83	40.49	39.56	41.81	41.08	42.28	41.69
Station Vietnam	66.68	64.27	63.10	64.64	63.76	65.09	65.44

Table 6 Extreme wave characteristics of 6 locations in present days

Station name	NCEP 1981-2000			ECHAM 1981-2000			GFDL 1981-2000		
	mean intensity [m]	mean duration [hr]	Storm freq [1/yr]	mean intensity [m]	mean duration [hr]	Storm freq [1/yr]	mean intensity [m]	mean duration [hr]	Storm freq [1/yr]
Petchaburi	0.21	5.98	4.05	0.11	8.51	4.10	0.12	8.19	3.35
Chumphon	0.41	10.77	2.75	0.45	11.05	3.15	0.52	12.47	2.70
Cambodia	0.44	6.84	3.40	0.31	9.11	3.50	0.29	8.32	3.65
Botru	0.39	7.00	3.15	0.42	10.07	2.45	0.42	9.27	2.50
Malaysia	0.62	11.45	1.90	0.38	12.43	1.90	0.59	13.45	1.65
Vietnam	0.49	9.29	2.55	0.47	10.70	2.25	0.59	11.36	2.00

Table 7 Extreme wave characteristics of 6 locations in future climate

Station name	ECHAM 2041-2060			ECHAM 2081-2100			GFDL 2041-2060			GFDL 2081-2100		
	mean intensity [m]	mean duration [hr]	Storm freq [1/yr]	mean intensity [m]	mean duration [hr]	Storm freq [1/yr]	mean intensity [m]	mean duration [hr]	Storm freq [1/yr]	mean intensity [m]	mean duration [hr]	Storm freq [1/yr]
Petchaburi	0.10	6.41	4.20	0.08	6.23	3.85	0.08	7.28	3.25	0.10	6.05	3.10
Chumphon	0.54	9.91	3.95	0.51	12.82	3.50	0.43	10.42	2.70	0.41	9.92	4.80
Cambodia	0.36	9.55	3.00	0.28	13.10	3.75	0.36	9.55	3.00	0.26	9.02	4.40
Botru	0.60	12.21	2.15	0.53	14.65	4.50	0.35	8.37	2.25	0.54	14.92	4.50
Malaysia	0.63	12.00	1.45	0.50	11.97	2.75	0.35	10.35	1.55	0.47	12.91	3.45
Vietnam	0.79	12.09	1.65	0.63	13.65	3.55	0.37	7.64	2.10	0.54	12.54	3.05

Designed wave height in the present and future climate

Fig.11 describes return value of wave height at the stations in Malaysia and Vietnam by ECHAM 5 simulations from present to future data where solid line is GEV fitted values. It shows that there is small different of small return period from 1 to 3 years. The change is remarkably noticed when return period increases to be 10 years. The significant design wave height for near future and far future does not alter much but both is significant increased from the values at present time. Generally, the return values increase noticeably from present to future time slice 2041-2060 data. Particularly, GFDL dataset indicating significant wave height at Botru, Chumphon, Malaysia and Vietnam could reach above 4 m for more than 50 year return period. In this computation, the GEV also fit with the GFDL results better than ECHAM but there is higher uncertainty in both upper and lower bound in most of the stations.

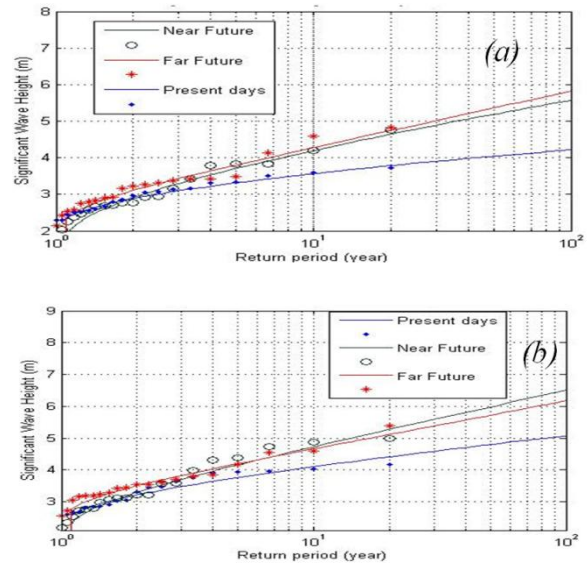


Fig.11 Designed wave height at (a) Malaysia (b) Vietnam for ECHAM5

There is an increasing spatial trend of significant wave height along the coast of Thailand from the Upper Gulf (Petchaburi), Lower Gulf (Chumphon), Botru (Songkhla) to the South coast (Malaysia) for 20 and 50 years return period as shown in Fig. 12. The geography around the gulf, especially Cape Ca Mau in Vietnam protecting wave to intrude into Thailand, significant wave height is then not high. Malaysia is not in the shadow zone of such cape, and it exposes to northeast monsoon; therefore wave height is high. The impact of climate change to extreme waves can be examined with design wave height at far future for ECHAM 5 in Fig. 13. Interestingly, Petchaburi wave height corresponding to 20 and 50 year return period has been witnessed less changing of about 0.3% in the future. It keeps increasing to 4%, 17% and 33% at Chumphon, Botru and Malaysia. The present wave height at Malaysia with 50 year return periods is 4.05 m will increase to 5.38 m in the far future. On the other side of the gulf, increment of significant wave height at stations Cambodia to Vietnam is 3% to 19% at maximum which is less than that of the southern part of Thailand, 33%. The present significant wave height at Vietnam at 100 years is 5.31 m is likely to increase to 6.17 m or 16% increased. One more important location is at Rayong where a number of Industrial Estate Authority of Thailand (IEAT) is located with an important port, Map Ta Phut. Increase design wave height at a location of 58 m water depth and 90 km from shoreline varies from 10 to 13% for 20 and 50 year return period. Structures located at intermediate and deep water depth in exposed sea is likely to encounter the increased design wave height. The present structures should be revisited for its safety with increased extreme waves driven from climate change.

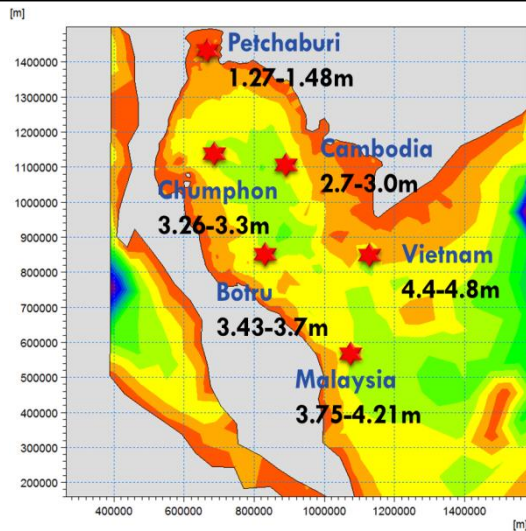


Fig.12 Significant wave height at 20 and 50 year return period at present time

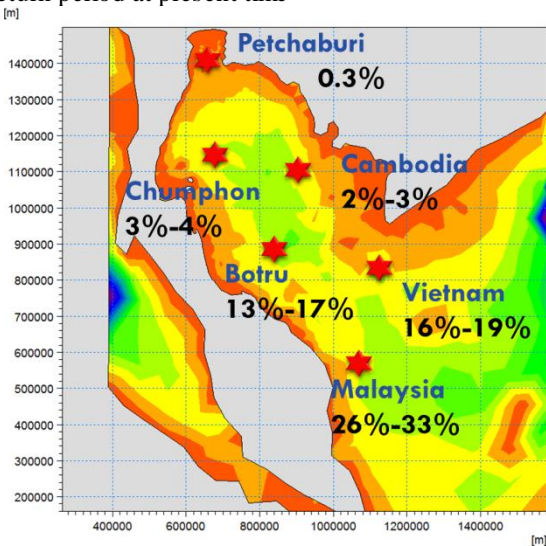


Fig.13 Increment in percentage of significant wave height at 20 and 50 years return period from present to far future ECHAM 5

Summary and conclusions

Wave directions in the gulf of Thailand are likely to change towards near-northeast direction and numbers of waves from west are reduced. Similar pattern of changing of wave direction for present and far future can be found outside GoT.i.e Malaysia and Vietnam.

Two GCMs perform comparable results of wave height and wave direction. Furthermore, the average intensity of extreme events is getting higher from 1 to 4 storms/year to 2 to 5 storms/year at half studied locations. Also, the mean storm duration becomes longer from 10 hours to 14 hours in the future at most of locations.

Spatial increment of significant design wave height in the far future can be found along gulf of Thailand and extended to Malaysia and Vietnam. The highest increased percentage is 33%. The structures can be examined for their safety and robustness

through engineering design with this increased of wave height.

Acknowledgement

Authors would like to acknowledge National Research Council of Thailand (NCRT) for providing measured wave data from oceanographic buoys.

References

- Grabemann I., and Weisse R. (2008). Climate change impacts on extreme wave conditions in the North Sea: an ensemble study. *Ocean Dynamics*, 199-212.
- Hemer M.A., McInnes K.L. and Ranasinghe R. (2012). Projections of Climate Change-Driven Variations in the Offshore Wave Climate Off South Eastern Australia. *International Journal of Climatology*, DOI : 10.1002/joc.3537.
- Hien N.T. (2016). Analysis of Nearshore Waves and Morphology under Extreme Climate Change in the Gulf of Thailand. AIT Thesis, 105 p.
- Kaushalya, W. L. (2011). Effect of future climate on the offshore wave characteristics at Songkhla in Gulf of Thailand, Master Thesis WM10-04, Bangkok, Asian Institute of Technology.
- Mori N., Yasuda T., Mase H. Tom T. and Oku Y. (2010). Projection of Extreme Wave Climate Change under Global Warming. *Hydrological Research Letters* 4, p.15-19.
- Slott, J.M. Murray A.B., Ashton A.D. and Crowley T.J.9. (2006). Coastline Responses to Changing Storm Patterns. *Geophys. Res. Lett.*, 33, 6 p.
- Sriumpoldech, C. (2012). Variability of nearshore wave and longshore sediment transport due to future climate change in the Lower Gulf of Thailand, Master Thesis WM12-14, Bangkok. Asian Institute of Technology.
- Wang X.L., Feng Y. and Swail V.R. (2014). Changes in Global Ocean Wave Heights as Projected Using Multimodel CMIPS Simulations. *Geophys. Res. Lett.*, 41, p.1026-1034.

Analysis of Farmers' Choice of Adaptations to Climate Change at Nong Sua District, Rangsit Canal, Thailand

Ashraf Sheikh Zeeshan^{1,a}, Sutat Weesakul^{2,b*}, Nalinrat Kalampabut^{3,c} and Sanidda Tiewtoy^{4,d}

Abstract The study investigated the farmer's perception towards climate change and examines that how farmers perceived trends in climatic parameters recorded at meteorological stations. The surveyed data from questionnaires are collected in 2015 to 16 at farm level for 208 households with 95 percent confident levels consisting of the farmer's households belonging to two sub districts i.e Bung Cham Aor (BCA) and SalaKru (SLK) sub districts, NongSua district, Pathumthani, Thailand. Average temperature is increased with increased number of hot days and reduced number of cold days with 66% to 76 % respondents. Annual rainfall, rainfall duration and its frequency are decreased with 69% respondents while length of dry period is extended with 75 % respondents. It shows that short memory in recent severe climate which strongly affect their productivity has influenced their perceiving for long term climate change. In total, 71% of farmers in study area adapt to climate change. Farmers prefer agricultural adaption as the most selected choice with 69 % compared to financial, technology and external adaptations. This study also identified the major agricultural adaptations used by the farmers. Changing in sowing and planting date, use of fertilizer and pest management practice, and change in cropping pattern are the most fours adaptations that local farmers practically used in the field. Independent factors affecting the choice of agricultural adaptations are identified using multivariate probit model for discrete choice at farm level. It is confirmed that experience, farm size, income, climate information and noticing climate change are the four important ascending factors affecting the farmer's choice to farm-level adaptation. Income represents wealth which is normal hypothesized to adopt agricultural technologies requiring sufficient financial support.

Levels of satisfaction are also evaluated, it is clearly shown that BCA has significant satisfactory than SLK sub districts with average score 3.60 compared to 2.82 for income and agricultural yield aspects. This is because the development of community water resources management at Bung Cham Aor to plan and use effectively available water. Using science and technology approach with strong participation from community, farmers can learn to use data and develop their own system for water management for climate adaptation and enhance the level of satisfaction.

Keywords *Farmer perception, agricultural adaptation, multivariate probit mode, community water resources management*

¹Graduate Student AIT
Punjab Irrigation Department (PID)
Pakistan

²Hydro and Agro Informatics Institute (HAI) and
Asian Institute of Technology (AIT)
Thailand

³Hydro and Agro Informatics Institute (HAI)
Thailand

⁴Department of Civil Engineering, Raja mangala
University of Technology Thanyaburi, Thailand

^axee.civil@yahoo.com

^bsutat@haii.or.th

^cnarinrat@haii.or.th

^dsanidda.t@en.mutt.ac.th

Introduction

Climate change has become a challenge globally specially in developing countries and it has become an essential component for food production and sustainable development. Agriculture is an important sector in Thailand employing 23 million people or 37% of total population, covering 46% of country area. Chaowiwat *et al.* (2016) stated that in the future year 2015 to 2039, rainfall in Thailand tend to decrease 14.1% to 22.7% for Representation Concentration Pathways (RCP) 4.5 and 13.7% to 24.5% for RCP8.5. The future temperatures tend to decrease 0.62°C to 0.88°C in RCP4.5 and 0.69°C to 0.93°C in RCP8.5. The present agriculture average water demand is 97,174 MCM/year. The overview of future water demand in year 2015 to 2039 tends to increase 15.7% in RCP4.5 and 15.5% in RCP8.5, respectively. It is then clearly seen that agricultural water has significantly and strongly impacted from climate change and more agricultural demand is needed at 15%. In an irrigation project, Plaichumpol Irrigation Project, Thailand, Koontanakulvong *et al.* (2013) stated that farmers 84 % noticed climate change. They focused in agricultural water allocation and agricultural adaptation to cope with future climate variability. ADB (2010) show an example of impact of climate change to

agricultural sector in southeast Asia that higher temperature by 2100 are likely to cause rice yield potential to decline by up to 50% on average compared to 1990 levels. In addition, the region must increase rice production by an average of 2.5% per year and double palm oil production. This intensification will lead to the conversion of land to cultivation. ADB has strength policies, governance and capacities in support of climate change adaptation.

Adaptation to climate change is one of the policy options to reduce adverse impact of climate change. Farmers can cope with climate change by necessitating adaptation. Agricultural adaptation to use new crop varieties, crop diversification, changing planting dates that are appropriate to drier or wetter conditions as described by Nhemachena and Hassan (2007), Kurukulasuriya (2008). Multiple cropping has also proven to be beneficial as an adaptation option to climate change as described by Nendel, et al., (2014) and Waha, et al., (2013). In addition, farmer’s perception on climate change is initially important step prior to responding to changes through adaptation. Farmer’s perception of climate change was significant related to the age of the head of the household, wealth, knowledge of climate change, social capital and agro-ecological setting as explained by Deressa et al. (2010). A number of studies have been conducted to analyze the effect of choice of adaptation which is normally dictated by a host of socio-economic and environment factors. These knowledge can assist policy to strengthen adaptation through investing on these factors. Lastly, the level of satisfaction will be determined and compared between two communities with and without science and technology approach for agricultural water management. This is to examine that the result of adaptations enhanced by science and technology to climate change can bring in the levels of life satisfaction.

The objectives of study are to analyze farmers’ perception on climate change, selecting choices of adaptations, determination of factors affecting agricultural adaptation and evaluation level of satisfaction.

Methodology

1. Study area

Two sub-districts namely Bueng Cham Aor (BCA), RangsitKlong 7 to 8 and SalaKru (SLK) of NongSua District, RangsitKlong 11 to 12 are selected as study area. The Bueng Cham Aor community is already equipped with irrigation water and community managed water resource (CMWR) project under Hydro and Agro Informatics Institute (HAII) whereas SalaKru community is having only irrigation water. BCA sub-district has an area of approximately 48.85 km². There is a canal basin area having three streams and the area is sandwiched between two lines and canal in many villages making them suitable for agriculture. There are

12 number of villages in BCA with a population of 8,624 people with 1,425 households. SLK sub-district is located in east of North East of district NongSua about 14.7 kilometers and 62.7 kilometers away from Pathumthani having an area of approximately 49.65 km². SLK consists of 10 villages and has a total population of 5181 people with 1,493 households. Figure 1 shows locations of both sub-districts.

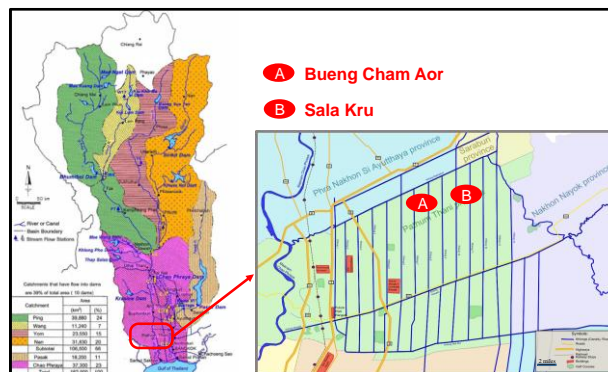


Fig. 1 Locations of Two sub-districts in Study area

2. Data Collection

To collect the information at household level regarding the farmer’s socio-economic characteristics, perception to climate change, strategies to deal climate change, barriers to adaptation, adaptation measures and level of satisfaction a qualitative household survey was conducted using household questionnaire survey with detail in Zeeshan (2016). The data from questionnaires are collected in 2015 to 16 at farm level for 208 households with 95 percent confidence levels consisting of the farmer’s households belonging to two sub-districts i.e. Bung Cham Aor (BCA) and SalaKru (SLK) sub-districts, NongSua district, Pathumthani, Thailand. Focus Group Discussions were conducted by farmers to generate information on the perception towards climate change on the community as well as to cross-check the information collected from the face-to-face interview sessions. Key informant interview is conducted and used to get the in depth information about the recent climatic extremes, current adaptations measures practiced, land use change and the government policies towards climate change. Data collected from survey were also validated through key informant interviews.

Secondary daily meteorological data are collected from Thailand Meteorological Department (TMD) and agricultural data from Hydro and Agro Informatics Institute (HAII). Figure 2 shows locations, period of data collection and type of data at meteorological stations.

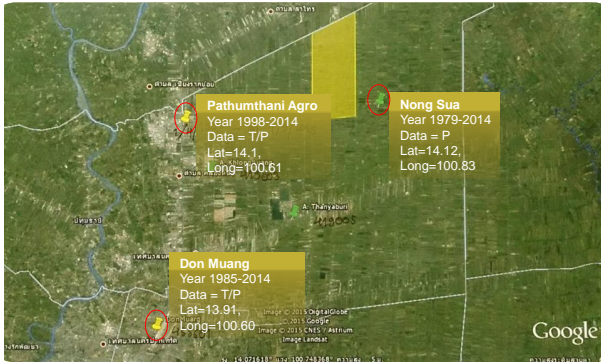


Fig. 2 Location of meteorological stations (T:Temperature, P: Precipitation)

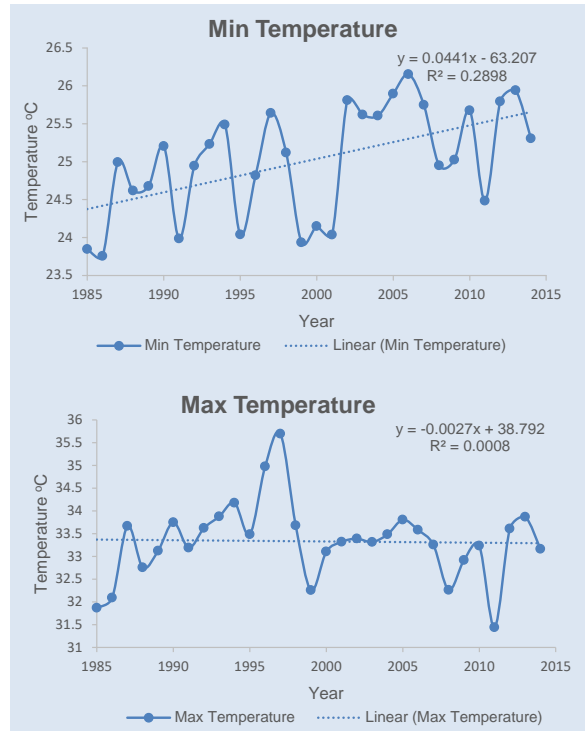
2.3 Analysis Tools

Trend analysis and Rclimdex are used to analysis the climate change. Mann-Kendall test is used to identify the significant of that in analysis of farmer perception. Multivariate Probit (MVProbit) model is applied to determine the main factors affecting the choice of adaptions measure, using the independent variables which are level of education, farmer’s information on climate change, notice about climate change, household’s size, household farm income, sex of household, farm size, distance to market, farming experience and sub district , and dependent variables as adaptions measures. Determinants of farmer’s choice can be made and analyzed. The major barrier identified in the focus group discussions were listed in the questionnaire and the farmers were asked to rank the listed barriers based on the severity they perceived about them. WAI (Weighted Average Index) technique was used to get the priority of the barriers. The respondents from the two sub districts are interviewed by using a structured questionnaire to collect information related to quality of life and level of satisfaction. The satisfaction part of the questionnaire contained respondent’s dimensions of quality of life Flanagan (1978) constructed a measure that encompasses quality of life elements within 5 domains of physical and material well-being, relations with other people, social, community and civic activities, personal development and fulfillment and recreation. Likert scale analysis is used to determine influential factors on life satisfaction and testing the null hypothesis of same satisfaction across both the sub districts by using different statistical tests.

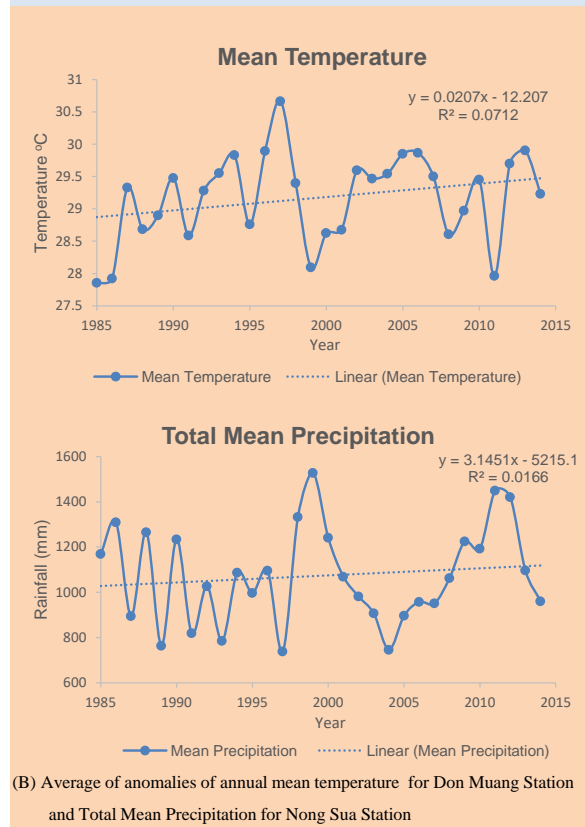
Results and Discussion

3.1 Trends Analysis of Annual and Extreme Indices

Figure 3 shows results of annual trend analysis and significant test. Minimum temperature and total or annual accumulated rainfall show significantly increase



(A) Average of anomalies of annual minimum and maximum temperature for Don Muang Station



(B) Average of anomalies of annual mean temperature for Don Muang Station and Total Mean Precipitation for Nong Sua Station

Fig. 3 shows results of annual trend analysis and significant test

accepted trend with 95 % confident level. It is noticed that there are locally reduced trend of accumulated annual rainfall in the last 3 years i.e. 2012 to 2014. The recent consecutive reducing rainfall may cause people percept in a different way compared with that of long , 35 years, 1979 to 2014. There are 27 indices which are used by RCLimDex and derived from the daily precipitation and temperature data which represents the extremes, frequency and persistence. Out of these 23 indicators were selected. Figure 4 summarize 5 variables having significant trends using Mann-Kendell test which are increased trend i.e. TNX (monthly maximum value of daily minimum temperature) , TN90p (warm night days) and SDII (simply rainfall intensity) while TN10p (cool night days) , DTR (diurnal temperature range) show reducing trend. This is to confirm considering from percentile based indices, TNX, TN90p and TN10p that the minimum temperature significantly increase.

At Don Mueng Station	
TNX	Monthly maximum value of daily minimum temperature (°C) Significant increase (28.3°C - 30°C)
TN90p	Percentage of days when TX > 90 th percentile (days) Warm nights significant increase (2 days to 17 days)
TN10p	Percentage of days when TN < 10 th percentile (days) Cool nights significant decrease (16 days to 3 days)
DTR	Monthly mean difference between TX and TN (°C) Diurnal temperature range significant decrease (9°C - 76°C)
At Nong Sua Station	
SDII	Annual total precipitation divided by number of wet days Simply daily intensity index significant increase (9mm/days to 12mm/days)

Fig. 4 summarize of RCLimDex having significant trends.

3.2 Farmer’s Perception on Climate

Perception on trend of average temperature had been accessed in the household questionnaire by asking three questions regarding temperature level, number of hot and cold days. In total of two sub-districts, about 74% of the respondents perceived long term changes in temperature. Most of them 63% perceive well that temperature is increasing as compare to the past. Only 10 % noticed to the contrary, a decrease in temperature. In addition, the increasing frequency hot days are also perceived by farmers and more than half of them have been experiencing gradual increase in temperature and hot days year after year with the response of about 76% and decrease in cold days by 67%. Figure 5 shows results of farmers’ perception on temperature.

Farmer perception to the trends in rainfall was calculated by questions. Majority of respondents perceived precipitation changes and put their answers under decreasing trends rather than increasing and no change. At BCA those who understands the climate change observed decrease in annual precipitation, timing of rain fall and frequency of rainfall by 68% , 68% and 67% respectively whereas for length of dry period 74% observed an increase and 4% reported a decrease in the dry spell. Results of farmers’ perception between SLK and BCA are similar. Figure 6 shows results of farmers’ perception on precipitation.

Regarding natural hazards, there is a mix response of flood and drought frequency and the intensity whereas in case of droughts there is a clear perception of the farmers of both the areas that there is an increasing trend for intensity and frequency of drought.

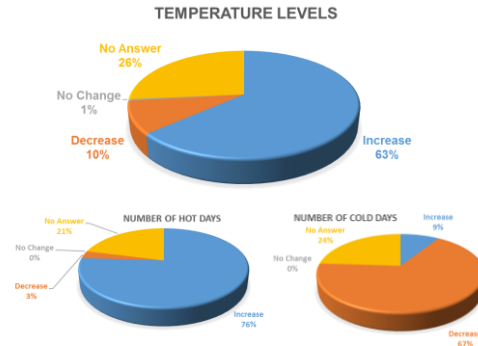


Fig. 5 Results of Farmers’ perception on Temperature

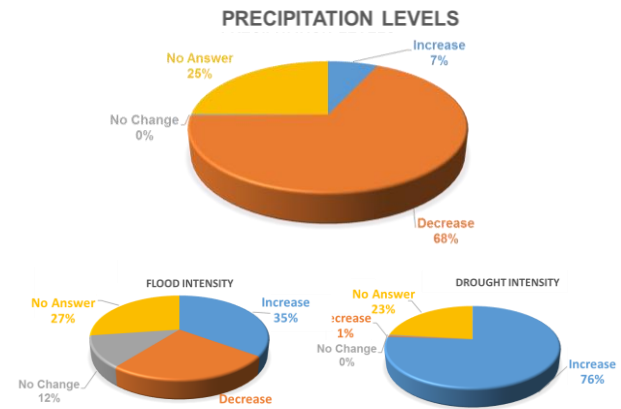


Fig. 6 Results of Farmers Perception on Precipitations

Regarding the climatic variations, a great majority, 72% of respondent perceive variation in environment and climatic pattern while 23% gives their response on the answer of not changing. There are a higher proportion of respondents in BCA than in SLK. It is noticed that SalaKru community is located in lower elevation and is more prone to floods as compared to BCA community that’s why they are well aware of climate change phenomena. Figure 7 shows summary of farmers’ understanding on climate change.

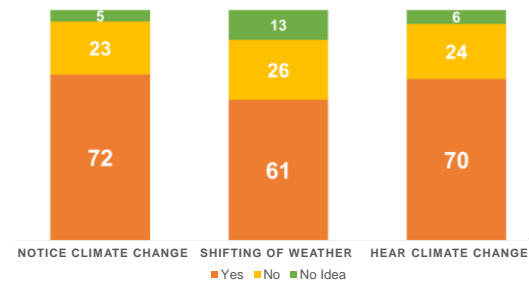


Fig.7 Farmers understanding towards climate change. It can be summarized as follows:

- The majority of farmers’ perception towards temperature change is in line with the temperature records that is increasing.
- A clear contradiction is observed between rainfall records and most farmers’ perception towards rainfall. All responses are towards the decreasing trends in precipitation and hence it cannot be validated with the metrological records.
- Rainfall perceptions can be explained by the fact
 - a) Rainfall trends are in continuous decrease from the last five years
 - b) Due to shift in climate rainfall does not fall enough in time of critical crop growth period

3.2 Climate Change Adaptation Practices

Corresponding to a question that “Have you adopted any measures/adjustment to cope with the effects of climate change?”. There are 70.7 % say yes and adopt measures while 29.43 % say no. Out of 70.7% of farmers 59.13 % (123 out of 208) reported to observe climate change and adopted accordingly. Whereas the rest of the farmers just copied the practice of others without knowing the reason behind that considering the profit to be their priority. Based on the results of focus group discussions and literature review various adaptations measures are grouped in to agriculture, external technological, no agricultural and local government role. Table 1 summaries type and percentage of adaptation. The highest percentage is Agricultural adaptation followed by role of government, external technology and non-agricultural.

Table 1: Summary types of adaptation

No	Types of adaptation	Percentage
1	Agricultural	70.7%
2	Role of Government	61.0%
7	External Technology	57.7%
8	Non - Agricultural	36.1%

3.2.1 Agricultural Adaptations

It is found based on the adaptation measures in the study area that majority of the farmers practiced change in sowing and planning, change in cultivation practice and change in crop variety. Also some farmers were hopeless and change their occupation to business or employment and some did nothing to deal with climate change. Results of agricultural adaptation are shown in Table 2.

Table 2: Agricultural adaptations practiced with respondents from farmers

No	Adaptation Categories	Percentage of respondents (%)	
		BCA	SLK
1	Change in sowing and planting dates	63.9	31
2	Change in cropping pattern/ Crop variety	37	34
3	Change in use of fertilizer	41.7	27
4	Pest management practice	45.4	23
5	Shading and Shelters (Trees etc.)	2.8	3
6	Change in the frequency of irrigation water	35.2	47
7	Reducing Farm Size	5.6	14
8	Agricultural allied activities (Livestock etc.)	1.9	8

Further discussions are conducted with the farmers to know more about the agricultural adaptations, farmers adopted *change in sowing and planting dates* because of changes in rainfall patterns and shortage of water. *Change in crop variety and patterns* is practiced as they observe frequent droughts and shortage of water forcing them to shift to the crops that use less water and short cropping periods. For example, reducing paddy field and concentrate on maize, lettuce and watermelon. The farmers are using mixture of chemical and organic *fertilizers* with amount ranging from 25-50kg./Rai and resulted in the increase of yield as compared to only chemical fertilizers. Chemical, biochemical and herbs are used as *pesticides* to control the insects. Chemical pesticides are reported to be more efficient but also having problems with the crop quality. One of the reasons that BCA has higher percentage of using pest management than SLK is that the productivity at BCA does not reduced much due to good management of agricultural water so that an insect including birds comes to eat their product. Some farmers are practicing *shading and shelter* technique like growing chilies under the shades of mango trees, using rice straw to cover the soil and growing bamboo to control seepage of water in to the soil. The farmers reported to reduce the *frequency of water* to be applied to the crops to manage water during drought and they are also using sprinklers and machines (boats) to apply water to fruits whereas for rice they have to flooding and require lots of water. Reduction of *frequency of water* and *reduce their farm size* are higher percentage at SLK because they do not have secondary storage of water or water management is poor. Farmers are farming frogs, chicken, duck and fish along with the agriculture activities and they are getting government support in this regard also.

3.2.2 Role of Local Government

When the individual adaptation is not much fruitful then intervention from government becomes important to effectively cope with the impacts of climate change. Sub-district Administrative Organization (SAO) along with external agency Hydro and Agro Informatics Institute (HAI) is leading in strengthen the community adaptive capacities including capacity building and hydro-information sharing, formation of community based water management groups and investment in research & development are the adaption options asked by the farmers in regard to the Local government support to climate change adaptation. It is clearly seen that capacity building and information sharing at BCA is significantly higher than SLK, 45.6 % compared to 25%. In this study 51% of respondents acknowledge the role of government and NGOs to effectively reduce the climate change impacts. Table 3 summaries detail of response from farmers for role of local government.

Table 3: Role of Local Government with respondents from farmers

No	Adaptation Categories	Percentage of respondents	
		BCA	SLK
1	Capacity building and information sharing	45.6	25
2	Formation of community based water management groups	50.9	43
3	Investment in research & development	21.3	8

3.2.3 External Technological Adaptations

In order to incorporate the technological trends used by the farmers, technological adaptations are also given which are change in land preparation (Equipment etc.), alternative supply of water and water harvesting and conservation to deal with climate change as shown in Table 4.

Table 4: External technological adaptations practiced with respondents from farmers

No	Adaptation Categories	Percentage of respondents	
		BCA	SLK
1	Change in land preparation (Equipment etc.)	25	7
2	Alternative supply of water	37.9	44
3	Water harvesting and conservation	22.2	37

Moreover while conducting the survey, the use of telemetric and media box by HAI are also reported by the farmers of BCA. HAI has installed telemetric system at the main canal and farmers in the area are

capable to have the information for the flows and water levels in the canals. Weather forecasting in 7 days ahead is disseminated and broadcasting in television at sub-district office administration office using the media box. Farmers at BCA can use such data to manage their crops accordingly. There is no technology at SLK. That is why SLK require more technology in their sub-district.

3.2.4 Non-agricultural adaptations

Apart from agricultural adaptations to climate change, there are many off farm non-agricultural adaptation to deal with climate change. After the preliminary survey of the site it is inferred that many farmers have inclinations towards non-agricultural adaptations which involves use insurances, borrowing credit, selling assets, migration to new place, business/ employment, religious practices and lease of land as shown in Table 5.

Table 5: Non-agricultural adaptations practiced with respondents from farmers

No	Adaptation Categories	Percentage of respondents	
		BCA	SLK
1	Use insurances	10.18	7
2	Borrowing Credit	6.5	18
3	Selling Assets	0.9	4
4	Migration to new place	0	2
5	Business/ employment	2.77	22
6	Religious Practices (Prayers, sacrifices)	0	6
7	Lease your land	0.95	12

In order to adapt to climate change it is imperative that the governmental policies should provide assistance to research and development which leads to better technologies. Therefore to increase the already existing capacity of the agricultural system these conscious policy decisions are taken by the government which include development of drought resistant crop varieties, increasing climate information by establishment of meteorological stations, monitoring of climate date and effective weather forecasts. Apart from that use of modern irrigation technologies is also planned by government. The objective of these policies is to increase the resilience of famers in response to climate change by enhancing their access to affordable credit.

3.3 Factor affecting farmer adaptation strategies

Technical, institutional, social economic and demographic factors influence adaptation behaviors of farmers in developing countries. Therefore it is

necessary to identify the response of farmers to type of agricultural adaptation strategies. Therefore to increase the effectiveness of farm level agricultural adaptations against threat of climate change it is necessary to rely on such factors which are statistically important in this regard. Significant policy information is obtained by identification of the determinants which play an important role in adoption of agricultural adaptation strategies. Therefore 8 agricultural adaptation measures in Table 2 are used as *dependent variables*. It is assumed by this statistical model that each adaptation option is linked to many socio economic factors and they correlate to the perceptions of farmers regarding climate. Farmer household characteristics are important factors in understanding the demand for these adaptation strategies which help in their effective use. These type of data is classified as *independent variables* as shown in Table 7. Education of household head is more than primary school. Literature indicates that when the household head is educated than the rate of adoption of better technology is increased positively along with rate of adaptation to climate change (Maddison 2006). Therefore, educated farmers adapt to climate change readily. Age of head of household is 52.19 years. Farming experience is 47.6 years. Farm size is 26.14 rai or 4.2 ha. Literature indicates that adoption to newer technologies is affected both negatively and positively by farm size showing that the effect of farm size is ambiguous. (Bradshaw *et al.* 2004). Since, larger farm indicated greater wealth therefore they can adapt to climate change in a better way. Wealthy household are in better position to adopt new farming technologies and their ability of bearing risks is increased.

Correlation of adaptations as dependent variables shows that they are correlated and then they are restructured and reduced into 5 adaptations. The parameter estimates from the multivariate probit determinants of adaptation measures are presented in table 7.

Age: The peasant age is one of the factors that is not being affected considerably. However, changing the planning pattern is general, negatively linked toward adaptation while others minor elements analysis shows less specific pattern.

Household size: Generally, in considering most of the adaptation strategies, the probability of adaptation reduces gradually when the household size increases. There is reverse relationship between household scale and adaptation as the size getting larger, the climate change adaptation capacity is going lesser. In addition, higher number of family members which is possible causing great pressure in income could also results in the shifting of labor force toward off-farm works. Furthermore, fertilizer and planning pattern changing, by contrast, are least adopted in growing household size.

Experience: It is strong confirmation that thorough experienced farmers are more likely to adapt in the

context of climate change as they are capable of considering and understanding all adaptation options. In other word, with more experiences, peasants are actually, gaining more knowledge and information about climate change and agricultures practices. As a result, they can utilize wisely these experiences in facing with fluctuations of climate or other socioeconomic situations. Moreover, they are normally, the leaders while rural communities are progressive farmers to encourage and support adaptation planning for others who have less experience or not yet adapting to climate change.

Farm Size: By comparison, this is important factor that positively correlate with the cropping pattern strategy consideration. Facts have shown that, with higher capital and resources, the large-scale farmer are able to adapt easily when they can upgrade the irrigation system at ease.

Distance from Market: There is significant relationship between the distance and the use of fertilizer. Therefore, it is likely to decrease the adaptation ability as the rising of remoteness from markets. The analysis indicates that more market interconnection fosters specialization in production and hence is an important area for public investment in adaptation infrastructure.

Agriculture Income: This is very clear cut-off factor in analyzing the adaptation capacity as wealthier household are better adapted. The survey of farm income also point out a positive and noticeable impact on changing in sowing and plantation date, using different crops, and pest management practices.

Climatic Information: It is important to notice the climate change context in planning adaptation measures. Similar to experience factor, the more awareness of climatic conditions changing, the higher chances of taking adaptive measures in response to changes for farmers. Particularly, the temperature and rainfall parameters are the most important information and having positive effects on the likelihood of adopting different adaptation plans specially change in use of fertilizer. It is therefore paramount acts from governments, meteorological departments, and ministries of agriculture in nurturing higher awareness of the changes in climatic conditions through appropriate communication pathways that are available and convenient to farmers.

Subdistrict Bueng Cham Aor: As analysis, different farmers living in different sub district employ various adaptation methods. Based on the multivariate probit model, the positive and significant parameter estimate on the Bueng Cham Aor Sub district dummy performs a higher likelihood of adopting change in sowing and plantation, fertilizer and pest management practice relative to Sala Kru Sub district

Education: As aforementioned, when analyzed farmer age and experience, it is believed that instead of education, age, experience is the most factor in adapting to climate change. The education level, thereby, didn’t impact significantly on the probability of choosing any adaptation technique.

Table 6 Descriptive of variables hypothesized to determine adaptation behavior, a brief description of each variable and its value in relation to various adoption options

Variable	Description	Value	Mean	Std. Dev.
Education of household head	Level of education of household head (Dummy)	1=Primary and 0=Other	2.47	0.78
Size of household	Number of family members of a household (Continuous)	Number	4.35	1.44
Gender of head household	Gender of the head of household (Dummy)	1=Male and 0=Female	0.537	0.501
Age of head household	Age of the head of household (Continuous)	Years	52.19	11.13
Farming experience	Number of years of farming experience for the household head (Continuous)	Years	47.63	12.41
Farm income	Income from the agriculture (Continuous)	Number	179294	108770
Climate change awareness	Information about climate change (Dummy)	1=Yes and 0=No	0.78	0.42
Farm size	Area of the farm for agriculture (Continuous)	Number	26.14	28.48
Distance to market	Distance from the farm to the output market (Continuous)	Number	7.83	4.93
Sub district	Sub district of respondent (Dummy)	1=BCA 0=SK	0.519	0.501

Table 7 Results of Multivariate Probit analysis for main factors affecting the choice of adaptation measure

	Change in sowing and plantation date	Change in cropping pattern	Change in use of fertilizer	Pest management practices	Change in frequency of irrigation water
Age of Household Head	0.0073 (0.0166)	-0.0288** (0.0141)	0.0145 (0.0133)	0.0028 (0.0133)	-0.0055 (0.0125)
Gender of Household Head	-0.6589** (0.3321)	0.4739* (0.2571)	0.117 (0.2685)	-0.4247 (0.2669)	0.2327 (0.2411)
Household Size	0.1554 (0.1033)	-0.2209*** (0.0845)	-0.3094*** (0.095)	-0.1216 (0.0809)	-0.0144 (0.0743)
Farming Experience	0.0105 (0.0104)	0.0232** (0.0097)	0.0093 (0.0092)	0.0012 (0.0089)	0.0021 (0.0082)
Education of Household Head	-0.1639 (0.3725)	0.4835 (0.3043)	0.465 (0.3135)	0.4424 (0.3257)	-0.2858 (0.2827)
Farm Size	0.0407** (0.017)	0.0089 (0.0071)	0.0144 (0.0108)	-0.0006 (0.0067)	0.0102 (0.007)
Distance from Market	-0.0119 (0.008)	-0.0027 (0.0074)	-0.0147* (0.0084)	-0.0084 (0.008)	-0.0008 (0.0071)
Agriculture Income	4.35e-6** (1.74e-6)	1.84e-6** (8.99e-7)	2.19e-6* (1.14e-6)	2.32e-6** (1.05e-6)	1.16e-6 (8.23e-7)
Access to climate change information	0.4401 (1.024)	1.0064 (0.988)	1.3123* (0.7811)	5.8839 (100.4644)	-0.0515 (0.7397)
Notice climate change	1.7469*** (0.3647)	-0.0943 (0.2665)	0.6727** (0.2723)	1.2446*** (0.2779)	-0.2859 (0.2498)
Sub district	0.0073 (0.0166)	-0.0288** (0.0141)	0.0145 (0.0133)	0.0028 (0.0133)	-0.0055 (0.0125)

Log likelihood = -389.34599
 Wald chi2(60) = 125.2
 Number of obs = 132
 Prob > chi2 = 0.0234

Likelihood ratio test of rho21 = rho31 = rho41 = rho51 = rho61 = rho32 = rho42 = rho52 = rho62 = rho43 = rho53 = rho63 = rho54 = rho64 = rho65 = 0
 Figures in parenthesis are standard errors. **, * and *** represents statistical significance at 10%, 5% and 1% level respectively.

3.4 Life Satisfaction

This section aims to approach life satisfaction whether people are satisfied with their life or not among two sub districts of BCA and SLK. The satisfaction questions

focus on items such as income/assets holding, agriculture, social aspects/ community and family characteristics. The Likert scale of 1 to 5 was used in analysis to indicate the satisfaction level for the questions, where 1 is not at all satisfied and 5 is highly satisfied for the statement that is being asked. Cronbach’s Alpha (α) is the most common measure of internal consistency (reliability) and is applied in this study to check the reliability of the scale for multiple likert questions. The results represent a value of 0.888 for BCA and 0.894 for SLK indicating a high level of consistency for our scale with this sample data.

The following section consisted of 11 Likert-type items designed to assess farmers’ overall life satisfaction. These items used a five point response scale (1= not at all satisfied and 5=highly satisfied) and prompted farmers to indicate the degree to which they agreed with each statement. Table 8 shows the mean and distribution of Likert scale score in percentage for both the sub districts of Bueng Cham Aor and SalaKru considering income/assets holding, agriculture, social aspects/ community and family characteristics aspects. It’s quite evident from the results that the farmers of BCA are more satisfied as compared with the SLK farmers with the major differences in income and agriculture.

Table 8 Difference in the level of satisfaction of farmers of Bueng Cham Aor and SalaKru

Statement	Likert Scale (Mean)		Percentage Difference
	Bueng Cham Aor	SalaKru	
Income/ Assets holding	3.7	2.85	23%
Agriculture	3.5	2.8	20%
Social Aspects /Community	3.67	3.23	11%
Family Characteristics	3.93	3.6	8.5%

Mann-Whitney U test is used to compare difference between two independent groups. We set our null hypothesis as the distribution of “Satisfaction is same across the sub district of BCA and SLK.” which can be concluded that that satisfaction level of farmers of BCA is significantly higher than the farmers of SalaKru for 95% confident level. Analysis detail is in Zeeshan (2016) The only reason and different factor from 2 sub-district is that BCA has worked out with HAI with science and technology approach for field/GIS data preparation by communities so that they can use water map to understand the existing conditions. Then community can make their own decision to strengthen water resources management by rehabilitating old irrigation infrastructures, monitor water level and

available water use. In addition, HAI provide them daily broadcasting of present and 7 days forecasting climate information so that community can plan and use available water wisely, even in drought year.

Summary and conclusions

- The farmers are well aware of climate change phenomena and their perceiving of temperature is validated with the past climatic data where as there is a contradiction in the trends of precipitation with the last 4 years of decline of trend.
- Majority of the farmers, 71 percent adopted some measures to deal with the effects of climate change and the results of the multivariate model reveals that experience, farm size, income, climatic information and noticing climate change have significant contribution to climate change adaptations while household size and distance from market negatively influence the adaptation. Therefore climate information is very important and required to be disseminated to farmers.
- Farmers of BCA are more satisfied significantly as compared to SLK based on their income on agriculture. This is on the basis of more versatile management of community water resources using science and technology approach.

Acknowledgement

The first author would like to acknowledge World Bank for financial scholarship to Asian Institute of Technology (AIT) through Punjab Irrigation Department, Pakistan. Authors would like to thanks Thai Meteorological Department (TMD) and Hydro and Agro Informatics Institute (HAI) for providing meteorological data for the present study. Officers at Sub-district Administration Office of Bueng Cham Aor and SalaKru are acknowledged for assistance and collaboration during data collection phase..

References

ADB (2010) “Climate Change in Southeast Asia : Focused Actions on the Frontlines of Climate Change”, Nov,32 p.

Deressa, T., R. Hassan, T. Alemu, M. Yesuf and C. Ringler (2008) Analyzing the Determinants of Farmers’ Choice of Adaptation Methods and Perceptions of Climate Change in the Nile Basin of Ethiopia. IFPRI Discussion Paper No.798. International Food Policy Research Institute, Washington DC

Deressa, T., R. Hassan, and C. Ringler (2011) “Perception of and Adaptation to Climate Change by Farmers in the Nile Basin of Ethiopia”, *Journal of Agricultural Science*, 149,23-31

Utokapat foundation (2016) “Application of Science and Technology for Community Water-Related Disaster Risk Reduction”, August, 107 p.

Nhemachena, C., Hassan, R., 2007. Micro-level analysis of farmers’ adaptation to climate change in Southern Africa. IFPRI Discussion Paper No. 00714. International Food Policy Research Institute, Washington, DC.

Zeeshan A.F. (2016) “Farmer’s Perceived Agricultural Adaptation to Climate Change Impact in Rangsit Canal Area of NongSua District, Thailand “, AIT Thesis, 87 p.

Flanagan J.C. (1978) “A Research Approach to Improving our quality of Life” ,*American Psychologist*,33,138-147.

Kurukulasuriya M.(2008) “ A Ricardian Analysis of the Impact of Climate Change on African Cropland”, *African Journal of Agricultural and Resource*,2 (1) p.1-23.

Nendel, C., Kersebaum, K. C., Mirschel, W., &Wenkel, K. O. (2014). Testing farm management options as climate change adaptation strategies using the MONICA model. *European Journal of Agronomy*, 52, 47-56.

Chaowiwat W. ,Boonya-aroonnet S., and Weesakul S. (2016) “Impact of climate change assessment on agriculture water demand in Thailand” *Naresuan University Engineering Journal*, Vol.11, Supplement 1, May 35-42.

Waha, K., Müller, C., Bondeau, A., Dietrich, J. P., Kurukulasuriya, P., Heinke, J., &Lotze-Campen, H. (2013).Adaptation to climate change through the choice of cropping system and sowing date in sub-Saharan Africa. *Global Environmental Change*, 23(1), 130-143.

Maddison, D. 2006. The perception of and adaptation to climate change in Africa. CEEPA Discussion Paper No. 10. Centre for Environmental Economics and Policy in Africa, University of Pretoria, South Africa.

Koontanakulvong S., Chaowiwat W. and Miyazato T. (2013) “Climate Change’s Impact on Irrigation System and Farmers’ response : a Case Study of the Plaichumpol Irrigation Project, Phitsanulok Province, Thailand, *Paddy Water Environ* , 14 p.

Bradshaw B., H. Dolan, and B. Smit. 2004. Farm-Level Adaptation to Climatic Variability and Change: Crop Diversification in the Canadian Prairies. *Climatic Change* 67: 119–141.

Change of the Probability Distribution of Annual Maximum River Discharge Derived from the d4PDF datasets at the Indochinese Peninsula

Patinya HANITTINAN^{1*}, Yasuto TACHIKAWA², Yutaka ICHIKAWA³ and Kazuaki YOROZU⁴

Abstract

This study investigates the differences in the probability distribution function of the future annual maximum river discharges (2051-2110) at the Indochinese Peninsula derived from the new climate datasets – database for Policy Decision making for future climate change (d4PDF). First, daily river discharge of the future period was simulated using the kinematic wave flow routing model, 1K-FRM. Based on this analysis, we combined fifteen 60-member ensembles separately for six different sea surface temperature (SST) patterns, which allows us to examine the statistical significant of the difference between the probability distribution. Then, we applied a non-parametric, two-sample Kolmogorov-Smirnov (K-S) test to the annual maximum river discharge produced by SST patterns in 15 groups. Finally, the results of each case indicate that the differences in probability distribution of the annual maximum discharges are statistically significant for the majority of the Indochinese Peninsula, except parts of the Mekong delta and southern Peninsulain Thailand. The implication of this finding should help underpin the case to merge the datasets from different SST patterns and fully utilize it in frequency analysis of extremely large datasets for a more credible hydrologic impact assessment.

Keywords *Climate change, Indochinese Peninsula, d4PDF, Kolmogorov-Smirnov test, 1K-FRM, Annual maximum daily discharge*

¹Patinya Hanittinan

Graduate School of Engineering, Kyoto University Kyoto, Japan, Hanittinan.patinya.77a@st.kyoto-u.ac.jp

²Yasuto Tachikawa

Graduate School of Engineering, Kyoto University, Kyoto, Japan, tachikawa@hywr.kuciv.kyoto-u.ac.jp

³Yutaka Ichikawa

Graduate School of Engineering, Kyoto University, Kyoto, Japan, Ichikawa@hywr.kuciv.kyoto-u.ac.jp

⁴Kazuaki Yoro zu

Graduate School of Engineering, Kyoto University, Kyoto, Japan, Yoro zu@hywr.kuciv.kyoto-u.ac.jp

Comparison of the Spatial Rainfall in Khun Dan Prakan Chon Reservoir by Spatial Interpolation Techniques

Peerapong Rattanaburi^{1,a,*}, Lerdphan Sukyirun^{2,b} and Wisuwat Taesombat, D.Eng. ^{3,c}

Abstract Comparison of the spatial rainfall in Khun Dan Prakan Chon Reservoir by spatial interpolation techniques aims to evaluate spatial interpolation techniques and compare different rainfall interpolation methods to produce spatial rainfall estimates. The interpolation methods used in this study were inverse distance weighting, kriging, Co-Kriging, isohyetal, Thiessen polygon and thin plate spline. Daily rainfall data from 21 rain gauges in Khun Dan Prakan Chon Reservoir surrounding point stations were used to estimate rainfall in September, 2008 and 2011. The accuracy of estimations was assessed through basic statistics, such as mean error (ME) and root mean square error (RMSE). Isohyetal has performed the lowest RMSE in Khun Dan Prakan Chon Reservoir and ME has provided positive value that is over-estimated rainfall.

Keywords *Rainfall, Spatial Rainfall, Khun Dan Prakan Chon Reservoir, Kriging, Co-Kriging and Interpolation Rainfall*

Peerapong Rattanaburi^{1,a,*}

¹Bureau of water management and hydrology
Royal Irrigation Department, RID
Bangkok, Thailand.

^apopirre60@gmail.com

Lerdphan Sukyirun^{2,b}

²Bureau of water management and hydrology
Royal Irrigation Department, RID
Bangkok, Thailand.

^bton0916@hotmail.com

Wisuwat Taesombat, D.Eng. ^{3,c}

³Department of irrigation engineering
Kasetsart University, KU
Bangkok, Thailand.

^cfengwwt@ku.ac.th

Introduction

Rainfall data accounts for one of crucial factors in implementing engineering works as well as in designing and planning the tasks in hydrology and water management. The data, which is collected from rain gauge tools, could continuously record the data in certain areas and this hence leads to the reliable data. When it comes to the utilization of both spatial and distributed rainfall data, it is important to analyze the data from several rainfall measuring stations to calculate the Spatial Interpolation in order to predict the amount of rainfall in the regions where the potential rainfall measuring stations are no longer available.

In Thailand, rainfall measurement system represents point data in rainfall and climate measuring stations: for example Meteorological Department and Royal Irrigation Department. The collected rainfall data only demonstrates the data in the measuring areas, which could not illustrate the data in other areas. To analyze the data regarding basin management, we adopt Geographic Information System (GIS) in Spatial Analysis. For this reason, it is required to evaluate the amount of rainfall in the areas in which the rainfall measuring stations are not installed. Furthermore, some factors such as the characteristics of rainfall distribution influenced by distance, time and rainfall intensity are all significant in generating the precise and correct measurement.

This research aims to study the estimation of the daily rainfall data in each methodology by applying Geographic Information System (GIS). GIS is adopted to analyze the measures in rainfall approximation in the zones of Bang Pakong river basin and KhundanPrakanchon reservoir in which the landscape of the areas is both plain and highland.

Study area

KhundanPrakanchon reservoir mainly covers the regions of NakhonNayok Province and partially covers Prachinburi Province. The landscape are the mountains with sharp slope. In this area, Dong Phraya Yen mountains (KhaoYai) is located in the northeast which is the collision front of the southwest monsoon. This collision front causes a huge rainfall during June to October in each year generating average rainfall around 2,600-2,900 mm/year. In the rainy season, there is a

great amount of rainfall water flowing from the southeast and suddenly decline in flowing levels before reaching the plains in NakhonNayok Province. Because of locating 3-4 meters above the mean sea level along with the great slope of waterway, these have led to the rapid and strong flow of water. As a result, in the rainy season, this has caused to the floods in the areas which could inundate agricultural areas as well as people's residents in the city. In addition, about 93% of the average annual runoff is from rainy season. For this reason, it is an undeniable fact that particular areas will face with the droughts in consumptive, agricultural and industrial sectors.

KhundanPrakanchon reservoir is located in the NakhonNayok basin, which is constituted as a sub-basin of Bang Pakong River. Looking into the details, NakhonNayok basin covers the entire 2,433 km-square and consists of numerous main rivers such as Samorpoon canal, Ta-Dan canal, and NakhonNayok river together with minor branches; Klong Nang Rong, Klong Wang Takhrai, Klong Ma-Duai, Klong Sumpung-haeng, Klong Bo, KlongSarika, Klong Si-Siad, KlongHuay-Saai, KlongHinKaew, and KlongBanNa, etc.(Fig.1)

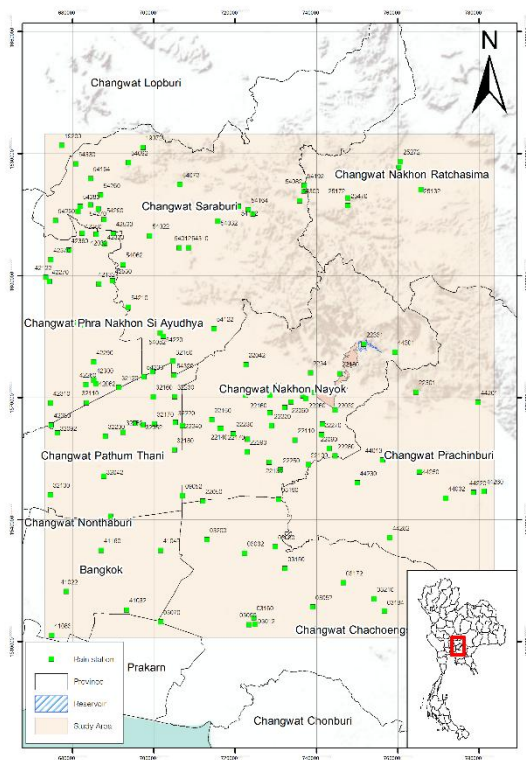


Figure 1 Study area

The purpose and scope of study

This research is the comparison between the spatial rainfalls in Bang Pakong River and the areas covered by KhundanPrakanchon reservoir. Also, the research utilizes spatial estimating techniques in order to make the results precise as well as reliable. The objectives are following:

1. To study spatial estimating techniques by the methodology of Inverse Distance Weighting, Kriging,

Co – Kriging, Isohyetal, Thiessen-polygon and Thin Plate Spline.

2. To compare the effectiveness of spatial estimation by adopting Inverse Distance Weighting, Kriging, Co – Kriging, Isohyetal, Thiessen-polygon and Thin Plate Spline.

The data used in this research is the collected daily rainfall between 2000 and 2014, from 138 stations (RID 89stations, Meteorological Department 49 stations and the other organizations 3 stations)

Methodology

1. Data collection and preparation

1.1 The data of this research must be from the slope and plain areas.

1.2 The geographic data used in this study are basin boundary the location of rainfall measuring stations in which they are from RID. In terms of data preparation, there are two main types:

Coordinate System, which has the unit in degrees in Grid Coordinate System. And the Projection UTM (Universal Transverse Mercator) Datum WGS84 Zone 47N, which has the unit in meters for the appropriateness in the study of how to approximate the amount of daily rainfalls by each methodology.

1.3 The daily rainfall data represent the study areas and the nearby regions in which they are collected between 2000 and 2014, from 138 stations (RID 89stations, Meteorological Department 49 stations and the other organizations 3 stations).

Regarding the record, the data is collected every day at 7 A.M. Also, each rainfall measuring station consists of station code and name, Latitude and Longitude.

1.4 In terms of Digital Elevation Model (DEM), the study consider and select the public data from NASA Shuttle Radar Topography Mission (SRTM) that have the resolution at 3 arc second or about 90 meter. This website <http://srtm.csi.cgiar.org> is the source where we can download the data.

2. Data selection in the study

2.1 On the initial step, the team of study examined rainfall data and other data from rainfall measuring stations by changing daily rainfall to cumulative annual data. Then, the team selected the missing data and the outliers.

2.2 Tested the reliability of rainfall data by utilizing Double Mass Curves. If the data are correct then the graph will be the linear function.

2.3 Filtered rainfall data from measuring stations during 2000-2014 to calculate cumulative monthly rainfall in each year and selected the data that possess the maximum cumulative monthly rainfall to study.

2.4 Calculated the elevation levels of the measuring stations from Digital Elevation Model, from SRTM, by applying ArcGIS when analyzing the correlation between heights and the amount of rainfall.

3. Data analysis and conclusion

3.1 Calculated spatial rainfall by using Inverse Distance Weighting, Kriging, Co – Kriging, Isohyetal, Thiessen-polygon and Thin Plate Spline. ArcGIS is also important in transforming the amount of rainfall from point data to either continuous spatial data or grid in geological system, which is required to adopt Geographic Coordinate System.

3.1.1 Created the boundaries that cover the study regions in the Polygon shape.

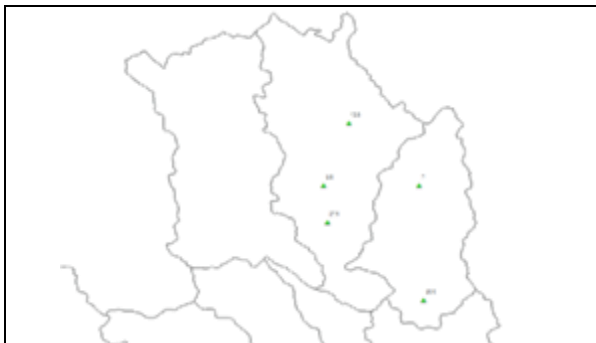
3.1.2 Imported the selected rainfall data, which is the daily rainfall from each measuring station. show on Pic 1. Sub (1)

3.1.3 Switched off certain rainfall measuring data stations that we would like to calculate the value. Then, we applied ArcGIS to generate spatial rainfall by these methodology: Inverse Distance Weighting, Kriging, Co – Kriging, Isohyetal, Thiessen-polygon and Thin Plate Spline., as shown in the picture. 1 Sub (2).

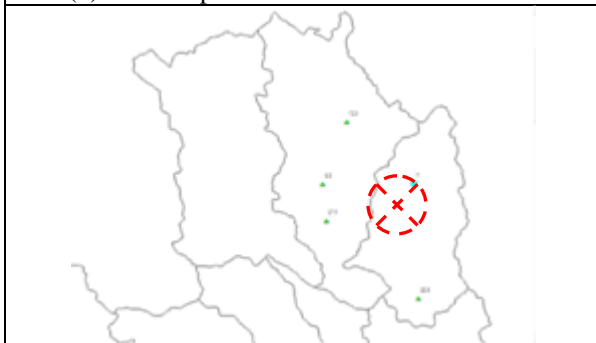
3.1.4 Finding the rainfall on the estimated position coordinates of the closing station in 3.1.3 and save the data for compare with the actual value of that particular station, as shown in pic 1 Sub (3)

3.1.5 Create a value of rainfall in every measuring station that we would like to know in one month.

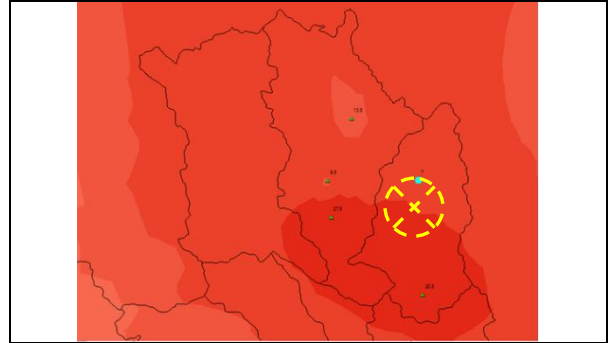
3.2 Verification of the result from each evaluation method and conclusion.



(1) Data Import rain chosen.



(2) Turn off the rain gauge station needs to know the value.



(3) Determine the amount of rain that falls on the estimated position coordinates of the measuring stations, the rain held off.

Figure 2 The spatial estimation.

By illustrating the distribution of rainfall from each statistically estimating methodology such as Mean Absolute Error (MAE), Root Mean Square Error (RMSE) and Mean Error. However, RMSE (shown in equation 1) is the measurement comparison between actual value and the estimated value. Also, if RMSE is relatively low, this means that actual value and the estimated value are quite similar.

$$RMSE = \sqrt{\frac{1}{n} \sum_{i=1}^n (x_i - x)^2} \quad (1)$$

RMSE = Error occurred.

x_i = actual value

x = the value from the estimate.

n = number whole data

The estimation from MAE (shown in equation 2) is the solution for solving the average of the absolute difference between actual value and the estimated value. If MAE is relatively low, this means that actual value and the estimated value are quite similar.

$$MAE = \frac{1}{n} \sum_{i=1}^n |x_i - x| \quad (2)$$

MAE = Error occurred.

x_i = actual value

x = the value from the estimate.

n = number whole data

The estimation from ME (shown in equation 3) is the solution for solving the average of the difference between actual value and the estimated value. If the value of ME is positive, this means that estimated value is lower than the actual one. But, if the value of ME is negative, this is implied that estimated value is greater than the actual value.

$$ME = \frac{1}{n} \sum_{i=1}^n (x_i - x) \quad (3)$$

ME = Error occurred.
 xi = actual value
 x = the value from the estimate.
 n = number whole data

Coefficient of Determination could be represented by “R²” (shown in equation 4). The coefficient demonstrates the regression that used in estimating certain values. Also, it could illustrate the variation of normal and independent variables in the models. The result from this methodology will be varied from 0 to 1, if the result is close to 1 this will reflect that the two variables have a positive correlation.

$$R^2 = \frac{SS_{Re\ g}}{SST} \quad (4)$$

R² = coefficient of determination.
 SSReg = the variance of y due to X's influence.
 SST = the sum of the difference between Yi and Y squared.

Results and discussion

1. Examination and selection of data in the study.

The testing of the reliability of rainfall data by Double Mass Curves methodology and the consideration of “R²” which is close to 1 (shown in table1) so that they can be further used in the study.

Table 1 summarizes the rain gauge stations.

No.	Detail	Study area
1.	Selected stations	21
	- Meteorologica l Department	21
	- R ²	0.9784 – 0.9994
2	DEM (m.)	4 – 493
3.	average annual rainfall (mm.)	1,224

In the study areas and the nearby, there are 21 selected stations which are under the control of the Meteorological Department. The 3 stations are in the NakornNayok basin, and the other 18 stations are located nearby. The R² from reliability testing by Double Mass Curves methodology is between 0.9784 – 0.9994 and this means that the reliability is acceptable. Regarding the study, we have found that the best rainfall data is from the Meteorological Department.

The study has selected the rainfall data in the year 2011, which has a huge amount of rainfall. Also, we chose the data from the year 2008 to compare. As a result, we found that the data show that the maximum cumulative monthly rainfall is in October 2011 (3,322 mm) and October 2008 (2,848 mm),so we select the

data in August to study about the spatial rainfall estimation.

Khun Dan Prakan Chon Reservoir has the elevation level from 4 – 493 meters. At the station no: 25172, it possesses the maximum height, at 493 meters while the lowest station is at the station number 44032. Most of these stations are not located on the slope of highland due to the fact that the majority of selected rainfall measuring stations are belonged to the Meteorological Department in which they will install the stations nearby villages or local authority. However, when considering the elevation in each station, we find that there is a great difference due to the landscape conditions of the stations.

2. The estimation results of spatial rain interpolation

During September 2008 to 2011, the entire average daily rainfall from the estimation is greater than the actual value. Especially, in the method of Thiessen Polygon which has the maximum value of average daily rainfall. In addition, Inverse Distance Weighting method is also high in its value when considering the day that has the maximum rainfall, on September 11th 2008. Thus, we found that Inverse Distance Weighting method has led to precise estimated value. Conversely, when it comes to the period that has lower rainfall, the approximated value is lower than the actual value.

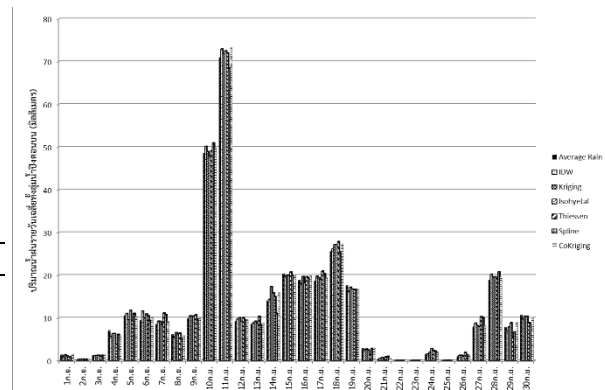


Figure 3 Shows the rainfall average daily in whole studies areas, September 2008.

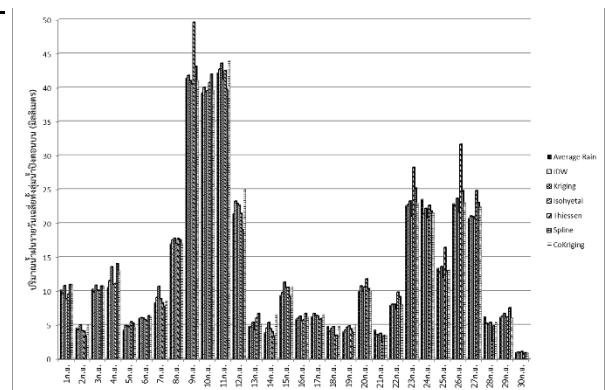


Figure 4 Shows the rainfall average daily in whole studies areas, September 2011.

The result from average daily rainfall estimation in the areas by several methods during September 2008 and 2011 could be summarized in the statistical data in the table no:2 and 3, respectively. Table no:3 demonstrates the approximation from each method in the Khun Dan Prakan Chon Reservoir

Table 3 Statistical in the estimation of each method of Khun Dan Prakan Chon reservoir aere

statistical	estimation	Khun Dan Prakan Chon reservoir aere	
		September 2008	September 2011
Mean Error (ME)	IDW	-5.53	-3.03
	Kriging	-10.50	-14.90
	Isohyetal	-7.61	7.46
	Thiessen	-9.30	-30.37
	TPS	-1.16	-10.19
	CoKriging	-11.64	-14.26
Mean Absolute Error (MAE)	IDW	252.30	356.22
	Kriging	262.45	364.76
	Isohyetal	266.04	348.51
	Thiessen	309.96	420.76
	TPS	328.15	420.53
	CoKriging	273.86	363.14
Root Mean square Error (RMSE)	IDW	351.34	500.44
	Kriging	363.79	520.62
	Isohyetal	356.86	473.00
	Thiessen	629.61	824.37
	TPS	562.02	704.66
	CoKriging	372.54	514.40

Table 4 Statistical in the estimation of each method of Khun Dan Prakan Chon Reservoir area. In case the maximum precipitation.

statistical	estimation	Khun Dan Prakan Chon Reservoir area	
		11-September. 2008	11-September. 2011
Mean Error (ME)	IDW	-2.00	-0.52
	Kriging	-0.85	-1.39
	Isohyetal	-1.55	0.97
	Thiessen	-1.07	-0.31
	TPS	2.41	2.44
	CoKriging	-2.29	-1.74
Mean Absolute Error (MAE)	IDW	28.01	19.83
	Kriging	28.64	19.30
	Isohyetal	29.23	19.36
	Thiessen	38.40	28.41
	TPS	48.34	21.73
	CoKriging	30.05	19.12
Root Mean square Error (RMSE)	IDW	79.66	33.92
	Kriging	77.89	35.74
	Isohyetal	74.28	30.43
	Thiessen	157.96	48.48

TPS	176.99	36.86
CoKriging	78.24	35.73

In the zone of Khun Dan Prakan Chon Reservoir, during September 2008, there are many statistical characteristics as shown in Table no: 3

We can summarize that Inverse Distance Weighting method could generate the minimum of both MAE(at 252.30) and RMSE (at 351.34), compared to other methods, as well as the value of ME, at -5.53(This implicitly means that the actual value is lower than the estimated value). Another methodologies are Isohyetal and Kriging. Looking into the details, during September 2011, we found that Isohyetal produces the minimum MAE (at 348.51), RMSE (473.00). Not only that, this method also engenders a positive ME(at 7.46) and this could be implied that the estimated values are lower than the actual values. As far as the Inverse Distance Weighting and the Kriging methods are concerned, when focusing on the maximum rainfall day (on September 11th 2008 in table no:4) we found that Isohyetal, Inverse Distance Weighting and Kriging all show a somewhat low MAE and RMSE, compared to other solutions.

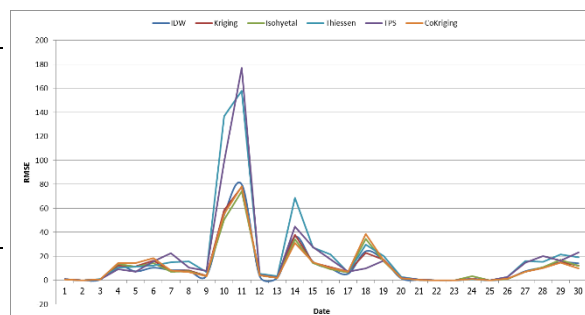


Figure 5 Shows a graph of the root mean squared error (RMSE) during September 2008 by precipitation from most to least.

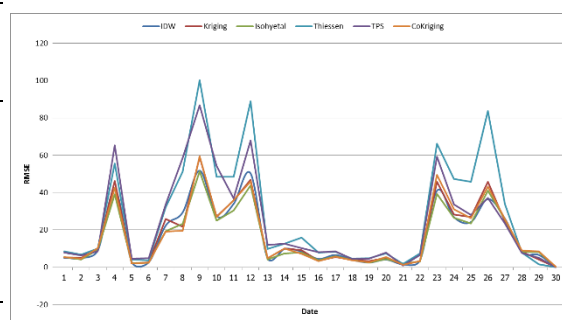


Figure 6 Shows a graph of the root mean squared error (RMSE) during September 2011 by precipitation from most to least.

When ordering rainfall data of September 2008 and 2011 from maximum to minimum (Figure 5 and 6) , it shows that estimated rainfall data are agreeable, excepting the Thiessen Polygon method which has a great error, especially in the day that huge rain occurs.

Summary and conclusions

From the estimation of spatial rainfall in the zone of Khun Dan Prakan Chon Reservoir, we can observe that rainfall data from the Meteorological Department has the best condition because the department is the main organization in collecting and keeping data. However, there are some limitations as well. For instance, the locations of numerous stations are located in the village areas as well as weather measuring stations in each province. For these reasons, they have led to the low density of rainfall which could further affect the calculation of spatial rainfall.

Regarding the estimated spatial rainfall value, there are some limitations and errors such as the occurrence of rainfall that the stations could not collect the amount of water. Thus, this allows the unreliable estimated value, which is obviously lower than the actual rainfall data. Also, the distances between certain and nearby stations are important in the calculation. We believe that if the density of rainfall measuring stations increases then the errors will definitely drop, as could be observed in the Thiessen Polygon method.

Table 5 Summarizes the estimation methods appropriate to the area.

Year	First		Second	
	Method	Estimation	Method	Estimation
2008	IDW	Higher	Isohyetal	Higher
2011	Isohyetal	Lower	IDW	Higher

The proper solution in estimating value in the area of Khun Dan Prakan Chon Reservoir for the rainfall data in 2008 and 2011 (shown in table no:5). It can be implied that the Inverse Distance Weighting and Isohyetal method are most suit because the estimated values are close to each other.

Acknowledgement

As a result, this research could effectively solve the raised issues. We would like to express our sincere gratitude to the Hydrology and Water Management Office (RID) that supported the research team a lot of significant data. Not only this, we would like to thank to Kasetsart University as our professional technical consultancy.

References

- Chang, C., Lo, S. and S. Yu. 2006. The parameter optimization in the inverse distance method by genetic algorithm for estimating precipitation. *Environmental Monitoring and Assessment*. 117: 145-155.
- Chang, Kang-tsung. 2002. *Introduction to Geographic Information Systems*. McGraw Hill Higher Education, New York.
- Chokngamwong, R. and L. Chiu. 2006. TRMM and Thailand daily gauge rainfall comparison, Conference proceeding in the 8th AMS Annual meeting, Atlanta Georgia, USA.
- Goovaerts, P. 2000. Geostatistical approaches for incorporating elevation into the spatial interpolation of rainfall. *J. Hydrology*. 288: 113-139.
- Hutchinson, M.F. 1995a. Interpolating mean rainfall using thin plate smoothing splines. *International Journal of Geographic Information Systems*. 19: 385-403.
- Hutchinson, M.F. and P.E. Gessler. 1994. Splines-more than just a smooth interpolator. *Geoderma*. 62: 45-67.
- Jacek, M. 1999. *GIS and Multicriteria Decision Analysis*. John Wiley & Son, Inc., New York.
- Johnston, K., M. Jay, V. Hoef, K. Konstantin and L. Neli. 2001. *Using ArcGIS Geostatistical Analyst*. California: ESRI USA. Inc.
- Sun X., M. J. Maton and E. E. Ebert. 2003. Regional rainfall estimation using double kriging of rain gauge and satellite observations. *BMRC research report No.94*.



Assessment of Satellite Rainfall Estimates as A Pre-Analysis for Water Environment Analytical Tools: A Case Study for Tonle Sap Lake in Cambodia

Arun. Chan. Phoeurn^{1,a*}, Sarann.Ly^{2,b}

Abstract

Tonle Sap Lake is the second main source of water supply and food security in Cambodia. However, this area is in the need for rainfall information which can cover the entire area for an accurate hydro-hydraulic modeling and climate modeling. In this case, Satellite Rainfall Estimates (SREs) would play a major role in the improvement of modeling. The study aims to assess the spatio-temporal performance of two high resolution satellite products such as TRMM 3B42V7 and CHIRPS V.2. One-hundred and sixty four (154) stations around the Tonle Sap Lake and Mekong River were selected for the pre-analysis prior input into the models within the study period of 2000 to 2004. After this, proper bias correction method is proposed. To do this, GIS and statistical indicators were used for the comparison.

Both TRMM and CHIRPS provide a good correlation with the gauge. Around 90% of stations have CC varies from 0.5 to 0.9. In addition, the median error of SREs are about 30 mm/month. Both satellite showed very similar pattern of bias spatially and temporally. This can be said that even though TRMM has the lower spatial resolution compared to CHIRPS, the performance of it is quite the same. However, high error for some stations still exist that could be cause due to the seasonal influence, topography, measurement error that need to be taken into account in the process of bias correction.

Keywords *CHIRPS, Hydraulic modeling, Remote sensing, Satellite rainfall estimates, TRMM, Tonle Sap Lake*

Chan Arun. Phoeurn and Sarann.Ly

Rural Engineering, Institute of Technology of Cambodia, Phnom Penh, Cambodia

Chanarun.p@gmail.com, ly.sarann@yahoo.com

Climate change and landslide risk assessment in Uttaradit province

Shotiros Protong

Abstract

The incidents of sudden landslides in Thailand during the past decade have occurred frequently and more severely. It is necessary to focus on the principal parameters used for analysis such as land cover/land use, rainfall values, characteristic of soil and digital elevation model (DEM). The combination of intense rainfall and severe monsoons is increasing due to global climate change. Landslide occurrences rapidly increase during intense rainfall especially in the rainy season in Thailand which usually starts around mid-May and ends in the middle of October. The rain-triggered landslide hazard analysis is the focus of this research.

The combination of geotechnical and hydrological data is used to determine permeability, conductivity, bedding orientation, overburden and presence of loose blocks. The regional landslide hazard mapping is developed using the Slope Stability Index SINMAP model supported on Arc GIS software version 10.1.

Geological and land use data are used to define the probability of landslide occurrences in terms of geotechnical data. The geological data can indicate the shear strength and the angle of friction values for soils above given rock types, which leads to the general applicability of the approach for landslide hazard analysis. In terms of hydrological data, the millimetres/twenty-four hours of average rainfall data are used to assess the rain triggered landslide hazard analysis in slope stability mapping. The period 1954-2012 is used for the baseline of rainfall data for calibration of present-day conditions. Future climate scenarios are simulated by spatial and temporal scales. The precipitation trends are needed to predict the future climate. The Statistical Downscaling Model (SDSM) version 4.2, is used to assess the simulation scenario of future change for latitudes $16^{\circ} 26'$ and $18^{\circ} 37'$ and between longitude $98^{\circ} 52'$ and $103^{\circ} 05'$; the study area is Uttaradit province, northern Thailand. The landslide hazard mapping will be compared and shown by areas (km^2) in both the present and the future under climate simulation scenarios A2 and B2 in Uttaradit province. The risk areas should be preserved for land use planning in order to reduce the high risk in hilly and mountainous terrain.

Assessment of an Urban Drainage System in Phnom Penh Using Storm Water Management Model

Sokchhay Heng^{1*}, Penghour Hong² and Sarann Ly³

Abstract The current climate change issue, commonly introducing more intense rainfall within a short time, together with a rapid population growth in Phnom Penh, the capital of Cambodia, have posed an accumulative stress on city drainage system. This study investigates the current capacity of sewage network with a diameter ranging from 0.8 to 2.0 m in a catchment of Chamkarmon district covering an area of about 1 km². Storm Water Management Model was selected to simulate the catchment runoff flowing into the drainage system. A questionnaire survey was carried out to determine the historical inundation situations. Such information is useful in judging the model performance. The study area was divided into 11 sub-catchments. The simulation was conducted for an extreme storm event occurring on 28 September 2014 with an intensity of 109.8 mm over a four-hour and a half period. Nine of 11 sub-catchments were found inundated and this result is similar to that obtained from the questionnaire survey. Four sub-catchments were inundated severely for a duration of 1.5–3.0 h. Two scenarios were proposed to improve the inundation conditions. Adding two new sewage lines in the downstream area was found as the optimum solution. It significantly reduces the inundation period of the severe sub-catchments to 0.63–2.95 h. The maximum overflow surcharge was also reduced relatively, from 3.18–7.08 m³/s to 1.55–6.40 m³/s. This modelling approach provides a sustainable solution to urban drainage management in Phnom Penh.

Keywords *Urban flood, urban drainage, SWMM*

¹ Sokchhay Heng

Department of Rural Engineering
Institute of Technology of Cambodia
Phnom Penh, Cambodia

* E-mail: heng_sokchhay@yahoo.com

² Penghour Hong

Department of Environmental Engineering
Chulalongkorn University
Bangkok, Thailand

³ Sarann Ly

Department of Rural Engineering
Institute of Technology of Cambodia
Phnom Penh, Cambodia

Introduction

Phnom Penh, the capital city of Cambodia, is located at the west side of the confluence of the Mekong River and Tonle Sap River. It is a rapidly growing city with a population increasing from 0.9 million in 1998 to 2.3 million in 2008, at a rate of 3.9% annually (NIS, 2008). Urbanization is also critical because of rural to urban migration which is one of the significantly social and environmental challenges. Urban drainage facilities in Phnom Penh draining storm water and domestic wastewater have been gradually improved in line with the development of the city. The sewer system has a total length of approximately 469 km of which 160 km is principally concrete sewer pipe with a diameter of 0.5–2.0 m (Ung, 1996; JICA, 2011).

Flood is a serious threat to Phnom Penh City in rainy season. It is certainly attributed to the poor inland drainage system, which may cause paralysis of urban function, thereby giving heavy damage to civic life. The drainage systems have to be changed frequently in order to cope with the flooding water caused by the poor urban planning. Compounding the issues of flooding is the lack of park space or open spaces to absorb rainy season waters. We observed that, although flooding in the city is rarely a direct cause of death, it often damages people's businesses, which they depend on to make a living.

Although, there were some studies on inundation in Phnom Penh for two times by JICA, with a purpose of urban drainage improvement, flood still occurs when there are heavy rains. Due to the lack of facilities and technical expertise, assessment of urban runoff has just been started for the development of the city. It showed that the management plan of storm water in the city could not be well understood. Therefore, the plan for proposing the assessment of runoff in Phase III of JICA's projects may be hampered by the absence of studies on the spatial and temporal variation of storm water characteristics (JICA, 2011). The temporal characteristics of storm water flow into different outfalls draining into Tum Pum and Tra Baek Lake has not been well studied, leading to a great concern on flooding in the areas during rainy season.

In order to plan for an effective urban development, including sustainable drainage system, it is necessary to characterize sewer flow spatiotemporally. Therefore, the objective of this

research are (1) to simulate flow in drainage by using Storm Water Management Model and (2) to propose a solution for reducing flood flow surcharge.

Materials and methods

Phnom Penh is divided into 12 districts. Chamkarmon, Daun Penh, 7 Makara and TuolKouk are the top four districts in term of populated area. The selected study area is situated in Chamkarmon District and covers 3 communes, namely ToulSvay Prey 1, ToulSvay Prey 2 and TumnobTeuk (Fig. 1). There are around 30,000 people living in this study area, extending over 1 km².

This study requires three main datasets for the analysis (Table 1). First, hydro-meteorological data including rainfall and inundation depth/extent is important for analyzing the runoff by any rainfall events and verifying the model results. Second, information of sewer system including diameter of pipe, location of manhole, length of conduit, flow direction, and invert elevation is important for hydraulic calculation. Third, topography or digital elevation model (DEM) is very important for determining the catchment slope gradient and flow direction. The data of inundation depth/extent was obtained by conducting a questionnaire survey because there is no historical records.

It is necessary to divide the study area into an appropriate number of sub-catchments for identifying the outlet point of each sub-catchment. Sub-catchments are hydrologic units of land whose topography and

drainage system elements direct surface runoff to a single discharge point. Discharge outlet points can be either nodes of the drainage system or other sub-catchments. Sub-catchments can be divided into pervious and impervious subareas. Surface runoff can infiltrate into the upper soil zone of the pervious subarea, but not through the impervious subarea. Impervious areas are themselves divided into two subareas - one that contains depression storage and another that does not. Runoff flow from one subarea in a sub-catchment can be routed to the other subarea, or both subareas can drain to the sub-catchment outlet. In this study the entire catchment area was divided into 10 sub-catchments (S1–S10) based on flow direction, drainage lines and catchment topography (Fig. 1). Moreover, it was assumed that all catchments have an imperviousness between 80% and 90%. There are in total 11 conduits namely C1–C11 and the corresponding junction of each conduits was denoted as J1–J11. J_{Outfall} represents the conduit junction located at the catchment outlet (Table 2).

The analysis framework of this research can be graphically represented by Fig. 2. The EPA Storm Water Management Model (SWMM) was used for the estimation of flow. It is a dynamic rainfall-runoff simulation model used for single event or long-term (continuous) simulation of runoff quantity and quality from primarily urban areas. The runoff component of SWMM operates on a collection of sub-catchment areas

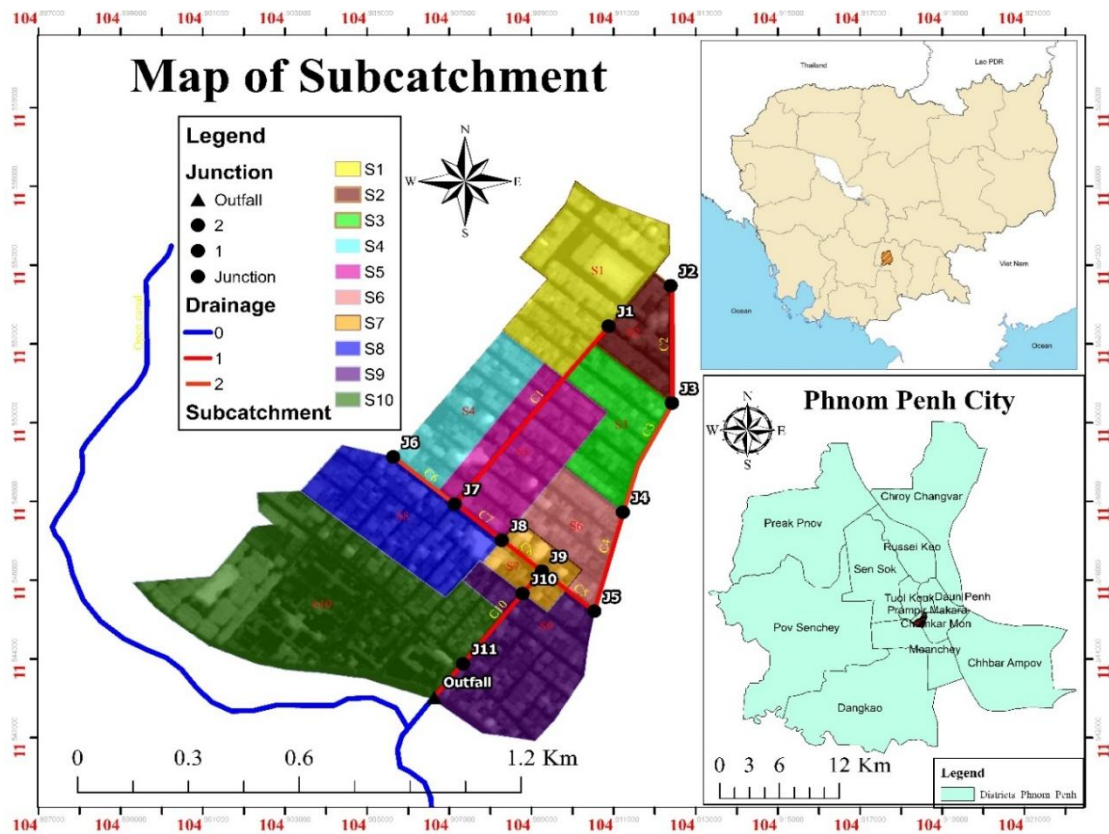


Fig. 1 Map of the study area

Table 1. Description of datasets

No.	Data	Source
1	Climate data including rainfall (5-minute temporal resolution) and inundation depth/extent	Institute of Technology of Cambodia and questionnaire survey
2	Sewer system data including size, length invert elevation, flow direction and location of manhole	Japan International Corporation Agency
3	Digital elevation model (2 x 2 m)	NTT DATA & RESTEC

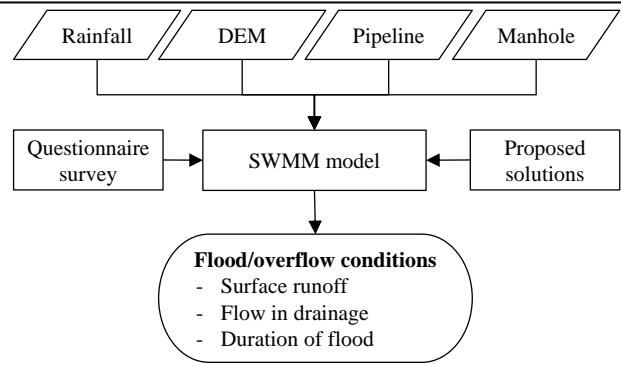


Fig. 2 Framework of the study

Table 2. Characteristics of conduits

Conduits	Description	Slope	Length (m)	Diameter (m)	Manning’s n value	Junctions for conduit
C1	Closed conduit (concrete pipe line)	0.10%	640	0.8	0.013	J1, J6
C2		0.10%	350	1.0		J2, J3
C3		0.07%	202	1.2		J3, J4
C4		0.06%	272	1.5		J4, J8
C5		0.07%	184	1.5		J8, J9
C6		0.13%	215	1.5		J5, J6
C7		0.13%	147	1.5		J6, J7
C8		0.06%	149	1.5		J7, J9
C9		0.04%	82	1.8		J9, J10
C10		0.04%	261	1.8		J10, J11
C11		0.04%	85	2.0		J11, J _{Outfall}

that receive precipitation and generate runoff and pollutant loads. The routing portion of SWMM transports this runoff through a system of pipes, channels, storage/treatment devices, pumps, and regulators. SWMM tracks the quantity and quality of runoff generated within each sub-catchment, and the flow rate, flow depth, and quality of water in each pipe and channel during a simulation period comprised of multiple time steps. Key equations which were built in SWMM and used in this research are:

- Continuity equation (James *et al.*, 2010)

$$\frac{\partial Q}{\partial x} + \frac{\partial A}{\partial t} = 0 \quad (1)$$

where Q is the flow rate, A is the wetted cross-sectional area, x is the distance along the conduit and t is the time.

- Momentum equation (James *et al.*, 2010)

$$\left[\frac{1}{A} \frac{\partial Q}{\partial x} \right] + \left[\frac{1}{A} \frac{\partial}{\partial t} \left(\frac{Q^2}{A} \right) \right] + \left[g \frac{\partial y}{\partial x} \right] - [g(S_0 - S_f)] = 0 \quad (2)$$

From left to right, the first term represents the local acceleration, the second term represents the convective acceleration, the third term represents the pressure force

and the fourth term represents the difference between the gravity and friction force.

The analysis was conducted for an extreme rainfall event which occurred on 28 September 2014. The recorded data is available at a 5-minute temporal resolution. The total rainfall depth is 109.8 mm. Since there is no observed data of inundation depth/extent, a questionnaire survey was conducted to obtain such information for verifying the model result. To ensure a good information can be obtained from the questionnaire survey, we considered only respondents with an age of 18 years old or more, living in Phnom Penh for at least 1 year and finished primary school education level. Regarding the location of samples, we primarily selected areas where there were flood occurrences in the past; this was based on literature review and experiences of research team. Spatial condition was also considered to avoid a redundancy of information provided by different respondents. Therefore, location of the next sample is dependent on that of the preceding sample. To achieve this, GPS was employed simultaneously to position the location of samples and analyze the spatial distribution during the survey.

Results and discussion

Fig. 3 illustrates an example of flow hydrograph in Conduit C1 obtained from the analysis using SWMM. Rainfall started at around 7:20AM and picked up at 7:50AM with an intensity of 17 mm within a period of 5 minutes. After 25 minutes of the rainfall, overflow at C1 began because the very heavy rainfall within such a short time empties the conduit capacity (0.57 m³/s). The maximum inflow reaches up to 3.75 m³/s, meaning that the maximum overflow surcharge is 3.18 m³/s. After picking up the inflow as well as the overflow surcharge decreases and increase following the rainfall pattern (Fig. 3). The total duration of flood/overflow occurred in the vicinity of Conduit C1 is about 2.18 h. For Conduits C2–C11, characteristics of the resulted inflow hydrographs and the overflow surcharges are summarized in Table 3. There is a flood/overflow for 9 conduits. The duration of flood/overflow is between 0.17 h (C1) and 3.00 h (C11). The maximum overflow surcharge ranges from 0.15 m³/s (C4) to 7.08 m³/s (C10).

- Conduits C1, C8, C10 and C11: the overflow surcharge is high for these conduits. The maximum overflow surcharge is up to 7.08 m³/s for C10 and this could be attributed to the cumulative inflow from the upstream areas together with a very small conduit capacity in comparison the total inflow.
- Conduits C2, C5, C7 and C9: overflow surcharge also occurs for these conduits but in a medium level. The maximum overflow surcharge is between 0.62 m³/s and 1.22 m³/s.
- Conduit C4: the overflow surcharge of this conduit is categorized as low with 0.15 m³/s of the maximum overflow surcharge.
- Conduits C3 and C6: there is no overflow for these 2 conduits. It means that they have enough capacity to drain out storm water falling with the sub-catchment and inflow from its upstream areas.

A total number of 100 citizens were interviewed for their experiences on flood situations.

The sample density is about 3.45 sample/km² which is reasonably enough for this kind of study. The questionnaire survey was conducted for a large area covering 4 most populated districts of Phnom Penh: Chamkarmon, Daun Penh, 7 Makara and TuolKouk. However, only information within the study area (3 communes of Chamkarmondistrict) was extracted for the verification with the model results (Fig. 4). The figure illustrates the variation of flood depth, which is not a result of a rainfall event but an experience of the citizens. That is why information of flood depth is classified in different ranges. It is impossible to verify flood depth in this study. Anyways, we can verify whether there is flood/overflow or not in the area of the 10 sub-catchments. By doing so, it can be concluded that the model results obtained from SWMM are comparable with that obtained from questionnaire survey. There are of course some bias because the model results is just for a specific event and the results depicted in Fig. 4 is from a spatial interpolation on the surveyed flood depths.

Based on the flood/overflow conditions of each conduit above, we propose to enlarge the diameter of Conduit C1 from 0.8 m to 1.2 m and the diameter of

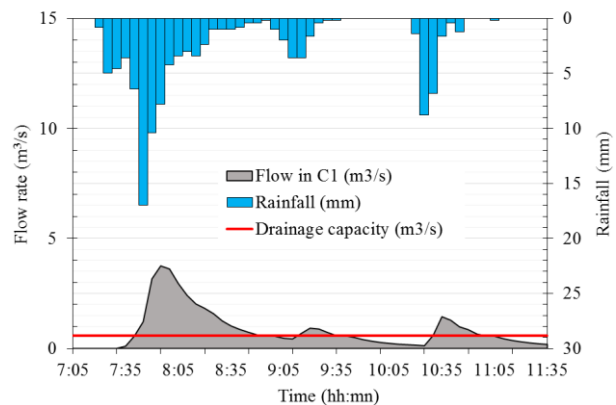


Fig. 3 Flow hydrograph in Conduit C1

Table 3. Summary of flow condition in each conduit

Conduits	Conduit capacity(m ³ /s)	Maximum inflow(m ³ /s)	Flood/overflow (Yes or No)	Duration of flood/overflow (h)	Maximum overflow surcharge(m ³ /s)
C1	0.57	3.75	Yes	2.18	3.18
C2	0.90	1.52	Yes	0.32	0.62
C3	1.04	0.92	No	-	-
C4	2.70	2.85	Yes	0.17	0.15
C5	3.11	4.33	Yes	0.38	1.22
C6	2.50	2.12	No	-	-
C7	3.81	5.01	Yes	0.35	1.20
C8	2.38	6.14	Yes	1.50	3.76
C9	5.74	6.74	Yes	0.45	1.00
C10	2.12	9.20	Yes	2.97	7.08
C11	3.11	7.43	Yes	3.00	4.32

Conduit C10 from 1.8 m to 2.0 m. This proposed solution is called Scenario 1. It should be noted that the based scenario represents the existing condition. As a result, Scenario 1 does not improve the flood/overflow situations overall because the fast outflow from the two conduits causes an increase in inflow to downstream conduits having the same capacity (Fig. 5). Much improvement is observed only at the Conduit C1 and C10 itself. For Conduit C1, the duration of flood/overflow is reduced from 2.18 h to 0.63 h and the maximum overflow surcharge is reduced from 3.18 m³/s to 2.07 m³/s. In case of Conduit C10, the duration of

flood/overflow is reduced from 2.97 h to 2.47 h and the maximum overflow surcharge is reduced from 7.08 m³/s to 6.40 m³/s.

Since Scenario 1 does not provide a good solution, we propose Scenario 2 which is an introduction of additional conduit lines, C12 and C13 (Fig. 6). The Conduit C12 has a length of 228 m, a diameter of 1.2 m, an inlet junction J12 and an outlet junction J13. The Conduit C13 is connected to C12 via Junction J13 and C10 via Junction J11; C13 has a length of 307 m, a diameter of 1.5 m, an inlet junction J13 and an outlet

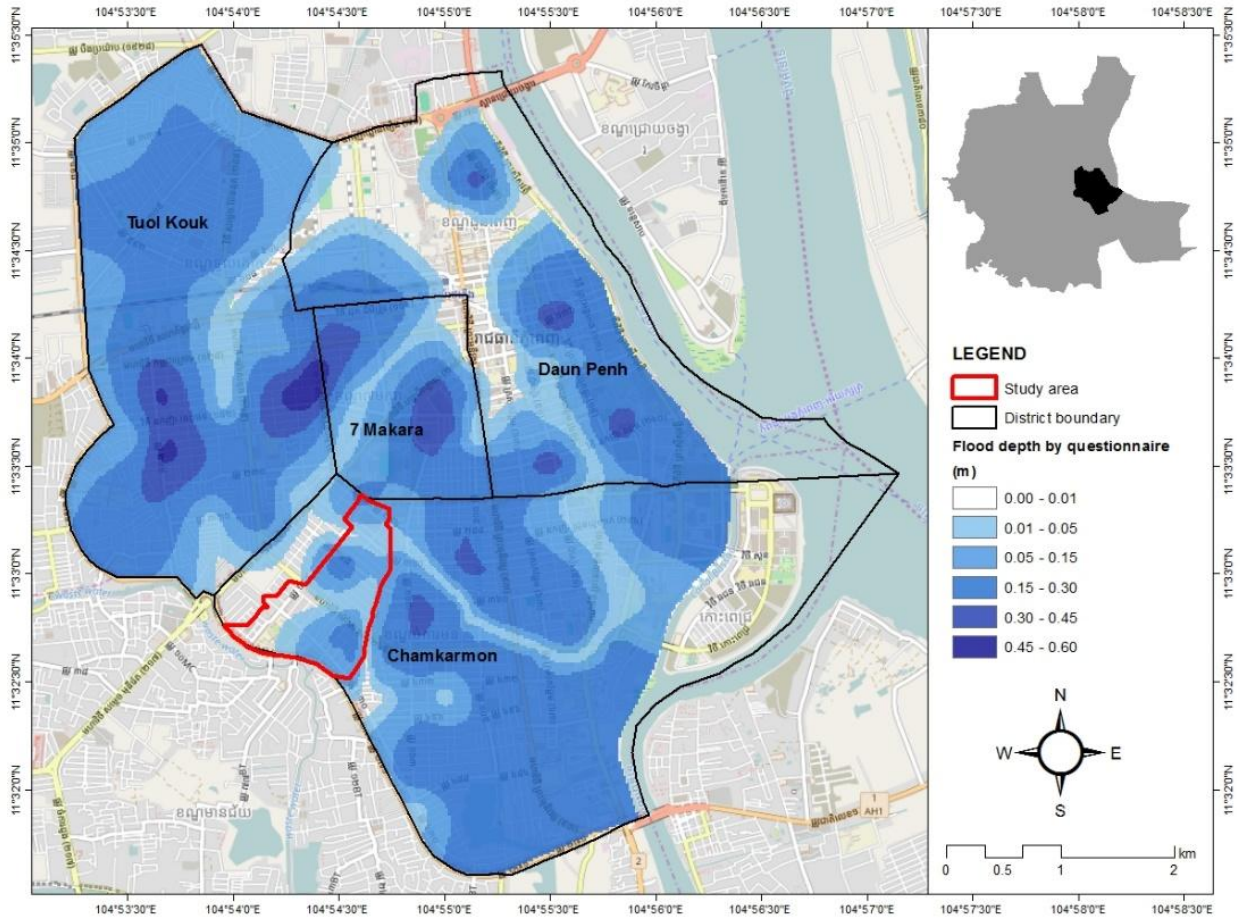


Fig. 4 Information of flood depth by questionnaire survey (100 samples)

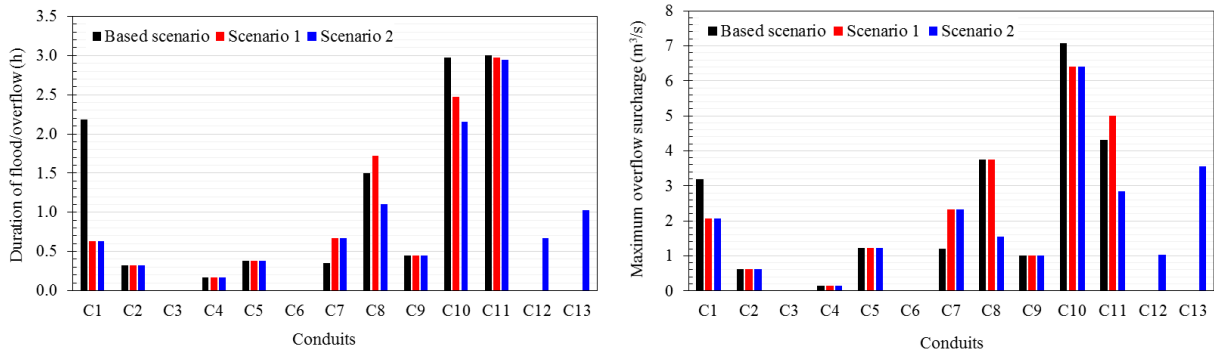


Fig. 5 Surcharge/overflow conditions of based scenario, Scenario 1 and Scenario 2

junction J11. The model results showed that Scenario 2 improves the flood/overflow situation better than Scenario 1, particularly for Conduit C1, C8, C10 and C11 where the existing flood/overflow situation is critical. For Conduit C1, the duration of flood/overflow is reduced from 2.18 h to 0.63 h and the maximum overflow surcharge is reduced from 3.18 m³/s to 2.07 m³/s. For Conduit C8, the duration of flood/overflow is reduced from 1.50 h to 1.10 h and the maximum overflow surcharge is reduced from 3.76 m³/s to 1.55 m³/s. For Conduit C10, the duration of flood/overflow is reduced from 2.97 h to 2.15 h and the maximum overflow surcharge is reduced from 7.08 m³/s to 6.40 m³/s. In case of Conduit C11, the duration of flood/overflow is reduced slightly from 3.00 h to 2.95 h and the maximum overflow surcharge is reduced from 4.32 m³/s to 2.85 m³/s. The flood/overflow situation can be improved more by introducing a pumping system but it is of economic concern especially on operation and maintenance cost. Therefore, we conclude Scenario 2 as an optimum solution to the existing flood/overflow situation in this study area.

Conclusions

The study firstly tried to apply Storm Water Management Model (SWMM) to analyze flow conditions in the sewer system of a small area in Chamkarmon district, Phnom Penh, Cambodia. The sewer system was divided into 11 conduit lines. Considering the rainfall event 28 September 2014, the model showed that there is occurrence of flood/overflow at 9 conduits and this result is comparable with that obtained from the questionnaire survey. The significant conditions are characterized by the duration of flood/overflow of 1.5–3.0 h and the maximum overflow surcharge of 3.18–7.08 m³/s. Secondly, by introducing 2 additional conduit lines, the flood/overflow situation at critical conduits was improved relatively. The significant duration of flood/overflow is reduced to 0.63–2.95 h and the maximum overflow surcharge is reduced to 1.55–6.40 m³/s. SWMM is a potential tool for the design of urban drainage in Phnom Penh. Using this modeling tool, we can foresee the impact of any proposed development or improvement projects of drainage system.

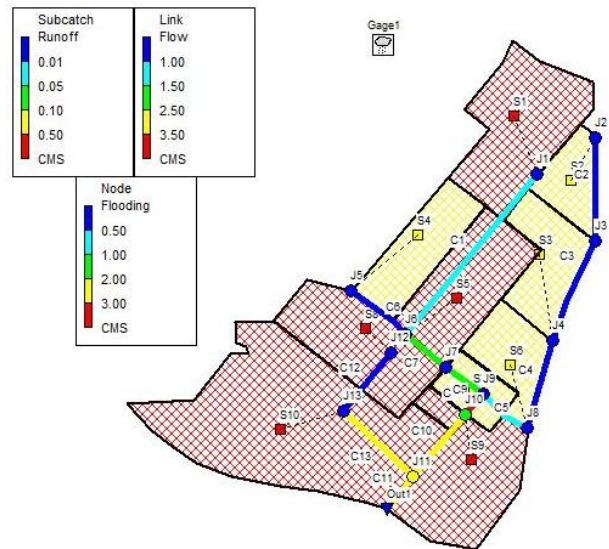


Fig. 6 Location map of addition conduits (C12 and C13) in Scenario 2

Acknowledgement

The authors would like to express high gratitude to JSPS Core-to-Core Program, B. Asia-Africa Science Platforms, for supporting this research study.

References

- James, W., Rossman, L.A. and James, W.R.C. (2010). User’s Guide to SWMM5, 13th Edition. CHI Press, Ontario.
- JICA (Japan International Cooperation Agency) (2011). Preparatory Survey Report on the Project for Flood Protection and Drainage Improvement in the Phnom Penh Capital City (Phase III) in the Kingdom of Cambodia. JICA, Phnom Penh.
- NIS (National Institute of Statistic, Cambodia) (2008). General Population Census of Cambodia - Final Census Results in 2008, Phnom Penh, Cambodia. NIS, Phnom Penh.
- Ung, P. 1996. The Environmental Situation in Cambodia, Policy and Instructions. Biopolitics, the Bio-Environment, and Bio-Culture in the Next Millennium, 5.

Development of Design Storm Pattern with Climate Change in Monsoon Asia

Muhammad Mudassar Rehan^{1,a,*}, Sutat Weesakul^{2,b}, Winai Chaowiwat^{3,c} and Wiwat Charoensukrungruang^{4,d}

Abstract General characteristics of rainfall in Asian monsoon climate have been studied and synthetic design storm pattern have been developed including climate change using field investigation data at Asian Institute of Technology (AIT). Recorded period of rainfall is 22 years from 1990 to 2007 and 2009 to 2012 with 5 minutes interval. Total numbers of selected storms are more than 600. Temporal distribution of rainfall in one day have been derived and it shows one peak at 18:00 to 20:00 contribute to 27 % of average temporal rainfall in one day. Recorded storm data have been extracted for 2, 5 and 10 years return period and used as data to derive a storm pattern. There are totally 49 storms ranging from 35 to 585 minutes. Criteria to select the appropriate storm pattern for the good fit compared to those selected one are the shape, peak intensity and time to peak. Among triangular shape, complex trapezoidal shape and a curved shape, the Chicago Design Storm (CDS) is found to be the best fit with proposed modified peak rainfall intensities by reduction to 5 and 10 minutes intensities. Results showed reduced absolute percentage errors are from 57% to 32% and 21 % respectively. This is a remarkably improve the peak intensity design. To take into account effect of climate change to design storm, the Equidistance Quantile-Matching method (EQM) is applied to modified IDF curve and their related parameters which is used in expression of a new storm pattern. Climate change is then reflecting in design rainfall pattern and shows intensity increasing 24% at most.

Keywords Synthetic storm pattern, Chicago design storm (CDS), Climate change and intensity-duration-frequency curve (IDF)

¹Graduate Student AIT
 Punjab Irrigation Department (PID)
 Pakistan

²Hydro and Agro Informatics Institute (HAII) and
 Asian Institute of Technology (AIT)
 Thailand

³Hydro and Agro Informatics Institute (HAII)
 Thailand

⁴Graduate Student AIT
 East Water Resources Development and Management
 PLC, Bangkok, Thailand

^aammrehan@gmail.com

^bsutat@hail.or.th

^cwinai@hail.or.th

^dwiwat_cha@eastwater.com

Introduction

Storm pattern is technically important and used in design of urban drainage system. Size of pipes in a conveyance system and volume of detention storage are influenced by such a pattern. Its shapes are different in countries and it depends on local climate and rainfall characteristics. A number of design rainfall patterns were studied and used in the design. Keifer et al. (1957) presented the Chicago Design Storm (CDS) developed from the total intensity-duration-frequency curve.

The location of the peak intensity (r) is found in one of two ways. The first is to study the location of the peak intensity within the duration t_d , and the other way is to evaluate the antecedent rain volume before the period t_d having the maximum average intensity. The synthetic storm pattern with " r " = 0.375 was found to be acceptable in the Chicago area. Equation described storm pattern can be divided into two parts, before the peak and after the peak, as following:

Before the peak

$$i_b = \frac{a \left[(1-b) \left(\frac{t_b}{r} \right)^b + c \right]}{\left[\left(\frac{t_b}{r} \right)^b + c \right]^2} \quad (1)$$

After the peak

$$i_a = \frac{a \left[(1-b) \left(\frac{t_b}{1-r} \right)^b + c \right]}{\left[\left(\frac{t_b}{1-r} \right)^b + c \right]^2} \quad (2)$$

$$t_d = t_a + t_b \quad (3)$$

$$r = t_a / t_d \quad (4)$$

$$i = \frac{a}{t_d^b + c} \quad (5)$$

Where i_b and i_a is the intensity before and after the peak, t_b is the time before the peak in minutes, t_a is the time after the peak in minutes and a , b and c are constants. t_d is rainfall duration. Chicago design storms have been used for design in different part in the world such as Bandyopadhyay (1972) in Gauhati, India, Water Development Consultant (1998) in Sukumvit, Thailand and Naksua (2001) West of Bangkok, Thailand. There are other shapes of rainfall pattern as summarized in Table 1. Sifalda (1973) proposed a shape S-type with long peak rainfall duration at the middle of total duration. This pattern is complex triangular-rectangular shape originated from Czechoslovakian.

Desbordes (1978) proposed the D-type, a complex triangular shape with bi-linear line for rising and recession parts. YEN et al. (1980) presented a simple triangular hyetograph to represent approximately the geometry of local rainstorm hyetographs for the design of small storm drainage systems. This shape derived from analyzing the hyetographs for 2, 3, 4, and 5 durations of rainfall using hourly precipitation of three stations in USA.

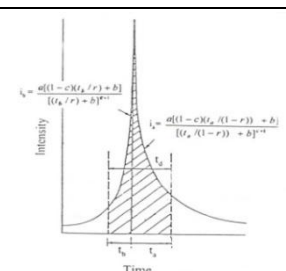
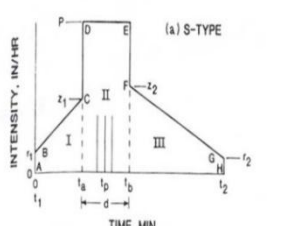
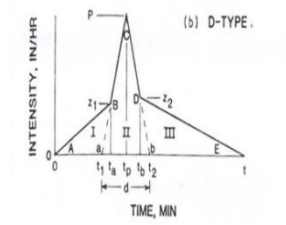
Watt et al. (1986) studied a 1-hr urban design storm which has been developed for a Canadian urban design storm. This design storm has two parts, the rising part of rainfall is linear and the recession part is exponential type. Extensive comparisons with observed 1-hr storms, both in the temporal domain and the frequency domain, indicate that the temporal design storm is capable of simulating individual rainfall events and an average or 'design' event for any particular site. The design storm model has been extended on a regional basis by evaluating the two parameters for each of 45 AES stations across Canada.

Van Nguyen et al. (2002) identified the most suitable temporal rainfall patterns for urban drainage design in southern Quebec, Canada. In total, seven popular design storm models were assessed based on the accuracy of their estimations of runoff peak flow and volume as compared to those values given by a set of 199 significant historical storm events that have been recorded in the region for the 1943-1994 periods. It shows significantly that Chicago design storm contains unrealistic high peak intensity. It is then modified using the peak intensity directly taken from the IDF relationships for next value, 5-minutes time interval.

The design rainfall pattern used in Thailand is CDS it requires technically research to support and validate it especially at the peak intensity because it shows overestimate in various locations in other countries..

Equidistant Quantile-Matching method (EQM) proposed by Li et al (2010) is used to derive Intensity-Duration-Frequency (IDF) curves with climate change effect. It is based on the principle that probabilities of sub-daily rainfall in the future are changed in a similarity of that for daily rainfall so that linear adjustment can be made. This method is so simple that it can be used in practice. Ashish et al (2015) determine IDF curves under climate change using daily rainfall in the future from stochastic weather generator and disaggregated into sub-daily using HYETOS model. Resulted IDF curves need to be adjusted using the present IDF otherwise it is underestimate especially for the case of duration less than 3 hours. The effect of climate change to rainfall enhances the extreme condition and it should be considered in urban drainage design. The objectives of present study are (1) to study the general characteristics of temporal rainfall in a sub-daily scale (2) to determine the appropriate shape for design storm pattern including the effect of climate change.

Table 1. Types of design storm pattern

Location	Shape	Type of Design Storms
Chicago		Chicago Design Storm (CDS) from Keifer & Chu (1957)
Czechoslovakia		Sifalda (1973)
France		Desbordes (1978)

Location	Shape	Type of Design Storms
Massachusetts, Illinois, and New Jersey		Triangular Yen & Chow (1980)
Canada		Design storm pattern from Watt et al. (1986)

Fig. 2. It shows one peak at 18:00 to 20:00 contribute to 27 % of average total rainfall in one day. Percentage of rainfall at day time (7:00 to 18:00) and night time (19:00 to 6:00) are 44 and 56 % respectively. It means that there is slightly more rainfall chance with higher percentage in the night time. Minimum accumulated rainfall is at 8:00 with 1.19 % and maximum one is at 19:00 with 9.0%.

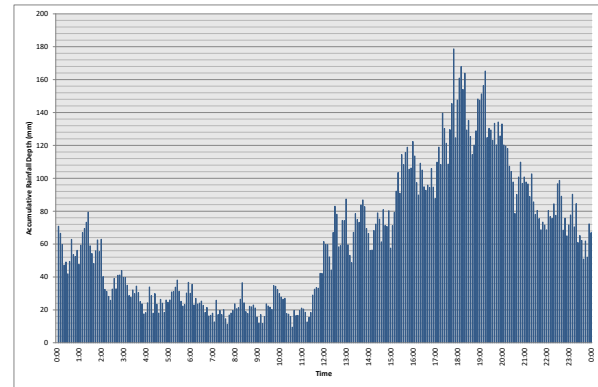


Fig.1 Accumulate temporal distribution of rainfall in a day at AIT station from 1990 to 2012 using 5 minutes interval

Methodology

In present study, synthetic storm pattern have been developed using field investigation data at Asian Institute of Technology (AIT), Pathumthani, Thailand. Recorded period of rainfall is 22 years from 1990 to 2007 and 2009 to 2012 with 5 minutes interval. Temporal analysis of distribution of rainfall in 1 day is conducted. Total numbers of selected storms are more than 600. Statistical analysis is carried to determine constants a , b and c in equation (3) and plotted for Intensity-Duration and Frequency Curve (IDF). Storms having accumulated rainfall corresponded to 2, 5 and 10 years are selected to be used in design storm analysis. There are totally 49 storms. Three storm patterns are validated for their similarity shape with those selected record rainfall. The first one is triangular shape from Yen & Chow (1980) because of its simple pattern. The second one is a complex trapezoidal shape from Sifalda (1973) in order to examine the peak intensity duration of rainfall. The last one is Chicago Design Storm (CDS) because it is the most popular used in Thailand. Criteria are the good fit for the shape of rainfall patterns; peak intensity and time to peak to be compared with recorded rainfall. CDS is a synthetic storm and it is developed for design purpose. When CDS peak intensity is not well determined, IDF should be checked and modification must be conducted. Equidistance Quantile – Matching Method (EQM) is used to compute IDF with climate changed and it will be input into the design storm equation.

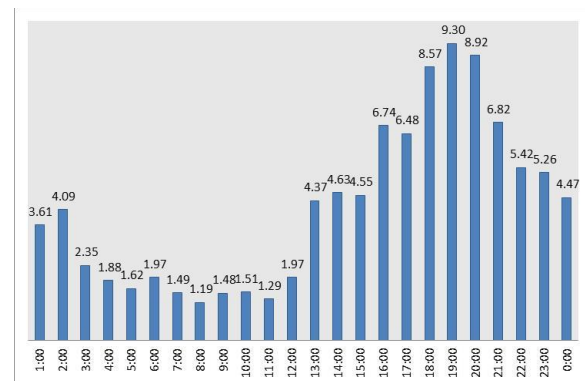


Fig. 2 Percentage of Rainfall Amount in a day over period 1990 - 2012

Results and Discussion

Temporal distribution

Plot of accumulated temporal distribution of rainfall in one day at 5 minutes interval have been derived as shown in Fig. 1. Summary of hourly rainfall is shown in

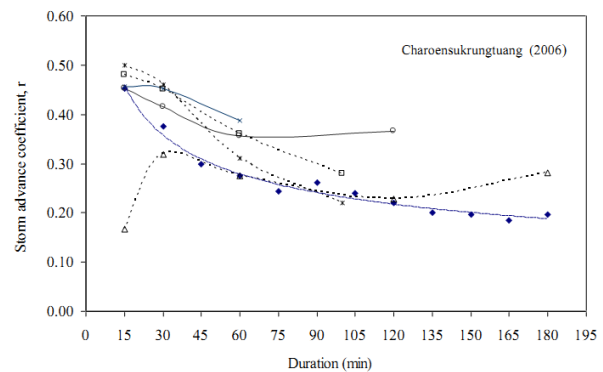


Fig.3 Relationship between duration and storm advance coefficient(Charoensukrungruang (2006))

Design Storm

Analysis of recorded rainfall has been conducted in order to obtain the IDF curve using Gumbel distribution. Table 2 shows results of IDF. Storm advanced coefficients (r) is derived as a function of rainfall duration with detail in Charoensukrungruang (2006) as shown in Fig. 3. Results of “r” values show that they vary with storm duration. The maximum is 0.49 while the minimum is 0.20. It means that design storm is almost symmetric for short duration. For longer duration, the timing of peak intensity will occur earlier but not less than 20% of rainfall duration. Recorded storm data have been extracted for 2 years return period for 42 storms ranging from 35 to 585 minutes. There are 5 and 2 selected storms corresponded to 5 and 10 years return period. The CDS is found to be the best fit using those three criteria when they are compared with 49 storms. Fig.4 shows one case of comparisons for 1 hour rainfall duration. The storm pattern can be observed virtually as in Fig. 4 that CDS is better than others. Times to peak are the same for all design storms for short duration. Peak intensity of Yen & Chow and Sifalda are always underestimated. In addition, results shows that the peak intensities derived by CDS are much higher than the measured peak on the average with 53% to 57%, therefore the CDS is needed to be modified.

Table 2 Intensity duration and frequency curves for AIT

Return Period (years)	Duration								
	5 min	10 min	15 min	30 min	1 hrs.	2 hrs.	6 hrs.	12 hrs.	24 hrs.
2	129.94	117.36	105.29	80.54	53.07	30.22	11.14	5.93	3.25
5	148.04	132.80	123.17	99.80	66.55	40.59	15.12	8.23	4.60
10	160.01	143.03	135.01	112.55	75.47	47.45	17.75	9.74	5.49
25	175.15	155.95	149.97	128.67	86.75	56.12	21.08	11.66	6.61
50	186.38	165.54	161.07	140.62	95.11	62.55	23.54	13.09	7.44
100	197.52	175.06	172.09	152.49	103.41	68.93	25.99	14.50	8.27

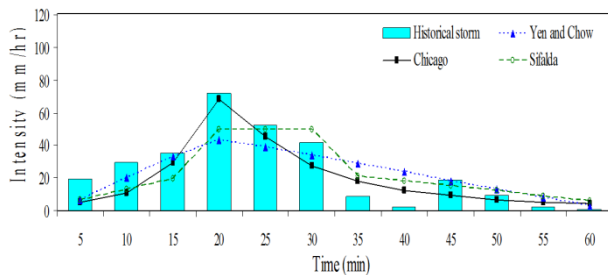


Fig.4 Comparison of three design storm with measured rainfall for 1 hrs. rainfall duration

Modified CDS

Table 3 shows results of Mean Absolute Percentage Error (MAPE %) for 2, 5 and 10 return period. A simple comparison of the peak intensities computed at 5 and 10 minutes interval show that the Mean Absolute Percentage Error (MAPE) are reduced from approximately 57% to 32% and 21% respectively.

Therefore the peak intensity of CDS is modified and reduced to be the appropriate value at 10 minutes. Fig.5 shows comparison of CDS and measured rainfall. In order to reduce peak intensity, IDF curve is modified from Eq. (5) to Eq.(6) and constants are shown in Table 4.

$$i = \frac{a}{(t_d + b)^c} \quad (6)$$

Table 3 Summary of Mean Absolute Percentage Error (MAPE) of Peak CDS

T _r (year)	Number of Storms	MAPE (%) at peak intensity		
		Peak	5 min	10 min
2	42	57.5	32.9	21.6
5	5	53.4	31.5	17.2
10	2	57.0	35.7	19.7
Average	49 (Total)	57	32.8	21.1

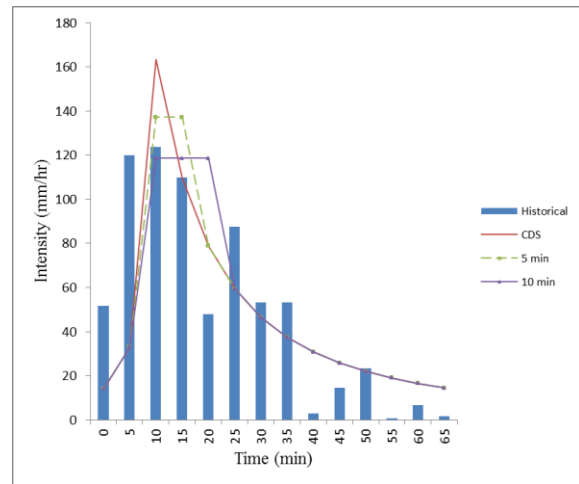


Fig.5 Comparison of CDS, Modified CDS and Historical storm dated 14-10-1998 (2 years return period)

Table 4 Constants for IDF Curves (Present)

T _r (year)	a	b	c
2	3,950	26	0.978
5	4,163	28	0.936
10	4,348	29	0.916

Design Storm with Effect of Climate Change

To take into account effect of climate change to design rainfall pattern, the Equidistance Quantile Matching method (EQM) was applied to updated IDF curve. Global Climate Model (GCM), Has GEM2-ES from Met Office Hadley Center with RCP4.5 year 2015-2039 is used. Table 5 shows new constants for IDF in the future climate. Detail can be found from Chaowiwat et al (2015). Fig. 6 shows comparison plots of present and future IDF curves for 2 and 5 year return period. Table 5

summarize results of all constants in future IDF curve. Fig. 7 shows comparison plots of present and future CDS. Peak intensities at 2, 5 and 10 years increase from 17% to 24% as shown in Table 6.

Accumulated rainfall in CDS increase 17 to 24% for 1 hour. It is clearly shown in Table 6 that rainfall occurred in 2 years return period in the future will be that of present 5 year return period. The present 5 years return period accumulate rainfall in the future will be that of present 10 years return period. This increasing peak intensity and accumulate rainfall with such percentage will have significantly effect to the design drainage in Bangkok having standard design for 2 and 5 years return period. In addition, the time of concentration in Sukumvit, highly urbanized area is approximately 3 hours, accumulated rainfall increase from 72 mm to 90 mm or 26% increase. It is expected that drainage improvement should be conducted to cope with future climate.

Table 5 Constants for IDF Curves (Future)

T _r (year)	a	b	c
2	4,469	26	0.940
5	5,924	28	0.950
10	6,919	29	0.956

Future: RCP4.5 (2015-2039)

Table 6 Comparison of Peak Intensity & 1 hours Rainfall for Present and Future

T _r (year)	Peak Intensity (mm/hrs.)			Rainfall (mm)		
	Present	Future	Difference (%)	Present	Future	Difference (%)
2	124	154	24	55	68	24
5	156	187	20	70	84	20
10	178	208	17	81	95	17

Future: RCP 4.5 (2015-2039)

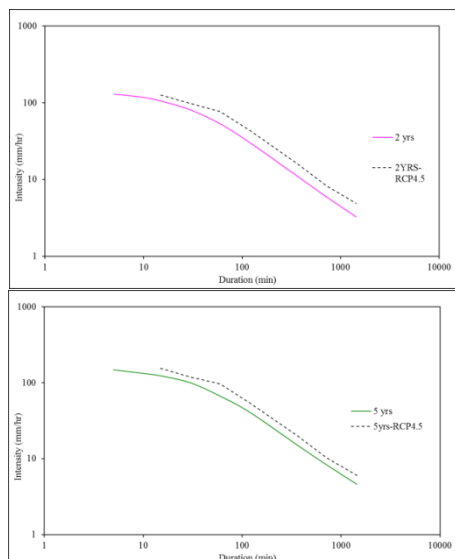


Fig. 6 Comparison of IDF curves for present and future 2015-2039 under RCP4.5

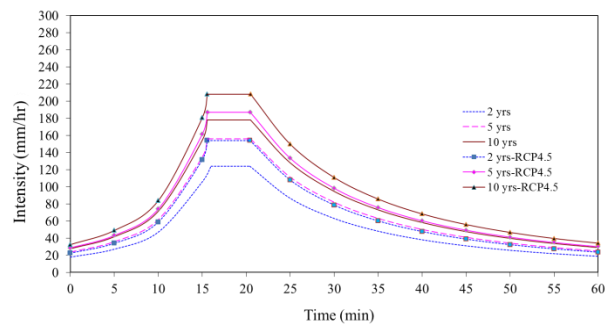


Fig.7 Comparison of Modified Chicago design storm for present and future 2015-2039 under RCP 4.5

Summary and conclusions

The present study can summarize the temporal rainfall characteristics in a daily time scale with statistically results to indicate one peak rainfall between 18:00 to 20:00. The design storm pattern has been developed and Chicago Design Storm (CDS) is the most appropriate one considering its shape, peak intensity and time to peak. Its peak is modified using 10 minutes rainfall intensity to match with the recorded values with reduced mean error from 57% to 21%. Climate change has been taken into account to IDF curve. Design storm pattern in the future climates (2015 to 2039) are derived with peak intensity increment 24% and same for accumulated rainfall. This condition can be used in designing measures for urban drainage in Thailand for the future.

Acknowledgement

The first author would like to acknowledge World Bank for financial scholarship to Asian Institute of Technology (AIT) through Punjab Irrigation Department, Pakistan. This work is under project “Climate Change Adaptation through Optimal Storm Water Capture Measures: Towards a New Paradigm for Urban Water Security”. Authors would like to acknowledge United Nations University, Japan for financial project support through Asia Pacific Network for Global Change research (APN).

References

Ashish S. (2013). Impact of Climate Change on Urban Flooding in Sukumvit Area of Bangkok, AIT Thesis, 114 p.

Ashish S., Weeakul S., Babel M.S. and Vojinovic Z. (2015). Designed Intensity-Duration-Frequency (IDF) Curves under Climate Change Condition in Urban Area. THA 2015 Conference, 6p.

Bandyopadhyay M. (1972). Synthetic Storm Pattern and Runoff for Gauhati, India. Journal of the Hydraulics Division, ASCE, 98(HY5), 845-857.

Charoensukrungruang W. (2006). Analysis of Rainfall Pattern for Urban Drainage Design, AIT Thesis, 92 p.



- Chaowiwat W., Charoensuk T., Weesakul S. and Boonya-Aroonnet S. (2015). Development of intensity, duration and frequency curve for climate change adaptation in Thailand. The 20th National Convention in Civil Engineering, 8-10 July 2015, Chonburi, Thailand.
- Desbordes M. (1978). Urban Runoff and Design Storm Modelling Proc. The first International Conference on Urban Storm Drainage, UK Pentech Press, London p.353-361
- Gillani S.N.A. (1980). A Mathematical Model for Storm Water Management. (Special Study No. WA-79-9, Asian Institute of Technology, 1970). Bangkok: Asian Institute of Technology.
- Keifer C.J. & Chu H.H. (1957). Synthetic Storm Pattern for Drainage Design. Journal of the Hydraulic Division, ASCE, 83 (HY4): 1332/1-1332/24.
- Naksua W. (2001). Improvement of Primary System and Its Operation in Ratburana and ThungKhru Areas by the MOUSE Model. Master thesis, King Mongkut's University of Technology Thonburi, 2001). Bangkok: King Mongkut's University of Technology Thonburi.
- Pothipiku K. (1993). A study of Rainfall on Bangkok Metropolitan Area. (Master thesis, Kasetsart University, 1993). Bangkok: Kasetsart University.
- Rattapan N. (1968). Bangkok Runoff Hydrograph. (Master thesis No. 225, Asian Institute of Technology, 1968). Bangkok: Asian Institute of Technology.
- Rehan M.M. (2016). Analysis of Rainfall Pattern and Validation of Design Storm Shape for Asian Monsoon. Asian Institute of Technology, Thesis, 143 p.
- Sifalda V. (1973). Entwicklung eines Berechnungsregens für die Bemessung von Kanalnetzen. Gwf-wasser/abwasser, 144(H9), 435-440.
- Van Nguyen V.T., Peyron N. and Rivard G. (2003). Rainfall Temporal Patterns for Urban Drainage Design in Southern Quebec. 9th International on Urban Drainage, Oregon, USA, 15p.
- Water Development Consultants Co., Ltd. (1998). Project for investigate and design drainage systems in Sukhumvit sub-catchments area in Bangkok. Bangkok: Department of Drainage and Sewerage.
- Watt W.E., Chow K.C.A., Hogg W.D. & Lathem K.W. (1986). A 1-Hour Urban Design Storm for Canada. Canadian Journal of Civil Engineering, 13(3), 293-300.
- Yen B.C., & Chow V.T. (1980). Design Hyetographs for Small Drainage Structures. Journal of the Hydraulics Division, ASCE, 106(HY6), 1055-1076.

Correlation Analysis Between Tsengwen-Wushantou Reservoirs Operation and Environmental Factors

Yi-Lung Yeh*, Sheng-Hsien Hsieh and Teng-Pao Chiu

Abstract Zengwen-Wushantou reservoir is the most important water supply system for the Chianan area as well as the irrigation water source of for the Chianan Plain, Taiwan. The water storage amount in the reservoir is affected by inflow and outflow. The inflow is affected by the rainfall amount in the catchment and the outflow is affected by the water evaporation and target water consumptions. This study collected water storage volumes of the reservoir in ten-day intervals from 1990 to 2014. The study also collected rainfall amounts in nine rainfall stations in ten-day intervals; these stations included Zengwen, Shuishan, Leye, Lijia, Biaohu, Matoushan, Longmei, Sanjiaonanshan, and Dadongshan. In addition, four target water consumption amounts were collected in ten-day intervals; these included rice, sugar, industrial, and population water consumption. We used correlation analysis to investigate the relationship between the water storage volumes, rainfall amounts in the rainfall stations, and the four target water consumptions. The dominant factors affecting the reservoir storage were determined by correlation analysis. These selected factors established the relationship between the water storage volumes and the main impact factors using multiple linear regression analysis. The results suggested that the main impact factor on the reservoir storage capacity was the rainfall amount, which has the highest effective rate in the Zengwen station, followed by Dadongshan station.

Yi-Lung Yeh

Department of Civil Engineering,
National Pingtung University of Science & Technology
Pingtung, Taiwan
e-mail: yalung@mail.npust.edu.tw

Sheng-Hsien Hsieh

Department of Civil Engineering,
National Pingtung University of Science & Technology
Pingtung, Taiwan
e-mail: tion388@gmail.com

Teng-Pao Chiu

Department of Civil Engineering,
National Pingtung University of Science & Technology
Pingtung, Taiwan
e-mail: ctp5559@gmail.com

The major factors that impact water storage were irrigation water for the rice, followed by industrial water. The significance test verified that reservoir storage capacity had a significant relationship with irrigation water for rice, industrial water consumption, and water used for sugar cane. The multiple linear regression of the water storage volumes with the main affecting factors can be determined by the following equation: $y = 177.3823 + 0.1189x_1 + 0.2061x_2 + 0.3275u_1 + 0.3585u_2 + 9.4545u_3 + 0.3665u_4$, in which y is the reservoir storage capacity, x_1 and x_2 are the rainfall amounts in Dadongshan and Zengwen stations, respectively, and u_1 , u_2 , u_3 , and u_4 are the water consumptions for rice irrigation, sugar cane irrigation, industrial water consumption, and the population consumption, respectively.

Keywords Zengwen-Wushantou reservoir system, environmental key factors, multi-Regression, water resources allocation

Introduction

The annual average rainfall in Taiwan reaches 2,500 mm, but the steep slope of riverbeds causes river flow and rainfall to rapidly flow into the sea that is very detrimental for water resources use. Zengwen and Wushantou reservoirs are two multi-objective reservoir systems in southern Taiwan. These reservoirs have operated in-series since 1974, mainly supplying water for irrigation, industry, and population water consumption. During a drought period, Zengwen-Wushantou reservoir operation will affect the supply of water resources in southern Taiwan. Therefore, it is necessary to master the factors influencing the reservoir water inflow and outflow to manage the water resources allocation of the reservoir.

In the face of climate change, different adaptation strategies for climate change adaptation and disaster mitigation strategies have been proposed. The adaptive strategies can be divided into following categories: flood disaster, debris flow disaster, storm surge causing flooding and coastal erosion, reservoir flood and siltation control, and safety and water resources operation and management [1-4]. In the case of the Zengwen-Wushantou reservoir, the irrigation project was planned by the Chianan Irrigation and Water Conservancy Association, Taiwan to plan the irrigation

water and water demand of each irrigation district in the same year [5].

This study collected storage volume, rainfall amounts, and water consumption from each target in ten-day intervals in the Zengwen-Wushantou reservoir. The relationship between water storage volume and water intake, and storage factors was analyzed using the Pearson correlation coefficient and gray relational analysis. The purpose was to investigate the dominant influence factor in reservoir water storage capacity.

Description of study site

Zengwen Reservoir and Wushantou Reservoir are the reservoirs used for multi-targets in southern Taiwan. The two reservoirs are currently operated in-series. The water is transported from Zengwen Reservoir to the Wushantou Reservoir with a tunnel for water consumption of irrigation, industrial water and population water consumption.

1. Zengwen Reservoir

Zengwen Reservoir is located at the upper reaches of the Zengwen River in the Liutengtang Gorge. It is a multi-target reservoir, including irrigation, public water, industrial water supply, hydroelectric power generation, and flood control. Power generation is needed to meet the irrigation and water supply. The reservoir began construction in 1967, was completed in October 1973, and in January 1974, it was an official power generation and water supply operation. The reservoir dam is a rolling soil type dam, 133 m high, 400 m long, with a crest elevation at 235 m, and a preventive wave wall at an elevation of 236.4 m. The reservoir catchment area is 481.16 km², the full water area is 17 km², and the total storage capacity is 708 million tons. The reservoir has been assailed by typhoons and heavy rains, and soil and sand deposition has made the reservoir storage capacity decrease. Hence, the reservoir effective storage capacity was 468 million tons in a 2015 measurement.

2. Wushantou Reservoir

Wushantou Reservoir is located at the west-south side of Zengwen Reservoir. It is an off-channel reservoir located at the upper reaches of Guantian Creek in the tributary of Zengwen River. Construction was started in January 1920 and was completed in May 1930. It has been operated in-series with Zengwen Reservoir since 1974. The catchment area of the reservoir is 60 km². The crest elevation is 66.66 m and the full water level is 58.18 m. In 1930, the total water storage capacity at full water level was 154.16 million tons, and the effective storage capacity in 2016 was 78.28 million tons. The water mainly comes from Zengwen Reservoir. It receives tail water from the power generation of Zengwen Reservoir in the East weir. The water passes through the Wushanling water diversion tunnel and is adjusted by a horn-type overflow port at the West side,

then water flows only into the Wushantou Reservoir. The water consumption of each target is supplied by Wushantou Reservoir.

3. Irrigation water supply system

The agricultural irrigation area of Zengwen-Wushantou Reservoir is the Chianan Plain, in the southwestern part of Taiwan (shown in Figure 1). The east side is the Central Mountain Range, the west side is the Taiwan Strait, the north side is Beigang Creek, Yunlin County, and the south side is Erren Creek nearby Kaohsiung Mountain. The area covers 71 km from east to west, 110 km from north to south and about 4,884 km² in the whole region, accounting for 14% of Taiwan's total island area. Although there are local irrigation facilities in the Chianan Plain, there are only about 5,000 hectares of irrigated land in the vicinity of the river or the pond. Due to the lack of comprehensive irrigation facilities, the farmers combined with the water supply system of Chianan Great Drainage Ditch to build the Wushantou Reservoir in the Guantian area at upper reaches of Zengwen River. In 1930, with the completion of the reservoir construction, it began to supply irrigation. In order to meet the sugar policy at that time, the implementation rotation-irrigation system in one-year irrigation periods, at three-year intervals, was first founded. In 1974, it combined with Zengwen Reservoir to operate in-series, and the original one-year irrigation period was changed to two-year irrigation periods at three-year intervals.

Analytical methods

This study collected total water storage volumes in ten-day intervals in Zengwen-Wushantou reservoir and nine rainfall stations including Zengwen, Shuishan, Leye, Lijia, Biaohu, Matoushan, Longmei, Sanjiaonanshan, and Dadongshan from 1990 to 2014. In addition, four target water consumption amounts including rice, sugar, industrial, and population water consumption were collected in ten-day intervals. Data in ten-day intervals served as a unit; the total water storage volume of the reservoir was taken the last day of the ten-day interval. Accumulated rainfall amounts were taken in the ten-day intervals, and accumulated water consumptions of the targets were counted at the end of the ten-day intervals.

The content format of collected data is shown in Table 1, where St is the total storage capacity of Zengwen-Wushantou reservoir, and R_i ($i = 1, 2, \dots, 8, 9$) represents the rainfall amounts in the nine stations: Zengwen, Shuishan, Leye, Lijia, Biaohu, Matoushan, Longmei, Sanjiaonanshan and Dadongshan. U_j ($j = 1, 2, 3, 4$) represents the water consumption of rice irrigation, sugar irrigation, industrial and population water consumption, respectively.

Table 1. Data collection format for Zengwen-Wushantou reservoir operation

Objective type														Time
U ₄	U ₃	U ₂	U ₁	R ₉	R ₈	R ₇	R ₆	R ₅	R ₄	R ₃	R ₂	R ₁	St	
U ₄₁	U ₃₁	U ₂₁	U ₁₁	R ₉₁	R ₈₁	R ₇₁	R ₆₁	R ₅₁	R ₄₁	R ₃₁	R ₂₁	R ₁₁	St ₁	1990-1
U ₄₂	U ₃₂	U ₂₂	U ₁₂	R ₉₂	R ₈₂	R ₇₂	R ₆₂	R ₅₂	R ₄₂	R ₃₂	R ₂₂	R ₁₂	St ₂	1990-2
U ₄₃	U ₃₃	U ₂₃	U ₁₃	R ₉₃	R ₈₃	R ₇₃	R ₆₃	R ₅₃	R ₄₃	R ₃₃	R ₂₃	R ₁₃	St ₃	1990-3
.....														...
.....														...
U _{4m-2}	U _{3m-2}	U _{2m-2}	U _{1m-2}	R _{9m-2}	R _{8m-2}	R _{7m-2}	R _{6m-2}	R _{5m-2}	R _{4m-2}	R _{3m-2}	R _{2m-2}	R _{1m-2}	St _{m-2}	2014-34
U _{4m-1}	U _{3m-1}	U _{2m-1}	U _{1m-1}	R _{9m-1}	R _{8m-1}	R _{7m-1}	R _{6m-1}	R _{5m-1}	R _{4m-1}	R _{3m-1}	R _{2m-1}	R _{1m-1}	St _{m-1}	2014-35
U _{4m}	U _{3m}	U _{2m}	U _{1m}	R _{9m}	R _{8m}	R _{7m}	R _{6m}	R _{5m}	R _{4m}	R _{3m}	R _{2m}	R _{1m}	St _m	2014-36

The collected water data were used in the following analysis:

1. Pearson correlation coefficient

The study used the Pearson correlation coefficient to find the correlation coefficients between the total storage volume and the rainfall amounts in the nine rainfall stations as well as the water consumption of the four targets. The Pearson correlation coefficient of the two variables X and Y is formally defined as the covariance of the two variables divided by the product of their standard deviations, and it can be equivalently defined by [6,7]

$$\gamma_{XY} = \frac{\sum(x_i - \bar{x})\sum(y_i - \bar{y})}{\sqrt{\sum(x_i - \bar{x})^2} \sqrt{\sum(y_i - \bar{y})^2}} \quad (1)$$

where $\bar{x} = \frac{1}{n} \sum_{i=1}^n x_i$ denotes the mean of x.

$\bar{y} = \frac{1}{n} \sum_{i=1}^n y_i$ denotes the mean of y. The coefficient

γ_{XY} ranges from -1 to 1 and it is invariant to linear transformations of either variables.

2. Multi-variable linear regression analysis

The variable of Zengwen-Wushantou reservoir storage capacity (y) had a linear relationship with the rainfall amount in the nine stations (R_i, i = 1,2, ..., 8,9), and water consumption of rice irrigation, sugar irrigation, industrial and population water consumptions (U_j, j = 1,2,3,4). The α times of the observed data can be expressed as Eq (2).

$$(y_\alpha ; R_{i\alpha 1}, U_{j\alpha 2}) \quad \alpha=1, 2, \dots, n; i=1, 2, \dots, 9; j=1, 2, 3, 4 \quad (2)$$

The equation of multiple-variable linear regression analysis can be expressed as Eq. (3).

$$\hat{y} = b_0 + b_{i1}R_{i1} + b_{j2}U_{j2} \quad i=1, 2, \dots, 9; j=1, 2, 3, 4 \quad (3)$$

where b₀, b_{i1}, and b_{j2} are regression coefficients and can be estimated by the least square method.

Results and discussion

From 1990 to 2014, the total water storage capacity and water supply standard limits at ten-day intervals of the Zengwen-Wushantou Reservoir is shown in Fig.1. In years 1994 and 2004, the water storage capacity of the reservoirs was lower than the low limit, which indicated the two periods were drought years. Fig. 2 shows the accumulated rainfall at the nine rainfall stations in the study area from 1990 to 2014; the rainfall in 2009 is very high. This is the heavy rainfall caused by the southwest airflow introduced by Morakot Typhoon. Fig. 3 shows the water consumption in the ten-day intervals of the researched targets from 1990 to 2014. It shows the main water consumption is for rice irrigation, followed by water consumption for sugar irrigation.

The correlation coefficients between the total storage capacity of the reservoir and the cumulative rainfall of each ten-day interval as well as the water consumption of each target were obtained from Pearson correlation analysis (Table 2). The results show that the amount of water used for rice irrigation was closely related to the amount of reservoir water storage in the previous ten-day interval. On the other hand, the rainfall amount was closely related to the amount of reservoir water storage in the next ten-day interval. The most significant relationship was the Zengwen rainfall station, followed by the Dadongshan station. The significance test verified that reservoir storage capacity had a significant relationship with the irrigation water for rice, industrial water consumption, and water used for sugar cane. The multiple linear regression of the water storage volume with the main affecting factors can be determined by the following equation: $y = 177.3823 + 0.1189x_1 + 0.2061x_2 + 0.3275u_1 + 0.3585u_2 + 9.4545u_3 + 0.3665u_4$, in which, y is the reservoir storage capacity, x₁ and x₂ are the rainfall amounts in Dadongshan and Zengwen stations, respectively, and u₁, u₂, u₃, and u₄ are the water consumptions for rice irrigation, sugar cane irrigation, industrial water consumption and the population consumption, respectively.

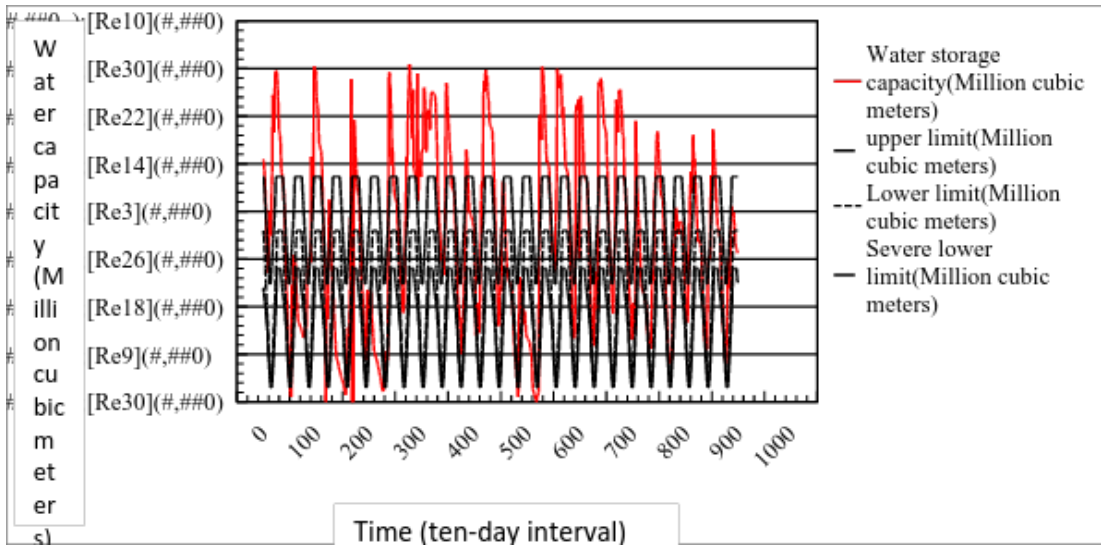


Fig. 1. The total water storage capacity and water supply standard limits at ten-day intervals of the Zengwen-Wushantou Reservoir from 1990 to 2014.

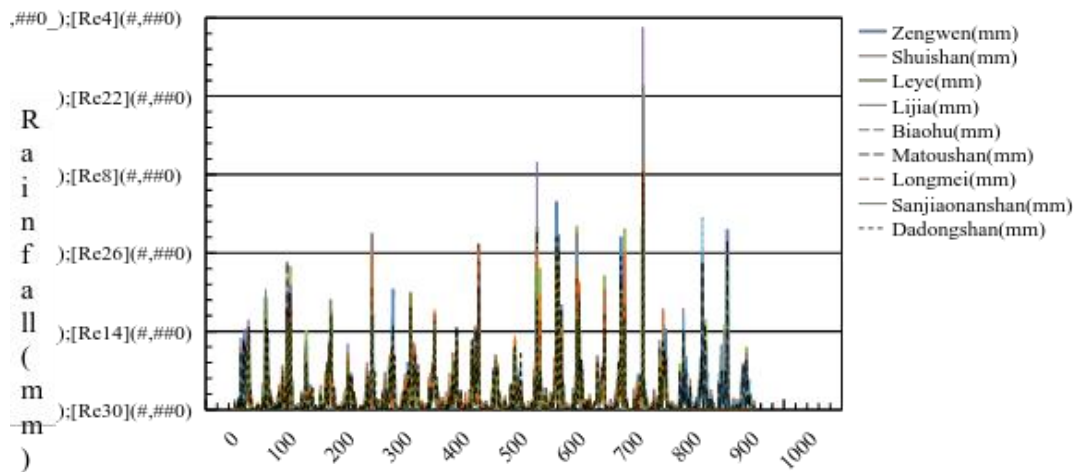


Fig. 2. The accumulated rainfall at the nine rainfall stations in the study area from 1990 to 2014.

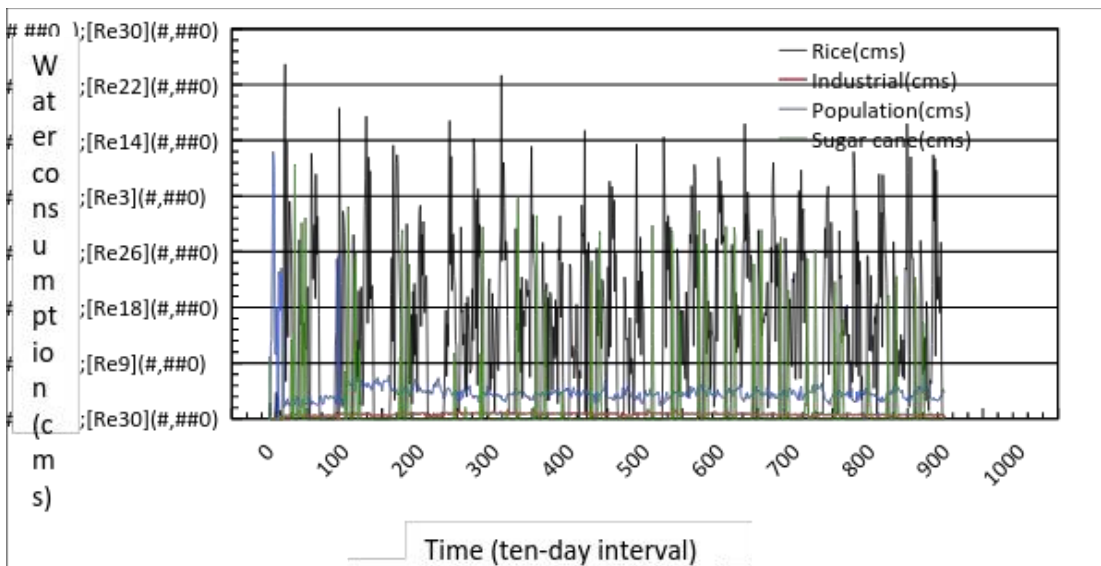


Fig. 3. The water consumption in the ten-day intervals of the rice, industrial, population, and sugar cane from 1990 to 2014.

Table 2. The Pearson correlation coefficient between total storage capacity of Zengwen-Wushantou reservoir and environmental factors

U ₄	U ₃	U ₂	U ₁	R ₉	R ₈	R ₇	R ₆	R ₅	R ₄	R ₃	R ₂	R ₁	St
0.109	-0.040	0.156	0.313	0.099	0.050	0.042	0.045	0.041	0.008	0.002	-0.010	0.077	St _{t-1}
0.054	-0.054	0.175	0.270	0.277	0.240	0.230	0.248	0.237	0.217	0.208	0.199	0.272	St _t
0.010	-0.058	0.189	0.286	0.313	0.270	0.258	0.285	0.282	0.250	0.242	0.236	0.303	St _{t+1}

St is the total storage capacity of Zengwen-Wushantou reservoir.

R_i(i=1,2,...,8,9) represents the rainfall amounts in the nine stations: Zengwen, Shuishan, Leye, Lijia, Biaohu, Matoushan, Longmei, Sanjiaonanshan and Dadongshan.

U_j (j = 1, 2, 3, 4) represents the water consumption of rice irrigation, sugar irrigation, industrial and population water consumption, respectively.

Conclusions

By analyzing the correlation between the water storage capacity of the Zengwen-Wushantou reservoir and the environmental factors, it was found that the main inflow factor was the rainfall amount at Zengwen rainfall station, followed by the rainfall amount at the Dadongshan station. The water storage capacity of the reservoir (outflow factor) was affected by the water for rice irrigation, followed by water for sugar irrigation. The water for industrial consumption was negatively correlated with the water storage capacity of the reservoir. The multiple linear regression of the water storage amount with the rainfall amounts in Dadongshan and Zengwen stations, and the water consumptions for rice irrigation, sugar cane irrigation, industrial water consumption and the population consumption was determined by the following equation: $y = 177.3823 + 0.1189x_1 + 0.2061x_2 + 0.3275u_1 + 0.3585u_2 + 9.4545u_3 + 0.3665u_4$.

References

- [1] G.H. Yu and S.P. Hsu, “The impacts of climatic change on water resources-rainfall analysis,” *Journal of Taiwan Agricultural Engineering*, vol.44, no.1, pp.9-24, 1998.
- [2] NCKU Research and Development, “Catchment conservation plan in Zeng-wen river,” Water Resources Agency, MOEA, Taiwan, 2011.
- [3] NCKU Research and Development, “A study on flood and soil and sand control for climate change in Zeng-wen river basin,” Water Resources Agency, MOEA, Taiwan,,2013.
- [4] NCKU Research and Development, “A study on climate change adaptation strategy of Zeng-wen river (1/3),” Water Resources Agency, MOEA, Taiwan, 2015.
- [5] Chianan Irrigation Association, “Irrigation planning in Zengwen-Wushantou irrigation system in 2011”, Tainan, Taiwan, 2011.
- [6] J.L. Rodgers and W.A. Nicewander, “Thirteen ways to look at the correlation coefficient,” *Am. Stat.*, no. 42, pp. 59-66, 1988.
- [7] H.M. Zhou, Z.H. Deng, Y.Q. Xia, and M.Y. Fu, “A new sampling method in particle filter based on Pearson correlation coefficient,” *Neurocomputing*, no. 216, pp.208-215, 2016.

Spatial heterogeneity and trans-boundary pollution: A case study on the 3S River Basin

Nguyen Thi Thuy Tranga^{1,a}, Sangam Shrestha^{2,b}, Manish Shrestha^{2, c*}, Avishek Datta^{2,d}, Akiyuki Kawasaki^{3,e}

Abstract We examine the current and the future water quality issues of the 3S (Sekong, Sesan and Srepok) River Basin of Southeast Asia. The 3S River Basin is a transboundary River between Cambodia, Laos and Vietnam and contributes 16% of the total annual flow to the Mekong River. Hydrological model SWAT was used to represent the hydrological process and nutrient loading of the basin. The nutrient loading map of the basin was developed and reveals that the highest contribution of the nutrient comes from Vietnam, upstream of Sesan and Srepok Rivers contributing more than 70% of the total nutrient loading. This can be attributed to intensive agriculture and urban areas in Vietnam. Similar results were obtained for the future periods under RCP 4.5 and RCP 8.5 scenarios. Therefore it can be summarized that human activities plays an important role in the occurrence of pollution in the basin and the lower part of the basin suffers from the dense populated upstream rather than pollution from the local source.

Keywords *Climate change, Discharge, Nutrient map, Transboundary, Water quality*

^{1,a} University of Yamanishi
Kofu, Japan
nguyenfiredragon@gmail.com

^{2,b} Asian Institute of Technology
Water Engineering and Management
PathumThani, Thailand
sangam@ait.asia

^{2,c*} Asian Institute of Technology
Water Engineering and Management
PathumThani, Thailand
manis_shrestha@live.com

^{2,d} Asian Institute of Technology
Agricultural Systems and Engineering
PathumThani, Thailand
avishek.ait@gmail.com

^{3,e} The University of Tokyo
Bunkyo-Ku, Japan
akiyuki@iis.u-tokyo.ac.jp

Introduction

The 3S Rivers (Sekong, Srepok and Sesan) are important transboundary tributaries of the Mekong River that flow through three countries, namely Laos, Vietnam and Cambodia and plays a significant role in the socio-economic development of the region. The water quality and quantity from the 3S Basin outlet directly impacts the water use in the Mekong Delta which plays a vital role in Vietnamese economy and food security as it is one of the largest producers and exporters of rice.

The Mekong River has been facing environmental degradation over the last 30 years due to multiple pressures such as rapid population growth, accelerated deforestation, industrialization and intensive agricultural development. Moreover, the water quality is also significantly affected by various anthropogenic activities including climate change (Tu, 2009) and the 3S basin is one of the climate change hotspot in the Lower Mekong Basin (LMB) (Hartman and Carlucci, 2014). Water quality can be directly affected through several climate related mechanisms on both the short-term and long-term basis (Tu, 2009; Jun et al., 2010). Therefore, water quality would be affected by global climate change. The changes in water quantity also modify water quality through impact of dilution or concentration of dissolved nutrients (Jun et al., 2010).

There are some studies on water quality related to the 3S Basin; however, most of these studies have been focused on an individual river of each country at local scale. Therefore, it is of utmost importance to study the water quality patterns at the whole basin scale in a holistic manner. In this regard, the aim of this study were to: (1) simulate the hydrology of the rivers of the 3S Basin; (2) develop the nutrient loading map of N and P in the 3S Basin from point sources and non-point sources pollution and (3) assess the impact of climate change on the water quality and quantity in the 3S River system.

Study area

The Sekong, Sesan and Srepok River Basin, also known as the 3S Basin, is located in the south-eastern part of the Mekong basin (Fig. 1). The total drainage area of the basin is 78529 km², which accounts for 10% of the

Mekong River Basin. The Sesan and Srepok Rivers originate from the central highlands of Vietnam whereas the Sekong River originates from the Annamite Mountain in Laos. The Sesan and Srepok Rivers flow through Cambodia, join the Sekong River and finally confluence to the Mekong River in Cambodia. The 3S Basin accounts for 16% of the total annual flow in the Mekong Delta (Räsänen et al., 2012). With an annual average rainfall of 2270mm and the average temperature of 22.5°C the average discharge of 3S River is 2386m³/s (Sekong 1040m³/s; Sesan 651 m³/s; Srepok 695 m³/s). The largest land-use area is the forest covering an area of 61712 km² accounting for 78.76% followed by agriculture 13.2%. The majority of the agriculture and urban area lies in the Vietnam upstream of Sesan and Srepok River. The urban area occupies only 1075 km² or 1.37% of the whole basin.

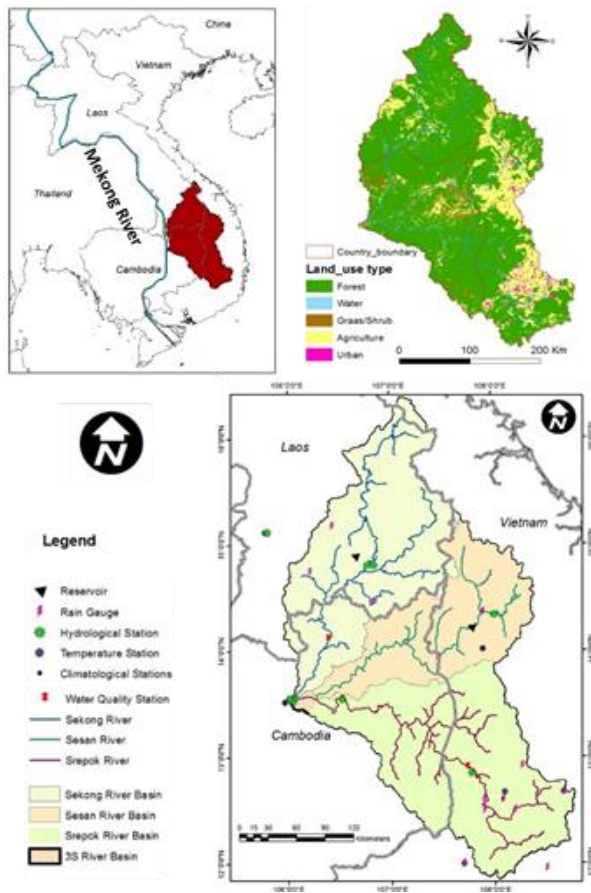


Fig. 1 Location of study area

Methodology

Semi distributed hydrological model SWAT was used to simulate the hydrology and water quality of the 3S basin. The input required for SWAT, DEM, Landuse, soil map, climate data, water quality and hydrology data were all collected from Mekong River Commission (MRC). The model was first calibrated and then validated against the observed discharge data at 8 hydrological stations followed by calibration and

validation against water quality parameters at 5 water quality stations. Both visual and statistical parameters (NSE, R² and PBIAS) were used to evaluate the model. The future climate data of the basin were extracted from 5 GCMS (CanESM2, CNRM-CM5, HadGEM2-AO, IPSL-CM5A-LR, MPI-ESM-MR) and bias corrected using perturbation method. RCP 4.5 and RCP 8.5 scenarios defined by AR5 was selected as these storyline represents the medium and high concentration of GHG in the future. The data was then used as an input to simulate future hydrology and water quality of each of the rivers in 3S Basin.

The following equations below is used for perturbation method:

For temperature,

$$CF_k = T_k^{GCMfut} - T_k^{GCMref}, T_{k,i}^{fut} = T_{i,k}^{obs} + CF_k \quad (1)$$

For precipitation,

$$CF_k = \frac{P_k^{GCMfut}}{P_k^{GCMref}}, P_{k,i}^{fut} = P_{i,k}^{obs} * CF_k \quad (2)$$

where CF_k = monthly mean change factor at month k , T_k^{GCMfut} = GCM-simulated temperature for the future period at month k , T_k^{GCMref} = GCM-simulated temperature for the reference period at month k , $T_{k,i}^{fut}$ = future temperature at day i and month k , $T_{i,k}^{obs}$ = observed temperature at day i and month k , P_k^{GCMfut} = GCM-simulated precipitation for a future period at month k , P_k^{GCMref} = GCM-simulated precipitation for the reference period at month k , $P_{k,i}^{fut}$ = future precipitation at day i and month k , $P_{i,k}^{obs}$ = observed temperature at day i and month k .

Results and discussion

Calibration and validation of model

There was a good agreement between the simulated and the observed flow at the outlet and Bandon station (See Table 1). In contrast, the model performance in Attapeu and Kontum was only satisfactory based on the R² and NSE factor. The reason could be due to the lack of precipitation data at those areas. Although the agreement between the observation and the simulation was achieved, the stream flow peak was not well fit and was mostly underestimated for all stations (Figure 2). However, the objective of this study was not to predict the flood; therefore, the mismatch in peak flow is not a significant concern. The model was also able to capture the trend of water quality simulation at different station for different water quality parameters.

Development of nutrient loading map

The spatial distribution of the average annual total N and P in the 3S Basin is illustrated in Fig. 3. The analysis shows that the highest contribution of TN and TP came from Vietnamese upstream of Sesan and Srepok Rivers. These loadings could come from intensive agriculture and urban areas in Vietnam. The pollutant will not only impact the discharging area upstream but will also have an adverse effect on the whole basin.

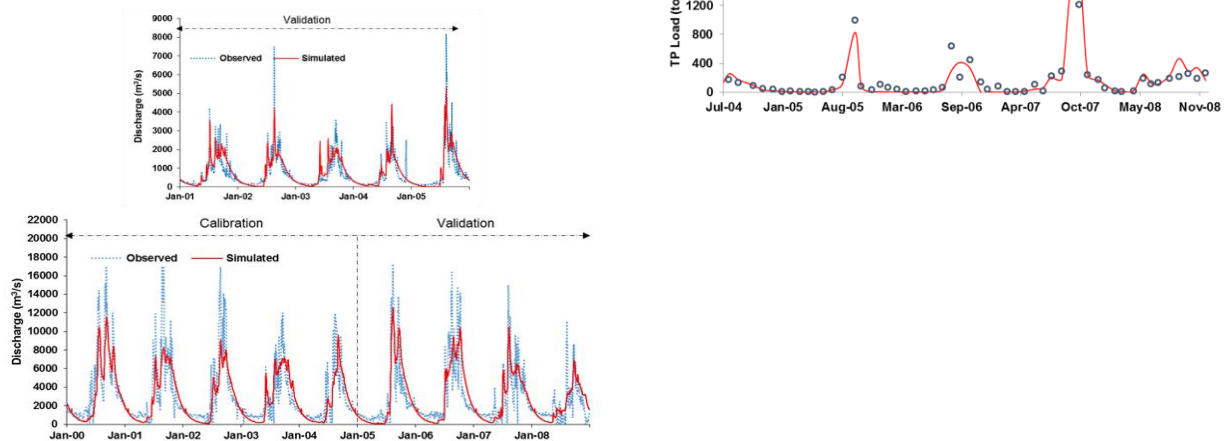


Fig. 2 The observed and the simulated daily discharge hydrograph (1st column) at B. Veunxhene and 3S Basin outlet and water quality (2nd Column) at Siem Pang and Bandon station.

Table 1: Performance of SWAT model

Hydrology							
Station	Time period	Calibration			Validation		
		R ²	NSE	PBIAS	R ²	NSE	PBIAS
Chantangoy	V: 1994–1999	-	-	-	0.59	0.65	1.61
Attapeu	C: 2000–2005	0.56	0.49	-9.36	-	-	-
B. Veunxhene	V: 1994–1999	-	-	-	0.8	0.80	8.01
Ban Kamphun	V: 1994–1999	-	-	-	0.80	0.80	8.01
Kontum	C: 2000–2005	0.61	0.45	-7.46	0.58	0.60	24.41
Lumphat	V: 1994–1999						
	C: 2000–2005	0.54	0.54	-6.90	0.58	0.57	-3.82
Bandon	V: 2006–2008						
	C: 2000–2005	0.74	0.65	-8.30	0.77	0.80	-0.83
	V: 1994–1999						
3S Basin outlet	C: 2000–2005	0.72	0.72	8.21	0.68	0.68	-2.86
	V: 2006–2008						
Water Quality							
Station	Parameter	Calibration (2004–2006)			Validation (2007–2008)		
		R ²	NSE	PBIAS	R ²	NSE	PBIAS
Siem Pang	NO ₃ ⁻	0.83	0.79	27.12	0.70	0.69	-4.61
Lumphat	NO ₃ ⁻	0.79	0.63	38.54	0.81	0.74	-21.1
Lumphat	NH ₄ ⁺	0.70	0.64	33.32	0.55	-1.51	25.46
Pleiku	P	0.85	0.80	1.25	0.78	0.61	-14.43
Bandon	P	0.84	0.81	24.57	0.84	0.60	-28.31

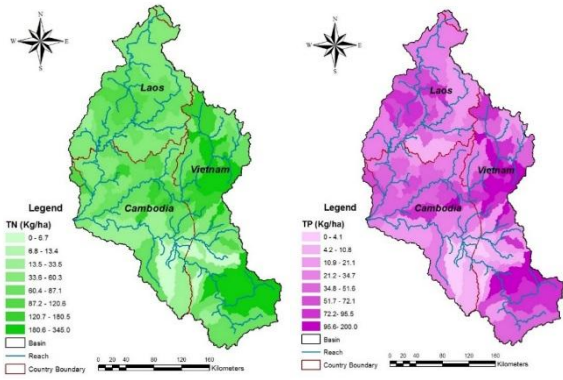


Fig. 3 Spatial distribution of annual total N [TN] and total P [TP] during the periods of 2004–2008.

The annual total N and P discharge was calculated as 732674 T/year and 360336 T/year, respectively. Figure 4 shows the percentage of nutrient load from each land-use type of the basin. It can be seen that forest and agriculture were the two major sources of nutrient pollution accounting for 70.86% N and 70.24% P and 11.74% N and 12.01% P, respectively, of the total nutrient load in the 3S Basin. However in terms of the load rate, urban area exported the highest rate of the pollutant load (Figure 5). The N loading rate of the urban area was nearly three times and agriculture land was nearly two times compared with forest area. It can be summarized that the human activity plays an important role in the occurrence of point sources and non-point sources pollution in the 3S Basin.

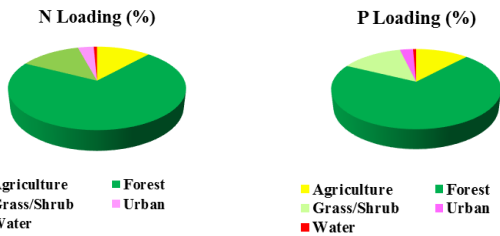


Fig. 4 The contribution of N and P loading from each land-use type.

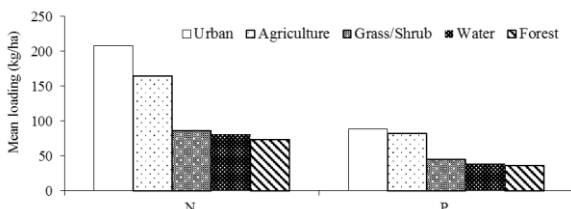


Fig. 5 N and P loading rate of each land-use type.

Climate change impact

It can be seen that the temperature has an increasing trend in both scenarios for three considered periods in every month. The basin average temperature is projected to increase by 0.89°C and 1.05°C in 2030s, 1.59°C and

2.31°C in 2060s and 1.97°C and 3.81°C in 2090s under RCP4.5 and RCP8.5, respectively, compared with the baseline period.

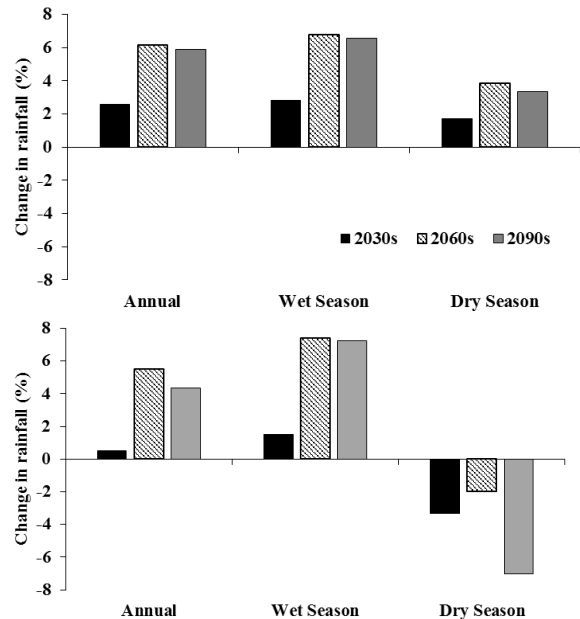


Fig. 6 Changes in seasonal rainfall for the period of 2030s, 2060s and 2090s compared with the baseline period under (a) RCP4.5 and (b) RCP8.5 scenarios.

The change in seasonal rainfall compared with the baseline period is shown in Fig. 6. It has been observed that the annual rainfall increases more under RCP4.5 than RCP8.5 scenarios. The highest increase of rainfall has been found in 2060s under RCP4.5. Rainfall changes during the wet season (May to October) within a range from 2.80% to 1.50% for the 2030s, 6.75% to 7.39% for the 2060s and 6.54% to 7.22% for the 2090s. In the dry season, rainfall change ranges from 1.72% to -3.31% for the 2030s, from 3.86% to -1.95% for the 2060s, and from 3.36% to -7.00% for the 2090s under RCP4.5 and RCP8.5, respectively. Overall, under the climate change scenario RCP4.5, rainfall is expected to increase for the entire period. Rainfall is predicted to decrease during the dry season and increase during the wet season under RCP8.5 scenario.

Impact on hydrology

The annual discharge of the basin is expected to increase under both RCP 4.5 and RCP8.5 scenarios (Figure 7). The increases of discharge can be explained by increases in precipitation during the wet season. During the wet season, discharge can increase upto 20.35% during the period of 2060s. However, the basin may face decrease in discharge during the dry season.

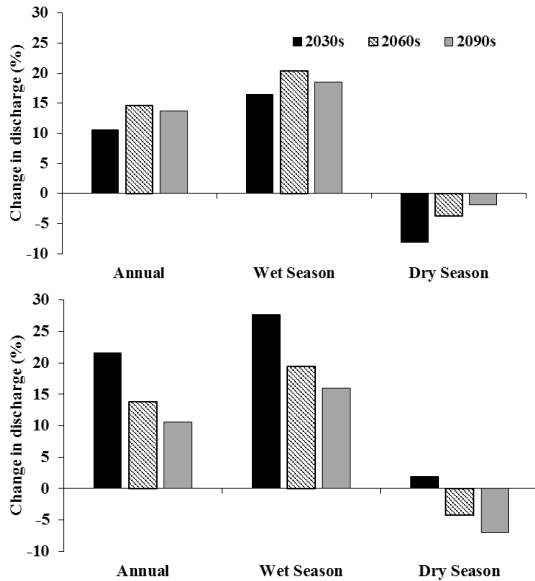


Fig. 7 Changes in discharge at the 3S Basin outlet under (a) RCP 4.5 and (b) RCP 8.5 scenarios.

Impact on nutrient loading

In order to perceive the change of nutrient loading by climate change, landuse and other factors were kept constant. The annual nutrient loading is predicted to increase under both climate change scenarios. The highest increase in N loading occurs in 2060s whereas the greatest increase in P loading occurs in 2030s only under RCP8.5 scenario.

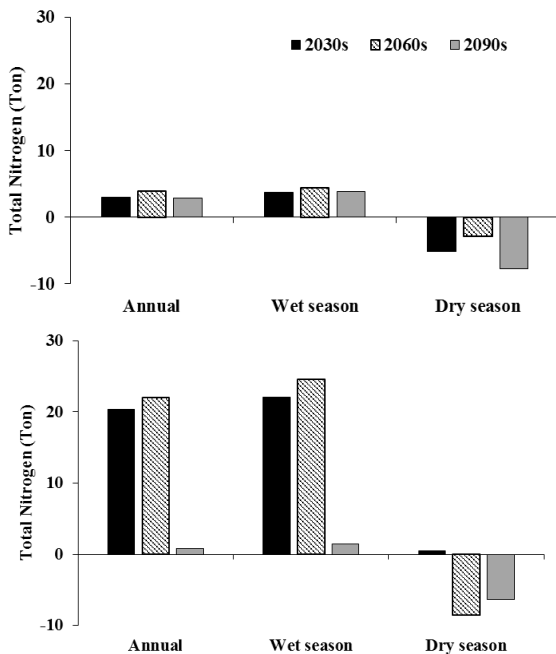


Fig. 8 Change in total N loading compared with the baseline period under RCP4.5 (1st row) and RCP8.5 (2nd row) scenarios.

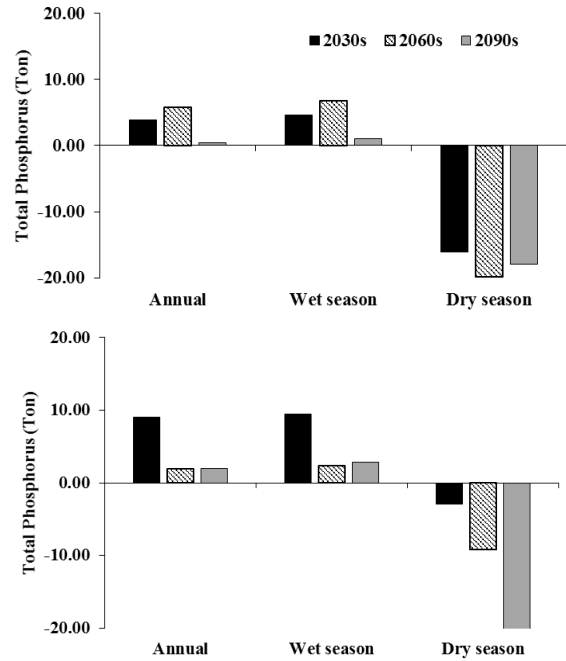


Fig. 9 Change in total P loading compared with the baseline period under RCP4.5 (1st row) and RCP8.5 (2nd row) scenarios.

The change of TN and TP loading in the future compared with the baseline period is presented in Figs. 8 and 9. In general, the trends of change in TN and TP are similar as basin discharge and rainfall. In terms of seasonal change, TN and TP are predicted to increase by 1.47% to as high as 24.57% and 1.08% to as high as 9.43%, respectively, in the wet season. In the dry season, TN is projected to decrease up to 8.52% whereas TP is projected to decrease up to 23.32% under RCP 4.5 scenario. In summary, the pollution loading is projected to increase in the early and midcentury and decrease in the late century. The annual loading increase is mostly contributed by the increase in loading during the wet season.

Among the three Rivers, Srepork River contributes the highest amount of N and P to the basin followed by Sesan River since both of the rivers originate from intensively cultivated areas in Vietnam. More than 70% of the total nutrient loading comes from these two rivers. Sekong River contributes on an average of 27% of the total nutrients in the basin. Similarly, the contribution share of Sesan and Sekong Rivers are around 33% and 40%, respectively. Similar trends can be observed in the future under both the climate change scenarios (Fig. 8).

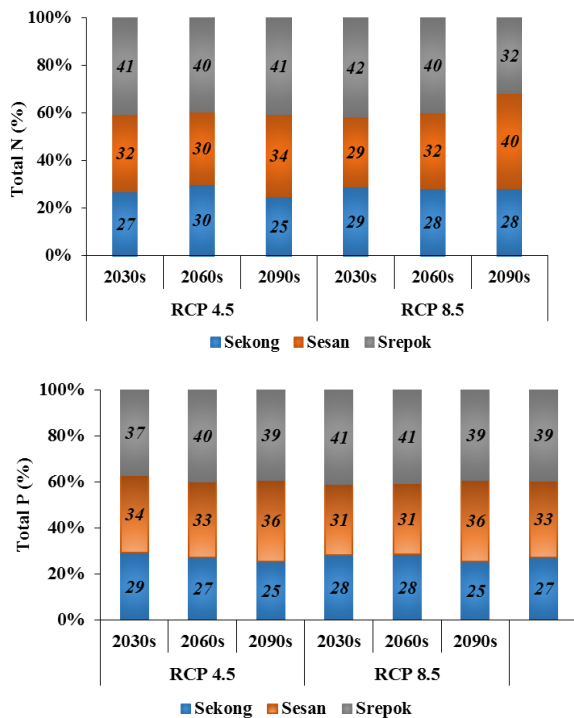


Fig. 10 Percentage contribution of (a) Total N (%) and (b) Total P (%) by Sekong, Sesan and Srepok Rivers under two climate change scenarios.

Summary and Conclusions

In this study, the Arc-SWAT model was applied to assess the potential impact of global climate change on water quality and quantity of the 3S River Basin. The model was calibrated against eight hydrological stations and four water quality stations spread within the basin. The calibrated model was then used to estimate the discharge, TN and TP in the future under the climate change scenarios of RCP4.5 and RCP8.5 for the three periods of 2030s, 2060s and 2090s. Data from five GCMs were bias corrected to forecast the future climate condition of the 3S Basin.

The analyses suggest that both temperature and rainfall is expected to increase in the future compared with the baseline period. The magnitude of increase varies and is dependent on the future time period and RCP scenario in question. However, rainfall is predicted to decrease during the dry season under RCP8.5. With respect to change in temperature and rainfall, water discharge and water quality also alter significantly. The annual water availability of the basin is expected to increase in the future. The increase of discharge can be explained by increase in precipitation. This increase comes mainly from increase in discharge during the wet season. However, the discharge is expected to decrease during the dry season.

The nutrient loading map of the basin reveals that the highest contribution of TN and TP comes from Vietnam, upstream of Sesan and Srepok Rivers. These two rivers contribute more than 70% of the total nutrient loading. This can be attributed to the intensive

agricultural and urban areas in Vietnam. Analyses also show that urban area exports the highest rate of the nutrient followed by agriculture in terms of the loading rate. It can be summarized that human activity play an important role in the occurrence of point sources and non-point sources pollution in the 3S Basin. It is also observed that the trends of change in TN and TP occur are similar as basin discharge and rainfall. In terms of seasonal change, TN and TP are predicted to increase in the wet season whereas it is projected to decrease under RCP4.5 scenario.

The results of this study would be useful to understand the potential impact of global climate change on both water quantity and quality of the 3S Basin. With increasing discharge and nutrient loading in the future proper adaptation strategies should be implemented to minimize the negative impact of climate change. Improvement in water quality in the 3S Basin would be a major challenge and a strong support and participation from the people and governments of the three nations living in the basin is urgently needed to enhance the effectiveness of the existing monitoring programs and future management plans in the basin.

Acknowledgement

The authors would like to thank the Greater Mekong Subregion (GMS) for providing the fund required for the research. The authors would also like to acknowledge Dr. Dao Nguyen Khoi from the Centre of Water Management and Climate Change (WACC), Vietnam National University for facilitation this research work.

References

- Hartman, P., Carlucci, K., 2014. Climate Change Impact and Adaptation Study for the Lower Mekong Basin. Key final results USAID Mekong Adaptation and Resilience to Climate Change (USAID Mekong ARCC). Thailand: Bangkok. <http://icem.com.au/wp-content/uploads/2014/02/Key-Results-10pgs-lowres.pdf>.
- Jun, X.I.A., Shubo, C., Xiuping, H.A.O., Rui, X.I.A., Xiaojie, L.I.U., 2010. Potential impacts and challenges of climate change on water quality and ecosystem: Case studies in representative rivers in China. *J. Resour. Ecol.* 1, 31–35. <http://www.jorae.cn/fileup/PDF/2010010104.pdf>.
- Räsänen, T.A., 2012. Baseline hydrology of the 3S basin: Sesan-Sekong-SrepokVMod hydrological modelling report: Challenge Program on Water & Food Mekong project MK3 “Optimizing the management of a cascade of reservoirs at the catchment level”. Hanoi, Vietnam : ICEM-International Centre for Environmental Management.



Tu, J., 2009. Combined impact of climate and land use changes on streamflow and water quality in eastern Massachusetts, USA. *J. Hydrol.* 379, 268–283. <http://dx.doi.org/10.1016/j.jhydrol.2009.10.009>.

Change of water budget between 1960's and 2000's at the seasonal tropical forest in Northern Thailand

Katsushige SHIRAKI^{1,a,*}, Chatchai TANTASIRIN^{2,b} and Nobuaki TANAKA^{3,c}

Abstract Lack of the long-term observation data of rainfall and runoff at watershed, especially in tropical rainforests, prevent us from estimating the future influence for the climate change, because it is difficult to separate the degree of influence of long-term change of meteorology and runoff characteristic. We have observed rainfall and runoff at the Kog Ma D seasonal tropical forested watershed, near Chiang Mai, northern Thailand in 2000's and compared them with the previous series of rainfall and runoff observation conducted in 1960's (previous period) by the Kasetsart University researchers. It was revealed that the distributions of very thick topsoil depth make the stable base flow together with the fractured bedrock in this watershed. The stable base flow makes the stable swamp area near the weir. These constant saturated area make the quick runoff while raining. These runoff characteristics are the same among 2000's and previous observation period. Although the annual rainfall decrease in 2000's, the amount of rainfall in the dry season increase slightly. At the same time, annual runoff showed the decrease tendency. The water loss that is calculated by subtracting runoff amount from rainfall showed almost the same among 2000's and previous observation period. We could conclude that the difference of these two observation period can be summarized by the decrease of rainfall and show the commonality of the water loss and runoff characteristics.

Keywords long-term observation, runoff characteristics, annual rainfall, Kog Ma watershed, water loss.

¹Faculty of Agriculture
 Tokyo University of Agriculture and Technology
 Tokyo, Japan

^ashirakik@cc.tuat.ac.jp

²Faculty of Forestry
 Kasetsart University
 Bangkok, Thailand

^bfforct@ku.ac.th

³University of Tokyo Forests
 The University of Tokyo
 Aichi, Japan

^ctanaka@uf.a.u-tokyo.ac.jp

Introduction

It is widely announced that we are suffered from the crisis of climate change and also said that the frequency of heavy rainfall will increase. In particular, tropical forest has great impact to the global warming and also be influenced on it. Moreover, the mountainous watersheds play important roles for supplying available water to the lower land. However, there is few report that shows the actual long-term change of rainfall and runoff at the tropical mountainous watershed. One of the reason must be the difficultness to obtain the long-term rainfall and runoff data. At the Kogma D watershed, rainfall and runoff have been observed precisely from 1966 to 1984, and restarting the observation since 1997. Therefore we can compare the temporal change of rainfall and runoff simultaneously. At the same time we compare the rainfall amount among flatland (Chiang Mai city) and mountainous field (Kogma). The rainfall-runoff mechanism at the mountainous watershed have been also checked for analyzing the temporal runoff change.

Site description

Kogma D watershed (N18°49' E98°54', 1290-1440m above sea level, basin area is 8.6 ha), in the field station of the Kasetsart University, northern Thailand (Fig.1). The Kog Ma watershed is located about 10 km west from the Chiang Mai city and mountainside of the Mt. DoiPui (Fig.2). This watershed is inside of the DoiSuthep-Puinalational park. There is distinct

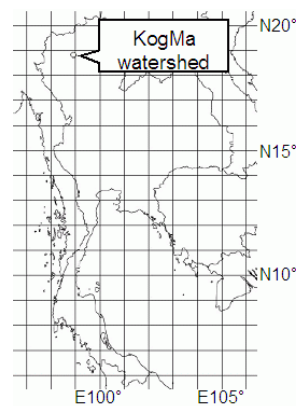


Fig.1 Location of Kogma

differentiation between wet season and dry season. Approximately, wet season begins from late April and

dry season begins from November every year (Shirakiet. *al*, 2008). The vegetation type is evergreen forest and the crown is almost closed. We judged that the forest condition have not been changing for our analyzing period, because there have been no human treatment such as thinning and planting except constructing research tower.

The rainfall data at the flatland in Chiang Mai city have been observed at the weather station (N18°47' E98°58', 314m above sea level, see Fig.2) by the Thai Meteorological Department (TMD), and situated about 10 km east of the Kogma site (Komatsu *et. al* 2010).

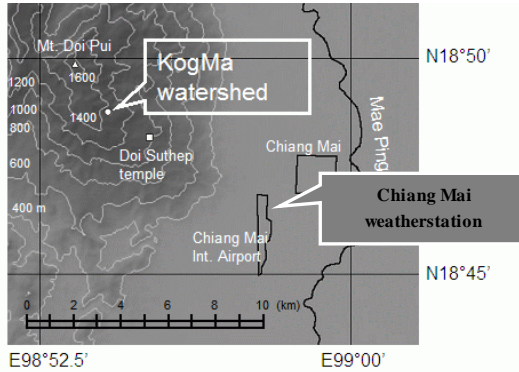


Fig.2 Location of the Chiang Mai weather station and Kogma

Observation of rainfall and runoff at the Kogma D

Stream water runoff is observed with a v-type weir by recording the water height at the weir pool at the outlet of the Kogma D (Fig.3). There are two periods of observation at this site. The 1st period was 1966-1984, and 2nd period was 1998-present. The 120 degree triangle weir have been used at the 1st period and the weir was replaced into 90 degree triangle type at the beginning of the 2nd period observation. The runoff amount is calculated from the water height with the H-Q formula that has been confirmed through discharge flow check executed manually several times. Three rain gauges have been set at an open field inside the watershed near the weir at the 1st period and one rain

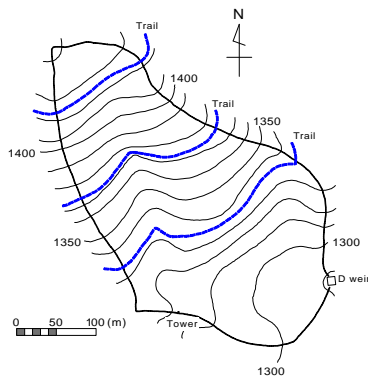


Fig.3 Topographical map of Kogma D

gauge about 30 m west of the weir with a tipping bucket type and a storage type rain gauge at the 2nd period. In this study, average of three rainfall amount were used for the analyses for the 1st period.

Rainfall and water height at the weir have been recorded every 10 minutes at the 2nd period. Runoff values are calculate by interpolating every one minute. Monthly rainfall and runoff data have been stored for the 1st period observation.

Result

1) Hydrograph and hyetograph at the Kogma D

The hydrograph and hyetograph of the year of 2001 is shown on Fig.4 for the typical example. Direct runoff was generated quickly while raining. On the other hand, very stable base flow was also generated while dry

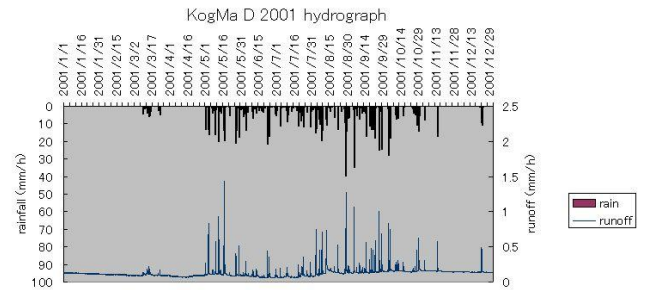


Fig.4 Example of hydro and hyetograph of Kog Ma D watershed

season.

2) Long-term rainfall change

Temporal change of annual rainfall is shown on Fig.5. Because of the effect of elevation difference, the amount of rainfall in the Kogma is always larger than those of Chiang Mai city. The range of rainfall difference is about 600 to 700 mm. By viewing the data of Chiang Mai rainfall as long-term, slight tendency of decreasing of rainfall can be observed.

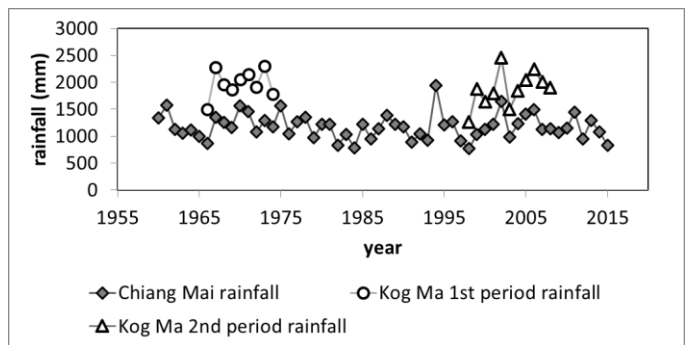


Fig.5 Temporal change of annual rainfall at Chiang Mai city and Kogma

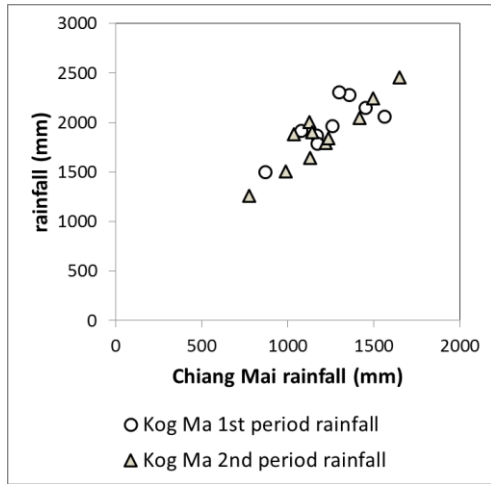


Fig.6 Relationship of annual rainfall among Chiang Mai and Kogma

There shows close relationships among Chiang Mai and Kogma rainfall, when the annual rainfall is small in the

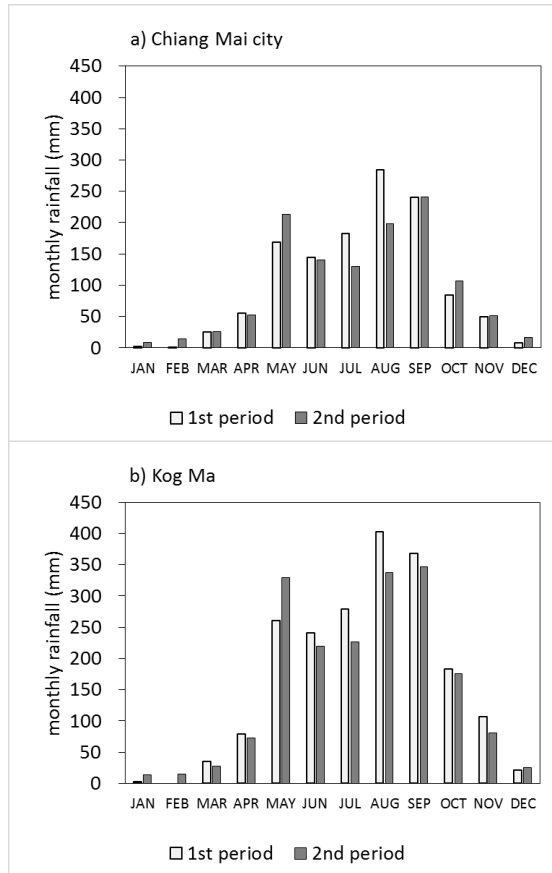


Fig.7 Monthly change of rainfall a) Chiang Mai city b) Kogma

Chiang Mai, those of Kogma also show the comparatively small amount (Fig.6).

The relationships of Chiang Mai annual rainfall and Kogma have not shown significant difference between 1st observation period and 2nd.

Monthly rainfall change between 1st period and 2nd period is shown on Fig.7. There observed almost no rainfall on January and February at the 1st period both Chiang Mai and Kogma, but small rainfall have started to be observed at the 2nd period at both sites. While the rainfall in May is significantly increased at the 2nd period, the rainfall in July and August have been decreasing at both sites.

3) Long-term water budget change

Fig. 8 and Table 1 show the change of annual water budget at Kogma watershed and change of Chiang Mai annual rainfall. The annual water loss is calculated by subtracting the annual runoff from rainfall. The water loss is composed of evaporation loss, transpiration loss from the soil surface, crown interception loss while rainfall, and deep infiltration into mountain.

Average of annual rainfall at Chiang Mai city is decreasing by 45 mm, approximately, while decrease of those of Kogma is about 100 mm from 1st to 2nd period. Average of annual runoff at Kogma is also decreasing by 100 mm in these period. Therefore, water losses at Kogma watershed show almost the same value between 1st and 2nd period.

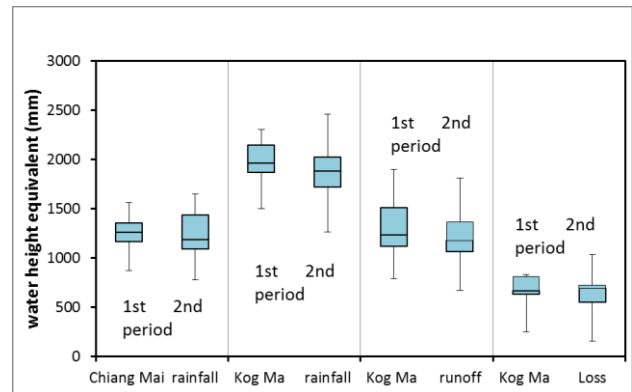


Fig.8 Water budget change at Kogma and change of Chiang Mai rainfall

Table 1 Annual change of water budget at Kogma and change of rainfall in Chiang Mai

	rainfall		runoff		loss		unit (mm)
	1st period	2nd period	1st period	2nd period	1st period	2nd period	
Chiang Mai	1246.8	1201.7					
Kog Ma	1978.9	1870.5	1329.6	1229.2	649.2	641.2	

Discussion

The long-term change of decreasing tendency of the rainfall at the Kogma watershed has been shown. Although the runoff value was decreased simultaneously, water loss has not changed.

In order to check the rainfall to runoff processes, topsoil distribution was observed by using the knocking cone penetrating device. This device can measure the topsoil depth by making the impacting of 5 kg and 50 cm free

weight drop power. The cone edge stops when it reaches bedrock and topsoil depth, the length from the surface to bedrock can be measured. The topsoil distribution is shown on Fig.9. The average topsoil depth has showed over 5 m, it was revealed that this watershed has the thick topsoil layer. And ground water table on the bedrock have hardly observed along the middle of stream line. That indicated that the bedrock layer is permeable. On the other hand, there is a stable swamp (saturated) area near the weir.

Those facts indicates the rainfall to runoff process at the Kogma D watershed shown as Fig.10. Thick topsoil layer and fractured permeable bedrock make the very slow soil water movement. These water make the stable swamp area at the lower place in the basin. The rainfall falling on the swamp produces the quick runoff while raining. The existence of these slow water movement means that watershed contains plenty of soil water. Therefore it is considered that evapo-transpiration loss has not been affected by the decreeing of rainfall because of the abundant soil water. These suggestions shows good agreement with the sap flow observation at late dry season and soil water simulation with SPAC model which resulted that the trees use the deeper soil water in this watershed (Tanaka K *et. al* 2004 or Kume T *et. al* 2007).

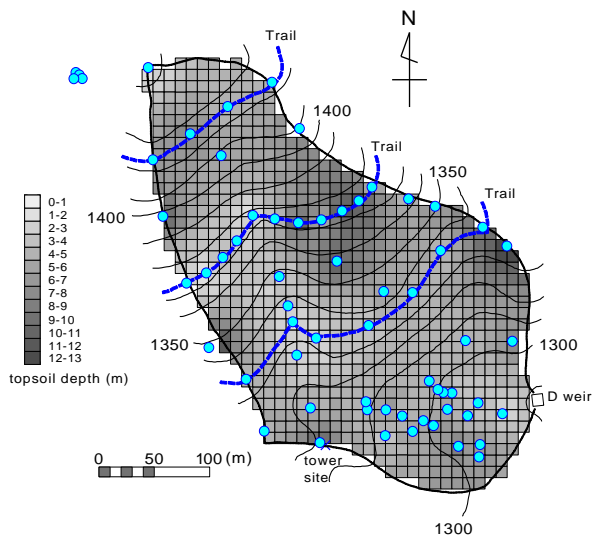


Fig.9 Distribution of topsoil depth at Kogma D watershed. Circles indicate

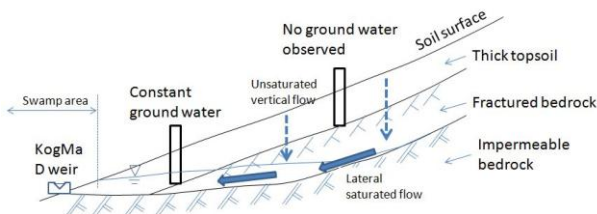


Fig.10 Chart drawing of Kogma rainfall to runoff process

Conclusion

We compared rainfall and runoff amount at two period, the first is 1960's and the second is 2000's at the mountainous watershed and low and flat land. Rainfall at the flat land has the slight decreasing tendency by these period. Annual average showed about 45 mm decrease of rainfall at flat land, while the decrease of those of mountainous field showed 100 mm. At the mountainous area, annual runoff amount also decreased 100 mm, that meant the water loss has not changed during these period.

This mountainous watershed is considered to contain much soil water at the thick topsoil layers and bedrock layers.

References

- Komatsu *Het. al* (2010). Modeling Seasonal Changes in the Temperature Lapse Rate in a Northern Thailand Mountainous Area. *Journal of Applied Meteorology and Climatology*, 49, 6, 1233-1246
- Kume T, Takizawa H, Yoshifuji N, Tanaka K, Tanaka N, Tantasirin C, Suzuki M (2007) Impact of soil drought due to seasonal and inter-annual variability of rainfall on sap flow and water status of evergreen trees in a tropical monsoon forest in northern Thailand, *Forest Ecology and Management*, 238:220-230
- Shiraki K, Takakura S, Chatchai T and Suzuki M (2008). Rainfall runoff process at the Kog Ma D watershed in northern Thailand. *FORTROPII*, proceedings.
- Tanaka K, Jianqing Xu, Takizawa H, Chatchai T, Kume T, Suzuki M (2004) The impact of rooting depth and soil hydraulic properties on the transpiration peak of an evergreen forest in northern Thailand in the late dry season, *Journal of Geophysical Research-Atmospheres*, Vol.109, D23107, doi:10.1029/2004JD004865

Stochastic Simulation and Frequency Analysis of the Concurrent Occurrences of Multisite Extreme Rainfalls

Ke-Sheng Cheng

Abstract Traditionally, hydrological frequency analyses were independently conducted at individual sites using annual maximum rainfalls. While this approach can provide useful results for site-specific design rainfall depths, it fails to offer insightful information about the return period of the concurrent occurrence of multi-site extreme rainfalls. There have been many evidences that a single major storm can result in annual maximum rainfalls of different durations at several sites, as demonstrated by the Typhoon Morakot in 2009. Thus, spatial correlation of the same-event rainfall depths at different sites plays an essential role in characterizing the concurrent occurrences of multi-site extreme rainfalls. In this study, we propose an innovative approach of multi-site storm rainfalls simulation, aiming to tackle the problem of frequency analysis of multi-site extreme rainfalls. The approach is composed of four major components: (1) delineating homogeneous regions within the study area using K-means cluster analysis, (2) standardizing and modeling the same-event rainfall depths at different sites by a Pearson Type III random field, (3) stochastic simulation of multi-site storm rainfalls using a covariance matrix conversion algorithm, and (4) determining the return periods of concurrent occurrences of multi-site extreme rainfalls. Using historical hourly rainfall records available at 25 rainfall stations in southern Taiwan, site-specific rainfall depths of different durations and return periods of this study were found to be very close to results of a previous study of single-site frequency analysis, indicating good applicability of the proposed approach. Additionally, the return period of four specific sites within the Kao-Ping River Basin (Shan-di-men, Ah-li, Jia-sian and Chi-shan) exceeding 1000 mm rainfalls in a 24-hour period, a scenario similar to rainfalls of Typhoon Morakot, was found to be only 514 years, as oppose to more than 2000 years or even higher by other previous studies.

Keywords *Stochastic simulation, Multi-site extreme rainfalls, Frequency analysis, Semi-variogram modeling, K-means cluster analysis*

Ke-Sheng Cheng
Dept. of Bioenvironmental Systems Engineering
National Taiwan University
Taipei, Taiwan
rslab@ntu.edu.tw

Introduction

Rainfall extremes of certain design durations and return periods are essential elements in hydrological design. Traditionally, such rainfall extremes are required at individual rainfall stations and are determined by single-site frequency analysis. However, there have had many evidences that a major storm in Taiwan (such as Typhoon Morakot of 2009) can result in extreme rainfalls at several neighboring stations and the return period of such concurrent occurrences of multi-site rainfall extremes cannot be determined by single-site frequency analysis. A unique feature of the concurrent occurrences of rainfall extremes is the significant spatial correlations among rainfalls of different stations. Taiwan has experienced increasing intensity, longer duration, and more extensive rainfall extremes of typhoons in recent years. Thus, it is due necessary for hydrological frequency analysis considering concurrent occurrences of multi-site rainfall extremes. In this study, we propose a new stochastic approach for simulation of event-specific multi-site maximum rainfalls with respect to certain design durations. The proposed approach is capable of generating large number of realizations of multi-site typhoon rainfalls which can then be used for multi-site frequency analysis of rainfall extremes.

Study area and data

Forty-six years of hourly rainfall data available at twenty-five rainfall stations in southern Taiwan were collected (Figure 1). Since almost all long-duration (longer than 12 hours) rainfall extremes were produced by typhoons, we firstly extracted hourly rainfall series of individual typhoon events at different rainfall stations. From these data, event-maximum rainfalls of 8 design durations (1, 2, 6, 12, 18, 24, 48 and 72 hours) of individual typhoons at all rainfall stations were obtained. Event-maximum rainfalls at individual stations were then standardized with respect to their long term averages and standard deviations. These duration-specific standardized event-max rainfalls have zero expectation and unit variance and their spatial variations were modeled as a Pearson type III random field.

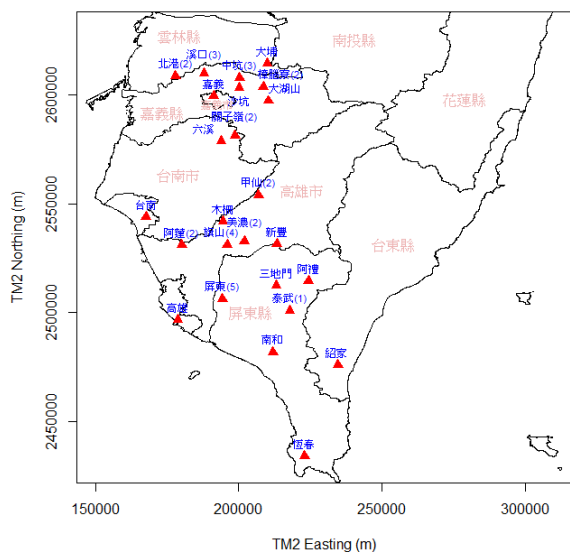


Figure 1. Rainfall stations used in this study.

Methodology

Standardized event-maximum rainfall (SEMR) at different stations were modeled by a Pearson type III (PT3) random field with marginal density of zero expectation and unit variance. Parameters of the marginal PT3 density at individual stations were estimated using the method of L-moments. Regional parameters were then calculated as the sample-size weighted average. Spatial covariance structure of SEMR is modeled by variogram analysis. An exponential semi-variogram model was used to fit the experimental variograms of SEMR of various design durations. Spatial covariance (correlation) function is then derived from the semivariogram. Stochastic simulation of the PT3 duration-specific SEMRs were conducted by transforming the PT3 random field (X) to a corresponding standard Gaussian random field (Z). Stochastic simulation of standard Gaussian random field was conducted by sequential Gaussian simulation (Liou et al., 2012; Hsieh, et al., 2014). Finally, the SEMRs were calculated through a frequency factor conversion. The event-maximum rainfalls at individual stations were then obtained by statistical denormalization of SEMRs using the station-specific means and standard deviations of event-maximum rainfalls.

Results and discussion

For each of the eight design durations, a total of 10,000 realizations of multi-site event-maximum rainfalls were generated by the proposed stochastic simulation approach. On average, the study area experiences 2.44 typhoon events every year. A major advantage of the stochastic simulation approach presented in this study is its capability of characterizing the concurrent occurrences of rainfall extremes at different stations. Such capability enables the approach to offer an estimate of the return period for a multi-site extreme event. This is demonstrated using the 24-hour extreme

rainfalls observed at several stations within the Kao-Ping River Basin during the Typhoon Morakot. Four rainfall stations within the Kao-Ping River Basin observed near or higher-than 1000 mm rainfall depths in a 24-hour period during Typhoon Morakot. Assuming a multi-site extreme event having higher-than 1000 mm rainfalls at the four stations, we found 8 out of the 10,000 simulated events met the requirements. It is equivalent to a return period of approximately 512 ($\approx 10,000/8/2.44$) years.

Conclusions

Concurrent occurrences of rainfall extremes at several rainfall stations are commonly observed in Taiwan. The multi-site stochastic simulation approach proposed in this study is capable of generating realizations of multi-site event-maximum rainfalls with respect to given design durations. Such realizations preserve not only the marginal densities but also the spatial correlation structure of the duration-specific event-maximum rainfalls. We also demonstrate that the proposed approach can be applied to estimation of the return period of multisite rainfall extremes.

References

- Cheng, K.S., Hou, J.C., Liou, J.J., Wu, Y.C., Chiang, J.L., 2011. Stochastic Simulation of Bivariate Gamma Distribution – A Frequency-Factor Based Approach. *Stochastic Environmental Research and Risk Assessment*, 25(2): 107 – 122, DOI 10.1007/s00477-010-0427-7.
- Liou, J.J. Su, Y.F., Chiang, J.L., Cheng, K.S., 2011. Gamma random field simulation by a covariance matrix transformation method. *Stochastic Environmental Research and Risk Assessment*, 25(2): 235 – 251, DOI: 10.1007/s00477-010-0434-8.
- Hsieh, H.I., Su, M.D., Cheng, K.S., 2014. Multisite Spatiotemporal Streamflow Simulation - With an Application to Irrigation Water Shortage Risk Assessment. *Terrestrial, Atmospheric, Oceanic Sciences*, 25(2): 255-266.

Climate Extremes, People's Perception and Adaptation in Lower Songkhram River Basin, Thailand

Pisinee Bariboon^{1,a *}, Sangam Shrestha^{2,b}

Abstract There is a growing concern on the impacts of climate change and climate variability on water resources, agriculture, fisheries, and consequently livelihood of local people in Lower Songkhram River Basin of Thailand. Thus, it is important to examine the people's perceptions on climate change and climate variability and its impact on their livelihood. In addition, this research will help the policy makers to scale up innovative adaptation measures by study the local people adaptation. As a result, the objectives of this study are to analyze the recent and future trend in hydro-climatic and water quality, to examine the level of people's perception of climate change and climate variability at the household level, and study the people adaptation strategies against the climate change impacts on water availability and agriculture production. The trends of climate data have been calculated by Mann-Kendall test and Sen's slope. In part of precipitation indices, it shows significant trends in six indices from seven indices but different station in recent trend. Mostly, there are significant trends under RCP8.5 during 2055 s. For RCP4.5, there are trends only in Sakon Nakhon province. In part of temperature indices, it shows significant trends in some indices in recent trend. For the future trend, mostly have significant trend under RCP8.5 during 2085 s. Moreover, there are some trends lightly in another future period. To understanding the rural farming community's perception of climate change impacts on their socio-economic activities and environment, their adaptation at the household level and opinions on government mitigation measures. This study is based on both primary and secondary data collected via a survey of 25 households in three villages. The results show that people can perceive the change in rainfall and temperature but they cannot perceive the change in season. In terms of adaptation options, there is government came to give a recommendation to local people about the change of weather and climate, but not every people can get that. Finally, results will show local people perceive climate change acutely and respond to it, based on their own indigenous knowledge and experiences. It is expected that this study will help policy makers to develop more appropriate adaptation policies in Lower Songkhram River Basin.

Keywords *Climate change, RCLimdex, Trend Analysis, People's Perception, Adaptation, Lower Songkhram River Basin, Thailand*

Pisinee Bariboon

Department of Water Engineering and Management
Asian Institute of Technology
Pathumthani, Thailand
b.pisinee@gmail.com

Sangam Shrestha

Department of Water Engineering and Management
Asian Institute of Technology
Pathumthani, Thailand
sangamshrestha@gmail.com

Introduction

Climate change and variability, its impacts and vulnerabilities are growing concern worldwide. The climate of the Lower Songkhram River Basin (LSRB) is changing and it is becoming more unpredictable every year. Hazards like floods and droughts, which are aggravated by climate change and its variability being experienced more frequently in LSRB than ever before. As the great majority of the people in this area is depends on agriculture and fisheries for their livelihood, crop agriculture in this region is highly susceptible to variations in the climate system. It is anticipated that crop production would be extremely vulnerable under climate change scenarios. For this reason, the food security of the region will be at risk. Furthermore, climate change may affect agriculture and water resources. This will decrease the amount of water, affect agricultural production, particularly rice, the main crop and requires a certain amount of water, sunlight, soil moisture, and temperature to some extent (Thailand Environment Foundation, 1998).

Hydrometeorological time series (floods, droughts, heat waves, etc.) include recent trends, especially over the past 30 years, as a result of climate change impact according to the Intergovernmental Panel on Climate Change (IPCC). If climate change is not taken into account, then such changes or variability can lead to underestimation/overestimation of parameters for the design and operation of water infrastructures, water shortages, water stresses, and agricultural failures.

Scientific studies projects a global increase in the frequency and impact of climate related natural disasters, a trend that is likely to continue as climate change increases the threat of disasters such as droughts and floods (IPCC, 2012).

The sector therefore needs better support from policy makers, service providers, and development agencies to remain the engine for rural development. Analysis of climate trends in relation to regional production sectors such as crops using available scientific tools would create opportunities to incorporate relevant adaptation measures from the planning stages. This study will help the policy makers to scale up innovation and adaptation measures people are practicing in response to climate change and climate variability.

In conclusion, the impacts of climate change and variability on poor communities are varying greatly. But in general, climate change is superimposed on existing vulnerabilities. Climate change will further reduce access to drinking water, negatively affect the health of poor people, and will pose a real threat to food security in many countries.

Study area

The Songkhram River Basin, located in northeast Thailand. The basin area is 13,081 km² and mainstream flows is 420 km from the western Phu Pan Mountains in Sakon Nakhon province through Udon Thani province before reaching the Mekong River at Ban Chaiburi and Nakhon Phanom province. Along most of its lower reaches it meanders over an extensive floodplain at an altitude of between 145 and 160 meters above sea level and a gentle gradient of about 1:30,000 (Blake & Pitakthepsombut, 2006). The water from Mekong River which causes supplementary water of Songkhram River in the wet season to be very spatially and temporally as well as wetlands season in the basin.

The Lower Songkhram River Basin covering an area of 3157.73 km², it is 24% approximately of Songkhram River Basin. This basin includes parts of twelve districts in three provinces, namely:

Bung Kan Province – Bung Khong Long, Phon Charoen, and Seka

Nakhon Phanom Province – Ban Paeng, Na Thom, Phon Sawan, Si Songkhram, and Tha Uthen

Sakon Nakhon – Akat Amnuai, Ban Muang, Kham Ta Kla, and Wanon Niwat

The Lower Songkhram River Basin (Figure.1) experiences a tropical, semi-arid climate, with three distinct seasons. This area has more serious droughts in sunny season and more floods in rainy season. There are six to seven rainy season months (May-October). The rainy season normally peaks in August to September, when floods reach their maximum extent. The cool season extends from November to February and it marked by generally dry and cool air from the northeast monsoon. Minimum temperatures rarely fall below 12°C

in the cool season. The hot season extends from March to mid or late May, if the rains arrive late. The early part tends to be very dry and warm, marked by occasional thunderstorms, and as maximum daytime temperature climb to over 40°C by mid to late April, the intensity, and frequency of thunder showers increase. The annual evaporation rate ranges from 100 to 165 mm.

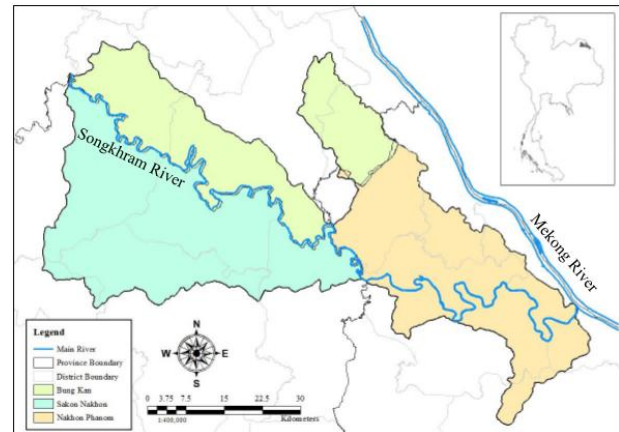


Fig. 1 Lower Songkhram River Basin

The Lower Songkhram wetland is a permanent flood plain with freshwater swamp forests, marshlands, and small streams. The swamp forests provide livelihoods for people living in this area by over 120,000 people. It is the important sources for wastewater dilution, recreation, raw water for municipal water supply, agriculture, and aquaculture, contains rich biodiversity that includes over 180 species of fish, more than 100 species of birds and vegetation, countless species of amphibians, reptiles and invertebrates associated with the wetlands and provides habitat for the globally significant and critically endangered Mekong Giant Catfish. Major economic activities at present include paddy rice farming, fishery, and field crops e.g. corn, cassava, sugarcane, and soybean. Moreover, at present the eucalyptuses and rubber plantation to be varying spatially which cause reduced wetland area in Songkhram River Basin.

The wetland is important not only for the sustenance that it provides area communities but it is also important for its biodiversity and providing feeding grounds for birds traveling along the East Asian-Australasian flyway. A management plan is in place for wise use of the site but currently does not include water usage. Furthermore, The LSRB is one of the wetland area in Thailand which has strong of climate change, so the study on climate change condition is helpful at the moment.

Methodology

Bias correction: Linear scaling method

The linear scaling approach aims to perfectly match the monthly mean of corrected values with that of observed

one. It operates with monthly correction values based on the differences between observed and raw data (Lenderink, et al., 2007). Precipitation is typically corrected with a multiplier and temperature with an additive term on a monthly basis;

$$P_{cor,m,d} = P_{raw,m,d} \times \frac{\mu(P_{obs,m})}{\mu(P_{raw,m})}$$

$$T_{cor,m,d} = T_{raw,m,d} + \mu(T_{obs,m}) - \mu(T_{raw,m})$$

where $P_{or,m,d}$ are corrected precipitation on the d th day of m th month

$T_{cor,m}$ are corrected temperature on the d th day of m th month

$P_{raw,m}$ are the raw precipitation on the d th day of m th month

$T_{raw,m}$ are the raw temperature on the d th day of m th month

μ represents the expectation operator

RCP scenarios

This study considered RCP4.5 and RCP8.5 under ECHAM6. The RCP4.5 and RCP8.5 are named after a possible range of radiative forcing values in the year 2100 relative to preindustrial values +4.5 and +8.5 W/m², respectively. RCP4.5 peak around 2040, then downwards. In contrast, RCP8.5 continue to rise throughout the 21st century.

Survey methodology

The results from hydro-climatic trend analysis will show a change of climate change parameters. From the results of the previous step is coming from a computer model, not from people. Therefore, balancing people’s perception with scientific evidence for climate change provides important insights into climate change impacts and the way people respond to it while simultaneously guiding future climate change adaptation processes (Kuruppu & Liverman, 2011). Furthermore, evaluation of people’s perception using available physical data confirms the results in rainfall and temperature.

Questionnaire design

The questionnaire design is one of the effective instruments of data collection. It is primary data (Quantitative data) which are to be collected for the first time and generated to meet specific requirements of investigation at hand. This survey refers to the method of securing information concerning a phenomenon under study from all and produce information that is inherently statistical in nature.

For this study will use both of “open-ended question” and “close-ended question”. The selection of survey mode depends on the topic, local feasibility, goal, and budget of the study. In order to allow the

investigator to collect the most accurate data from a target population, a questionnaire must be unbiased.

A questionnaire can obtain information about what people do, what they have, what they think, know, or feel. Knowledge questions offer choices such as correct vs. incorrect or accurate vs. inaccurate. Opinions questions refer to psychological states which the perceptions people hold, their thoughts, feelings, ideas, judgments, or ways of thinking. Questions on behavior ask people what they have done in the past, or do now. For the attribute questions will ask about person’s personal or demographic characteristics (age, education, or occupation) and ask people about who they are, rather than what they do.

To write meaningful questions, be clear about the objectives of this study and type of information desired. The information is about knowledge, opinions, behavior, and attributes. The words used in the questions should be simple, familiar and unsuspected to the target population. The length of the questionnaire should be short in order to avoid response fatigue and skipping questions tendencies. Pay careful attention to the wording. On the contrary, questions about knowledge, behaviors and attributes are more straightforward. Furthermore, the questionnaire may elicit opinions when the actual intent is to document behavior.

Results and discussion

Precipitation indices

In this study, seven precipitation indices were done using RCLimdex that shows a significant trend for six extreme climate indices: consecutive wet days (CWD), number of very heavy precipitation days (R20mm), very wet days (R95p), extremely wet days (R99p), maximum 1 –day precipitation amount (RX1day), and maximum 5 –day precipitation amount (RX5day). These results are separate in two parts which are recent period and future period.

Recent trend of precipitation indices

The recent trend of precipitation indices was analyzed from 1976-2010. Most of the indices in Bung Kan and Sakon Nakhon province shows a significant trend. Nakhon Phanom province is only one station which has one index shows a significant trend.

The consecutive wet days (CWD) index shows decreasing trend in Bung Kan province. This index has a range of 3-67 days. The lowest number of consecutive wet days is in 1988 with a total of 3 days, while the greatest number of consecutive wet days is in 1985 with a total of 67 days.

The annual frequency of very heavy rainfall (R20mm) index show increasing trend in Bung Kan, Nakhon Phanom, and Sakon Nakhon province. This index has a range from 4 to 56 days. The lowest number

of days is in Bung Kan province with a total number of 4 days in 1977 while the highest number of days is at the same point with a total number of 56 days in 2008.

The number of very wet days (R95p) and the number of extremely wet days (R99p) indices are used to measure heavy precipitation that exceeds the 95 and 99 percentile thresholds. This index shows a significant trend in Bung Kan and Sakon Nakhon province. The number of very wet days index show increasing trend and the number of extremely wet days index also show an increasing trend in Bung Kan and Sakon Nakhon province. Bung Kan province is the highest number of very wet days and extremely wet days, which is 1290.9 mm and 529.0 mm, in 2001.

The monthly maximum 1 –day precipitation (RX1day) index shows the highest amount of precipitation in a single day of each year. This index show increasing trend in Bung Kan and Sakon Nakhon province. This index has a range from 25.5 to 201.4 mm. The lowest number is in 1977 and the highest number is in 1994, in Sakon Nakhon province.

The monthly maximum consecutive 5 –day precipitation (RX5day) index shows the increasing trend in Bung Kan and Sakon Nakhon province. This index has a range from 71.0 to 380.5 mm. The lowest number is in Sakon Nakhon province with a total number of 71.0 mm in 1977. The highest number is in Bung Kan province with a total number of 380.5 mm in 1997.

Future trend of precipitation indices

The future trend of precipitation indices was analyzed from 2011-2100 by divided into three parts as 2025s, 2055s, and 2085s. There is no evidence that there is a trend for any indices during 2025s. Moreover, during 2055s and 2085s, there are increasing significant trends in a number of very heavy precipitation days (R20mm), very wet days (R95p), extremely wet days (R99p), maximum 1 –day precipitation amount (RX1day), and maximum 5 –day precipitation amount (RX5day).

The annual frequency of very heavy rainfall (R20mm) index shows the increasing trend in Nakhon Phanom province. This index has a range from 25 to 51 days for 2055s under RCP8.5. The lowest number of days is in 2048 and the highest number is in 2067.

The number of very wet days (R95p) index shows the increasing trend in Bung Kan and Sakon Nakhon province, during 2055s under RCP8.5. This index has the lowest number is 53.8 mm in Sakon Nakhon province, in the year 2050. The highest number of this index is 625.9 mm in Bung Kan province, in the year 2066.

The number of extremely wet days (R99p) index shows the increasing trend in Nakhon Phanom province during 2055s under RCP8.5. The highest number is 604.1 mm in 2052. During 2085s under RCP4.5, there is an increasing trend for Sen’s slope estimator with 4.411 mm/year in Sakon Nakhon province. The highest number is 534.8 mm in 2094.

The monthly maximum 1 –day precipitation (RX1day) index shows the increasing trend in Sakon Nakhon province during 2085s under RCP4.5. This index has a range from 52.2 to 345.7 mm. The lowest number is in 2082 and the highest number is in 2094.

The monthly maximum consecutive 5 –day precipitation (RX5day) index shows the increasing trend in Sakon Nakhon province during 2055s under RCP4.5, and during 2085s under RCP4.5. This index has a range of 91.5 in 2043 and 1102.2 mm in 2051 from 2055s under RCP4.5. Moreover, during 2085s under RCP4.5, it has a range of 121.5 mm in 2082 and 350.6 mm in 2094.

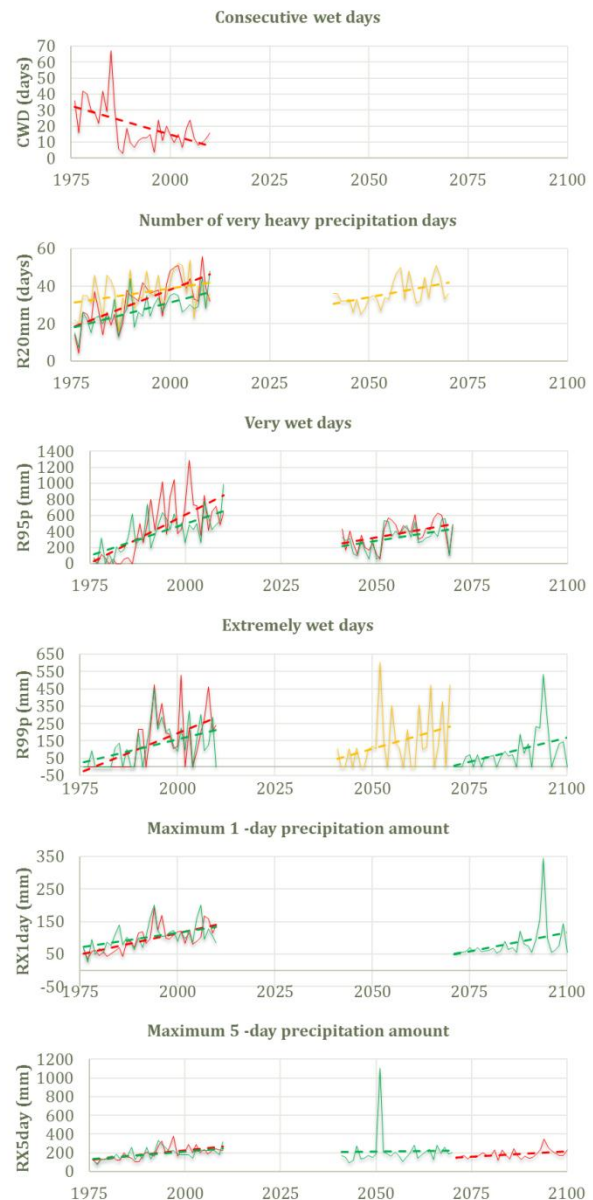


Fig.2 The graph shows trends in each precipitation indices where the red line is Bung Kan province, yellow line is Nakhon Phanom province, and green line is Sakon Nakhon province.

Temperature indices

In this study, seven temperature indices were done using RClimdex that shows a significant trend for six extreme climate indices: warm nights (TN90p), coolest night (TNn), hottest night (TNx), warm days (TX90p), hottest day (TXx), and warm spell duration indicator (WSDI).

Recent trend of temperature indices

The percentage of days when TN>90th percentile (TN90p) index shows the increasing trend in Bung Kan province and Sakon Nakhon province. This index has a range from 2.45 to 35.87%. The lowest percentage is in Sakon Nakhon province in the year 1976. The highest percentage is in Bung Kan province in the year 2010.

The percentage of days when TX>90th percentile (TX90p) index shows the increasing trend in Bung Kan, Nakhon Phanom, and Sakon Nakhon province. This index has a range from 1.61 to 36.10%. The lowest percentage is in Bung Kan province in the year 1976. The highest percentage is in Sakon Nakhon province in the year 1998.

The warm spell duration indicator (WSDI) index shows 0 days/year for Sen’s slope estimator in Bung Kan province. Accordingly, there is no evidence that there is a trend for this index in any situation.

Future trend of temperature indices

The percentage of days when TN>90th percentile (TN90p) index shows the increasing trend during 2025s under RCP4.5 in Nakhon Phanom and Sakon Nakhon province. Including an increasing trend during 2055s under RCP8.5. Also, during 2085s under RCP8.5 in Bung Kan, Nakhon Phanom, and Sakon Nakhon province. The highest values during 2025s under RCP4.5 in Sakon Nakhon province in the year 2040. For 2055s under RCP8.5, this index has a range from 0.65 to 74.46%, which are in Nakhon Phanom province in the year 2056 and Sakon Nakhon province in the year 2059.

The monthly minimum value of daily minimum temperature (TNn) index shows the increasing trend in Sakon Nakhon province during 2055s under RCP8.5. This index has a range from 8.48 to 15.48°C. The lowest values are in 2065 and the highest values are in 2067.

The monthly maximum value of daily minimum temperature (TNx) index shows the increasing trend in Bung Kan, Nakhon Phanom, and Sakon Nakhon province during 2085s under RCP8.5. This index has a range from 28.89 to 36.85°C. The lowest value is in the year 2073, the highest value is in the year 2098. Both of values is in Nakhon Phanom province.

The percentage of days when TX>90th percentile (TX90p) index shows the increasing trend during 2085s under RCP8.5 in Bung Kan, Nakhon Phanom, and Sakon Nakhon province. This index has a range from 15.72 to 159.05%. The lowest percentage is

in Nakhon Phanom province in the year 2072. The highest percentage is in Bung Kan province in the year 2092.

The monthly maximum value of daily maximum temperature (TXx) index shows the increasing trend during 2085s under RCP8.5 in Bung Kan, Nakhon Phanom, and Sakon Nakhon province, respectively. The lowest value of this index is 38.70°C in Sakon Nakhon province in this year 2073. The highest value of this index is 47.75°C in Bung Kan province in the year 2098.

The warm spell duration indicator (WSDI) index shows the increasing trend in every province during 2085s under RCP8.5. This index has the highest values is 134 days in Nakhon Phanom province in the year 2092.

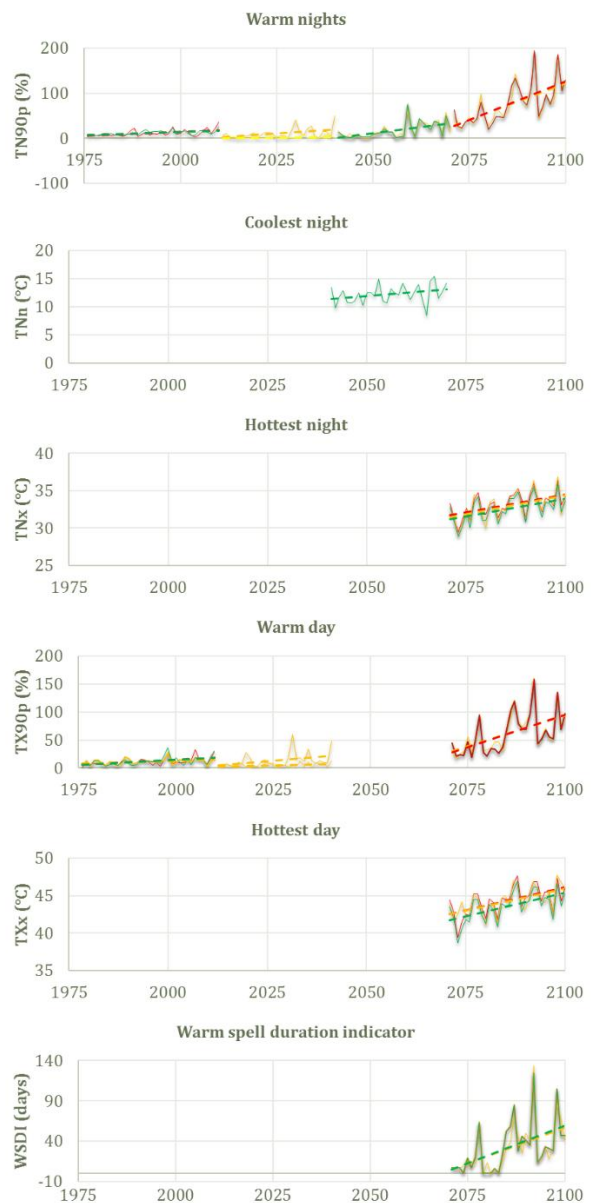


Fig.3 The graph shows trends in each temperature indices where the red line is Bung Kan province, yellow

line is Nakhon Phanom province, and green line is Sakon Nakhon province.

People’s perception on climate change

These three villages are near the Khong river. Every activity in Lower Songkhram and Khong river are related to each other. Climate change is not a new thing for people in this area. There is much organization came to this area for developing water use management plan because this area is benefitted to local communities and improve ecosystem connectivity from the tributaries to the Khong river.

The results from field survey shown that all of the people in Ban Had Paeng have perceived climate change in their area. In Ban Pak Yam, people have perceived climate change 88.89% in their area. On the other hand, Ban Tan Pak Nam got the lowest value of perceived climate change, which is 66.67%. For all the results, it appeared that respondents have perceived climate change.

Table 1. People’s perceived on climate change

	No		Yes		WAI score	Overall assessment
	N	%	N	%		
Ban Pak Yam	1	11.11	8	88.89	88.89	People perceive climate change
Ban Had Paeng	0	0.00	7	100.00	100.00	
Ban Tan Pak Nam	3	33.33	6	66.67	66.67	
Average	1.33	14.81	7	85.19	85.19	

(Source: Field survey, 2016)

People’s perception on rainfall

In last 5-10 years, respondents think the rainfall are becoming less frequent. However, the percentages of respondents who think the rainfall are becoming more frequent in Ban Pak Yam are higher than Ban Had Paeng and Ban Tan Pak Nam. Results can be like this because Ban Pak Yam may in the upper part than another two villages.

Table 2. People’s perceived in rainfall

	More		No difference		Less		Don’t know		WAI score
	N	%	N	%	N	%	N	%	
Ban Pak Yam	2	22.22	0	0.00	5	55.56	2	22.22	66.67
Ban Had Paeng	0	0.00	1	14.29	5	71.43	1	14.29	78.57
Ban Tan Pak Nam	0	0.00	0	0.00	8	88.89	1	11.11	88.89
Average	0.67	7.41	0.33	4.76	6	71.96	1.33	15.87	78.04

(Source: Field survey, 2016)

People’s perception on temperature

From the field survey, the temperature is becoming higher in last 5-10 years. On the other hand, 55.56% in Ban Tan Pak Nam cannot perceive the changes of temperature. Respondents said not only in summer which has a high temperature but in winter is strongly cold likewise. Small wonder that temperatures are become more extremes nowadays.

Table 3. People’s perceived in temperature

	More		No difference		Less		Don’t know		WAI score
	N	%	N	%	N	%	N	%	
Ban Pak Yam	6	66.67	2	22.22	1	11.11	0	0.00	83.33
Ban Had Paeng	5	71.43	2	28.57	0	0.00	0	0.00	85.71
Ban Tan Pak Nam	3	33.33	1	11.11	0	0.00	5	55.56	38.89
Average	4.67	57.14	1.67	20.63	0.33	3.70	1.67	18.52	69.31

(Source: Field survey, 2016)

Adaptation Strategies

Adaptation to climate change may include many measures. One of these is policy reform to adapt to climate change. Individuals, households, government, or any stakeholders can implement effective adaptation strategies to adjust the climatic variations and uncertainties based on the resources availability and social conditions.

Assessments of Impacts and Adaptations to Climate Change has given general recommendations to adapt to climate change: 1) adapt currently, 2) make favorable situation to enable adaptation, 3) incorporate adaptation with development, 4) increase awareness and knowledge level, 5) strengthen institutions, 6) safe guard natural resources, 7) provide financial assistance, 8) involve those at risk, and 9) use location specific strategies. As a step forward in the process of adaptation to climate change financial resources need to be strengthened, natural resources need to be protected and adaptation needs to be integrated with development (Leary, et al., 2007)

Climate change is already making itself felt across Lower Songkhram River Basin and the rest of the world. Extreme weather events are becoming more frequent or more intense, causing loss of life, and damaging economic infrastructure. To study adaptation options in this study area, questionnaire surveys were used. Furthermore, given the paradox between views of present day helplessness and historical adaptability, it is vital to investigate how exposure to climatically driven changes in the environment can affect both its use and people’s livelihoods. An investigation is framed to enhance understanding of how societies may adapt to future climate change. Moreover, progressing understanding of both the science of climate change and societal responses in fraught with theoretical, conceptual and empirical challenges.

The recent expansion of para rubber is an example of the adaptive capacity of both government agencies and of local people. Para rubber has been strongly promoted by provincial agriculture agencies and has attracted considerable interest from local people. In this study has one person who is para rubber planter, he has this occupation as a minor occupation. It can say that para rubber is becoming more popular in a few years after this.

Summary and conclusions

Lower Songkhram River Basin is an important branch of the Mekong River in Northeast of Thailand. Agriculture is important for this area. Most people do

farming, fishing, and the occupations which are not related to weather/climate. From questioned, people can perceive the change of season, rainfall, and temperature. Local people graduated from primary school and they can do agriculture from their skills which are from their parents or observing and remembering. However, adaptation options from suggested of government cannot use in this area because the constraints of money.

Trend analysis shows the change of extreme events: rainfall, maximum temperature, and minimum temperature. The extreme event analysed under this study have represented the trends in seven annual extreme indices for rainfall and seven annual extreme indices for temperature in Lower Songkhram River Basin. The analyzes have been carried out for three rainfall stations, and three meteorological stations, for a period between 1976-2010, which characterizes a long-term period which represents the occurrence, frequency, and changes of the events were significant or not. In addition, a period between 2011-2100 was analyzed as same as the recent period below to represents the trends in the future.

Mostly, there is a significant increase, only for consecutive wet days during 1976-2010 in Bung Kan province is decreased. The indices which show the significant increase are same in three stations are the annual count of days when rainfall ≥ 20 mm, and warm days. In shorts, those trends are the same as local people said. It means local people can perceive the change of temperature and rainfall.

Adaptation options in these areas are various. Local people can use local wisdom to relieve the change of climate. For example, change the crop calendar, change an occupation, or have a variety of occupation which can get income in every month. This area is an area for researching because it is an abundant wetland. Many researchers came to do research and develop this area at the same times.

There have government came to this study area for a survey about people livelihood and suggest them how to adapt to the change of climate. Local people said not every people can do as the government suggested. The problem is money. People have to spend too much money if they would like to follow government's suggestion. With this reason, local people are group together and find the best way to adapt themselves to the change of environment. Lack of education is not a big issue; they can continue improving even they are not graduated in high school.

Acknowledgement

I would like to thank Thailand Development Research Institute (TDRI) and International Development Research Center (IDRC) to providing student research grants for this research according to the research project named “Improving Flood Management Planning in Thailand”. My sincere thanks also goes to local people in Ban Pak Yam, Ban Had Paeng, and Ban Tan Pak Nam, where is the study area for questionnaire surveys.

Also, great thanks to all World Wide Fund for Nature (WWF) team, who supported a convenience way to contact to local people. Of course, this acknowledgement would no be complete without sincere gratitude to a beloved and deep respect my family, who gave me a good education and always supportive patient to make my study complete successfully in AIT.

References

- Blake, D. J., & Pitakthepsombut, R. (2006). *Situation Analysis Lower Songkhram River Basin, Thailand*. Bangkok, Thailand: Mekong Wetlands Biodiversity Conservation and Sustainable Use Programme.
- Kuruppu, N., & Liverman, D. (2011). Mental preparation for climate adaptation: The role of cognition and culture in enhancing adaptive capacity of water management in Kiribati. *Global Environmental Change*, 21(2), 657-669.
- Leary, N., Adejuwon, J., Barros, V., Batimaa, P., Biagini, B., Burton, I., . . . Wehbe, M. (2007, May). A Stitch in in Time: Lessons for Climate Change Adaptation from the AIACC Project. *AIACC Working Paper No. 48*.
- IPCC. Climate Change. (2012) — Managing the Risks of Extreme Events and Disasters to Advance Climate Change Adaptation (SREX). A Special Report of Working Group I and II of the intergovernmental Panel on Climate Change. Field, C. B., V. Barrors, T. F. Stocker, D. Qin, D. J. Dokken, K. L. Ebi, M. D. Mastrandrea, K. J. Mach, G-K. Plattner, S. K. Allen, M. Tignor, and P. M. Midgley (eds.). Cambridge Univ. Press, Cambridge, UK, and New York, NY, USA.
- Thailand Environment Foundation. (1998) Reporting policies and strategies under Climate Change for Thailand. URL : http://ebooktei.org/document/HTML/123_HFR-123.html

Assessment of Water Resources During the 21st Century in Northern Thailand with Focus on Ping River Basin

Srisunee Wuthiwongyothin^{1,a,*}, Su-Hyung Jang^{2,b}, Kei Ishida^{3,c} and M. Levent Kavvas^{4,c}

Abstract The effects of climate change on the hydrology and water resources of the upper Ping River basin, Thailand are assessed by utilizing the IPCC SRES-climate scenarios during the 21st century from the ECHAM5 and the CCSM3 global climate model (GCM). The hydrologic response of streamflow in the upper Ping River basin to the climate change is performed under A1B, A2 and B1 with total 12 projections. The Watershed Environmental Hydrology-Hydro Climate Model (WEHY-HCM) is used to perform dynamical downscaling from the global atmospheric scale (~200 km) to the regional atmospheric scale over the study basin via the MM5 regional atmospheric model at 9 km grid resolutions and hourly time intervals. The watershed module then couples the atmospheric and the land surface hydrology processes with its physically based model feather, and simulates the watershed flows. The Global Climate Model (GCM)-historical control runs (1971 to 2000) were downscaled, corrected for their bias, and tested for the models' performance by a goodness of fit of model and observed flow via cumulative distribution functions. From the established GCMs' reliability in producing future climate variables, the future hydrologic flows of the study area can be generated and the effects of the climate change can be studied. Based on the ensemble average of 12 realizations, the results (2016-2099) show that toward the end of the 21st century, future projected flows yield a significant upward trend with 95% confidence level. The study basin will have a streamflow increase of 17.3% (6.36 billion m³) on average, compared to the average flows from 1988 to 2015 (5.24 billion m³). This key model results show that the projected flows under the future climate change conditions are changing, and this change will directly affect the hydrology and water supply of the upper Ping River basin and the Bhumibol Dam. Thus, the need for newly adjusted water policies and management options must be investigated further in more detail due to the effect of climate change conditions.

Keywords *Climate change, Global Climate Models, Dynamical downscaling, Ping basin, Bhumibol Dam*

^aCivil Engineering, Burapha University, Saen Suk, Chonburi, Thailand. E-mail: srisunee.wu@eng.buu.ac.th

^bSenior Researcher, Korea Institute of Water and Environment, Korea Water Resources, Deajeon, Korea.

^cManager, Hydrologic Research Laboratory, UC Davis, CA, USA. Email: kishida@ucdavis.edu

^dDistinguished Professor, Civil and Environmental Engineering, UC Davis, CA, USA. Email: mlkavvas@ucdavis.edu

Introduction

As the future evolution in nature and earth climate is changing, the assessment of its potential impacts on water resources is justifiably a necessary action to take. Its impact is foreseen to increase water stress globally as evidenced by occurrences of more extreme hydrological events such as an increasing number and intensity of heavy rain events that induce floods, and an increasing number with increasing intensity of droughts in many regions of the world (Trenberth, 2008). Therefore, climate change effect on hydrology will affect water resources planning and management that involve substantial work dealing with many socioeconomic and engineering development activities in order to ensure meeting of water needs, and to secure from water-related disasters. The present research emphasizes the need to assess climate change impact on hydrological change and water resources during the 21st century in Thailand focusing on the Ping River basin. The Ping basin is a significant head watershed and essential water supply to a major rice bowl area, Chao Phraya River System, in central Thailand. In order to investigate the change, the future climate conditions provided by the Intergovernmental Panel on Climate Change (IPCC), is considered. The IPCC had developed various scenarios mainly by the quantification of future global greenhouse gas emissions (Nakicenovic and Swart, 2000). To

simulate the future hydro-climatic conditions under IPCC scenarios over a specified region, outputs from General Circulation Model (GCM) climate simulations are required.

This research will focus at the watershed scale in the Ping Basin necessitating the downscaling of a GCM climate projection to this specified region. A typical GCM's grid-box is about 2° latitude by 2° longitude (~200-250 km x 200-250 km) in horizontal direction and 1 km or more in vertical direction. This GCM-coarse grid cannot represent the small-scale spatial climate variability. A methodology to refine the spatial scale from the GCM output, called “downscaling”, is necessitated, and it has been widely applied to date for most user applications (Cozzetto et al., 2011). The downscaling technique is essential to bridge the gap of the mismatched scales between GCM-supplied climate variables and the required detailed information of a region, especially at a watershed scale for studying the impact of climate change on hydrology and water resources. Generally, two broad categories of downscaling methods can be classified as statistical downscaling and dynamical downscaling. The statistical downscaling concept is based on empirically-based techniques by finding a relationship of the large scale atmospheric variables, predictors, and local/small scale climate variables, predictands (Wilby and Wigley, 2000). By this way, it allows the modelers to not have to directly solve the physical processes of land-atmosphere interactions that are basically based on energy and mass balance transfer between the land and the atmosphere (Jang and Kavvas, 2013). The dynamical downscaling is based on a process based technique considered over a nested area or limited area by means of a regional climate model (RCM) to extract the local-scale climate data from the large-scale GCM's information (Xu, 1999). Dynamical downscaling, by using regional climate models (RCMs) is able to solve land-atmosphere interaction under physical principles, conservation of mass, energy and momentum (Jang and Kavvas, 2013). In other words, dynamical downscaling by means of RCMs relies on dynamics and physics of the climate processes at very fine spatial and temporal scales that can gain incorporate physical information over a watershed scale, and allows more understanding of hydrologic impact studies. Therefore, using downscaling methods to refine the GCM climate data before using such data as the input to a hydrologic model now is the best choice that seems to be rendering more precise information on the impact of various climate scenarios on hydrologic regimes and water resources availability under climate change. The overview concept and comparison of statistical and dynamical downscaling approaches can be found in the literature (Fowler et al., 2007; Jang and Kavvas, 2013; Murphy, 1999; Schmidli et al., 2007). However, GCMs or RCMs still contain model bias due to the knowledge base and technological limitations. Such biases are

generally remedied by applying bias correction, but still there remains the challenge of accurate decision of future variability of the projected data.

In this research, dynamical downscaling by means of the Fifth Generation Mesoscale Model (MM5) developed at Penn State University and NCAR (Dudhia and Bresch, 2002; Grell et al., 1994) was performed to refine the GCMs output of climate projections in time at hourly intervals and space at 9 km grid size over the Ping River basin. MM5 is able to translate the physical conditions of climate, as simulated by GCMs at coarse grid size to a finer scales as low as 0.5 km. It is noted that at a 9 km grid size is a compromise between resolving cumulus clouds and having to include uncertain cloud microphysics details coupled with greater computational demand.

Study area

Thailand is known as one of the top rice exporters in the world, and rice is the country's most important crop. The major “rice bowl” of Thailand's agriculture area is in the Chao Phraya River system located in the central region. Like all countries that rely heavily on agricultural production, for Thailand water is a vital resource. Consequently, water availability is truly essential, especially in agriculture-dominated areas. An important headwater of the Chao Phraya River system is the Ping River (about 35,000 km², 22% of the Great Chao Phraya area), the second largest of the four upstream basins. The upper Ping Basin area, a watershed of approximately 26,111 km² that comprises 75% of the Ping Basin area, conserves freshwater in a multipurpose dam, Bhumibol. The Bhumibol Dam, together with the Sirikit Dam (located in Nan Basin), are the two major reservoirs in the northern region of Thailand. Together they supply water to the downstream area, the lower Chao Phraya Basin in the central region.

The Ping River basin lies in Northern Thailand with geographical coordinates of latitude 15.7°N to 19.75°N and longitude 98.10 °E to 100.20°E. The watershed covers parts of five provinces in the region: Chiang Mai, Lamphun, Tak, KamphaengPhet, and NakonSawan. It functions as a major water supply for the central region of Thailand (the Chao Phraya area) via water storage and releases from the Bhumibol Dam.

The topography of Ping basin (Figure.1), is mostly hilly and mountainous. The highest altitude, approximately 2,595 meters above sea level (m a.s.l.), is at Doi Inthanon in Chiang Mai. The lowest elevation is approximately 300 m a.s.l. From the North to the South the hill ridges are oriented in parallel from the west to the east, intersected by a number of major valleys. Land coverage within the basin is dominated by subtropical forest (about 80%). Mountain ranges in the eastern and the western sectors of the region host several important tributaries

of the Ping River. These characteristics contribute to the feather-like shape of the Ping watershed, narrow in width (about 86 km.) and much longer in length (about 740 km.). As one of the two largest dams in Northern Thailand, Bhumibol Dam is the main water storage structures in the basin. The dam was completed and started to store water in 1964, and it divides the Ping Basin into the upper Ping Basin (26,111 km²) and the lower Ping Basin (8,889 km²). The dam was designed to serve as a multi-purpose reservoir, serving mainly for irrigation supplies, electricity generation, flood protection, domestic and industrial water supply, navigation, environmental conservation and recreation. The reservoir has a live storage capacity of 9.7 billion cubic meters (bm³) and a total capacity of about 13.5 bm³. Average annual inflow is 6.6 bm³. Hydroelectric generation capacity is approximately 713 MW. Hence, the protection and maintenance of the capacity of this dam is strategically important, especially in the upper portions of the Ping River basin, which is the focus of this research.

have been investigated. These future climate projections are based on the assumption of increasing greenhouse gas emission due to developments in global and regional economies together with the change in world demography and environment technology innovation. ECHAM5 has generated three different initial conditions for scenarios A1B, A2 and B1, thus providing nine total future climate projections of A1B1, A1B2, A1B3, A2-1, A2-2, A2-3, and B1-1, B1-2, B1-3 (Table 1). Meanwhile, CCSM3 simulated only one initial condition and provided a total of only three different projections of A1B, A2 and B1 (Table 1). In addition, historical control run data (focusing in 1971-2000) from the two GCMs is used to quantify model historical climate simulations that contain biases due to model uncertainties. In this study, ECHAM5 and CCSM3 are the two selected GCMs because these models have provided four-dimensional atmospheric data at a six-hour time scale, which are required as realistic boundary conditions for regional atmospheric model simulations.

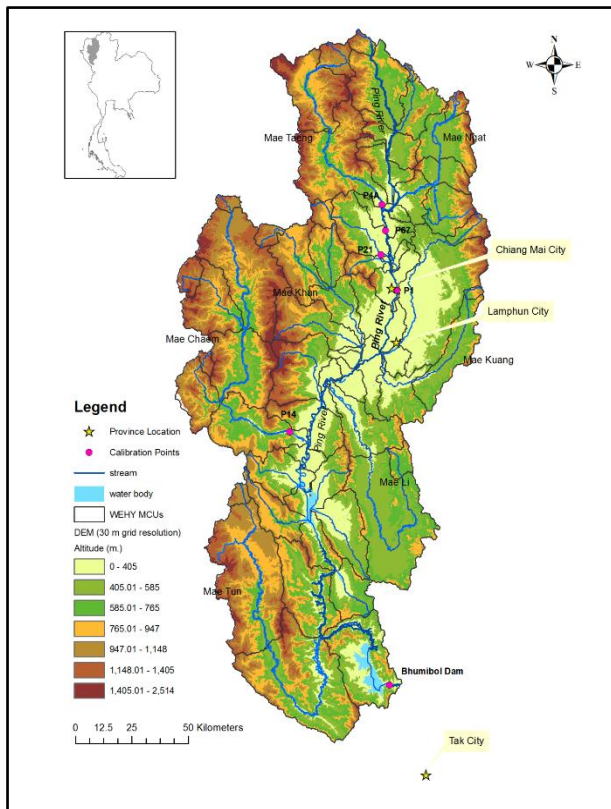


Fig.1 The upper Ping River Basin Topography

GCM Climate Projections

To evaluate the impacts of climate change on hydrologic system of the upper Ping River basin, future climate change scenarios from the special report on emissions scenarios (SRES) A1B, A2 and B1, acquired by two GCMs of ECHAM5/MPI and CCSM3, resulting in a total 12 future projections

Table 1. GCMs’ climate projections

GCMs	SRES Emission Scenarios		Total Scenarios
	Family	Scenarios	
ECHAM5	A1	A1B1, A1B2 and A1B3	3
	A2	A2-1, A2-2 and A2-3	3
	B1	B1-1, B1-2 and B1-3	3
CCSM3	A1	A1B	1
	A2	A2	1
	B1	B1	1

The ECHAM5 GCM is the fifth generation atmospheric general circulation model, and it has been developed at the Max Planck Institute for Meteorology (MPIM) in Hamburg, Germany (Roeckner et al., 2003; Roeckner et al., 2006). The model has been improved to have a horizontal resolution of T63 with a grid size of 1.9° x 1.9° at the equator and a vertical resolution of L31 (31 layers). A comprehensive description of ECHAM5 GCM can be found in Roeckner et al. (2003; 2006).

The CCSM3 GCM is the Community Climate System Model version 3.0 (CCSM3), a general circulation model of the US National Center for Atmospheric Research (NCAR). The CCSM3 has been improved to have a high resolution of T85 with a grid resolution in the atmosphere at about 1.4° x 1.4° in horizon, 26 levels in vertical resolution with the top two model hybrid level midpoints at 3.54 and

7.39 hPa. A detailed description of CCSM3 GCM can be found in Collins et al. (2006).

Methodology

Generation of the projected water supply begins by obtaining initial and boundary conditions to the regional climate model (RCM) downscaling from a total of 12 climate projections by two GCMs under A1B, A2 and B1 scenarios. These GCMs supply a historical control runs (1971-2000) and future global meteorological data (2001-2099) that are then dynamically downscaled to a spatial resolution of 9 x 9 km over the upper Ping River basin, covering 26,111 km² at an hourly time scale. The MM5, can be used to bridge the gap between the coarse resolution from GCMs and the fine time-space resolution climate data that is necessary to perform engineering water resource studies over a geographical region or a specific area. Optimal MM5 configuration is set by focusing on the simulation of precipitation in selected locations, on the basis of a one-year simulation during 2004, driven by NCEP/NCAR reanalysis data. The spatially varying precipitation time series data set from the dynamical downscaling by MM5 required statistical bias correction before being input into the upper Ping watershed hydrologic system. The simple multiplicative monthly bias factor is applied and can be defined as follows:

$$F_i = \frac{\bar{P}_{obs,i}}{\bar{P}_{his,i}}, \quad i=1,2,\dots,12 \text{ month}$$

Among the many complexities of studying climate change effects on hydrology, one key issue is the interactive processes between atmosphere and land surface hydrology. WEHY-HCM, as a new development in watershed-scale hydro-climate modeling, was developed to consider the interaction between the atmospheric and land hydrologic processes, in which the hydrologic cycle is closely related to the atmosphere and is a part of the earth's atmospheric system. Moreover, the model is useful at watersheds that naturally have non-homogeneous topography and land use/cover, because the model is based on areally averaged, scalable conservation equations and parameters in order to quantify and account for the effect of heterogeneity within watersheds. WEHY-HCM is able to model vertical interaction with the atmosphere (precipitation, radiation, wind, sensible heat flux, evaporation/ET, and vertical soil water flow), lateral hydrologic processes (subsurface storm flow, overland flow, groundwater flow) at hillslope scale, and dynamic interaction of the open channel flow and groundwater flow at the watershed scales (Kavvas et al., 2013). The WEHY-HCM has been developed at the Hydrologic Research laboratory (HRL), UC Davis. The detail description of the WEHY-HCM model are given by

Kavvas et al. (2004; 2006; 2013) and Chen et al. (1994a; 1994b).

Once the downscaled climate input data of the specified watershed were obtained the Watershed Environmental Hydrology (WEHY) model is used to estimate the hydrologic processes within the study area. The overall procedure of studying the impacts of future climate change on hydrology and water resources in the upper Ping Basin is presented in Figure 2.

Results and discussion

MM5 model configuration

Because MM5 has several physical parameterization options, the model must be calibrated to obtain an optimal configuration. To determine the optimal configuration, the combination of the MM5 model options were simulated, and those downscaled precipitation results were then compared to available observed rainfall at specific grid points. The data used for this comparison is retrieved from NCEP/NCAR reanalysis1 coarse-resolution climate data, and compared with observed rainfall for the year 2004. To find the best combination of MM5 physical options in this study, the options for the cumulus parameterizations, the microphysics processes, and planetary boundary layer (PBL) scheme were varied. The best combination option (Kain-Fritsch 2, Reisnergraupel, and MRF) can simulate precipitation driven from NCEP/NCAR reanalysis1 data and then was compared to the observed rainfall in a monthly time scale ranged from acceptable to very good at the selected grid points, with the correlations ranging from 0.70 to 0.93 in the upper Ping area. Thus, this physical options can produce reliable atmospheric variables over the upper Ping Basin.

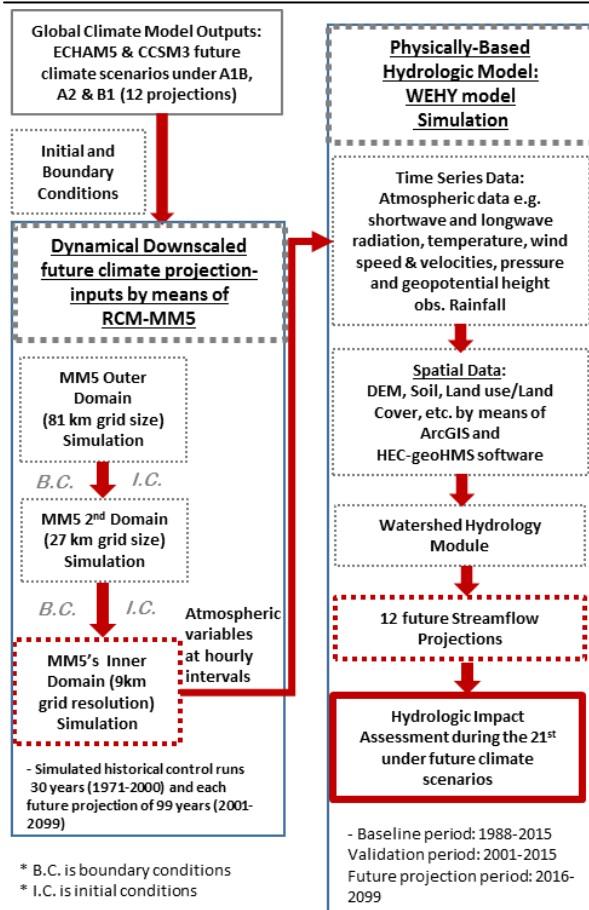


Fig.2 Schematic description of study procedure

WEHY model calibration and validation

After preparing the physical parameters and the hydro-meteorological time series required by WEHY model as shown in figure2, calibration and validation were performed. The calibration and validation are needed to evaluate model performance and reliability. Calibration was completed by adjusting and/or refining the corresponding parameter set (e.g. initial soil moisture condition, Chezy and Manning's roughness coefficients at each stream network segment in each model computational unit) to fit the hydrologic processes (by comparison with the watershed runoff observations) of the upper Ping watershed. Validation is necessary to confirm that the model can represent the study area's hydrologic system well and is reproducing realistic hydrologic projections. The WEHY model is a physically-based hydrologic model, and therefore the estimation of model parameters is largely from compiled land information (e.g. soil and vegetation parameters), rather than from fitting by a rainfall-runoff exercise (Chen et al., 2004a) as is traditionally performed in calibrating other hydrologic models. In this research of the upper Ping Basin, the WEHY hydrologic module was calibrated during 2004-2006 (3 years). Another critical step to assure the model accuracy is by validation, which was performed during 2000-2012 (10 years excluding 2004-2006). The calibration

and validation results were compared with the observed stream discharge at six stations. The plot for the calibration and validation period are displayed in Figures 3.

These graphs demonstrate that most daily simulated hydrograph flows are reasonably well matched with the observed flows in both their timing and peak discharge magnitude. For calibration, the correlation coefficient (r) ranges from 0.72-0.91, and the Nash-Sutcliffe efficiency (NSE) ranges from 0.51-0.81 (not shown in Fig.4). The validation results show a reasonably well matched hydrograph between simulated and observed flow as well, with r values ranging from 0.73-0.90, and the Nash-Sutcliffe from 0.49-0.90. At some points (e.g. P4A, P.14) do not show statistical values well, especially in the upstream area covering by mountain range. This is due to inadequate and sparse rain gauges, specifically in the mountain areas. There are denser networks in the lowland areas for which the statistical analysis is more favorable (e.g. P.1, Bhumibol Dam). Furthermore, the mountain areas are typically effected by orographic forcing, which can cause differences between light rainfall at the lee side (rain shadow) and heavy rain at the upwind side. Overall, the goodness of fit of the model calibration and validation results can accurately replicate the hydrologic system in the upper Ping River basin. Therefore, the WEHY-HCM model can produce very promising runoff results for the the upper Ping Basin and due to the model's high performance, it can be used to project future runoff under various climate scenarios.

Downscaled GCMs' historical runs' validation

In order to simulate the 21st century future climate projections, it is necessary to test the GCMs' downscaled climate data after bias correction. Typically, a GCM historical period is simulated to obtain a realistic initial condition before simulating the future climate scenarios and it can be employed to quantify the model biases. The present study, bias factors are estimated by comparing the average monthly rainfall of the upper Ping Basin from the GCM-simulated historical data to the observed data. The corrected rainfall data, along with other atmospheric variables, are fed into the WEHY-HCM which simulates the basin hydrologic flows. By comparing the simulated flows with inputs from the corrected GCM-simulated historical control run climate data, with the observed flows during 1971-2000, the GCM's performance can be evaluated to determine whether the downscaled bias-corrected GCM data can achieve consistency and reliability in producing future climate variables. In this manner, the performances of the two GCMs were evaluated by the cumulative distribution function of the

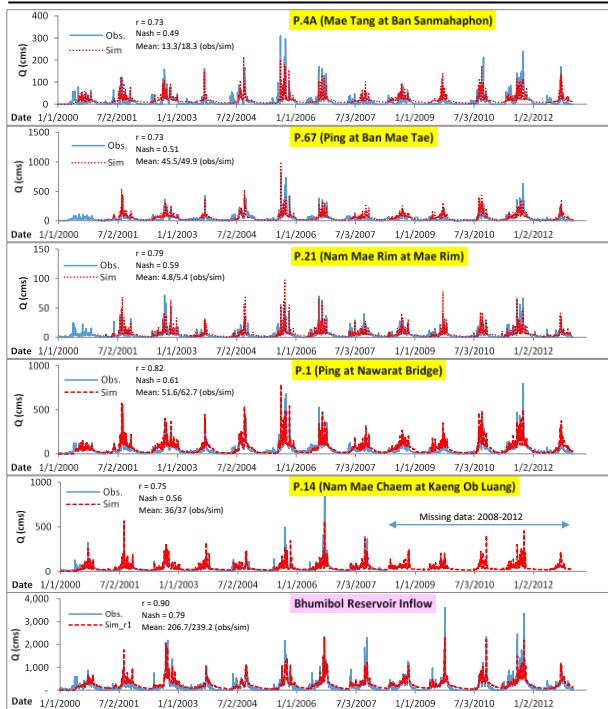


Fig.4 WEHY hydrology model calibration and validation by comparing the daily mean discharge between simulated and observed flows

GCM-based historical simulated flows and the observed flows of the upper Ping Basin at its outlet (the Bhumibol Dam) (nam as shown in Figure 5).

Since the ECHAM5 and CCSM3 GCMs provide the climate change projections from 2001 to 2099, the generated flows during 2001-2015 can be extracted and compared to the observations in order to verify the performance of these GCMs. It is noted that the future projected flow simulations driven by GCMs are based on climate driving forcing assumptions, which are not for climate forecast or prediction purposes. Hence, the expectation is that the future hydrologic flows under various climate scenarios should give a plausible range covering the observed flows instead of providing accurate forecasts for flows. Thus, these two GCMs' performance can be presented as in Figure 6 for the 15-year average monthly flows. The graph shows that the GCM-projected flows from both ECHAM5 (average from 9 projections) and CCSM3 (average from 3 projections) cover the observed flows, and that their correlation r with the observation is about 0.99 and 0.98 respectively. In addition, the generated flows from GCMs also fall within the 95% confidence band of the observed flows. Thus, the ECHAM5 and CCSM3 can represent and project the future water flow during the 21st century for the upper Ping River basin.

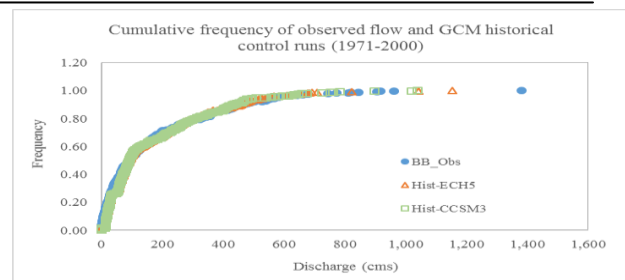


Fig.5 Comparison of simulated flow based on GCM historical control runs and observed flow at the upper Ping Basin outlet

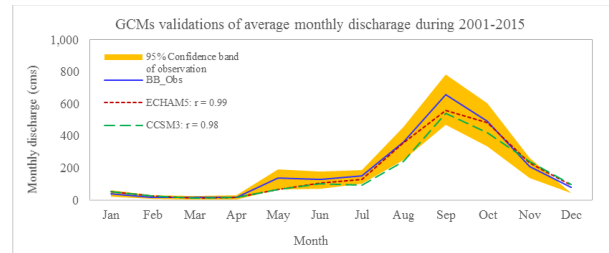
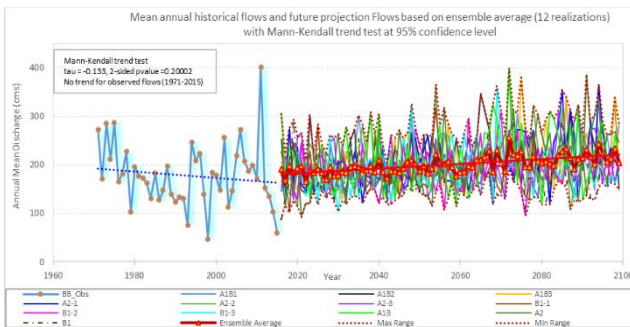


Fig.6 Comparisons of mean monthly flow of ECHAM5-average and CCSM3-average flows with the observed flow during 2001-2015

Future projected flows of the 21st century at the upper Ping River basin

As stated earlier, climate change is expected to impact the hydrologic flows in the Ping River basin and one of the most important functional hydraulic structures, Bhumibol Dam. The future projected flows from the upper Ping River basin are considered as the dam inflows. Various future projected monthly inflows into the Bhumibol Dam from 2016 to 2099 by the different GCMs and climate projections, as well as the ensemble average of all 12 realizations are plotted in figure 7. The figure depicts the trends of the historical observed streamflows as well as the ensemble average of the future flow projections including the maximum and minimum bands of projection scenarios based on an annual time scale. The plots clearly show that the future projected flows based on the ensemble average from the 12 projection flows have an upward trend toward the end of the 21st century. However, the historical observed flows appear to have a downward trend, which is not statistically significant based on the non-parametric Mann Kendall trend test at the 95% confidence level. Hence, from this result can be concluded that toward the end of the 21st century in the upper Ping River basin, there will be higher streamflow values due to climate change. Note that the ensemble average of the future projected flows has a smoother trend because the average itself smooths out all the fluctuations, whereas a single observation data set as in the historical observed data will show much greater fluctuations. For example, historically, a distinct extreme flood occurred in 2011, and the two most droughts appeared in 1998 and 2015. In addition, the

historical data set has only short-time memory (45 years), while the ensemble average of future projections contains much longer period (84 years) with total 12 realizations. These can create a distinct break between the observed and simulation trends. The maximum and minimum bands reveal the plausible range or the worst case that could happen in the future. Figure 8 displays the overall 21st century mean monthly hydrograph based on ensemble averaged of the 12 projection realizations and compared with based line period (1988-2015). The figure also shows the mean monthly maximum and minimum range of the ensemble average together with the maximum and minimum range of the 12 projected flows.



- Chen, Z. Q., et al. (2004b). "Watershed Environmental Hydrology (WEHY) Model: Model Application." *Journal of Hydrologic Engineering*, 9(6), 480-490.
- Collins, W. D., et al. (2006). "The community climate system model version 3 (CCSM3)." *Journal of Climate*, 19(11), 2122-2143.
- Cozzetto, K., et al. (2011). "Examining Regional Climate Model (RCM) projections: What do they add to our picture of future climate in the region?" *Intermountain West Climate Summary*, 7(5).
- Dudhia, J., and Bresch, J. F. (2002). "A Global Version of the PSU-NCAR Mesoscale Model." *Monthly Weather Review*, 130(12), 2989-3007.
- Fowler, H. J., et al. (2007). "Linking climate change modelling to impacts studies: recent advances in downscaling techniques for hydrological modelling." *Int. J. Climatol.*, 27(12), 1547-1578.
- Grell, G. A., et al. (1994). "A description of the fifth-generation Penn State/NCAR mesoscale model (MM5)."
- Jang, S., and Kavvas, M. (2013). "Some Issues on the Downscaling of Global Climate Simulations to Regional Scales: Statistical Downscaling versus Dynamical Downscaling." *Journal of Hydrologic Engineering*, 0(ja), null.
- Kavvas, M. L., et al. (2004). "Watershed environmental hydrology (WEHY) model based on upscaled conservation equations: hydrologic module." *Journal of Hydrologic Engineering*, 9(6), 450-464.
- Kavvas, M. L., et al. (2006). "Watershed environmental hydrology model: Environmental module and its application to a California watershed." *Journal of Hydrologic Engineering*, 11(3), 261-272.
- Kavvas, M. L., et al. (2013). "WEHY-HCM for Modeling Interactive Atmospheric-Hydrologic Processes at Watershed Scale. I: Model Description." *Journal of Hydrologic Engineering*, 18(10), 1262-1271.
- Murphy, J. (1999). "An Evaluation of Statistical and Dynamical Techniques for Downscaling Local Climate." *Journal of Climate*, 12(8), 2256-2284.
- Nakicenovic, N., and Swart, R. (2000). "Special Report on Emissions Scenarios." *A Special Report of Working Group III of the Intergovernmental Panel on Climate Change*. Cambridge University Press: Cambridge, 599.
- Roeckner, E., et al. (2003). "The atmospheric general circulation model ECHAM 5. PART I: Model description."
- Roeckner, E., et al. (2006). "Sensitivity of simulated climate to horizontal and vertical resolution in the ECHAM5 atmosphere model." *Journal of Climate*, 19(16), 3771-3791.
- Schmidli, J., et al. (2007). "Statistical and dynamical downscaling of precipitation: An evaluation and comparison of scenarios for the European Alps." *Journal of Geophysical Research: Atmospheres*, 112(D4).
- Trenberth, K. E. (2008). "The impact of climate change and variability on heavy precipitation, floods, and droughts." *Encyclopedia of hydrological sciences*.
- Wilby, R. L., and Wigley, T. M. L. (2000). "Precipitation predictors for downscaling: observed and general circulation model relationships." *Int. J. Climatol.*, 20(6), 641-661.
- Xu, C.-y. (1999). "From GCMs to river flow: a review of downscaling methods and hydrologic modelling approaches." *Progress in physical Geography*, 23(2), 229-249.



Session B

Participatory Management for Water and Irrigation Project



Invited Papers



PRINCIPLES AND METHODS FOR PIM IN ACTION IS THE JAPAN'S MODEL EXCEPTIONAL?

Masayoshi Satoh

Abstract

Improving water management in irrigation projects is believed to be of urgent importance after so much investment on the projects. One of the effective methods for the improvement is Participatory Irrigation Management (PIM), for which big efforts have been made in the past decades and not seen remarkable successful in the world yet.

Development of practical methods for PIM implementation is strongly required. We may get some useful lessons for that from successful cases in the world. Although the cases are limited in number, the Japanese model may be one of them. The question is whether the major reason for the success exists in the local and indigenous conditions or in common principles that are applicable to other localities.

This presentation shows the background conditions of Japanese irrigation, and clarifies that the widely believed reasons for success, 1) 1,800 mm of yearly rainfall making its irrigation less important, 2) the cooperative nature of the Japanese farmers making conflict resolutions easy, are not correct. It also introduces the role-sharing between governments and farmers in large scale irrigation projects, followed by discussion on the Japanese system to encourage the farmers to participate in the projects and to form and manage their WUA (Land Improvement District, LID) under the conditions of conflicts among different local farmers. It concludes that this Japanese model is based on the common principles such as information dissemination, accountability, equity, and transferring decision making power to farmers, thus the governments are successful in involving farmers into the projects and water management to most effectively and efficiently achieve the government objectives.

Masayoshi Satoh

Prof. Emeritus, University of Tsukuba



Papers

Water-Food Nexus: Water Use Efficiency in Central Asia

JUNG Younghun^{1*}, LEE Eulrae², CHOI Byungman³

Abstract The excessive water use of Central Asian countries have brought the environmental disaster in Aral Sea. Two transboundary rivers in Aral Sea basin are main sources of the shared water resources in Central Asian countries. In this regard, they need to improve the efficiency in using the shared water resources to overcome their environmental and economic difficulties. Accordingly, the twin objectives of this study were firstly to analyze the challenges of water resources in the Aral Sea Basin and secondly to estimate the efficiency of agricultural water use according to the crop types and the irrigation methods. The results showed that the economic efficiency of water use in Central Asian countries was lower than other Asian countries. Furthermore, climate change has increased temperature which can induce evapotranspiration and snow- or glacier-melting in the Aral Sea Basin. Finally, this study illustrated that the selection of the crop types and irrigation methods can improve the quantitative and economic efficiency of water use. However it is asked as a necessary preliminary to provide a clear outline of interaction to avoid hierarchy and failure of coordination and collaboration for regional win-win approach. In such outline, this study will deliver valuable information on water efficiency in Aral Sea basin.

Keywords *water-energy-food nexus, climate change, sustainable development, assessment tool*

JUNG Younghun (ph.D)
Water Resources Research Center
K-water Institute
Daejeon, Korea
erlee@kwater.or.kr

LEE Eulrae (ph.D)
Water Resources Research Center
K-water Institute
Daejeon, Korea
erlee@kwater.or.kr

CHOI Byungman (ph.D)
Water Resources Research Center
K-water Institute
Daejeon, Korea
bmchoi@kwater.or.kr

Introduction

Central Asia countries have to hurdle over many fences for successful economic growth in the Central Asia, but substantial environmental and economic pressures are on them. To resolve this issue, they need to pursue enabling growth potentials and minimizing risks on the ecosystem in long-term. For example, the concept of Green Growth or Green Economy could be one of several good suggestions to overcome the complex problems facing the Aral Sea Basin because it is very relevant to the purposes that the region has pursued (Mathew, 2012; Resnick et al., 2012). Also, such concept may be an appropriate approach as a solution for water-energy-food security nexus, one of the global issues (Hoffman 2011; Waughray 2011; Bazilian et al. 2011). However, water-energy-food security in transboundary river basin can lead to excessive water competition at the regional scale. Therefore, more effort and time are needed to move gradually towards achieving water-energy-food security in Aral Sea Basin.

This study focused on efficiency in the water use for water-energy-food security nexus in Aral Sea Basin. In this regard, the objectives of this study are 1) to analyze the challenges of water resources in Aral Sea basin in terms of climate and economy and 2) to quantify the quantitative and economic efficiency of agricultural water use for the selections of crop types and irrigation methods. To reach this objective, we investigated the water status of five Central Asia countries (Kazakhstan, and Kyrgyzstan, Tajikistan, Turkmenistan, and Uzbekistan) in Aral Sea basin at the regional level.

Overview of Aral Sea Basin

Aral Sea Basin is consisted of Kazakhstan, Kyrgyzstan, Tajikistan, Turkmenistan, Uzbekistan, Afghanistan, Iran and China. However, five Central Asia countries (Kazakhstan, Kyrgyzstan, Tajikistan, Turkmenistan, and Uzbekistan) were mainly treated in this study due to difficulty in access of data in other countries.

Aral Sea Basin are morphologically divided into plain zone in central and western part of the Basin and mountain zone in the east (Dukhovny and Sokolov, 2003) (Fig.1). The plain zone has two main deserts: the Kara Kum desert in the western and the south-western parts and the Kyzyl Kum desert in the northern part. While, the mountain area includes two main mountain

ranges: the Tien Shan and Pamir. Hydrologically, these two mountain ranges are a very important role of water supply in Aral Sea Basin because two main transboundary rivers (the Syr Darya and the Amu Darya) are fed by the water melted from snows and glaciers (Sorg et al., 2014; Hagg et al., 2013; Bernauer and Siegfried, 2012).



Fig. 2 Location of Aral Sea basin (CAWATERinfo)

This study tries to apply surface irrigation and drip irrigation to cotton and wheat which account for more than 50% of agricultural lands in five countries, and thereby analyze the water use and economic profit of each method. For an irrigated area, there is no land use information on cotton and wheat in each country. Therefore, an agricultural area ratio was set to an irrigated area for each crop [Table 1]. For water use, yield productivity, and economic efficiency according to irrigation methods, this study applied the ratio of drip irrigation to surface irrigation in irrigated area and productivity and the ratio of wheat to cotton in irrigated area and economic benefit, developed by Ward and Pulido-Velazquez [2008] with the measure data of the semi-arid regions Texas, USA and Ciudad Juarez, Mexico [Table 2]. To minimize the uncertainty arising from the point that Central Asia and actually measured places have different climate and economic conditions, the assumption was presented with ratios. In addition, the economic benefit in Table 4 does not include installation and maintenance costs for irrigation methods because of a lack of materials.

Table 1. Irrigation status in the Aral Sea basin

	Total		Cotton	Wheat
	Irrigated Area	Irrigated Water	Area (CA)	Area (WA)
Kazakhstan	750	5.9	168.0	70.5
Kyrgyzstan	407	2.3	24.8	22.4
Tajikistan	802	9.3	134.7	316.8
Turkmenistan	1,869	22.5	758.8	852.3
Uzbekistan	4,373	51.6	1,132.6	1,150.1
Aral Sea basin	8,201	91.6	2,219.0	2,412.0

Table 2. Relative efficiency ratio of drip irrigation to surface irrigation for cotton and wheat [Ward and Pulido-Velazquez, 2008]

	Irrigated Water per Unit Area		Yield Productivity per Unit Area		Economic benefit per Unit Area
	Surface	Drip	Surface	Drip	
Cotton	1 (1)	0.54 (1)	1	1.25	(1)
Wheat	1 (0.89)	0.56 (0.93)	1	1.25	(0.46)

where, () indicate the relative efficiency ratio in irrigated water and economic benefit between wheat and cotton without consideration of costs for installation and maintenance.

Quantification of Efficiency in Water Use in the Aral Sea Basin

This study calculated quantitative efficiency (QE) Eqs. 1 when drip irrigation was installed in cotton and wheat at the same ratio and cotton to wheat (CTW) or wheat to cotton (WTC) conversion was made in an irrigated area of crop in each country (Table 3). On the assumption that the irrigation water for each crop in each country is in proportion to a land use area and the current irrigation is all controlled by surface irrigation technique, Eqs. 1 and 2 are formulated based on values in Table 4.

QE_{CTW} (Eq. 1a) represents QE at the time of converting a cotton irrigated area into a wheat one in the current status, and QE_{WTC} (Eq. 1b) is QE at the time of converting a wheat irrigated area into a cotton one. Accordingly, when QE is 1, each one means water use and economic benefit in the current status. The smaller QE is, the larger water use efficiency is.

$$QE_{CTW} = \frac{\left((CA \times (1 - CTWcr) + CA \times CTWcr \times 0.89 + WA) \times S \right)}{\left((CA \times (1 - CTWcr) \times 0.54 + CA \times CTWcr \times 0.56 \times 0.89 + WA \times 0.56) \times D \right)} \quad 1a)$$

$$QE_{WTC} = \frac{\left((WA \times (1 - WTCcr) + WA \times WTCcr / 0.89 + CA) \times S \right)}{\left((WA \times (1 - WTCcr) \times 0.56 + WA \times WTCcr \times 0.54 / 0.89 + CA \times 0.54) \times D \right)} \quad 1b)$$

where, D is the ratio of the drip irrigation to total irrigation, S is the ratio of the surface irrigation to total irrigation, CA and WA are the irrigated areas for cotton and wheat, respectively. Also, CTWcr and WTCcr are conversion ratios from cotton to wheat and from wheat to cotton, respectively. D, CTWcr and WTCcr are ranged from 0 to 1.

This study calculated quantitative efficiency (QE) in water use of each country according to crop types and irrigation methods (Tables 8-10). From the perspective of quantitative efficiency, when cotton was fully converted into wheat in drip irrigation status of all countries, the efficiency was the highest (0.52-0.54), whereas when wheat was fully converted into cotton in the current irrigation method (surface irrigation), the efficiency was the lowest (1.04-1.09) (Table 8). In this study, regarding the efficiency through the change in crop types and irrigation methods in the Aral Sea basin, QE was calculated to be 0.53-1.06 (Tables 8). Fig. 5 illustrates the efficiency according to the change in crop and irrigation in the Aral Sea basin.

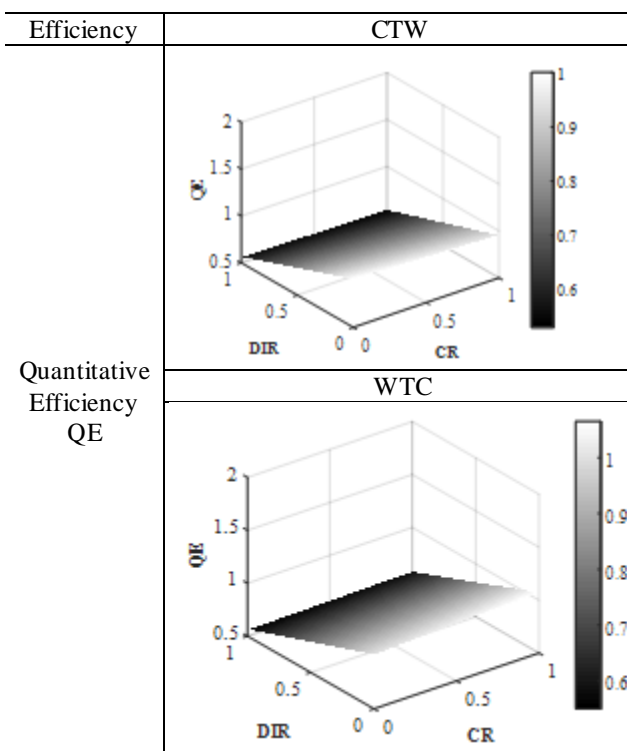
Table 3. Quantitative efficiency (QE) in water use according to change of crop type and irrigation method
 a) Cotton to Wheat

Country	Conversion Ratio (CR)			
	0 %	100 %	0 %	100 %
	Drip Irrigation Ratio (DIR)			
	0 %		100 %	
Kazakhstan	1	0.92	0.55	0.52
Kyrgyzstan	1	0.94	0.55	0.53
Tajikistan	1	0.97	0.55	0.54
Turkmenistan	1	0.95	0.55	0.53
Uzbekistan	1	0.95	0.55	0.53
Aral Sea basin	1	0.95	0.55	0.53

b) Cotton to Wheat

Country	Conversion Ratio (CR)			
	0 %	100 %	0 %	100 %
	Drip Irrigation Ratio (DIR)			
	0 %		100 %	
Kazakhstan	1	1.04	1	0.56
Kyrgyzstan	1	1.09	1	0.57
Tajikistan	1	1.09	1	0.59
Turkmenistan	1	1.07	1	0.58
Uzbekistan	1	1.06	1	0.57
Aral Sea basin	1	1.06	1	0.57

Figure 4. Efficiency of water use in Aral Sea Basin according to change of crop type and irrigation method.



Conclusion

Now we are preparing for a new water agenda in response. This study revealed that the selection of crop types and irrigation methods helps to improve quantitative and economic efficiency in water use. However, in making such a selection, it is also necessary to take into account economic condition, food and energy security, technology, education, employment, geographical condition, population, and legal system in each country in order to improve water use efficiency. Improvement of the efficiency in water use will provide more various options for the successful regional water governance in the Aral Sea Basin..

Reference

Bazilian, M., Rogner, H., Howells, M., Hermann, S., Arent, D., Gielen, D., et al. (2011) Considering the energy, water and food nexus: towards an integrated modelling approach. *Energy Policy* 2011, 39:7896–906.
 Bernauer, T. and Siegfried, T. (2012) Climate change and international water conflict in Central Asia. *Journal of Peace Research*, 49(1): 227-239.
 CAWATERinfo. Available online: <http://www.cawater->

-
- maps.net/ara1_sea_basin_en/ default.aspx
(accessed on 7 February 2015).
- Dukhovny, V. and Sokolov, V. (2013) Lessons on cooperation building to manage water conflicts in the Aral Sea Basin. UNESCO-IHP: Paris, France.
- Hagg, W., Hoelzle, M., Wagner, S., Mayr, E., and Klose, Z. (2013) Glacier and runoff changes in the Rukhik catchment, upper Amu-Darya basin until 2050. *Global and Planetary Change*, 110: 62-73
- Hoffmann, U. (2011). Some reflections on climate change, green growth illusions and development space. UNCTD Discussion Paper, UNCTD, Geneva.
- Mathews, J. A. (2012). Green growth strategies—Korean initiatives. *Futures*, 44(8): 761-769.
- Resnick, D., Tarp, F., and Thurlow, J. (2012). The political economy of green growth: Cases from Southern Africa. *Public Administration and Development*, 32(3): 215-228.
- Sorg, A., Mosello, B., Shalpykova, G., Allan, A., Clarvis, M. H., and Stoffel, M. (2014). Coping with changing water resources: the case of the Syr Darya river basin in Central Asia. *Environmental Science & Policy*, 43: 68-77.
- Ward, F. A. and Pulido-Velazquez, M. (2008) Water conservation in irrigation can increase water use. *Proceedings of the National Academy of Sciences*, 105(47): 18215-18220.
- Wegerich, K. (2004) Coping with disintegration of a river-basin management system: multi-dimensional issues in Central Asia. *Water Policy*, 6(4): 335-344.

Improving Crop Water Use with the use of Efficient Irrigation Technologies and Coconut Mulch Husk: A study on long-bean production

Keouangchai Keokhamphui¹, Corentin Clement², Khamkeng Chanthavongsa¹, Iep Keovongsa¹, Sern Singthong¹, Syphanxai Norlasin¹

¹National University of Laos, Faculty of water resources, Tadthong campus, Vientiane capital.

²International water management institute, Vientiane capital, Lao PDR.

Abstract This study investigated the applicability of coconut husk mulch and irrigation techniques for long bean production in Laos. The objectives are to determine the efficiency of water irrigation techniques and soil moisture content for long bean cultivation. This study uses experiments by applying coconut mulch cover and uncover the long bean pilot plots with different drip irrigation techniques. This study also monitored the environmental aspects such as temperature, evaporation, precipitation, and groundwater level. The results showed that long beans grew well across different temperature and moisture conditions. The best system of water irrigation was found to be the drip technique with coconut husk in which coconut husk could better absorb water and infill to the soil as nutrients which proved by the crop growth stages. In addition, the drip system with coconut husk also reduces water quantity as compared to water irrigated to the certain period. This can be said that it is an alternative for farmers to plant cash crop in drought areas affected by climate change by using abundant groundwater resources in the country.

Keywords *cash crop, Long-bean, irrigation, coconut mulch husk.*

Keouangchai Keokhamphui¹

Khamkeng Chanthavongsa¹

Iep Keovongsa¹

Sern Singthong¹

Syphanxai Norlasin¹

¹National University of Laos, Faculty of water resources, Tadthong campus, Vientiane capital.

Corentin Clement²

²International water management institute, Vientiane capital, Lao PDR.

1. Introduction

Climate change has led to an increase in irregular weather events such as extreme drought and severe floods, storms, cyclones and heat waves, which have had a significant impact on agricultural production, the environment, economic growth and the society as a whole. The severity and frequency of floods and droughts have increased in the Lao PDR, with a significant impact on agriculture.

Cultivation, breeding animals and fishery are the main daily activities of Lao's people (WREA, 2010). The domestic income from agricultural production for national economic and social development is covered 50% in 2001 (WB, 2008). Most of the agriculture activities depend on rainfall with the traditional technique causes to the low harvest and against to climate change. Moreover, no soil improvement and use the repetitive seed causes to get low quality of product which it is not reach the market standard and consumers (WB, 2014).

Groundwater plays the important role for water consumption and agriculture in the dry countries. Especially, the countries located in the desert region, about 40% of groundwater was supplied for irrigation (Plusquellec, 2002). However, Lao PDR has the surface water sufficiently for agriculture but it does not cover all area in country, some is facing to water shortage and drought events. Therefore, finding technology is very important for new innovation to respond to the sustainable consumption. Especially, the plants consume much water (Kima et al., 2014). The drip technique is very efficient on the different geography level due to it is difficult to supply water along the land surface (Albaji et al., 2015).

To find the solution for low harvesting and sustainability of soil improvement, this research was used coconut husk mulch to cover the long-bean plot with different water irrigations. The general purposes of this research are to reduce the coconut waste and find the optional utilizing coconut husk waste for soil improvement. The specific objectives were to evaluate the efficiency of drip irrigation techniques and soil moisture contents for

enhancing crop production by using coconut husk cover and promote the cultivation technique of gardeners.

2. Materials and Methods

2.1. Materials

Experiment site, in the faculty of water resources, Tadthong campus, Sykhottabong district, Vientiane, Lao PDR, was located at 17°59'23.70" N and 102°30'14.71" E. The area covered 1,600 m² which it is fine sand mixed with reddish clayey, it poorly absorbs water and nutrients. The experiment was used coconut husk cover the long-bean pilot trial. The weather station and rain gauge were installed in the experiment site to monitor the evaporation, temperature, wind speed, and precipitation. The water meter was installed at each row of long-bean plot to measure and control the water irrigation. Moreover, the groundwater level was recorded by Heron Instrument Dipper Logger and Barlog. For the measurement of moisture content in soil before and after irrigation was used RIXEN M-700S. The coconut husk was collected from coconut shop in the Otxy market, Sikhottabong district, Vientiane capital. It was chopped into small pieces for covering the long-bean plots. The experiment was divided into two systems; 1) the long-bean plots without covering coconut husk, 2) the long-bean plots were covered by coconut husk

2.2. Methods

Drip irrigation techniques were provided by dividing in three different pilot plots and types 1) drip technique without coconut husk, 2) pipe drip with coconut husk, 3) drip technique with coconut husk. The long-bean pilot plots were prepared by the area of 0.6x8 m, the distance between each was 0.5 m.

The experiment was conducted and divided into two systems; drip and pipe systems. The drippers were connected to pipe with distance of 0.5m in the drip system. The holes, in the pipe drip, were drilled with distance 0.5m. Two times a day for water irrigation, in the morning and evening. The irrigated water rate was controlled by water meter in drip technique for 10 minutes, and 5 minutes for pipe drip technique, respectively. In order to inspect the moisture content before and after irrigated water, this research was also conducted daily soil moisture content test by using moisture meter (model M-700S).

3. Results and Discussion

3.1. Effect of temperature, evaporation and rainfall

Fig 1. Demonstrated the relationship of temperature, evaporation and rainfall during long-bean growth period.

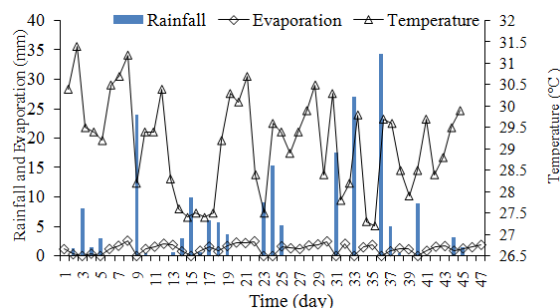


Figure 1. The relationship of temperature, evaporation and rainfall effect to plant growth

The average temperature was about 29.09°C, the day before rain it was higher which effects to water evaporation from soil, plants, and others that water contained in. However, the temperature decreased after rain cause to water evaporation decreased as well. Lalić et al., (2014) found the relationship between temperature and production, the yield was decreased when the temperature increased especially in dry season.

3.1. Effect of moisture content

The water contains in soil is an important parameter that many researchers focused on. Especially, the ability of keeping water and allow water to flow through (John et al., 2015). Fig 2. showed the percentage of moistness in soil, it was increased from the original soil of 42.7 to 47.2%, 42.6 to 47.5% and 42.4 to 47.8% in the drip technique without coconut husk, pipe drip with coconut husk and drip technique with coconut husk, respectively. Tao et al (2007) stated that the moistness plays the important role for plant growth, due to the important nutrients for plants might contain in water

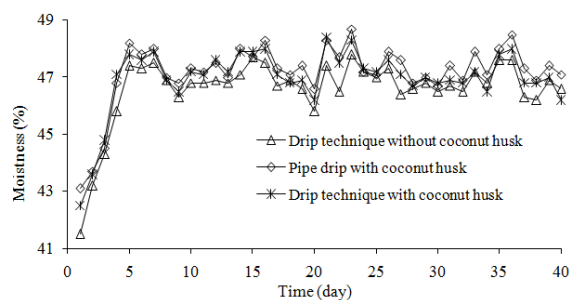


Figure 2. The percentage of soil moisture

3.2. Crop growth apparent

The cultivation technique is very important for getting higher benefit of production. It improved production yield and save water. As early mentioned there are three systems of this study,

the growth rate of each system was not far different (Fig.3), it seems the pipe system with coconut husk grew well in the first period and slowly growth then.

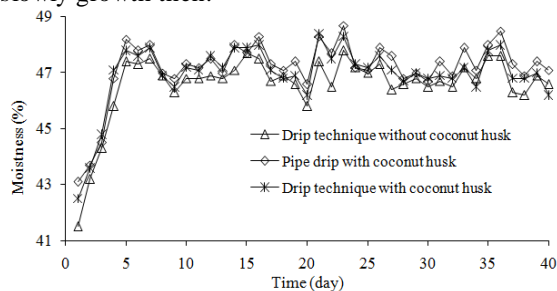


Figure 3. growth rate of long bean

This might cause from swelling water in the soil and coconut husk which opposite to drip technique without coconut husk, it might lack of water. So, the drip system with coconut husk clearly resulted that the long-bean grew well with the higher yield contrast to the rest techniques. Adams (2001) found that plants grow well when it consumed sufficient water, however the others fundamental factors are needed as well such as temperature, sunlight, rainfall, etc.

3.3. The comparison of water irrigation efficiency

The sufficiently and efficiently water irrigation is the important part for growing process of plant which it will be replaced into evaporated water (Allen et al., 2006). So, this study was focused on water irrigation technique appropriately such as drip technique without coconut husk, pipe drip with coconut husk and drip technique with coconut husk. The result showed in Fig4, demonstrated that the drip technique with coconut husk and drip technique without coconut husk used water in quite similar amount which different from the rest technique.

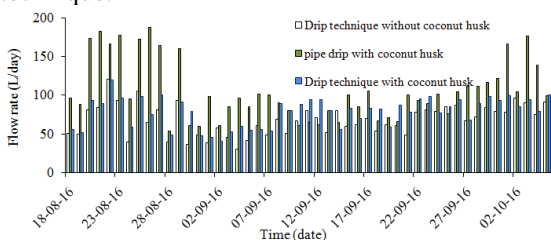


Figure 4. The difference water irrigation of each technique

3.4. Economic evaluation

The results of the study were showed in Fig5. Based on the planting area of 4.8 m² of each long-bean garden. So, in 1 Rai we can plant long-bean around 872.72 m²/rai or 5,436.36 m²/ha. The drip technique without coconut husk, pipe drip with coconut husk and drip technique with coconut husk resulted the production in one long-bean plot of 4.667 kg, 4.333 kg, and 7.167 kg, and evaluate in one hectare is 5.303 tone, 4,923 tone and 8.144 tone, respectively. The long-bean price in the local

market in Laos is around 1 USD/kg. From the results, the drip technique with coconut husk had higher capacity to produce long-bean.

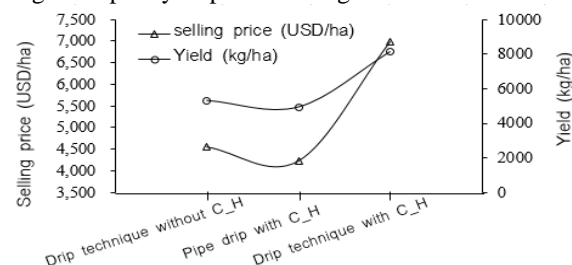


Figure 5. selling price and yield of long bean production

3.5. Changes of groundwater level

Groundwater is the new source for agriculture in Laos. So, its monitoring or measurement is important to identify the level of it for sustainable use (see Fig6). During the cultivation period, the groundwater level changed between 1-2 m which changed in the morning and evening because these times were extracted for long bean watering. Hagose and Mamo (2005) stated that groundwater supplies for consumption of human against to climate change. So, from the groundwater monitoring of this experiment proved that the groundwater was sufficient for planting.

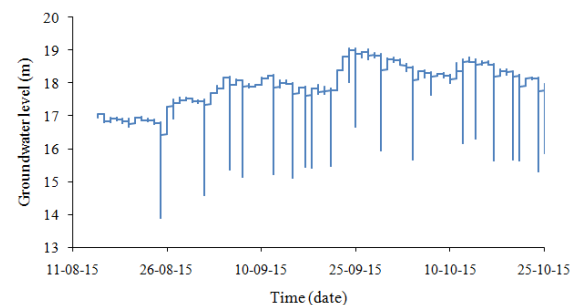


Figure 6. Groundwater level measurement

4. Conclusion

This research was conducted with the different water irrigations for growing long-bean in which the growth rate, soil moisture content, evaporation, soil characteristic and daily temperature included changes of groundwater level were needed. The results showed that long bean grew well across different temperature and moisture conditions. The best technique of water irrigation was found to be the drip technique with coconut husk in which coconut husk could keep moisture well and be mixed into soil as nutrients. However, the drip system with coconut husk could reduce water quantity applied for plant and reduced coconut waste, which can be an alternative for farmers to plant cash crop by using abundant groundwater resources in the country.



Acknowledgement

The researcher team would like to thank the Australian Centre for International Agriculture Research (ACIAR), a researcher from International Water Management Institute (IWMI) for advice and Faculty of Water Resources, National University of Laos for providing support the experiment site.

References

- Adams, S. R., Cockshull, K. E., & J. Cave, C. R. (2001). Effect of Temperature on the Growth and Development of Tomato Fruits. *Annals of Botany*, (88), 869-877. Retrieved from http://www.oxfordjournals.org/our_journals/annbot/access_purchase/price_list.html
- Albaji, M., Golabi, M., Boroomand Nasab, S., & Zadeh, F. N. (2015). Investigation of surface, sprinkler and drip irrigation methods based on the parametric evaluation approach in Jaizan Plain. *Journal of the Saudi Society of Agricultural Sciences*, 14(1), 1-10. doi:10.1016/j.jssas.2013.11.001
- Allen, R. G., Pereira, L. S., Rase, D., & Smith, M. (2006). *Crop Evapotranspiration (Guidelines for Computing Crop Water Requirements)* (56). FAO Irrigation and Drainage Paper.
- Department of water resources water resources and Environment Administration (DWREA). (2008). *the Nam ngum river basin development*. Vientiane capital: Asian Development bank and Francaise de developpement.
- Hagos, F., & Mamo, K. (2014). Financial viability of groundwater irrigation and its impact on livelihoods of smallholder farmers: The case of eastern Ethiopia. *Water Resources and Economics*, (7), 55-65.
- John Panuska, Scott Sanford and Astrid Newenhouse, (2015). *Methods to Monitor Soil Moisture*. University of Wisconsin Extension.
- Kima, P. E. (2014). Leishmania molecules that mediate intracellular pathogenesis. *Microbes and Infection*, 16(9), 721-726. doi:10.1016/j.micinf.2014.07.012
- Lalić, B., Eitzinger, J., Thaler, S., Vučetić, V., Nejedlik, P., Eckersten, H., ... Nikolić-Djorić, E. (2014). Can Agrometeorological Indices of Adverse Weather Conditions Help to Improve Yield Prediction by Crop Models? *Atmosphere*, 5(4), 1020-1041. doi:10.3390/atmos5041020
- Plusquellec, H. L., & Food and Agriculture Organization of the United Nations. (2002). *How design, management, and policy affect the performance of irrigation projects: Emerging modernization procedures and design standards*. Bangkok, Thailand: FAO.
- Tao, H., Dittert, K., Zhang, L., Lin, S., Römheld, V., & Sattelmacher, B. (2007). Effects of soil water content on growth, tillering, and manganese uptake of lowland rice grown in the water-saving ground-cover rice-production system (GCRPS). *J. Plant Nutr. Soil Sci.*, 170(1), 7-13. doi:10.1002/jpln.200625033.
- World Bank. (2008). *Lao People's Democratic Republic: Policy, Market and Agriculture Transition in the Northern Uplands*. DC: Washington.
- World Bank. (2014). *Enhance the work efficiency to widely development (ACS9577)*. world bank.

Participatory Water Management in the Specific Locale of Sub-watershed: Negotiation Process and Institutionalization.

MAN PUROTAGANON, PhD.^{1, a *}

Abstract This article will present the application of the framework: 'stakeholders' analysis' which will help understand the complex relationships among water users, and the application of conceptual framework of 'institutionalization' in understanding the cooperation and negotiation processes among multi-stakeholders in water management. Examples will be taken from five sub-watersheds: Upper Loei; Lower Huayluang, Udonthani; Huaysaneng, Surin; Middle reach of Moon River, Roi-et; and Chi, Mun and Khong River, Ubonratchathani.

Keywords *stakeholders' analysis, institutionalization, multi-stakeholders, negotiation process, water management, multi-stakeholders' platform.*

Man Purotaganon, PhD. (Author)
Thai Water Partnership
ThaiWP
Bangkok, THAILAND
purotaganon@gmail.com

Introduction

Water Institution: Conceptual frame

Water Institution, the conceptual frame for understanding of water management institutions is the perspective which needs to cover macro level, national or regional level, and specified at formal perspective. It is broader than organizational structure. This is because 'institution' covers legislative conceptual frame, policy regime, and organizational administration. With this conceptual frame, water institution' composed of key factors: water laws, water policy, and water administration, which are interrelated and cannot be separated. Thus, in this study, 'institution' is identified as integrated system which covers organizational environment and management.

Over the time, water management has been influenced by the governmental system in every context. Government has become active actor in taking control over water management. Thus, the interest of organizational administration has focused on planning, budgeting and disbursement, and competing among agencies rather than undertaking major task for efficient water management and water allocation. Then in people's perspective, responsible unit for water management when in practice is necessary, no matter whether the government agencies will take responsible or not.

The idea for the integration of water institutions concept must be achieved by analyzing three main elements: water laws; water policy, and water management. The analysis of three main elements must be done separately from social context to understand how that system and the proceeding of water institutions be affected by various external factors as well as strict limitations from government water resources section. Remarkable attributes of water institutions, different from those of socio-economics institutions in general, that they are informal, and faster to respond to changes of their rules at local and cultural environment than rules and regulations at macro level which surrounded by political economy and limitations of the governmental system.

Cases and Areas of study

Table 1. Summary of information on physical, situation-issues/threats and crucial management issues of 5 areas, represented of local researches in watershed eco-system, the Northeast, Thailand.

Case/study area	Watershed	Situations-Threats	Water management Issue
1) Kudkhakeem Middle reach, Mun River, Roi-et	NumMun Basin	low lying land and food plains ecosystem. land and resources utilization and local livelihoods, affected by Rasrisalai Dam construction. Conflicts between local stakeholders and government agencies.	Land and resource use by local users as Local livelihoods and different ways of water management.
2) Upper Loei	NumKhong	- Upstream: Forest and land cover drastically loses for agricultural activities. - Middle range: deteriorating water quality due to polluted water released from residential area and chemical application. - Downstream: water pollution and environmental degradation due to mining industry.	Land and resource use at basin level. Long-term land use planning for better water management and restores water quality.
3) Huaysaneng, Surin	NumMun	- Upstream: Intensification of chemical use. - Middle range: excavation of canals upstream affected bank erosion and deteriorating of watershed ecosystem -- Downstream: flooding at connecting area of Huaysaneng reservoir, water polluting and competing use of water between households consumption and agricultural use.	Competing water use between residential area and agricultural use. Multi-stakeholders have proposed plan for holistic water management at basin level.
4) Lower Huayluang, Udonthani	NumKhong	- Upstream: water contaminated by intensified chemical use in agriculture. - Middle range: extension of residential and farming areas, competing use of water, flooding, and water polluting . Downstream: flood plains area turned to second rice fields.	Proposed strategic plan for water management at basin level. Long-term land use planning should be implementing for better water management and restores water quality.
5) Chi, Moon and Khong Rivers, Ubonratchathani	Num Chi-Mun and NumKhong	Local organizations prioritize allocation of water for consumption and water for agricultural use. This water management approach has been interrupted by overlapping authority of local organizations.	Water management across different administrative boundaries.

Three steps of study process are as follows: 1). Documentary or literatures review in order to select the issues and study site, 2). Summarize the lessons learned with the research projects-organize the forum to analyze the research issues and knowledge from the researches, for examples, learning process, water management in different forms and their mechanism as groups/networks/nodes, and 3) Research team with local leaders analyzed the overview of 5 cases, and organized the forum to discuss and analyze crucial issues of water management in the Northeast, composed of a) local

knowledge in water management, b) water institutions in the Northeast, and c) guidelines to develop institutions cooperatively and /or in negotiating, including to link knowledge with the social context for water management in the Northeast.

Table 2. Major attributes of the Management Units in the basin ecosystem.

Watershed Management Unit	Typical area(km ² .)	Influences of impervious cover	Primary Planning authority	Management Focus
Micro-watershed	0.05-0.50	Very strong	Property owner/local	Exploitation-maintenance
Sub-watershed	1-10	strong	Local government	Basin classification and integrated management
Watershed	10-100	moderate	Local or multiple local government	Land use planning - design
Sub-basin	100-1,000	weak	local-province-region	Basin planning
Basin	1000-10000	Very weak	Province-provinces	Basin planning

(adjusted from *Watershed Management Approaches, Policies and Operations: Lessons for Scaling Up, The World Bank Washington, DC, 2008*)

Considering information from Table 1., most of watershed management units in the study areas fall under Micro-Watershed with the typical area between **0.05-0.50** km². and some are classified as Sub-watershed, of **1-10** km². Scale and boundary (Typical area) is crucial attribute which will identify the relation of watershed with the eco-system in various aspects, such as Hydraulic system, Flow rates, speed of the flow, runoff. In this study, priority was given to the knowledge on watershed eco-system, which can be explained and understood by tools and local knowledge.

Types of networks of Basin management in the study areas:

The mechanism and network of are different and can be categorized into 3 groups as follow:

1. **Group/Network of Water Management:** It composed of relatives, or groups in the same social domain. This is limited to small scale water management. Networks of Basin Resources Users (water/land/forest) which are various based on various kinds of resources and how they are used, for examples:
 - Water management in kinship groups where they have rice fields in the same vicinity. They have set agreement to use water together.
 - Water users groups at local level, use the same water sources, with management system and common agreement.
 - Occupational groups benefitted from basin resources, for examples, cattle groups, mat weaving group, fishery group, and wetlands ecological group.

This type of networks is based on relationship among members and physical condition of the areas with main purpose to use the resources.

2. **Network-Committee for water management:** It aims to manage the overall water management system involved water account, water allocation, and environmental services.

It is based on the social relations and common agreements among water user groups and with local communities as support mechanism. Examples as in Loei Basin Committee, and using the networks to communicate, negotiate with the government and private sector as in Kudkhakeem and Huaysaneng (Surin) Networks.

3. **Multi-stakeholders Network:** This network covers the areas larger than 10 km². It links the structures at local, provincial and watershed levels and aims to mobilize resources, negotiate for the resources use, and communicate with publics on watershed management. Examples are:

- Mechanism to develop management system for Phan Reservoir with MoU of three TAOs.
- Mechanism to develop water management system in the trans-boundary areas of Khothong sub-district, undertaken with the MoU of PAOs Ubolrachathani, Yasothorn, and two TAOs.
- The movement for provincial development strategic plan of Surin by Huaysaneng Basin Network in the Forum for Health Assembly.
- Campaigning for the monitoring of Loei Basin Network by Youth Network, and Loei Basin Committee (from Civic Group).

In categories 1 and 2, it is limited boundary to within 10 km² at local level, while the third is more complex with multi-stakeholders and varied objectives for water use. The case will reveal how ‘Stakeholders’ analysis’ and ‘Institutionalization’ facilitate the researchers and water managers to better understand the complicated problems in water management.

Table 3. Pattern-Structure of organization/Institution in the Study Area

Area/ Watershed	Pattern- Structure	Roles and Functions	Relationship/ Key Actors	Co-operation/ Negotiation	Link w/ government agencies	Policy Implications
Upper Loei	Local Network	Water management at local level	Occupational groups/local networks and leaders.	Plan for Co-operation-local user groups and TAO.	Co-operation between local users and TAOs.	-Community Rights -Plan to restore environment and water quality.
Lower Huayluang, Udornthani	Local groups/Network (Phan Reservoir Committee comprises of 3 TAOs)	Water management at local level (committee: representatives of parties involved)	Occupational groups/local network – leaders and government agencies.	Plan for Co-operation-local user groups and Negotiation process w/local, and provincial authorities.	- Co-operation between local users and TAOs	-Co-operation Plan across administrative boundaries. - Common agreement at local level.
Huaysaneng, Surin	Local groups/Network (Health Assembly Committee- Provincial level)	Water management at local level, Strategic Plan proposed by Multi-stakeholders at provincial level.	Occupational groups/local network – leaders and government agencies at provincial level.	Co-operation among different users and campaigning of River Basin Issues through Health Assembly Committee (Provincial level).	-Local Authority legislation process. - Health Assembly at provincial level.	-Water quality effects to health and environment. -Priorities set for water allocation between urban and agricultural use.
Kudkhakeem Middle reach of Mun River, Roi-et	Local groups/Network	Water management at local level	Occupational groups/local networks – leaders	Co-operation among user groups to manage water at local level, supported by government agencies.	- Planning and Budgeting support by TAOs. - Co-operation between local users and agencies.	-Integrated land and resource planning to restore local livelihood and ecosystem.
Chi Moon and Khong River, Ubonratchathani.	Local groups/Network (MOU-agreement and compliment of TAOs-PAO)	Water management at local level, Common agreements of Local users and TAOs under support of PAO)	Occupational groups/local network – leaders local organization ,gov. agencies and two PAOs.	Co-operation among user groups to manage water at local level, Common agreement and Co-operation Plan across constituencies.	-Planning and Budgeting supported by TAOs. -Co-operation between TAOs and PAO	Common agreement and Co-operation Plan across constituencies.

Multi-Stakeholders Processes-MSPs and Negotiation Process

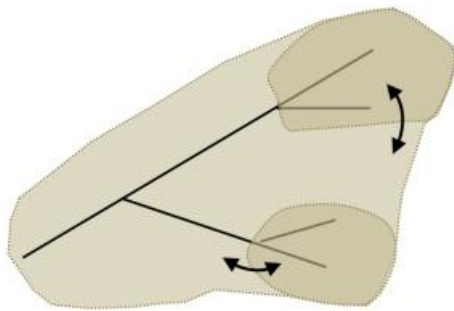
‘Multi-Stakeholders Processes-MSPs’ means communication process, learning process to consult with stakeholders in the use and management of natural resources in order to facilitate quality decision making and with more choices. It is ensured that opinions of direct stakeholders are listened to and considered in the process for decision making through negotiation and careful consultation. MSPs are intended to build trust among stakeholders involved in the decision making for

the highest benefit in the natural resources management. Negotiation Process is the key factor when

there are many different stakeholders with various objectives and interests. Choice must be made. Negotiation process is the effort to help compromise among different stakeholders. Main objective of the ideal negotiation is to achieve the practical common agreement which is acceptable to various all involved: individuals, groups, communities, NGOs, academia, private sector, and facilitators as representatives of groups/organizations, and networks’ cooperation. There are necessary conditions for negotiation process, for examples, various interests of participated stakeholders. Imperative conditions are composed of: Various interests of different stakeholders; Independences of the stakeholders; and Communication process Effective communication can facilitate better understanding of the

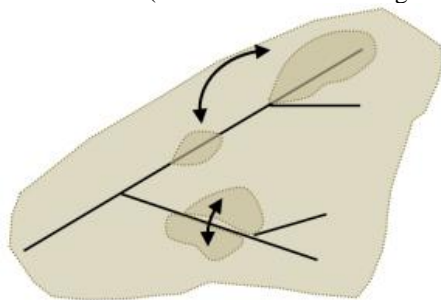
involved parties, which will lead to quality and practical choices to solve their water management problems they are facing.

However, this paper would like to make a link between the constructing process of practical knowledge and the practice of local knowledge as well as explaining the phenomenon resulting from learning process of water management in various dimensions horizontally how the networking of different stakeholders is extended, and vertically how water institutions have structured and linked to daily practices, beliefs, and norms of different user groups. This is necessary to employ the Political Ecology (applied social science) framework to understand the overlapping and dynamics of local areas’ water management issues linked with different dimensions in Scale, Position, and Spatial dimension.



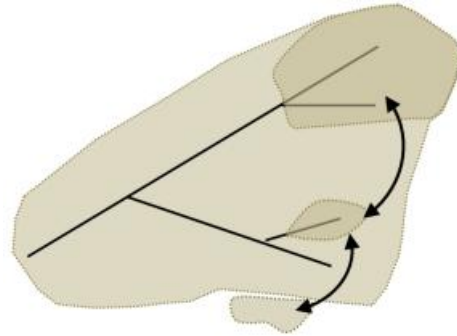
ที่มา: Lebel, L., P. Garden, and M. Imamura. 2005.

Scale: In general, we believe that big scale water management by the government, through plan and management system at national level should ensure that people will have equal access to water. In principle, public tend to trust the government in managing water with high hope for the fair and good service. However, by the empirical data of academic research revealed the success of small scale community based irrigation scheme in the North (traditional water management).



ที่มา: Lebel, L., P. Garden, and M. Imamura. 2005.

Position: Naturally, water runs from high place to low lying land, this has made differences on water users’ location, and it is unavoidable to create inequality of access to water. It is the same as when the water allocation project has set the criteria to supply piped water to urban dwellers before planning to distribute water to agricultural sector.



ที่มา: Lebel, L., P. Garden, and M. Imamura. 2005.

Spatial dimension: Large scale water management needs to engineering technology to adjust the different and disadvantages in spatial dimension which impacted stakeholders in different physical locations. Water users at the downstream usually face negative impacts of water management/allocation the most and this has caused endless water conflicts

Conclusion

Five cases presented in this article, has revealed that water management in small scale basin eco-system in the Northeast Thailand has been managed by local knowledge together with modern technology developed by practical solutions to problems at different levels. It also includes skills in groups/organizations’ administration suitable to social context at local level and trans-boundary. However, conventional organizational analysis has limitation as it only focuses on the practices of mechanism or organizations at local level. This article proposes to apply the concept of institutions in understanding the learning process, social relations in both collaboration and negotiation among multi-stakeholders. This is not to limit only to understanding of formal organizational structure or explanations only related laws and regulations. Institutional analysis will help elaborate for us to see various water users in scale, position, and spatial dimensions, and then to understand their process of cooperation/collaboration and negotiation. This new perspective of ‘Institutions’ can link social practice to a wider context in legal aspect and policy covered at basin, regional, and national levels.

References

Christensen, S. R., & Areeya Boon-long. (1993). Institutional Problems in water Allocation: Challenges for New Legislation. *TDR Quarterly Review*, 8(3), 3-8.

Coward, E. W. (Ed.). (1980). *Irrigation and Agricultural Development in Asia: Perspectives from the Social Sciences*. Ithaca, NY: Cornell University Press.

Dore, J. (2007). Mekong Region Water-Related MSPs-Unfulfilled Potential. In J. Warner (Ed.), *Multi-*



- Stakeholder Platforms for Integrated Water Management*. Aldershot, UK: Ashgate.
- Dore, J., Robinson, J., & Smith, M. (Eds.). (2010). *Negotiate – Reaching agreements over water*. Gland, Switzerland: IUCN.
- FAO (Food and Agriculture Organization). (1995). *Water sector policy review and strategy formulation: A general framework*. Rome, Italy: Author.
- Faysse, N. (2006). “Troubles on the way: An analysis of the challenges faced by multi-stakeholder platforms”. *Natural Resources Forum*, 30, 219-229.
- Global Water Partnership. (2003). *Water Management and Ecosystems: Living with Change. Technical Advisory Committee (TAC) Background Paper no.9*. Stockholm, Sweden.
- Grimble, R. J., & Chan, M. K. (2000). "Stakeholder analysis for natural resource management in developing countries: Some practical guidelines for making management more participatory and effective". *Natural Resources Forum*, 19(2), 113-124.
- Hemmati, M. (2002). *Multi-stakeholder processes for governance and sustainability: beyond deadlock and conflict/ Minu Hemmati; with contributions from Felix Dodds, Jasmin Enyati, and Jan McHarry*. London, UK: Earthscan.
- Lebel, L., P. Garden and M. Imamura (2005). “The politics of scale, position, and place in the governance of water resources in the Mekong region.” *Ecology and Society*, 10(2).
- Molle, F., Floch, P., Promphakping, B., & Blake, D. H. (2009). The 'greening of Isaan': Politics, ideology, and irrigation development in the Northeast of Thailand. *Contested waterscapes in the Mekong region: Hydropower, livelihoods and governance*, 253-282.
- Purotananon, M., & Schmidt-Vogt, D. (2014). Agricultural Intensification In The Bang Phluang Irrigation Scheme, Prachinburi Sub-basin, Thailand, And Its Impacts On Water Management[J]. *International Journal Of Water Resources Development*, 30(2), 308-321.
- Warner, J. (2005). *Multi-Stakeholders Platforms: Integrating Society in Water Resource Management*. Ambiente e Sociedad

WATER QUALITY PROFILES AND THE RESERVOIR UTILIZATION WITH SPECIAL REFERENCES TO JATILUHUR, CIRATA AND SAGULING RESERVOIRS

Luki Subehi

Research Centre for Limnology, Indonesian Institute of Sciences, Cibinong 16911, Indonesia; ²Laboratory of Water Environment, University of Tsukuba, Tsukuba, Japan

Email :luki@limnologi.lipi.go.id

Abstract Reservoir is one of the unique ecosystems which are functioning in both ecological and economic services. The objective of this study is to analyze the hydrological characteristics represented by Jatiluhur, Cirata and Saguling as cascade reservoirs. Surveys at Jatiluhur, Cirata and Saguling reservoirs were conducted on July 2014, March 2015 and September 2015, respectively. Meanwhile, the results on the survey in Jatiluhur, Cirata and Saguling reservoirs showed that the average depths are 32.9m, 34.9m and 17.9 m, respectively. Jatiluhur reservoir covers 7,780 ha of area with maximum depth of 90 m. Meanwhile, Cirata reservoir covers approximately 6,200 ha of area with maximum depth of 106 m. In addition, Saguling reservoir covers approximately 4,869 ha of area with maximum depth of 90 m. All of those reservoirs serve as important hydroelectricity power. Next, the percentage value of fish cages at Cirata reservoir was larger (3.95%) than those at Jatiluhur (1.00%) and Saguling (0.70%) reservoirs. It indicated the potential impact from fish cages as pollutant at those reservoirs. In addition, based on water quality profiles (dissolve oxygen/DO, Chl-a and temperature), upwelling caused water quality degradation. In order to maintain the sustainability of the lake, basic ecological information is necessary for the next study.

Keywords *Jatiluhur reservoir – Cirata reservoir – Saguling reservoir - Water quality – Fish cages*

Introduction

Water is our most valuable natural resource. The availability and quality of inland waters not only impact human health and wellbeing, but also the functioning of essential ecosystems, including rivers, wetlands, lakes and coastal ecosystems. Without sound water resources management, human activities can upset the delicate balance between water resources and environmental sustainability.

The strategic functions of the Citarum River basin and Jatiluhur, Cirata and Saguling reservoirs at the national scale (Presidential *Decision* of the *Republic of Indonesia No.12/2012*) and its socio-environmental problems are two important reasons why the locations have been selected here. Several key environmental issues for the Jatiluhur and Cirata reservoirs and the Upper Citarum River basin are described below: land degradation, flood, soil erosion and sedimentation, water quality deterioration and water supply fluctuations.

Citarum River basin is one of main river basins in Indonesia which experience flood problem. Furthermore, the topographic condition and geographical location also contribute to the occurrence of flood disaster in Citarum River basin. The upper Citarum River basin is also recognised as an area with some of the most persistently active landslides in Indonesia. The floods that trigger the landslides occur almost every year and cause extensive damage. The Citarum River is of vital importance for West Java Province and Jakarta City, Indonesia, in terms of economic development and the prosperity of the people.

The Jatiluhur and Cirata reservoirs were constructed in 1967 and 1988, respectively. In Jatiluhur reservoirs used for power generation that installed capacity of 150MW. On the other hand, Cirata and Saguling reservoirs are used for power generation those installed capacity of 500MW and 700 MW, respectively (Sembiring 1985; Gamo 2002). In addition, the condition of the upper river basin is an important factor in controlling its hydrological response, including floods, soil erosion,

landsliding, and sediment input to the Saguling Reservoir.

Eutrophication and toxic algal blooms have restricted the function of those reservoirs. Pollution originates mainly from the upper catchment and mostly from improperly treated urban and industrial sewage, agriculture and land-use transformation due to urbanization and deforestation. A significant nutrient source for eutrophication is the internal load from the sediments that intensively accumulate at the bottom of the reservoir from the ever-expanding traditional fish cage culture.

An increasing trend of high water supply fluctuations from the basin between wet and dry seasons restricts continuous hydropower generation. Water deficiency during the dry season disrupts hydropower generation, resulting in the application of costly rain-harvesting techniques. Reservoir degradation is rooted in socio-economic problems. The objective of this study is to analyze the water quality related to the reservoir morphometry and fish culture conditions at both sites.

Methods

We conducted survey at Jatiluhur and Cirata reservoirs to know water quality conditions (Fig. 1). Not only survey at field, but also to collect the secondary data for supporting the analyze.

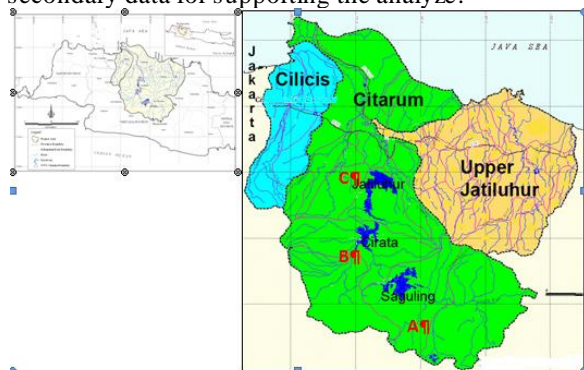


Fig. 1 Locations of study area: Saguling (A), Cirata (B) and Jatiluhur (C) reservoirs (source: PJT II Jatiluhur-PU, 2013)

Water samples at Jatiluhur and Cirata reservoirs were taken on July 2014 and March 2015, respectively. We used ringko profiler, supported by University of Tsukuba, Japan. The logger version CTD profiler with optical fast DO sensor RINKO-Profilier was used for survey. Depth (semiconductor pressure sensor with ranged 0 to 600 m and resolution 0.01m), temperature (thermistors with ranged -3 to 45°C and resolution 0.001°C) and dissolved oxygen/DO (phosphorescence with ranged 0 to 20 mg/L and resolution 0.001mg/L) were obtained at each station. Measurements were carried out until to the depth of 72.7 m (Jatiluhur reservoir) and 80.8 m (Cirata reservoir) with an interval of 10 cm.

Finally, fish aquaculture cages established at both reservoirs were also observed. In 2008,

at Jatiluhur and Cirata reservoirs, there are 15,810 and 49,985 unit fish culture cages, respectively (Machbub B, 2010). In general, the size of fish culture cage is 7 x 7 m (Director General of Aquaculture, Ministry of Marine Affairs and Fisheries 2013).

Results and Discussion

Jatiluhur reservoir is located at an altitude of 111 m above sea level with a surface area of 7,780 ha and an average depth of 32.9 m. Meanwhile, Cirata reservoir is located at an altitude of 200 m above sea level with a surface area of 6,200 ha and an average depth of 34.9 m. Both of reservoirs are multipurpose cascade dams. The source of water comes from the Citarum river with a basin area of 660,000 ha with a length of 270 km where flowing to Saguling, Cirata and Jatiluhur reservoirs. The magnitudes of outflow discharge and hydroelectric power were described in Fig. 2.

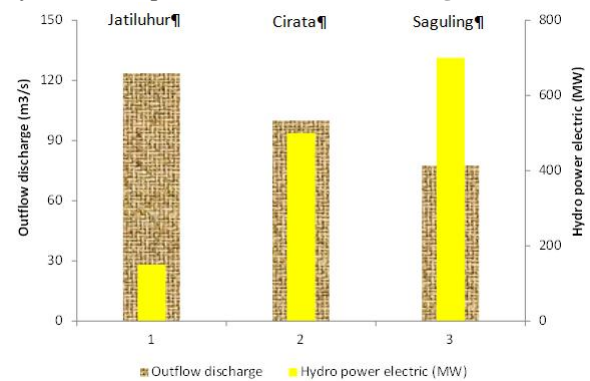


Fig. 2 Outflow discharge and hydroelectric power in 2008 at three sites (modified after Machbub B, 2010)

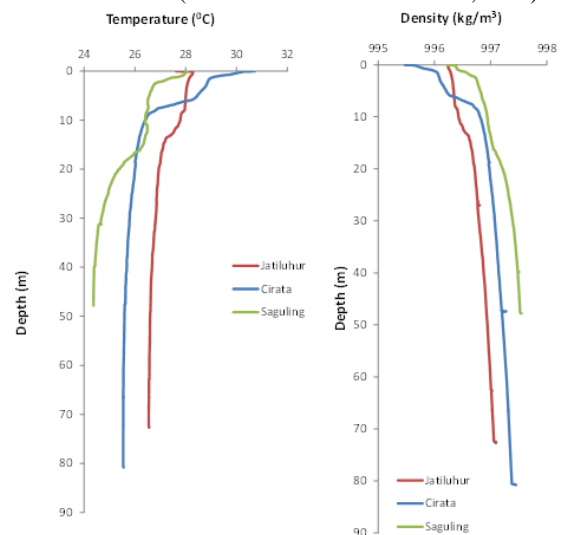


Fig. 3 Temperature and density profiles at Jatiluhur (July 2014), Cirata (March 2015) and Saguling (September 2015) reservoirs

Figure 3 refers to the water column at Cirata reservoir was divided into two primary layers: epilimnion characterized as a column of hot water and less dense at the surface to a depth of 5 m and hypolimnion cooler denser deeper divided between the average depths of 10 m to 80.8 m. Between

the two layers, there is a layer that resembles metalimnion layer indicated by a sudden drop in temperature between the average 28⁰C to 26⁰C from an average depth of 5m to 10m. The top of this layer bordering the epilimnion constantly changing depth, while the bottom layer adjacent to hypolimnion remained stable at an average depth of 80.8 m.

In contrary, there were not so large changes in temperature for Saguling and Jatiluhur reservoirs. It could be explained that the mixing of water column were easier at Saguling and Jatiluhur reservoirs than that at Cirata reservoir. In addition, from Fig. 3, the density at Cirata reservoir was more stratified than those at Saguling and Jatiluhur reservoirs. In addition, the characteristics of density were related to temperatures profile (Subehi et al. 2014).

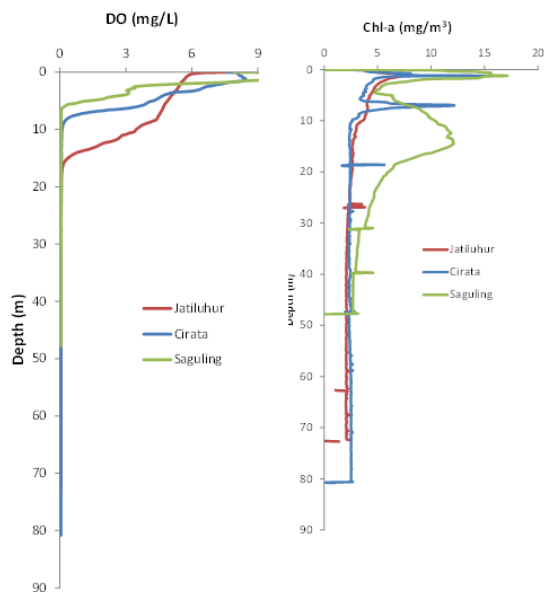


Fig. 4 Dissolve oxygen (DO) and Chl-a profiles at Jatiluhur (July 2014), Cirata (March 2015) and Saguling (September 2015) reservoirs

Based on **Fig. 4**, the average dissolved oxygen (DO) from surface until 5 m at Cirata reservoir was relative larger than those at Jatiluhur and Saguling reservoirs. In contrary, the values of DO at Jatiluhur reservoir were larger at depth of 10 m than those at Cirata and Saguling reservoirs. It suggested the water quality at Jatiluhur reservoir relative was better condition.

In case at Cirata reservoir, high dissolved oxygen content in the surface layer and the base of diminishing. Dissolved oxygen from the surface layer to a depth of 5 m, and from a depth of 10 m to the policy did not differ significantly ($p > 0.05$) among the research stations at the same depth and has a low variation during the study. In contrast to the average depth of 3 m to 10 m, the variation shown is high due to the different recorded at each sampling interval. In addition, the concentration of chl-a at Cirata reservoir was also relative higher than that at Jatiluhur

reservoir. More specifically at Saguling reservoir, the concentration of chl-a was higher at depth of 10 m to 40 m than those at Cirata and Jatiluhur reservoirs. It could be suggested the high potential eutrofication at Saguling reservoir.

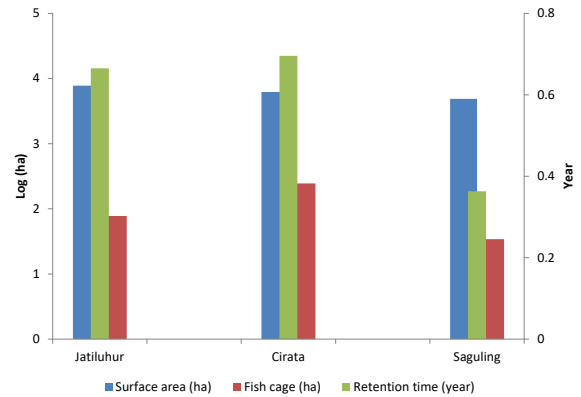


Fig. 5 Comparison among surface area, fish cage area and retention time in 2008 at three sites (modified after Machbub B, 2010)

Based on our survey and secondary data, in **Fig. 5** showed the surface area, fish cage area (unit ha) in logarithm and retention time (year) at all sites. The percentage value of fish cages at Cirata reservoir was larger (3.95%) than that at Jatiluhur (1.00%) and Saguling (0.70%) reservoirs. It indicated the potential impact from fish cages as pollutant with the length of retention time was larger at Cirata reservoir than those at Jatiluhur and Saguling reservoirs. Moreover, the condition of DO, Chl-a concentration and stratified layer also influenced the water quality of the reservoirs.

Conclusion

Jatiluhur, Cirata and Saguling reservoirs function in ecological and economic services as in other tropical reservoirs. The different characteristics and utilizations of reservoirs have resulted in various problems. It found the percentage value of fish cages at Cirata reservoir was higher (3.95%) than that at Jatiluhur (1.00%) and Saguling (0.70%) reservoirs. Based on those ratios, the density of aquaculture which indicated the potential impact i.e. pollutants from fish cages at Cirata reservoir was higher than those at Jatiluhur and Saguling reservoirs. Consequently, in order to maintain the sustainability of these reservoirs, basic ecological information is necessary for the next study.



References

- Director General of Aquaculture, Ministry of Marine Affairs and Fisheries (2013) Kebijakan pengelolaan perikanan budidaya di perairan umum daratan. Seminar Nasional Limnologi VII, 16 September 2014 di LIPI. Cibinong, Bogor.
- Garno YS (2002) Beban pencemaran limbah perikanan budidaya dan eutofikasi di perairan waduk pada DAS Citarum. Jurnal Teknologi Lingkungan Vol.3 No. 2: 112 – 120.
- Machbub B (2010) Model perhitungan daya tampung beban pencemaran air danau dan waduk. Jurnal Sumber Daya Air Vol. 6 No. 2: 103-204
- PJT II Jatiluhur– PU presentation file. 2013. LIPI, APCE and ILEC Meeting, July 13, 2013
- Sembiring S (1985) Water quality in three reservoirs on the Citarum river, Indonesia.
<http://hydrologie.org/ACT/Marseille/works-pdf/wchp3poster4.pdf>
- Subehi L, Ridwansyah I, Nor Aisyahbinti Omar, Muzalifah Abd Hamid, Mashhor Mansor (2014) The Utilization and problems in tropical lakes with special reference to lake Maninjau (Indonesia) and lake Temengor (Malaysia). International Conference on Ecohydrology – November 2014, Yogyakarta.

Proposal of a reservoir management method based on the observed accumulated areal mean rainfall for the Sirikit reservoir in the Chao Phraya River basin, Thailand

Kentaro Dotani^{1,a,*}, Masashi Shimosaka^{1,b}, Taichi Tebakari^{1,c} and Shuichi Kure^{1,d}

Abstract The Chao Phraya River basin (CPRB) in Thailand has been confronted with serious drought situation since 2012. Historically, the CPRB also has drought risk in every single dry season. On the other hand, the CPRB had a massive flooding in 2011, which affected on not only Thai socio-economics but also global supply-chain of industrial production. Even though the CPRB has two multi-purpose and large-scale reservoirs, Bhumibol and Sirikit reservoirs, serious both flooding and drought has been existed from ancient times.

The purpose of this study is to propose a new reservoir operation system on science-based which can be easily put into practice; we studied a reservoir optimum operation for large scale reservoir considering the country's situation. This study proposed the new reservoir operation method for reducing risks of drought and flood. The method was determined characteristics of rainfall in the target basin using historical inflow data on reservoir and historical rainfall data on catchment area of reservoir. In our proposal method, daily release was decided by using accumulated daily rainfall data, daily inflow data and storage volume. The usefulness of the reservoir operation method was verified using historical inflow data on reservoir and daily rainfall data on catchment area of reservoir. This proposed method was applied for the Sirikit reservoir. The proposed reservoir operation method could contribute stabilization of release discharge and storage volume. It means that the risk of drought is low. In addition, the method could control release discharge without rising risks of flood in lower section of the basin.

Keywords *Accumulated areal mean rainfall, Reservoir management, The Sirikit reservoir, The Chao Phraya River basin.*

Kentaro Dotani
Graduate School of Engineering, Toyama Prefectural University
Imizu, Toyama, Japan
t557008@st.pu-toyama.ac.jp

Masashi Shimosaka
Graduate School of Engineering, Toyama Prefectural University
Imizu, Toyama, Japan

Taichi Tebakari
Graduate School of Engineering, Toyama Prefectural University
Imizu, Toyama, Japan

Shuichi Kure
Graduate School of Engineering, Toyama Prefectural University
Imizu, Toyama, Japan

Introduction

In 2011, historical flooding occurred in the Chao Phraya River Basin (CPRB), Thailand. The unprecedented flood damage had a large effect on the Thai economy. By contrast, the basin suffered severe droughts in the early 1990s. In addition, the two largest reservoirs in the CPRB, the Bhumibol and Sirikit Reservoirs, have suffered serious water shortages for the past 3 years. In Thailand, a very large proportion of the population is still involved in agriculture, although agriculture is gradually contributing less to the Gross Domestic Product. Consequently, drought has a huge effect on the economy of Thailand. Therefore, integrated watershed management, including flood control and water usage, is necessary for the CPRB.

The CPRB has two large multi-purpose reservoirs: the Bhumibol and Sirikit dam reservoirs (named after King Bhumibol and Queen Sirikit). Tebakari *et al.* (2005) showed that these reservoirs contributed to ensuring a stable water supply and decreased the frequency of floods in the lower basin. Even in the flood of 2011, both reservoirs maintained flood control functions to an extent. Komori *et al.* (2013) evaluated the operation of these reservoirs using the probability of inflow into the reservoirs and showed that it is too difficult to control flooding and maintain irrigation capacity in the CPRB using only these reservoirs. Concerning the watershed management, the influence of reservoir management is significant, and it is necessary to optimize the management of these reservoirs.

The runoff characteristics of the CPRB have been modelled (Kure and Tebakari, 2012). However, none of these studies achieved a concrete means of watershed management. As a practical method of optimizing reservoir management in Japan, the prior flow method has been developed and put to practical use (Shimosaka

et al., 2008). In theory, this method improves flood control without decreasing water use.

Our group has studied reservoir operations for the CPRB based on Shimosaka *et al.* (2008) (Tebakari *et al.*, 2015). This study proposed a method for operating a large reservoir based on the prior flow method and validated the effectiveness of the method using dam reservoir and observed rainfall data.

Sirikit Reservoir

The CPRB, the largest river basin in Thailand, is located in north-central Thailand. It covers 157,925 square kilometers and 29 provinces, almost 30% of the country’s area. As of 2016, there were nine dams in the CPRB, with a total storage capacity of 25.4 billion cubic meters. Sirikit Dam Reservoir, the second largest reservoir in CPRB is controlled and managed by the Electricity Generating Authority of Thailand (EGAT). As already reported, the Sirikit Dam Reservoir is controlled using a storage rule curve (Tebakari *et al.*, 2015). Here, these curves are referred to as the upper rule curve (URC) and lower rule curve (LRC). In addition, the minimum release volume is determined by the water supply needs of the lower basin, the provision of navigable river depth, and other factors. As Tebakari *et al.* (2005) discussed, the release volume during the dry season is determined in conformity with the irrigation release volume established by the Royal Irrigation Department (RID). Since they are explained in Tebakari *et al.* (2015), the actual historical storage volumes and release volumes are omitted here. Historically, the storage volume remained significantly lower than the LRC in some years, and the actual release volume during the dry season was significantly below the irrigation demand volume for several years.

Proposed Method

We propose a new reservoir management method that optimizes the current rule curve management. The irrigation capacity of the Sirikit Dam Reservoir is mainly used for irrigation water during the next dry season. The main goal of reservoir management is to meet the storage target by December 31 each year, while securing a suitable flood control capacity. The proposed method identifies probable inflows to the reservoir until December 31 from the observed areal rainfall. The inflow is calculated using its relationship with the areal rainfall. In our proposed method, the calculated probable inflows in excess of the storage target will be released. This is explained in detail below. As an indicator of excess of storage volume, S' is defined as follows:

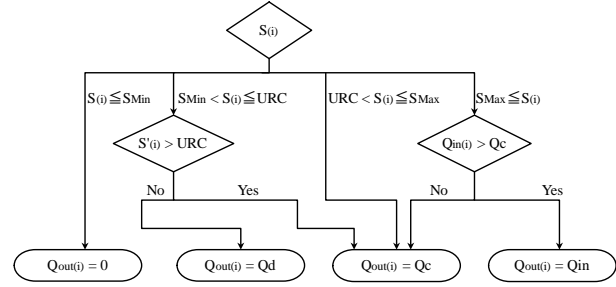


Figure 1 Flow chart used for determining the daily discharge

$$S'(i) = S(i) + V(i) \quad (1)$$

$$V(i) = R(i) - \sum Q(i) \quad (2)$$

Here, $S(i)$ is the storage volume on the i^{th} day of the year from January 1, $R(i)$ is the probable inflow in the year, and $\sum Q(i)$ is the accumulated observed inflow from January 1 to the i^{th} day (all in cubic meters). $R(i)$ is calculated from the relationship between rainfall and inflow to the basin, and is explained below. In equation (2), $V(i)$ is the probable inflow from the i^{th} day to December 31. By comparing S' with the storage target, one can judge the excess of storage volume and start flood control operations sooner than when judged using only the storage volume.

Validation of Proposal Method

Using historical data for the dam reservoir and the observed areal mean rainfall, we validated the proposed reservoir operation method from January 1, 2011 to March 31, 2016. The daily discharge $Q_{\text{out}(i)}$ (m^3) is determined from the relationship between the storage volume $S(i)$ and URC or between $S'(i)$ and URC (Figure 1). Here, S_{max} is the storage capacity of the reservoir, $Q_{\text{in}(i)}$ is the daily inflow volume on the i^{th} day, Q_c is the daily release volume capacity, URC is the value of URC on the i^{th} day, I is the storage target of the reservoir, Q_d is the value of the release demand on the i^{th} day, and S_{min} is the minimum storage volume of reservoir (all in m^3). URC is a value applied from 1995 through 2011 on reservoir operations. The release volume capacity is a limit of the release volume that considers the downstream discharge capacity. Considering discharge capacity of lower basin, Q_c was set to 40 MCM/day. In equation (1), $R(i)$ is determined by the relationship between the areal rainfall and inflow derived from historical data. Here, data for 1974 to 2010 (referred to as the reference period in the following) were used to derive $R(i)$ in the validation. Figure 2 is a scatterplot of the relationship between the total areal mean rainfall for 365 days from January 1 each year and the total 365-day inflow to the Sirikit Reservoir from January 1 each year.

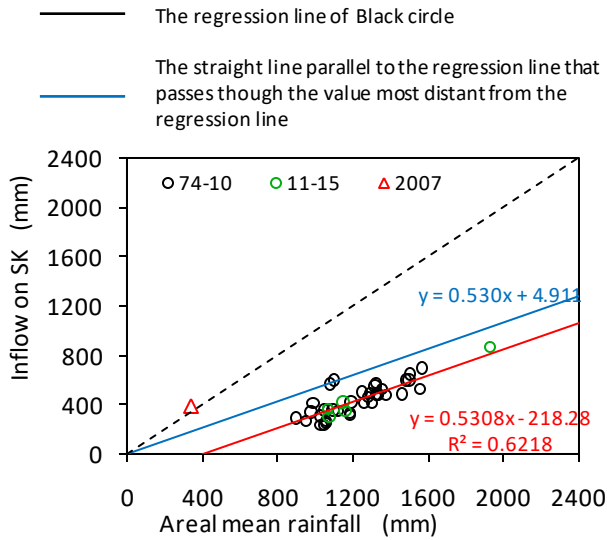


Figure 2. Scatterplot of the 365-day accumulated areal mean rainfall from 13 December and 365-day accumulated inflow to the Sirikit Reservoir from the following 1 January

Table 1. $R(t)$ determination in each scenario

	Equation used to derive $R(t)$
Case A	$R(t) = (0.5308 \times \sum r + 4.9111) \times A/1000$ Red line in Fig. 2
Case B	$R(t) = (0.5308 \times \sum r - 218.28) \times A/1000$ Blue line in Fig. 2
Case C	Without probable inflow

Black and green circles show the values for the reference and validation periods, respectively. Red triangle shows the value of 2007. In 2007, there is a lot of data missing day in the rainfall data. Therefore, the data of 2007 was excluded from reference period data. The red line in the figure is the regression line for the reference period data. The blue line is a straight line parallel to the regression line that passes through the value most distant from the regression line in the positive direction in the reference period.

The red and blue lines were used to determine $R(t)$, which was calculated as follows:

$$R(i) = A \times \left(k \sum r(i) - L \right) \div 1000 \quad (3)$$

Here, A is the catchment area of Sirikit dam (km^3), $\sum R(t)$ is the accumulated areal rainfall from January 1 to the i^{th} day (mm), and k and L are values determining the relationship between the areal rainfall and inflow on Figure 2. The blue line covers all inflow for the accumulated rainfall in the reference period. Therefore the probable inflow $R(i)$ become over estimate in several years. In this validation, the upper limit of $V(i)$ was set for each case (Table 1).

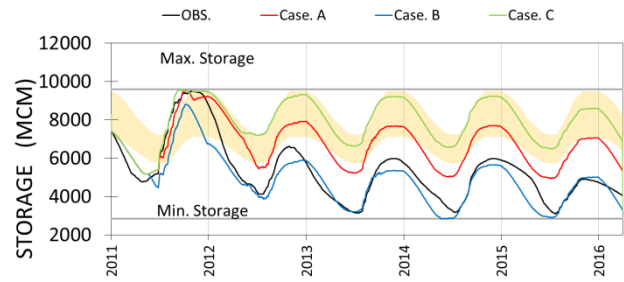


Figure 3. The calculated storage volumes of the Sirikit Dam Reservoir for Cases A to C

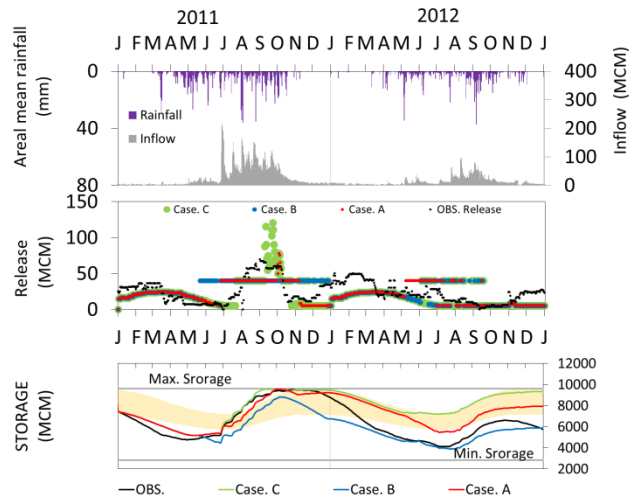


Figure 4. The observed areal mean rainfall, inflow to the reservoir, and the results of the calculations for 2011 and 2012

Validation Results

Figure 3 shows the results of the calculated storage volumes of the Sirikit Dam for Cases A to C. The solid black line shows the actual storage volume of the reservoir, while the straight grey lines above and below indicate the maximum and minimum storage volumes. The yellow area means the range between URC and LRC. The reservoir storage tended to be the smallest in Case B, followed by Cases A and C. The storage volume in Cases A and C were larger than the actual storage volume. The storage volume in Cases B was smaller than the actual storage volume from 2014 to 2015, and it reached the minimum storage volume from February 2016. This suggested that the probable inflow in Case B was overestimated, and the storage volume did not recover as estimated.

Figure 4 shows the observed areal mean rainfall, the observed inflow to the reservoir, and the results of calculations for 2011 and 2012. In Cases A and B, flood control operations determined by $S'(i)$ were conducted in 2011. In 2011, the inflow was. In Cases A and B, the release volume increased in order to prepare the free capacity in March and June respectively before the peak of inflow. In Case B, the release volume was controlled under the daily release volume capacity. In Case A, the

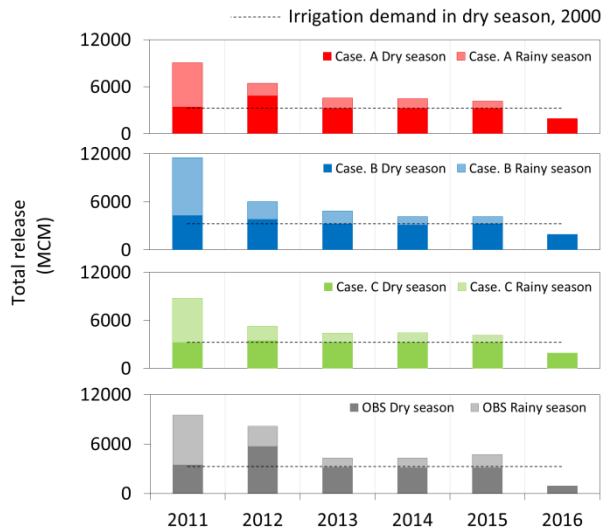


Figure 5. The total volume released during the dry and rainy seasons in Cases A to C and the actual total volume of water released from the Sirikit Reservoir

release volume was controlled under the daily release volume capacity expect 8 days. In addition, the peak of the release volume in Cases A and B was smaller than the peak of the release volume in Cases C. That suggests the proposed method could improve the flood control function. In Case C, the release volume didn't increase in July and August and the storage volume reached the maximum storage volume in September 2011. That caused to release large volume over daily release volume capacity in September and October. In 2012, the storage volumes in cases A, and B were less than Case C. In cases A and B, the release volumes were increased in August and September despite their storage volume less than URC. This is due to the overestimate of probable inflow.

Figure 5 shows the total volume released during the dry season (January 1 to June 30) and rainy season (July 1 to December 31) in Cases A to C and the actual total volume of water released from the Sirikit Reservoir. The dotted lines in the figure indicate the dry season irrigation demand in 2000. The value of 2016 shows the total release volume from January 1 to March 31. While the actual total dry season release volume was slightly below the irrigation demand in 2014 and 2015, the total dry season release volume in Cases A and C satisfied the demand in both years. And the total dry season release volume in case B was slightly below the irrigation demand in 2014 and 2015. In Case B, the excess of release volume in 2012 had not been recovered. That caused less of the storage volume in 2015. Therefore, in Case B, the total release volume in 2015 was smaller than the other scenarios. However, in cases A and B, the proposed method succeeded in improving flood control without losing the annual total release volume.

Conclusion

This paper proposes a new method for operating large reservoirs in the CPRB, Thailand based on a prior flow method, and validates the effectiveness of the proposed method by using historical data. The proposed method estimates the future probable inflows from the observed areal rainfall, and then the excess storage volume is determined from the probable inflows, in addition to the actual storage volume.

We validated the effectiveness of the new method by applying it to the Sirikit Dam, examining the changes in the storage volume and then verifying the appropriateness of the total volume released in the dry season. The validation was conducted for the period from January 1, 2011 to March 31, 2016. We also compared the results of the calculation with historical records. The probable inflow is determined using the relationship between rainfall and inflow into the basin. In each year, the accumulated areal rainfall has the greatest correlation with the total annual inflow. The relation between the areal rainfall and inflow from 1974 to 2010 was used to derive the probable inflow in the validation.

Our validation findings suggested that the proposed method improves flood control by increasing the release volume and reaching free capacity before the peak of inflow. Furthermore, in the validation period, the enhanced flood control function with the proposed method will not result in a loss of irrigation in the dry season.

Next, to improve the estimation of probable inflow, we need to develop more suitable derivation method. Nevertheless, the proposed method enhances flood control function using simply observed data.

Acknowledgments

This study was partially funded by the Japan Society for the Promotion of Science KAKENHI Grant Number 15H05222.

References

- Komori D, Mateo C M, Satani A, Nakamura S, Kigchi M, Klinkhachorn P, Sukhapunnaphan T, Champathong A, Taketani M, Oki T. 2013. Study on large scale reservoir operation for seasonal scale considering both flood control and water resources using probability analysis: Proceedings of the 21st Symposium on Global Environment, 115-125.
- Kure S, Tebakari T. 2012. Hydrological impact of regional climate change in the Chao Phraya River Basin, Thailand, Hydrological Research Letters 6, 53–58.
- Shimosaka M, Kure S, Toyota H, Yamada T, Kikkawa H. 2008. A study on new determination method of dam reservoir discharge for flood control capacity improvement of existing dam, Proceedings of



Hydraulic Engineering, JSCE, Vol. 52, 511-516.
(in Japanese with English abstract)

Tebakari T, Yoshitani J. 2005. Effect of the Large-Scale Dams on the Hydrological Regime; A Case Study in Chao Phraya River Basin Kingdom of Thailand: Journal of Japan Society of Hydrology and Water Resources, 18(3), 281-292. (in Japanese with English abstract)

Tebakari T, Dotani K, Kure S, Suvanpimol P. 2015 A NEW OPTIMAL OPERATION METHOD FOR LARGE SCALE RESERVOIRS IN THE CHAO PHRAYA RIVER BASIN, THAILAND, The 3rd International Conference on Water Resources, ID 166.



Session C

Emerging Technologies in Water Management and Environment Towards Nexus (WEF)



Invited Papers



WATER-ENERGY-FOOD NEXUS: THE ROADMAP IN KOREA

Choi Byung-man

Abstract

Water, energy and food (WEF) are essential for human well-being, poverty reduction and sustainable development. However, experts expect that demand for freshwater, energy and food will increase significantly over the next decades due to population growth, economic development, urbanization and climate change. The interdependence of these three resources is known as the water-energy-food (WEF) nexus. The WEF nexus complicates addressing these resources' scarcity independently, as actions taken with regard to one resource are likely to affect the other two. Moreover, it is recommended developing a proper and tailored concept of the WEF nexus and assessment tool to aid its harmonious development and to meet the global environmental standard. The development of the WEF nexus concept and assessment tool is necessary to understand the interconnections in quantitative way and have better chance to improve the management of those valuable resource for future security. Recently K-water launches a research program to establish a roadmap on the WEF nexus to cope with a water shortage caused by a severe drought, energy and food crisis in future. The roadmap includes: (i) assessment of current status of water, energy and food sector (ii) suggestion of efficient management practices of water, energy and food (iii) development of database on nexus elements and assessment tools for policy implementation based on nexus approach (iv) new technologies of the nexus and determine sites of the nexus test-bed. With the recent water-energy-food nexus technology innovation, much attention has been paid into water and energy efficiency improvement and cost saving technologies such as floating photovoltaic power plant, reuse and recycling technologies of waste water & waste heat, smart farming by ICT & IoT.

Keywords *sustainable development, interdependence, nexus approach*

Choi Byung-man

K-water Institute, 125, 1689 beon-gil, Yuseong-daero,

Yuseong-gu, Daejeon, 34035, Republic of Korea

bmchoi@kwater.or.kr

SMART URBAN WATER SYSTEMS – IN PRACTICE

Sten Lindberg*1a, Morten Rungø2 and Somchai Chonwattanam3c

Abstract

Providing sufficient and safe drinking water and collecting and treating the used water and storm water in ever growing cities was already a few decades ago a very complex management and technical challenge. The climate changes have added further complexity to this challenge. Changes in annual rainfall depths, more high intensity rainstorm – combined with the continued growth of the cities call for smarter solutions. The advances within sensors, communication, models, web-technology and knowledge make it feasible to combine the elements into integrated urban water management systems - IUWMS.

The presentation describes examples of IUWM deployed or under preparation in Thailand and Vietnam. Reference is made to cities where IUWM is an established management element.

Bangkok Metropolitan Administration, with financial support from the UN program CTCN, are currently implementing an operation Urban Flood Warning system. Based on actual measurements of water levels in channels (klong) and Chao Phraya river combined with information from a number of rainfall gauges and short term rainfall forecasts, the system evaluate flood risk in the selected focus area. The results – in terms of maps with flood prone areas are continuously updated and displayed on a web-portal, accessible for the citizens of Bangkok.

The climate changes and the growing cities makes it even more important to have efficient water distribution systems. The loss of water, due to low effective management or physically deteriorated pipe- and pump-systems is excessively high in many cities. The presentation includes examples of the use of smart technology in reducing the water losses.

Keywords *Smart water cities, urban flooding, flood warning, Integrated Urban Water Management, water efficiency, non-revenue water*

¹DHI, Ager Allé 5, DK 2970 Hørsholm, Denmark

²DHI, Ager Allé 5, DK 2970 Hørsholm, Denmark

³DHI Thailand, Asian Institute of Technology (AIT), WEM/SET, P.O. Box 4, Klong Luang
12120 Pathumthani, Thailand

^asl@dhigroup.com, ^bmor@dhigroup.com, ^csch@dhigroup.com

Achieving Sustainable Resources Security through the Water-Energy-Food Nexus

LEE Eulrae^{1*}, CHOI Byungman², JUNG Younghun³

Abstract Climate Change, Urbanization, and Population growth are global stressors that are increasing the uncertainty of resource which is necessary for human activities. OECD(2012) predicted that resources demand of water, energy and food will be increased by 55%, 80%, 60% respectively in 2015. Resource security has been threatening by this uncertainty and aggravation of imbalance between the supply and demand of resources. Especially, climate change, which is very impactful to global water crisis, is the most critical crisis and common challenge for humanity. Much effort has been made to achieve the Sustainable Development Goals (SDGs) and the Water-Energy-Food (WEF) Nexus has attracted worldwide attention as a new paradigm to reach the resource security goals established in the SDGs. WEF Nexus is begun to be discussed at Bonn 2011 international conference in earnest and on the rise as concept of the most interested to resource security in the world.

WEF Nexus has to be considered secure sustainable resources and create a new industrial eco-system by incorporating the strategies of the WEF Nexus. The strategies mainly consist of these key concepts. These are Nexus DB system, impact assessment tool, the Nexus element technology and legal and institutional systems.

To achieve these strategies, we are in the process of quantifying the trade-offs or synergy effects through big data analyses to detect correlations between resources. The technologies of Nexus can be classified into two groups: 1) Element technology and 2) Connection technology. Element Technology means the increasing the 1st efficiency through improvement & development of element technologies and connection technology means the maximizing 2nd efficiency by interconnecting individual element technologies. Moreover the legal and institutional backgrounds should be supported to reflect these technologies through policy.

Finally, we will prepare a plan that leads to a win-win strategy for both the legal & institutional systems which prevents resources conflicts. We expect that WEF Nexus technology will help to overcome the existing resource crisis and establish a stable economic foundation for future generations.

Keywords *water-energy-food nexus, climate change, sustainable development, assessment tool*

LEE Eulrae (ph.D)

Water Resources Research Center
K-water Institute
Daejeon, Korea
erlee@kwater.or.kr

CHOI Byungman (ph.D)
Water Resources Research Center
K-water Institute
Daejeon, Korea
bmchoi@kwater.or.kr

JUNG Younghun (ph.D)
Water Resources Research Center
K-water Institute
Daejeon, Korea
younghun@kwater.or.kr

Introduction

Climate change and resource depletion are expected to accelerate and intensify as water, energy and food demand increase and supply shortages are expected due to global population growth and urbanization and industrialization. In particular, as the demand for water increases, but the supply is limited, it is necessary to find out the correlation between energy and food problems, which are essential to human beings for sustainable mankind survival, and to develop and policy for effective water utilization.

In particular, 70% of the world's water supply is spent on agriculture and 15% on energy. In Europe and the United States, 43% and 50% of the total amount of fresh water is used as cooling water for power generation. In the world, the disparity in supply and demand of water, food and energy is intensifying and mutual crisis is amplifying.

Currently, the three crises that are absolutely necessary for human life are combined and the mutual crisis can be amplified. However, the management and operation technology of individual resources is quite high in Korea, but the linkage of Energy-Food Nexus is low condition. Since the situation of the linkage of three

resources internationally is large in the developed countries and in the regions where the natural conditions such as the desert region are poor, the crisis-related relation between the resources is high, so Korea can accurately understand the crisis of this situation. It is necessary to establish countermeasures against environmental changes. However, current water management and management of water supply facilities are not properly implemented in Korea. As a result, there is a fear of water shortage in food production over the medium to long term. In addition, data on water - energy - food linkages and policy - making are absolutely lacking at administrative intervals between ministries, so systematically building DBs based on big data and defining inventories are absolutely necessary at present.



Fig. 1 The uncertainty of future resources (OECD-FAO, 2012)

<p>Population Growth</p>	<p>Recently, the world population has exceeded 7 billion the total world population will be 8.1 billion in 2025 and it will reach to 9.6 billion in 2050</p>
<p>Energy Demand</p>	<p>From 2011 to 2030, the world's main energy consumption is increasing 1.6% every year. It is predicted to be almost 36% until 2030.</p>
<p>Water Demand</p>	<p>If the efficiency improvement is not realized under the current growing trend, it is forecasted that the water demand will be increased from 4.5 trillion m³ to 6.9 trillion m³.</p>
<p>Urbanization</p>	<p>Currently, above 50% of world's population lives in cities and acceleration of urbanization leads industrialization required more water usage.</p>
<p>Food Demand & Changing Meals</p>	<p>The meat intake of world's population was 37kg per person in 2000 and it will be increased to 52kg per person in 2050. Under this situation, around 50% of grain production should be transferred to animal feeds.</p>

Fig. 2 The perspective of water, energy food demand

Water-Energy-Food Correlation

Research on WEF Nexus is being actively pursued at the Bone2011 conference. The WEF was discussed in 19 programs at the 7th World Water Forum in 2015. In general, WEF Nexus examines the connectivity of water, energy and food resources. And it means integrated management technology to utilize resources efficiently. In other words, it can be seen that other resources are closely related to the production, supply and consumption of each resource. In this way, it is possible to efficiently manage the production, supply, and consumption of the three resources by accurately

grasping and quantifying the status of other resources consumed until production and supply of each resource. The US NIC presented a future outlook report. Here we present the four mega-trends that have a large impact on human life by 2030, including the WEF Nexus. The report emphasized customized technological innovation to overcome these four megatrends.

To identify water consumption for energy and food production, water footprints and virtual water, which are national water use indicators, can be utilized. This is an indicator introduced to measure actual water consumption by country and to prepare for future water shortage efficiently. Water footprint is calculated by tracking the amount of water needed to produce goods and services consumed by people living in the country to be. According to UNESCO-IHP research data released in 2004, South Korea is ranked 15th among the 100 countries to be evaluated as having a high water import rate (65%). In the case of Korea, the export of high value-added goods is high, while the majority of low-value-added products such as agricultural products and crude oil depend on imports, which means that they are very vulnerable to weaponization and protection trade in food. It can be said that 1.4 times more water is needed than water.

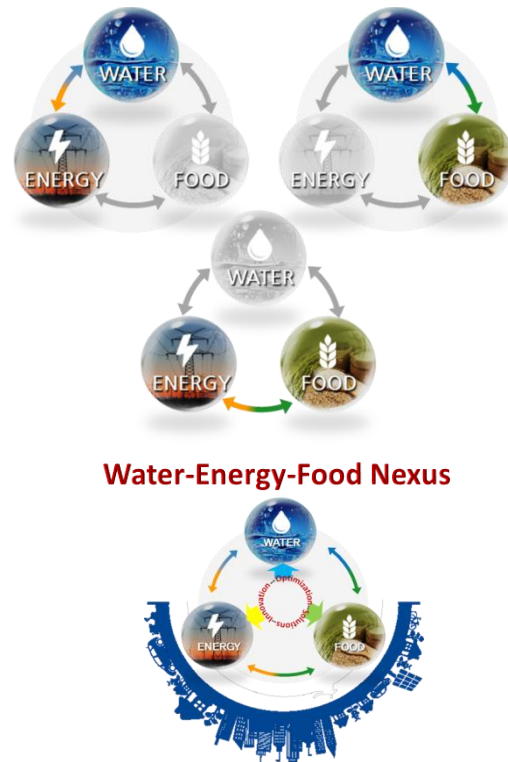


Fig. 3 Water-Energy-Food Correlation

Water - Energy - Food Security

Securing security between each resource is absolutely necessary for sustainable securing and proper allocation. Water security is a water quality that has adequate quality and quality to preserve ecosystems for political stability and climatic peace, to prevent water-borne pollution and water-related disasters for livelihoods,

human happiness, socio-economic development (UN Water, 2014), and food security is sufficient and sufficient to ensure that everyone is always able to satisfy their ingestion and food preferences in order to lead an active and healthy life (FAO, 2014) where nutritious food can be obtained physically, socially and economically. Energy security also represents the sustainable supply availability of energy (IEA, 2014) at an acceptable price level. In order to secure the security of each resource, it is necessary to accurately determine the production, consumption, and supply systems of each resource and fully examine and apply mutual connectivity to each resource.

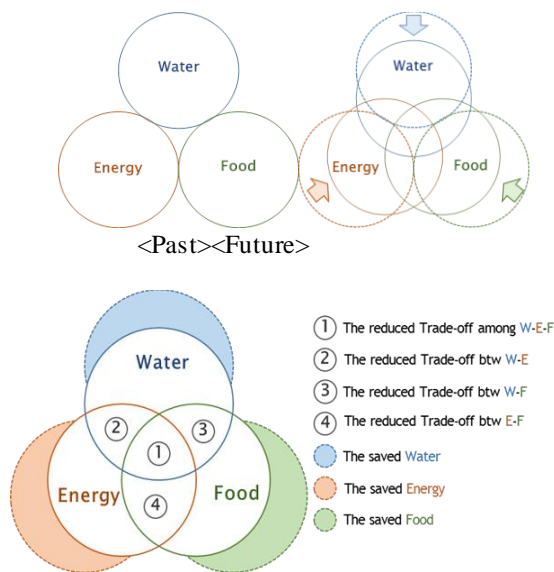


Fig. 4 Concept of Water-Energy-Food

Market trends in the water sector

70% of the world's water supply is for agriculture, and 15% is consumed by the energy industry (FAO, 2014). According to GWI (Global Water Intelligence), the global water market in 2010 is estimated at \$482.8 billion, with annual average growth of 4.9%, to \$865 billion in 2025. Water use in the domestic agricultural sector accounts for 62% of the total water use, and aging of the water supply facilities is intensifying, and if not improved, the overall supply disruption of agricultural water is expected to be mid- to long-term. Especially, due to the increase of climate change and weather volatility, difficulties in management of water resources are increasing, but the development of new water resources is in a stagnant condition, and there is a possibility of regional water shortage in the future.

Market Trends in the Energy Sector

Globally, resource development such as petroleum, gas and coal mining, and cooling water for nuclear power and thermal power generation are the major water consumption areas. In particular, Europe and the United States use 43% and 50% of the total amount of fresh

water for power generation, respectively (UN Water 2014 statistics). In Korea, 7% of domestic electricity consumption is spent on operation of waterworks facilities.

Globally, resource development such as petroleum, gas and coal mining, and cooling water for nuclear power and thermal power generation are the major water consumption areas. In particular, Europe and the United States use 43% and 50% of the total amount of fresh water for power generation, respectively (UN Water 2014 statistics). In Korea, 7% of domestic electricity consumption is spent on waterworks facilities, annual electricity consumption 1,315 million kWh in the water intake plant, 1,117.6 million kWh in water treatment plant annual water use, 32.4 million kWh in industrial water treatment plant, 32.4 million kWh in annual water usage, kWh. In particular, Korea is in the 103rd place among the 129 countries because the energy security situation is very weak.

Market Trends in the Food Sector

The world's major grain prices have risen 2-3 times over the past 10 years (Park, Pyungsik, et al., 2008). The constant risks of over-weather and supply-demand structural risks are expected to increase, and water and food supply is threatened by the production of bio-fuels such as corn, wheat and sugar cane. In Korea, food self-sufficiency rate, declining land area, and grain shortage are becoming more and more vulnerable to the supply and demand of food. In order to cope with this, research on the efficiency of water management, overseas agricultural strategies in terms of resource security, and strengthening the supply / demand control function of the domestic food market should be pursued. Domestic agriculture is pursuing its development while pursuing the 6th industry, but there is much room for improvement in terms of efficient use of water and energy for food production. In particular, it reduces energy loss in processing and distribution. The development of technology that can be done is urgent, and the economical burden of the common people can be increased due to the uncertainty of crop price instability due to uncertain future climate change.

Water - Energy - Future Directions for Food Nexus

Now it is time for the WEF Nexus Country Action Plan as a water-based agenda for future climate change response and national essential resource security system. As it is difficult to utilize limited resources efficiently in order to cope with future changes in the environment such as population growth, economic growth, and climate change, it is required to secure sustainable resource security that utilizes the linkage among resources. In order to secure sustainable resources, it is necessary to identify the interrelationships and increase the efficiency of resource utilization through linking production and consumption among resources and secure resources for the next generation. In order to

achieve this, it is necessary to establish a plan for integrated linkage of government-led management systems for each resource and plan for implementation, and improvement of resource independence through WEF Nexus should be promoted. Stable resource management efforts to cope with hydro-meteorological variability due to global climate change and resource security using resource linkages due to environmental changes such as population change, land use change, urbanization and industrial advancement are needed. It is necessary to predict changes in resource linkage of new concepts according to the form of resource consumption due to changes in national life patterns, forecast resource consumption and resource supply management strategies. And it is required to realize the creative economy through the convergence of technologies for smart water industry in the future. In order to prepare for climate change and water shortage, integrated management system including climate, environment, industry, and technology policy is needed to break away from existing water management and secured WEF Nexus technology centered on technology convergence due to expansion of global water market opening. Urgent. It is necessary to create synergies such as achieving national resource security through Nexus and discovering new markets, building a demand management market using ICT, fostering new service industries, and contributing to job creation. We need to predict the impact of economic, water, energy, and food interactions on economic growth, and look for ways to respond in the long term. In addition, it is urgent to acquire technologies and operating tools for technology-convergence-type water-energy-food linkage. An integrated operation management system is needed to track the production and consumption traces of the resource market due to the expansion of the global resource market. The development of linking technologies and operational tools that enable each resource for sustainable water-energy-food security linkage to be delivered to other resources should be undertaken.

Maximization of efficiency and promotion system between resources

To realize WEF Nexus, it is necessary to maximize efficiency among resources. In the past, if we pursued securing of individual resources, we must secure the linkage between the resources through mutual win- In order to achieve this, it is necessary to take into consideration the problems of securing the current resources, to ensure efficiency through interconnection, and to make synergy effects by affecting the efficiency of each resource. Table 1 presents the concrete method of implementation of these measures.

The connectivity between each resource in a given watershed is composed of smart grids. Water, energy, and food can be thought of as grids that are linked to human life, plant operations, fuel production, and

ecosystems. Therefore, in this system, when emphasizing only specific resources and pursuing development, it is possible to cause imbalance of supply and demand in other resources. Therefore, development considering all resources can be the most important paradigm of securing future resources. Figure 5 shows the actual linkage and application between each resource. Based on this, it is important to secure the security of resources by reflecting the smart grid in order to increase the efficiency among each resource. Table 2 provides a description of these specific implementation systems and methodologies.

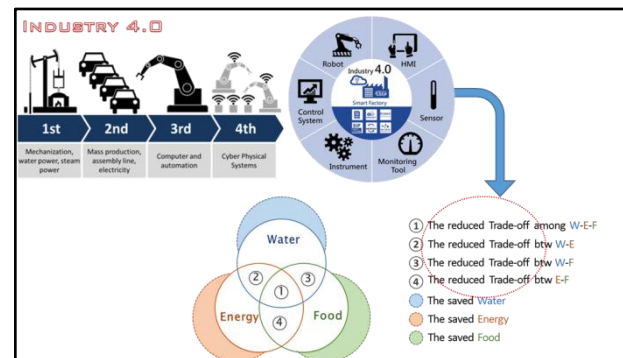


Fig. 5 Industry 4.0 and WEF Nexus

Past Hardware-oriented	<ul style="list-style-type: none"> Water securement with the construction of infrastructure such as dams, weirs, etc. Water securement to ensure the nation's economic foundation with nation-centered and industry-centered methods Problem: Environment issues, deterioration, limitation of national land area
Present Software-oriented	<ul style="list-style-type: none"> Water securement by increasing water use efficiency through the operation of dams and water supply networks Operation of dams considering natural sluice effects (Safety securement)
Future Humanware-oriented (Nexus perspective)	<ul style="list-style-type: none"> Water securement through demand management of the whole water supply process from source to consumer (e.g. Controlling water consumption required for the production of essential resources such as energy and food) Increasing water efficiency with the development of element technologies applied to production Positive effect of water securement and efficiency improvement for the securement of other resources and their efficiency Increase of sustainability in water security by connecting the infrastructure with existing Hardware and Software and Industry 4.0 based technology

Fig. 6 Nexus Future Perspective

Case Study in Korea

Providing cooling-heating systems using ground source heat in horticultural greenhouses

In the agricultural sector of Korea, interest in substitute heat source is lacking. And when using greenhouses, there is a limited active supply of cooling-heating facilities that use ground source heat due to the relatively heavy initial investment costs compared to hot-air furnaces or hot water boilers.

In terms of the total management cost of the horticulture sector, heating expenses account for 19~58% of the costs depending on type of cultivated crops

※ About 92% of the heating energy source used is fossil energy, specifically oil.

(Initial investment cost recovery) Initial investment cost is recovered at 7 years (2,376m² plastic greenhouse) and 2 years (9,384m² plastic greenhouse)

System of Rice Intensification(SRI)

The SRI is rice cultivation method for agriculture water reductions of rice paddies and production improvements. The example in Korea (Ministry for Agriculture, Food and Rural Affairs, Korea Rural Community Corporation, 2011) has the amount of irrigation water used compared to practice, 49.4% reduction in agricultural water usage. The harvest amount : Compared to practice, 109-120 % (white rice), 120-130 % (head rice)

Greenhouse gases : Compared to practice, reduction in 71.8% of greenhouse gas

If approx. 40% of agricultural water is reduced by applying the SRI method to all rice paddies, about 5.1 billion tons of water can be secured



Fig. 7 SRI(System of Rice Intensification)

Cooling-heating system of water-thermal energy of The Second Lotte World Building.

The Principle of water-thermal energy is system used for cooling-heating and providing hot water in a building by collecting the temperature energy of water included in river water, lake, sea water, and etc. directly or by heat pump.

※ Energy-saving effect of 20~40% compared to existing cooling-heating systems

In Korea, at 2nd Lotte World, the K-water is proceeding with joint development using lake water from a dam, raw water in a wide area and etc.



Fig. 8 Cooling-heating system of water-thermal energy of The Second Lotte World

Conclusion

Now we are preparing for a new water agenda in response to population growth and climate change, and we must ensure resource security by fully considering the interrelationship of energy and food, which is an essential resource centered on water resources. The

following three points can be considered. First, it is necessary to find humanitarian step-by-step projects for solving North Korea's water-energy-food problems and support for unification. Based on this, it is time to develop and apply an infrastructure package model that is linked with the project to recreate the Korean peninsula considering resource efficiency and effectiveness. Second, it is the contribution of the international community. In order to realize the new global agenda, SDGs, the demand of the international society to meet the economic scale of Korea is increasing. Accordingly, there is an obligation to establish a strategic and systematic infrastructure for developing water resources and securing food and energy in developing countries in connection with ODA projects. Third, the growth of the industry is fostering. The global water industry is shifting from infrastructure building to water efficiency, integrated management, and inter-industry linkage to application / convergence technologies. Water scarcity, social and technological change, as well as water-energy-food linkage, Traffic, public health, and environmental protection. The disparity in supply and demand of water, food, and energy is intensifying in the world, and mutual crisis is also amplifying. Therefore, it is necessary for the Korean government to recognize the crisis situation and to prepare countermeasures against it. Nexus between resources needs to be developed as a platform for integrated sustainable strategy, crossing the boundary between academic and government departments, and interdepartmental interconnection is important. In addition to national technology, it is necessary to develop sustainable development policies, and the water-energy-food issue can be solved most effectively when policies are integrated. In order to maximize efficiency at minimum cost, to deliver efficiency among resources, and to create synergy, it is necessary to develop tools suitable for domestic integration for integration, analysis, evaluation and decision making. Through these various efforts, we believe that sustainable energy production and supply will be possible based on the linkage of each resource.

Reference

Allan, J. A. (1998) Virtual water: A strategic resource global solutions to regional deficits. *Groundwater*, 36(4), 545-546.

FAO (2014) The Water-Energy-Food Nexus: A new approach in support of food security and sustainable limits to freshwater withdrawal and use. *Proceedings of the National Academy of Sciences*, 107(25), 11155-11162.

Hellegers, P., Zilberman, D., Steduto, P., & McCormick, P. (2008) Interactions between water, energy, food and environment:



evolving perspectives and policy issues.
Water Policy, 10, 1.

IEA (2014) Energy Supply Security 2014

IRENA (2015) Renewable Energy in the Water,
Energy & Food Nexus

NIC (2012) GLOBAL TRENDS 2030 :
ALTERNATIVE WORLDS

OECD-FAO (2012), "OECD FAO Agricultural
Outlook 2013-2022", OECD,
Paris, [www.oecd.org/site/oecd-
faoagriculturaloutlook/highlights-2013-
EN.pdf](http://www.oecd.org/site/oecd-faoagriculturaloutlook/highlights-2013-EN.pdf).

Pimentel, D., & Pimentel, M. H. (Eds.).(2007)
Food, energy, and society.CRC press. New
York, USA.

UN water (2014) Water Security & the Global
Water Agenda : A UN-Water Analytical
Brief

World Energy Council (2013) World Energy
Trilemma 2013: Time to get real - the
agriculture, Food and Agriculture
Organization of the United Nations, Italy.

Gleick, P. H., & Palaniappan, M. (2010) Peak
water

case for sustainable energy investment, World
Energy Council, UK.

World Water Forum (2015) Water-Energy-Food
Nexus

Characteristics of CH₄ Flux from Paddy Field Adopting the Intermittent Irrigation Technique during the Winter-Spring and Summer-Autumn Seasons in the Red River Delta, Vietnam

Fumiya Inagaki^{1,a,*}, Kimihito Nakamura^{1,b}, Le Xuan Quang^{2,c}, Pham Thanh Hai^{3,d}, Nguyen Dang Ha^{4,e}, Tran Hung^{2,f}, Shinji Fukuda^{5,g}, Junya Hirata^{5,h} and Hiroataka Komatsu^{5,i}

Abstract Methane (CH₄) emission from paddy contributes to increasing the total global warming potential in Vietnam. It is important to implement eco-friendly paddy water management (e.g. alternate wetting and drying (AWD)) to reduce greenhouse gas emissions in Vietnam. The study on the application of intermittent irrigation technique has been done in the Red River Delta, Vietnam. The objectives were to investigate the temporal changes in CH₄ fluxes from six paddy plots in the winter-spring season and the summer-autumn season and to specify the influential factors to CH₄ emissions using multiple regression analysis (MRA). The cumulative CH₄ flux in the winter-spring season was one quarter of that in the summer-autumn season (9.0 g m⁻² in the winter-spring season (91 days) and 37.3 g m⁻² in the summer-autumn season (85 days)). The percentage of CH₄ flux in intermittent irrigation period to the total cropping period was 11% in the winter-spring season and 49% in the summer-autumn season, respectively. Though the improved paddy water management may be effective in the winter-spring season due to less rainfall, the countermeasures for the summer-autumn season is also important. The results of MRA show the correlations between CH₄ fluxes and the influential factors (the paddy ponding water level, the soil water content at 5 cm deep, the soil temperature, electrical conductivity, pH, redox potential (Eh) of upper soil layer) are low in the both seasons. However, the CH₄ fluxes decrease when the volumetric water content at a depth of 5 cm is under 0.25 and when the Eh is above 220 mV.

Keywords *paddy water management, methane emission, intermittent irrigation, multiple regression analysis, Vietnam*

1 Graduate School of Agriculture, Kyoto University, Kitashirakawa Oiwake, Sakyo, Kyoto, Japan

2 Institute of Water Environment, 165/2 Chua Boc Str., Hanoi, Vietnam

3 Faculty of Hydrology and Water Resources, Thuy Loi University, 175 Tay Son Str., Hanoi, Vietnam
4 Investment Construction Management Board No 3, 668 Ba Trieu Str., Thanh Hoa Province, Vietnam
5 Kitai Sekkei Co., Ltd., 1030 Kamitoyourazuchi, Omihachiman, Shiga, Japan

ainagaki.fumiya.26n@st.kyoto-u.ac.jp,
bnakamura@kais.kyoto-u.ac.jp,
clequangiwe.vawr@gmail.com,
dpthaiavn@gmail.com, edanghaban3@gmail.com,
franhung25282.com, gs-fukuda@kitai.co.jp,
hj-hirata@kitai.co.jp, ih-komatsu@kitai.co.jp

Introduction

It is essential to conduct "water saving management" in rice crops in order to alleviate problems such as food and water resource shortages that are global concerns in the future. Furthermore, inappropriate water management places a heavy burden on the environment, such as water pollution accompanied by the discharge of fertilizer and agricultural chemical ingredients, release of greenhouse gases, etc. Therefore, the practice of "eco-friendly and water saving management" becomes an important issue. In recent studies on eco-friendly and water saving management in paddy field, the keyword is alternate wetting and drying (AWD) that is an intermittent irrigation technique that repeats flooding and non-flooding by avoiding flooding at all times and irrigating after disappearance of flooding. For example, it was found that AWD in China could reduce water usage, surface drainage, and fertilizer component outflow associated with surface drainage without reducing yield (Liang et al., 2013). AWD is also considered a promising irrigation technique to reduce greenhouse gas (GHG) emissions (Richards and Sander, 2014). Intermittent irrigation (Minami, 2003) and midterm drying (Minamikawa, 2006) can contribute to reduce CH₄ emissions. Carbon dioxide (CO₂) and nitrous oxide (N₂O) emit at the time of drainage of ponding water, and CO₂ is stored at the time of irrigation (Minamikawa, 2006). Iida et al. (2007) measured the emission of CH₄ and N₂O in relation to intermittent irrigation, and Kudo et al. (2012) examined

the optimal intermittent days based on the measurements of CO₂, CH₄ and N₂O emissions and yield. It is clear that eco-friendly water saving management is possible by water management including intermittent irrigation. However, these are the results of small plot-scale experiments, and there is no report on the practical implementation at the district level that is handled by the farmer. The significant problem at the present stage is how to put the new water management technology into action, and it is required to present effective means as a model case for that. Moreover, by specifying parameters that affect GHG emissions from paddy fields, it is possible to clarify the qualitative standards or indices for intermittent irrigation management.

In this study, conventional block, weak-dry block and strong-dry block were set up in the paddy field district, and water saving management was practiced by using small several gates controlling irrigation water flow. We investigated the temporal changes in GHG fluxes from six paddy plots in the winter-spring season and the summer-autumn season in 2015, analyzing factors that affect GHG emissions from paddy in the Red River Delta, Vietnam. Here, we focused on only CH₄ because the amount of CH₄ emission was much larger than N₂O.

Exploring the way of eco-friendly paddy water management in Vietnam is considered to be able to provide useful knowledge to other Southeast Asian regions as well which are the major rice producing countries.

Materials and methods

Experimental area

The field experiment was conducted at paddy fields in Phu Thinh commune, Kim Dong district, Hung Yen province, Vietnam (21°25'N, 105°46'E) (Fig. 1). This commune is on the Red River Delta. The field area is about 70 ha. Paddy water is irrigated from water courses by using pump, and then it drained to the same water courses, i.e. dual-purpose canal. This area has rainy and dry seasons. The rainy season usually lasts from the end of April to October. Rainfall during the rainy season accounts for 70% of total annual rainfall. The average annual rainfall is 1,500 mm, the average temperature is 23.2°C, and the average relative humidity is 83%.

In Phu Thinh, rice is produced twice a year; the winter-spring season and the summer-autumn season. In the winter-spring season, rice was transplanted on Mar. 6, and harvested on Jun. 4 in 2015. In the summer-autumn season, rice was transplanted on Jun. 26, and harvested on Sep. 22 in 2015.

Paddy water management

The experimental area was divided into three blocks. Different water management was set for each block experimentally: Conventional block, Weak-dry block, and Strong-dry block. Conventional water management was traditional and conventional in this district; weak-dry type water management included short intermittent irrigation; and strong-dry type was long intermittent irrigation. In weak-dry type block, water was irrigated when the water level in a pipe buried in a paddy plot lowered to a depth of -5cm. In strong-dry type block, water was irrigated when the water level lowered to a depth of -15cm. We kept soil condition wet during 1 month after transplanting and between the panicle



Fig. The study area. Phu Thinh commune is under the Red River Delta, and the natural topography is relatively flat.

formation period and ear emergence season. Figure 2 shows the ideal ponding water depth in each water management practice. Two observation plots were set up in each water management block: C1 and C2 for conventional block, W1 and W2 for weak-dry block, S1 and S2 for strong-dry block. Temporal changes in ponding water depth and soil conditions were measured at each plot. Gas sampling and rice yield survey were conducted at each plot.

In order to control the irrigation water flow in this district and to flow to each experimental block, we constructed two weirs and eleven gates in water canals in the district. Observation pipes installed in each plot were used to check the water level in the plot. According to the water management plan, the farmers of the local commune operated the gates.

Measurement

Meteorological data were measured at the rooftop of a house near the pilot area. The height of the observation point was about 10m above the ground. A rain gauge (ECRN-100, Decagon Devices, Inc.), Davis cup anemometer (Decagon Devices, Inc.), a solar radiation sensor (PYR, Decagon Devices, Inc.), and a humidity temperature and vapor pressure sensor (VP-3, Decagon Devices, Inc.) with a radiation shield were installed. These data were collected every 10 minutes through a

Gas samplings for estimating GHG emissions were conducted almost 7 days interval using chamber method. Chamber, a box with lids (60×60×100cm), was put on each observation plot. Gas samples from the chamber headspace were collected at 10-min intervals using 15-ml plastic syringes during a 20-min period after the chamber closure. Almost every sampling was conducted in the morning (8:30–11:00 am).

CH₄ concentrations were measured by gas chromatographs equipped with flame ionization detectors (FIDs) (Itoh et al., 2011). The gas emission flux was calculated from the gradient of temporal change in the gas concentrations as the following equation,

$$f = \frac{dc}{dt} M \frac{273}{22.4} \frac{1}{273 + T} \frac{V}{A} \quad (1)$$

where f is the CH₄ flux (mg m⁻² h⁻¹), c is the gas concentration (ppm), t is the time (h), M is the molecular weight (g mol⁻¹), T is the air temperature in chamber (°C), V is the volume of air in chamber (m³),

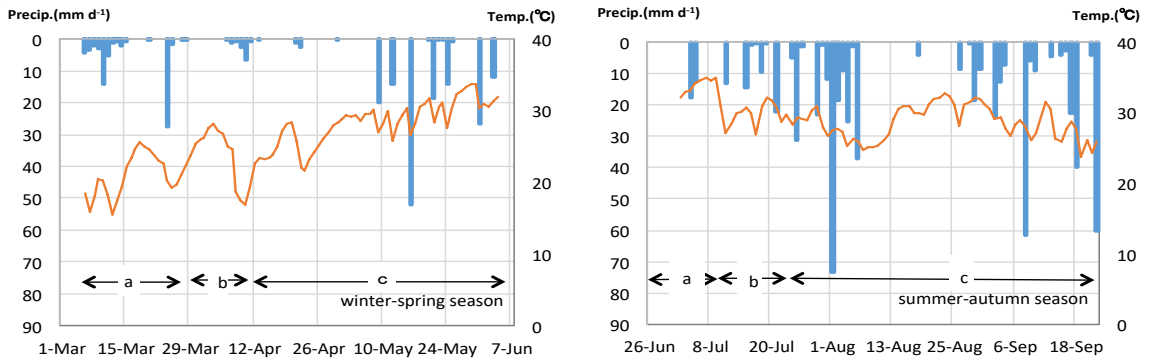
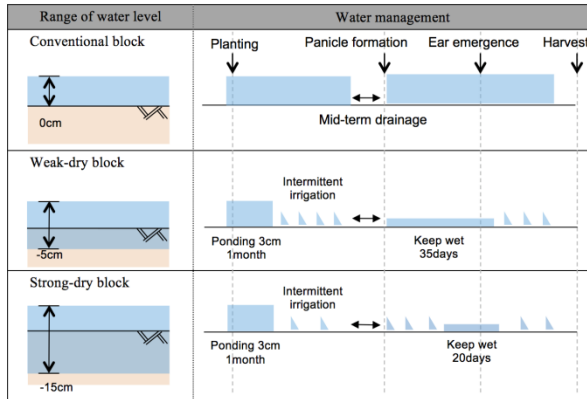


Fig. Daily precipitation and average air temperature in 2015. a: ponding period, b: midterm drainage period, c: intermittent irrigation period.

data logger (Em50, Decagon Devices, Inc.)

Water gauges (S&DL mini, Oyo Corp.) were installed to some gates in canal to measure water level of canal. Paddy ponding water depths were measured using water level sensors (WT-HR, Intech Instruments LTD). Tensiometers (DIK-3046, Daiki Rika Kogyo Co., Ltd.) were installed to depths of 5 cm and 15 cm at C1, W1, and S1 plots at intervals of 30 minutes. Soil moisture sensors (5TE, Decagon Devices, Inc.) for measuring the soil water content, the soil EC and the soil temperature were installed to depths of 5 cm and 15 cm in C1, W1, and S1 plots and to a depth of 5 cm in C2, W2, and S2 plots at intervals of 10 minutes.

and A is the cross-sectional area of chamber (m²).

Soil pH and Eh were measured by sensors (PRN-41, Fujiwara Scientific Co., Ltd.) at the same time as gas sampling.

Multiple regression analysis

Using multiple regression analysis (MRA), we investigated the influential factors on CH₄ emission from paddy field. One variable was deleted from the variables with high P -value, and MRA was performed until the number of variable became one. The optimal regression was the case that the explanatory variable selection criterion (R_u) was maximum.

$$R_u = 1 - \left(\frac{1 - R^2}{n - k - 1} \right)^{n + k + 1} \quad (2)$$

where R is multiple correlation coefficient, n is the number of data, and k is the number of independent variables. Investigated variables were the paddy water level, the soil temperature at surface and a depth of 5cm, the soil pH, the soil electrical conductivity, the air temperature, and the temperature in chamber.

Results and discussion

Meteorological conditions

Figure 3 shows daily precipitation and average daily air temperature in both seasons. The total precipitations were 244.6mm in the winter-spring season and 634.8mm in the summer-autumn season. Each season was divided into three periods: the ponding period before the midterm drainage (winter-spring season: Mar.6 to Mar. 29, summer-autumn season: Jun.26 to Jul.13), the midterm drainage period (winter-spring season: Mar. 30 to Apr. 9, summer-autumn season: Jul.14 to Jul.25), and the intermittent irrigation period (winter-spring season: Apr. 10 to Jun. 4, summer-autumn season: Jul.26 to Sep.22). The rainfall amounts during three periods were 68 mm, 5.4 mm, and 171.2 mm in the winter-spring season and 44.2mm, 85.6mm and 505mm in the summer-autumn season, respectively. Average air temperatures were 25.7°C in the winter-spring season and 29.3°C in the summer-autumn season.

Paddy water level

Figure 4 shows paddy water level in each plot. In the winter-spring season, paddy ponding water kept about more than 5cm depth before the midterm drainage. After the midterm drainage, it was estimated from measured data of paddy water levels and canal water levels that

there were three to five times of irrigation except S2 plot, and only twice irrigations were conducted at S2 plot. A farmer of plot S2 appeared to try strong-dry water management, but the first planned water management at W1, W2, and S1 plots were not implemented properly. After May 9, paddy water levels increased sometimes by rainfall events. The artificial water management in the intermittent irrigation period was found to be difficult, and planned water management failed to conduct due to frequent rainfall events.

In the summer-autumn season, almost every plot was flooded during the planned midterm drainage because of rainfall. The artificial water management in the summer-autumn season was found to be more difficult than the winter-spring season due to frequent rainfall.

CH₄ flux

Figure 5 shows seasonal dynamics of CH₄ flux. In the winter-spring season, CH₄ flux was higher at all plots before the midterm drainage. It was negligibly small in the midterm drainage and the intermittent irrigation periods. On the other hands, in the summer-autumn season, CH₄ flux was almost positive until the end of August. Especially, much CH₄ emitted during late-July to mid-August. After the end of August, the flux were zero at all plots.

The cumulative CH₄ flux, which was calculated by assuming the constant flux was kept during the measurement intervals, in the winter-spring season was one quarter of that in the summer-autumn season (9.0 g m⁻² in the winter-spring season (91days) and 37.3 g m⁻² in the summer-autumn season (85days)). The percentage of CH₄ flux in intermittent irrigation period to the total cropping period was 11% in the winter-spring season

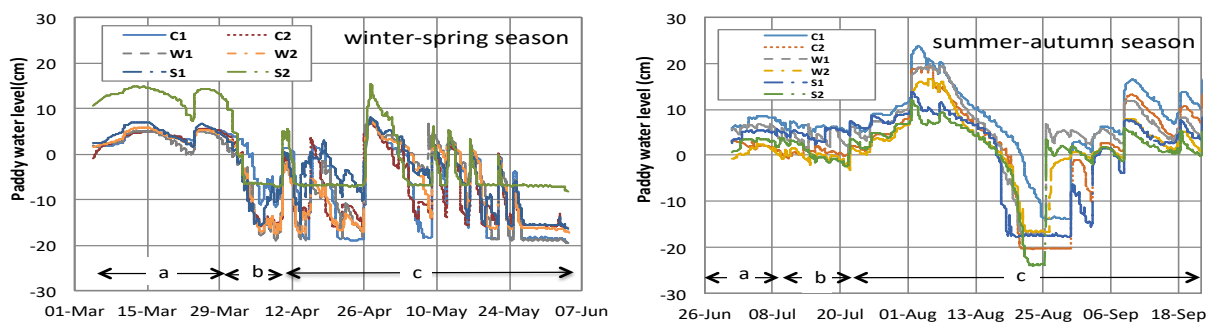


Fig. Water levels in paddy plots during water management experiments in 2015. a: ponding period, b: midterm drainage period, c: intermittent irrigation period.

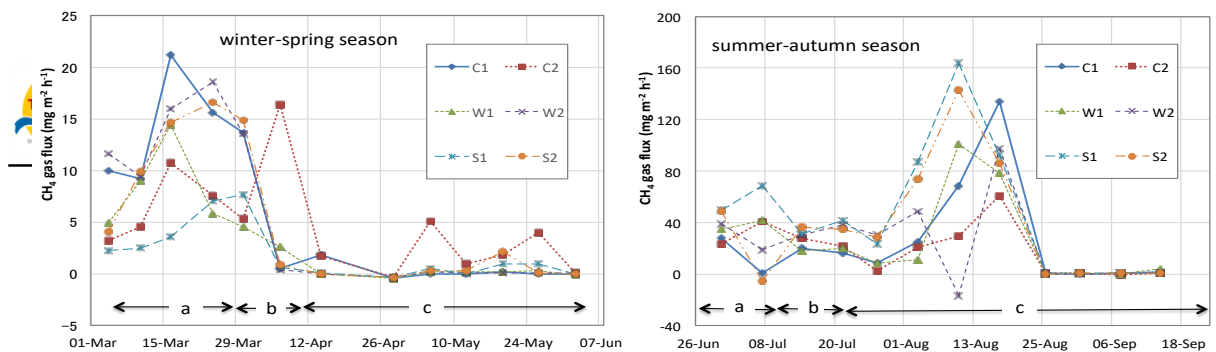


Fig. CH₄ emissions during water management experiments in 2015. a: ponding period, b: midterm drainage period, c: intermittent irrigation period.

and 49% in the summer-autumn season, respectively. Though the improved paddy water management may be effective in the winter-spring season due to less rainfall, the countermeasure for the summer-autumn season is also important.

Influential factors on CH₄ emission

The explanatory variable selection criterion (R_u) reaches the maximum value when the paddy water level, the soil temperature at a depth of 5cm, and the soil pH are taken as independent variables in the winter-spring season and when the water content at a depth of 5cm, paddy water level, soil EC, soil Eh are taken as independent variables in the summer-autumn season (Table 1). In the winter-spring season, the partial regression coefficient of the soil temperature at a depth of 5cm is negative and that of the soil pH is positive. The independent variable commonly seen in the both seasons is only the paddy water level. However, the partial regression coefficient is positive in the winter-spring season and negative in the summer-autumn season. This is because, paddy fields in the winter-spring season became non-flooded due to the midterm drying or intermittent irrigation, although which in the summer-autumn season were flooded through almost the entire period. Therefore, decreasing in the paddy water level did not cause CH₄ emission in the summer-autumn season. For the same reason, the partial regression coefficient of soil moisture content at a depth of 5cm in the summer-autumn season was negative. The correlation coefficient, the multiple correlation coefficients and R_u are low hence the influential factor with high importance are not be found in both seasons.

The correlation diagrams between Eh, pH, soil moisture content and methane flux are shown in Fig. 6. Connell and Patrick (1969) presented CH₄ is generated actively with Eh less than 150 mV, though CH₄ occurs mainly when Eh is under 220 mV in this survey. The fact that CH₄ emissions under 10mV of Eh were low is unaccountable. CH₄ emissions decrease when the soil water content at a depth of 5cm is about 0.25 or less. Oremland (1988) observed that CH₄ emission increases at

pH 6 to 8, and this trend was also recognized in this survey. No characteristic trend was found from the correlation diagram with other influential factors.

It is considered that more precise management of gates during no rainfall period is necessary for achieving the significant decrease of CH₄ emission from paddy plot. One of the targets is to lower soil water content at a depth of 5cm to 0.25 or below.

Table Parameters of the results of multiple regression analysis with maximum R_u in both seasons.

winter-spring season ($R_u=0.372$, $R^2=0.433$, $n=78$)				
	PRC	SE	t	P-value
paddy water level (cm)	0.002	0.001	2.064	0.043
soil temperature (°C)	-0.007	0.002	-4.228	0.000
soil pH	0.029	0.015	1.867	0.066
summer-autumn season ($R_u=0.357$, $R^2=0.564$, $n=26$)				
	PRC	SE	t	P-value
paddy water level (cm)	-4.018	1.196	-3.361	0.003
soil water content at 5cm	-0.027	0.011	-2.517	0.020
EC (mS cm ⁻¹)	0.452	0.264	1.713	0.101
Eh (mV)	-0.002	0.001	-2.463	0.023

PRC : partial regression coefficient

SE : standard error

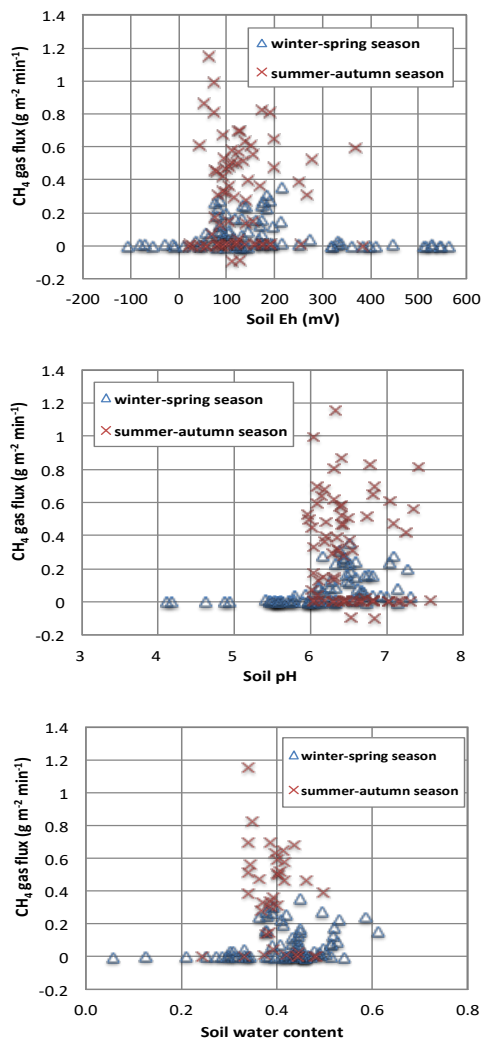


Fig. Correlation of CH₄ flux with soil Eh, soil pH and soil water content at a depth of 5cm.

Conclusions

In this research, we have adopted intermittent irrigation to paddy fields in the Red River Delta, Vietnam. However, since rainy weather continued through the summer-autumn season and some rainy days in the winter-spring season, intermittent irrigation was found difficult to carry out. In actual situations, it is difficult to manage the water level in order to realize the target paddy water management due to rainfall events.

Methane emission in the summer-autumn season is four times more than which in the winter-spring season, accounting for 49% of the total methane emission in the intermittent irrigation period. Therefore, the importance of reducing the amount of methane generated from paddy fields in the rainy season is also expected.

No parameter with high influence on methane emission was found in multiple regression analysis. Nevertheless, we found that CH₄ emission decreases when the volumetric water content at a depth of 5 cm is under 0.25 and when the Eh is above 220 mV, and it increases when the pH scale ranges from 6 to 8.

Acknowledgements

This work was supported by JSPS KAKENHI Grant Number 16H05799.

References

Connell, W. E. and Patrick, W. H. Jr. (1969) Reduction of sulphate to sulphide in waterlogged soil, *Soil Sci. Soc. Am. Proc.* 33(5), 711-715

Iida, T., Kakuda, K., Ishikawa, M. and Okubo, H (2007) Variation in methane and nitrous oxide emission from practical paddy fields with intermittent irrigation, *Trans. of JSIDRE* 247, 45-52

Itoh, M., Sudo, S., Mori, S., Saito, H., Yoshida, T., Shiratori, Y., Suga, S., Yoshikawa, N., Suzue, Y., Mizukami, H., Mochida, T. and Yagi, K. (2011) Mitigation of methane emissions from paddy fields by prolonging midseason drainage, *Agriculture, Ecosystems and Environment* 141, 359-372

Kudo, Y., Noborio, K., Kato, T. and Shimoozono, N. (2012) Effects of difference in water management on greenhouse gas emissions of direct and indirect in rice paddy field, *Trans. of JSIDRE* 282, 43-50

Liang, X.Q., Chen, Y.X., Nie, Z.Y., Ye, Y.S., Liu, J., Tian, G.M., Wang, G.H. and Tuong, T.P. (2013) Mitigation of nutrient losses via surface runoff from rice cropping systems with alternate wetting and drying irrigation and site-specific nutrient management practices, *Environ. Sci. Pollut. Res.* 20, 6980-6991

Minami, K. (2003) Tropical agriculture and environmental conservation, *Japanese society for Tropical Agriculture* 41(3), 115-124

Minamikawa, K. (2006) Appropriate farm works to mitigate greenhouse gases emission from paddy fields, *Japanese Journal of Farm Work Research* 41(3), 115-12

Oremland, R. S. (1988) Biogeochemistry of methanogenic bacteria, in: Zehnder A.J.B.(ed.),



Biology of anaerobic microorganisms, John Wiley,
New York, 641

Richards, M. and Sander B. O. (2014) Information note
on alternate wetting and drying in irrigated rice,
Implementation guidance for policy makers and
investors, CGIAR, CCAFS, IRRI

Water Energy Carbon Nexus in Urban Water Supply System of Kathmandu Valley

Mimansha Joshi

Abstract Urban water services are challenged from different dimensions of sustainability. Although not evident, water services consume a considerable amount of energy through extraction, treatment, distribution and conveyance. While a myriad number of studies have been carried out globally to quantify WEC nexus in urban water supply systems, only a handful of studies have been carried out in Asia. In order to bridge this gap, this study estimated the existing energy and carbon footprint from the cycle, which further expands to examining how the energy implications change when new planned water supply is operational in Kathmandu valley. It uses secondary data achieved through interactions with concerned stakeholders and through best estimations and assumptions.

The study revealed that about 250 GWh – 286 GWh of energy is used for water supply in Kathmandu valley, accounting for 0.04% of total energy consumption of Kathmandu.

Households and private tankers were found to be very energy intensive. On assuming that water distribution through private tankers are eliminated after planned water supply system is operational, the valley can save about 140 GWh of energy and about 35 ktCO₂e carbon emissions as the energy intensity decreases from 12.77 kWh/m³ to 2.72 kWh/m³. Furthermore, as groundwater extraction gets reduced by 12% after MWSP, Kathmandu will be able to save about Rs. 7 million a year.

As a result, the study aims to contribute to the formulation of a policy in water and energy sectors to reduce GHG emissions.

Keywords *Water, Energy, Carbon, Urban Water Cycle, Kathmandu, Climate Change, Sustainability*

Introduction

Despite adequate water availability, water security remains a pressing problem in Nepal with growing demands and insufficient infrastructures. Access to water resources remains primitive in Nepal, with a severe lack of rural infrastructure, power and technology to redistribute water to high demand areas. With only 24 percent of arable land being irrigated and 28 percent of population still lacking access to safe potable water supplies, the rising population in Nepal is at increasing pressure on resources and associated water risk (Bartlett et al., 2010). In line with water insecurity, Nepal also has a darker problem in parallel- energy security. Energy resource insufficiency to support electricity or to avail water resources has hindered Nepal's development as water and energy is poorly managed and substantially underused.

Nepal also lacks effective governance for progressing in livelihood enhancing technologies to improve access to water and energy. Since a good infrastructure is dependent on good institutional governance and sustainability, there

is a need to quantify water and energy footprints to support policy discussions and mitigate the effects of climate change in parallel.

Study Area Description

Kathmandu Valley covers the capital city, Kathmandu and two surrounding metropolitan cities known as Lalitpur and Bhaktapur. Kathmandu Valley is the largest urban settlement of Nepal, having an area 49.45 km² and is home to 2.5 million inhabitants (9.1 % of total country population). Other municipalities within the valley are Kirtipur and Madhyapur Thimi. The valley consists of major rivers like Bagmati, Bishnumati and Manohara with Bishnumati, Manohara, Dhobikhola, Nagmati and Balkhu rivers being the main tributaries of the Bagmati River.

Kathmandu Valley lies in the Warm Temperate Zone (elevation ranging from 1,200–2,300 meters (3,900–7,500 ft), where the climate is fairly temperate. Under Köppen's climate classification, portions of the city with lower elevations have a humid subtropical climate, while portions of the city with higher elevations generally have a subtropical highland climate. In the Kathmandu Valley, the average summer temperature varies from 28–30 °C (82–86 °F). The average winter temperature is 10.1 °C (50.2 °F). Rainfall is mostly monsoon-based about 65% of the total concentrated during the monsoon months of June to August. Rainfall has been recorded at about 1,400 millimeters (55.1 in) for the Kathmandu valley, and averages 1,407 millimeters (55.4 in) for the city of Kathmandu. On average humidity is 75%. The annual amount of precipitation was 1,124 millimeters (44.3 in) for 2005, as per monthly data.

Water Demand, Supply and Management in Kathmandu

The present population of the Valley water supply service area is estimated to be 2.7 million with a water demand of 370 MLD. The total water production in the wet and dry seasons is about 142 and 98 MLD, respectively (KUKL, 2015).

Given the above numbers, the water supply operator, Kathmandu UpatyakaKhanepani Limited (KUKL), which is the prime body for supplying water is clearly not being able to meet the demand. Added to the supply has 38 percent of leakage, which is one of the biggest challenge for the supply. However, KUKL has considered on addressing this problem with a fifteen-year long project for replacing old pipes in the valley with new ones for leakage control, estimated to be complete in 2025 (Manandhar, 2013). This can help replace improve the water supply and reduce waste likewise.

Kathmandu receives its water supply from surface sources and groundwater sources. Out of total water supplied by the water supply operator Kathmandu UpatyakaKhanepani Limited (KUKL), surface water counts for 80% in wet season and 54% for Dry season (KUKL, 2015). The remaining of the supply is through the ground source i.e. wells and tube wells which are mostly situated at the northern area of Kathmandu Valley. Thus, most of the surface sources are being tapped for the water supply in Kathmandu Valley (Manandhar, 2013). Surface water accounts for 116 MLD during wet season and 64 MLD during dry

season. KUKL is using 35 surface sources including small tributaries. KUKL, in its 10 systems, gets water from surface sources like Shivapuri, Bishnumati, Alley, Boude, Nagmati, Shyalmati, Doodhpokhari, Lunhkot, Nakhu, Sesh Narayan, Nallu, MahadevKhola and Devki rivers.

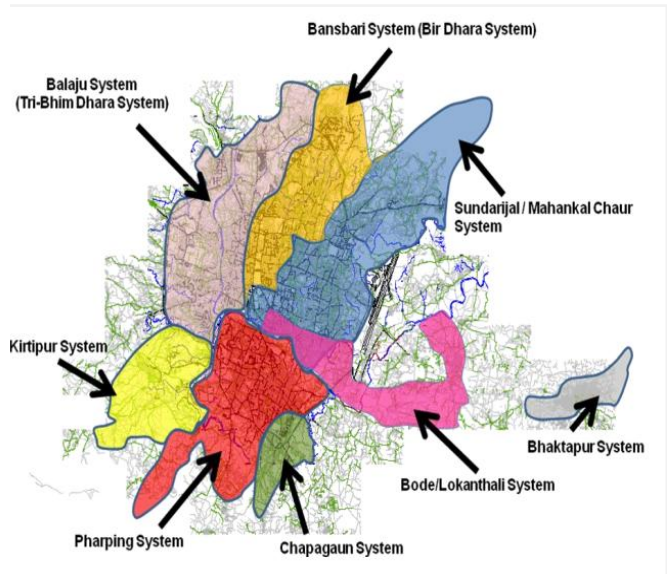


Fig.1 KUKL’s Water distribution systems

Source: GRDB

Groundwater abstraction started in 1980 A.D. and became the most reliable sources for water consumption. However, the abstraction rate has been exceeding the recharging rate lately, thereby depleting the groundwater level considerably. When JICA (1990) conducted the modeling of deep aquifer system to estimate sustainable withdrawal of water, the study suggested a safe withdrawal of 0.027 million m³/day. However, with the current recharge being up to 15 mm/year (0.04 to 1.2 million m³/year); extraction rate is 20 times of this amount; and reserves will be used up within 100 years at current rate of extraction (Pradhanang, 2012). While unmet demands have been one of the major concerns in water supply system of Kathmandu, the quality and quantity of water have been equally problematic. These unmet demands have led to adding pipelines beyond KUKL’s systems as per request of communities. Hence, there is an unplanned distribution of water that does not follow the plan, making Kathmandu’s water distribution network more complex and ad hoc.

Private tankers also provide water during peak demand as per the request of individual households and communities based on their needs.

Kathmandu also consists of registered wells that supply water for commercial and industrial use. These sectors mainly comprise of banks, housing, hotels and other industries.

Additionally, households also extract water as road networks in Kathmandu are usually planned for pedestrian movements which may not accommodate trucks and private tankers to pass through the households that need water. As a result of lack of municipal water supply and costly water transport from private tankers, households have opted for private dug wells and tube wells in their respective land areas. This is also one of the main source of water for household construction purposes, which can easily serve the homes after construction of their dwelling (Manandhar, 2013). These dug wells have not been monitored by the government, but according to Manandhar, there are about 10,000 dug wells in the valley.

However, in every household, dug wells or tube wells are being used for household activities. Water supply from KUKL or private tankers are first collected in underground water tankers with the capacity of about 9000 liters- 12000 liters, from which they pump the same water to their roof-top water tankers which has the capacity of about 500-2000 liters. Water is then accessible through gravity. As per the need, households also pump water from their dug wells to separate rooftop water tankers for other purposes.

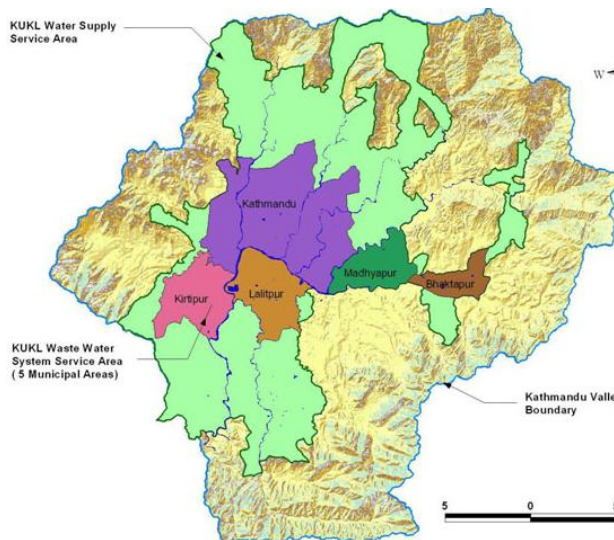


Fig.2 Kathmandu Valley and KUKL Service area

Source: KUKL (2011)

To deal with increasing water supply deficit and water scarcity in the valley, Melamchi Water Supply Project (MWSP) is underway to bring water from off-the-

valley sources. After completion of the project, water supply quantity is expected to be improved.

This study used the water and energy data for the urban water cycle from KUKL to quantify and analyze the water-energy-carbon nexus from water utilities. At its completion, it will have built a scenario for post-Melamchi to compare the energy use and greenhouse gas emissions after its outset.

Data Collection

The data used for this research are mostly secondary data that are obtained from literature review and through the correspondence with respective data distributors from Water Management and Supply sectors in Kathmandu. Also, the range of values for energy footprint of water treatment and production is adopted from a set of values from different literatures. All data regarding KUKL’s water supply and Melamchi’s plans are collected from KUKL’s annual reports and through interviews with the corresponding engineers. The statistics related to water discharge, operation hours for registered wells are collected from KVWSMB. Other data related to carbon emission factors for different sources of energy are obtained from International Energy Agency.

Results and Discussion

Quantifying energy and carbon intensities from urban water supply cycle is generally difficult, especially in the context of Kathmandu due to difficulty in finding information and specific data on several parameters which have not been considered for measurement. Data availability and quality has been the most common and critical issue in conducting this research although this research would require high-quality data collected in a consistent manner. But, even so, there is a growing advantage of this integrated study in Kathmandu as water, energy and carbon issues are adjacent at the institutional level. This study hence considers in giving a generic analysis and estimation by organizing available data from existing publications and Water Supply sources into a dataset to give streamline the link between water, energy and carbon from urban water supply cycle.

Apart from the centralized water system, there are also private tankers, households and registered wells in Kathmandu through which water is supplied. The energy used in water production from these areas vary in several ways. Hence, it is imperative to compare the

energy and carbon intensity for these different water supply systems.

Energy Consumption in KUKL Water Supply

KUKL system is being managed by 10 branch offices of KUKL, with six of them for the Kathmandu Metropolitan City area and adjoining VDCs, one for Lalitpur and adjoining VDCs, one for Bhaktapur and adjoining VDCs, one for Kirtipur and adjoining VDCs and one for MadhyapurThimi and adjoining VDCs (ADB, 2006).

Other temporary populations and VDCs are able to obtain water from sources without treatment like traditional waterspouts, ground water wells, rivers, streams, etc.

Energy consumption is accounted for in four different stages of water supply, namely: abstraction, or raw water intake, water conveyance, water treatment and water distribution. The amount of water extracted, efficiency of pumps, pump horsepower and average daily operation hours are governing factors for finding the energy use. The study assumed that the pump efficiency varied from 65% to 85%, and hence found a range of energy intensity with corresponding efficiencies.

The energy intensity is higher for abstraction and distribution processes, i.e., 0.26 kWh/m³- 0.30 kWh/m³ and 0.12kWh/m³ – 0.42 kWh/m³ respectively as it involves pumping and hence uses a lot of energy (Table 1). Energy intensity from treatment was extracted using the range of values provided by Wilkinson for a definite value of water treated. In Kathmandu, 90% of water is distributed by gravity, with only three out of nine branches having two reservoirs that use booster pumps. Expert interviews and discussions led to conclusion that Kathmandu’s distribution system accounts for 35% loss. Hence, the study calculated energy intensity for three scenarios- 0% loss, 15% loss and 35% loss with 65% and 85% pump efficiencies. The overall energy intensity for water supply from KUKL is 0.45 kWh/m³ – 0.87 kWh/m³. The total carbon footprint is 26.6 TCO₂e – 47.2 TCO₂e, calculated from the emission factor for Nepal from electricity generation being 0.003 kgCO₂/kWh (IEA, 2014).

As most of the water is conveyed from groundwater to treatment plants and from surface water to treatment plants through gravity, the energy intensity and carbon

footprint from water conveyance is effectively zero in the case of Kathmandu Valley.

Table1 Estimation of total energy intensity, energy consumed and carbon emissions at different stages of KUKL water supply

S N	Parameter	Volume (MLD)	KUKL Energy Use Intensity (kWh/m ³)	Energy Consumption (kWh/day)	Carbon Emissions (tCO ₂ e/year)
1	Raw Water Intake	78.8	0.26 – 0.30	18800-22810	22-25
2	Conveyance	0	0	0	0
3	Treatment	64.8	0.14 – 0.15	8270 – 15894	0.9-17.4
4	Distribution	0.21 – 0.27	0.12-0.42	3396 – 4440	3.72-4.86
	Total		0.45 – 0.87	30,466 – 22600	26.6 – 47.2

Energy Intensity and Carbon Emissions from other sectors of water supply

The total energy consumption by private tankers from groundwater extraction ranged from **827 kWh/yr - 1081.5 kWh/yr**. The energy intensity for abstraction by private tankers is **0.09 kWh/m³ - 0.12 kWh/m³**. Carbon Emissions from groundwater extraction for private tankers varied from **1 tCO₂e/year to 2.5 tCO₂e/yr**. Private tankers were seen to be very energy intensive when distributing the water to households, as their energy intensity is **9.97 kWh/m³** and carbon emissions is **34.9 MtCO₂e/yr**.

Similarly, the industrial, commercial sectors and housing consumes **4805 kWh/yr - 6283.7kWh/yr**. Given that the total volume of water extracted is **25844.5 m³**, the energy intensity for abstraction by registered wells varied from **0.19 kWh/m³ – 0.24 kWh/m³**. Carbon emissions for this sector varied from **5 – 7 tCO₂e/yr**.

Although the KUKL pipeline is reported to be available to most of the households in Kathmandu, many households cannot acquire the connection due to lack of connectivity and functionality. According to KUKL, water supply is delivered at an average of 2-3 days a

week. However, this number is due to vary with location and availability. Also, most of the households although have a private connection to the piped water system, many households only receive water scantily suffering from negative pressures and chronic contaminations. To combat this problem of water scarcity, households engage in several coping behaviors like collecting water from public taps, purchasing it from vendors and neighbors and investing in storage tanks, etc. The household water abstraction is also complex due to problems like leaking pipes, sharing with neighbors and community, stealing from the system and performing illegal pumping from distribution mains.

Only accounting for legal practices, the study found the total energy consumption to be 25.8 kWh/yr – 128.5 kWh/ yr. The energy intensity was found to vary from 0.37 kWh/m³– 1.86 kWh/m³. Carbon emissions varied from 78 ktCO₂e/yr – 385 ktCO₂e/yr. The high and low estimations account for households extracting water through use of pumps with 1 HP capacity 2 – 7 days in a week.

If we compare the energy intensity for water supply in different cities as shown in Table 2, the intensity for Kathmandu’s water supply is quite low. The energy intensity of Kathmandu for abstraction being 0.92-2.52 kWh/m³ could be a result of use of inefficient pumps that are energy intensive with a deep static groundwater table depth. The pumps might also be used for extracting lower volumes of water, resulting in higher energy intensity.

Water distribution in Kathmandu is energy intensive if we account for private tankers too. However, only accounting for piped water distribution system, we can see that Kathmandu’s water distribution through networks is almost comparable to that of Delhi.

Similarly, treatment energy intensity in Kathmandu is estimated to be 0.14 kWh/m³, which is almost similar to that of Sydney and Delhi.

According to the study, “Water-Energy-Carbon Nexus in Cities: Cases from Bangkok, New Delhi, Tokyo”, it was found that Delhi’s water tanker service consumes about 526 MWh/day, which is quite close to that of Kathmandu, which consumes 380 MWh/day.

Table 2 Comparison of Kathmandu’s Energy Use and intensity with various water supply sources/ stages in different regions

Water supply sources/stages	Region	Purpose	Energy Use	References
Ground water extraction	California, USA	Groundwater pumping	0.14-0.69 kWh/m ³	Plappally and Lienhard (2012)
	Central Arizona, USA	Lifting groundwater	3.3 kWh/m ³	Perrone et al. (2011)
	USA	Whole water supply system	1.02 kWh/m ³	Sattenspiel and Wilson (2009)
	USA	Groundwater pumping	0.18-0.49 kWh/m ³	EPRI (2002)
	Chino Basin, Southern California	Groundwater pumping	0.79 kWh/m ³	Wilkinson, 2005
	Australia	Groundwater pumping	0.48-0.53 kWh/m ³	Rocheta and Pearson (2011)
Water distribution conveyance	Tokyo	Groundwater pumping	1.78 kWh/m ³	Shrestha S. et al. (2015)
	Kathmandu, Nepal	Groundwater pumping	0.91-2.52 kWh/m ³	
	Northern California		0.04 kWh/m ³	CEC (2005)
	Southern California		2.4 kWh/m ³	CEC (2005)
	Bangkok	Piped Networks	0.081 kWh/m ³	Shrestha S. et al. (2015)
	Delhi	Piped Networks	0.5 kWh/m ³	Shrestha S. et al. (2015)
	Tokyo	Piped Networks	0.13 kWh/m ³	Shrestha S. et al. (2015)
	Kathmandu, Nepal	Water distribution through pumping and transporting	10.12 – 10.38 kWh/m ³	
	Kathmandu, Nepal	Water distribution through piped networks	0.42 kWh/m ³	
	Australia	Raw water treatment	0.1-0.6 kWh/m ³	Marsh, 2008
Water treatment	USA	Raw water treatment	0.027-4.32 kWh/m ³	Sattenspiel and Wilson (2009)
	Northern and Southern California, USA	Raw water treatment	0.027 kWh/m ³	CEC (2005)
	Sydney Australia	Raw water treatment for 2006/07	0.1 kWh/m ³	Kenway et al. (2008)
	Bangkok	4 WTPs	0.047 kWh/m ³	Shrestha S. et al. (2015)
	Delhi	10 WTPs	0.17 kWh/m ³	Shrestha S. et al. (2015)
	Tokyo	11 WTPs	0.29 kWh/m ³	Shrestha S. et al. (2015)
	Kathmandu, Nepal	Conventional Water Treatment	0.14 kWh/m ³	

Discussions and Major Findings

In Kathmandu, water extraction mostly depends on the static depth of the groundwater table, head of pumps, efficiency of pumps, discharge of water through the pumps and number of hours of operation. Since the water is conveyed to treatment plants through gravity,

no energy is consumed during this process, but treatment largely depends on the kinds of technologies used while chemical dosing. Around 90% of water is distributed through gravity in Kathmandu, but only 10% is distributed by the use of pumps.

Joshi’s study found that Kathmandu consumes about 690 MWh/day- 784 MWh/day of energy for water supply and distribution. Similarly, the total energy intensity was in the range for Kathmandu is about 11.1 kWh/m³- 12.8 kWh/m³. The total carbon emissions are in the range of 35 kTCO₂e – 35.4 kTCO₂e per year.

Decision-makers can integrate the energy issues into water policy decision-making as looking at both these components can generate valuable insights that may not rise from separate policy analyses of water, energy and climate change. On so doing, Kathmandu’s policy makers can find better methods and ways to link decisions between water energy and carbon in order to maximize the benefits, address the increasing financial costs while also identifying new partnerships and ideas. For example, policy-makers can make their sustainability plans where they can make decisions like eliminating diesel-based transportation to serve water, improving water quality, managing leakage and reducing groundwater pumping to yield effective solutions.

Policy makers can also help to make improvements on management practices. On recognizing that energy considerations in managing water can lead to energy and cost savings, plans and policies that incorporate improvement of energy efficiency, and better technologies can bring about remarkable results. For example, leakage management practices if carried out by testing and benchmarking pump stations for water agency like KUKL to check their performance, a good amount of energy can be reduced throughout this good practice.

Clearly, transitioning to a sustainable water supply system needs cooperative and innovative policy-making which cannot happen overnight. However, on understanding the benefits incurred, policy makers can implement this integrated approach between the three components to reduce energy and water demand.

References

- Barlett, R., Pant, L., Hosterman, H., & McCormick, P. (2010). Climate Change Impacts and Adaptation in Nepal. *IWMI*, 139.
- Dixit, A., & Upadhaya, M. (2005). *Augumenting Groundwater in Kathmandu Valley: Challenges and Possibilites*. Kathmandu: Nepal Water Conservation Foundation.
- KUKL. (2011). *Kathmandu Upatyaka Khanepani Limited at a Glance*. Kathmandu.
- Manandhar, I. (2013). *Sucess to Abundant Water Supply in Kathmandu Valley*. University of Minnesota. Minnesota: University of Minnesota.
- MWSDB. (1998). *Melamchi Water Supply Project - Information Brochure*. Nepal: Melamchi Water Supply Development Board (MWSDB).
- Joshi, Mimansha. *Water, Energy and Carbon Nexus in Urban Water Supply System of Kathmandu*. Thesis. Asian Institute of Technology, 2015. Print.
- JICA. (1990). *Groundwater Management Project in the Kathmandu Valley Final Report*. JICA.
- Pradhanang, S. (2012). *Comprehensive Review of Groundwater Research in Kathmandu Valley, Nepal*. *Research Gate* .
- Shrestha, D. (2011). *State and Services of Private Water Tanker Operation in Kathmandu*. *Interdisciplinary Water Resources Management* .

Satellite based sub-daily downscaling of gauged rainfall for flood analysis via fully distributed hydrological model

Pallav Kumar Shrestha^{1,*}, Sangam Shrestha¹ and Sarawut Ninsawat²

Abstract Flood events bear pronounced sub-daily variations originating from the variation of rainfall during storm events. Hence, correct flood simulations require sub-daily gauged rainfall which may not be available in all cases. This study proposes to route this issue thru a satellite based approach wherein daily gauged rainfall is downscaled to three hourly (3-h) resolution using diurnal variability of Tropical Rainfall Measurement Mission's (TRMM) 3B42 level 3 data (R_{sat}). Three rainfall datasets – TRMM-downscaled rainfall (R_{ds}), R_{sat} and daily gauged rainfall downscaled uniformly at 3-h intervals (R_{uni}) – are then forced into a fully distributed model, SHETRAN, which is pre-calibrated with gauged hourly rainfall ($R_{control}$) for 2011-12. R_{ds} shows improved degree of agreement and correlation to $R_{control}$ compared to R_{sat} and R_{uni} . Evaluation of the 2-year hourly hydrograph shows R_{ds} clearly outperforming R_{uni} (hourly Nash-Sutcliffe Efficiencies of 0.72 & 0.64 respectively). Correlation analysis of Q_2 flows (magnitudes that are exceeded only 2% of the time) shows R_{ds} to simulate flood events more accurately than R_{uni} (correlation coefficient of 0.57 & 0.35 respectively). Comparison of flood peak magnitudes (forty flood events in Q_2) without timing consideration shows R_{ds} outperforming R_{uni} and performing on par with $R_{control}$ (correlation coefficient of 0.84, 0.39 & 0.88 respectively) in flood peak simulation. However, R_{ds} yielded a varying peak flood timing error which could be attributed to various factors including the satellite's sensing mechanism. This study concludes that satellite based sub-daily downscaling of daily gauged rainfall could be a good option for flood analyses in cases where sub-daily gauged measurements are not available.

Keywords *Gauged rainfall, satellite rainfall, sub-daily downscaling, flood analysis, TRMM, distributed hydrologic model*

Pallav Kumar Shrestha, Sangam Shrestha

Water Engineering and Management

Asian Institute of Technology

Pathumthani, Thailand

*pallav@ait.asia

SarawutNinsawat

Remote Sensing and Geographic Information Systems

Asian Institute of Technology

Pathumthani, Thailand

Introduction

Rainfall monitoring is an integral part of meteorological science. It is a common case that countries (especially from under-developed regions) have only a 'one time a day' manual reading of precipitation record. However, advanced research and development studies demand finer resolution datasets.

Flood is a one of the most afflicting natural disaster worldwide. They are triggered by high intensity/duration precipitation during wet seasons and thus have direct correlation to the storms. The relation between the storm and the resulting flow rate in the river has been studied immensely in past and led to development of various rainfall-runoff models. Physically based fully distributed models are the most sophisticated tools present today for studying river hydrology. They solve the analytical equations at each grid of the model that trace the movement of water in the basin and thus is able to simulate river flow from input meteorological data. However, these advanced tools require finer data input in order to avoid instability issues of the model solvers. In addition, floods themselves beckon for finer (sub-daily) resolution rainfall information since floods bear pronounced sub-daily variations originating from the rainfall variation over time.

Satellites are wonders of human technological advancement. The idea of monitoring rain from space paved way to a list of research innovation as the satellites started global rainfall monitoring at desired frequency and spatial resolution. Numerous satellites have been observing rainfall remotely with their own interpreting algorithm, out of which arguably, Tropical Rainfall Measurement Mission (TRMM) project initiated by NASA and Japanese Aerospace Exploration Agency (JAXA) and its products might be the most popular of them all. With sub-daily high resolution rainfall measurements, TRMM offers a good opportunity to explore its utility in flood simulation analysis.

Most of the past studies with application of satellite data in the field of hydrology have been using them with models of simpler mechanism and/or at daily time scale at most. Studies pertaining to real-time forecasting of flood are mainly focused on the use of the satellite product directly rather than utilizing the forgotten value of daily gauged rainfall alongside. This study presents a satellite based sub-daily downscaling of daily gauged rain data and evaluates it from hydrological and flood analysis standpoint. The conclusions of this research could evolve into a working component for extreme flood studies and flood forecasting studies (real-time/ stochastic) under scenarios analysis amongst others.

Study area

The Kathmandu Valley (602 km²) is the headwaters catchment of the Bagmati River Basin (refer Fig.). Located in the middle mountainous physiographical region of Nepal, this small basin has a rather flat central area with urban cover while the terrain shows steep elevation rise towards the rim of the valley (ranging from 1279 to 2600 meters above sea level). The land cover of the basin consists mainly of urban area, cultivated land and forest cover constituting 19%, 59% and 22% of the total basin area respectively. Although several Himalayan peaks are observable from Kathmandu in days with clear skies, the valley itself has a non-snowed hydrology with all of the precipitation occurring as rain. The basin receives an average annual rainfall of about 1550 mm with high spatial variation. In year 2012, the annual precipitation ranged from 867 mm (KTM Airport) to 2077 mm (Sundarija). The valley rain climatology also exhibits heavy downpour during the

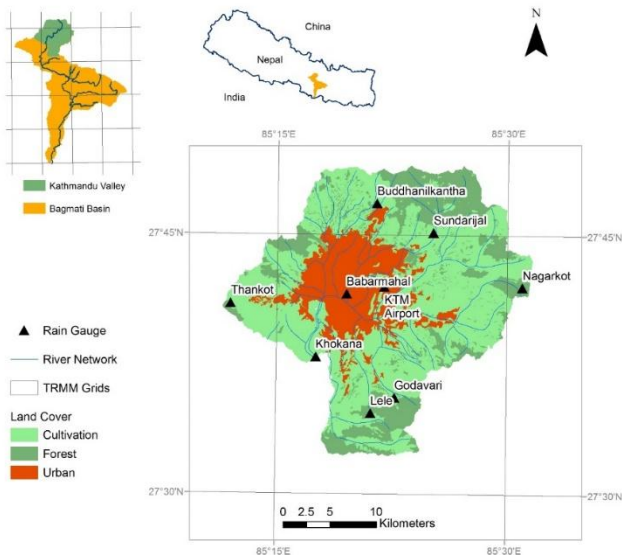


Fig. 2 Location Map of Kathmandu Valley

rainy season. In 2011 alone, 7 out of 9 rain gauge showed maximum hourly intensities greater than 40

mm/hr with values up to 52 mm/hr (19:00 – 20:00 hrs June 17, Khokana). The high intensity storm events and the spatial variation of rainfall thus makes the Kathmandu valley a good basin choice for storm-flood relation study as in present research case.

Rainfall datasets

Hourly (1-h) Gauged Rainfall, $R_{control}$

Fig. shows the hyetographs for storm event of 1 July 2011 for all the rainfall data sets used in this study. The hourly gauged rainfall data is the blue hyetograph and denoted by $R_{control}$ for simplicity. $R_{control}$ is considered as the actual rainfall and the performance of the remaining rain datasets are evaluated against it.

Daily Gauged Rainfall, R_{daily}

The main discussion of this paper is evaluation of alternatives in cases when hourly rain datasets are

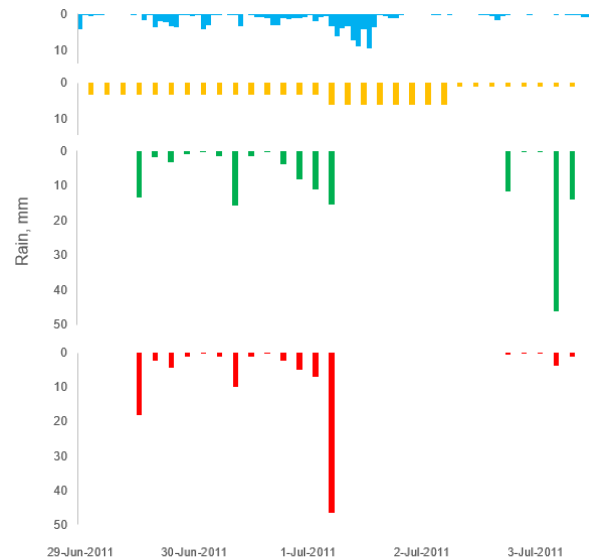


Fig.1 Observed hourly rain (blue, $R_{control}$) and other rainfall datasets evaluated in the study (yellow - R_{uni} , green - R_{sat} , red - R_{ds}). Values shown for the storm event of 1 July 2011

unavailable. In order to mimic that situation, $R_{control}$ is aggregated to 24-hour rainfall to get the daily gauged rainfall dataset (R_{daily}). R_{daily} is used to develop the two out of three rain dataset alternatives (discussed in following text) evaluated in this study.

Uniformly-downscaled daily gauged rainfall (3-h), R_{uni}

The first and the simplest of the sub-daily alternatives to $R_{control}$ is uniform temporal downscaling of R_{daily} at sub-daily intervals. Since the other two alternative rain datasets used in this study have 3 hourly (3-h) resolution, R_{daily} is downscaled uniformly at 3-h to get uniformly-downscaled daily gauged rainfall, R_{uni} (yellow hyetograph in Fig.).

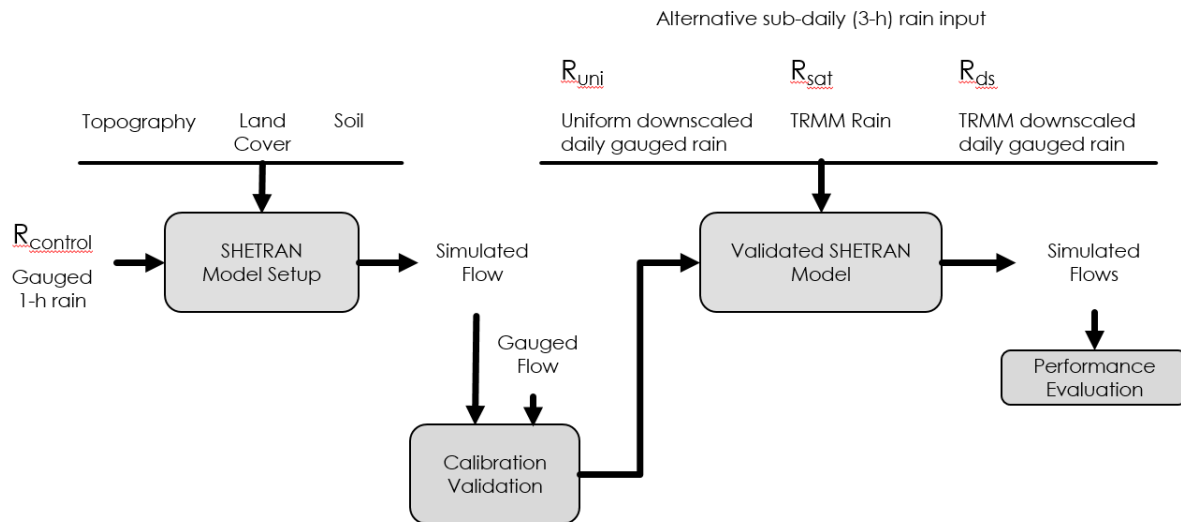


Fig. 3 Methodology framework

TRMM Rainfall Product, R_{sat}

The second and the remotely sensed sub-daily alternative to $R_{control}$ is the 3-h TRMM satellite observations denoted by R_{sat} in this study (green hyetograph in Figure 2). TRMM consists of satellite based observations of 4D distribution of rain and latent heat. The satellite data’s space domain covers major tropical areas of the Earth (350 N to 350S latitudes) while its time domain spans from the years 1998 till 2014. The project database offers a range of products out of which 3B42 level 3 product having spatial resolution of 0.250 and temporal resolution of 3-h was considered in this study.

rainfall volume same as the blue or the yellow hyetograph) but the sub-daily variation will comply with R_{sat} (the green hyetograph).

Distributed Hydrological Model – SHETRAN

SHETRAN is a physically-based, distributed, deterministic, integrated surface and subsurface modeling system, designed to simulate water flow, sediment transport, and contaminant transport at the catchment scale. It is designed to have the capability to predict the consequences of given changes in climate and land use (Ewen *et al.*, 2000). The water flow component of SHETRAN is an updated version of the Système Hydrologique Européen (SHE) (Abbott *et al.*, 1986). For technical details please refer document manuals (2013 a; 2013 b; SHETRAN, 2013 c).

TRMM-downscaled daily gauged rainfall (3-h), R_{ds}

The third and the hybrid sub-daily alternative to $R_{control}$ is the 3-h TRMM-downscaled daily rain datasets (R_{ds} – red hyetograph). R_{ds} is obtained by temporal downscaling of R_{daily} using R_{sat} i.e. R_{ds} has same 24-h cumulative volume as R_{daily} or R_{uni} or $R_{control}$ (i.e. daily

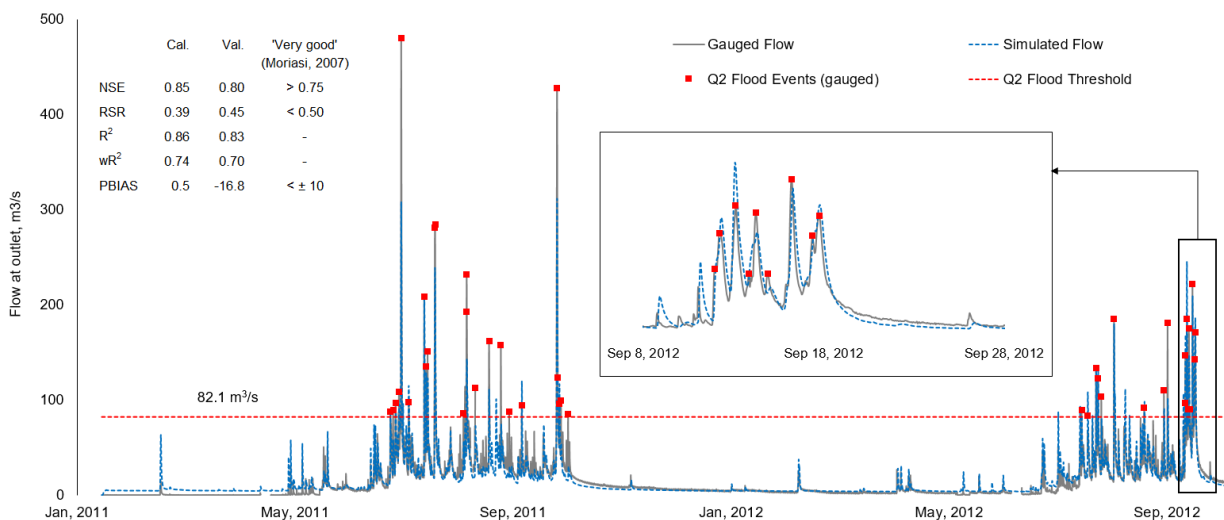


Fig. Hydrograph simulation performance for model calibration and validation using $R_{control}$ for year 2011 and 2012 respectively. Inset - the corresponding performance statistics

Methodology

Methodology Framework

The methodology framework followed in this study is presented in Fig. . The framework consists of two main components – 1) model calibration and validation, and 2) evaluating hydrological performance of alternative sub-daily datasets using the validated model.

Model Calibration and Validation

The hydrological response for the Kathmandu Valley catchment is calibrated using the hourly outlet flow time series for the year 2011 and then validated with the flow for the year 2012. Due to the hourly meteorological input requirement of SHETRAN and availability of only two years of data from the Flood Forecasting Project of DHM (establishment in 2011), one year each was used for calibration and validation of the model. The initial values of model parameters for calibration are taken from literature and SHETRAN manuals (SHETRAN, 2013 a). During calibration, the simulated discharge hydrograph at the outlet of the catchment is assessed using the Nash Sutcliffe Efficiency (NSE), RMSE-Standard Deviation Ratio (RSR), Coefficient of Determination (R^2), Weighted R^2 (wR^2) and percentage volume bias (PBIAS).

Performance Evaluation

The three alternatives of sub-daily rain datasets are evaluated for their meteorological performance (before forcing into the calibrated model) and hydrological performance. For the meteorological performance evaluation, the wet day frequency and statistical parameters including mean, standard deviation, correlation (r), and degree of agreement (d) are compared. For the hydrological performance of the corresponding rain forced models, the rain datasets are evaluated for the visual match of the hydrograph, evaluation statistics as mentioned in previous section, correlation to Q_2 flows, correlation to major flood events and their timing.

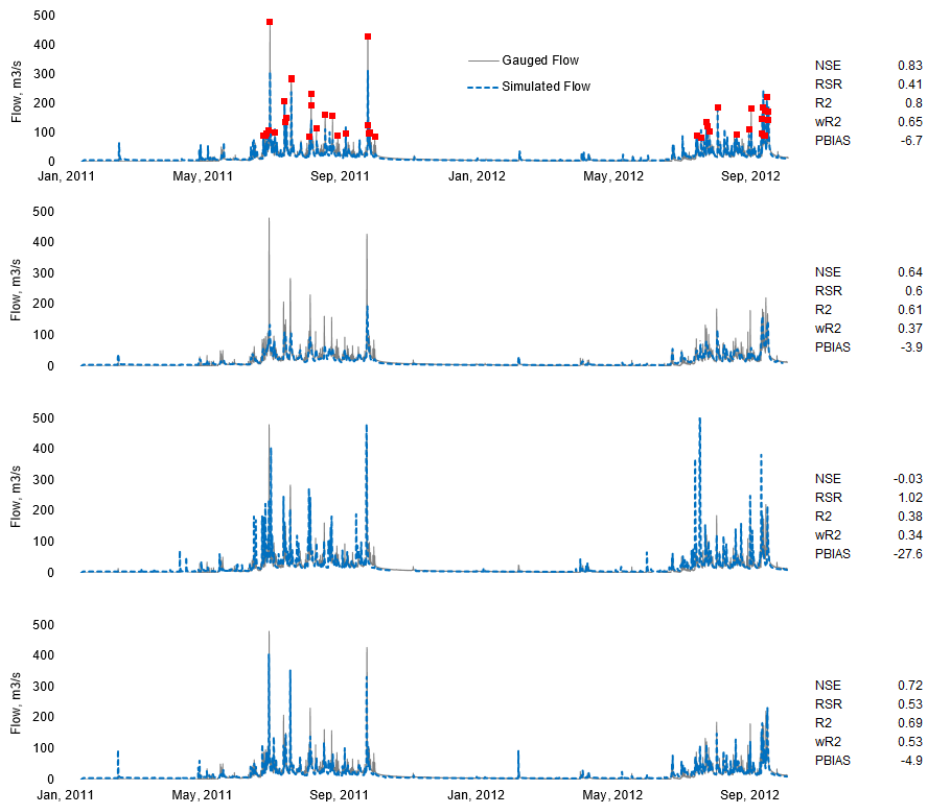


Fig. Hydrograph simulation and hourly performance statistics for $R_{control}$ (top) and its comparison with R_{uni} (2nd), R_{sat} (3rd) and R_{ds} (4th) for 2011-12 at the basin outlet

Results and discussion

Model Calibration

The model calibration and validation hydrograph is illustrated in Fig. 1. It is seen that the simulations (blue) are able to capture the gauged flow (grey) in both the periods. The corresponding hourly statistics of model simulation performance (Fig. 1 inset) also shows that the model is able to capture the peaks (very good NSE and RSR), pattern (very good R^2), and the volume (very good wR^2 , good PBIAS) of flow time series, even by daily scale standards. The mentioned benchmarks of statistics are taken from Moriasi *et al.* (2007).

Meteorological Evaluation of R_{uni} , R_{sat} , and R_{ds}

The evaluation made at the initial stages of R_{sat} dataset usage, before further processing, was to check the dry day/ wet day agreement with $R_{control}$. It was observed that R_{sat} had good agreement with $R_{control}$. The two datasets agree 79% of the time which was a good correlation to initiate work on testing applicability of TRMM in hydrology. After development of R_{ds} its performance improvement was compared with R_{sat} . It was seen that the large mean bias error and volume underestimation present in R_{sat} was eliminated (by definition of R_{ds}) while the sub-daily correlation coefficient and degree of agreement also improved after downscaling.

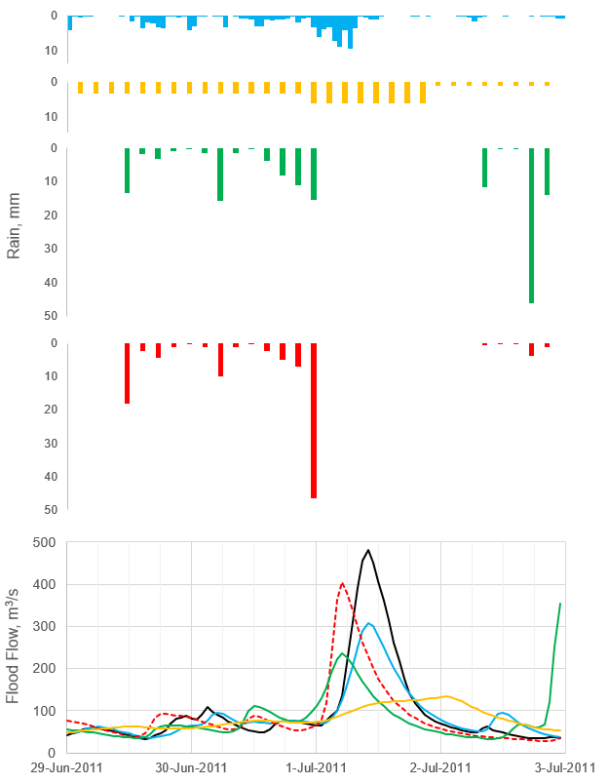


Fig. Comparison of the flood event of 1 July, 2011 simulated by $R_{control}$ (blue), R_{uni} (yellow), R_{sat} (green) and R_{ds} (red) against the gauged flow (black). The corresponding storm hyetographs are also depicted in their respective colors.

Hydrological Evaluation of R_{uni} , R_{sat} , and R_{ds}

The three alternative sub-daily rain datasets were individually forced in to the validated model of the Kathmandu Valley for the whole two-year period from

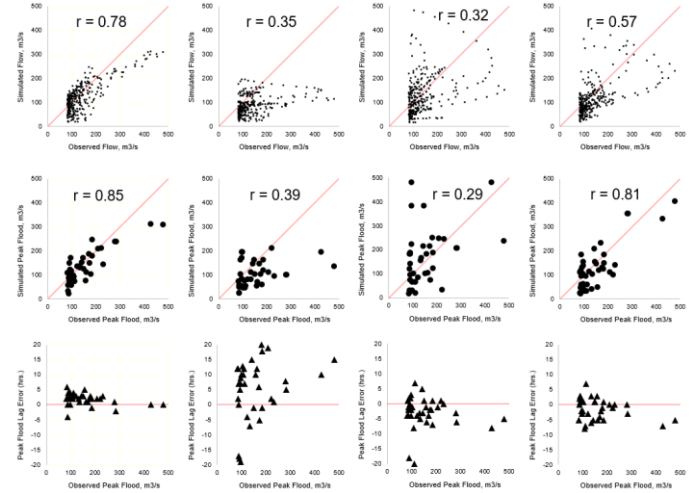


Fig. *top row* – Correlation of Q_2 flows between gauged flow and $R_{control}$ (1st column), R_{uni} (2nd column), R_{sat} (3rd column) and R_{ds} (4th column). *middle row* – Correlation of forty flood peaks of Q_2 flows between gauged and simulated flows without considering timing error. *bottom row* – Flood peak timing error in simulating Q_2 flood peaks.

2011 to 2012. The results (Fig. 2) show that out of the three options, R_{ds} is the best alternative in absence of $R_{control}$ with best values for all statistics except for PBIAS for which R_{uni} performed slightly better. The visual fit of the hydrograph also shows that model forced with R_{ds} would give the best hydrological fit. It can also be noted from Fig. 2 that the peak floods simulated by R_{ds} match quite well with gauged flow and in some cases even better than $R_{control}$. After R_{ds} , its R_{uni} which performs the second best in terms of hydrological simulation and the corresponding statistics.

Flood Simulation Performance

The major objective of this study was to check the applicability and value of R_{ds} on flood events. Flood events exhibit sub-daily characteristics in terms of magnitude and timing. Whereas TRMM downscaled R_{ds} also possess the diurnal variability of d_{sat} which could prove useful for flood magnitude and timing related analysis.

Individual analyses of biggest flood events (one example is Fig. 4) at the basin outlet and their simulation by $R_{control}$, R_{uni} , R_{sat} and R_{ds} shows that, in terms of magnitude, R_{ds} is able to simulate the magnitude of the flood and as good as $R_{control}$. R_{uni} on the other hand is not able to generate comparable flood peaks. This is understandably due to lack of sub-daily variation in the input storm estimation which allowed the rain water to percolate rather than forming the direct runoff hydrograph. R_{sat} on the other hand showed better performance than R_{uni} with peaks agreeing with $R_{control}$.

However, R_{sat} was also accompanied by several spurious peaks due to bias in intensity and/or timing. In case of the example shown in Fig.4 one of such spurious peak appears at the end of 2nd July 2011.

The correlation of Q_2 (refer Fig.3) i.e. flow magnitude exceeded only 2% of the time (in this case 82.1 m³/s as depicted in Fig.1), between the gauged flow and the simulated flow shows R_{ds} to perform better than R_{uni} and R_{sat} . However, this value is much lower compared to performance of $R_{control}$ (0.78) which is to be attributed to the timing error of the flood peak. Q_2 flows consisted of 40 flood events (refer Fig.1 and Fig.3). The simulated magnitudes of the peak of these forty flood events were analyzed and found that R_{ds} (r 0.84) could perform on par with $R_{control}$ (r 0.88) for magnitude only analysis (without timing consideration).

The same correlation analysis also shows that R_{uni} (r 0.39) to be better than R_{sat} (r 0.29) in terms of correlation of peaks without timing consideration. However, the peak timing error for these two clearly shows that in fact it is R_{sat} which is the better option for flood simulations out of the two due to better peak timing accuracy (this point is referable in Fig.4 as well).

Summary and conclusions

Using a robust distributed hydrological flood simulation model of the Kathmandu Valley, this study concludes that out of the three alternatives to measured sub-daily rain datasets, R_{ds} ranks first in terms of hydrological as well as flood simulation performance. R_{sat} performed quite poorly in hydrological simulation performance (general hydrograph) due to bias in intensity and/or occurrence of rain events in the region. However, in terms of flood event analysis it turned out to be the second best rain input alternative after R_{ds} . The third approach, R_{uni} , is also a doable approach for achieving moderate hydrological performance but may not be up to the mark for flood magnitude and/ or timing analysis. The major finding of this study is that when it comes to flood simulation and analysis, R_{ds} performs on par with $R_{control}$ for simulating the flood magnitudes. This results could be applied to in future for flood peak magnitude related studies such as return period analysis under future scenarios. However, it was also noted that, at least for this case study, the use of R_{ds} was accompanied by slight flood peak mistiming. One of the major area to track and work on to find a solution for this issue could be the sensing mechanism of the TRMM satellite and probable time errors incurred.

Acknowledgement

The authors are thankful to the Flood Forecasting Project under Department of Hydrology and

Meteorology of Nepal for providing us the hourly hydrometeorology data. We would also like to thank Rocky Talchabhadel and Vishnu Prasad Panday for their assistance in data access.

References

- Abbott, M. B., Bathrust, J. C., Cunge, J. A., O'Connell, P. E., and Rasmussen, J. (1986), An introduction to the European Hydrological System - Systeme Hydrologique Europeen, 'SHE', Journal of Hydrology (87), 61-77.
- Ewen, J., Parkin, G., and O'Connell, P. E. (2000), SHETRAN: Distributed River Basin Flow and Transport Modelling System, Journal of Hydrologic Engineering, 5, 250-258.
- Feddes, R. A., Kowalik, P., Neuman, S. P., and Bresler, E. (1976), Finite difference and finite element simulation of field water uptake by plants, Hydrological Science Bulletin (21), pp. 81 - 98.
- IDC. (2009), Study on the status of groundwater extraction in the Kathmandu Valley and its potential impacts, Final Report, Groundwater Resources Development Board (GWRDB).
- KUKL. (2011), Kathmandu Khanepani Upatyaka Limited (KUKL) at a glance, Third Anniversary report, Kathmandu.
- Monteith, J. L. (1965), Evaporation and environment. The state and movement of water in living organisms, Proceeding of 15th symposium, Society of Experimental Biology, pp. 205 - 234. Swansea.
- Moriasi, D. N., Arnold, J. G., Van Liew, M. W., Bingner, R. L., Harmel, R. D., Veith, T. L. (2007). Model evaluation guidelines for systematic quantification of accuracy in watershed simulations. Transactions of the ASABE, 50: 885-900.
- Pandey, V. P., Shrestha, S. and Kazama, F. (2012), Groundwater in the Kathmandu Valley: Development dynamics, consequences and prospects for sustainable management, European Water, 37: 3 - 14.
- Rutter, A. J., Kershaw, K. A., Robins, P. C., & Morton, A. J. (1971/72), A predictive model of rainfall interception in forests, Agricultural Meteorology, 9, 367 - 384.
- SHETRAN. (2013 a), Data Requirements, Data Processing and Parameter Values.
- SHETRAN. (2013 b), SHETRAN water flow component equations and algorithms. School of Civil Engineering and Geosciences, Newcastle University.
- SHETRAN. (2013 c), SHETRAN Standard Version - V 4.4.1: User Guide and Data Input Manual.

A Case Study on Industrial Mismanagement of Tanneries in Hazaribagh: Water Pollution and Chromium Poisoning in Dhaka, Bangladesh

Nilay Kumar Sarker

Abstract Tanneries of Hazaribagh produce large amount of liquid and solid wastes. Nature of liquid waste shows it is highly polluted; BOD (Biological Oxygen Demand) - 1823 ppm, COD (Chemical Oxygen Demand)- 3662 ppm, TDS (Total Dissolved Oxygen)- 16358 ppm, DO (Dissolved Oxygen)- 0.0, pH - 4.05, Cr - 987 ppm. Liquid waste is disposed to Buriganga river without any treatment. Solid wastes are comprised of raw trimmings, salt, hair, lime and unhairing sludge, fleshing, splits/trimming and processed skin waste. Workers of these tanneries are not paid well, they work in an unsafe and unhealthy environment, child labor and gender discrimination is a common scene. Workers suffer from various diseases due to pollution caused by tanneries. From fleshing and chromium contaminated trimmings Shutki is produced, it is used for chicken and fish feed and through chicken and fish chromium poisoning occurs to human body. Burning of processed skin waste is responsible for chromium poisoning via air.

Keywords *Hazaribagh, Tannery, Waste, Shutki, Chromium poisoning, Water pollution*

Nilay Kumar Sarker
Energy Field of Study
School of Environment, Resources and Development (SERD), Asian Institute of Technology (AIT)
Pathumthani, Thailand

Introduction

Tannery is one of the oldest industrial sectors in Bangladesh. Every year Bangladesh earns a lot of foreign currency by exporting leather and leather goods. The export quality leathers are the product of tanneries. Raw materials of export quality leather goods also come from tanneries. Growth of tannery sector took place in Bangladesh centering two areas - Hazaribagh of Dhaka city and Kalurghat of Chittagong city. In terms of financial returns and social benefits, leather sector is a potentially rich manufacturing sector. Bangladesh earned 402 million US dollar in 2009 - 2010 from this sector [1]. Leather sector has a significant contribution in national GDP of Bangladesh, contribution to total GDP was 0.47% in 2006 - 07, 0.33% in 2007 - 08, 0.19% in 2008 - 09, 0.20% in 2009 - 10 [1]. About 741000 people are employed directly and indirectly in leather and its sub-sectors [1].

In Hazaribagh there are around 400 tanneries, about 95% of total number of tanneries in Bangladesh [1]. Hazaribagh is situated at the south-east part of Dhaka city. In tannery, cattle skins and hides are transformed into leather through tanning process, a good number of chemicals are needed to complete this transformation process and it produces heavily polluted, colored and foul smelling waste water and also solid wastes like trimmings, hair, fleshing etc. Transformation of every kilogram of raw hides to processed leather causes generation of 30 liters of waste water [2]. Everyday tanneries of Hazaribagh collectively dump 77000 m³ untreated waste water into Buriganga river and also produce 88 metric tons of solid wastes [3].

Objective

Mismanagement means that is careless and/or inefficient. Some examples of industrial mismanagement in tannery sector in Bangladesh are handling liquid waste water and solid waste in improper way, employment of child labor, paying salary to the workers irregularly etc. Tanneries in Bangladesh release uncontrolled liquid and solid wastes. Hazaribagh is the place where maximum number of tanneries are located. So, pollution in and around of Hazaribagh is beyond imagination. Additionally, chromium poisoning is spreading in Dhaka city due to solid wastes, which is

a direct consequence of industrial mismanagement of these tanneries. Moreover, industrial mismanagement is also responsible for sufferings and risks to the workers of these tanneries. Main purpose of this article is to highlight on these factors.

Description and History of Tannery Industry in Hazaribagh

The urban area of Dhaka is surrounded by Turag river, Buriganga river and Dhaleshwari river in the west and north west, Balu river and Lakhya river in the east and Turag river in the north connecting river Balu and Turag [1]. Buriganga river is the most used waterway to Dhaka. Most of the drinking water of Dhaka urban area is also supplied by Buriganga river. It was once the main source of fish of Dhaka city. Hazaribagh is situated on the south-west part of the Dhaka city. The Buriganga river is flowing on the western side of Hazaribagh. Total households of this area are more than 25900 units and total population is more than 127000 [3]. Tannery industrialization started in this area in 1940-50s. Owners of the "Noor Vai Tannery Ltd." from India established a Tannery in Hazaribagh in 1947. It was the first tannery in this area. It used vegetable tanning process. Numbers of tanneries started increasing at the end of 1960s. In 1965, there were 30 tanneries in Hazaribagh. Most of them were established by west Pakistani businessmen. Bangladesh achieved liberation in 1971 from Pakistan and in 1972 all tanneries of this area nationalized. The government formed "Bangladesh Tanneries Corporation" (BTC) with 24 tanneries in 1972. Then these tanneries started facing management crisis. So, these tanneries were brought under "Bangladesh Chemical Industries Corporation" (BCIC). But problems were not solved and tanneries failed to make profit. At last, government returned the tanneries to the private owners. In Hazaribagh number of tanneries was around 250 in the late 1990s and around 400 in 2010 [3].

Data Collection

To perform this study data was mainly collected through direct interviews and survey. Some data and information was collected from related journals and publications. To measure the composition of liquid and liquid waste from tanneries experiments were performed in laboratory.

Experiment

Waste water: Waste water is collected from several tanneries. Then BOD, COD, TDS, DO and pH are measured for each sample and then mathematical average is calculated. Composition of pollutants of tannery waste water is shown in Table-1. For measurement of BOD a mixture of solution is prepared with 0.3 ml of Phosphate buffer solution, 0.3 ml of CaCl_2 solution, 0.3 ml of MgSO_4 solution, 0.3 ml of FeCl_3 solution and 0.3 ml of seed water. Then 300 ml of sample is mixed with this solution mixture and aerated

for 20-25 minutes. After completion of aeration, DO is measured of this solution with Hach DO meter, this is the DO of day-1. Then this solution is kept at 20°C for 5 days and then again DO is measured. This is the DO for day-5. Difference of DO between day-5 and day-1 is BOD of this sample. For measurement of COD, a solution mixture is prepared with 4 ml of digest solution, 3 ml of reagent and 2 ml of deionized water (this is called blank solution) and another solution mixture is prepared with 4 ml of digest solution, 3 ml of reagent and 2 ml of sample. Then these two solutions are heated at 150°C for 2 hours. Then using Hach COD meter, COD of this sample is measured. DO, TDS and pH is measured directly by Hach DO meter, Hach TDS meter and Denver pH meter.

Solid waste: Solid wastes are collected from several waste dumping points of Hazaribagh. Then mass composition of each component is measured for each waste dumping point. Finally average mass composition is measured mathematically. Average composition of tannery solid waste is shown in Table-2.

Reagent preparation

To prepare Phosphate buffer solution 8.5 gm KH_2PO_4 , 21.75 gm K_2HPO_4 , 33.4 gm $\text{Na}_2\text{HPO}_4 \cdot 7\text{H}_2\text{O}$ and 1.7 gm NH_4Cl are dissolved in 500 ml deionized water and then diluted to 1000 ml. pH of this solution reaches to 7.2. To prepare MgSO_4 solution 22.5 gm $\text{MgSO}_4 \cdot 7\text{H}_2\text{O}$ is dissolved in 1 litre deionized water. For preparation of CaCl_2 solution 27.5 gm CaCl_2 is dissolved in 1000 ml deionized water. To prepare FeCl_3 solution 0.25 gm $\text{FeCl}_3 \cdot 6\text{H}_2\text{O}$ is dissolved in 1 litre deionized water. Source of seed water is sewerage water of Berger Paint Ltd. Bangladesh and rotten foods.

Tannery wastes

Two types of waste are emitted from tanneries - 1. Liquid waste and 2. Solid waste. Liquid waste contains unacceptable amount of BOD, COD, DO, TDS, TSS (Total Suspended Solid), pH, Cr, color, odor, chloride, sulfide, phenol compounds, oil and grease etc. Solid waste contains trimmings, hair, fleshing, salt, lime, unhairing sludge etc.

About all liquid waste is directly disposed to Buriganga river. Among solid wastes trimmings (locally it is called "Shaving Waste") and fleshing are used as raw materials of producing "Shutki", which is used to make a component of poultry and fish feed. After being processed, skin is sized and cut to make bags, shoes, sandals, belts, jackets and other leather products. This produces huge amount of processed skin wastes. This waste burns easily and is sold in market as fuel at a cheaper rate. Other solid wastes are dumped randomly here and there.

Table-1: Composition of pollutants of tannery waste water

	Tannery waste water	Department of Environment Standards [4]
BOD	1823 ppm	50 ppm (inland surface), 250 ppm (irrigated land)
COD	3662 ppm	200 ppm (inland surface), 400 ppm (irrigated land)
TDS	16358 ppm	2100 ppm
DO	0.0	4.5-8 ppm
pH	4.05	6-9
Cr	10.009 ppm [4]	0.5 ppm

Table-2: Composition of tannery solid waste

Name of the components	Composition % (mass)
Raw Trimmings	25
Salt	8
Hair	3
Lime and unhairing sludge	12
Fleshing	18
Splits/trimming	16
Processed skin waste	18

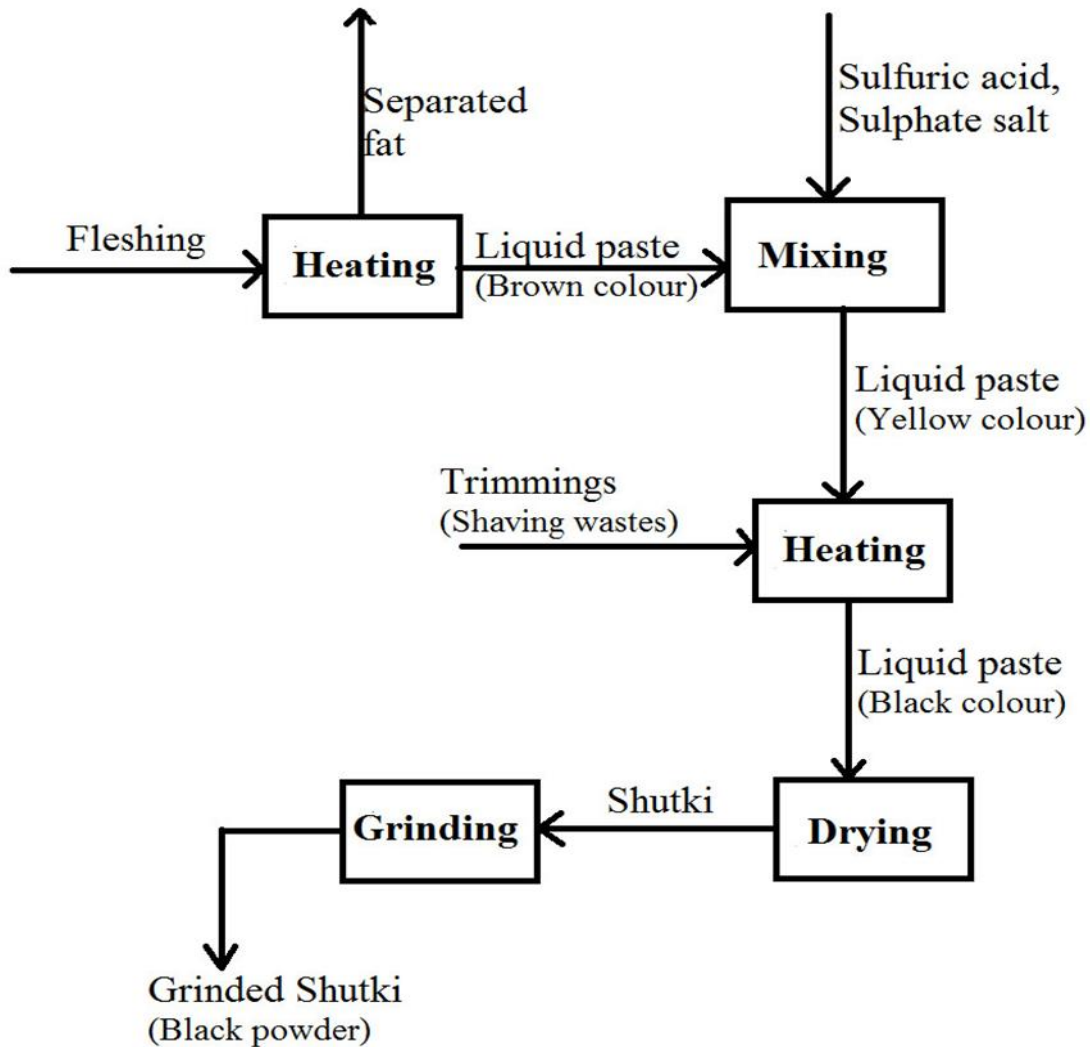


Figure-1: Process flow diagram of Shutki production

Shutki production

Shutki producers buy fleshing and trimmings from tanneries. At first, fleshing is heated at high temperature, so that fat is separated and rest portion is converted into brown color paste. Then sulfuric acid and sulphate salt are mixed with this brown paste, this results a liquid of yellow color. After that trimmings/shaving wastes are mixed with this yellow liquid and they are heated again. Finally, it turns into black colored paste. This black paste is dried for several days and then sold to grinding mills. Then it becomes reddish black powder. After being grinded, this reddish black powder is bought by dealers and they sell it to the feed markets as “Meat and Bone meal”. Main reason to use Shutki as meat and bone meal is, it is cheaper. Previously meat and bone meal was imported. Ten years ago price of imported meat and bone meal was 9 - 10 taka per kg. Now its price is 40 - 45 taka per kg while price of meat and bone meal from Shutki is 16 - 20 taka per kg. Figure-1 shows the process flow diagram of Shutki production.



Figure-2: Grinded Shutki

Mechanism of chromium poisoning from tanneries to human body

Main reason of chromium contamination to human body is poultry, layer and fish feed. In Bangladesh, two types poultry and layer feeds are available - 1. ready-feed and 2. hand-made feed. To prepare hand-made feed, farmers buy components from market, then mix them and finally feed to the poultry and layer. Ready-feed is directly fed and it does not need any mixing process. Most of the ready-feeds are produced by industries, some ready-feeds are imported and they are more expensive than hand-made feeds. In Dhaka city and its surrounding areas more than half of the farmers feed their poultry and layer hand-made feeds. About all fish feeds fed by farmers are hand-made feeds. Table-3 shows name and amount of the components of broiler feed, layer feed and fish feed for 100 kg feed. This data was collected from the chicken and fish feed sellers of Nimtole Market, it is located near ChankharPul, Lalbag of Dhaka. Before chromium poisoning in human body chromium contamination occurs in cattle hides in tanneries for chromium tanning. Shaving wastes or trimmings, one type of solid waste of tanneries are produced from these contaminated hides are used for Shutki production and this Shutki is one of the important components of “Meat and bone meal”. Table-3 shows that meat and bone meal is used for preparation of Poultry feed, Layer feed and Fish feed at a significant percentage. Thus Poultry and Layer chickens, eggs and fishes produced in farm become poisoned with chromium. These are most common and popular protein source for the people of Dhaka city and its surrounding

small towns and villages. Human body can get poisoned with chromium by consuming these foods and this poisoning can cause cancer or other diseases related to liver and kidney [8]. Presence of chromium in chickens that consume feed manufactured with tannery waste is 249 microgram (mg) to 4,561mg per kg [9], for human beings, tolerance level is only 0.5-2 mg [8]. Figure-3 shows the flow chart of the process of chromium poisoning from tanneries to human body.

Condition of the Tannery Workers

About 20000-22000 workers are employed in Hazaribagh tanneries. More than 25% of these workers are children and about 15-20% workers are women. Wage of workers vary from tannery to tannery. Maximum wage for a worker in Hazaribagh tannery does not exceed 360 dollar (27000-28000 taka) though usual work time is 10-11 hours, sometimes workers have to work 14-15 hours. Many adult workers of Hazaribagh started working in tanneries when they were only 11 or 12 years old. Children workers of 11-14 years old earn wage 40-55 dollar (3000-4000 taka) per month, though they have to work full time (10-11 hours) like adult workers. Women workers face same type situation. They get paid not more than 60-65% of a male worker, although they do not work less than a male worker. For some tannery owners, children and women are cheaper labor source and they even do not complain much if they are not paid regularly. Another tragic event is, workers have no safety in work places. Many workers have to handle machines without enough technical

knowledge and training, this causes sometimes limb amputations, many workers have to handle hazardous chemicals with very little or no safety, this causes skin diseases, respiratory problems, fever often to the workers. These tannery authorities do not provide proper training and do not supply sufficient protective equipment, rather they compel workers to work with hazardous chemicals and aging, low efficient machinery in this risky working environment. Tannery authorities do not allow sick leave often and not giving any compensation to the workers who get injured during work is very common scene here. At least 90% of the Hazaribagh tannery workers die before age of 50 due severe unhealthy environment of working-place, 58.10 % of workers suffer from ulcer, 31.28 % have skin diseases, 16.76 % suffer from malnutrition, 11.73 % have high blood pressure and 10.61 % suffer from rheumatic fever [3]. They also suffer from dizziness, headache, weakness, eye problems, abdominal pain, nausea, diarrhea, allergy, burning sensation in the chest, throat, palm and toes, urinary problems and pain in the body, waist, legs, back, throat, neck, shoulder and ankles [3].

Health problems of the Hazaribagh dwellers

Tanneries cause direct pollution to land and water. This pollution causes health problems to the Hazaribagh inhabitants. Many people suffer from diarrhea and fevers often. A lot of people have respiratory problems. People living near Buriganga river suffer from skin

diseases. Another dangerous health problem is chromium poisoning via air. Dry processed skin waste is a popular fuel for cooking and other activities, because it is cheap and burns well. As processed skin contains chromium, when this waste is burnt green smoke is produced. Many housewives and female members of the families who use processed skin waste as fuel for cooking suffer from asthma and digestive problems. The reason of green color is presence of chromium. Chromium poisoning is also caused through chicken and fish feed and it affects the whole Dhaka city and its surrounding areas. Chromium is contaminated to chicken and fish feed through Shutki.

Conclusion

Hazaribagh is an over populated area of 20 hectares of land. In this 20 hectare area there are about 400 tanneries. Industrial mis management has made this area quite unsuitable to live. Intolerable bad smell is everywhere. Physical look of this area is not pleasant at all. Water of Buriganga river is not suitable to use for any single purpose and main reason is these tanneries. These tanneries are also the root of chromium poisoning in Dhaka city and its surrounding areas. Both workers and dwellers in these area undergo several health problems. According to Bhowmik and Islam 2009 et al., government has approved a plan for relocation of tanneries of Hazaribagh to the Hemayetpur area of Savar

Table-3: Amount of the components of broiler, layer and fish feed for 100 kg feed

Broiler feed		Layer feed		Fish feed	
Component	Amount	Component	Amount	Component	Amount
Rice bran	5 kg	Rice bran	12 kg	Rice bran	30 kg
Pea	60 kg	Pea	50 kg	Maize	10 kg
Soybean meal	20 kg	Soybean meal	22 kg	Soybean meal	20 kg
Protein	5 kg	Protein	5 kg	Mustard oil cake	15 kg
Meat and Bone meal	10 kg	Meat and Bone meal	3 kg	Meat and Bone meal	15 kg
		Pearl Grinding	8 kg	Fish meal	10 kg
Total	100 kg	Total	100 kg	Total	100 kg

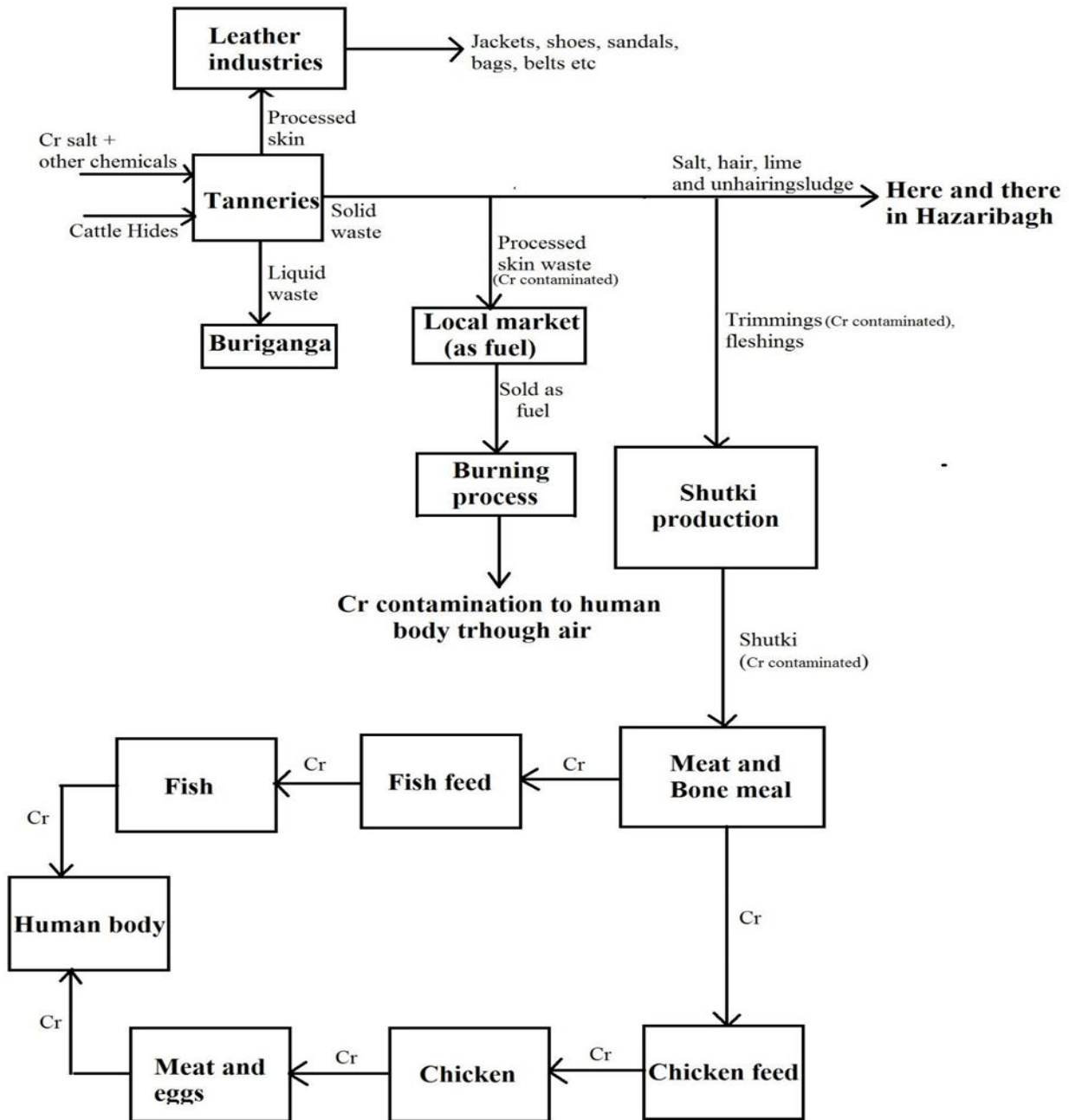


Figure-3: Process flow diagram of chromium poisoning from tanneries to human body

But there was no suggestion to revive the polluted land of Hazaribagh with highly toxic wastes. Rather relocation can cause creation of another brown field in Hemayetpur due to processing mismanagement and waste disposal without any treatment. Still no plan has been made yet to stop chromium poisoning. According to the government officials, the mills involved with Shutki production are not registered or do not take permission from any legal authority, so operation of this mills is illegal. Sometimes police shut down one or two mills and arrest some people but these mills again start operation within one or two weeks and police let go the arrested people and this happens for political influence. Without proper attention of government, definite

planning of concerned authority and effective activity of law enforcement agencies, chromium poisoning problem will not be solved.

References

[1] Biswas, B. and Hamada, T. (2012). Relation between Hazaribagh Tannery Industry Development and Buriganga River Pollution in Bangladesh. International Journal of Environment, 2(2): 117– 127.

- [2] MIDHA, V. and DEY, A. (2008).
BIOLOGICAL TREATMENT OF TANNERY
WASTEWATER FOR SULFIDE REMOVAL.
International Journal of Chemical Science: 6(2), 472-
486.
- [3] Bhowmik, A. K. and Islam, M. S. (2009).
Environmental Concerns regarding Hazaribagh Tannery
area and Present Relocation Scenario. Nagar Shoilee 4.
- [4] Rouf, M.A., Islam, M.A., Haq, M.Z., Ahmed,
N. and Rabeya. T. (2013). Characterization of effluents
of leather industries in Hazaribagh area of Dhaka city.
Bangladesh J. Sci. Ind. Res. 48(3), 155-166.
- [5] Baruthio, F (1992). Toxic Effects of Chromium
and its Compounds; Biol. Trace Elem. Res., 32:145-153.
- [6] Hossain, M.A. and Hassan, Z (2014). Excess
Amount of Chromium Transport From Tannery to
Human Body Through Poultry Feed in Bangladesh and
its Carcinogenic Effects. International Journal of Civil,
Structural, Environmental and Infrastructure
Engineering Research and Development. 4(4): 1-10.
- [7] Hossain, A.M.M.M., Islam, M.S., Rahman,
M.M., Mamun, M.M., Kazi, M.A.I. and Elahi, S.F.
(2009). Assessment of Tannery Based Chromium Eco-
toxicity through Investigating Regional Bio-
concentration in Commercially Produced Chicken Eggs
and Their Physical Properties. Bangladesh J. Sci. Ind.
Res. 44(1), 11-30.
- [8] Abedin, M.J., Akter, S and Arafin, S.A.K.
(2015). Chromium Toxicity in Soil Around Tannery
Area, Hazaribagh, Dhaka, Bangladesh and its Impacts
on Environment as well as Human Health. International
Journal of Innovative Research in Advanced
Engineering. 2(4): 119-122.
- [9] Hossain, A.M.M.M., Monir, T. Rezwan-Ul-
Haque, A.M., Kazi, M.A.I., Islam, M.S. and Elahi, S.F.
(2007). Heavy Metal Concentration in Tannery Solid
Wastes Used as Poultry Feed and the Ecotoxicological
Consequences. Bangladesh J. Sci. Ind. Res., 42(4): 397-
416.

Quantifying climate change impact on rice production in Northeast of Thailand: a critical review through water footprint concept

Miss. Ranju Chapagain

Abstract Climate change impact on rice yield and its corresponding water footprint was investigated for a case study in Northeast of Thailand. CERES-Rice crop growth model was used to simulate rice production which was set up and validated using yield data during 2009-2013. Three different rice varieties (KDML 105, RD 6 and ChaiNat-1) were considered in the study. The present water footprint (green, blue and grey) of rice, defined as amount of water evaporated during growing period of rice, was then calculated for irrigation area. To quantify potential impact of climate change on rice production in future, climate scenarios from three were downscaled and bias corrected for Nam Oon Basin and then supplied to CERES-Rice model. The future reference time was divided into three time slices; early future (2020s), mid future (2050s) and far future (2080s) and studied. At all-time slices, yield decreased for KDML 105 and RD6, resulting in increased water footprint potential future scenarios of decreasing precipitation and increasing temperature. This may be due to increased evapotranspiration, higher irrigation demand and lower final yield. On contrary, crop yield increased resulting in decreased water footprint for ChaiNat-1 under increasing summer temperature and decreasing precipitation for all periods. Since, ChaiNat-1 is a drought resistant variety, thus it could bear the harsh effect of in temperature increase resulting in higher water productivity. The study also showed blue footprint will be very large as compared to green and grey water footprint; huge amount of irrigation water will be needed to meet the evaporation demand in future. The results obtained from study highlights need for proper adaptation strategies to reduce or maintain acceptable water footprint under future climate.

Keywords *Climate Change, Food Security, Rice Production, Water Footprint*

Miss. Ranju Chapagain

Asian Institute of Technology/ Water Engineering
Department/ Water Engineering and Management,
AIT

Introduction

Agriculture sector is the major withdrawer of the freshwater resource. It is anticipated that by 2025, water use in agriculture sector is expected to increase by 19% (WWAP, 2012). Climate change mostly revolves around water and is most likely to give rise to water crisis in future. Therefore, water management strategies and policies is a must to meet the rapidly growing food demand.

Rice is the staple food of Thailand and is also one of the top exported goods from Thailand. About 10.5% is contributed to the total Thai GDP from agriculture sector (World Bank, 2014). As compared to other crops, rice is the most water intensive using 2-3 times more water. The north-east region is mostly rainfed; 85 % of land is rainfed paddy area during the wet season and 15 % is irrigated paddy field. It is estimated that Northeastern Thailand produces approximately 80% of all jasmine fragrant rice (Thanawong et al., 2014). However, this region has been hit by severe drought in the recent years reducing its annual rice production. The rapid demand of energy crops also adds increment to water stress. Therefore, for proper planning of water resources, information related to water required by crops and water availability is vital.

The water footprint (WF) is referred as volume of water used to produce a good (Hoekstra, 2003; Hoekstra & Chapagain, 2004). Green water footprint (amount of rain water evaporated to produce a crop), blue (amount of surface water evaporated to produce a crop) and grey (water to dilute pollutants) water footprints are the three components of water footprint (Hoekstra et al (2011)). There have been few researches that have considered water footprint of maize and energy crops cassava and sugarcane for Thailand (Kaenchan & Gheewala, 2012; Kongboon & Sampattagul, 2012; Nilsalab et al (2012); Sukumalchart et al (2011)). Therefore, the main objective of this paper is to assess climate change

impact on water footprint of rice in Northeast region of Thailand.

Material and Methods

Study Area

Among the various large scale irrigation projects in the Northeast of Thailand, Nam Oon River Project is also one which diverts water from Nam Oon river (Figure 1). Nam Oon river is one of the tributary of Nam Songkram river. The main purpose of Nam Oon Irrigation Project is to help in increment of agricultural productivity and as well as increase social security. The project area is 32,480 ha and irrigation area in wet and dry seasons are 29, 728 ha and 16,000 ha respectively

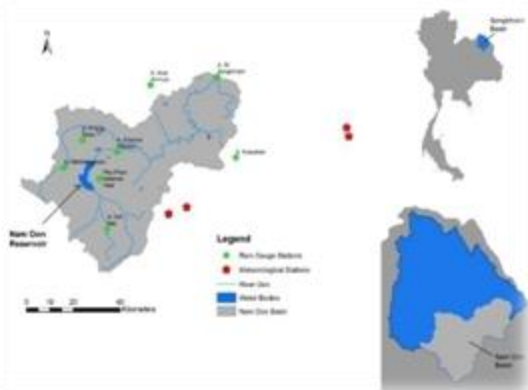


Figure 1: Location map of Nam Oon river basin (Northeast of Thailand)

The region where Nam Oon Irrigation Project is located has tropical climate. The maximum temperature ranges 28.5oC to 35 oC and minimum temperature ranges from 14.73 oC to 25.08 oC. The annual average precipitation is about 1400mm. The crops are mostly grown in wet season (June-October) as about 85% of total rainfall occurs in this season. Soil texture comprises of silty clay and has problem of alkalinity and salinity.

There are two main cropping season. In the first rice season (also known as wet rice), famous, common rice varieties of this region are KDML 105 and RD6. Since, rice can be harvested in around 120 days, there is second growing season (also known as dry season) which starts in January and ends in May. Due to the recent drought, these regions have been facing, ChaiNat-1 have been started to be preferred in the dry season.

Methodological Flowchart

Bias, from outcomes of two regional concentration pathways scenarios RCP 4.5 and RCP 8.5, of three RCMs were removed using quantile mapping method to project future precipitation, maximum and minimum temperature of the study area. The future time was divided into 2020s, 2050s and 2080s. The

climate of these periods was compared against baseline of 1976-2005. The bias-corrected variables were then fed into calibrated DSSAT (CERES-rice) model (Hoogenboom et al., 2003, Hoogenboom et al., 2015) to simulate future rice yield and water footprint for all time slices (Figure 2).

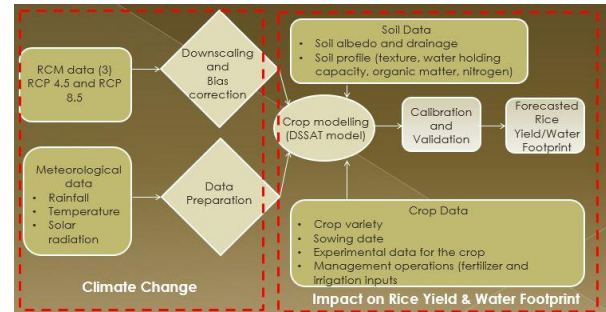


Figure 2: Research methodology used in the study

Results and Discussion

In this section, projected future rice yield and impact of climate change on water footprint will be analyzed.

Climate Change Impact on Rice Yield

DSSAT model is calibrated for three rice varieties (KDML 105, RD6 and ChaiNat-1) from 2009-2013 and validated using field data of 2014. The outcomes of our simulation reveal that rice yield is going to decrease significantly under potential climate change for KDML 105 and RD6. The decrease for KDML 105 is 32.94%, 35.31% and 37.22% for RCP 4.5 and 34.72%, 36.92% and 38.23% for RCP 8.5. The rice variety RD6 also faces decrease of 10.72%, 11.62% and 12.79% for RCP 4.5 and 11.39%, 12.70% and 17.55% for RCP 8.5. However, for ChaiNat-1, simulation results showed increase by almost 50% as compared to baseline i.e. 78.46%, 75.86% and 73.36% for RCP 4.5 and 76.05%, 72.02% and 59.35% for RCP 8.5. Since, ChaiNat-1 is a drought resistant variety, therefore using ChaiNat-1 will increase the rice yield. Our results comply with the findings of Babel et al. (2011) where, the rice yield of KDML-105 and RD 6 is forecasted to have declination and have suggested ChaiNat as an alternative variety against climate change. The results of Deb et al (2014) also reveal sharp maize yield declination of 33.9 to 44.2% maize yield in Sikkim under climate change.

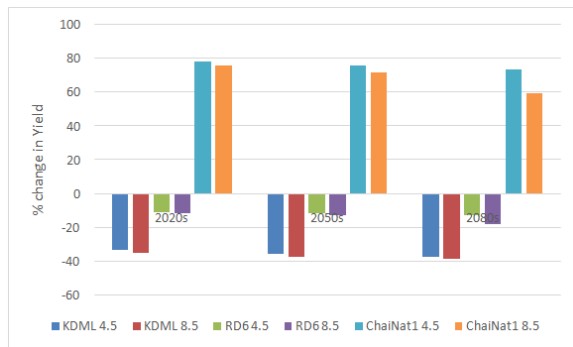


Figure 3: Percentage change in rice yield

ChaiNat-1 is a drought resistant variety and is suitable to grow in places which have less rainfall as well. Since, the magnitude of rainfall is increasing during dry period, thus the yield is increasing at a significant percentage. As for KDML 105 and RD6, they are popular rice varieties which are grown in rainfed conditions and require ample rainfall to maintain same yield. So, when the temperature will be increasing and precipitation decreasing, the yield of these varieties is automatically effected.

Climate Change Impact on WF

The effect of climate change on total water footprint will depend on the rice varieties used in the study area. In case of our study, there is significant increment in the water footprint of KDML 105 and RD6. However, there is decrement in the water footprint of ChaiNat-1 (Table 2).

Since, the results of projected future climate show increase in maximum and minimum temperature and decrease in precipitation for the study area, thus this will affect rice yield. With the climate change, the evapotranspiration demand of rice will also have significant rise. Hence resulting in increased water footprint for KDML 105 and RD6. However, since yield of ChaiNat-1 is significantly increasing, thus the WF of ChaiNat is decreasing with respect to baseline.

Table 2: Projected Future water footprint

Period	KDML 105		RD 6		ChaiNat-1		
	WF (m ³ /t)	Change (%)	WF (m ³ /t)	Change (%)	WF (m ³ /t)	Change (%)	
Baseline	3429.53		3150.38		1780.35		
RCP 4.5	2020s	5369.03	56.55	4018.44	27.55	1032.32	-42.02
	2050s	5847.75	70.51	4036.03	28.11	1058.27	-40.56
	2080s	6592.42	92.23	4087.22	29.74	1077.93	-39.45
RCP 8.5	2020s	5879.46	71.44	4028.53	27.87	1094.29	-38.53
	2050s	5792.68	68.91	4067.84	29.12	1130.08	-36.52
	2080s	6052.92	76.49	4335.37	37.61	1216.23	-31.69

Conclusions

Water footprint of rice were projected and investigated using quantile mapping bias correction method and DSSAT(CERES-rice) model. The investigation on projected future climate reveals that temperature (both maximum and minimum) will increase in future and under same changing climate precipitation will be decreasing. This would in turn lead to decrease rice yield for KDML 105 and RD6 and significant increase of total water footprint of rice production. On contrary, ChaiNat-1 will have increase crop yield and decrease water footprint for the future period under both RCP 4.5 and RCP 8.5 scenarios. The results show that future yield and water footprint will highly vary depending on the cultivar used. Since, the green water will not be able to meet the evapotranspiration demand, blue water requirement by crops will almost double for the common varieties KDML 105 and RD6. Adaptation strategies against climate change will be a must in the Northeastern Thailand to maintain yield and reduce water footprint in future.

Acknowledgement

Sakon Nakhon Rice Research Center, Thai Meteorological Department and Land Development Department are kindly acknowledged for helping with the necessary data.

References

- Babel, M. S., Agarwal, A., Swain, D. K. and Herath, S. (2011). *Evaluation of climate change impacts and adaptation measures for rice cultivation in Northeast Thailand*. Climate Research, 46(2), pp. 137- 146.
- Bocchiola, D., Nana, E. and Soncini, A. (2013). *Impact of climate change scenarios on crop yield and water footprint of maize in the Po valley of Italy*. Agricultural Water Management, 116, pp.50-61.
- Brown, A. and Matlock, M. D. (2011). A review of water scarcity indices and methodologies. White paper, 106, 19.
- Chapagain, A. K. & Hoekstra, A. Y. (2004). Water footprints of nations. Value of Water Research Report Series No. 16, The United Nations Educational, Scientific and Cultural Organization- International Institute for Hydraulic and Environmental Engineering (UNESCO-IHE): Delft.
- Chapagain, A.K., Hoekstra, A. Y., Savenije, H.H.G. and Gautam, R. (2006) *The water footprint of cotton consumption: An assessment of the*

- impact of worldwide consumption of cotton products on the water resources in the cotton producing countries.* Ecological economics, 60(1), pp. 186-203.
- Chapagain, R. (2016). Climate Change Impact on Water Footprint of Rice Production in Nam Oon Irrigation Project of Thailand (published master's thesis). Asian Institute of Technology, Thailand.
- Deb, P., Shrestha, S. and Babel, M. S. (2015). *Forecasting climate change impacts and evaluation of adaptation options for maize cropping in the hilly terrain of Himalayas: Sikkim, India.* Theoretical and Applied Climatology, 121(3-4), pp. 649-667.
- Gheewala, S. H., Silalertruksa, T., Nilsalab, P., Mungkung, R., Perret, S. R. and Chaiyawannakarn, N. (2014). *Water footprint and impact of water consumption for food, feed, fuel crops production in Thailand.* Water, 6(6), pp. 1698-1718.
- Hoekstra, A. Y. (2003). Virtual water: An introduction. In Virtual water trade: Proceedings of the international expert meeting on virtual water trade. Value of water research report series 11, pp. 13-23.
- Hoekstra, A. Y., Chapagain, A., Aldaya, M. and Mekonnen, M. M. (2011). *The water footprint assessment manual: Setting the global standard.* Routledge.
- Hoogenboom, G., Jones, J.W., Wilkens, P.W., Porter, C.H., Batchelor, W.D., Hunt, L.A., Boote, K.J., Singh, U., Uryasev, O., Bowen, W.T. and Gijsman, A.J. (2004). Decision support system for agrotechnology transfer version 4.0. University of Hawaii, Honolulu, HI (CD-ROM).
- Hoogenboom, G., Jones, J.W., Wilkens, P.W., Porter, C.H., Boote, K.J., Hunt, L.A., Singh, U., Lizaso, J.I., White, J.W., Uryasev, O. and Ogoshi, R. (2015). Decision Support System for Agrotechnology Transfer (DSSAT) Version 4.6 (www.DSSAT.net). DSSAT Foundation, Prosser.
- Kaenchan, P. and Gheewala, S. H. (2013). *A review of the water footprint of biofuel crop production in Thailand.* Journal of Sustainable Energy & Environment, 4(2).
- Kongboon, R. and Sampattagul, S. (2012) Investigating the Water Footprint in Bio-ethanol Crops Production in the Northern of Thailand. Paper presented to Conference on Green and Sustainable Innovation, Chiang Mai, Thailand.
- Mekonnen, M. M. and Hoekstra, A. Y. (2011). *The green, blue and grey water footprint of crops and derived crop products.* Hydrology and Earth System Sciences, 15(5), pp. 1577-1600.
- Nilsalab, P., Gheewala, S. H. and Mungkung, R. (2012). *Water Assessment of agrofuels feedstock cultivation: Methodology approaches.* Environ. Nat. Resour. J, 10, pp. 11-20.
- Shrestha, S., Deb, P. and Bui, T. T. T. (2016). *Adaptation strategies for rice cultivation under climate change in Central Vietnam. Mitigation and Adaptation Strategies for Global Change,* 21(1), pp. 15-37.
- Sukumalchart, T., Pornprommin, A. and Lipiwattanakarn, S. (2011) Monthly Water Footprint of Maize in Major Cultivated Areas of Thailand. Paper presented to Conference on Water Resources Management under Risk of Natural Hazard and Data Uncertainty, Phetchaburi, Thailand.
- Teutschbein, C. and Seibert, J. (2012). *Bias correction of regional climate model simulations for hydrological climate-change impact studies: Review and evaluation of different methods.* Journal of Hydrology, 456, 12-29.
- Thanawong, K., Perret, S. R., & Basset-Mens, C. (2014). Eco-efficiency of paddy rice production in Northeastern Thailand: a comparison of rain-fed and irrigated cropping systems. Journal of Cleaner Production, 73, 204-217.
- World Bank. (2014). *Agriculture, value added (% GDP).* Retrieved from <http://data.worldbank.org/indicator/NV.AG.R.TOTL.ZS>
- World Water Assessment Program (WWAP). (2012). *Managing Water under Uncertainty and Risk.* The United Nations World Water Development Report 4, Volume 1. Paris, France.



Session D

Disaster Management / Groundwater Management



Invited Papers

Japan's Policies and Technical Works for Flood Damage Reduction under Climate Change

Takafumi Nakui¹, Hirotada Matsuki²

Abstract Flood disasters had occurred frequently all over Japan while Disaster Risk Reduction governance and river management facilities were poor. People thought it natural for them to prevent their community from floods and took measures with their self-responsibility. After that, flood and water resource managements in a whole basin came into action under river authorities, and the Disaster Management Basic Act and relative regulations have been developed based on the experiences of huge flood disasters of ISEWAN Typhoon(1959) and others.

Under the Acts, all thinkable measures decreased flood damages and the victims slightly, and improved water use and promoted environmental conservation have been also promoted efficiently. However large-scale disasters have occurred again and again. In September 2015, a dyke-break and huge flooding occurred at Kinugawa river, which flows in the outer metropolitan area of Tokyo. It is predictable that enormous disasters which exceed the scale of past disasters will increase gradually under changing climate. On this occasion, river authorities, residents and relatives have to recognize the following mind, 'Unexpected scale floods surely occur and exceed limited capacity of river facilities'. And they also have to proceed integrated measures against such enormous disasters by structural and non-structural measures. In this paper, the transition of regulations on water-related disasters would be explained from the viewpoint of Japan's climate and historical background, and various challenging measures against large-scale water disasters in recent years would be introduced.

Keywords *Climate change, Unexpected scale disaster, Restructure, Disaster Management Policy*

Takafumi Nakui

Senior Deputy Director of International Affairs Office, River Planning Division, Water and Disaster Management Bureau, MLIT, Tokyo, JAPAN
nakui-t2kf@mlit.go.jp

Hirotada Matsuki

Director of International Affairs Office, River Planning Division, Water and Disaster Management Bureau, MLIT, Tokyo, JAPAN
matsuki84@gmail.com

Introduction

In old Japan, which had not started modern river improvement yet and people had been suffered from frequent flood disaster, the Heads of each region administrated their own territory and each community implemented river management and flood control within each region. And most of the people recognized it natural to deal with disasters by themselves, such as making a shelter on mound and equipping a boat under the eaves etc.

The first River law was established in 1896. The law defined a river manager, its role and management section in each river. As the river manager, government or prefecture are responsible for river facilities and water resources management.

After that, water rights and environment conservation were added in the river law to integrate water management system.

As the frequency of water disasters became decreased by their efforts, the social mind also changed to rely on the public sector.

On the other hand, larger-scale disasters beyond expectation have occurred by climate change recently. In September of 2015, eastern area of Japan (Kanto and Tohoku region including Tokyo metropolitan area) were attacked by the record breaking heavy rain and flood disaster. Especially severe overtoppings and dyke breaches along Kinugawa river made about 10,000 houses flooded and over 4,000 people isolated in their houses.

And in September of 2016, three typhoons attacked northern area of Japan (Hokkaido region) where typhoon rarely came so far, and left severe damage on people's lives and economy.

Based on these cases, it is understandable that huge disasters would occur and exceed the current function of river facilities in the future. Against the disasters, river managers, residents and relatives have to recognize the following mind, 'Unexpected scale floods surely occur and exceed limited capacity of river facilities', and they have to work with coalition to prevent such disasters.

Based on the situation, MLIT reviewed the strategy and measures against such huge disasters with experts and regional leaders, and proclaim the 'Rebuilding Flood-Conscious Society' as a policy against the huge

water disasters by climate change in December 2015. Details of this policy are introduced as follows.

Rebuilding Flood-Conscious Society

This vision is consisted the following three subjects.

1) Non-structural measures with residents’ perspective

River managers have implemented various measures to prevent and recover from flood disasters until now, but this policy promote the resident’s self-action based on the manager’s supports. And it focuses on the non-structural measures with resident’s perspective in order for people to understand the risk on their own initiatives and to take actions for evacuation. River managers disseminate the following information to residents and promote their self-action for evacuation and other measures.

- Publish the anticipated flood risk zone in danger of house collapsing which require eviction for evacuation.
- Improve a hazard map that is easy to understand and use for residents.
- Hold an explanatory meeting for real estate business operations.
- Establish a Timeline focused on evacuation activities and execute a roll playing training with having mayor’s participation.
- Set up observation equipments such as water gauges and live cameras in high risk areas for flooding.
- Positive distribution of flood forecast information by optimizing various devices like s martphone etc.

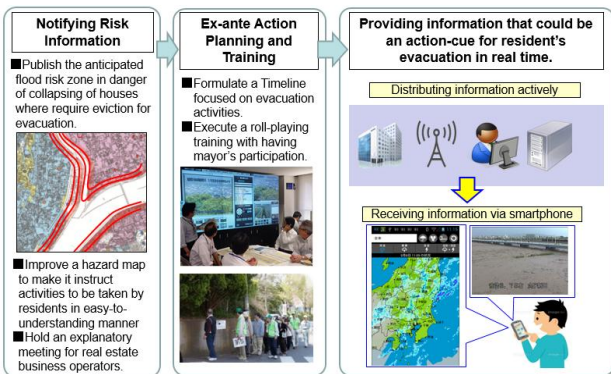


Fig.1 Non-structural measures with residents’ perspective

2) Structural measures to prevent outflow

Structural measures will be implemented preferentially in the areas where there are great concerns for flood disasters as follows in five years (about 1,200km in total).

- Piping prevention measures for levees where there are any concerns of collapsing by piping in the trace of old river channel etc (about 330km in total).
- Constructing levees and excavating river channel in the areas where the discharge capacity is not enough (about 760m in total). It would be promoted in consideration of the balance between upstream and downstream.
- Erosion and Scour prevention measures in the area where there are concerns of riverbank erosion and revetment collapse by water hammer or deep digging etc. (about 110km in total).



Fig.2 Structural measures to prevent outflow

3) Structural measures for crisis management

Improvement measures of levees will be promoted to extend the time of levee breach as long as possible within five years in a zone which is unavailable to construct new levees in consideration with the balance between upstream and downstream though there is risk of flood disasters.

- Protecting levee crest with asphalt and other materials to control the infiltration of rain water into levee, or delaying the time of breaking progression of levee top when an overflow disaster occurs (about 1,310km in total).
- Reinforcing the foot of back slope with blocks to delay the time of progression for deep excavation when an overflow disaster occurs (about 630km in total).

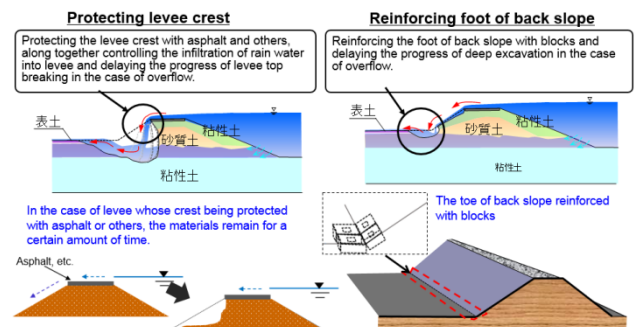


Fig.3 Structural measures for crisis management



System construction to promote disaster measures based on the Vision

To promote restructuring the Flood Fighting Conscious Society, a conference will be established in cooperate with river managers, prefectures, municipalities and other relatives in each area of overflowing. The goal for disaster mitigation will be shared and the discussion for promoting structural and non-structural measures integrally and systematically will be implemented in this conference. The conference will be coordinated in cooperate with other areas depending on the situation of the region, and promote the following measures.

1) Sharing a current information and measures against the risk of water disaster of the region

Government, prefectures and municipalities had promoted each disaster prevention and mitigation measures for reach until now. To implement disaster measures more effectively, they have become sharing the risk information of water disasters such as anticipated inundation area etc. And they also share the current status of disaster mitigation measures such as information exchange, evacuation plan, flood fighting system, drainage system and operating facilities for inundation, constructing river management facilities etc.

2) Formulating local disaster mitigation policy

River managers will formulate regional policies based on the characteristic of each region about evacuation, floodfighting, draining etc. that should be achieved in five years to mitigate water disaster. Details are as follows but they will depend on the situation of each region.

i) Smooth and rapid evacuation

- Information exchange and evacuation plan
- Information transfer, education, training in normal period
- Constructing facilities for smooth and rapid evacuation

ii) Accurate and rapid flood fighting

- Efficiency of flood fighting activities and strengthen of the system
- Promoting self-flood fighting system at municipality's building and disaster base hospital

iii) Draining and operating facilities of overflowing water

3) Following up the policies

River managers review and follow up the policies about each policy in the conference every year. Especially in the region which was damaged by the

flood disaster of 2015, Emergency actions for promoting early evacuation was made and will be followed up with other policies before flood season of each year as follows.

i) Conducting high level seminar for decision makers

River managers confirm with mayors how to deal with the information about flood forecast and flood emergency call provided from river managers to mayors during the flood.

ii) Joint inspection and dissemination to residents

River managers, prefectures, municipalities and relatives inspect the zones where there are high risks of flooding, such as the zone where the capacity of discharge is not enough and the points where water leakage occurred in the past, and share the information each other with residents.

MLIT ordered all river managers to establish conferences to implement the Vision at December 2015. Now the conference were established in 130 regions and the efforts for disaster mitigation are being undertaken based on each regional situation. The Vision will be completed in all regions until 2020.

Other technical efforts against disaster prevention and mitigation

To promote each measure of this Vision more effectively, other organizational and technical measures are being promoted in parallel as follows.

1) TEC-FORCE

Since before establishing the Vision, the Expert dispatching system has been established for the smooth and rapid recovery from the damages by huge disasters. The expert team is called 'TEC-FORCE'. TEC-FORCE is consisted of MLIT's technical staffs specialized in various fields such as river, road, sabo, ports and harbors, architect, electric machinery, sewer etc.

And each team is organized by proper staffs depending on the situation.

When the huge disaster occurred or is predicted to occur,

TEC-FORCE will be dispatched to the damaged area with necessary equipments and materials, and they will support recovering measures of prefectures and municipalities.

They catch the needs of damaged municipalities rapidly and specifically, and they inspect the damaged state and advice technically to prevent secondary disasters and to promote smooth

recovering.



Fig. 4 TEC-FORCE activities

TEC-FORCE will be dispatched not only in Japan but overseas. Some team were dispatched to Thailand with drainage pump vehicles in 2011 and supported to drain the overflow water in Bangkok and other cities.

2) Integrated Disaster Information Mapping System (DiMAPS)

MLIT are developing system to collect real time information from disaster sites and to lap the necessary information on a map. The system can coordinate some information visually and it will help getting situation smoothly and implementing a quick response in the damaged areas.

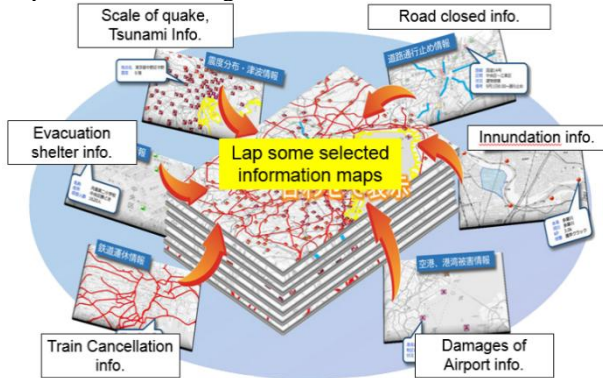


Fig. 5 DiMAPS

Conclusion

Flood disaster can easily exceed assumed scale anywhere in the world under changing climate. We should rebuild our mind from ‘Prevent outflow by facilities’ to “Prepare emergency action against huge flood”. That is the way of damage reduction. So it is necessary to study the character of each river and the risk in each region, and to think and implement most effective measures conducted by the river managers, responsible authorities and local residents.

References

Council for Social Infrastructure (2015).
 The measure state against huge inundation disaster - To restructure flood fighting conscious society by the change of fundamental attitudes - MLIT Report (2016)
 The activities of TEC-FORCE
 Geospatial Information Authority of Japan Report (2015)
 Integrated Disaster Information Mapping System (DiMAPS)

Prediction of extreme floods and risk curve development under a changing climate

Yasuto TACHIKAWA, Tomohiro TANAKA, Hiromasa HAYASHI, Kazuaki YOROZU, and Yutaka ICHIKAWA

Abstract To estimate probabilistic characteristics of extreme floods and to predict the magnitude of largest-class floods under a changing climate are key issues for impact assessment studies on water resources. In this research, a non-stationary hydrologic frequency analysis was introduced to future extreme rainfall GCM outputs to evaluate the change of extreme rainfall and flood characteristics. Then, a physically-based method to estimate a probable largest-class flood was shown. Finally, a probabilistic method to evaluate economical loss due to flood inundation was proposed to assess adaptation measures to cope with flood disasters.

Keywords *Climate change; non-stationary hydrologic frequency analysis; largest-class flood; flood risk curve*

Yasuto TACHIKAWA, Tomohiro TANAKA
Kazuaki YOROZU, Yutaka ICHIKAWA
Department of Civil and Earth Resources Engineering,
Kyoto University
Kyoto, Japan
tachikawa@hywr.kuciv.kyoto-u.ac.jp

Hiromasa HAYASHI
Ministry of Land, Infrastructure, and Transportation
Tokyo, Japan

Introduction

To estimate probabilistic characteristics of extreme floods and magnitudes of largest-class floods under a changing climate is a key issue for building up an adaptation strategy. To evaluate the change of extreme rainfall and flood characteristics, a non-stationary hydrologic frequency analysis was applied to future extreme rainfall outputs projected by MRI-A GCM 3.2S, 20km resolution atmospheric general circulation model developed by Metrology Research Institute in Japan (Mizuta *et al.*, 2012). The results showed that the magnitudes of the annual maximum short-term rainfall increase for the near future in most parts of Japan and this tendency was intensified in the end of the 21st century (Hayashi *et al.*, 2014).

As well as a non-stationary hydrologic frequency analysis, the magnitudes of largest-class floods caused by typhoons under a changing climate scenario were examined by using numerical typhoon simulation outputs. The rainfall data used for the flood simulation was developed by a physically-based course ensemble typhoon experiment for the Ise Bay Typhoon in 1959 under a pseudo global warming condition (Takemi *et al.*, 2013). The simulated rainfall data was given to a distributed rainfall-runoff model considering flood regulation with dam reservoir operations and flood control basins. It was revealed that the largest flood discharge at the Hirakata station, located at the upper part of the Osaka City area happened at the flood simulation using the typhoon course closest to the best track of the Ise-Bay Typhoon, which means the actual Ise Bay Typhoon course was the worst course for flood disaster in the Osaka area; the peak discharge in the pseudo global warming experiment showed 10% increase than the control experiment.

Finally, a method to construct a flood risk curve, a relation between the annual maximum damage due to flood inundation and its exceedance probability, was developed for a probabilistic assessment of economic loss by flood disasters (Tanaka *et al.*, 2015, 2016; Tanaka, 2016). The flood risk curve was obtained by integrating the exceedance probability of the annual maximum rainfall that causes a given inundation damage for all historical spatio-temporal rainfall patterns. A flood risk curve was constructed in the Yodo River basin using the latest climate change projection database, d4PDF, the database for Policy Decision making for Future climate change (Mizuta *et al.*, 2016).

Non-stationary hydrologic frequency analysis

Non-stationary hydrologic frequency models with time dependent parameters (Coles, 2001) were introduced to assess the change of probabilistic characteristics of extreme rainfall (Hayashi *et al.*, 2014). The non-stationary hydrologic frequency models used here were a non-stationary GEV model, a non-stationary Gumbel model, a non-stationary SQRT-ET model, and a non-stationary lognormal model. A cumulative distribution function (CDF) and a probabilistic distribution function (PDF) for these models are represented as below:

1) CDF of the non-stationary GEV model

$$F(x_{t_i}|\theta) = \exp\left\{-\left[1 + \xi\left(\frac{x_{t_i} - \mu(t_i)}{e^{\sigma(t_i)}}\right)\right]^{-1/\xi}\right\}$$

2) CDF of the non-stationary Gumbel model

$$F(x_{t_i}|\theta) = \exp\left[-\exp\left(-\frac{x_{t_i} - \mu(t_i)}{e^{\sigma(t_i)}}\right)\right]$$

3) CDF of the non-stationary SQRT-ET model

$$F(x_{t_i}|\theta) = \exp\left[-e^{a(t_i)}\left(1 + \sqrt{e^{b(t_i)}x_{t_i}}\right)\right. \\ \left.\times \exp\left(-\sqrt{e^{b(t_i)}x_{t_i}}\right)\right]$$

4) PDF of the non-stationary lognormal model

$$f(x_{t_i}|\theta) = \frac{1}{\sqrt{2\pi}e^{\sigma(t_i)}x} \exp\left[-\frac{1}{2}\left(\frac{\log x - \mu(t_i)}{e^{\sigma(t_i)}}\right)^2\right]$$

The time dependent model parameters for each hydrologic frequency model are modeled using the polynomial equation as

$$\mu = \mu(t_i) = \sum_{k=0}^p \mu_k t_i^k, \quad \sigma = \sigma(t_i) = \sum_{k=0}^q \sigma_k t_i^k$$

The coefficients of the polynomial equation were identified by using the maximum likelihood method. The best fitted model was selected using the Takeuchi information criterion TIC and the Akaike information criterion AIC, which were analytically confirmed for model selection criteria for non-stationary sequences.

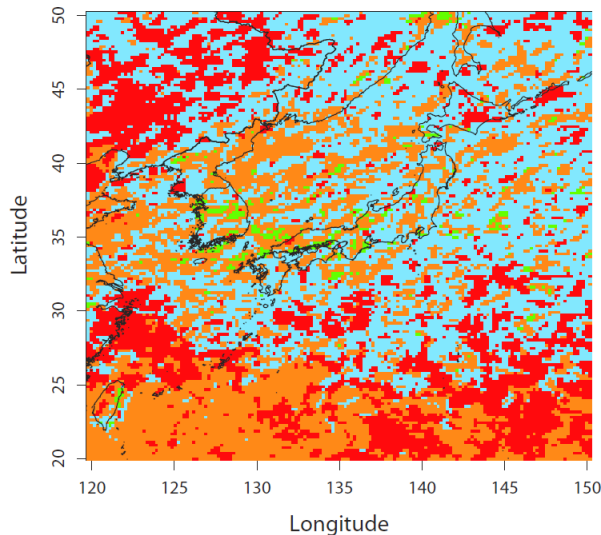


Fig. 1 The best fitted non-stationary frequency model for the annual maximum daily rainfall projected by MRI-AGCM3.2S with 20km spatial resolution. Red: non-stationary GEV model; Green: non-stationary Gumbel model; Right Blue: non-stationary SQRT-ET model; and Orange: non-stationary lognormal model. The non-stationary four models were applied to GCM rainfall time series to examine the future change of extreme rainfall intensity. The GCM outputs used were the time series of annual maximum daily rainfall data having 20km spatial resolution for the present climate

experiment (1979-2003), the near future climate experiment (2015-2044) and the end of the 21st century climate experiment (2075-2099) projected by MRI-AGCM3.2S (Mizuta *et al.*, 2012).

Figure 1 shows the spatial distribution of the best fitted non-stationary frequency model evaluated by the AIC for the annual maximum daily rainfall of each grid having 20km resolution. Using the best fitted model, the change of the 100-year annual maximum daily rainfall was analyzed as shown in Figure 2.

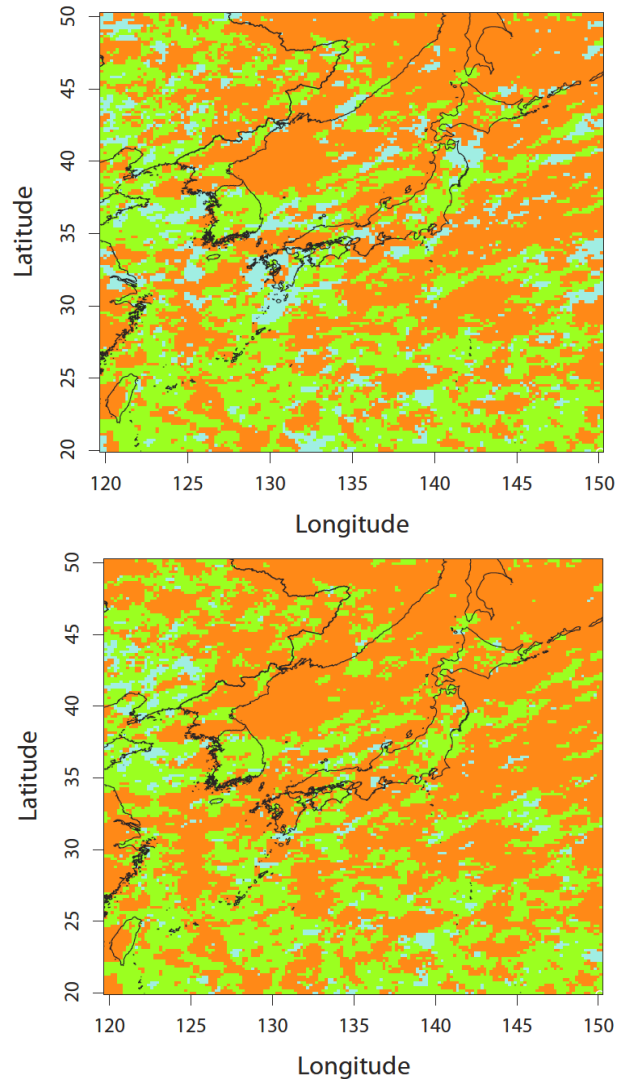


Fig. 2 Change of the 100-year annual maximum daily rainfall. Orange, green, and right blue show increase, no change, and decrease, respectively. The above figure shows the change between 2029 at the middle of the near future experiment and 1993 at the middle of the present climate experiment. The below shows the change between 2089 at the middle of the end of the 21st century climate experiment and 1993.

As shown in Figure 2, we found that the annual maximum daily rainfall around Japan shows an increase tendency and the increase tendency is intensified at the end of 21st century.

Largest-class flood prediction

A largest-class flood caused by a typhoon under a climate change condition at the Yodo River basin is examined by using rainfall data developed by a physically-based course ensemble typhoon experiment for the Isewan Typhoon in 1959 and a distributed rainfall-runoff model including flood regulation with dam reservoir operation (Tachikawa *et al.*, 2014, Miyawaki *et al.*, 2016).

Takemi *et al.* (2013) developed a heavy rainfall dataset based on an ensemble simulation of the historical extreme typhoon, the Ise-Bay Typhoon (1959) using a meso-scale meteorological model, the Weather Research Forecasting (WRF) model version 3.1.1. The ensemble simulation method realizes to generate different typhoon tracks perturbed from the original track of the typhoon by applying a potential vorticity inversion (PVI) method (Ishikawa *et al.*, 2012). Figure 3 shows the typhoon tracks simulated by the PVI method for the Ise-Bay Typhoon in 1959. The ensemble simulation approach was also applied to the typhoon under a pseudo global warming condition by setting a different sea surface temperature. The difference of the sea surface temperature was given based on the difference of the monthly mean SST in September between the end 21st century climate experiment (2075-2099) and the present climate experiment (1979-2003) simulated by MRI-AGCM3.2 (Mizuta *et al.*, 2012).

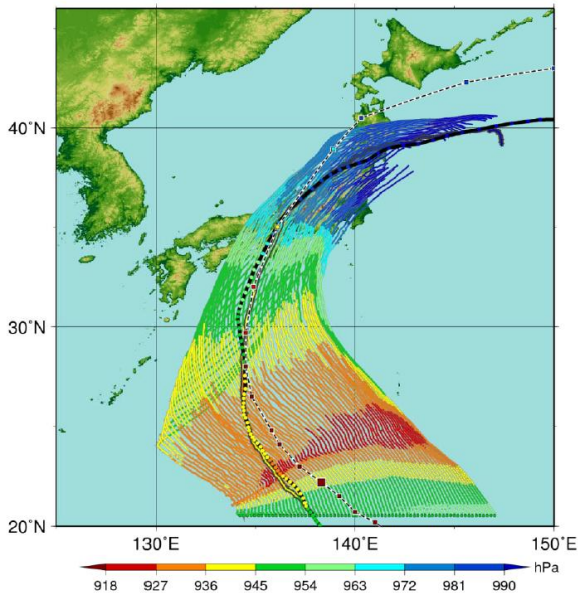


Fig. 3 Virtual shifting of typhoon's initial position for the Ise-Bay Typhoon in 1959 (Takemi *et al.*, 2013).

The simulated rainfall data was given to a distributed rainfall-runoff model with 1km spatial resolution, 1K-DHM (Tachikawa and Tanaka, 2014) developed for the Central and Kansai regions in Japan as shown in Figure 4. The simulated discharge for each typhoon track was stored with about 1km grid resolution. Figure 5 shows the largest river discharge at

the Hirakata station (7,281km²) in the Yodo River basin for each typhoon track.

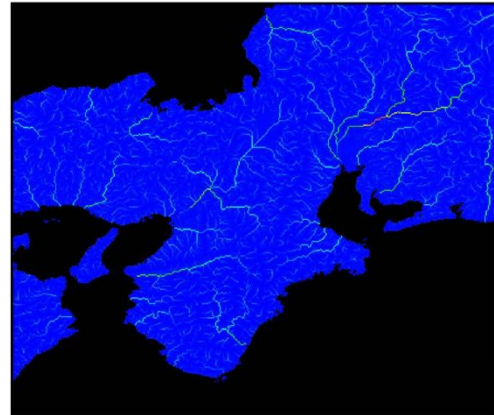


Fig. 4 Spatially distributed river flow for the Central and Kansai regions in Japan simulated by a distributed hydrologic model, 1K-DHM.

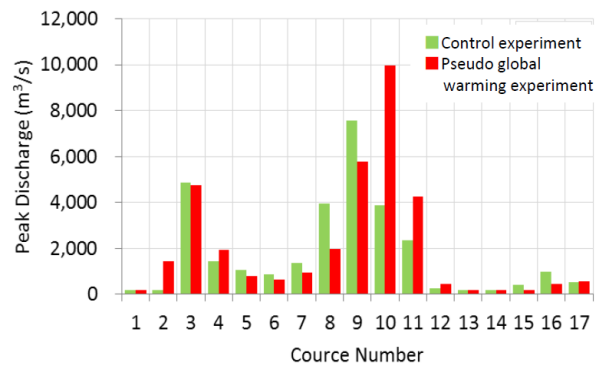


Fig. 5 The largest river discharge at the Hirakata station (7,281km²) in the Yodo River basin for each typhoon track.

We found that the simulated typhoon track No. 9 which caused the largest river discharge at the Hirakata station was the closest track to the best track of the Isewan Typhoon in 1959, which means the Isewan typhoon took the worst course for the Yodo River basin; and the largest river discharge at the Hirakata station under a pseudo global warming condition showed about 10% increase. We also found that the peak flood discharge at the Typhoon 18 in 2013 was larger than the largest peak discharge estimated by the Isewan Typhoon course ensemble simulation under a pseudo global warming condition.

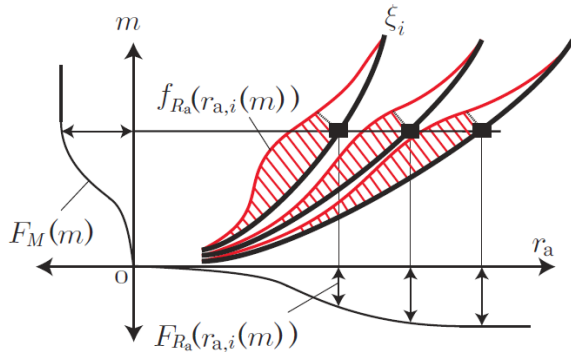


Fig. 6 Schematic explanation of the translation of a distribution function of the D -day annual maximum rainfall r_a to a distribution function of inundation damage m through various rainfall patterns (Tanaka *et al.*, 2015).

Development of flood risk curve: probabilistic assessment of economic loss due to flood

To realize an integrated economic risk assessment by flood disasters, a flood risk curve plays an important role. A flood risk curve provides a relation between economic loss due to flood disaster and its exceedance probability. A method to obtain the flood risk curve considering the uncertainty of spatio-temporal rainfall distribution is newly proposed (Tanaka *et al.*, 2015, 2016; Tanaka, 2016).

A flood risk curve is generated from a probability distribution function of the annual maximum rainfall distribution through the following processes (Figure 6): 1) to prepare typical extreme rainfall patterns ξ_i ; 2) to obtain a probability distribution of the annual maximum rainfall $F_R(r_a)$ from the historical data; 3) to obtain relations between T -year annual maximum rainfall and the maximum inundation water depth through a rainfall-runoff and inundation simulation; and 4) the economic damage m is estimated for each maximum inundation depth caused by the T -year annual maximum rainfall r_a . These procedures are conducted for each typical extreme rainfall pattern. Finally, the relation between economic damage m and its exceedance probability $F_M(m)$ is obtained by integrating the exceedance probability of each inundation damage. This method requires many rainfall-runoff and inundation simulations, thus a nesting runoff-inundation simulation method to reduce computational costs was also developed.

The method was applied to the Yodo River basin in Japan (Figure 7). Rainfall-runoff simulation was applied to the entire Yodo River basin using a distributed hydrologic model 1K-DHM with about 1km spatial resolution. Then, inundation simulations were applied to the central part of the Yodo River basin which is the most vulnerable area for flood inundation. The estimated spatial distributions of inundation depth were used to calculate the economic loss due to inundation using a guideline to estimate the economic damage (MLIT, 2005).

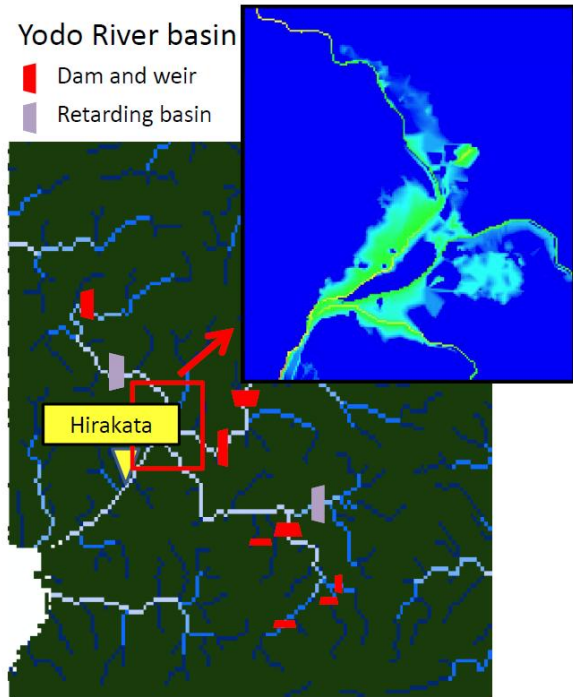


Fig. 7 Yodo River basin and an example of estimated inundation at the central part of the Yodo River basin.

To estimate the risk curve, the latest climate change projection data, d4PDF (database for Policy Decision making for Future climate change (Mizuta *et al.*, 2016)) was used. The d4PDF was simulated by using MRI-AGCM3.2H and 3.2S, which includes the historical experiment from 1951 to 2011 with 50 ensemble members which is equivalent to 3,000 years simulation. For the future experiment, d4PDF assumes the four degrees increase condition, which corresponds to the end of 21st century of the RCP8.5 scenario experiment. The future data consists of 15 ensemble experiments from 2051 to 2111 for six different SST patterns, which means 900 years simulation for each SST pattern.

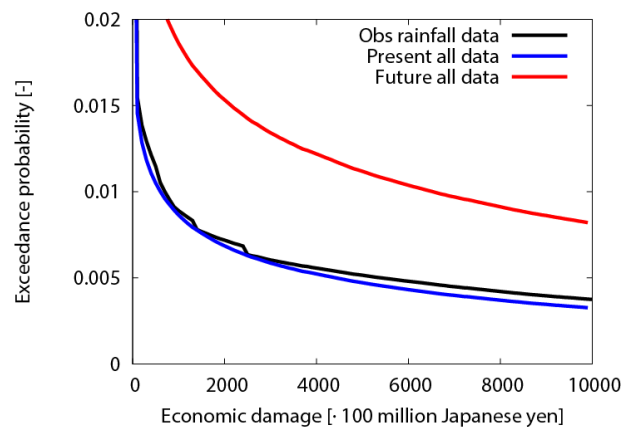


Fig. 8 Estimated flood risk curve at the Yodo River basin.

Figure 8 show a flood risk curve at the central part of the Yodo River basin derived using the observed rainfall data and d4PDF rainfall projection data. The flood risk curve estimated by using observed rainfall data well matched to the one using the d4PDF historical data set. Figure 8 clearly shows that the predicted economic loss due to flood inundation becomes larger at the end of the 21st century under the climate change scenario.

Summary and conclusions

In this study, characteristics of extreme rainfall under a climate change scenario was analyzed using a non-stationary hydrologic frequency analysis. It is found that the annual maximum daily rainfall around Japan shows an increase tendency and the increase tendency is intensified in the end of 21st century. Then, a largest-class flood was estimated using a rainfall-runoff simulation with the multi-track ensemble numerical typhoon simulation under a pseudo global warming condition. It is found that the Isewan typhoon took the worst course for the Yodo River basin and the largest river discharge under a pseudo global warming condition showed about 10% increase. Finally, a probabilistic method to evaluate economical loss due to flood inundation was demonstrated using the latest climate change projection data d4PDF.

Acknowledgement

This research was conducted under the framework of the "Precise Impact Assessments on Climate Change" supported by the SOUSEI Program of the Ministry of Education, Culture, Sports, Science, and Technology, Japan. Prof. Takemi for providing the dataset of the multi-track ensemble numerical typhoon simulations was also acknowledged.

References

- Coles, S. (2001) An introduction to statistical modeling of extreme values, Springer.
- Hayashi, H., Tachikawa, Y. and Shiiba, M. (2015) Non-stationary hydrologic frequency analysis using time dependent parameters and its model selection, *Journal of Japan Society of Civil Engineers, B1(Hydraulic Eng.)*, 71(1), 28-42 (in Japanese).
- Ishikawa, H., Oku, Y., Kim, S., Takemi, T. and Yoshino, J.(2013) Estimation of a possible maximum flood event in the Tone River basin, Japan caused by a tropical cyclone, *Hydrological Processes*, 27(23), 3292–3300.
- Ministry of Land, Infrastructure, Transport and Tourism of Japan, Water and Disaster Management Bureau (2005) A guideline of economic survey for flood control (in Japanese).
- Miyawaki, K., Tachikawa, Y., Tanaka, T., Ishii, D., Ichikawa, Y., Yorozu, K., Takemi, T. (2016) Flood runoff simulations in the yodo river basin assuming largest-class typhoons, *Journal of Japan Society of Civil Engineers, Ser. B1 (Hydraulic Engineering)*, 72(4), I_31-I_36 (in Japanese).
- Mizuta, R., Yoshimura, H., Murakami, H., Matsueda, M., Endo, H., Ose, T., Kamiguchi, K., Hosaka, M., Sugi, M., Yukimoto, S., Kusunoki, S. and Kitoh, A. (2012) Climate simulations usingMRI-AGCM3.2 with 20-km grid. *J. Meteor. Soc. Japan*, 90A, 233-258.doi:10.2151/jmsj.2012-A12.
- Mizuta, R., Murata, M., Ishii, M., Shiogama, H., Hibino, K., Mori, M., Arakawa, O., Imada, Y., Yoshida, K., Aoyagi, T., Kawase, H., Mori, M., Okada, Y., Shimura, T., Nagatomo, T., Ikeda, M., Endo, H., Nosaka, M., Arai, M., Takahashi, C., Tanaka, K., Takemi, T., Tachikawa, Y., Temur, K., Kamae, Y., Watanabe, M., Sasaki, H., Kitoh, A., Takayabu, I., Nakakita, E., and Kimoto, M. (2016) Over 5000 years of ensemble future climate simulations by 60 km global and 20 km regional atmospheric models, *Bulletin of the American Meteorological Society*, BAMS-D-16-0099.
- Tachikawa, Y., Ishii, D. and Yorozu, K. (2014) Probable maximum flood estimation by extreme typhoons under a changing climate, *International Conference on Ecohydrology (ICE) in Conjunction with the 22nd Meeting of UNESCO IHP Regional Steering Committee (RSC) for South Asia and Pacific*, Yogyakarta, Indonesia, 10-12, November 2014.
- Tachikawa, Y. and Tanaka, T. (2014) 1K-FRM/DHM, A distributed river discharge simulation model based on kinematic wave theory using HydroSHED topography data, <http://hywr.kuciv.kyoto-u.ac.jp/products/1K-DHM/1K-DHM.htm>.
- Takemi, T., Ishikawa, T., Oku, Y. and Okada, Y (2013) Ensemble experiment for the Ise-Bay Typhoon, SOUSEI Program for Risk Information on Climate Change, Research Report, Heisei 24, 16-18 (in Japanese).
- Tanaka, T., Tachikawa, Y. and Yorozu, K. (2015) A flood risk curve development for inundation disaster considering spatio-temporal rainfall distribution, *Journal of Japan Society of Civil Engineers, Ser. B1 (Hydraulic Engineering)*, 71(4), I_1483-I_1488 (in Japanese).
- Tanaka, T., Tachikawa, Y., Ichikawa, Y., and Yorozu, K. (2016) A flood risk curve development using conditional probability distribution of rainfall on duration, *Journal of Japan Society of Civil Engineers, Ser. B1 (Hydraulic Engineering)*, 72(4), I_1219-I_1224 (in Japanese).
- Tanaka, T. (2016) Development of a flood risk curve considering spatial-temporal rainfall variability and its application to actual river basins, *Dissertation for Doctor of Engineering, Kyoto University, Japan*.



Papers

Groundwater balance and river interaction analysis in Pleistocene aquifer of the Saigon River basin, South of Vietnam by stable isotope analysis and groundwater modeling

Tran Thanh Long^{1,a,*}, Sucharit Koontanakulvong^{1,b}

Abstract Groundwater is playing an important role in water extraction and utilizations especially in mega city such as Ho Chi Minh City, Binh Duong City. The excessive-extraction of groundwater and land subsidence of these cities are dramatically increased because of high water demand for domestic and industrial fields meanwhile Saigon River basin significantly contribute to balance the surface water and groundwater. Land surface recharge is considerably sensitive driving force to the groundwater reserves which is not fully understood. The study tries to explore the sources from land surface and river in the Saigon River basin, South East of Vietnam. First, the groundwater balance is contributed via groundwater modeling during 1995-2015. Second, the relationship between surface hydrology and groundwater is detected from surface and groundwater analysis. Final, the sources from land and river recharges are recognized by combination of isotope analysis and groundwater modeling. The sources of both recharges will be helpful for groundwater modeling researches and effective master planning of integrated water resources management in Saigon River Basin.

Keywords *Saigon River Basin, MODFLOW, stable isotopes, sources land and river recharge*

Tran Thanh Long
Department of Water Resources Engineering
Faculty of Engineering, Chulalongkorn University
Bangkok, Thailand
Email: tlongdcbk@yahoo.com

SucharitKoontanakulvong
Department of Water Resources Engineering,
Faculty of Engineering, Chulalongkorn University.
Bangkok, Thailand
Email: sucharit.k@chula.ac.th

Introduction

Saigon River basin has been well-known as the fastest growing economy of Vietnam, since 2004, its contributed 37.40% of the national GDP, and 55.76% of government budget. Under pressure from population appropriate of more than 14 million people (in 2014), and high population density (595 person/km²), groundwater has been utilized as a primary solution to meet water demand in areas after surface water. Since 1995, groundwater extraction has increased rapidly and declining groundwater levels now pose an immediate threat to drinking water supplies, farming systems, and livelihoods in the delta. The excessive-extraction of groundwater and land subsidence of these cities are dramatically increased because of high water demand for domestic and industrial fields, meanwhile Saigon River basin significantly contribute to balance the surface water and groundwater. Land surface water and river interaction with groundwater is considerably sensitive driving force to aquifers. Recently, the groundwater flow model in the Saigon river basin determined the amount of land recharge accounting for 0 to 10.3%, and river leakage accounting for 18.54% to 21.41% of the groundwater storage (Lanh Do T (2010), Chan N D (2011)). Likewise, the river recharges is estimated at 29% of total groundwater reserve in Ho Chi Minh and surround area by applying recharge function from effective rainfall (Khai (2015)). Nonetheless, the sources of land and river recharge are not fully sighting. This paper focus on exploring the sources of land surface and river in the Saigon River basin, South of Vietnam. First, the groundwater balance is contributed via groundwater modeling during 1995-2015. Second, the relationship between surface hydrology and groundwater is detected from surface and groundwater analysis. Final, the sources from land and river recharges are recognized by a combination of isotope analysis and groundwater modeling. The sources of both recharges will be helpful for groundwater modeling researches and effective master planning of integrated water resources management in the Saigon River Basin.

Study area

Study area stretches from latitude 10.320 E to 11.201 E and from longitude 106.215 N to 107.024 N with an area of 6,640 km². It covers all area of Ho Chi Minh City and some districts of Dong Nai, Binh Phuoc, Binh Duong, Long An and Tay Ninh Province. The area has a tropical climate, specifically a tropical wet and dry climate, with an average humidity of 75%. The year is divided into two distinct seasons. Mean annual rainfall is at 1,612mm and mean annual temperature is at 27°C. Terraced plain mainly characterizes the topography of the area with elevation vary from 0 MSL to 70 MSL. In the area, there are 3 major rivers as Sai Gon River, Vam Co Dong River, and Dong Nai River. Regarding Hydrogeology, there are 3 aquifers interacted with river system, and distributing from top to bottom respectively as follows: upper-Pleistocene (qp₃), Upper Middle Pleistocene (qp₂₋₃), Lower Pleistocene (qp₁), and 1 aquifers disconnected with river system: Holocene (qh). Piezometer head of upper-Pleistocene (qp₃), Upper Middle Pleistocene (qp₂₋₃), Lower Pleistocene (qp₁) are oscillated follow the fluctuation of rainfall and river stage. Under increasing abstraction rapidly, groundwater levels in all of aquifers are declining with annual rate 0.04m in upper Pleistocene aquifer and 0.9m in lower Pleistocene aquifer. In currently, the abstraction is estimated at 600,000 m³/day and occupies 34% of water supply.

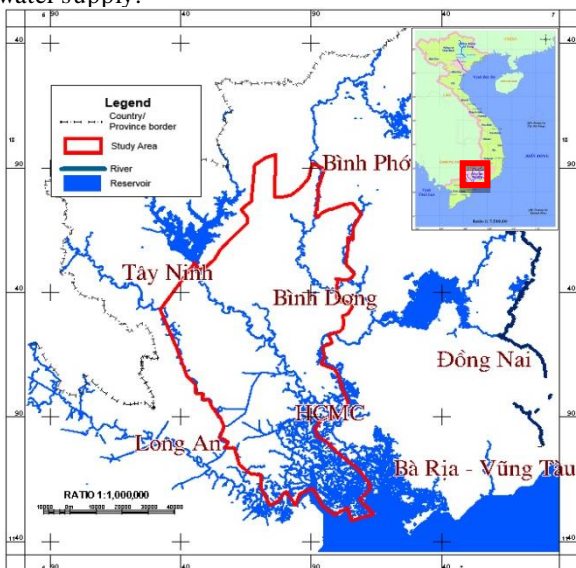


Fig. 1 The study area

Daily observed precipitation, temperature, river water level data are collected at Southern Regional Hydrometeorology Center, groundwater monitoring and Hydrogeology data area collected at Division for Water Resources Planning and Investigation for the South of Vietnam (DWRPIS) and Groundwater abstraction and water use are collected at Department of Resources and Environmental. The data are collected in period 1995 - 2015.

Methodology

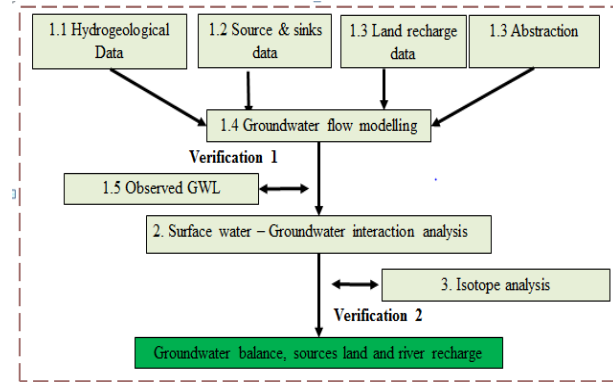


Fig. 2 Research methodology

In order to explore the sources of recharges, the methodology involves in 3 sub-tasks: First, water balance is estimated from groundwater model. The hydraulic conductivities of aquifers are generated by applying geo-statistic. The input conductance coefficient of river was applied from previous groundwater model (Boehmer, 2000), (Tuan, 2016). Daily observed precipitation, temperature, river stage data are collected at Southern Regional Hydrometeorology Center, the record piezometric head, and hydrogeology data collected at Division for Water Resources Planning and Investigation for the South of Vietnam (DWRPIS) and Groundwater abstraction and water use are collected at Department of Resources and Environmental. The calibration and verification are proceeded during period 1995-2006, and 2007- 2015, respectively. Second, the river and groundwater interaction is analysis from water balance and flow direction. Final, the stable isotope analysis is applied to verify the river and groundwater interaction.

Groundwater modeling

Groundwater-flow models are used to simulate aquifer response, in terms of head (ground water level) and fluxes into and out of an aquifer, to natural and human-induced stresses; The governing equation represents in three-dimensional movement of ground water is

$$\frac{\delta}{\delta x} \left[K_{xx} \frac{\delta h}{\delta x} \right] + \frac{\delta}{\delta y} \left[K_{yy} \frac{\delta h}{\delta y} \right] + \frac{\delta}{\delta z} \left[K_{zz} \frac{\delta h}{\delta z} \right] + W = S_s \frac{\delta h}{\delta t} \quad (0)$$

where

K_{xx}, K_{yy} and K_{zz} are the values of hydraulic conductivity along the x, y, and z coordinate axes and h is the potentiometric head (hydraulic head)

W is a volumetric flux per unit volume representing sources and/or sinks of water, where negative values are water extractions, and positive values are injections/recharge. It is a function of space and time (i.e. W = W(x, y, z, t)).

S_s is the specific storage of the porous material and may be function of space.
 t is time.

Kriging method

Presentation errors map and variance reduction in weighting for estimating is the benefits of Kriging against others interpolation methods. Errors in this method are independency from variable and dependent to spatial location and it cause to predict the best location sampling is possible. Variogram relationship based on the measured points is as follows:

$$\gamma(h) = \frac{1}{2n(h)} \sum_{i=1}^{n(h)} [z(x+h) - z(x)]^2 \quad (1)$$

where $\gamma(h)$: is the variogram for a distance (lag) h between observations $z(x)$ and $z(x+h)$.

$n(h)$: is the number of pairs of observations which are at distance h . $z(x)$: the observed variable.

$z(x+h)$: the observed variable is the h distance from $z(x)$ and variogram $\gamma(h)$.

Natural Neighbor

Based on the natural neighbor coordinates, Robin Sibson developed a weighted average interpolation technique that he named natural neighbor interpolation (Sibson, 1980, 1981)

$$G(x, y) = \sum_{i=1}^n w_i f(x_i, y_i) \quad (1)$$

where: $G(x,y)$ is the NN estimation at (x,y) ;
 n is the number of nearest neighbors used for interpolation;
 $f(x_i,y_i)$ is the observed value at (x_i,y_i) ; and
 w_i is the weight associated with $f(x_i,y_i)$.

Isotopes Mass Balance Analysis Method

$$C = A(1-X) + BX \quad (1)$$

Where:

A is the stable isotope value of first source recharge;
 B is the stable isotope value of second source recharge;
 C is the stable isotope value of destination flow;
 V_A is the amount of first source recharge;
 V_B is the amount of second source recharge;
 X is the recharge proportion of river water; and $(1-X)$ is the recharge proportion of precipitation.

Results and discussion

Hydraulic conductivity estimation

Table. Comparison Krigging method and Natural Neighbor method for estimated hydraulic conductivity

	Aquifer 2		Aquifer 3		Aquifer 4	
	Krig	NN_gr	Krig	NN_gr	Krig	NN_gr
Min	27.86	29.45	26	25.83	27.1	25.68
Max	4.36	3.49	1.7	0.36	6.5	8.32
ME	0.2	0.99	0.38	0.53	0.13	0.14
MAE	2.33	2.6	3.2	3.35	1.45	1.55
RMSE	3.44	3.61	4.26	4.47	2.05	2.6

As result of table 1, the mean error of krigging is in range 0.13 – 0.38, meanwhile, the natural neighbor is 0.14 – 0.99. In addition, RMSE of the krigging is better than natural neighbor 0.2. According to good performance, krigging method is selected to interpolate hydraulic conductivity in the groundwater mode as Fig 3.

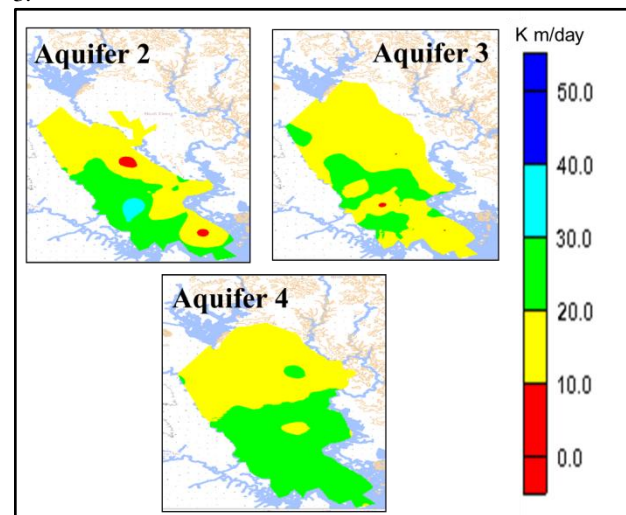


Fig. 3 Estimated hydraulic conductivity distribution

The hydraulic conductivity is from 5 m/day to 40 m/day. The hydraulic conductivity in the upper part is lower than the lower part. So, the groundwater flows in upper part circulate less than the down part.

Calibration/Verification Groundwater Model

Groundwater flow model (MODFLOW) was simulated conditions in the area during the period 1995 – 2015. The land recharge and conductance in river was calibrated during period 1995-2006 and verified in 2007- 2015. Result of calibration and verification indicate that the computed and observed are correspondence. The ME is from 0.03 to 0.77. Likewise, RMSE is from 0.4 to 1.61.

Table ME, MAE, RMSE value of aquifers in comparison with observed data

	Aquifer 1	Aquifer 2	Aquifer 3	Aquifer 4
Calibration (1995-2006)				
Max E	0.97	2.64	2.22	0.98
Min E	-0.64	-1.3	-1.25	-0.95
ME	0.1	0.31	0.13	0.03
MAE	0.33	0.95	0.68	0.45
RMSE	0.4	1.12	0.81	0.53

	Verification (2007-2015)			
Max E	1.58	1.98	2.25	0.79
Min E	0.04	-1.56	-1.46	-0.99
ME	0.77	0.08	0.03	-0.18
MAE	0.85	1.43	1.13	0.53
RMSE	0.91	1.61	1.32	0.61

River and groundwater interaction analysis

Year	River	Land recharge	Storage	Boundaries
1996	49,877 m ³ /day (14%)	61,999 m ³ /day (18%)	24,939 m ³ /day (7%)	195,942 m ³ /day (57%)
2002	124,288 m ³ /day (21%)	51,179 m ³ /day (9%)	17,140 m ³ /day (8%)	333,616 m ³ /day (57%)
2012	259,764 m ³ /day (24%)	76,190 m ³ /day (8%)	130,605 m ³ /day (12%)	616,238 m ³ /day (56%)



Year	River	Abstraction	Storage	Boundaries
1996	53,644 m ³ /day (16%)	58,847 m ³ /day (17%)	8,914 m ³ /day (3%)	223,317 m ³ /day (65%)
2002	34,342 m ³ /day (6%)	230,127 m ³ /day (39%)	5,941 m ³ /day (1%)	317,745 m ³ /day (54%)
2012	31,349 m ³ /day (3%)	529,263 m ³ /day (48%)	8,408 m ³ /day (1%)	522,920 m ³ /day (48%)

Fig.4 Groundwater balance in year 1996, 2002, 2012

According to water balance in Fig.4, under the increasing abstraction from 58,847 m³/day (17%) to 529,263 m³/day (48%), the river leakage intensified rapidly from 49,887 m³/day (14%) to 299,764 m³/day (24%). Correspondingly, the discharge from groundwater to river diminished from 53,644 m³/day (16%) to 31,349 m³/day (3%). Meanwhile, with the range 61,999 m³/day to 76,190 m³/day, the land recharge seem not to fluctuate as increasing river leakage. Hence, the river recharge play major role to balance the groundwater reserve in this area.

The groundwater flow demonstrated in the Fig. 5. The flow processed from the hill innorth westto sea in south East. According to the different piezo metric head, the groundwater discharges to river in section 1 and section 3, nevertheless, river will discharge to groundwater in section 2. The river recharge occurs in the middle part of Saigon river. The verification river recharge, land recharge and groundwater interaction by stable isotope analysis is showed as Fig . 6.

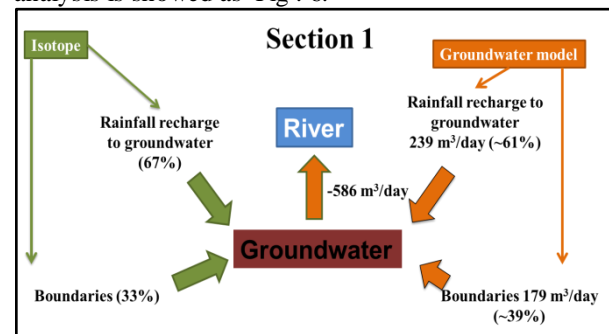
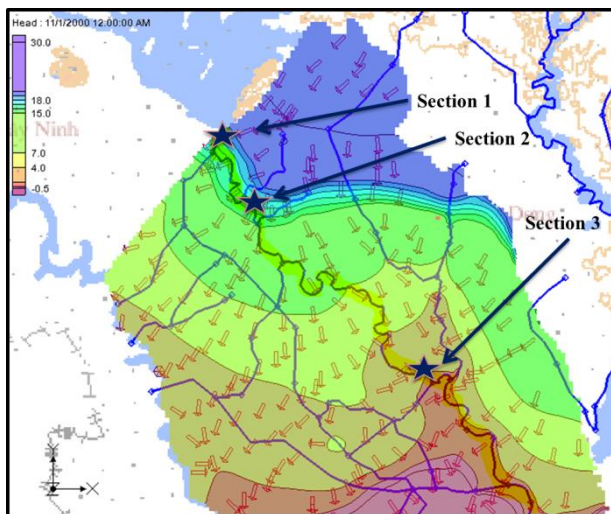


Fig.5 Flow direction and section sample isotope

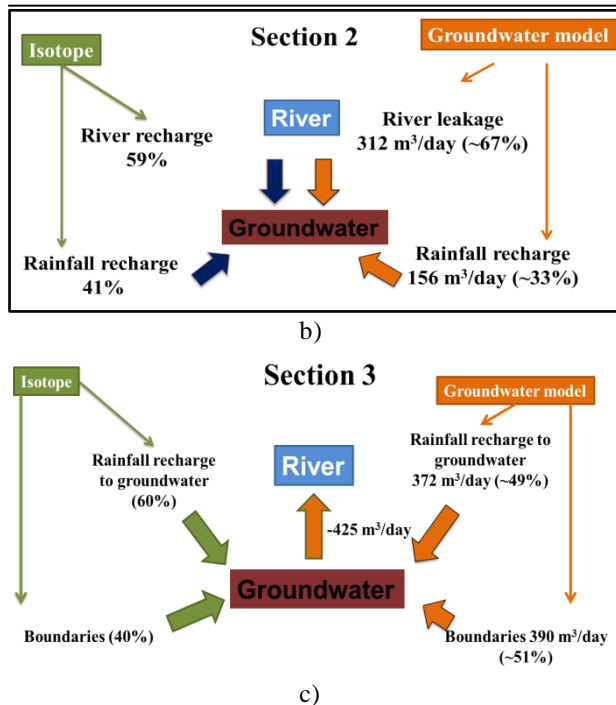


Fig.6 Proportion land recharge and river recharge by isotope

In 3 sections, the results of stable isotope analysis and groundwater model are coincident. In section 1 and 3, the rainfall recharge play the major recharge to groundwater reserves as 60%. Besides, in section 2, the proportion river recharge and rainfall recharge is 51:41 via isotope sample and 67:33 via groundwater model. Hence, this method can help to explore the sources of recharge from rainfall and river to groundwater reserve. With the verification of stable isotope, the groundwater in upper part gains recharge from rainfall and discharge to river. The river recharge occurs in section 2 and potential in middle part of Saigon River. The further research should extend the stable isotope investigation in the middle part of Saigon River to clarify the sources of recharge and proportion of rainfall and river recharge in this area.

Summary and conclusions

This study showed the interactions of river and groundwater in Saigon River basin from groundwater model and isotope analysis. The combination of isotope analysis and groundwater model indicates that the groundwater gain the rainfall recharge and discharge to river in the north west. While, with groundwater model, the river recharge to groundwater occurs in middle part of Saigon river.

The paper showed that the river recharge increase with same proportion of growing abstraction which induce more river recharge. In currently, the river recharge plays a major role in groundwater balance in Saigon river basin.

The results also prove that the method Kriging can apply in this area to interpolate hydraulic conductivity with good performance.

To understand fully the surface and groundwater interaction in this area, this approach could apply to explore more sources of land and river recharge to groundwater reserves in study area.

Acknowledgement

This paper could not be accomplished without the support of Ph.D sandwich program scholarship from AUN – Seed net and the Water Resources System Research Unit of Faculty of Engineering, Chulalongkorn University. The authors also thank to the staff at Division for Water Resources Planning and Investigation for the South of Vietnam, Southern Regional Hydrometeorology Center Department of Resources and Environmental, Center for Nuclear Techniques in Ho Chi Minh City for data collection.

References

- Arlen W. Harbaugh (2005) *Modflow-2005*, the U.S. geological survey modular ground-water model, the ground-water flow process, techniques and methods, USA.
- Boehmer, W. (2000). Groundwater study Mekong delta. HASKONING B.V Consulting Engineers and Architects: HASKONING B.V Consulting Engineers and Architects.
- Chan.N.D, K. N. V. H. D. T. (2011). Generating sources of exploitable groundwater reserves in Saigon river basin area. Vietnam National University-Ho Chi Minh City, Doctorate dissertation (ID:62.85.15.01).
- Chinh, N. K. (2012). Use of the isotope techniques to study Groundwater Recharged Availability in Hochiminh City Area: Department of Isotope Hydrology, Center for Nuclear Techniques in Ho Chi Minh City.
- Khai, H. Q., & Koontanakulvong, S. (2015). Impact of Climate Change on groundwater recharge in Ho Chi Minh City Area, Vietnam. THA 2015 International
- Long, T. T., & Koontanakulvong, S. (2014). SW-GW Interaction Analysis for Drought Management in Con Son Valley, Con Dao Island, Ba Ria-Vung Tau Province, Vietnam. Paper presented at the The 1st AUN/SEED-Net Regional Conference on Natural Disaster, Universitas Gadjah Mada, Yogyakarta, Indonesia.
- Lanh Do T, C. N. D. e. a. (2010). Integrated Management and Water Resources Reasonable Usage on Dong Nai River system. Ministry of Science and Technology, KC08 18/06-10.



- M. Moradi , D. Ghonchehpour , A. Majidi , V. MahmoudiNejad , "Geostatistic Approaches for Investigating of Soil Hydraulic Conductivity in Shahrekord Plain, Iran", *American Journal of Mathematics and Statistics*, Vol. 2 No. 6, 2012, pp. 164-168. doi: 10.5923/j.ajms.20120206.01
- Vuong. (2010). Reconstruction of Geology map, Hydrogeology map, and Geotechnical map with scale 1:50.000. Division for Water Resources Planning and Investigation for the South of Vietnam., Report 2010.
- Yeh, H.-F.; Lin, H.-I.; Lee, C.-H.; Hsu, K.-C.; Wu, C.-S. Identifying Seasonal Groundwater Recharge Using Environmental Stable Isotopes. *Water* 2014, 6, 2849-2861.

Estimation of river conductance values along Saigon River, Vietnam

Tuan Pham Van^{1,a*}, Sucharit Koontanakulvong^{2,b}

Abstract The Saigon River system is one of the largest resources contributing water supply for domestic and industrial fields at Ho Chi Minh City and Binh Duong Province, which has been facing the drought issue at downstream in recent years. To manage the water resources in Saigon Basin effectively, the groundwater and river interaction parameters need to be assessed seriously. However, in the past researches, the parameters seem to be less described with fully understanding. In this study, a groundwater modeling of the main stream of Saigon River using local boundary conditions derived from the regional groundwater flow model is used to estimate the river recharge to the aquifer. The conductance values of river bed based on soil type are defined at a selected river stretch (Thudaumot area) through calibrated and verified by the groundwater model using the observed piezometric heads during 2000 to 2007. The estimation of conductance values are applied for interaction analysis between Saigon River recharge and groundwater reserve.

Keywords *Saigon River, Groundwater Model, Conductance, Pumping rates, Interaction.*

Tuan Pham Van
Department of Water Resources Engineering
Faculty of Engineering, Chulalongkorn University
Bangkok, Thailand
Email: phamtuanld8@gmail.com

Sucharit Koontanakulvong
Department of Water Resources Engineering
Faculty of Engineering, Chulalongkorn University
Bangkok, Thailand
Email: sucharit.k@chula.ac.th

Introduction

In hydrologic cycle, the groundwater and river interaction is one of important parts. The interconnection of river and groundwater take many forms. In many situations, river gain water and solutes from ground-water systems and in others. The river is a source of ground-water recharge and causes changes in groundwater quality (Winter 1998). Lateral flow and transportation between groundwater and river water through the subsurface interaction zone, in particular, is a major pathway for energy, water and gas transfer between terrestrial and aquatic systems. Pollution of surface water can cause degradation of ground-water quality and conversely pollution of ground water can degrade surface water. So, the effective land and water management requires a clear understanding of the linkages between ground water and surface water as it applies to any given hydrologic setting. In Viet Nam, groundwater and river system are two main parts of water resources systems. So, issues related to water supply, water quality, and degradation of aquatic environments are importance concerns of the Nation or Region. The Saigon River system is the second largest river supplying domestic water to Ho Chi Minh City after the Dong Nai River, which has been in high pressure on water quality due to the effect of wastewater from industrial, domestic and agricultural activities. The groundwater recharge from river occupied until 29% (about 623,247 cubic meter per day) of total flow in groundwater storage in Ho Chi Minh area (Khai 2015). Especially, the impact of salt water intrusion is being an extremely serious problem in the South of Viet Nam, and Saigon basin is one of regions most affected. Thus, groundwater and river interaction has been shown to be a significant concern in many of these issues at Saigon River.

The understanding about groundwater and river interaction parameter plays a key part in water resources management at the Saigon river basin. Therefore, the purpose of this study is to analyze groundwater and river interaction parameter at the lower of Saigon River by groundwater model and groundwater balance of the middle Pleistocene (qp2-3) aquifer in the study area.

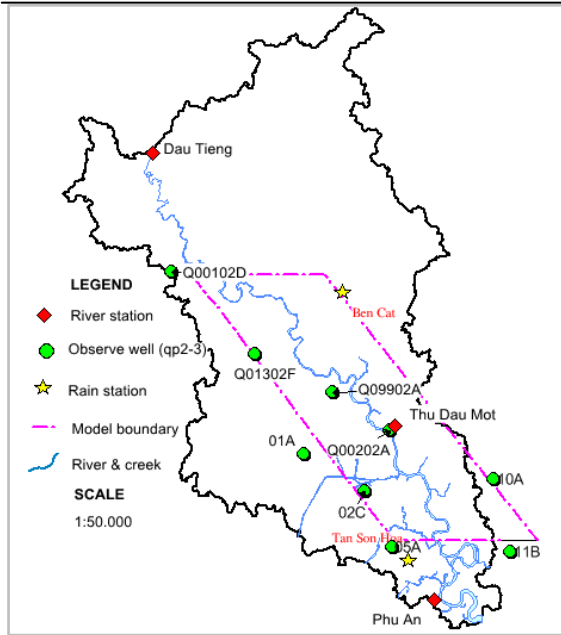


Fig. 3 Groundwater model area

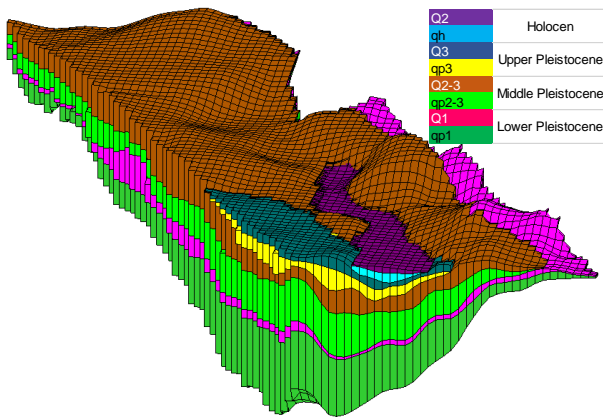


Fig. Simulation of geological strata at the study area

Table. 1 Pumping rates distribution of aquifer qp2-3 at the study area from 2000 to 2007

Time	Population (person)	Abstraction per person (m ³ /person/d)	Pumping rate (m ³ /d)
2000	272,156	0.086	23,418.4
2001	272,307	0.086	23,418.4
2002	298,092	0.086	25,635.9
2003	326,262	0.086	28,058.5
2004	326,643	0.119	38,870.5
2005	351,090	0.119	41,779.7
2006	380,056	0.119	45,226.5
2007	409,792	0.119	48,911.7

Model calibration

The calibrated steady-state model is evaluated using residuals between computed and observed heads of

aquifer qp2-3, where out of four wells (Figure 5). Mean error (ME) is 0.46 and root mean square error is 0.6 in January 2000.

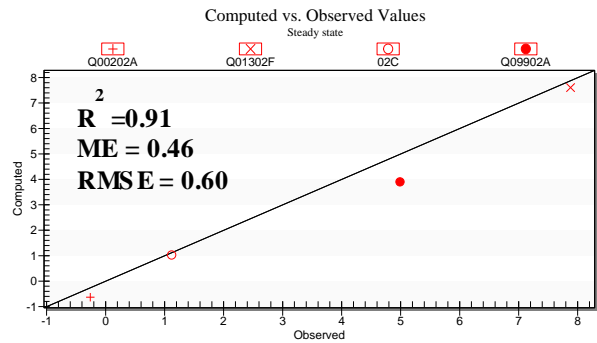


Fig. 5 Correlation between observed and computed groundwater head of aquifer qp2-3 in steady state (1/2000).

Results of calibration model show that computation values have close relations with observation data (Figure 6) and expressed by average RMSE range from 0.5 to 1.02 m in three aquifers and R² range from 0.58 to 0.92 (Table 2).

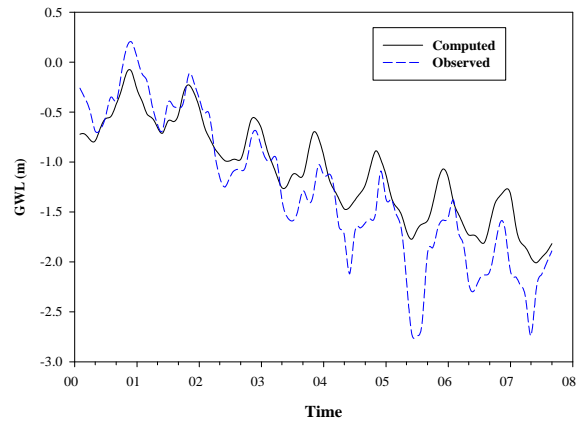


Fig. 6 Observed and computed groundwater level in period 2000- 2007 (Q00202A)

Table. 2 Model errors in transient state (1/2000 – 9/2007)

ID	Obs Aquifer	R ²	ME	RMSE
Q011020	qp3	0.78	0.4	0.5
Q00902A	qp2-3	0.86	0.47	0.67
Q00202A	qp2-3	0.83	0.82	0.85
02C	qp2-3	0.80	0.75	0.9
Q01302F	qp2-3	0.58	0.32	0.37
Q00204A	qp1	0.82	0.97	1.02
Q040300	qp1	0.92	0.84	1.01
01B	qp1	0.89	0.82	0.95

Results and applications

Conductance calibration

Bottom of river at Thudaumot area located in Middle Pleistocene aquifer with the depth around 18 MSL. Both the fluctuation of river water level (Thudaumot station) and groundwater level (Q00202A) are homogeneous and ultimately depend on precipitation. However, whereas river water levels did not have much change, the groundwater levels tend to go down with rapid drop in the period from 2000 to 2007 (Figure 7).

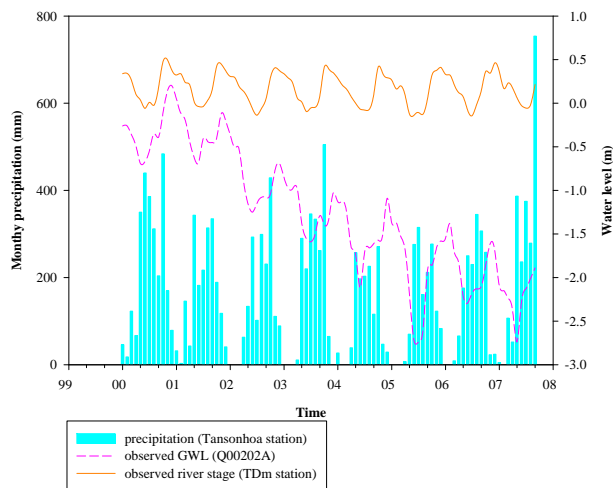


Fig. 7 Records of riverwater level, groundwater and precipitation at Thudaumot area during 2000 to 2007

The conductance of river stretch at TDM area was calibrated by observed piezometric heads (Q00202A) during 2000 to 2007 and the values were changed from 0.2 to 5 (Figure 8). Results of model verification show that the model generally have appropriate prediction when compared model value with observation (Q00202A) (Figure 9).

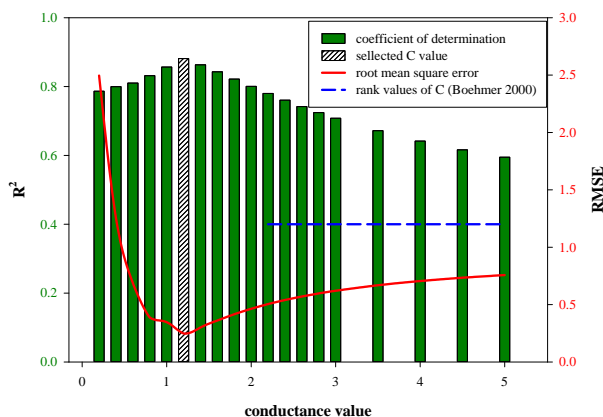


Fig. 8 Records of coefficient of determination and root mean square error of conductance calibration at the monitoring well (Q00202A)

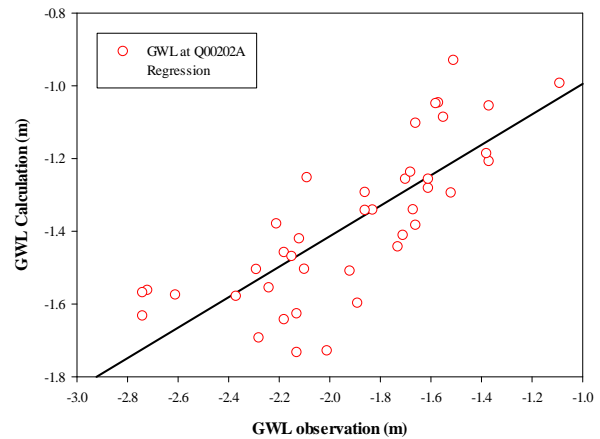


Fig. 9 Cogression of observed and computed groundwater head during period 2000-2007

In groundwater modelling, the flow across riverbed is represented by the following equation:

$$Q_{riv} = C_{riv} \times (H_{riv} - h) \quad (eq. 1)$$

where:

Q_{riv} is the flow between the river and the aquifer, taken as positive if it is directed into the aquifer (L^3T^{-1}),

H_{riv} is the water level (stage) in the river (m),

C_{riv} is the hydraulic conductance of the river-aquifer interconnection,

h is the head at the node in the cell underlying the river reach (m)

From groundwater modelling, hydraulic conductivity of riverbed was determined by hydraulic gradient and river recharge as function below:

The conductance, C for each cell along the river is given by:

$$C = \frac{K \times L \times W}{M} \quad (eq. 2)$$

So, by combining equation (1) and (2) the hydraulic conductivity of riverbed can estimated as:

$$K = \frac{Q}{\Delta H} \times \frac{M}{L \times W} \quad (eq. 3)$$

K is the hydraulic conductivity of river bed (L/T)

W is the width of riverbed (L)

L is the length of river section (L)

M is the thickness of riverbed (L)

The main materials of river bottom at Thudaumot area are silt, losses and silty sand with range of hydraulic conductivity from 10^{-4} to 5 (Heath, Ralph C, 1983. Basic Groundwater Hydrology Book– Page 13). Compared with the hydraulic conductivity calculation from groundwater model using scattered plot, the values range from 0.005 to 0.007 (average = 0.0061) (Figure 10).

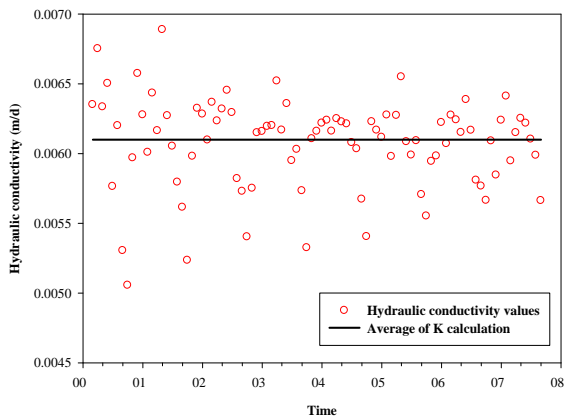


Fig. 10 Scattered plots of hydraulic conductivity of riverbed during period 2000-2007

Application 1: Effect to water balance of aquifer qp2-3 in the study area due to pumping and river leakage

In 2001, the model estimated total inflows to be 13 % groundwater recharge, 36% boundary recharge and 33 % river leakage. In the meanwhile, the model estimated outflows to be 19 river leakage, 27 % pumping discharge, 54 % boundaries discharge (Figure 11). In the period from 2000 to 2007, while ratio of pumping rate increase 7% in 2004 and 9% in 2006, ratio of the river leakage went up 4% in 2004 and 5% in 2006, respectively (Figure 12, 13)

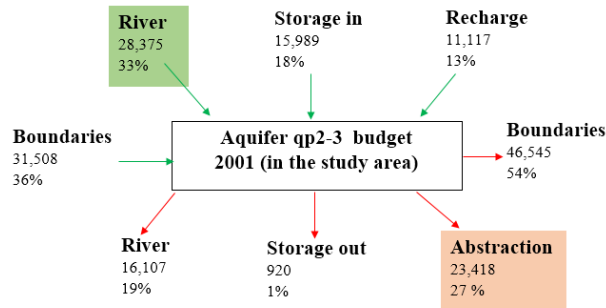


Fig. 11 Water balance of aquifer qp2-3 in study area (2001)

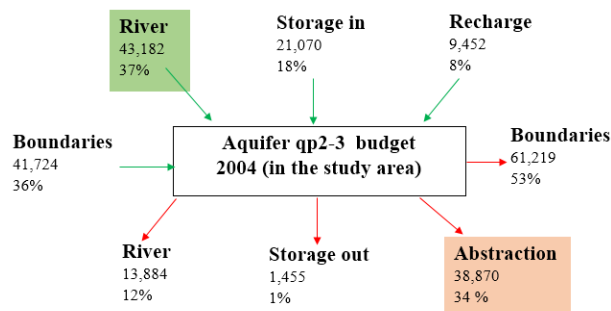


Fig. 12 Water balance of aquifer qp2-3 in study area (2004)

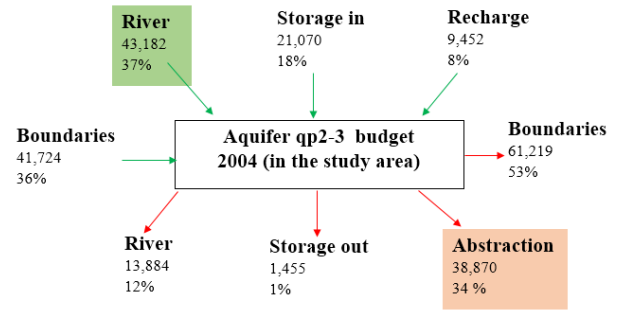


Fig. 13 Water balance of aquifer qp2-3 in study area (2006)

Application 2: River and aquifer qp2-3 interaction

The river recharge in wet season always was higher the one in dry season in the period from 2000 to 2007 with average difference ratio between two seasons approximately 7% (Figure 14). Pumping induced more river recharge and gave the same to tendency to increase rapidly from 2000 to 2007. In contrast, the changing storage declined from 8,340 m³/d in 2000 to 24,129 m³/d in 2007 (Figure 15).

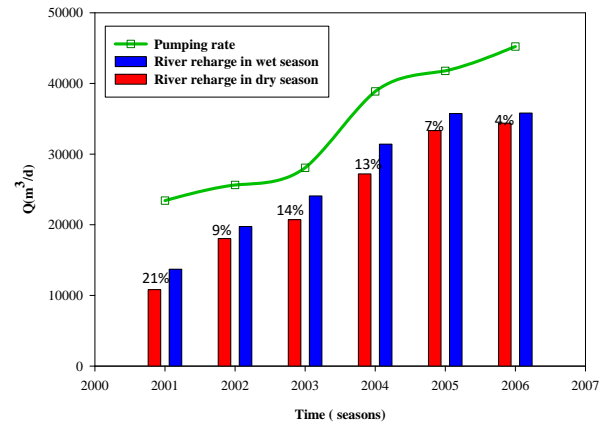


Fig. 14 Comparison of river recharge and pumping rate in dry season and wet season during 2000 to 2007 (Figure)

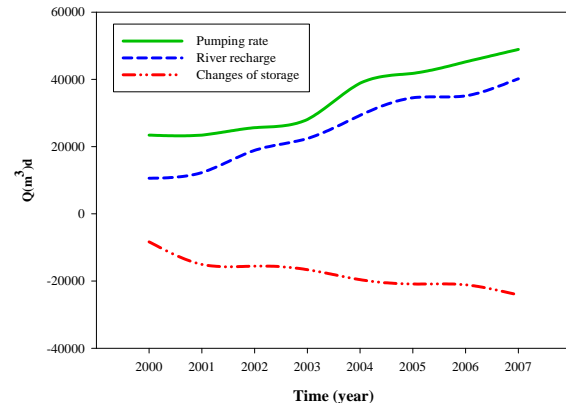


Fig. 15 Comparison of pumping rate, river recharge and changes of storage in period 2000 - 2007

Conclusions

From groundwater modeling, hydraulic conductivity estimation of riverbed in the study area is 0.0061. Besides, The values of the conductance value in the range of 1.1 to 1.3 and can be applied for future groundwater modeling in Saigon River area.

In aquifer qp₂₋₃, pumping rate went up rapidly, so the changes of groundwater storage also has negative values and decreases every year during the period from 2000 to 2007. The accumulative changes of groundwater storage reduces from -8,340m³/d in 2000 to -24,129m³/d in 2010, the decrease rate is 15,790 m³/d.

Acknowledgement

The author would like to acknowledge the support from the Department of Water Resources Engineering, Chulalongkorn University. This paper is developed as a part of master programme funded by 72nd King's Birthday Scholarship of Chulalongkorn University. This research cannot be concluded without data from the Division for Water Resources Planning and Investigation for the South of Vietnam (DWRPIS) and therefore we would like to extend appreciation to DWRPIS for the support.

References

- Boehmer, (2000). Surface water data and processing for the hydrogeological model of the Mekong delta. Haskoning B.V. Consulting Engineers and Architects, in association with Division for Water Resources Planning and Investigation for the South of Viet Nam.
- Chan, N. D. (2008). Applied Groundwater modeling method to estimate Groundwater reserves on Ho Chi Minh City and Neighborhoods area. 6949/KQ-TTKHCN. V. N. Division of Water Resources Planning and Investigation for the South of Vietnam. Ministry of Natural Resources and Environmental.
- Chan, N.D. (2015). Water resources planning in Binh Duong province. Division for Water Resources Planning and Investigation for the South of Viet Nam.
- Chinh, N. K. (2012). Use of the isotope techniques to study Groundwater Recharged Availability in Hochiminh City Area: Department of Isotope Hydrology, Center for Nuclear Techniques in Ho Chi Minh City.
- Heath, Ralph C. Basic ground-water hydrology. Vol. 2220. US Geological Survey, 1983.
- Fox, Garey A., Derek M. Heeren, and Michael A. Kizer. Evaluation of a stream-aquifer analysis test for deriving reach-scale streambed conductance. Transactions of the ASABE 54.2 (2011): 473-479.
- Khai, H. Q. (2015). Impact of climate change on groundwater recharge in Ho Chi Minh city. Master Thesis, Chulalongkorn University.
- Lackey, G., R. M. Neupauer and J. Pitlick (2015). Effects of streambed conductance on stream depletion. Water 7(1): 271-287
- Long, N. T. (2014). Water resources development planning under surface water and groundwater interaction assessment in Con Son Valley, Con Dao Island, Ba Ria-Vung Tau province, Viet Nam. Master, Chulalongkorn University.
- Qiu, Shuwei, et al. Numerical Simulation of Groundwater Flow in a River Valley Basin in Jilin Urban Area, China. Water 7.10 (2015): 5768-5787.
- Pérez-Paricio, A., et al. Estimation of the river conductance coefficient using streambed slope for modeling of regional river-aquifer interaction. Proc., 18th Int. Conf. on Water Resources, International Center for Numerical Methods in Engineering, Barcelona, Spain, Google Scholar. 2010.
- Winter, T. C. (1998). Ground water and surface water: a single resource, DIANE Publishing Inc.
- Yager, Richard M. Estimation of hydraulic conductivity of a riverbed and aquifer system on the Susquehanna River in Broome County, New York. No. 2387. USGPO; US Geological Survey, Book and Open-File Report Sales [distributor], 1993.
- Vuong, B.T. (2010). Reconstruction of Geology map, hydrology map, and Geotechnical map with scale 1: 50.000. Division for Water Resources Planning and Investigation for the South of Viet Nam.

Estimation of Hydrological Parameter Distribution by Geostatistical methods in the Upper Central Plain, Thailand

Pwint Phyu Aye ^{1,a *}, Sucharit Koontanakulvong ^{2,b}

Abstract Thai farmers traditionally relied on rain and flood water for crops, but the water amount needed for rice cultivation was not adequate in dry years and, thus, used groundwater as supplement. Groundwater model is necessary to assess the groundwater potentials in this area. Groundwater flow models require specification of several input parameters. The problem of estimating hydrological parameter distribution, in particular, hydraulic conductivity, from input-output measurements is re-examined in a geostatistical framework. The structure of the parameter field is identified, mathematically representations of the semivariogram. Linear estimation theory is applied to provide minimum variance and unbiased point estimates of hydrogeological parameters ('Kriging') to obtain the distributed conductivity field. This study used the bore logs data of 1128 observation wells in the area. The estimated hydraulic conductivity distribution are verified with the observed piezometric heads and simulated values from the regional groundwater model. This study focuses on the estimation of hydrogeological parameter distribution in regional groundwater modeling in the study area. The estimated hydrogeological parameter distribution will improve the quality of groundwater modeling in the study area.

Keywords *hydrogeological parameter, distribution, geostatistical method, groundwater modeling*

Pwint Phyu Aye
Department of Water Resources Engineering
Faculty of Engineering, Chulalongkorn University
Bangkok, Thailand
Email: pwintphyuaye89@gmail.com

Sucharit Koontanakulvong
Department of Water Resources Engineering
Faculty of Engineering, Chulalongkorn University
Bangkok, Thailand
Email: sucharit.k@chula.ac.th

Introduction

Upper Central Plain is the most important area for Thailand's economy. It is also the most agriculturally productive area without its own large water sources. Demand for water in this area far exceeds locally available supply. The area therefore depends heavily on water from river basins upstream. Groundwater in this area is mainly recharged by rainfall and stream seepages. Aquifers supply a large amount of water throughout Thailand. There is limited information on groundwater extraction rates at the national level. A number of canals had been constructed in the Central Plain and other canals were dug. The canals did not form a controlled irrigation system, however, but simply a distribution net, and whether additional water could be made available depended on the level of the rivers. The local farmers depended on both surface water and groundwater sources especially in the dry season. Most farmers turned to use groundwater to supplement irrigation water. Farmers cultivate paddy all year round and need irrigation water supply to match with crop requirement all time. They face the water shortage from surface water allocation in these areas. The purpose of this paper is to analysis regional groundwater model with the geostatistical method for parameter estimation. This paper focuses to estimate the hydrological parameter distribution, in particular, hydraulic conductivity, from input-output measurements by applying MODFLOW and using the geostatistical framework.

Study area

The study area, Upper Central Plain is located in the Northern part of Chao Phraya Plain covering the areas of Sukhothai, Phitsanulok, Kamphangphet, Pichit, and Nakornsawan Provinces. Total area is 47,986 square kilometres. Average height is approximately 40-60 meters above mean sea level. It is composed of five basins that are Lower Ping basin, Lower Yom basin, Lower Nan basin, Upper Sa-Gae-Grang basin, and Upper Chao Praya basin. The main rivers in the study area are the Yom River (West) and the Nan River (East) which are parallel flow from North to South, as shown in Fig. 1.

Aquifer Characteristics

The aquifer system in this study was defined as semi unconfined layer with three deposit types whereby the thickness is 40m. The 3D block-cent red grid model representing the groundwater basin has a grid size 10km ×10km, resulting in 672 elements in the layer. (Fig. 2) The western, eastern and northern borders of the model assumed as an impermeable consolidated rock and were defined as specific inflow boundaries (total 587 million m³/year) derived from the available head distribution along these boundaries. The southern

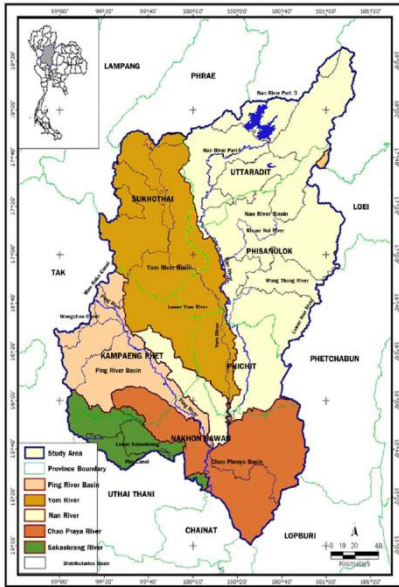


Figure 1. Upper Central Plain Basin

boundary, which is partially blocked by impermeable rocks and forms a narrow trough between the mountains in the east and west, was set as an outflow boundary. (Koontanakulvong S, et.al, 2006). In this study, there are 1128 of well data, 108 of monitoring wells and 10 full pumping test wells to be used for calibrations.

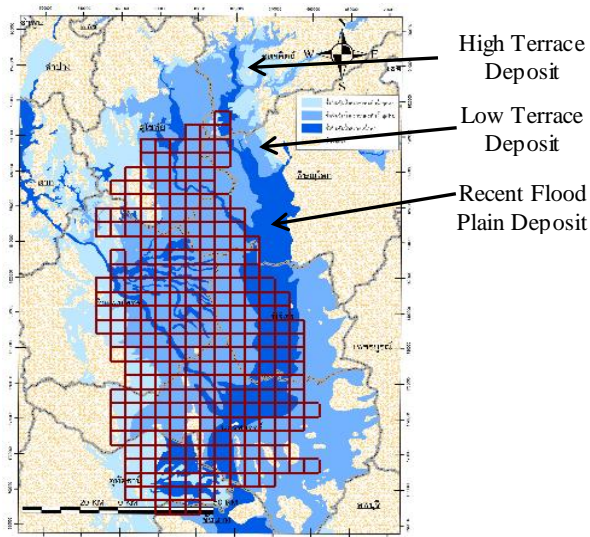


Figure 2. Model Grid Design and aquifer characteristics

Methods and Equation Used

Hydrogeologic approaches were employed to estimate the values of aquifer parameters such as specific yield (S_y), transmissivity (T), and hydraulic conductivity (K) from pumping test. Groundwater levels were taken from historical records during 1993 - 2003. In order to explore the model, we estimated the transmissivity from well data (with low pump test data) and pump test (full pumping test) data due to limited pumping test data by using this equation and find constants (a and b).

$$T = a(S_c)^b, \quad (1)$$

$$S_c = \frac{Q}{\Delta S \times L} \quad (2)$$

where,
 Q = discharge (m³/d)
 ΔS = drawdown (m)
 L = screen length of the well (m)
 T = Transmissivity

The hydraulic conductivities are generated from the aquifer data and optimize the hydraulic conductivities in the steady state with known observed peizometrics. Transient state regional model calibrations are preceded by using geostatistical tools to distribute hydraulic conductivities in the model area and selected the appropriate methods and hydraulic conductivity distribution for regional groundwater modeling. Finally the regional groundwater flow model was computed with best geostatistical interpolation.

Groundwater modeling

Groundwater model is used to predict aquifer response, in terms of head (ground water level) and fluxes into and out of an aquifer, to natural and human induced stresses. The three-dimensional movement of ground water of constant density through porous earth material may be described by the partial differential equation.

$$\frac{\partial}{\partial x} \left[K_{xx} \frac{\partial h}{\partial x} \right] + \frac{\partial}{\partial y} \left[K_{yy} \frac{\partial h}{\partial y} \right] + \frac{\partial}{\partial z} \left[K_{zz} \frac{\partial h}{\partial z} \right] + W = Ss \frac{\partial h}{\partial t} \quad (3)$$

Where

K_{xx} , K_{yy} and K_{zz} are the values of hydraulic conductivity along the x , y , and z coordinate axes and are function of space. h is the potentiometric head (hydraulic head).

W is a volumetric flux per unit volume representing sources and/or sinks of water, where negative values are water extractions, and positive values are injections. It may be a function of space and time (i.e., $W = W(x, y, z, t)$).

S_s is the specific storage of the porous material and is function of space and t is time. The Equation, together with specification of flow and head conditions at the boundaries of aquifer system and specification of initial head conditions, constitutes a mathematical representation of groundwater flow system.

Kriging Method

Kriging is one of the important geostatistical techniques which have been applied to many hydrogeologic problems for estimation and sampling purposes. This algorithm is basically a statistical interpolation technique. Presentation errors map and variance reduction in weighting for estimating is the benefits of Kriging against others interpolation methods. Errors in this method are independency from variable and dependent to spatial location and it cause to predict the best location sampling is possible. Variogram relationship based on the measured points is as follows:

$$\gamma(h) = \frac{1}{2n(h)} \sum_{i=1}^{n(h)} [z(x+h) - z(x)]^2 \quad (4)$$

where:

$\gamma(h)$ is the variogram for a distance (lag) h between observations $z(x)$ and $z(x+h)$.

$n(h)$ is the number of pairs of observations which are at distance h .

$z(x)$ is the observed variable. $z(x+h)$: the observed variable is the h distance from $z(x)$ and variogram $\gamma(h)$.

Natural Neighbor Method

Based on the natural neighbor coordinates, Robin Sibson developed a weighted average interpolation technique that he named natural neighbor interpolation (Sibson, 1980, 1981)

$$G(x,y) = \sum_{i=1}^n W_i f(x_i,y_i) \quad (5)$$

where:

$G(x,y)$ is the NN estimation at (x,y) ;
 n is the number of nearest neighbors used for interpolation;

$f(x_i,y_i)$ is the observed value at (x_i,y_i) ; and
 w_i is the weight associated with $f(x_i,y_i)$.

Inverse Distance Weight Method

Inverse Distance Weighting (IDW) is one of the interpolation techniques. It explicitly implements the assumption that things that are close to one another. It assumes each measured point has a local influence that diminishes with distance. It weights the points closer to the prediction location greater than those farther away, hence the name inverse distance weighted. Weight of each sample point is an inverse

proportion to the distance (Peter K. Kitanidis and et. al., 1983). IDW is given by

$$W_i = \frac{1/(d_i)^p}{\sum_{i=1}^n (1/(d_i)^p)} \quad (6)$$

where,

d_i is the distance between the estimated point and the sample, and (p) is an exponent parameter.

Results and discussion

(1) Steady State

The hydraulic parameters estimated from Equation (1) (with $a=14.05077$, $b=1.1477$) were put into the model and by using optimization scheme; the computed heads were compared with the observed data. Results of recalibration model show that simulation values were closed with observation data compared with the former and pumping test in Equation (1) for hydrological parameters estimation in steady state.

The model was calibrated in the steady state and, after optimization, gave the good performance when compared with the observed data (Figure 3).

(2) Geostatistical Interpolation

The main procedures are the Kriging methods by using variogram, to know how similar or dissimilar the measurement values of adjacent data points are as a function of their distance from each other. Correlation to the prior estimate is accomplished by adapting observed system response data from the true system, merging the model calculated and observed values. This correlation depends on the uncertainly attached to both the prior estimate (the model results) and the true values (the observations form the true system). The correlation made to the model calculated values by the observed values is dictated.

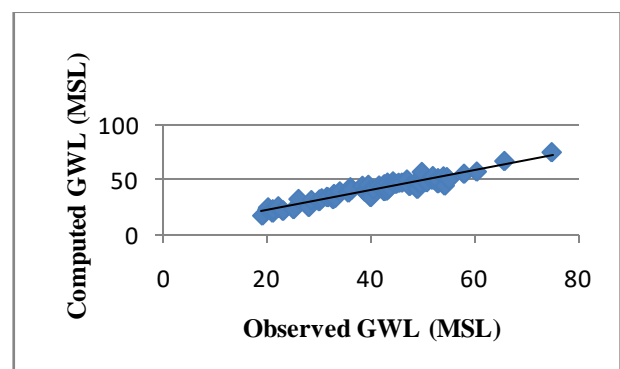


Figure 3. Comparison of computed and observed GWL in the steady state

(3) Hydraulic Conductivity Estimation

Estimated hydraulic conductivity distribution by using geostatistics methods such as IDW, NN and Kriging with steady and transient and choose the good method based on mean error is shown in table 1. The mean error is range from 0.1 to

0.4. But a result of Kriging is better than natural neighbour and inverse distance weight. According to good performance, Kriging method is selected to interpolate hydraulic conductivity in the groundwater model as Figure 4.

Table 1. Comparison among methods for hydraulic conductivity distribution

	IDW	Natural Neighbor	Kriging
Minimum	3.671874	2.7	4.449543
Maximum	24.72096	28.46214	18.54053
Mean Error	0.362889	0.20012	0.104132
Mean abs. error	3.62037	3.72547	3.51397
Root Mean Square Error	5.79154	5.97338	5.49893
Rank of performance	3	2	1

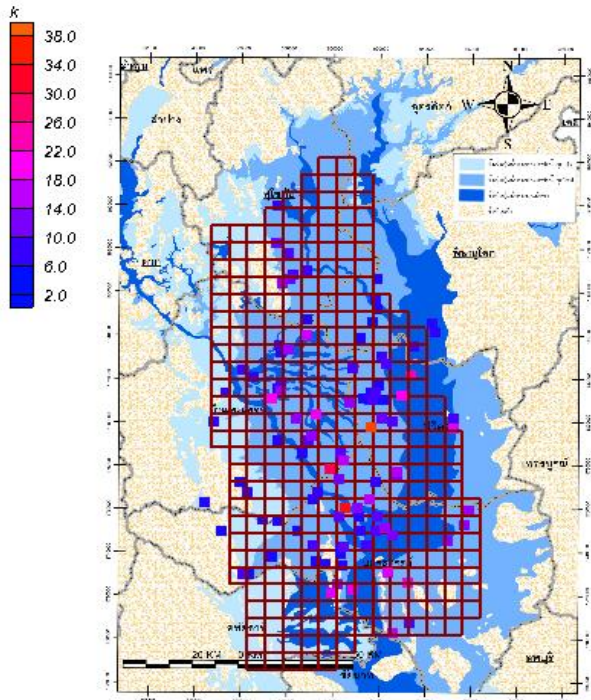


Figure 4. The distribution corresponded well with aquifer characteristics.

The hydraulic conductivity along the river is higher than in the mountains. The hydraulic conductivity value in the river is from 14 to 36 m/d. While in mountains area, hydraulic conductivity distribute from 2 to 14 m/d. The distribution of hydraulic conductivity with Kriging method in the study area is shown in Figure 5 and is similar to the observed data.

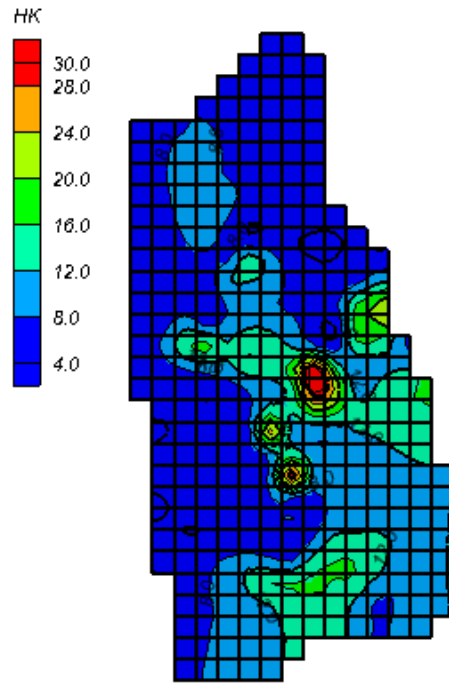


Figure 5. Hydraulic Conductivity Distribution with Kriging Method

(4) Groundwater model calibration

Groundwater flow model (MODFLOW) was used to simulate groundwater flow conditions in the area during the period 1993-2003. This model was developed by Koontanakulvong S., et.al. 2006. Input data included river water level, observation groundwater level and hydraulic conductivity. In this study, the model was recalibrated and compared with observation data using hydraulic conductivity.

(5) Transient State

Similar with the result in the steady state, the computed GWL values are closely relation with the observed data in the transient state. The total error summary is shown in Table 2. The mean error in the both states is -0.5 which means the simulation is corresponded with the actual observed data. Hence, the Kriging Method can be applied to estimate the hydraulic conductivity in this area for further groundwater study in this area (Figure 6).

Table 2. Error Summary of Calibration Result

Error (m)	Steady State	Transient State
Mean Error	-0.43	-0.58
Mean Abs. Error	2.8	4.58
RMSE	3.42	6.85

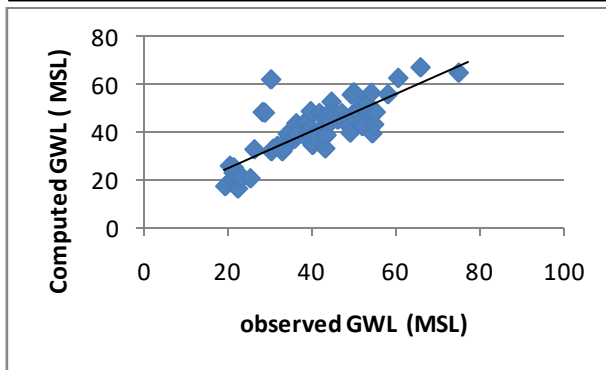


Figure 6. Comparison of computed and observed GWL in the transient state

Conclusions

This study estimate the transmissivity from well data and pumping test results due to limited pumping data by using the derived empirical formula and it was found that the empirical formula fairly estimate the transmissivity values of the well in the study area. The main procedure for hydrological parameter distribution is the Kriging method by using variogram, to know how similar or dissimilar the measurement values of adjacent data points are as a function of their distance from each other. Model calibration was preceded with steady and transient states. Estimated hydraulic conductivity distribution by using geostatistical methods is better represented by the mean error. The estimated hydrogeological parameter distribution improved the quality of groundwater modeling in the study area.

Acknowledgement

This paper could not be accomplished without the support of Ph.D. Sandwich Program scholarship from AUN/SEED-Net. The authors wish to thank the staff at the Water Resources System Research Unit, Chulalongkorn University. We also acknowledge the assistance of the Royal Irrigation Department for providing useful information on the study area. The study cannot be concluded without historical record data from the Department of Groundwater Resources.

References

- Peter K. Kitanidis and et. al., 1983, “A Geostatistical Approach to the Inverse Problem in Groundwater Modeling (steady state) and One Dimensional Simulation”, Institute of Hydraulic Research, vol. 19. No.3. pages 677-690.
- David M. Nielsen, 1991, “Practical Handbook of Groundwater Monitoring”, National Water Well Association, p17-67, 239-331, 367-395.

- Anderson, M.P., Woessner, W.W. (1992) Applied Groundwater Modeling, Academic Press, San Diego.
- Belaine, G., Peralta, R.C., Hughes, T.C. (1999) Simulation/optimization modeling for water resources management. *J. Water Res. Plann. Manage.* 125 (3), pp. 154–161.
- Arlen W. Harbaugh (2005) Modflow-2005, the U.S. geological survey modular ground-water model, the ground-water flow process, techniques and methods, USA.
- Koontanakulvong S., et. al. (2006) “Groundwater modeling for conjunctive use patterns investigation in the upper Central Plain of Thailand”, Department of Groundwater Resources. Chulalongkorn University.
- M. Moradi , D. Ghonchehpour , A. Majidi , V. Mahmoudi Nejad, 2012, "Geostatistic Approaches for Investigating of Soil Hydraulic Conductivity in Shahrekord Plain, Iran", *American Journal of Mathematics and Statistics*, Vol. 2 No. 6, pp. 164-168. doi: 10.5923/j.ajms.20120206.01

Mechanism of land subsidence due to groundwater production.

PongsakPhongprayoon

Non-affiliated, Bangkok, Thailand.E-mail: pongsakpyn@gmail.com

Abstract The major land subsidence in Bangkok and vicinity areas was thought to be due to the overexploitation of groundwater of Chao Phraya groundwater basin. The rapid declined of the piezometric pressure of the aquifers led to believe that the major land subsidence came from fine-grained compaction of aquitards that squeezed out pores water. But from the analysis of previous data, it led to another conclusion of the major land subsidence causes by coarse-grained compaction within the aquifer and supplement with fine-grained compaction from aquitards on top of the major one. Major land subsidence causes by high-capacity production well at great- depth, due to their small cross-section area of screen and without filter-pact or with inefficient filter-pact. The well of high capacity pump, small-screen area will create higher velocity of flow in the aquifer to rush through the well-screen and also bring about an aquifer sands into well causing cave and cave-in close to screen. The space of cave and high velocity of turbulent water flow to well enable the sand grains to slip or move and with the stressed of overburden pressure will compact the sand layer of the aquifer. With repeated action of sand production will lead to more sand compaction near well and spread out radially causing a depression of 1 to 2 km. in diameter in long run. The more compaction of the aquifer at each steps will create higher velocity of water that rush into the well with the same pump, the higher velocity at each steps will lower the piezometric pressure accordingly. Furthermore, the lengthy lowering piezometric pressure of the aquifer will supplement with fine-grained compaction of the enclosed and included aquitards with minor degrees of compaction. If this type of wells happened to situate nearby, it could form a network of regional depression or land subsidence like Ramkumhaeng- Bangkokapi – Ladpraow area.

Keywords *Bangkok Land Subsidence, Mechanism of Land Subsidence, Deep Well Construction*

Introduction

Chao Phraya River basin or Lower Central Plain issituated north of the Gulf of Thailand. The length of the basin is approximately 220 kilometers and 155 kilometers width covering an areal extend approximately 35,000 square kilometers. The basin was deposited with fined-grained and coarse-grained clasticsediments, in alternating and/or interbedding sequences by fluvial and flooded plain deposits, cover large portion of the central basin from north to south and extend out to intercalated with alluvial fan deposits on both sides of basin borders. There are 8 confined-aquifers that can be distinguished from the Quaternary deposits with more than 600 meters thick and thinning out into alluvial fan deposits of unconfined aquifers on east and west borders. The Bangkok and its vicinity are underlain by eight – confined aquifers system that extending to depth of > 640 m.The name of each aquifer from top to bottom are as followed:

	approximated level
1 Bangkok aquifer	30 – 60 m.
2 PhraPradaengaquifer	60 – 120 m
3 NakhonLuang aquifer	120 – 180 m.
4 Nonthaburiaquifer	180 –280 m.
5 SamKhok aquifer	280 – 360 m.
6 Phaya Thai aquifer	360 – 430 m.
7 ThonBuri aquifer	430 – 480 m.
8 Pak Nam aquifer	480 - >600 m.

Land subsidence was the case that given public attention since early 1970. The academics and authorities concernbelieved, that land subsidence almost at center of the metropolitan are caused by the over exploitation of groundwater. The lowering of piezometric pressuresgenerally related to the area of large amount or heavy groundwater production but there are also evidences indicated that the single heavy production well with some small groundwater producing wells nearby can also cause high rate of land subsidence. The phrase of “ over exploitation “ were stated or emphasized without mentioned or related to the groundwater reserves of the basin. Since there are several evidences contradicted to the assumption of land subsidence as a result of aquitard compaction related to the lowering of piezometric pressures, such as the average high rate of land subsidence at 5 cm./per annum occurred around 1978 – 1982 which groundwater production per day less than one million cubic-meters, and while average groundwater production lied in

between 1 – 2 million cubic meters the average rate of land subsidence become less at 2 cm./year, furthermore at the peak of groundwater production of 2.4 million cubic meters, the average rate of land subsidence is 1 cm./year. At some places the piezometric level from the monitor wells are high up, but rate of land subsidence also increased. All of these evidences indicates that, there must be other cause than simply over production of groundwater result to the aquifer to lose its piezometric pressure to squeeze out aquifer water and compacted.

Groundwater reserves vs. Safe Yield

In the past there are little data on groundwater reserves of Chao Phraya river basin available, on 1998 Ramnarong and others (in Thai), introduced the figure of groundwater reserves of Chao Phraya basin as $6,470 \times 10^6$ cubic meters with safe-yield of 3.5 million cu.m./day. Later on in 2005, another figures of groundwater reserves from DGR, were 277,900 million cu.m., with the annual recharge or safe yield of 15,341 million cu.m. (42 million cu.m./day). However, JICA in 1995 introduced the figure of reserve of the aquifers underlain Bangkok and its vicinity, covering an area of 7,923 sq.km. (without Nakhon Pathom) by using effective porosity (0.20) instead of average porosity (0.30) in calculation and obtained 391,074 million cu.m. Lately in 2015, DGR made some modification of groundwater reserved figure to be 269,313 million cu.m. and the annual recharge of 20,575 million cu.m., but safe yield was reduced to 15,431 million cu.m. (42 million cu.m./day)

Merely with the information of large amount of groundwater produced along with the continually declining of piezometric level without any collaboration with the amount of total reserves and/or annual recharge capability, result land subsidence had led public to be genuinely believed that we are over exploitation our groundwater resource or mining the resource. Upon groundwater reserve, let looks at the authority figure 269,313 million cu.m., which are under the basin coverage of 35,000 sq.km. in comparison with JICA's data which is 391,074 million cu.m. (using effective porosity) or could be 586,610 million cu.m. (using an average porosity), which are under the areal coverage only 7,923 sq.km., central of the basin. Base on JICA's data, groundwater resource's reserve of Chao Phraya basin, are certainly, more than trillion cubic meters or could be as high as 2 trillion cubic meters since their study area covered less than one-fourth of the basin.

Safe yield in the past is used the same figure as annual recharge but, social and economic development drove many countries to redefine their safe yield to use higher number such as 10 %, 20 % or even 30% of total reserves. But Thai authority preferred to use the figure of safe yield as 1.25 million cu.m./day, which

derived solely from mathematical modeling without any other consideration of total reserve or annual recharge or even safe yield obtained by other methods.

Causes of Land Subsidence

There must be two main causes that operated on the aquifers with the process of compaction. The first one is the major cause of land subsidence, originated from poorly designed and constructed well and send the effects down hole to the aquifer to compact sand grains of aquifer called coarse-grained compaction. The second is less intense effected on compaction, occurring slowly on the declining of piezometric pressure of the aquifer which assisted the overburden pressure to squeeze out water from aquitards that included or enclosed the aquifer to be compacted, called fine-grained compaction

The major cause (coarse – grained compaction)

During the peak period of groundwater production, more than 11,000 wells are in operation within Bangkok and its vicinity areas covering 10,300 sq.km., may be only a few tens of deep wells with high production capacity that could have caused the aquifer to be compacted, and resulted with a significant land subsidence. These wells need to have some essential parameters, such as a deep to very deep wells (<100 to 600 m), short screens length or small screen areas for water entrance, attached with high capacity pump (100 – 300 cu.m./hr.), the well may not have filter-pack or with filter-pack but wrong size or even miss-placed. These are the essentials characters of deep wells and their production that capable to lower land surface with least time. This type of compaction cause high rate of land subsidence with local coverage of 1 to 2 km². of land depressed surface, but they could be allied or connected as network if they are located nearby each other, resulted in large shallow bowl shape depression covering a few tens square kilometers.

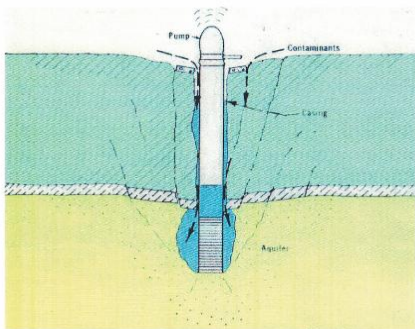
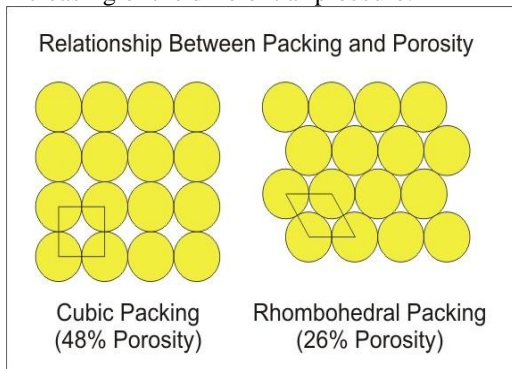
The minor cause (fine – grained compaction, supplement to the major cause)

The land subsidence result from the compaction of aquitards (fine-grained compaction) which are included and or enclosed the aquifers, are caused by decrease in the volume of the reservoir system. As water was withdrawn from the aquifer, pore-pressure decreased subjected to some deformation or compaction of the system. The land surface depression, caused by fine-grained - compaction are extensive and shallow, tens of kilometers width with low depressed center basin. However, this extensive shallow subsidence bowl accommodated several deeper local depressions formed by coarse-grained compaction within.

Mechanism of Land subsidence.

Coarse – grained compaction.

When deep wells (<150 -600 m.) with small diameter production pipe(6-8”dia.), attached with high capacity pumps(150 -300 cu.m/hr.) and also with screens of small entrance area(screen-pipe length 6-12 m.), mostly without filter-pack protection, are in operation, it will bring down the well water level rapidly. The lowering of well pressure result to the differential pressure increase between aquifer and pumping well, this will force water to rush into well faster and faster according to the increasing of the differential pressure.-

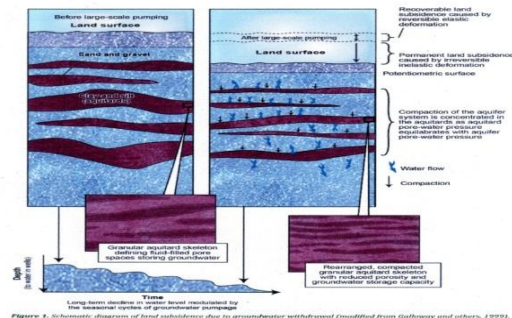


If the production well is operated with high differential pressure, the high velocity of water in turbulences form rush entrance well-screen will also help sand grains passing screen into well and some might got stuck at screens, and the reducing of screen entrance area will increase flow velocity to well. After some period of time, this sand production well, will be able to create a caving space around screens, which means the aquifer sand can withstand high stressed of overburden load because they are blocking and interlocking with another grains, but now there are some free space for sandgrains to move, by force of water that rush into well. When the outer most grains next to free space move, the next and next can be moved or slipped easily, then coarse-grained compaction is started and send the effects to spread out radially, upon the repeated process, as long as the well is in used, area surrounded will also continue to subside into a local depression. The coarse- grained compaction can be seen as similar process to cubic packing in a confined walls with 48% porosity, if the confined wall is slightly moved to provide some free space to grains, then flowing water to lubricate with dynamic force, the grains will slip to form rhombohedral packing, result to thickness and porosity reduction. Since, coarse – grained

compaction occurred within the aquifer, it also caused serious and permanent damaged to aquifers, such as porosity reduction will lead to reduced groundwater storage, and also reduced hydraulic conductivity of aquifer. Furthermore, the reduction of porosity and hydraulic conductivity combined with the operation of the same high capacity pump, producing less volume of water into well, will lead to the lowering drastically of well water level, which induced groundwaterflow to pumping well with higher speed. The high rate of declining piezometric pressure does not caused by over exploitation of our resource but came from coarse-grained compaction of aquifer, that forced water to flow faster into well, the increasing velocity of flow in the system with less volume, is the main mechanism that caused piezometric pressure to decline rapidly.

Fine – grained compaction.

Land subsidence associated with groundwater withdrawal is caused by the reduction of porosity in the aquifer system. Whenpores fluid of the aquifer move into well in high speed will add up inversely effected to fluid pressure of the aquifer, aside from the reduction of fluid volume. The difference between the total overburden stress and pore - fluid pressure determine deformation of porous media or compaction of the system, which occurred mainly to fine-grained of aquitards. However, Holzer (1981) showed that many aquifer systems in subsidence areas prior to groundwater development had naturalpreconsolidation stresses that typically required water levels to decline more than 30 m. before significant subsidence could begin.



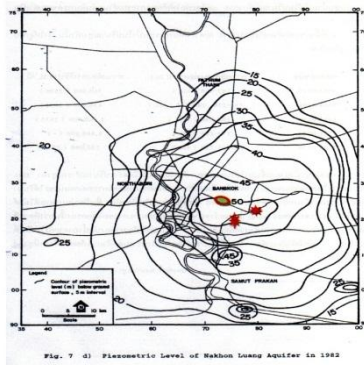
Causes of subsidence in Bangkok

The process of land subsidence is a complex phenomenon, but in Bangkok, there are two main causes to the problem.

1. Sub-standard designs and construction well, attached with high capacity pump (coarse -grained compaction).
2. Rapid decline of piezometric pressure of the aquifers cause by all wells of both up to standard and sub-standard(fine-grained compaction).

Land subsidence from deep well pumping has been affecting Bangkok for the past four

decades. Most academics and public seem to convince that land subsidence result from over-production of groundwater resource.



Around 1970 there were several housing development projects for middle to high income classes located in east and northeast of central Bangkok. The housing projects seem to be located nearby each other into cluster of build-up area. The development area did not have any provision of main-water service, each schemes had to construct their own deep-well to service communities. Many deep well were designed and constructed rather carelessly to save costs by using small size well-tube, short-length screen pipe some well without filter-pack to preventsand production, but most wells equipped with high production capacity pumps. It took a few years for the housing development projects to be completed, then most of the deep wells were operated in full capacity, some depression around wells were observed during rainy season, but nothing to be alarmed off. Finally, in 1983, when Bangkok were hit with precipitations from several storms and depressions of bad weather, the deepest flooded water(more than 2 m.depth) occupied around services well of the village(Seri Village, next to Ramkumhaeng University) where on the main road of Ramkumhaeng less than a kilometer away, water covered only 30 cm. above surface. The next well of the network cluster was belonged to a beverage company of Coke, further on 1-2 km. at LumSalee intersection, another beverage company of Fanta and Green Spots. Next, to the north approximately 1 km. closed to Bangkapi district office, there are National Housing Complexes which accommodated tenants around 20,000 – 30,000 people which also have to depend on water from deep wells. From Bangkapi along Ladpraow road to the west, there were also several deep wells of several housing villages to give services their tenants. These are an example of deep well clustered, they were attached with high capacity pumps, and most of them had history of sand as co-

production, pump-motors burnt out, deepening their suction pipes of the wells. All these evidences indicated that coarse-grained compaction originated from poorly designed and construction of deep wells to cause local, high rate of subsidence and rapid decline of piezometric pressure(additional lowering of pressure come from increasing velocity of flow to wells upon coarse-grained compaction).

Conclusion.

1. There are 2 main causes of land subsidence in Bangkok, Thailand.
 - A. Coarse-grained compaction originated from high production capacity, poorly constructed deep wells, this cause can be prevented or reduced to minimum by better designs and more careful with construction.
 - B. Fine-grained compaction cause according to the amount of water removed from aquifers, but there are some additional effects on compaction of aquitards derived from coarse-grained compaction. To keep coarse-grained stable, this additional part can be reduced or prevented.
2. There are huge amount of groundwater reserves, 1-2 trillions cubic meters lied under Chao Phraya basin, waiting to be used in needed on social and economic development.
3. Safe Yield is needs to be reconsidered more carefully with the figures recommended.

References

- Holzer, T. L., 1981. Preconsolidation Stress of Aquifer Systems in Areas of Induced Land Subsidence, *Water Resource Research* 17, no. 3 p.693-704.
- Holzer, T. L., and D. L. Galloway. 2005. Impacts of land subsidence caused by withdrawal of underground fluids in the United States, in Ehlen, J., Haneberg, W.C., Larson, R.A. (eds.), *Humans as Geologic Agents: Reviews in Engineering Geology*, 16, 87-99, doi:10.1130/2005.4016(08)
- JICA., 1995, *The Study on Management of Groundwater and Land Subsidence in the Bangkok Metropolitan Area and Its Vicinity*, Department of Mineral Resources, Bangkok, Thailand.
- Jorgensen, Donald G., 1980, *Relationships between Basic Soils-Engineering Equations and Basic Groundwater Flow Equations*; U.S. Geological Survey Water-Supply Paper 2064
- Nutalaya, P., 1989, *Land Subsidence in Bangkok during 1978-1988. Workshop on Bangkok Land Subsidence – What's next?*, 1-48..
- Price, Michael., 1996, *Introducing Groundwater*, 2nd edition, 2-6 Boundary Row, London, Chapman & Hall.
- Sucharit Koonthanakulvong, et al., 2008, *Assessment of Impacts on Enforcement of Laws on*



Establishment of Groundwater Conservation Fees in the Critical Zone of Bangkok Metropolis, Water Resources Management Research Unit, Water Resources Engineering Department, Faculty of Engineering, Chulalongkorn University.

Yong, Raymond N., Maathuis, Harm., 1995. Groundwater abstraction-induced land subsidence prediction: Bangkok and Jakarta case studies, Land Subsidence(Proceedings of the Fifth International Symposium on Land Subsidence, The Hague, October 1995). IAHS Publ. no. 234, 1995.12

Flow budget of groundwater system and conjunctive use pattern under climate change in Upper Central Plain, Thailand

Chokchai Suthidhumrajit^{1,a*}, Sucharit Koontanakulvong^{2,b}

Abstract In the Upper Central Plain of Thailand, the farmers rely on both surface water and groundwater. Because the allocated water from the Bhumibol and Sirikit Dams is limited which caused water shortage in the dry years. Most farmers turn to use groundwater to supplement irrigation water in the dry years. This study aims to understand flow budget of surface water and groundwater system and the conjunctive use pattern under climate change scenarios. The conjunctive use pattern of surface water as well as groundwater were investigated by field surveys and groundwater flow modeling. This study used the MODFLOW model for applying groundwater flow model to simulate the groundwater movement over the 10 years, and also used the bias-corrected MRI-GCM data to project the future climate condition (during 2015 -2039 and 2075-2099) and to assess the impact on groundwater system. The conjunctive use pattern of surface water use and groundwater system and the flow budget, in this study, were analyzed in term of water demand, rainfall, reservoir storage, groundwater recharge, groundwater storage and groundwater pumping in each water year pattern. The study shows the flow budget, conjunctive use pattern of each season and water year in the past and in the future under climate change scenarios.

Keywords *flow budget, conjunctive use, pattern, climate change, Upper Central Plain, Thailand*

Chokchai Suthidhumrajit
Department of Water Resources Engineering
Faculty of Engineering, Chulalongkorn University
Bangkok, Thailand
Email: chokchai.s@chula.ac.th

Sucharit Koontanakulvong
Department of Water Resources Engineering, Faculty of
Engineering, Chulalongkorn University.
Bangkok, Thailand
Email: sucharit.k@chula.ac.th

Introduction

The Upper Central Plain of Thailand covers the areas of Uttaradit, Sukhothai, Pitsanulok, Kamphangphet, Pichit, and Nakornsawan Provinces, where farmers depended on both surface water and groundwater. Because the allocated water from the Bhumibol and Sirikit Dams is limited which caused water shortage in the dry years. Most farmers turn to use groundwater to supplement irrigation water in the dry years. This also caused groundwater drawdown and make farmers to dig deeper (shallow) wells which made more cost for agriculture (Chulalongkorn, 2010). It is difficult for the downstream area to receive irrigation water through canal, thus farmers dig their own groundwater wells in their paddy fields and pumped groundwater individually to compensate surface water shortages. The focus of the paper is to understand the flow budget and conjunctive use pattern of surface water and groundwater at present and climate change impacts on flow budget and conjunctive use pattern of groundwater system in the study area.

Study area

The Upper Central Plain is in the Northern part of Chao Phraya Plain covering the areas of Uttaradit, Sukhothai, Pitsanulok, Kamphangphet, Pichit, and Nakornsawan Provinces. Total area is 47,986 square kilometers or 29,991,699 rai. Average height is approximately 40-60 meters above mean sea level. The areas consist of sediments. These sediments were generated from erosion and decay of rock, then accumulated and generated as plain, terrace, and swamp. The climate of the study area is under the influences of monsoon winds i.e. southwest and northeast monsoon. From the meteorological point of view, the climate can be divided into three seasons, i.e., summer season (mid-February to mid-May), rainy season (mid-May to October), and winter season (November begin to mid-February). The study area is composed of 5 basins that are Lower Ping basin, Lower Yom basin, Lower Nan basin, Upper Sa-Grae-Grang basin, and Upper Chao Phraya basin, as shown in Fig. 1.

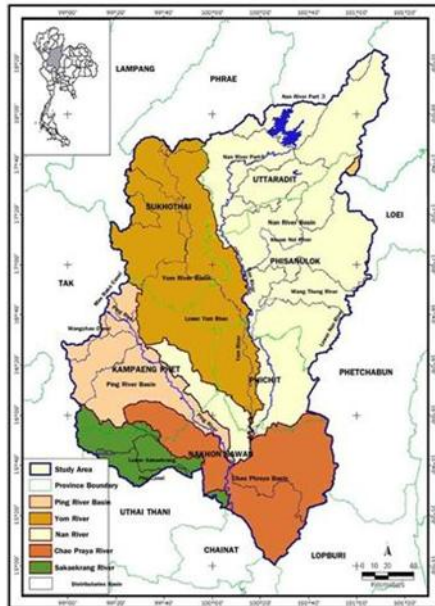


Fig.1 Upper Central Plain Basin

The main rivers in the study areas are the Yom and the Nan River which flow parallel from North to South and join at Chumsang District, Nakornsawan Province. In addition, there is the Ping River which flows from west side and joins with the Yom and the Nan River at Paknampho District, Nakornsawan Province. They become the Chao Phraya River, which continuously flow to the Central Plain. From daily and monthly rainfall data of rainfall stations (68 stations) that collected during 1974 to 2003, the amount of rainfall in the Upper Central Plain is between 900 to 1,450 mm/year. From 52 station runoff data of Royal Irrigation Department that collected during 1994 to 2003, the total runoff 15,481.9 million cubic meters per year, divided into rainy season 13,625 million cubic meters, 88% of total runoff, and dry season 1,856.9 million cubic meters, 12% of total runoff.

Methodology

To understand flow budget and the conjunctive use pattern, there are two steps in this study, i.e., first step is to simulate the impact towards flow budget and conjunctive use pattern by using the projected bias corrected the MRI GCMs climate data (Koontanakulvong S., et.al., 2011) in two future time frames, i.e., near future (2015-2039) and far future (2075-2099) periods. The improved groundwater model (MODFLOW) was applied to assess the impact of climate change on flow budget (groundwater recharge and ground water table) in the study area and to find the impact on flow budget and conjunctive use pattern. The second step is to analyze conjunctive use pattern. The conjunctive use pattern is described in term of the ratio between each water supply sources and water demand. The water supply sources are surface water, groundwater and the other. The surface water used data from the previous study (Koontanakulvong S., et. al. 2006). The

groundwater data used the groundwater model given from the first step. The other means water from other sources included water deficit which was calculated by water demand minus surface water and groundwater.

Groundwater model

The three-dimensional movement of ground water of constant density through porous earth material may be described by the partial-differential equation in the MODFLOW model.

$$\frac{\partial}{\partial x} \left[K_{xx} \frac{\partial h}{\partial x} \right] + \frac{\partial}{\partial y} \left[K_{yy} \frac{\partial h}{\partial y} \right] + \frac{\partial}{\partial z} \left[K_{zz} \frac{\partial h}{\partial z} \right] + W = S_s \frac{\partial h}{\partial t} \quad (1)$$

where

K_{xx} , K_{yy} and K_{zz} are the values of hydraulic conductivity along the x, y, and z coordinate axes (space function).

h is the potentiometric head (hydraulic head).

W is a volumetric flux per unit volume representing sources and/or sinks of water, where negative values are water extractions, and positive values are injections. It may be a function of space and time (i.e. $W = W(x, y, z, t)$).

S_s is the specific storage of the porous material (space function).

t is time.

Recharge equation

From the water budget analysis in the soil layer, The recharge can be approximated simpler by using the following equation

$$R/P = a_i * (P - ET) / P + b_i \quad (2)$$

where

R is recharge,

P is precipitation,

ET is evapotranspiration,

a_i and b_i are constant and can be found by using goodness fit test for each soil group. (Suthidhumrajit, C., Koontanakulvong, S. 2015)

Groundwater use

The total number of shallow wells in the study area in 2003 has been 78,114 with a ratio of agricultural to domestic consumption wells of 1:3 (Koontanakulvong S., et. al. 2006) and an average daily domestic consumption of 0.71 m³/well, amounting to a total domestic-consumption from wells of 15 million m³/year in 2003. The major groundwater use in this area is for agriculture. Agricultural wells' records often do not exist and the pumping behavior is unknown, for this reason, the investigation results of the actual water use pattern, farmers' behavior and constraints, has been used to estimate the groundwater use for agriculture. The major pumping statistics retrieved from the survey which can conclude that the average pumping capacity per well is 41 m³/hour, whereas the average pumping rate per well is 79 m³/day inside the irrigation project,

and 76 m³/day outside (Bejranonda, W., Koontanakulvong, S., Koch, M., Suthidhumajit, C., 2007). The historical yearly record of the wells in each province during 1993-2003 has been converted to a growth rate of the wells for the future. As mentioned, besides the seasonally agricultural water use, the latter depends on the surface water supply available during the time which is related to the actual storage of two main upstream reservoirs (Koontanakulvong S., et. al. 2006), the Bhumibol and Sirikit reservoirs.

Results and discussion

Groundwater model calibration

Groundwater flow model (MODFLOW) was used to simulate groundwater flow conditions in the area during the period 1993-2003. Input data included river water level, observation groundwater level, and well abstraction used from the former project (Koontanakulvong S., et. al., 2006). The layer aquifer conceptual model and model grid design as show in Fig. 2. In this study, the model was calibrated compared with observation data using recharge equation derived. Model calibration and verification/prediction was performed in steady state as well as in transient state. Following the seasonal crop pattern, the seasonal stress period was used in the calibration of two years of recorded historical groundwater levels. Calibration in transient state has been carried out, using the 1993-2003 historical water levels, whereby groups of specific storage have been calibrated. Results of calibration model (Fig.3) show that simulation values were closer with observation data the root mean square calibration error is 3.70 m in steady-state mode and 3.9 m in transient model.

Flow Budget

Fig. 4 is the groundwater flow budget in dry season, it show that in the 1st layer, the average land recharge was 0.003 MCM/day, which lower than the discharge to the river, the average river recharge was -2.543 MCM/day. The average groundwater pump age was 2.584 MCM/day. For the 2nd layer, the average land recharge was 0.032 MCM/day, which lower than the discharge to the river, the average river recharge was -0.12 MCM/day. The average groundwater pump age was 0.125 MCM/day. The flow in boundary and flow out boundary were 0.16 MCM/day, 0.003 MCM/day and -0.241 MCM/day, 0.156 MCM/day in 1st layer and 2nd layer, respectively, and the interaction between 2 layer, there was 0.102 MCM/day flow from 2nd layer to 1st layer.

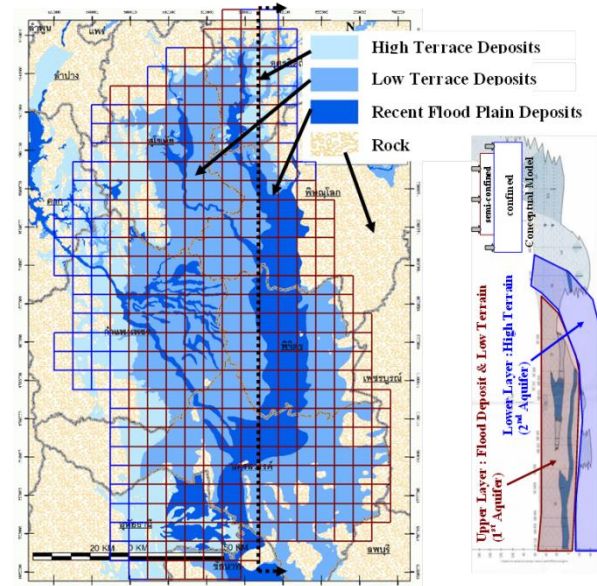
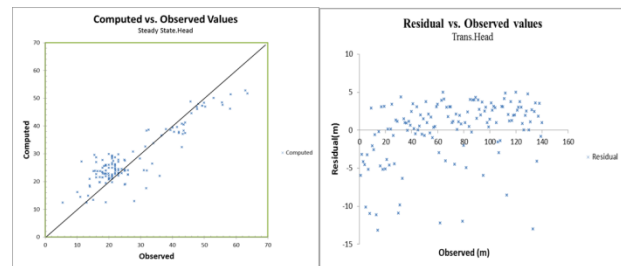


Fig.2 Layer aquifer's conceptual model and grid design



a) steady state b) transient state
Fig.3 Computed vs. Observed values in steady state and transient state

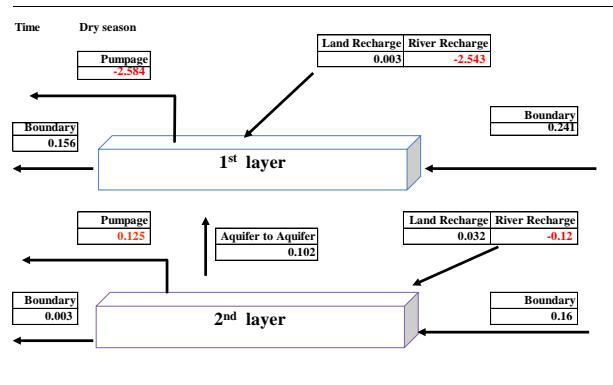


Fig.4 The flow budget in the groundwater system in dry season

From the model results of the 1st layer, which is the important layer that the farmers pumped water for their paddy field, the seasonal and annual groundwater system situations are shown as Table 1 and Fig.5. The average land recharge was 0.901, 0.011 and 0.456 MCM/day in wet season, dry season and annual respectively. But the river recharge was different from land recharge. It recharged to aquifer in wet season (0.778 MCM/day) but it received water from aquifer in dry season (-1.594 MCM/day). The average recharged rate were 0.778, -1.594 and -0.408 MCM/day

in wet season, dry season and annually respectively. The average groundwater pumpage was very high, nearly 2.0MCM/day in dry season. For these reasons, the average groundwater storage change decreased to 1.064 MCM/day annually. This was the reason that the average groundwater level in this area decreased.

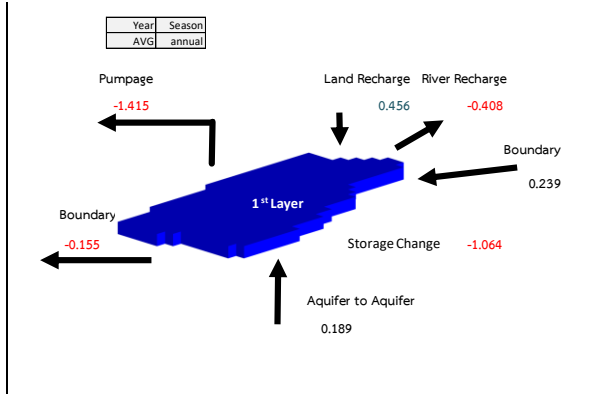


Fig. 5 The annual flow budget of groundwater system (the 1st layer) in the Present period

Table 1 The seasonal flow budget of groundwater system in the Present period (the 1st layer)

Time Period	Present Period (MCM/day)		
	wet	dry	annual
River recharge	0.778	-1.594	-0.408
GW_Storage change	1.143	-3.271	-1.064
Land recharge	0.901	0.011	0.456
GW_Pumpage	-0.838	-1.991	-1.415
Flow in (Boundary)	0.240	0.239	0.239
Flow out (Boundary)	-0.153	-0.156	-0.155
From the 2 nd layer	0.177	0.201	0.189

Impact of climate change on flow budget of groundwater system and conjunctive use pattern

Fig. 6 shows that recharge tend to decrease in the periods of both near future and far future and will be lower than in the past because of the increase of the evapotranspiration (due to higher temperature). The ratio of average recharge rate in near future and far future compare with present is 0.42, and 0.50, respectively. The heads of groundwater in the selected stations in the study area are shown in Fig. 7. It can be seen that climate change will induce lower water table in the north due to higher temperature, the water table will decrease approximately 0.23, 0.16 m/year in near future and far future periods, respectively.

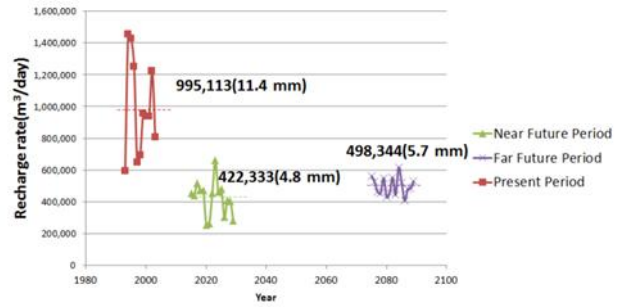


Fig. 6 The average groundwater recharge rate from projected future climate data

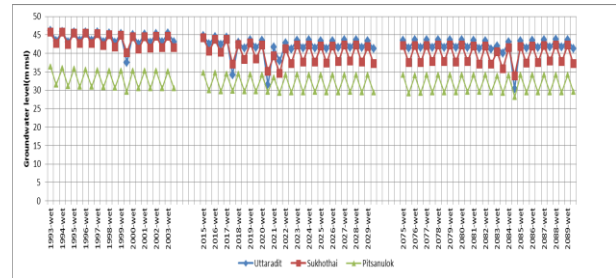


Fig. 7 The groundwater levels at selected locations

From Fig. 8, the hot spot of lower water level will occur in some part of Utrarat, Sukhothai, Phisanulok, Kamphaengphet, Pichit and Nakhonsawan Provinces, especially in upper part of Plaichumpol Irrigation Project, the decrease of water level is up to 10 m

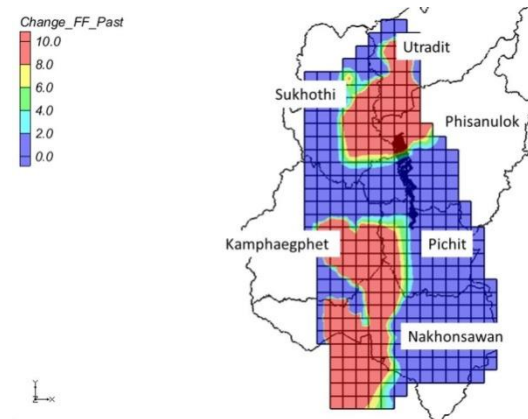


Fig. 8 The change of water level (in meter) in the aquifer by the end of far future period

The seasonal flow budget of groundwater system in the near future and far future (shown in Table 2 and Fig. 9) will be impacted from the climate change and the average groundwater pumpage will be 1.855 MCM/day in near future and it will be 1.767 MCM/day in far future, it will slightly decrease in the near future. The annual river recharge will be 0.464 MCM/day and -0.086 MCM/day in near future and far future, respectively. From these results, the groundwater storage change will be -1.128 MCM/day and -0.648 MCM/day in near future and far future period, respectively. When focused in dry season, the river recharge will be -2.923 MCM/day and -2.364 MCM/day

which means that the groundwater will recharge to the river in dry season which will gain to surface water in dry season.

other ratio and water situation from 1993-2003. In average, the ratio of groundwater use and surface water use were 0.12 and 0.63 respectively. In drought year, the ratio of groundwater use was highest (0.13-0.17) and the lowest was in wet year (0.06-0.09)

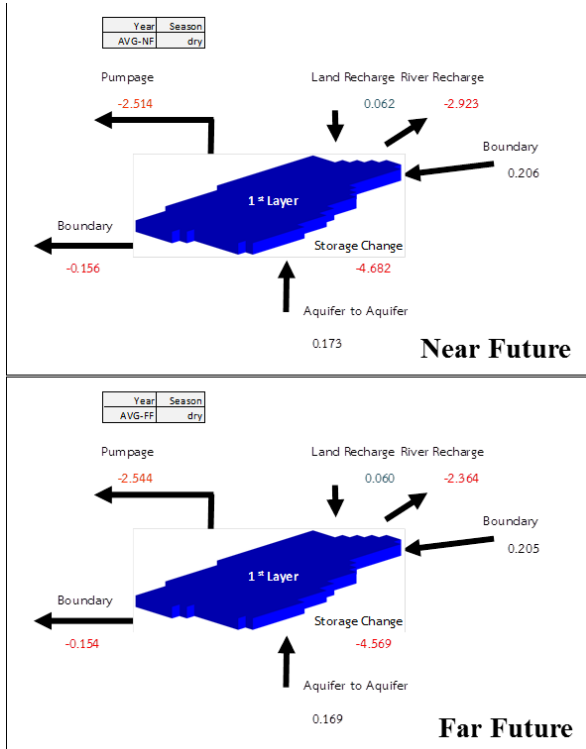


Fig.9 The flow budget of groundwater system (dry season) in near future and far future period

Table 3 The water demand, the conjunctive use pattern and water situation in 1993-2003

year	Water Demand (MCM)	GW-ratio	SW-ratio	Other	water situation
1993	3,885	0.12	0.63	0.25	Dry
1994	4,617	0.13	0.53	0.34	Drought
1995	3,775	0.09	0.68	0.23	Wet
1996	4,757	0.08	0.74	0.18	Wet
1997	4,873	0.12	0.66	0.22	Normal
1998	4,701	0.13	0.52	0.35	Normal
1999	4,535	0.17	0.64	0.19	Drought
2000	4,588	0.14	0.67	0.19	Normal
2001	4,804	0.08	0.64	0.28	Wet
2002	5,445	0.07	0.63	0.30	Wet
2003	6,159	0.06	0.63	0.31	Wet
Average	4,740	0.12	0.63	0.25	

Table 2 The seasonal flow budget of groundwater system in the near future and far future periods

Time Period	Near Future			Far Future		
	wet	dry	annual	wet	dry	annual
River recharge	2.750	-2.923	-0.086	3.293	-2.364	0.464
GW_Storage change	2.427	-4.682	-1.128	3.274	-4.569	-0.648
Land recharge	0.538	0.062	0.300	0.635	0.060	0.348
GW_Pumpage	-1.197	-2.514	-1.855	-0.990	-2.544	-1.767
Flow in (Boundary)	0.197	0.206	0.201	0.197	0.205	0.201
Flow out (Boundary)	-0.153	-0.156	-0.154	-0.154	-0.154	-0.154
From Aquifer 2	0.159	0.173	0.166	0.154	0.169	0.162

The conjunctive use patterns in the future are demonstrated in Fig.10 and Table 4. The ratio of groundwater use tends to increase in the future. The groundwater ratio will increase to 0.20 and 0.27 in near future and far future period respectively. These are attributed to the increase in water demand in the near future and far future. It means that the groundwater will have more role to mitigate the drought and as an adaptation option to climate change.

The conjunctive use pattern of the present period is showed in Table 3 and Fig.10. The table described the water demand, groundwater ratio, surface water ratio,

Table 4 The average water demand, the conjunctive use pattern in present, near future and far future periods

Time Period	Water Demand (MCM)	GW-ratio	SW-ratio	Other-ratio
Present	4,740	0.12	0.62	0.26
Near Future	5,111	0.20	0.65	0.15
Far Future	5,353	0.27	0.57	0.16

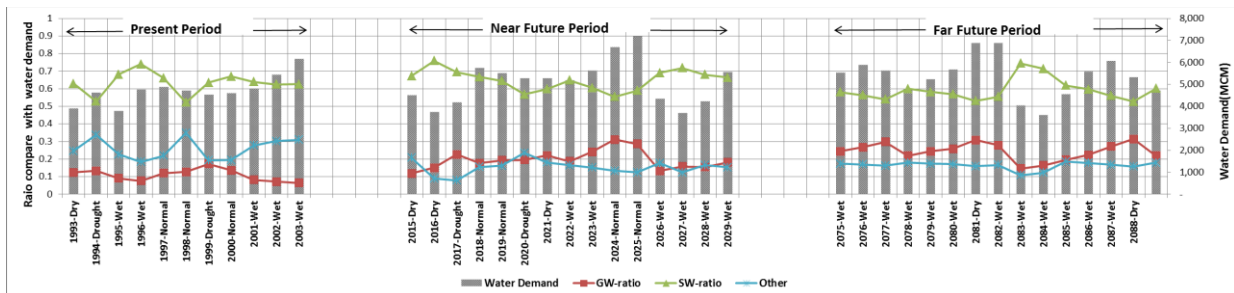


Fig. 10 The water demand, the conjunctive use pattern in Present, Near Future and Far Future Periods

Conclusions

For the flow budget of the groundwater system situation in present period, the average land recharge were 0.901, 0.011 and 0.456 MCM/day in wet season, dry season and annual respectively. But the river recharge were different from land recharge. It recharged to aquifer in wet season(0.778 MCM/day) but it received water from aquifer in dry season(-1.594 MCM/day). The 0.778, -1.594 and -0.408 MCM/day in wet season, dry season and annual, respectively. The average groundwater pump age was very high, nearly 2MCM/day in dry season. For these reasons, the average groundwater storage change will decrease to 1.064 MCM/day in annual. This was a reason that the average groundwater level in this area decreased.

The flow budget of groundwater system in the near future and far future, which was impacted from the climate change condition, show that the average groundwater pumpage will be 1.855 MCM/day in near future and it will be 1.767 MCM/day in far future. It will slightly decrease from near future. The annual river recharge will be 0.464 MCM/day and -0.086 MCM/day in near future and far future. For these results, the groundwater storage change will be -1.128 MCM/day and -0.648 MCM/day in near future and far future period respectively. When focused in dry season, the river recharge will be -2.923 MCM/day and -2.364 MCM/day which means that the groundwater will recharge to the river in dry season and this will gain to the surface water in dry season.

In the study, the conjunctive use pattern of surface water and groundwater at present was described in term of the ratio compared with the water demand. The ratio of groundwater use was highest in drought year(0.13-0.17) and the lowest was in wet year (0.06-0.09). The conjunctive use pattern in the future shows the increase in the ratio of groundwater use. Thus water use in the future will depend more on groundwater and may need more demand side management measures.

Acknowledgement

The article could not be concluded without data from various government agencies, e.g., Meteorological Research Institute (MRI, Japan), Thai Royal Irrigation Department (RID) and Thai Meteorological Department (TMD). This research has been partially support by Office of Thailand Research Fund (TRF). The research was also done under the Water Resources System Research Unit (CU_WRSRU) of Department of Water Resources Engineering, Faculty of Engineering, Chulalongkorn University.

References

- Bejranonda W., Koontanakulvong S., Koch M., Suthidhumajit, C. (2007) Groundwater modeling for conjunctive use patterns investigation in the upper Central Plain of Thailand, International Association of Hydrogeologists selected papers, Aquifer Systems Management: Darcy’s Legacy in a World of Impending Water Shortage, Taylor & Francis Group, London, UK
- Bejranonda W., Koontanakulvong S., Suthidhumajit C. (2008) Study of the Interaction between Streamflow and Groundwater toward the Conjunctive use Management: a Case Study in an Irrigation Project. 1st NPRU Academic Conference, Oct. Annals, pp. 59-67.
- Bejranonda W., Koch M., Koontanakulvong S. (2011) Surface water and groundwater dynamic interaction models as guiding tools for optimal conjunctive water use policies in the central plain of Thailand. Environ Earth Sci, 8pp.
- Chulalongkorn, Groundwater Use and Potential Study in the Lower Central Plain (2005) submitted to the Thailand Research Fund.
- Phaichumphol Irrigation Project, Phitsanulok (2009) (<http://irrigation.rid.go.th/rid3/chumpol/staff.html>).
- Chulalongkorn (2010) The Impact of Climate Change on Irrigation Systems and Adaptation Measures (Case Study: Plaichumphol Irrigation Project, Thailand), presented at JIID Seminar on Impact of Climate Change on Irrigation Systems, Bangkok, Jan 26.
- Koontanakulvong S., et. al. (2006) The study of Conjunctive use of Groundwater and Surface Water in Northern Chao Phraya Basin, Final Report. Department of Groundwater Resources. Chulalongkorn University
- Koontanakulvong S., Chaowiwat W. (2011) GCM Data Comparison and its application to water disaster adaptation measures in Thailand. Technical Report, Chulalongkorn University, March.
- Koontanakulvong S., Chaowiwat W., Mizayato T. (2013) Climate change’s impact on irrigation system and farmers’ response: a case study of the Plaichumphol Irrigation Project, Phitsanulok Province, Thailand. Paddy and Water Environ. doi: 10.1007/s10333-013-0389-8
- Koontanakulvong, S., & Suthidhumajit, C. (2015). The Role of Groundwater to mitigate the drought and as an Adaptation to Climate Change in the Phitsanulok Irrigation Project, in the Nan Basin, Thailand, In Jurnal Teknologi (Sciences & Engineering), Vol76:1No.15, 89–95
- Suthidhumajit, C., Koontanakulvong, S. (2015). Climate Change impact on groundwater recharge in Upper Central Plain and Plaichumphol Irrigation Project, Thailand, THA 2015 International Conference, 28-30 January 2015, Bangkok, Thailand

Flood Mapping along the Lower Mekong River in Cambodia

Sarann Ly, Lengthong Kim, Séverine Demerreand Sokchhay Heng

Abstract

Located in Southeast Asia, Cambodia is one of the most disaster prone countries, where flooding rank the top of the natural disaster. Flood affects and threatens not only humans' and animal's life, properties, infrastructures, but it is also an obstacle to the current development. Furthermore, without having the efficient modern technology to predict flood situation in Cambodia, the disaster in this country become more serious. The objective of this research study is to simulate flood inundation area by using software HEC-RAS. HEC-RAS is a hydraulic model software capable of calculating any hydraulic river study including flood. In this study, the Lower Mekong River with approximately 50 km length was selected to delineate flood map from 2000 until 2013 and also 10-year return period map. The available data are 11 years of the measured water level at the upstream and downstream stations, 18 surveyed cross-sections and DEM with grid cell size 30 m x 30 m were used to understand the recurrence of the floods in the study area. The output from the model was delineated into map including flood extent and flood depth from 2000 until 2013 (without 2009, 2010 and 2012). The results show that flooding varied from year to year; however, the greatest flood was during 2000 and again in 2011. The simulated flood maps were compared with observed data to figure out that the model was accurate for flood mapping. These results will be useful for river engineers, experts, and decision makers to manage river floods.

Keywords *Flooding, Flood Map, HEC-RAS Model, Mekong River, Return Period*

Sarann Ly et al., Department of Rural Engineering, Institute of Technology of Cambodia (ITC), Phnom Penh, Cambodia, ly.sarann@itc.edu.kh

Drought Risk Assessment of Irrigation Project Areas in a River Basin

Tawatchai Tingsanchali^{1*}, Thiantheera Piriyawong²

Abstract A model is developed for drought risk estimation in a river basin with an irrigation project. Drought risk is expressed as a product of drought hazard, exposure and vulnerability. Drought hazard is a function of rainfall, groundwater potential, groundwater quality and water storage in reservoirs. Exposure is the presence of irrigation system and crop areas inside or outside the irrigation project. Vulnerability or the lack of resistance damages due to drought depends on types of irrigation system, types of crop and their economic values. Vulnerability and exposure can be combined as consequences. The product of normalized hazard and consequences is called risk. The model is applied to assess drought risk in drought year of 2015 in the Munbon-Lamsae River Basin in Northeast Thailand. Monthly data in the past 30 years are collected. This includes rainfall, stream flow, groundwater potential and groundwater quality; and available water storage in reservoirs. Maps of hazard, consequences and risk conditions of the study area are computed in drought months such as in June 2015. The maps are calibrated for consistency with the actual field conditions by adjusting the weighting factors or coefficients of the model parameters. The developed model is further applied to estimate change in drought risk due change of irrigation system, for example when the types of irrigation system is changed from surface irrigation system to sprinkler irrigation system. The drought risk in the study area is significantly reduced because the sprinkler system can supply irrigation water more efficiently with less water loss.

Keywords *Drought hazard, vulnerability, exposure, risk, irrigation, Munbon-Lamsae river basin*

Introduction

Unlike floods, droughts occur slowly and their impacts can be severe and last much longer. Only limited number of research and studies on droughts has been done in the past, therefore the present study is carried out to develop a model to assess drought hazard, drought vulnerability, exposure and drought risk. Knowing drought risk in a study area, management plan to mitigate drought impacts can be setup in advance with sufficient lead time. Both structural and non-structural measures can be implemented for the purpose of drought preparedness and according to priority setting in relation to risk assessment and actual needs of the people. The developed model is a semi-empirical model considering various factors that have influence on droughts. The model requires input data commonly available, assumed values of parameters of the semi-empirical model parameters, the model results can be verified with actual field conditions. After verification, the model can be applied to predict the change in drought risks under various scenarios for decision making on drought mitigation measures. The model can be applied to other irrigation project areas for drought risk assessment and management.

Purpose of study

The main purpose of this study is to develop a model to determine drought hazard, exposure and vulnerability; and drought risk in a river basin with irrigation projects. Other purposes are to apply the model to a case study of Munbon-Lamsae River Basin in Northeast Thailand and to illustrate how the model can be used as a tool in decision making for drought mitigation in a river basin.

Study area

The Munbon-Lamsae River Basin is selected as a study area. The river basin is an upstream catchment of the Mun River Basin in Northeast Thailand. The drainage area of the Munbon-Lamsae River Basin is 2,521 km² which is a small portion of the main drainage area of 119,000 km² of the Mun River. The Munbon-Lamsae basin mainly covers Koraburi District and Chokchai district of Nakhon Ratchasima Province. The topography of the river basin slopes downward from hilly area in the south toward the

¹*TawatchaiTingsanchali

Water Engineering and Management
Asian Institute of Technology
Pathumthani, Thailand
Email: tawatchai2593@gmail.com

²ThiantheeraPiriyawong

Water Engineering and Management
Asian Institute of Technology
Pathumthani, Thailand
Email: tateetien@gmail.com

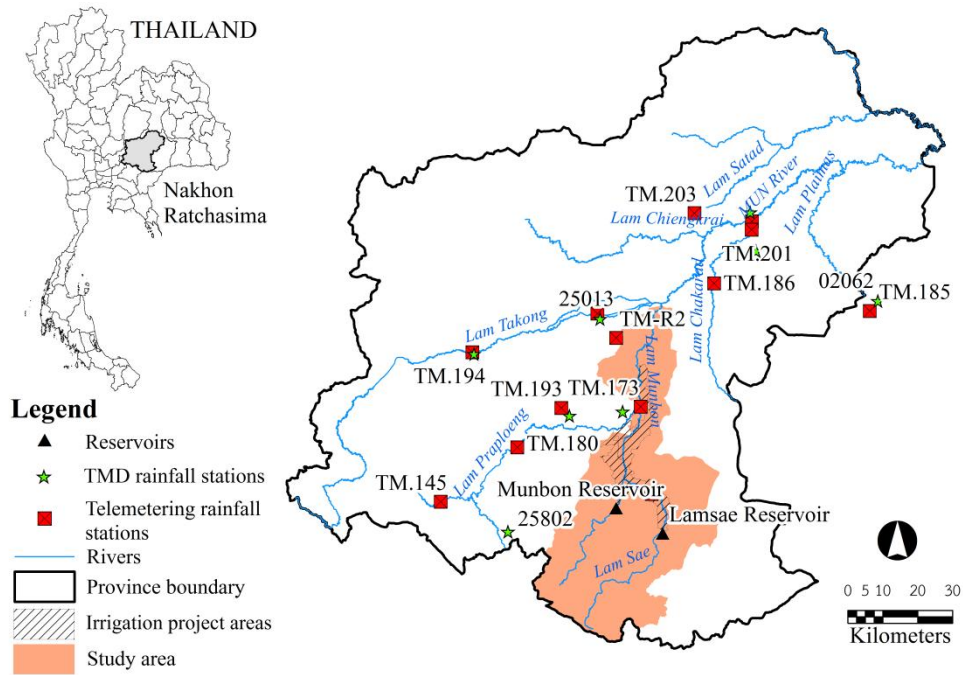


Fig.1 Munbon – Lamsae River Basin, the study area with two reservoirs and rainfall stations

plain area in the north. The Munbon River is the main river of the river basin. It is joined by its tributary namely the Lamsae River on its way as it flows downslope before joining with its mother river: the Mun River. The overbank areas on both sides of the Munbon and Lamsae Rivers are flat near the rivers and then slowly sloping upward away from the river banks on both sides.

The Munbon-Lamsae River Basin is under the influence of tropical monsoons and tropical cyclones in which rainy season starts from mid of May to end of October. The average annual rainfall in the river basin is about 1,150 mm and annual evaporation is 1600 mm. There are two reservoirs for irrigation project of Royal Irrigation Department (RID) in the river basin namely Munbon reservoir with a storage capacity of 141 MCM and Lam Sea reservoir with a storage capacity of 275 MCM. The two reservoirs supply water for irrigation project areas of 72,222 and 18,210 hectares respectively. The map showing the river basin, the rainfall stations and the irrigation project area is given in Figure 1.

The data collected in this study includes monthly rainfall in the study area in the past 30 years; the reservoir operation data of the Munbon reservoir and the Lamsae reservoir; groundwater level and groundwater quality data; land use data; irrigation water use and type of crops, crop water requirement and crop prices.

Rainfall deficit

Over the years, many drought indices were developed and used by meteorologists and climatologists around the world (Ceglar, 2008). Those ranged from simple indices such as percentage of normal precipitation and precipitation percentiles to more complicated indices

such as the Palmer Drought Severity Index. However, it is realized that an index needed to be simple, easy to calculate and statistically relevant and meaningful. This led to the development of Standard Precipitation Index (SPI) by McKee, Doesken and Kleist (1993 and 1995). SPI is used as an indicator for estimation of deficit of rainfall or precipitation on droughts. SPI is a powerful, flexible index that is simple to calculate. Due to its reliability and high efficiency, SPI has been used by National Drought Mitigation Center of U.S.A. for drought forecast and warning. SPI is calculated by using only rainfall data to indicate effect of rainfall deficit on soil moisture, stream flow, reservoir water storage, and ground water level at different time periods. In this study, 3-month SPI values are computed for drought analysis according to user guide of WMO (1992) to show short term impact of rainfall deficit to drought condition.

Estimation of drought hazard, exposure, vulnerability and risk

Drought hazard

Drought hazard is the likelihood that a drought may occur. Here it is computed as a function of the weighted sum of four components by the following equation:

$$\text{Hazard} = R1.w1 + R2.w2 + R3.w3 + R4.w4 \quad (1)$$

Where $R1+R2+R3+R4 = 1$

Table 1. Weights and coefficients of input parameters for estimating drought hazard and consequences

No.	Parameters	Weight (R)	Conditions	Coeff. (w)			
1	SPI <-2 -1.5 to -1.99 -1.00 to -1.49 -0.01 to 0.99 >0	R1 = 0.50	Hazard	w1			
			Extremely dry	1.00			
			Severely dry	0.90			
			Moderate dry	0.80			
			Near normal	0.30			
Wet	0.00						
2	GW yield (m³hr.) <2 2 -10 10 - 20 >20	R2 = 0.10	Hazard	w2			
			Very High	1.00			
			High	0.80			
			Moderate	0.50			
			Low	0.00			
3	Total dissolved solid (mg/ l) >1,500 750 -1,500 <750	R3 = 0.10	Hazard	w3			
			High	1.00			
			Moderate	0.30			
			Low	0.00			
4	Shortage of Reservoir water Outside irri. project Inside irri. project Where D = % of available water storage with the respect to reservoir full capacity	R4 = 0.30	Hazard	w4			
			High	1.00			
5	Irri. Systems Surface irri. (furrow/border/ basin) Sprinkler Drip	R5 = 0.50	Consequences	w5			
			High	1.00			
			Medium	0.50			
			Low	0.00			
6	Crop sensitivity to drought (FAO,1989) banana, fresh green, vegetables, paddy rice, potato, sugarcane beans, cabbage, maize, onion, peas, pepper tomato, melon groundnuts, soybean, sugarbeet, sunflower, wheat cassava, cotton millet, pigeon pea, sorghum	R6 = 0.25	Consequences	w6			
			High	1.00			
			High/ Moderate	0.75			
			Low/ Moderate	0.50			
			Low	0.25			
			7	Crop price Sugarcane (9,000*) Cassava (8,510*) Corn (4,110*) Rice (3,300 *)	R7 = 0.25	Consequences	w7
						High	0.90
						High	0.85
						Moderate	0.41
						Low	0.33

*Price in Baht/rai/crop; 35 Baht=1 US dollar and 1 rai = 0.16 hectare

The principal weights R1, R2, R3 and R4 are the weights that share the influences of the following parameters on drought hazard namely: rainfall deficit, groundwater potential, groundwater quality (Total dissolved solid: TDS) and potential shortage of reservoirwater storage for crop areas inside or outside the irrigation project area respectively. The weight R1 which is related to rainfall deficit is represented by Standard Precipitation Index (SPI) as described above. While the adjusting coefficients w1, w2, w3 and w4 for the weights R1, R2, R3 and R4 are considered to have the values in the range of 0 and 1. The values of R's and w's under various conditions are given in Table 1.

In this study the values of R1, R2, R3 and R4 are assumed according to the outcome of questionnaire surveys with farmers and field conditions and their values are taken to be 0.5, 0.1, 0.1 and 0.3 respectively. The weight w1 is set according to the SPI values, while the weights w2, w3 and w4 are assigned according to the variations with time and locations of groundwater level, the amount of dissolved solids in groundwater and the available water storages in the reservoirs. The range values of w1, w2, w3 and w4 are between 0 and 1 and are shown in Table 1. The computed hazard obtained from Eq.1 over the study area is normalized between the range of its maximum and minimum values, taking the maximum equal to 1 and minimum equal to 0.

Drought exposure and vulnerability

According to IPCC (2012) and Kron(2015), exposure is the presence of people/property, vulnerability is the lack of resistance to damaging forces on human health and wellbeing; on structural or physical integrity; and on financial wealth. Vulnerability and exposure can be combined and called consequences. In this study, consequences is computed as the weighted sum of three components by the following equation

$$\text{Consequences} = R5.w5 + R6.w6 + R7.w7 \quad (2)$$

Where $R5+R6+R7=1$

The weights R5, R6 and R7 are the weighting factors of the parameters that have influences on drought consequences namely: types of irrigation systems, crop sensitivity to drought which varies with land use area and prices of crops respectively. The coefficients w5, w6, and w7 of R5, R6 and R7 are considered to have the values within the range of 0 and 1. The values of R's and w's under various conditions are given in Table 1. As shown in Table 1, the values of R5, R6 and R7 are assigned according to the outcome of questionnaire survey with farmers and field conditions. The values of R5, R6 and R7 are taken as 0.5, 0.25 and 0.25 respectively. The coefficients w5, w6 and w7 for the weights R5, R6 and R7 are specified according to the conditions of various types of irrigation systems, types of crops and prices of crops. The computed consequences obtained from Eq.2 are normalized

between the range of its maximum and minimum values, taking the maximum as 1 and minimum as 0.

Drought risk

Drought risk is defined as the product of drought hazard and consequences (Kron, 2003 and 2015) and IPCC (2012), i.e.

$$\text{Risk} = \text{Hazard} \times \text{Consequences} \quad (3)$$

The hazard, consequences (vulnerability and exposure) and risk vary with locations within the study area and with time (months). Where there are no people or values that can be affected by a natural phenomenon, there is no risk. Three basic maps can be prepared to illustrate the spatial distributions of hazard, consequences and risk for each month throughout the period of study.

For relative comparison with other case studies, the computed risks obtained from Eq.3 are normalized between the range of its maximum and minimum values, taking the maximum as 1 and minimum as 0.

Results of model application and discussions

Drought hazard maps

From the computed drought hazard over the study area, a drought hazard map is developed using ArcGIS software with a pixel size of 100 m x 100 m. Figure 2 shows an example of drought hazard map of the river basin for the month of June 2015, the month that has the most critical drought condition. As presented in the figure, the spatial distribution of drought hazard is classified by different color shading as low, moderate, high and very high. The regions of high drought hazard are in the area upstream of the Munbon and Lamsae reservoirs and also in the area far downstream outside the irrigation project. Where in the area of irrigation project, the hazard is mainly moderate and the hazard increases to high in the area outside the irrigation project area on both sides of the two rivers.

Far away from the river banks on both sides within the irrigation project, the hazard is moderate or low. The magnitude of hazard follows mainly the trend of rainfall deficit and to a lesser extent on availability of groundwater resources and groundwater quality.

Drought consequences maps

From the computed drought consequences, the drought consequences map is developed as shown in Figure 3 for example in the month of June 2015. The drought consequences are classified into low, moderate, high and very high. The spatial distribution of drought consequences in the river basin is shown by using different color shadings in the same figure. It can be seen that the region of highest consequences is mainly in the south eastern region of the river basin upstream of the reservoirs except in the area far upstream of the

reservoirs where the area is mainly forest and there is no data on the consequences. Other areas with highest drought consequences are in the far downstream areas of the Munbon and Lamsae reservoirs outside the irrigation project areas. In the irrigation project areas, the drought consequences are low compared to the surrounding region outside the irrigation project area. For the areas along both sides of the river outside the irrigation project area, the consequences are moderate.

The magnitude of consequences follows mainly the trend of type of irrigation system and to a lesser extent on types of crops and prices of crops.

Drought risk maps

The computed drought risk in the river basin area is shown in Figure 4. Same as in the hazard and consequences maps, the risk level is classified into low, moderate, high and very high. The risk levels are shown by using different color shadings. The highest and high drought risk areas scatter around in the regions just downstream of the dams. While in the irrigation project areas downstream of the dams, and along the both banks of the two rivers, the risk is low. The areas of moderate risk exist along the right bank of the Lamsae River downstream of the dam to the middle part of the irrigation project areas. The magnitude of drought risk is described by the products of hazard and consequences. Since there is no data on consequences in the forest area upstream of the reservoirs, hence the risk in this area is not calculated.

In view of risk mitigation, the risk can be reduced by introducing more efficient use of irrigation water such as by introducing sprinkler irrigation system to replace the existing surface water irrigation system.

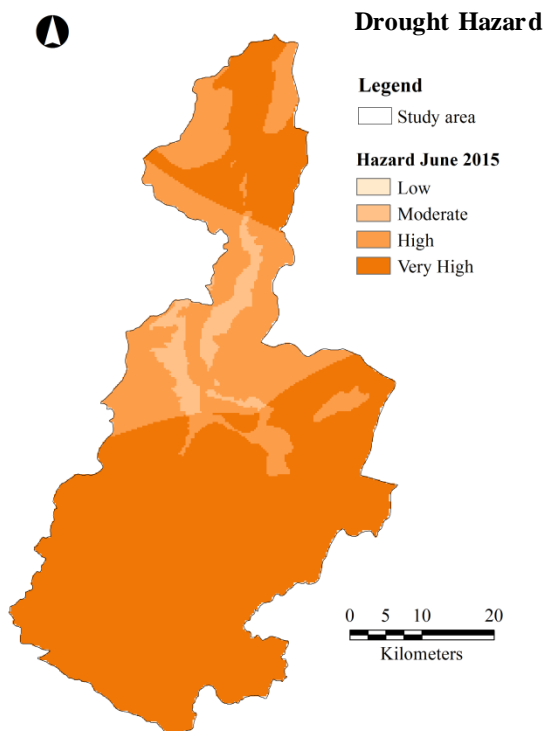


Fig.2 Drought hazard map of the study area in June 2015

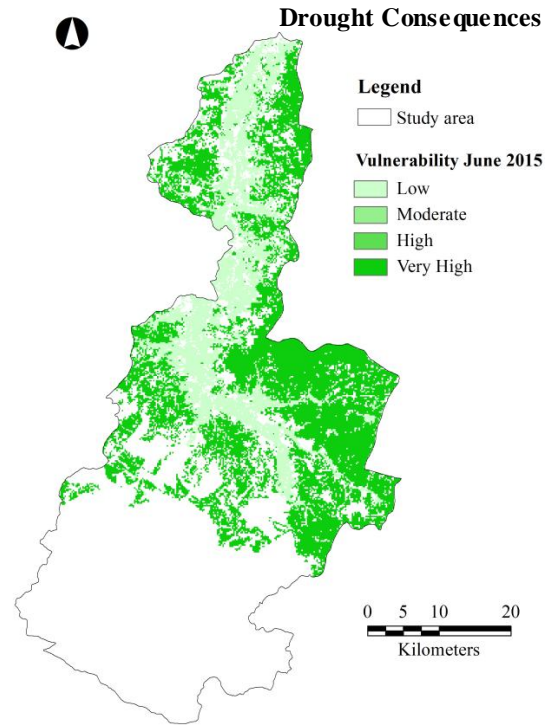


Fig.3 Drought consequences map of the study area in June 2015

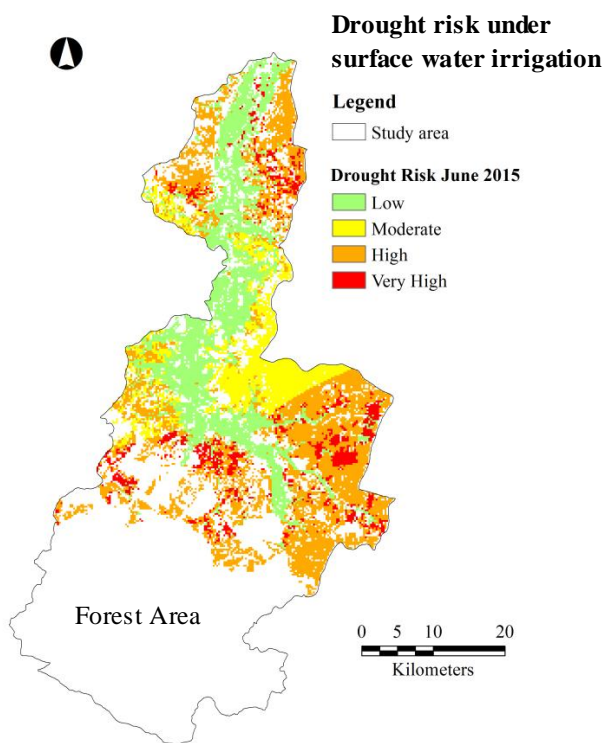


Fig.4 Drought risk map of the study area in June 2015 under surface water irrigation system

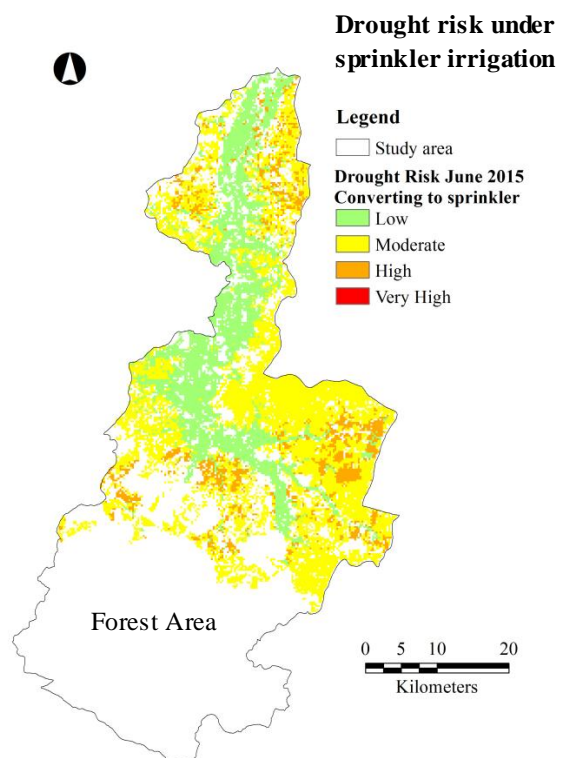


Fig. 5 Reduction in drought risk due to change of irrigation system from surface water irrigation to sprinkler irrigation system

Estimation of drought risk reduction by mitigation measures

To show how the developed model can be applied to estimate the effect of drought mitigation measures, an investigation is carried out by considering replacing the original surface water irrigation system by the sprinkler irrigation system throughout the areas inside and outside the irrigation project. Originally the area inside the irrigation project is supplied by surface water irrigation system and the area outside the irrigation project is rain fed. Groundwater is used to supplement the irrigation water where there is a need. The main crops grown in the study area in June is cassava and sugar cane. The calculation considers the same input parameters as in the original base case except the change in irrigation system as mentioned above. The results in Figure 5 show that the area outside the irrigation project which originally has very high or high values of consequences and risk, now has mainly moderate consequences and risk. Whereas in the area inside the irrigation project, the drought consequences and risk which are originally low remain unchanged. This is because the sprinkler system distributes water supply to crops more effectively and efficiently with less irrigation water losses.

Drought risk reduction can be done in many other ways such as change in types of irrigation system, types of crops, change in crop calendar, reservoir operation as well as supplementing irrigation supply by other alternative water resources.

Conclusions and recommendations

The study presents a model which can be used in determining drought hazard, consequences and risk in a river basin with irrigation project area. The method takes into account the effects of various input parameters such as rainfall deficit, groundwater storage, ground water quality and available reservoir water storage, etc. for hazard estimation. On consequences estimation, the method takes into account the effects of type of irrigation system, types of crop and crop prices, etc. The drought risk is computed as product hazard and consequences in which vulnerability and exposure are combined. The method can estimate change in consequences and risk due to change in the input parameters such as type of irrigation system from surface water to sprinkler irrigation. The computed drought risk is useful for setting up priority for drought preparedness plan and implementation. An example of application in this study provides a useful illustration how the model can be applied to determine reduction in drought consequences and drought risk. The model developed provides a useful decision making tool in assessing drought mitigation measures for irrigation projects in a river basin.

References

- Ceglar, A. (2008) Drought indices. Drought Management Center for Southeastern Europe, Biotechnical Faculty, University of Ljubljana, Slovenia.
- FAO (1989) Irrigation water management: Irrigation scheduling. www.fao.org/docrep/t7202e/t7202e00.HTM Training Manual No. 4, Natural Resources Management and Environment Department, Italy.
- IPCC Intergovernmental Panel on Climate Change (2012) Managing the Risks of Extreme Events and Disasters to Advance Climate Change Adaptation. A special Report of Working Groups I and II of IPCC/SREX/2012. Field, C. B., Barros, V., Stocker, T. F., Qin, D., Dokken, D. J., Ebi, K. L., Mastrandrea, M. D., Mach, K. J., Plattner, G. K., Allen, S. K., Tignor, M. and Midgley P. M. (eds.), Cambridge and New York: Cambridge University Press.
- Kron, W. (2003) Flood catastrophes: causes – losses – prevention from an international re-insurer's viewpoint, International Workshop on Precautionary Flood Protection Europe, Bonn, Germany, 16 p.
- Kron, W. (2015) Global aspects of flood risk management, Journal of Hydraulic Engineering, 1, David Publishing, New York, U.S.A., pp. 35-46, doi: 10.17265/2332-8215/2015.01.004.
- McKee, T.B., Doesken, N.J. and Kleist, J. (1993) Drought monitoring with multiple time scales. Ninth Conference on Applied Climatology, American Meteorological Society, Dallas, TX, U.S.A., pp.233-236.
- McKee, T.B., Doesken, N.J. and Kleist, J. (1995) The relationship of drought frequency and duration of time scales. Eighth Conference on Applied Climatology, American Meteorological Society, Anaheim CA, U.S.A., pp.179-186.
- RID Royal Irrigation Department, Munbon and Lamsae Irrigation Project, Regional Irrigation Office 8, Thailand (website <http://www.rid8.go.th/>)
- WMO World Meteorological Organization (2012) Standardized precipitation index, User Guide (M. Svoboda, M. Hayes and D. Wood). (WMO Report No. 1090), Geneva, Switzerland.

Assessment of rainfall-runoff models for streamflow predictions in the Nam Song River basin

Bounhome Kimmany^{1,a*}, Supattra Visessri^{2,b}

Abstract Flood disaster is one of the problems threatening sustainable water resources management in many parts of the world. The Nam Song River basin in Lao PDR has long been affected by floods. The severity of major floods continues to increase in recent years. This is probably be a result of changes in the pattern and amount of rainfall which is highly variable in monsoon regions. The issue is aggravated by scarce meteorological and hydrological gauges and unequally distributed of the gauges over the basin. Reliable predictions of streamflow and flood for improved water resources management in the Nam Song basin are therefore particularly challenging. The overall aim of this study is to assess the performance of rainfall-runoff models for streamflow and flood predictions under the limitation of data scarcity. Three rainfall-runoff models, HEC-HMS, IFAS and SWAT, with different complexities were tested. The hydrological data used in this study were obtained from four rainfall gauges and two streamflow gauges. The period of the study was from 1996 to 2013. The calibration period was from 1996 to 2004 for parameter estimation and sensitivity analysis and the validation period was from 2005 to 2013. The performance of the models were evaluated at two temporal resolutions including daily and monthly scales. The correlation coefficient (r) and Nash-Sutcliffe efficiency (NSE) were used as performance indices. While all the rainfall-runoff models tested in this study performed equally well for predicting daily and monthly streamflow time series, they had different capabilities in prediction high flows that might lead to flooding. IFAS outperformed HEC-HMS and SWAT when predicting high flows. Due to its best performance in predicting high flows and overall streamflow time series, IFAS was considered to be more suitable than HEC-HMS and SWAT models for flood prediction applications for the Nam Song River Basin.

Keywords ungauged basin, Nam Song River basin, rainfall estimation, rainfall-runoff model

^{1,a*} Bounhome Kimmany

Department of Water Resources Engineering
Faculty of Engineering, Chulalongkorn University
Bangkok, Thailand
bounhomekmm@gmail.com

^{2,b} Supattra Visessri

Department of Water Resources Engineering
Faculty of Engineering, Chulalongkorn University
Bangkok, Thailand
supattra.vi@chula.ac.th

Introduction

Rainfall and flow are the most important data for hydrological planning and water resources management. Given poor network of hydrological gauges and short historical records in some areas, spatial and temporal variability of rainfall cannot be well captured. Thus, modeling hydrological processes or disasters, such as flood and drought, which rely heavily on good information about rainfall as input is still a challenge.

Most natural disasters especially flooding and drought are caused by weather. Floods are the most frequent natural disasters globally (40%) followed by tropical hurricanes (20%), earthquakes (15%), and drought (15%) (CFE-DMHA 2014). The natural disasters cause loss of life and property and even causes severe economic setback especially in developing countries. Impacts of natural disasters affecting developing countries are considerably more than those of the developed countries in terms of social and economic and the situation is not likely to change in the foreseeable future (Phommachanh 2003). The Nam Song basin is one of the worst affected by the natural disaster especially flooding. In the past, Nam Song has been affected by flooding due to tropical storms causing millions in damages. The physical characteristics of the area are mountainous area in the upstream and the wetland covering the area of Vangvieng district, Vientiane Province, Laos (Phommalin 2014). The Nam Song diversion dam is located at the Nam Song River to divert water to Nam Ngum dam for generating hydropower and the release flows to the original river for multi-purposes uses. For dam operation, streamflow data are required for planning and management to reduce natural disaster. The Nam Song basin is an ungauged or poorly gauged basin. Furthermore, some existing monitoring sites are affected by human influences such as upstream abstraction. Consequently, the method for streamflow predictions is needed. Increased accuracy of rainfall estimation in this area is also contributed to an improvement in streamflow prediction (Yoshida 2016).

There are a number of rainfall-runoff models which can be applied to a basin for streamflow prediction ranging from mathematical model, statistical model, and Artificial Neural Network (ANN) model. Each model has different property, capability and complexity (represented here as the numbers of model parameters). The mathematical model uses physical and hydrological characteristics to create the relationship between rainfall and runoff. The statistical model such as multiple regression and time series analysis applies the principle of statistics to meteorological and hydrological data to generate streamflow. The ANN (Jafar, Shahrour, & Juran, 2010) model simulates complex flow behavior with non-linear regression which can be changed by time, but does not consider the basic of physical relationship of variables or statistical analysis. Model selection for streamflow analysis depends on a number of factors such as the purpose of simulation, ability of the model to serve the purpose of simulation, and researcher discretion for model application in accordance with the nature of work (Champhangkham 2012).

According to the information and problems mentioned above, this study is conducted to predict streamflow in a poorly gauged basin using rainfall-runoff models with different number of parameters. Selected models are HEC-HMS, IFAS, and SWAT models. The performances of the models are measured using r^2 and NSE. This study also investigates different methods for rainfall estimation that possibly have significant impacts on streamflow prediction. The framework proposed for this study is expected to be applicable to other basins with similar hydrological characteristics for improved planning and management of water resources at present and for the future.

Study area

Nam Song Basin as presented in **Figure 1** is a tributary of the Nam Lik River situated in Vangvieng district, Vientiane province, Lao PDR. It is the basin which receives water from the Nam Song River. The Basin area covers six districts in three provinces which are: Vientiane, Luangphabang and Xaysomboon. The maximum and minimum elevations are 1,992 m.a.s.l. (Meter Above Mean Sea Level) and 183 m.a.s.l. respectively. The Nam Song River originates from Phoukeo and flows to the west to Phatang for an approximate distance of 17 km and then flows straight to south of Vangvieng. From the south of Vangvieng to the confluence with Nam Lik at Hineheup, the river meanders along a narrow valley. The basin is located between latitudes 18°55'24"N to 19°16'00"N and longitudes 102°15'00"E to 103°38'00"E covering the total area of 1,258 km². The length of the Nam Song River to Vangvieng is about 36 km of the total length 80 km (Phommalin 2014).

The northern region of the basin is defined by extreme topography with slopes exceeding more than 30% in some areas. The southern areas from Vangvieng and

toward the Nam Lik are rolling hills that support agriculture, rice production and plantation. The major land cover of the Nam song basin approximately 40% is forest. About 25% of the area is used for agriculture, 20% for upland crop, 8% for urban, 1% for lake and river, and 6% for other uses. The dominant soil type in the upper of basin is sandy loam covering 81% of the basin. In the lower area about 11% is covered by clay loam and 4% is covered by loam. The distribution of daily rainfall over the Nam Song River Basin is highly varied. The average daily rainfall was 6.83 mm and maximum rainfall was 263.7 mm. The daily average discharge is 48.53 m³/s while the maximum and minimum are 799 m³/s and 4 m³/s respectively.

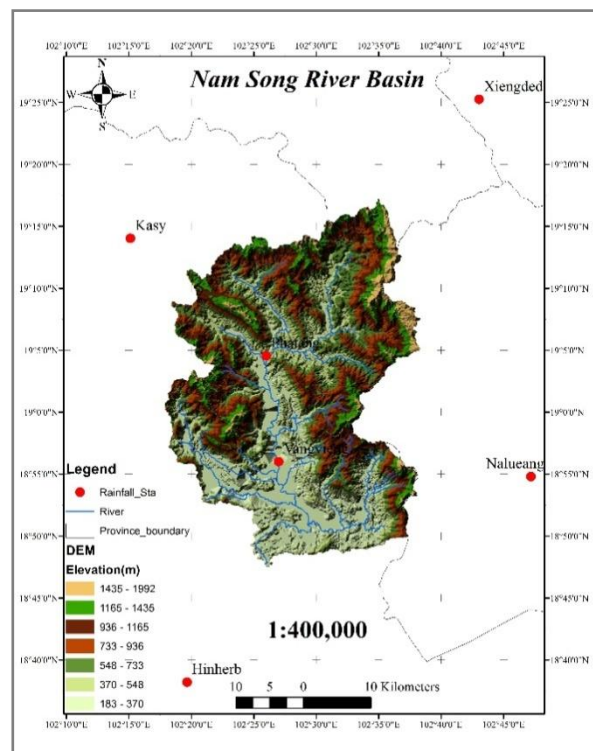


Figure 1 Nam Song River Basin

Rainfall-runoff model

HEC-HMS model

HEC-HMS (Hydrologic Engineering Center - Hydrologic Modeling System) model was developed by the US Army Corps of Engineers (Feldman 2000) that could be used for many hydrological simulations. The model of a watershed is based on water balance concept. The mathematic model is based on mass and energy flux in hydrologic cycle. Each mathematic model is included into the program for using in different environments and under different conditions. Many alternative methods are included for transforming excess precipitation into surface runoff such as unit hydrograph method, by Clark, Snyder synthetic unit hydrograph, and SCS techniques (USACE, 2010). HEC-HMS model is a lumped model designed to simulate both event and continuous simulation. HEC-HMS is comprised of a graphical user

interface, integrated hydrological analysis components, data storage and management capabilities, and graphic and reporting facilities (Beil 2001).

IFAS model

Integrated Flood Analysis System (IFAS) was developed by a collaborative research team of International Centre for Water Hazard and Risk Management (ICHARM), the Public Works Research Institute (PWRI) (ICHARM 2009). IFAS is a succinct tool with a Graphic User Interface (GUI) for building analysis distributed rainfall-runoff model. The model comprise of distributed hydrological model based on the tank model and routing model and also based on kinematic wave hydraulic model. The model provides user-friendly graphic interface for data input and output presentation, model constructing module, parameter setting function and rainfall-runoff analysis. Some input for the model such as DEM is downloadable via the model. This is therefore possible for applying it for streamflow predictions even in poorly gauged basin (ICHARM 2011). To simulate streamflow process, IFAS uses the theoretical of tank model, Manning’s law, Darcy’s law and kinematic wave methods.

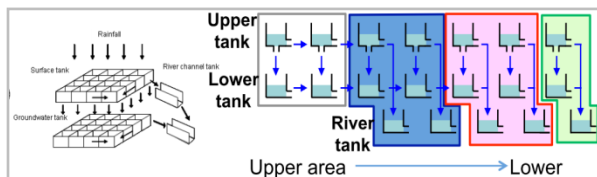


Figure 2 Schematic of distributed hydrological model (ICHARM 2011)

IFAS model Version 1 contains three layers included surface tank, unsaturated tank and groundwater tank. According to the results from previous users (ICHARM, 2011), the unsaturated tank does not need for this model so that, Version 2 contains configuration of two tanks on vertical direction. Version 2 was used in this study. Direction of streamflow is routed from upstream to downstream area by the surface and aquifer tank as shown in the Figure 2. For the river channel tank distribution is set according to four cell types and only starts in the cells defined as upstream cells.

SWAT model

Soil and Water Assessment Tool (SWAT) model was developed by the Backland Research Center (BRC), United State Department of Agriculture - Agriculture Research Service (USDA-ARS) and Texas Agriculture Experiment Station (TAES) (Koonto 2012). SWAT model was developed to predict the impact of land management on water resources, sediment chemical yield from agricultural practices in the large-complex watershed with varying of soil, land use and management over the long period of time. The model can simulate physical systems occurred over basin by dividing the large basin into sub-basins of similar land

use characteristics. In each sub-basin has at least a HRU, a main channel, a tributary channel or reach (Suwanertcharoen 2011). Hydrologic response units are a part of a sub-basin that process land use and soil attributes. An HRU is the total area in the sub-basin with particular land use and soil classes. HRUs with similar land use and soil classes are lumped together into a single response unit (S.L. Neitsch 2011). Streamflow is generated for each HRU and summed over the basin area. Figure 3 summarizes main processes for SWAT modeling.

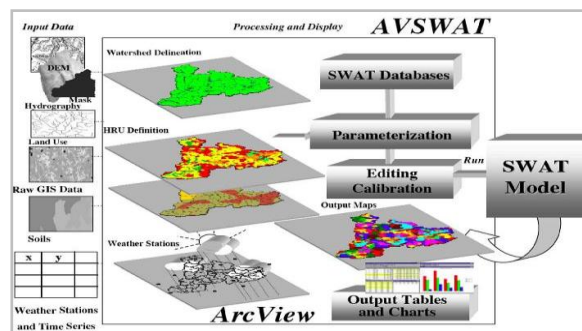


Figure 3 Processing of SWAT model (Dile 2016)

Methodology

Rainfall interpolation

Rainfall data used for this study were from 1996 to 2013 from a network of six gauge stations that located in and around the Nam Song River basin. This point rainfall data was used for estimating the average rainfall over the Nam Song River Basin by using Thiessen polygon methods.

Parameter sensitivity analysis

Sensitivity analysis was perform to evaluate the impact of model parameters on the model outputs. It was also used as a tool to assess model behavior and particularly the importance of parameterizations within the model. Generally, sensitivity analysis is widely used in the model calibration process and attempts to identify the most important parameters for hydrologic model calibration (Vilaysane 2015). Some hydrological change indices, such as discharge total volume, and peak flow (Shrestha 2016), were used for sensitivity analysis. The criteria of parameter sensitivity used in this study is shown in Table 1 defining level of sensitivity into three groups which are high, medium and low (Maharjan and S. 2015, Ram-indra T. 2015).

Table 1 Parameter sensitivity criteria

Level of change	Correlation coefficient change (%)	Nash-Sutcliffe Efficiency change (%)
Low	< 0.01	< 0.01
Middle	0.01 - 10	0.01 - 10
High	> 10	> 10

Model calibration and validation

The calibration was made for the average daily streamflow and was performed by trial and error by changing one parameter at a time and then analyzing the results. Generally, the parameter adjusting to analyze the sensitivity of model could range from +20% increasing to -20% decreasing the value of single parameter in the same proportion (Ercan 2014). Parameters were calibrated through the adjustment values until a good agreement between the observed and simulated hydrographs were achieved. For HEC-HMS and IFAS models, parameters were calibrated by trial and error method. For SWAT model, SWAT-CUP, an interface that was developed for automatic calibration for SWAT model based on the deterministic and stochastic methods, was used. A set of parameter value was initially selected for streamflow calibration as suggested by the model. Simulation streamflow were compared with observed flow.

Validation was performed by applying calibrated parameters to predict streamflow time series for the period that was not used for calibration. A testing data set was from 2005 to 2013 for validation of the model. Graphical comparisons and statistical test methods were used for evaluating the relationship between the observed and simulated flows.

Model evaluation

Several quantitative variables were used to measure model performance. By comparing observed and simulated streamflow. Choice of quantitative variables could be different depending on a number of factors such as the purpose of modeling and the preference of the modeler. For this study, the performance of the model in calibration and validation periods is assessed based on statistical measures such as correlation coefficient (r) (Takahashi & Kurosawa, 2016) and Nash-Sutcliffe Efficiency (NSE) (J. E. NASH and J. V. SUTCLIFFE).

$$r = \frac{\sum_{i=1}^n (x_i - \bar{x})(y_i - \bar{y})}{\sqrt{\sum_{i=1}^n (x_i - \bar{x})^2 \sum_{i=1}^n (y_i - \bar{y})^2}} \dots\dots\dots(1)$$

$$NSE = 1 - \frac{\sum_{i=1}^n (X_{obs} - X_{model})^2}{\sum_{i=1}^n (X_{obs} - \bar{X}_{obs})^2} \dots\dots\dots(2)$$

Input data

Input data requirements for running the selected rainfall-runoff models are presented in Table 2. The period of 1998-2013 is selected for this study due to data availability and quality. Hydrological input data, i.e. precipitation, temperature and streamflow were obtained from the Department of Meteorology and Hydrology, Lao PDR. Geographical and geological data, i.e. soil, land use, basin boundary, DEM, are requested from

National Agriculture and Forestry Research Institute of Laos (2010).

Table 2 Minimum input data requirement

Model	Data type	Data
HEC-HMS	Local data	Soil information, Land use, daily Daily precipitation Daily streamflow Basin boundary
		Daily precipitation, Daily streamflow
IFAS	Local data	DEM, Land cover, Soil types
	Global ³	DEM, land use, Soil types, Daily precipitation, Maximum and minimum temperature Daily streamflow Solar radiation, Relative humidity, Wind speed
SWAT	Local data ¹	Daily precipitation, Maximum and minimum temperature Daily streamflow
	Default data ²	Solar radiation, Relative humidity, Wind speed

Note: ¹ Local data are data observed by some units in the target area.

² Default data are existing data in SWAT database.

³ Global data are downloadable from particular websites defined by IFAS model developer

Results and discussion

Sensitive parameter

HEC-HMS model

The results of sensitivity analysis of parameters influences on streamflow (Table 3) suggested that the highest sensitive parameter were Curve Number (CN) in loss model and Muskingum X in Routing model. Curve Number (CN) affected hydrograph peaks while Muskingum X affected the time of for generating peak flows. Other parameters are categorized as middle to low sensitivity.

Table 3 Sensitivity analysis for HEC-HMS model

Parameters model	Definition	Level of sensitivity
Loss	Curve Number	high
Routing	Muskingum X	high
	Muskingum K (hr)	middle
Baseflow	Initial Discharge (m3/s)	middle
	Recession Constant	low
Transform	Lag Time (min)	low

IFAS model

The results of sensitivity analysis of parameters influences on streamflow (Table 4) suggested that the highest sensitive parameters are Final infiltration capacity (SKF) in the surface tank model and Manning’s coefficient of roughness (RNS) in the river channel tank model. Other parameters, i.e. Surface roughness coefficient (SNF), Runoff coefficient of groundwater (AGD), were found to have middle level of sensitivity. Rapid intermediate flow Regulation coefficient (FALFX) is slightly sensitive to streamflow simulation.

Table 4 Sensitivity analysis for IFAS model

Parameter	Level of sensitivity
SKF (cm/s)	high
RNS	high
AGD	middle
SNF	middle
HCGD (m)	middle
FALFX	low

SWAT model

The results of sensitivity analysis of parameters influences on stream flow suggested that the highest sensitive parameters are SCS runoff curve number (CN2), Base flow alpha factor (ALPHA_BF). Available water capacity of the soil layer (SOL_ACW), Manning’s “n” value for the main channel (CH_N2) and Saturated hydraulic conductivity (SOL_K) area moderately sensitive to predicting stream flow. Other parameters, i.e. Depth of water in the shallow aquifer required for return flow (GWQMN), Soil evaporation compensation factor (ESCO), and Surface runoff lag time (SURLAG) have little influence on simulating stream flow values. Sensitive parameters are described in Table 5

Table 5 Sensitivity analysis for SWAT model

Parameters	Level of sensitivity
CN2	high
ALPHA_BF	high
SOL_ACW	middle
CH_N2	middle
SOL_K	middle
GWQMN	low
ESCO	low
SURLAG	low

Calibration results

The results of model calibration from three selected models indicated that the simulated and measured daily streamflow values were well fitted. Statistical indices including Correlation coefficient (r), Nash-Sutcliffe coefficient (NSE), % Error on total volume and % Error

on peak flow were used to assess model performance. The values of performance indices are shown in Table 6.

Table 6 Performance indices of calibration period

Model	Performance indices			
	r	NSE	Total volume error (%)	Peak flow error (%)
HEC-HMS	0.85	0.75	7.17	5.71
IFAS	0.89	0.78	-7.81	-4.54
SWAT	0.81	0.7	6.55	5.27

Validation results

Based on the comparison between the simulated and observed daily stream flow, the performance of the three models in validation period was considered as good as that in calibration period. The daily simulation of HEC-HMS model was generally good. Based on the values of performance indices shown in Table 7, IFAS model outperformed HEC-HMS and SWAT when predicting high flows. The daily simulation of SWAT model slightly underestimated peak flow in low flow years and overestimated peak flow in high flow years. Statistical indices including Correlation coefficient (r), Nash-Sutcliffe coefficient (NSE), % Error on total volume and % Error on peak flow were used to assess model performance. The values of performance indices are shown in Table 7.

Table 7 Performance indices of validation period

Model	Performance indices			
	r	NSE	Total volume error (%)	Peak flow error (%)
HEC-HMS	0.81	0.72	1.88	6.66
IFAS	0.83	0.75	-7.15	-4.32
SWAT	0.77	0.68	9.06	7.35

Conclusion

The overall aim of this study is to assess the effectiveness of rainfall-runoff models for stream flow simulation under limitation of data scarcity. Three models, HEC-HMS, IFAS and SWAT models were used for rainfall-runoff simulation of the Nam Song River basin. The hydrological observed data used in this study were obtained from four rainfall gauges and two stream flow gauges. The period of the study was from 1996 to 2013. The training data set for parameter estimation and sensitivity analysis was from 1996 to 2004 and a testing data set was from 2005 to 2013 for validation of the models.

In over all, the three selected rainfall-runoff models (HEC, IFAS and SWAT) tested in this study performed equally well for predicting daily and monthly stream flow time series as presented in Table 6 and Table 7. However, they have little differences in predicting hydrograph components. HEC-HMS model slightly

underestimated peak flow in high flow years and overestimates low flow in recession periods. IFAS model slightly underestimated total streamflow volume in the low flow years, but it well predicted hydrographs in high flow years. SWAT model slightly underestimated streamflow volume in the low flow years and overestimates total streamflow volume in the high flow years. Focusing on the purpose of flood simulation, it might be considered that IFAS outperformed HEC-HMS and SWAT models. Due to its best performance in predicting high flows and overall streamflow time series, IFAS was considered to be the most suitable rainfall-runoff model for prediction flood in the Nam Song River basin.

Acknowledgement

First and foremost I wish to thank the AUN (ASEAN University Network) and SEED-Net (Southeast Asia Engineering Education Development Network) who has been supported scholarship for this study.

This thesis would not have been successful without data support of Department of Meteorology and Hydrology, Department of Geology and Minerals, and National Agriculture and Forestry Research Institute, Lao PDR. I am grateful to thank for supporting me the data.

I would like to thank my supervisor, Asst. Prof. Dr. Anurak Sriariyawat and Dr. Supattra Visessri whom have been given me valuable guidance and useful suggestion for my life and research.

Finally, I also would like to thank all teachers and official staff in Water Resources Engineering Department, Chulalongkorn University for their encouragement and insightful comments.

References

CFE-DMHA (2014). Lao PDR Disaster Management Reference Handbook. Center for Excellence in Disaster Management and Humanitarian Assistance.
 Champathangkham, S. (2012). Hydrological modeling of Xebangfai River Basin in Lao PDR using SWAT model. Master.
 Dile, Y. (2016). "Introducing a new open source GIS user interface for the SWAT model." *Environmental Modelling & Software* 85: 129-138.
 Ercan, M. B. (2014). "Calibration of SWAT models using the cloud." *Environmental Modelling & Software* 62: 188-196.
 Feldman (2000). Hydrologic Modeling System HEC-HMS: Technical Reference Manual, US Army Corps of Engineers, Hydrologic Engineering Center.
 ICHARM (2009). Integrated Flood Analysis Systems IFAS Version 1.2 User's manual. P. d. h. model.
 ICHARM (2011). Integrated Flood Analysis Systems (IFAS) System Instruction Guidebook.
 Jafar, R., Shahrou, I., & Juran, I. (2010). Application of Artificial Neural Networks (ANN) to model the

failure of urban water mains. *Mathematical and Computer Modelling*, 51, 1170-1180
 Koonto, S. (2012). Estimating water runoff from CA-MARKOV predicting land use using SWAT model: case study of Huaytunglung watershed in the Mun River Basin.
 Maharjan, M. et al. (2015). Impact of the Uncertainty of Future Climates on Discharge in the Nam Ou River Basin, Lao PDR.: 65-87.
 Phommachanh, B. (2003). Droughts and Flood in the Lao People's Democratic Republic, WAD, DOR, MCTPC, Vientiane Laos.
 Phommalin, L. (2014). Hydrological study in Nam Song River Basin by using HEC-HMS model. Bachelor, National University of Laos.
 Ram-indra, T. (2015). Spatial design rainfall for rainfall-runoff model in Yom River Basin. Master, Chulalongkorn University.
 Shrestha, M. K. (2016). "Assessing SWAT models based on single and multi-site calibration for the simulation of flow and nutrient loads in the semi-arid Onkaparinga basin in South Australia." *Agricultural Water Management* 175: 61-71.
 Suwanlertcharoen, T. (2011). Application of the SWAT Model to evaluate runoff and suspended sediment from a small watershed: A case study of Mae Phun Sub-watershed, Laplae District, Utradiit Province. Master, Kasetsart University.
 S.L. Neitsch, J.R. Williams (2011). Soil and Water Assessment Tool: Theoretical Documentation Version 2009. T. W. R. Institute. Blackland Research Center, Texas A&M University.
 Takahashi, A., & Kurosawa, T. (2016). Regression correlation coefficient for a Poisson regression model. *Computational Statistics & Data Analysis*, 98, 71-78
 US Army Corps of Engineers. (2010) HEC – HMS Hydrologic Modeling System. User's Manual.
 Vilaysane, B., Takara (2015). "Hydrological Stream Flow Modelling for Calibration and Uncertainty Analysis Using SWAT Model in the Xedone River Basin, Lao PDR." *Procedia Environmental Sciences* 28: 380-390.
 Yoshida, K., Shiozawa (2016). "Thermal variations of water in the Nam Song stream/Mekong River: II. Experimental data and theoretical predictions." *Sustainable Water Resources Management*: 135-141

An Assessment of Saltwater Intrusion in Cebu City Aquifers

Nelson Stephen L. Ventura¹, Nicole B. Mercado¹, Nicole H. Guerra¹, Raymond Albert L. Ng¹ and Mario P. de Leon, PhD¹

Abstract Constructing adequate models of the groundwater aquifer is an essential component of integrated water resources management, especially in the effort to curb the effects of saltwater intrusion in coastal areas. In the Philippines, the Department of Environment and Natural Resources has declared Cebu City as early as the year 2004 to be among the major cities in the country with the most critical balance conditions, suffering from the depletion of groundwater sources and the incidence of saltwater intrusion. However, save for the ongoing well-monitoring and plotting of isohaline contours by the Metro Cebu Water District (MCWD), in the years following the publication of DENR-CEST (2004) not much attention had been given to construct a groundwater model of Cebu City with updated data. In this light, an analytical model is useful for a quick assessment of the groundwater condition given limited access to data.

A simplified analytical model of the Cebu City aquifers is presented to determine the current position of the presumed sharp saltwater-freshwater interface, and visualize cones of ascension. Ten representative wells were assessed individually regarding the likelihood of saline contamination. Moreover, the cones of ascension of these ten wells have been simulated considering the effects of well interference. In defining the freshwater head and the distance of the toe of the freshwater-saltwater interface from the shore, the Glover relation was primarily used. Simulation results are illustrated by two- and three-dimensional representations.

Calculations and graphical representations were all carried out using Microsoft Excel spreadsheets. Three of ten wells were shown to be contaminated, while two more are threatened. Simulations with data gathered in the year 2014 also showed an alarming drawdown condition in the aquifer. Aside from the contribution to a greater public awareness of the threat of saltwater intrusion, the findings may serve to guide the policy-making of MCWD as to establishing allowable rates of groundwater extraction.

Keywords *Analytical model, Cebu, groundwater, saltwater intrusion*

¹ Civil Engineering Department,
De La Salle University,
Manila, Philippines

nelson_ventura@dlsu.edu.ph, raymond_ng@dlsu.edu.ph
nicole_mercado@dlsu.edu.ph
nicole_guerra@dlsu.edu.ph

Introduction

In the Philippines, Cebu City has been declared as among the major cities with the most critical balance conditions (DENR-CEST 2004), suffering from the depletion of groundwater sources and the incidence of saltwater intrusion. Moreover, according to the report of the Japan International Cooperation Agency (JICA) and the National Water Resources Board (NWRB) in 1998, the lowering of the water table results in inadequate water availability and saltwater intrusion in several areas in Cebu, including Cebu City. A report by the World Wildlife Fund and the Bank of the Philippine Islands (2011) also indicates that even though Cebu City is located at an average eighteen meters above sea level, some areas are barely one to two meters above mean sea level due to subsidence of the land level attributed to undue groundwater extraction, and indicated saltwater encroachment in coastal areas to an extent of five kilometers inshore.

Prior studies have determined the cause of saltwater intruding into the coastal freshwater aquifers of Cebu City to be the continuous, unregulated groundwater extraction (Abracosa et al., 2001; UNESCO-IHE, 2014). To compound the matter further, groundwater recharge is insufficient to replenish the supply: Maghaway Valley, for instance, only registered an annual rainfall rate of 1.4 million cubic meters with an addition inflow of 1.1 MCM from riverbeds, a figure considered by Abracosa et al. (2001) as inadequate in meeting the growing water demand from the many sectors of Cebu City.

Nonetheless, save for the ongoing well-monitoring and plotting of isohaline contours by the Metro Cebu Water District (MCWD), following the publication of DENR-CEST (2004) not much attention had not been given to possibly construct a groundwater model of Cebu City with updated data. In this light, an analytical model is useful for a quick assessment of the groundwater condition given limited access to data (Rushton, 2003).

The paper presents a simplified analytical model of the Cebu City aquifers to determine the current position of the presumed sharp saltwater-freshwater interface, as well as visualize the cross-sectional profiles of wells at drawdown and their cones of ascension. Ten representative wells were assessed individually

regarding the likelihood of saline contamination. Moreover, the cones of ascension of these ten wells has been modelled considering the effects of well interference. In defining the freshwater head and the distance of the toe of the freshwater-saltwater interface from the shore, the Glover relation was primarily used. Aside from the contribution to a greater public awareness of the threat of saltwater intrusion, the findings may serve to guide the policy-making of MCWD with regard to establishing allowable rates of groundwater extraction.

Methodology

Data from the 1980s and onwards was acquired from recorded water quality measurements of multiple wells across the study area, gathered from LWUA and MCWD. Sections of the study area were taken in order to visualize the groundwater profile. Changes in the profile over time are also observed. Analytical solutions were used to calculate and plot the profile of the saltwater-freshwater interface in the unconfined aquifer, both before and after the presence of pumping wells.

A study area was defined that encompassed a square region seventeen kilometers on each side, with vertical cross-sections taken at 2-kilometer intervals and oriented 128 degrees from the positive x-axis. Values had been set for the mass densities of freshwater ($\rho_{fw}=1.000 \text{ g/cm}^3$) and seawater ($\rho_{sw}=1.025 \text{ g/cm}^3$), the dimensionless relative density of saltwater ($\Delta\rho=0.025$), the horizontal flow of freshwater to the seaward direction ($q= 1.2864 \text{ m}^3/\text{day/m}$), and the hydraulic conductivity of the aquifer (limestone: $k= 5 \text{ m/day}$). Beginning with 1989 and for every five years hence, the extent of the cone of ascension of the saltwater-freshwater interface was considered. For each mark of the five-year time interval, the Glover relation was used as an analytical means of determining h_f , the head of fresh groundwater above mean sea level; z , the depth of the saltwater-freshwater interface from mean sea level; and x_o , the distance of the toe of the saltwater-freshwater interface from the shore. Contour lines of equal depths were generated for each of the vertical cross-sections of the study area, but prior to generating the contours, z values had been interpolated between every 25-m depth for a smoother curve.

Ten wells in the study area have complete characterization information – such as the specific capacity, well diameter, distance from the shore and well depth – and so they have been designated as the reference wells: around them was employed the Thiessen polygon method for interpolation of data (Boots, 1999), in particular, that of water level and yield/discharge.

The total drawdown is then computed as the quotient of the discharge and the specific capacity of the well. The study supposes a 2-km effective radius of influence and the 200-m aquifer thickness; the hydraulic conductivity

K is then determined by $K = \frac{Q \ln \frac{r_e}{r_w}}{\pi (h_u^2 - h_w^2)}$, which in turn is used to determine the drawdown H as in $H^2 - h_w^2 = \frac{Q}{\pi K} \ln \left(\frac{R}{r_w} \right)$.

It is a conservative assumption that the cone of ascension of saltwater is directly proportional to the drawdown of freshwater in the well despite the density difference. The depths of the points that comprise the sharp saltwater-freshwater interface are given by $x_o = \frac{\rho q}{2 \Delta \rho K}$, where x_o is the interface distance to the shore. The critical rise marks the boundary past which the saltwater in the particular scenario of the study would inevitably contaminate the pumping well. The profiles of the cones of ascension and critical rise per well were plotted for comparison and analysis.

Before plotting the drawdown contour maps from well interferences, the total drawdown from its average water level at every point in the 17 x 17-meter grid at 0.2-meter intervals was determined through $Z_{initial} =$

$\sqrt{\frac{2\rho q x}{\Delta \rho K} + \left(\frac{\rho q}{\Delta \rho} \right)^2}$; where z is the elevation. The logical if function of Microsoft Excel was used to interpolate the coordinates of elevations at 0.25 intervals downward. For each elevation, the X and Y coordinates from interpolation were gathered and arranged to form the contour line from these points as smooth line graphs. The smooth line graphs generated from each elevation were combined in one main graph for each year that corresponds to one main color legend. The 3D graph of each year from well interferences was generated through Microsoft Excel with the 17 x 17-meter grid at 0.2-meter intervals as X and Y values and total drawdown at each point as the Z values.

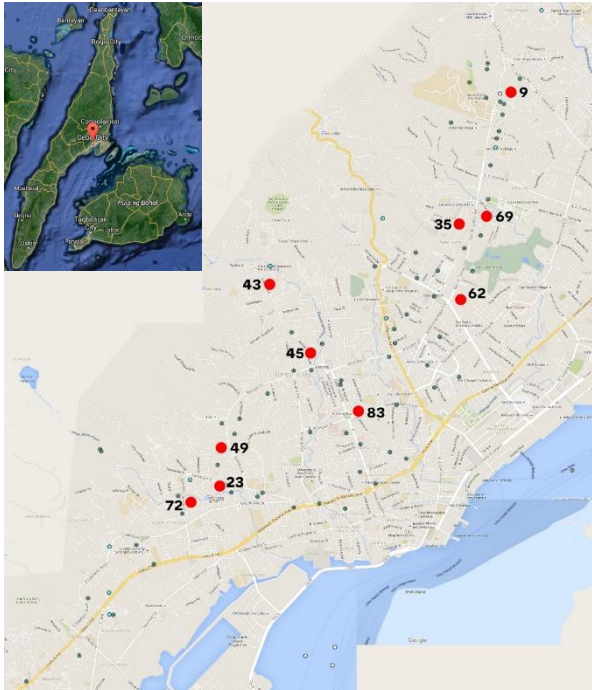


Fig. 1 The study area as the coast of Cebu City, capital of the island province of Cebu in the central region of the Philippines. A plot of representative wells for data.

Results and discussion

The analytical model was used to assess the extent of saltwater intrusion in three respects: the occurrence of saline contamination in an individual well; the over-extraction of wells beyond the maximum allowable discharge considering well interference; and the movement of the saltwater-freshwater interface.

Each well had been individually modelled using Glover’s relation and the Dupuit assumption in order to construct a profile of the drawdown and the corresponding upconing at each well. The peak of the cone of ascension is compared with the critical rise for the same well, where going beyond the critical rise indicates the occurrence of saline contamination in the well as projected by the model. It was found that Contour maps were generated from isohalines at different elevations for 1989, 1994, 1999 and 2004 (Fig. 72). Three-dimensional representations of the drawdown at the aforementioned years are also generated considering the effects of well interference among the ten representative wells.

Table 1 summarizes information of Well 9 for a span of 15 years at 5-year intervals, and shows the smallest gap between the peak upconing and the critical rise to be in 1989 with only a 9.27 m allowance. Despite the increase in discharge in the years 1989 to 2004, it was not the sole determining factor of threat of saline contamination, since the elevation of the critical rise also rose. Also noticeable is the rising of the peak of the upconing, which is attributed to the increase in the well drawdown (Eq. 9) that elicits the saltwater upconing

response of the aquifer. The increase in the well drawdown corresponds to the increase in the discharge.

Table 1. Summary of Well 9 Data.

YEAR	DISCHARGE, Q (CMS)	PEAK OF THE CONE OF ASCENSION (M)	ELEVATION OF THE CRITICAL RISE BOUNDARY (M)	GAP BETWEEN CRITICAL RISE AND THE PEAK OF THE CONE OF ASCENSION (M)
1989	0.014	-196.9	-187.63	9.27
1994	0.025	-194.59	-178.44	16.15
1999	0.026	-194.47	-194.55	16.53
2004	0.031	-193.34	-196.27	19.91

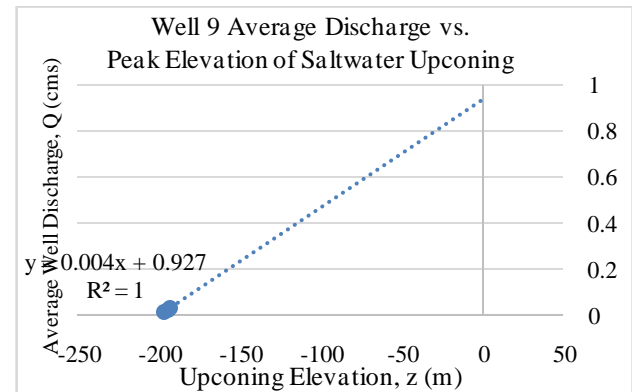


Fig. 2 Correlation of pumping rate with the cone of ascension.

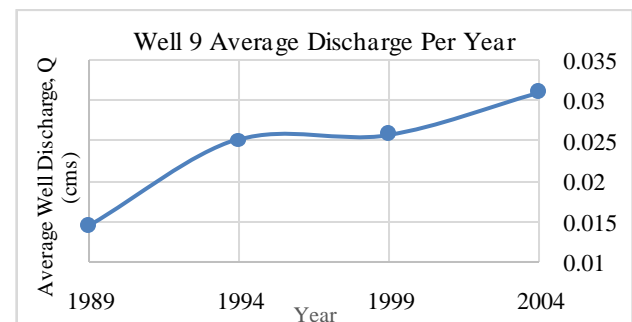


Fig. 3 Trend of Well 9 average pumping rates.

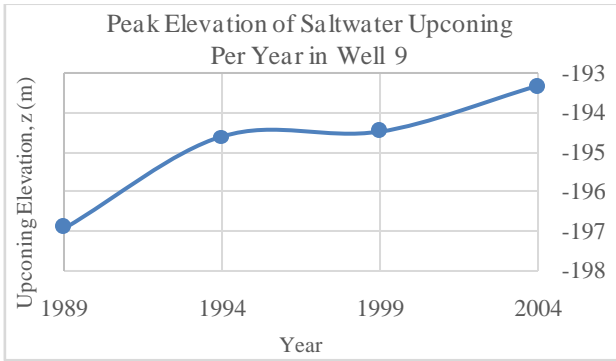


Fig.4 Trend of saltwater upconing in Well 9.

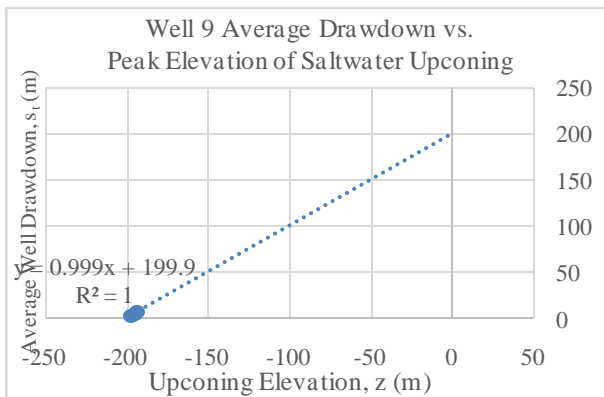


Fig. 5 Correlation of the extent of Well 9 drawdown and the cone of ascension.

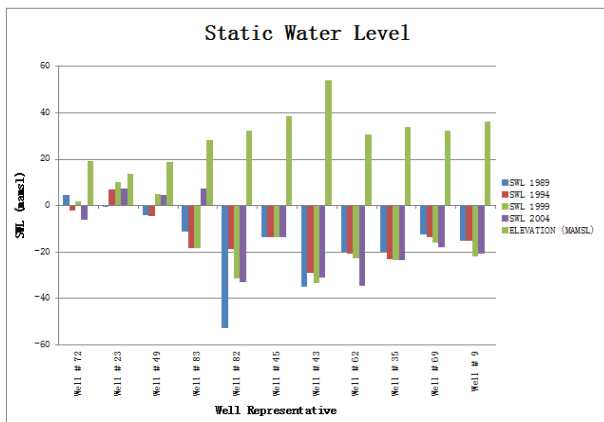


Fig. 6 Static water levels of the representative wells.

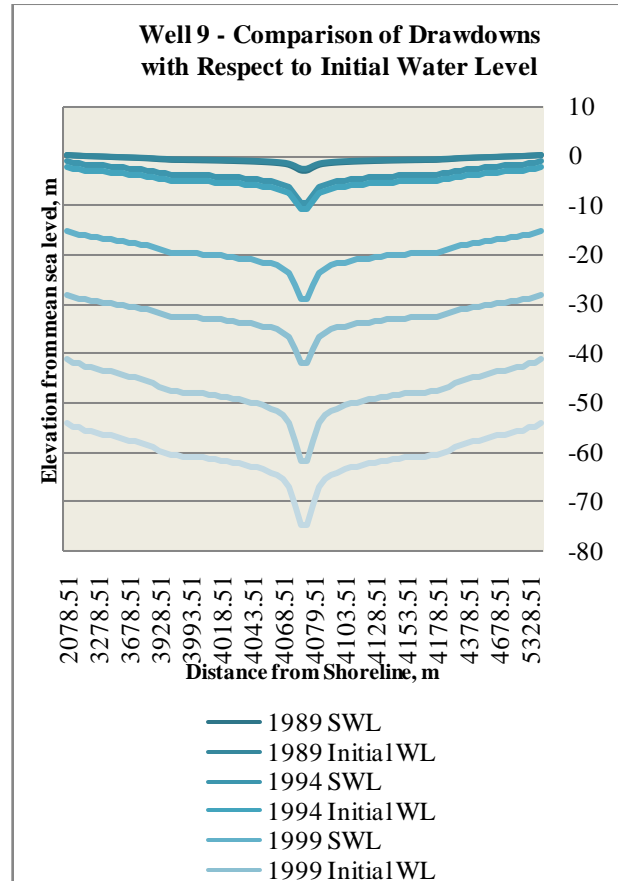


Fig. 7 Comparison of drawdowns of Well 9 per year.

The correlation between the peak upconing and the well discharge has been exhibited in Fig. 24, where a direct relationship is established with the equation $Q = 0.0046z + 0.9276$. The veracity of this direct relationship is further supported by a comparison of Fig. 25 and 26, where the trends of discharge and saltwater upconing are strikingly similar. Fig. 27 finally quantifies the relationship between well drawdown and saltwater upconing, and gives $H = 0.9995s_t + 199.9$, an alternative correlation that can be used to monitor saltwater upconing in the absence of discharge data.

Nonetheless it is evident that from 1989 to 2004, the rate of extraction of groundwater allowed for the corresponding drawdown and saltwater upconing, but without contamination of the well since the freshwater-saltwater interface had not yet reached the wells. Also the increasing distance between the peak of the saltwater cone of ascension and the critical rise from 1989 to 2004 indicates that a significantly larger extraction rate is required for seawater to encroach into Well 9.

According to Schmorak and Mercado (1969), maximum well penetration without saline penetration into the freshwater region is increased as permeability is decreased; this relation was only applicable to wells 9, 23, 35, and 43 from year 1989 to 2004. For the other wells, inconsistency respective to this theory was manifested, due to approximation of the data used.

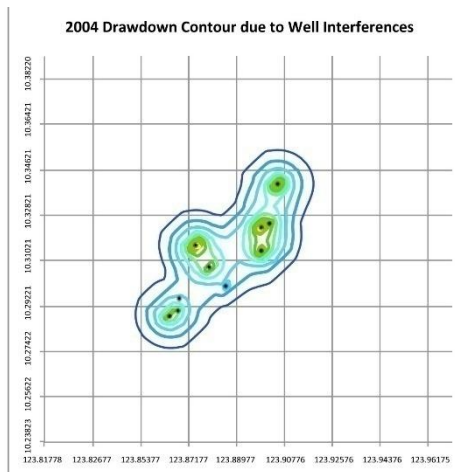
However, since it is not enough to merely assess saltwater contamination on a well-to-well basis as if

each well is independent of the others, simulations for saltwater cones of ascension are conducted for the wellfield of ten representative wells, considering well interference.

In creating the contour maps, all the representative wells were assumed to have an average water level of -0.5242 m, -2.2651 m, -3.8532 m, -1.5657 m for the years 1989, 1994, 1999, and 2004 respectively. These water levels are assumed to be the reference level before the drawdown occurs. The coordinates of the elevations at intervals of 0.25 m downward were plotted on the 2D contour maps using the results of elevation from

$Z_{initial} = \sqrt{\frac{2\rho q x}{\Delta\rho K} + \left(\frac{\rho q}{\Delta\rho K}\right)^2}$. If the water level of the well was already at a certain elevation of the assigned intervals, the coordinates of its location are interpolated and plotted. Then, these plots are connected to form the contour of each elevation.

Investigation of saline contamination in a well is based on the cone of ascension, which is assumed to be an inverted drawdown from the bottom of the aquifer. Once it crossed the critical rise level, it may be considered as a critical region for saltwater intrusion. However, since the critical rise is different per well, only 2D profiles were generated for this occurrence. The drawdown contour maps mainly show the behavior of well usage for the reason that the varying variable was the abstraction rate. The drawdown contours for 2004 is illustrated in Figures 8 and 9 below:



LEGEND:

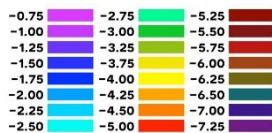


Fig. 8 Contours of drawdowns considering well interference.

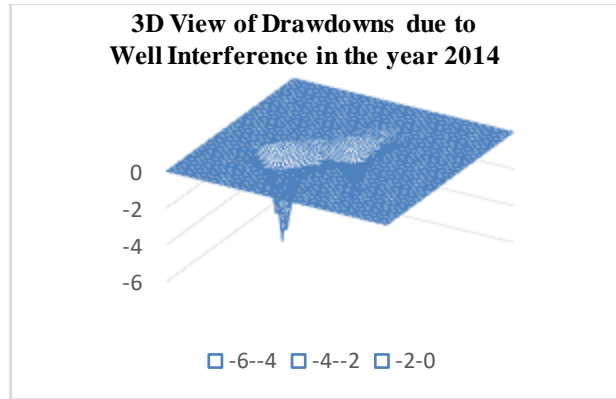


Fig.9A 3D View of the drawdown due to well interferences.

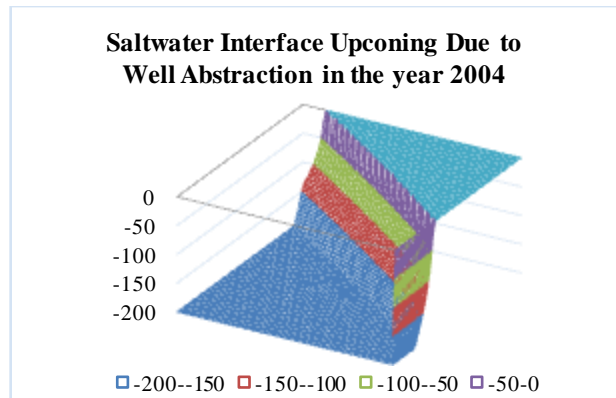


Fig.10 Cone of ascension of the Saltwater-freshwater interface in the year 2004.

Summary and conclusions

Simulated cones of ascension in three wells (Wells 43, 45 and 83) in 1989, 1994, 1999 and 2004 are observed to exceed the critical levels, thereby indicating their susceptibility to the intrusion of seawater. Extending the projection further, critical areas where saline intrusion may occur even after 2004 are Well Areas 23 and 35. This finding is further supported by the fact that within the vicinity are nine wells that were abandoned in 1992 because of confirmed saline contamination, where chloride concentration exceeded the 250-ppt limit set by the Philippine National Standards for Drinking Water. Well regions 9, 49, 62, 69 and 72 in Figure 1 are not yet considered critical areas since these areas recorded a projected distance from the peak of the cone of ascension to the critical rise of more than 5 m. Most of the well regions that were not yet considered under critical areas were located at the northeastern portion of Cebu City except for well regions 35 and 23.

Isohaline contours were generated to simulate the condition of simultaneous extraction of the ten representative wells in the years 1989, 1994, 1999 and 2004, and subsequently converted to three-dimensional renderings of the extent of groundwater drawdowns. Moreover projected drawdowns in 2009 and 2014 point to an alarming condition of the groundwater supply. The hypothesis that well abstraction contributes to the gradual advance of the saltwater-freshwater interface is

confirmed from the three-dimensional renderings of the extent of saltwater cones of ascension and its influence on the sharp interface. The merely gradual movement is attributed to the limitation of considering the effect of only ten pumping wells instead of the entire wellfield. Nonetheless it is also notable that the discharge rate is the primary determinant of the total drawdown, the level of the saltwater cones of ascension, and the gap between critical rise and peak of the cone of ascension as observed in the analysis of the drawdown and cone of ascension profiles of each of the representative wells considered.

Acknowledgements

Gratitude for the completion of this paper is owed to several persons whose contribution are inestimable: to research adviser Dr. Mario P. de Leon for his expertise, counsel and persistence through the arduous timeline of the study; to the staff of the Metro Cebu Water District for waiving fees for hydrochemical data; to the staff of the Local Water Utilities Administration for their generous assistance in providing water quality data; to Rafael Mercado, for aiding the group in data acquisition; to family, friends, and professors for their endearing support and assistance; lastly, to Almighty God for his Providence, without which our efforts would not have come to fruition.

References

Abd-Elhamid, H. F. and Javadi, A. A. (2008). "An Investigation into Control of Saltwater Intrusion Considering the Effects of Climate Change and Sea Level Rise." Retrieved from <http://www.swim-site.nl/pdf/swim20/file023-026.pdf>.

Abacososa, R., Clemente, R., David, C., Inocencio, A., & Tabios, G. (2001). *Metro Manila and Metro Cebu Groundwater Assessment*. Philippine Institute for Development Studies, 1-43.

Adrien, N. G. (2004). *Computational Hydraulics and Hydrology: An Illustrated Dictionary*. Boca Raton, Florida: CRC Press.

Barlow, P. M. (2003). *Groundwater in Freshwater-Saltwater Environments of the Atlantic Coast*. U.S. Geological Survey Circular: 1262.

Bear, J., Cheng, A. H. D., Sorek, S., Ouazar, D. and Herrera, I. (eds.). (1999). *Seawater intrusion in coastal aquifers – concepts, methods and practices*. Dordrecht, Netherlands: Kluwer Academic Publisher.

Berner, E. K., and Berner, R. A. (2012). *Global Environment: Water, Air, and Geochemical Cycles*, 2nd ed. Princeton, New Jersey: Princeton University Press.

Clemente, R. S. et al. (2001). "Metro Manila and Metro Cebu Groundwater Assessment." Discussion Paper Series No. 2001-05. Makati City, Philippines: Philippine Institute for Developmental Studies.

Costello, L. (1981). *Soil Survey Manual*. Bureau of Soil and Water Management.

Environmental Management Bureau (2005). *National Water Quality Status Report 2001-2005*. Quezon City: JICA.

Fisher et al. (1979). "Mixing in inland and coastal waters." New York: Academic Press.

Felisa, G., Ciriello, V. and Di Federico, V. (2013). "Saltwater intrusion in coastal aquifers: A primary case study along the Adriatic coast investigated within a probabilistic framework." In *Water* 2013, 5, 1830-1847. Retrieved from www.mdpi.com/2073-4441/5/4/1830.

Groundwater Management Coastal areas. (2015). Retrieved November 30, 2015, from <http://adb-knowledge-partnership.unesco-ihe/org.comparative-research-groundwater-management-0>.

Hathaway, D. and Grigsby, B. (2006). "Modeling Methodology: The simplicity of the Glover method." Technical note. S. S. Papadopoulos and Associates, Inc.: Colorado.

Henry, H. (1964). "Interfaces between salt water and fresh water in coastal aquifers" in *Sea Water in Coastal Aquifers*.

Houben, G. and Treskatis, C. (2007). *Water Well Rehabilitation and Reconstruction*. New York: McGraw-Hill.

Huyakorn, P. S., Park, N. S., Wu, Y. S. (1996). "Multiphase Approach to the Numerical Solution of a Sharp Interface Saltwater Intrusion Problem," in *Water Resources Research*, 32(1), 93-102.

Japan International Cooperation Agency (JICA) and National Water Resources Board (NWRB) (1998). *1998 Master Plan Study on Water Resources Management in the Philippines*.

Kaselow, M. (2001). *Applied Groundwater Hydrology and Well Hydraulics*, 2nd Ed. Highlands Ranch, Colorado: Water Resources Publications.

Kashef, A. I. (1971). "On the management of ground water in coastal aquifers," in *Groundwater*, 9 (2), 19-20.

Kashef, A. I. (1987). *Groundwater Engineering*. Singapore: McGraw-Hill.

Konikow, L. F. (1985). "Predictive Accuracy of a Ground-Water Model." In *Groundwater* Vol. 24, No. 2, March-April.

Kumar, C. P., "Management of Groundwater in Salt Water Ingress Coastal Aquifers", In: Ghosh, N. C., Sharma, K.D. (Eds), *Groundwater modelling and management*. New Delhi: Capital Publishing company; 2006, p. 540-560.

Kommadath, A. (2000). "Estimation of Natural Ground Water Recharge." In Section 7, *Ground Water and Hydrology*. Retrieved July 1, 2016 from <http://ces.iisc.ernet.in/energy/water/proceed/section7/paper5/section7paper5.htm>

Mantoglou, A. and Papantoniou, M. (2008). "Optimal Design of Pumping Networks In Coastal Aquifers Using Sharp Interface Models." *Journal of*

- Hydrology, doi:10.1016/j.jhydrol.2008.07.022,
ISSN 0022-1694.
- Melloul, A. J. and Zeitoun, D. G. (1999). "A Semi-Empirical Approach to Intrusion Monitoring in Israeli Coastal Aquifer." In Bear, J. et al. (eds.). *Seawater Intrusion in Coastal Aquifers*, 543-558.
- Michael, A. M., Khepar, S. D., and Sondhi, S. K. (2008). *Water Wells and Pumps*, 2nd Ed. New Delhi: McGraw-Hill.
- National Economic and Development Authority. (2011). *Philippine Development Plan 2011-2016*.
- National Water Resources Board. (2004). "Water Resources Assessment for Prioritized Critical Areas (phase 1)."
- Park, C. H. and Aral, M. M. (2004) "Multi-objective optimization of pumping rates and well placement in coastal aquifers." *Journal of Hydrology*, 290 (1), 80-99.
- Righetti, C., Gigliuto, A., Chini, A., and Rossetto, R. (2009). "Saltwater intrusion in a coastal contaminated aquifer density-dependent finite element model of flow and transport to assess remediation strategies and saltwater intrusion at a coastal gas plant site" Retrieved from http://www.dhigroup.com/upload/publications/dhiwasy/Righetti_2009.pdf.
- Shoemaker, W. B. (2004). "Important Observations and Parameters for a Salt Water Intrusion Model." *Ground Water* Vol. 42(5). p. 829 – 840. Retrieved http://fl.water.usgs.gov/PDF_files/GW_42_6_Shoemaker.pdf.
- The World Bank. Philippines Environment Monitor 2003: Water Quality. Retrieved on October 10, 2015, <http://www.worldbank.org.ph/WBSITE/EXTERNAL/COUNTRIES/EASTASIAPACIFICEXT/PHILIPPINESEXTN/0,,contentMDK:20209686~pagePK:141137~piPK:217854~theSitePK:332982~isCURL:Y,00.html>.
- Tomaszewski, D. H. (1996). "Distribution and Movement of Saltwater in Aquifers in the Baton Rouge Area, Louisiana, 1990-92." Baton Rouge, Louisiana: Louisiana Department of Transportation and Development.
- United States Geological Survey (2005). "Saltwater Intrusion in Los Angeles Area Coastal Aquifers – The Marine Connection." Retrieved on September 29, 2015 from <http://pubs.usgs.gov/fs/2002/fs030-02/>
- Walther, M., Bilke, L., Delfs, J., Graf, T., Grundmann, J., Kolditz, O., and Liedl, R. (2014). "Assessing the saltwater remediation potential of a three-dimensional, heterogeneous, coastal aquifer system: Model verification, application and visualization for transient density-driven seawater intrusion." In *Environmental Earth Science*. Berlin: Springer. DOI 10.1007/s12665-014-3253-2.

Flood Risk Maps and Its Applications

Ling Feng Chang¹, Wen-Tsun Feng², MingDaw Su^{3*},

Abstract Floods are among the most frequent and costly natural disasters in terms of human hardship and economic loss. Most of the governments invest heavy resources to provide information for impact mitigation of this natural disaster. Flood potential maps are the most common available information among this data category. Although flood potential maps provide precious information about flooding occurrences, its values and usefulness may be slashed with the absences of socioeconomic data and vulnerability models for damage assessment.

This paper presents three categories of flood risk map, which are flood hazard risk map for flooding occurrence potential, flood lose risk map for financial damages caused by flooding, and the flood resilience map to take into account the social vulnerability. These three flood risk maps can be overlaid with each other to produce four combinations providing spatial risk information for regional flood risk management. Taipei metropolitan area was used as an example study area for this proposed flood risk management framework and the interpretations of the proposed flood risk maps.

Keywords *Risk, Flood, Risk Map, Hazard, Exposure, Vulnerability, Resilience*

Ling Feng Chang, Ph.D

Associate Research Fellow,
Agricultural Engineering Research Center,
Tao Yuan, Taiwan
changlf@aecr.org.tw

Wen-Tsun Feng, Ph.D.

Research Fellow and Acting Director,
Agricultural Engineering Research Center, Taiwan
Tao Yuan, Taiwan
wtfang@aecr.org.tw

MingDaw Su, Professor

Dept. of Bioenvironmental Systems Engineering,
National Taiwan University,
Taipei, Taiwan.
sumd@ntu.edu.tw

Introduction

A natural disaster is caused by major adverse events in natural (hydrological, geological, or metrological) processes. An adverse event will not rise to the disaster level if it occurs in an area without vulnerable population or economic activities. In a vulnerable area, it can have disastrous consequences causing loss of life, property, and lasting damage, requiring years to repair. According to review on last 20-year records, the UNISDR shows that 90% of disasters are weather-related (floods, storms, droughts, etc.) and the rate of weather-related disasters is growing. Between 2005 and 2014, the annual average of weather-related disasters showed an increase of 14 percent from 1995 to 2004 and almost twice the average recorded from 1985 to 1995. Although the casualty from flood is reduced but it still affected more people than most of the other natural disasters (UNISDR,2015).

There is a growing importance and understanding that data collection, analysis, and management can help to identify disaster risks and make disaster management more efficient and effective. The need for systematic data for disaster mitigation and prevention is an increasing concern of both development and response agencies. According to Margareta Wahlström, UN Special Representative of the Secretary-General for Disaster: "Access to information is critical to successful disaster risk management. You cannot manage what you cannot measure." This paper proposed somerisk maps of flood disasters that may better identify the spatial distribution of flooding risk for more effective short/long terms flood risk mitigation planning.

Risk Management Framework

In the process of handling the natural disaster impact to the society, a risk management framework as shown in figure 1 is usually followed. Risk must be identified and evaluated so that impact mitigation may be planned. A monitoring system may be established for early warning as the hazardous event occurs to reduce the impacts or damages. The recovery stage will follow the event and eventually into the risk analysis stage for reinvestigate the risk for better future events. The risk analysis and mitigation planning will be referred as "risk management" and the preparedness and recovery as the "emergency response". Risk management is much more

important asset may reduce the panic and the severity of damages as the event hits.

The risk induced from natural disaster is quite different from other kind of risks like health, financial, IT systems, and environmental. The occurrence probabilities of the natural disaster events are better understood, especially for hydrological and meteorological disasters. These disasters can occur repeatedly at the same site within specific time period. And most of the damages caused by the disasters can be recovered and may be damaged again during the next attack. The risk of natural disaster (take flood as an example) can then be defined as the summation of the total damage under a single event ($H \cdot E \cdot V$) multiple by its occurrence probability for all the probable events in a specific period (e.g. a year).

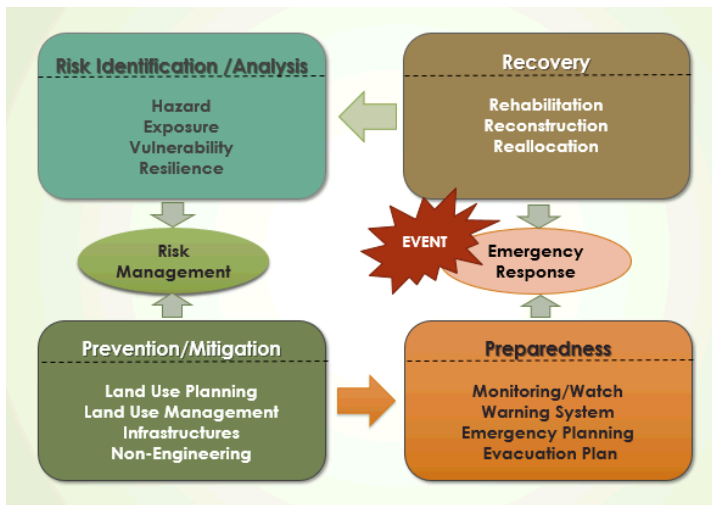


Fig. 1 The Risk Management Framework

Risk analysis is the key component in the risk management process and the analysis results will become vital basis for selection and implementation of disaster prevention and mitigation measures. The risk analysis of natural hazard composed of four components as hazard, exposure, vulnerability and resilience. The hazard may be defined as source of potential harm (ISO 31000, 2009). In flooding disaster, the hazard can be expressed as the inundation depths. And it is usually expressed as flood potential maps to show its spatial distribution. A flood potential map usually is associated with a specified event with designated severity and occurrence probability. The exposure is the extent to which an organization and/or stakeholder is subject to an event (ISO31000, 2009). In the case of flood disaster, the exposure is the population, housing, and other economic activities such as industry, commercial and agriculture that are inundated in the event. Vulnerability is the intrinsic properties of something resulting in susceptibility to a risk source that can lead to an event with a consequence. So it will be the relationship of the loss versus flooding depth for each categories of the above exposures. At last, resilience is the adaptive capacity of an organization in a complex and changing environment. In case of flood, resilience will be the capacity of the risk receptor to adapt to the disaster. The resilience can be viewed as the social vulnerability of the risk receptors because this will more related for socio-economical characteristics of the receptors. Some potential proxies for resilience are children, people with disabilities, elderly, minority, chronic and acute medical illness, social isolation, low-to-no income, and illiterate/low level of education. People with these above social factors have disproportionate exposure to risk and a decreased ability to avoid or absorb potential loss (Martin, 2015).

$$\text{Risk} = \text{SUM}(H \cdot E \cdot V \cdot Pr.) \dots\dots\dots (1)$$

Where:

Risk: Expected annual loss (in \$)

H: Hazard potential (inundation depth in flood)

E: Exposure (number of household, or acreage)

V: Vulnerability (Loss/Depth/unit household)

Pr: occurrence probability of the event

The above equation may be applied to a designated spatial unit, e.g. county, township, or unit grid in a mesh system (Figure 2), and the results from each unit in the region collectively produce a map showing the spatial distribution of the flood risk.

Risk Maps

Risk Map is a map showing the spatial distribution pattern of regional flood risk. As shown in Fig. 2, a mesh system was used to express the spatial distribution of hazard (flood depth), exposure (number of household). Equation (1) is applied to estimate financial loss for each grid at the flood depth (H) of an event with the exposed household (E) and associated damage estimating function (V).

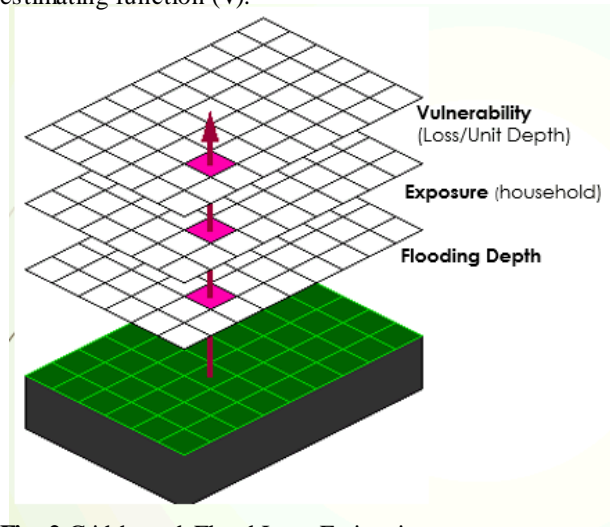


Fig. 2 Grid-based Flood Loss Estimation

The same process was done for some designated simulated flood events with a return period of 2, 10, 50, 100, 200, 500 years, and the flooding losses in each grid from different events were integrated together with its occurrence probability as shown in Fig. 3. Since we simulated the flood disaster with discrete events (RT=2,10,50...years), a transformed version of Fig 3 is shown in Fig.4. The financial-loss-based risk was estimated for each grid will finally be estimated. And all the grids collectively will show the spatial distribution of the flooding risk for the region.

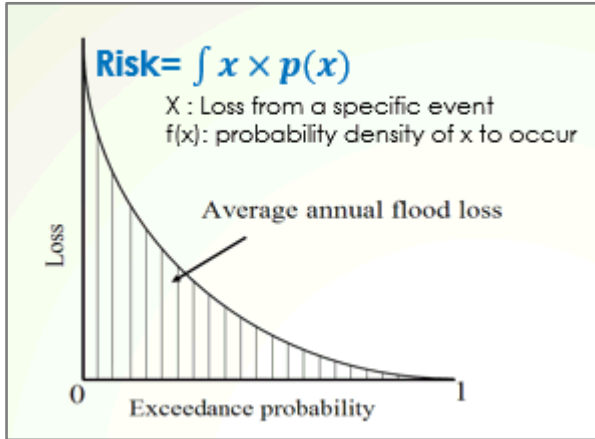


Fig.3 Risk as the expected annual loss

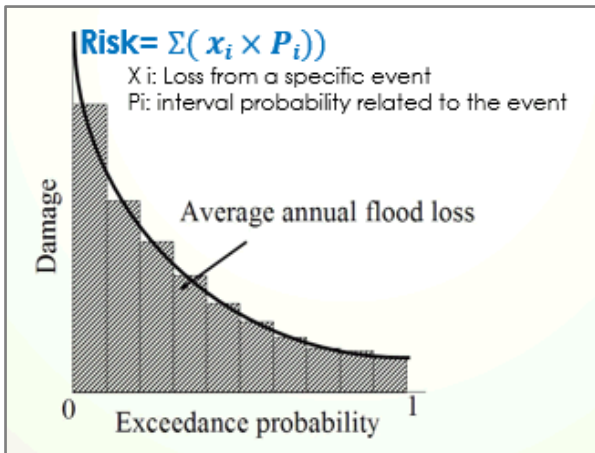


Fig.4 Estimating risk with discrete events

Taipei City, Taiwan was used as a demonstration area for this study (as shown in Fig.5). Taipei City with an area of about 272 sq.km and a population size of about 3 million is the Capital of Taiwan and the center of economy and political development. The average precipitation in the central Taipei City is about 2,500 mm/year and 68% of the annual rainfall is concentrated in the monsoon and typhoon season between May and October. Typhoons usually carry heavy rainfall in short time periods as intense as 100 mm/hr or 1,000 mm/day. Taipei City suffered from severe flood disaster in the old time. The situation is well improved from the major flood control plan for the Great Taipei Metropolitan in

the mid 70's last century, but it still attacked by flood disaster from the heavy rainfall in the urban watershed. As shown in Fig.5, it is the flood simulation for 1 event with return period of 500 years.

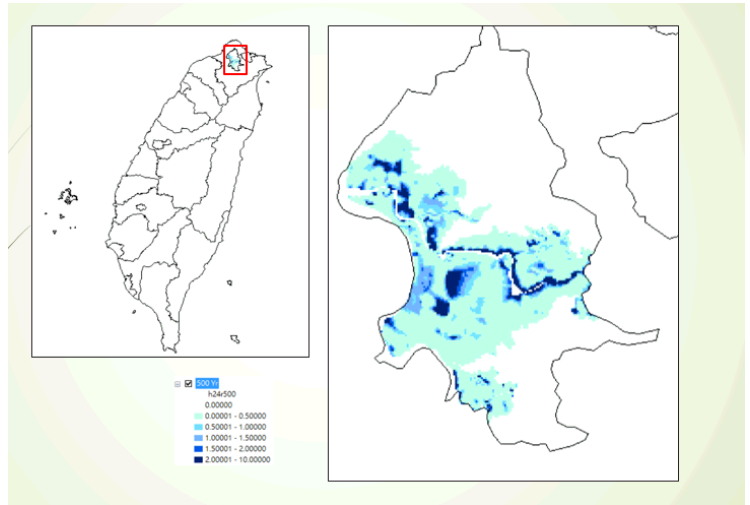


Fig.5 Taipei City, Taiwan with flood potential of event with 500 year return period

Fig.5 shows the hazard potential of a specific event, and this will be done for events with 2, 10, 50, 100, 200, years of return period. The exposure data of the area was then collected. Fig. 6 shows the density of buildings/households in Taipei city.

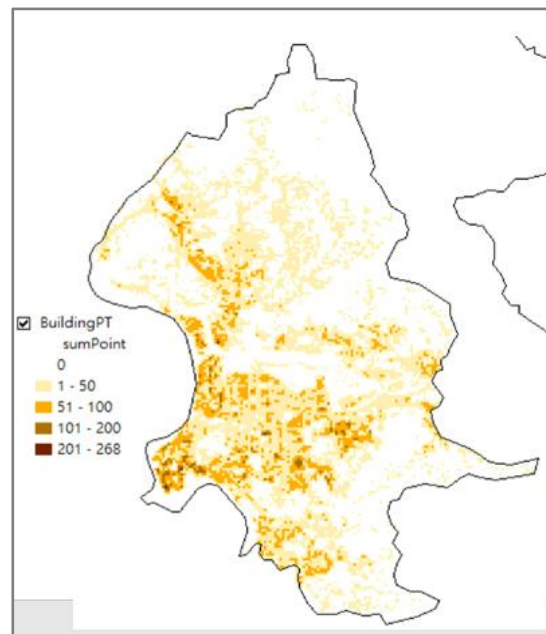


Fig.6 Exposure data

Each cell in Fig.6 contains the number of building/household within, and the flood-loss vs. flood-depth function was applied to each cell for the flood loss estimation of that cell. The results is shown as in Fig.7.

This process was executed for all the simulated events with 5, 10, 50, 100, 200 return years and were all integrated for each cell to assess the flood risk in that cell using method shown in Fig 4. The resulting map is shown in Fig. 8. This will be the first kind of flood risk map showing the expected annual loss due to flood for Taipei.

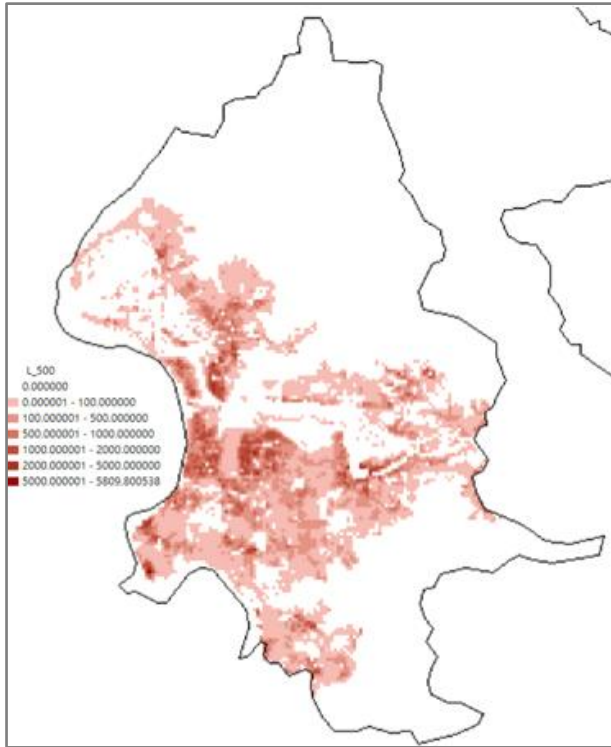


Fig.7 Flooding loss under a 500 year event

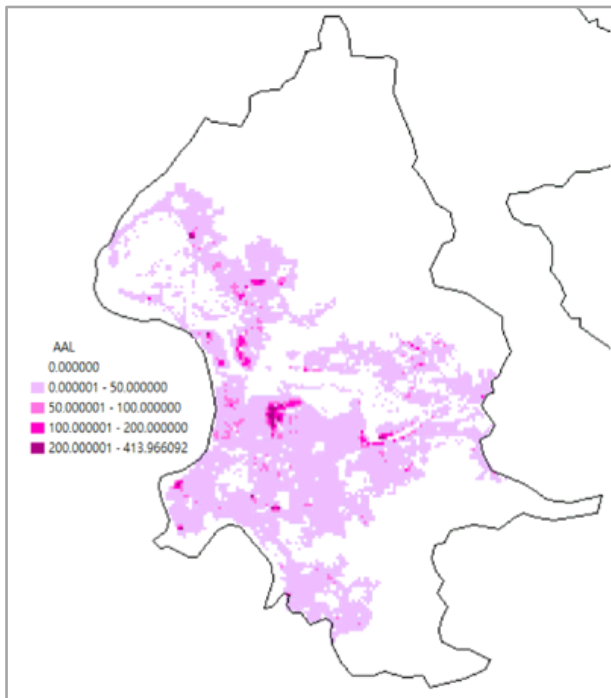


Fig.8 Risk Map based on expected annual loss

The risk map shown in Fig. 8 can be used to identified which part of the city will cause more financial loss due to the hit of flood in general. Since this risk is defined by Eq. (1), higher values of potential flood damages may not indicate high hazard potential, it may because the denser exposure in the vicinity. So this risk map may not be correct if a discriminated flood insurance premium scheme is to be set up. This paper proposed a second kind of risk map based on expected flood potential, that is defined as eq.(2) and (3) for continuous or discrete simulation..

$$EH = \int D * Pr(D) \dots\dots\dots (2)$$

$$EH = \sum (D_i * P_i) \dots\dots\dots (3)$$

Where the EH is the annual expected accumulated flooding depth, and will be a proxy for risk of potential hazard. The simulation result for Taipei city is shown in Fig. 9.

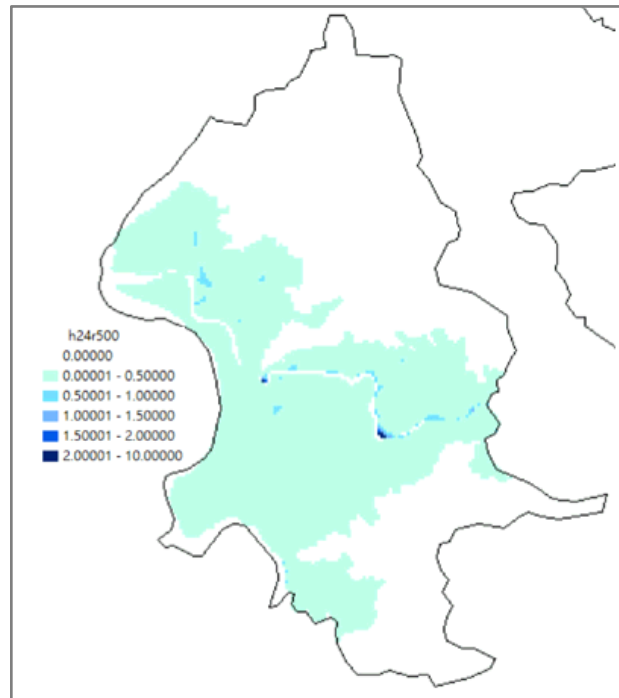


Fig.9 Risk map based on the annual expected hazard

The areas with darker blue in Fig.9 are expected to be suffered from more frequent/severe flooding hazard, and may be charged for higher premium for a flood insurance policy.

The Fig. 8 and Fig.9 were reclassified into a binary categories of High and Low Risk. The cutoff threshold for these binary classifications are set as the mean plus one standard deviation of the risk values for all the cell in each figures. The result is shown as in Fig. 10. The reason for these reclassifications is these two risk maps are to be overlaid so that more information about flood risk management can be extracted. The map shown in Fig.11 is the result of overlaying the hazard risk map on the loss risk map.

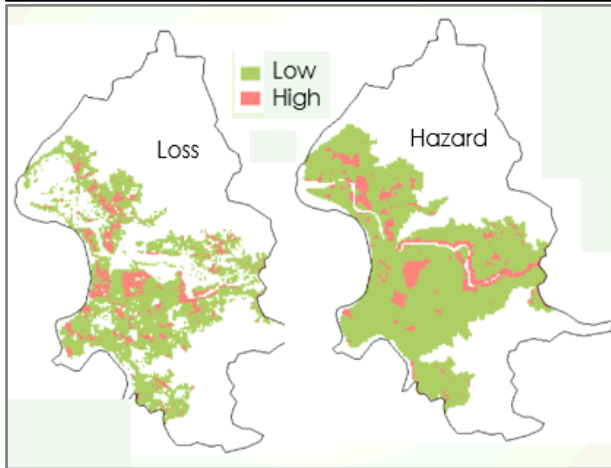


Fig.10 Risk Map Reclassified into H/L categories

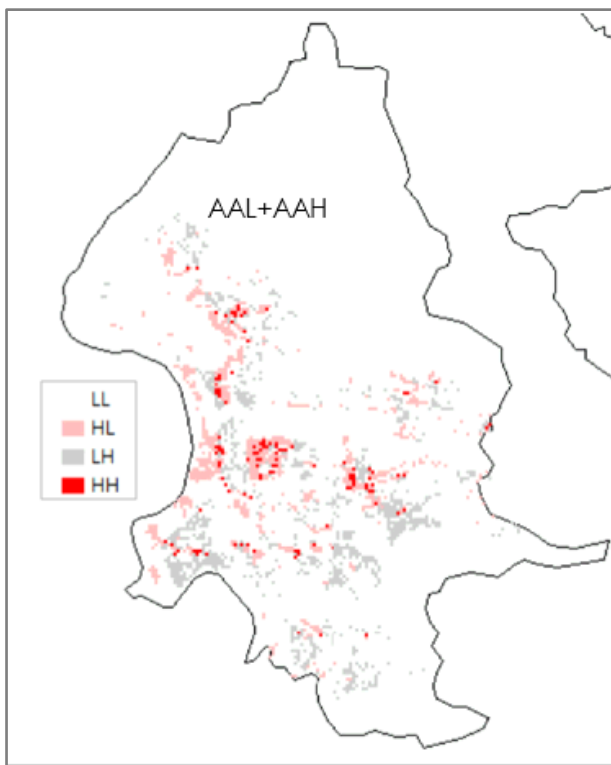


Fig.11 Overlay of hazard and loss risk maps

As shown in Fig.10, there are four categories that may have different interpretations and different measures may be proposed for the risk treatments as shown in Table1. As for the four categories, there are not much needs for discussion for category no.1 and 4. There is nothing needed to do for the first category where both risks are low. And for the 4th category, there is an immediate need to take actions with both engineering and non-engineering measure, such as potable pumping plant, drainage system augmentation, and even an emergent warning and evacuation plan. For category 3 where shows low potential of flood loss although the potential hazard is high, this may indicate that some minority or low income level people live on a flood prone area. This is not only an disaster problem but also a social equity one. Early warning system should be

established and some engineering measure to mitigate the flood hazard potential whenever the budget is allowed. The 2nd category is not likely to occur if a sound land use planning and management has been carried out. It usually indicates over-intense economic development in this region. Land use plan should be examined and adjusted. Some early warning system may help for the short term period before the land use pattern can be adjusted.

Table1 Risk classifications and suggestive actions (AL/AH)

Cat.	AL	AH	Remarks
1	L	L	OK (No action needed)
2	H	L	1. Setup early warning system 2. Land use review/adjust 3. Decrease economic intensity (Over/intensive development)
3	L	H	1. Setup early warning system 2. Engineeringmeasure (Minority living on flood-prone areas)
4	H	H	1. Need to take action immediately 2. Both engineering/Non-engineering measures 3. Emergency response plan

Note: AH= Expected Annual Accumulated Hazard
 AL= Expected Annual Accumulated Loss

Other than the two kinds of risk map based on annual expected loss and hazard, a third kind of risk map is proposed in this paper. It is the risk map base on the resilience. As discussed previous, resilience is defined as the adaptive capacity for the flood disaster. The resilience can be viewed as the social vulnerability of the risk receptors because the socio-economical minorities such ass low-income or low education level, ill or elderly or social isolated people will have more difficulties to adapt to or recover from the flood disasters. And the previous vulnerability of the financial loss can be viewed as bio-physical vulnerability. A risk map based on social vulnerability is shown in Fig.12 using the number of disable persons as a proxy.

All three kinds of risk map can be overlaid with each other or simultaneously together. In this paper. Only the results of overlay with all three risk maps are shown in Fig. 13. These overlays generated 8 categories as shown in Fig. 13 and Table 2. Similar as discussed above, these 8 categories from the overlays of risk maps based on loss, hazard, and social vulnerability can be examined and some mitigation actions suggested. With extra information from including the risk map based on social vulnerability, the high risk area (with HHH in all three categories) can be identified. and immediate actions be taken. The other categories are more similar to the discussion above; either is the over-development from missed or improper land use planning or the socio-economic vulnerable minority gathering on a flood prone areas can be taken care of as discussed above or as shown in Table 2.

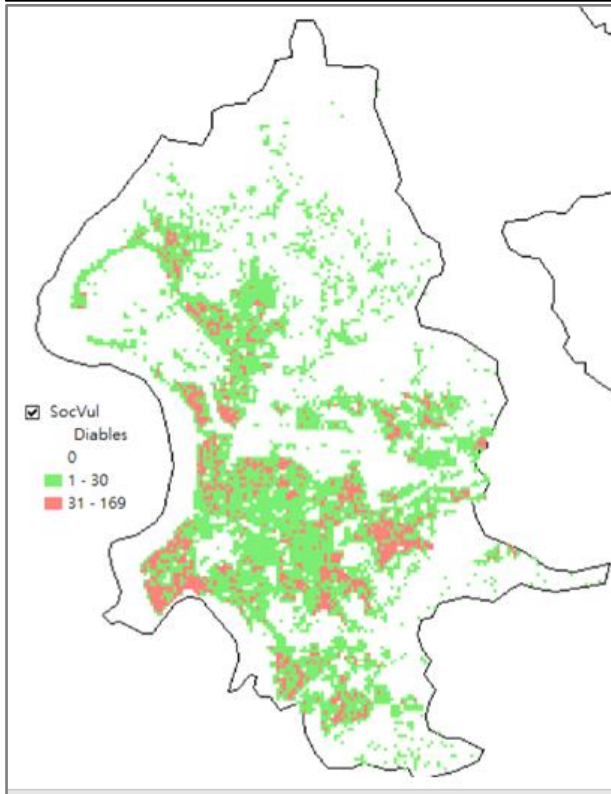


Fig.12 Risk map based on social vulnerability

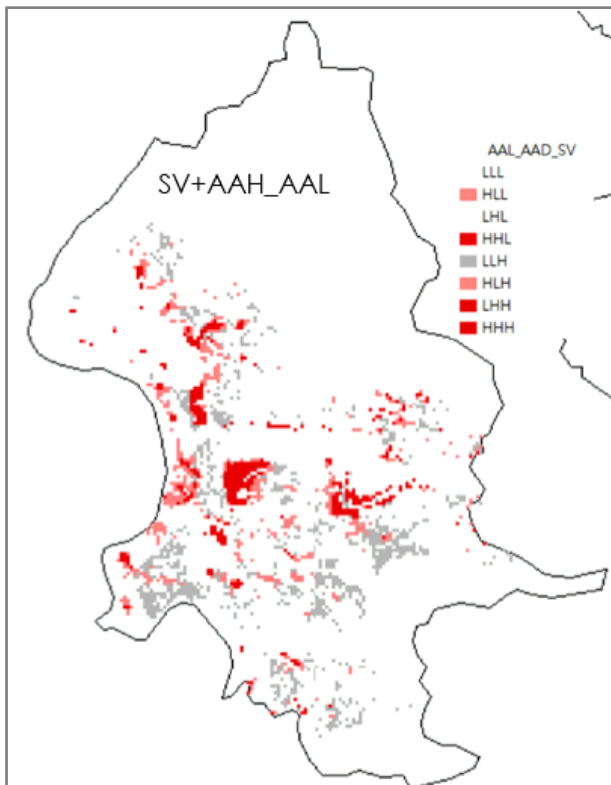


Fig.13 Overlay of all three risk maps

Summary and Discussions

This paper presents a general Risk Management Framework for natural disaster including the definitions

about hazard, exposure, vulnerability, resilience and risk. The Social Vulnerability other than the traditional bio-physical vulnerability discussed in most of the literatures is also proposed as a surrogate to the resilience

Table2 Risk classifications and suggestive actions (AL/AH/SV)

Cat	AL	AH	SV	Remark
1	L	L	L	OK
2	H	L	L	Warning system and Land use adjustment
3	L	H	L	OK or marginal land development with engineering measures
4	H	H	L	Warning system /Engineering measures
5	L	L	H	Warning system/Engineering measures
6	H	L	H	Warning/Engineering/Land use adjustment
7	L	H	H	Emergent Action (Social equity problem)
8	H	H	H	Action (Most urgent!)

Note: AH= Expected Annual Accumulated Hazard

AL= Expected Annual Accumulated Loss

SV= Social Vulnerability

There are three categories of flood risk maps presented, which are flood hazard risk map for flooding occurrence potential, flood lose risk map for financial damages caused by flooding, and the flood resilience map to take into account the social vulnerability. These three flood risk maps will be overlaid with each other to produce four combinations providing spatial risk information for regional flood risk management. Taipei metropolitan area was used as an example study area for this proposed flood risk management framework and the interpretations of the proposed flood risk maps.

References

ISO 31000, 2009, Guide 73:Risk management- Vocabulary, ISO GUIDE 73:2009

Martin, S.A., 2015, A framework to understand the relationship between social factors that reduce resilience in cities: Application to the City of Boston, I. J. of Disaster Risk Reduction 12(2015):53-80

UNISDR, 2015, Disasters in Numbers, http://www.unisdr.org/files/47804_2015disastertrendsinfographic.pdf

Analysis of Rainfall Induced Landslide Dam Geometries and Failures

XuanKhanh Do^{1,a}, Kahhoong Kok^{2,b}, Wansik Yu^{3,c}, and Kwansue Jung^{2,d*}

Abstract. Landslide dam is formed as consequence of natural disasters such as typhoon and earthquake. The water impounded behind the landslide dam in a river may inundate the upstream areas and thus the formation of landslide dam possesses hazardous risk to the areas in the vicinity of the landslide dam. Recently, the occurrence of landslide dam problems has been aggravated due to the effects caused by climate change and the further expansion of land use in mountainous areas. Landslide dam hazard is often analyzed as a single event. There is still no research describing landslide dam hazards as a cascading disaster which starts from the occurrence of landslide located near river banks, forms a dam in the river, and ends when the dam overtops. This paper investigates the failure process of rainfall induced landslide dam in 3-dimensions through laboratory experiments and numerical method. The results indicated that both bottom erosion and side bank erosion played an important role in the breach evolution process. By using the identical sediment and constant inflow rate, the dam height is directly proportional to the rate of erosion. The peak discharges maybe much greater than normal inflow rate. In the simulation, the outflow discharge and the variation of dam surface erosions were well estimated by the 2D surface flow erosion/deposition model.

Keywords. *Landslide dam, breach, overtopping, numerical simulation*

XuanKhanh Do
Phd, Department of Civil Engineering
Thuyloi University, Hanoi, Vietnam.
augustxk1982@gmail.com

Kahhoong Kok
Phd candidate, Department of Civil Engineering
Chungnam National University, Daejeon, South Korea.
kahhoong_kok@yahoo.com

Wansik Yu
Phd, Department of Civil Engineering
IWRRI, Chungnam National University, Daejeon, South Korea.
yuwansik@gmail.com

Kwansue Jung
Professor, Department of Civil Engineering
Chungnam National University, Daejeon, South Korea.
ksjung@cnu.ac.kr

Introduction

Landslide dam presents as a natural blockage of river by hill slope-derived mass movement (Costa & Shuster, 1988). Intense rainfall, rapid snow melts, volcanic eruptions, and earthquakes are the most common landslide dam triggering factors (Wieczorek, 1996). Most of landslide dam (90%) was reported to be triggered by either rainstorms/snowmelts or earthquakes (Schuster, 2000), while the other less common causes, such as volcanoes or even anthropogenic activities have been documented as well. Landslide dam may fail by a variety of processes including overtopping, abrupt collapse or progressive failure. However the most common type is overtopping (Takahashi, 1991). This failure is generally caused by water spilling over the dam crest and eroding a channel along the downstream face of the dam. Breach growth occurs by both fluvial erosion of the floor of the breach channel via sediment entrainment and slope failures of the breach sidewalls and downstream face.



Fig. 1 Landslide dam in Sunkoshi River, Nepal

This study aims to investigate landslide problem as a cascading disaster. Firstly, the geometry of a landslide dam will be determined in considering its mixed character between landslide and valley floor. Secondly, the failure by overtopping of landslide dam in 3D shape was examined. This study was completed through performing both laboratory experiments and numerical simulation of non-cohesive homogenous landslide dam.

Laboratory experiments on the failure of landslide dam by overtopping

The experiments were carried out in a flume with dimensions, 5.0 m long, 0.5 m wide, and 0.6 m deep. This one-side glass flume was fixed with a bottom slope (θ). The landslide dam was located at 2.0 m from the inlet of the flume. Fine sand of mean diameter 0.42 mm was used to prepare landslide dams in the flume. The geometry of the landslide dam was determined by the following parameter: the longitudinal base length (LB) was 90 cm, the width of landslide dam W was equal to the flume width (50cm), right height (hr) of the dam was fixed at 20cm while the left height (hl) of the dam was varied in each experiment (10cm or 15cm). A same constant inflow discharge of $233\text{cm}^3/\text{s}$ was supplied in all 3 experiments.

During the experiments, a grid size scale 5.0 cm long \times 2.0 cm height covering the shape of the landslide dam was set at the glass side wall to record the changes of dam surface at different time (Fig 2). A ruler was also placed near to the landslide dam to be able to measure the upstream stage hydrograph. In order to measure the outflow hydrograph, a series of buckets were prepared at the downstream end of the flume. The average discharge in every 5 second after the dam break was calculated by the volume of water collected by one bucket in the same 5 seconds period. The flume experiment set up is presented in Fig 2. Tab 1 illustrates the sediment parameters and Fig 3 depicts the grain size distribution of the sediment used to form the landslide dam.

Table 1. Sediment parameters used for the experiment

Sediment type	Sand
Saturated moisture content, θ_s	0.32
Residual moisture content, θ_r	0.02
Van Genuchten parameter, α	3.15
Van Genuchten parameter, η	5.25
Saturated hydraulic conductivity, K_s (m/s)	0.000142
Specify gravity, G_{sg}	2.65
Mean grain size, D_{50} (mm)	0.42
Angle of response, ϕ	34°
Porosity, n	0.32

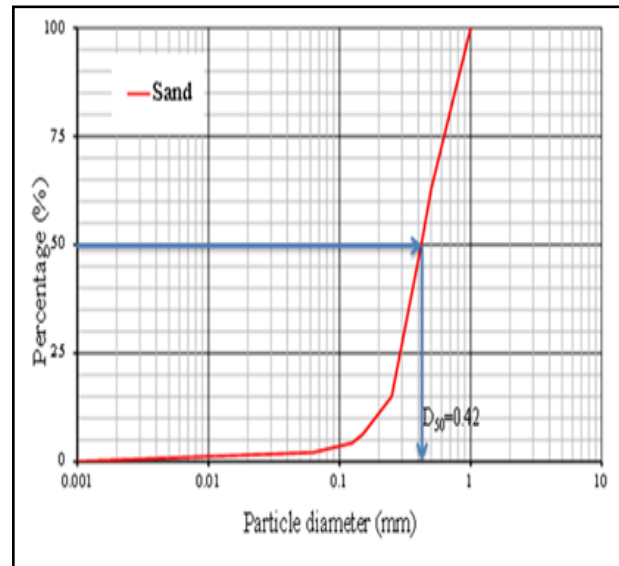


Fig. 3 Grain size distribution of the sediment used in the experiment

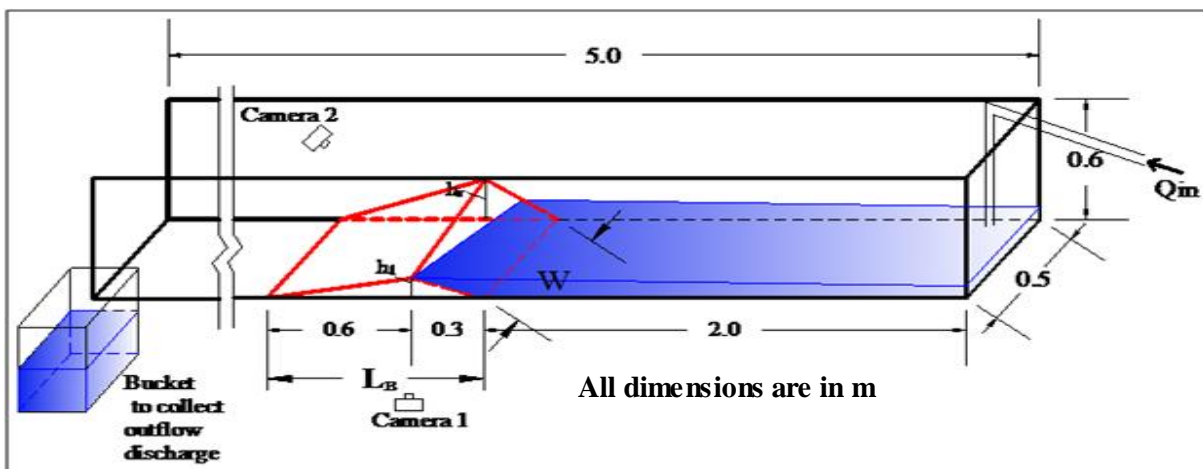


Fig. 2 Experimental set up of the failure of landslide dam by overtopping

Numerical model for landslide dam failure caused by overtopping

A 2-Dimensional surface flow erosion/deposition model developed by Takahashi et al (1992) was applied to perform the numerical analysis of the surface flow and erosion/deposition on the surface of the model slope. The depth-wise averaged 2D momentum equations for the x-wise (down valley) and y-wise direction directions are, respectively:

$$\frac{\partial M}{\partial t} + \beta \frac{\partial (uM)}{\partial x} + \beta \frac{\partial (vM)}{\partial y} = gh \sin \theta_{bx} - gh \cos \theta_{bx} \frac{\partial (h + z_b)}{\partial x} - \frac{\tau_{bx}}{\rho_t}$$

$$\frac{\partial N}{\partial t} + \beta \frac{\partial (uN)}{\partial x} + \beta \frac{\partial (vN)}{\partial y} = gh \sin \theta_{by} - gh \cos \theta_{by} \frac{\partial (h + z_b)}{\partial y} - \frac{\tau_{by}}{\rho_t}$$

The continuity equation of the total volume is:

$$\frac{\partial h}{\partial t} + \frac{\partial M}{\partial x} + \frac{\partial N}{\partial y} = i \{ c_* + (1 - c_*) s_b \}$$

The continuity equation of the particle fraction is:

$$\frac{\partial ch}{\partial t} + \frac{\partial (cM)}{\partial x} + \frac{\partial (cN)}{\partial y} = ic_*$$

The equation for the change of bed surface elevation is:

$$\frac{\partial z_b}{\partial t} + i = i_{sml} + i_{smr}$$

where $M (=uh)$ and $N (=vh)$ are the flow discharge per unit width in the x and y direction; u and v are the depth-averaged velocity in the x and y direction; h is the water depth; g is the gravitational acceleration; β is the momentum correction factor equal to 1.25 for stony type debris flow (Takahashi et al, 1992) and 1.0 for both an immature debris flow and a turbulent flow; θ_b is the bed slope; z_b is the erosion or deposition thickness measured from the original bed elevation; τ_{bx} and τ_{by} are the bottom shear stresses in the x and y direction, respectively; ρ_T is the mixture density; s_b is the degree of saturation in the bed; i is the rate of hydraulic erosion or deposition from the flowing water; c is the sediment concentration in the flow; c^* is the maximum sediment concentration in the bed; ρ is the density of water; σ is the density of the sediment particles; i_{sml} and i_{smr} are the mean recessing velocity of the left and right hand side banks of the incised channel. The cross section of the breach on the dam is shown in Fig. 4.

According to Takahashi et al (1992), the erosion and deposition rate at the bank and surface are:

$$\frac{i_b}{\sqrt{gh}} = K_e \sin^{\frac{3}{2}} \theta \left[1 - \frac{\sigma - \rho_T}{\rho_T} c \left(\frac{\tan \phi}{\tan \theta} - 1 \right) \right]^{\frac{1}{2}} \cdot \left(\frac{\tan \phi}{\tan \theta} - 1 \right) (c_\infty - c) \frac{h}{d_m}$$

$$\frac{i_s}{\sqrt{gh}} = \left(\frac{1}{2} \right)^{\frac{3}{2}} K_{es} \sin^{\frac{3}{2}} \theta \left[1 - \frac{\sigma - \rho_T}{\rho_T} c \left(\frac{\tan \phi}{\tan \theta} - 1 \right) \right]^{\frac{1}{2}} \cdot \left(\frac{\tan \phi}{\tan \theta} - 1 \right) (c_\infty - c) \frac{h}{d_m}$$

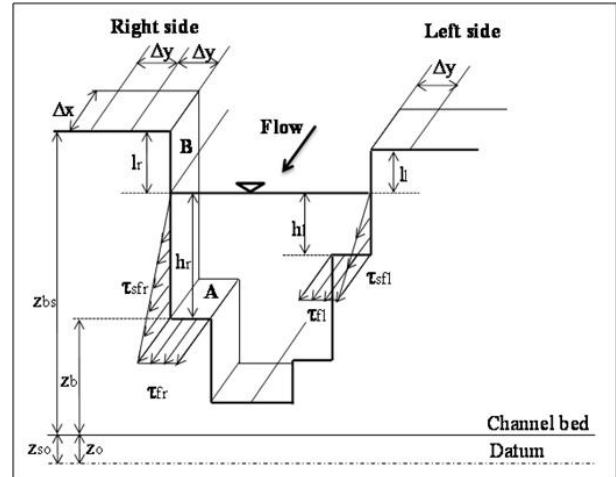


Fig. 4 Cross section of the breach on the dam

Results and discussion

After the construction of landslide dam, a steady discharge of 223cm³/s from the upstream part of the flume was supplied to create a reservoir behind the dam. The observed overtopping time and the final breach time (the time when the dam crest is eroded to bottom level) of three experiments were recorded in Tab. 2. Fig. 5 illustrates the failure process of landslide dam by overtopping at different time in experiment 1. The failure process was similar in all experiments. It started with the breach at the left side (the lowest point of the dam crest) by the overtopping flow. The flow then eroded the downstream surface of the dam creating an erosion gully. These gullies were gradually deepened continuously by bottom erosion and enlarged to the right bank by the effect of side bank erosion. The final breach width at the crest position was different in three experiments. They were 10.2 cm, 15.3 and 7.1 cm in Exp. 1, 2 and 3 respectively. The eroded channel was observed to be incised almost vertically.

Fig6 shows the comparison of the simulated and experimental outflow hydrographs in experiment 1. The main trend of these hydrographs and the peak discharges in all 3 experiments were well predicted. The Sutcliffe efficiency coefficients which present the accuracy of the simulated discharge are 0.880, 0.868 and 0.851 in experiment 1, 2 and 3, respectively. Calibration was also conducted for bottom erosion velocity K_e and side bank erosion velocity K_{es} for further enhancing the accuracy of the simulation results. The results of calibration for K_e and K_{es} for experiment 1 are illustrated in Fig 7 and Fig8. These calibrated parameters were

used to simulate the eroded shape of the landslide dam for experiment 1 as shown in Fig 9.

Table2 Observed overtopping time and final breach time

Exp. No	Bottom Slope	Right dam height (cm)	Left dam height (cm)	Discharge (cm ³ /s)	Overtopping time(s)	Final breach time (s)
Exp. 1	1/500	20	10	223	350	514
Exp. 2	1/500	20	15	223	625	810
Exp. 3	1/1000	20	10	223	400	580

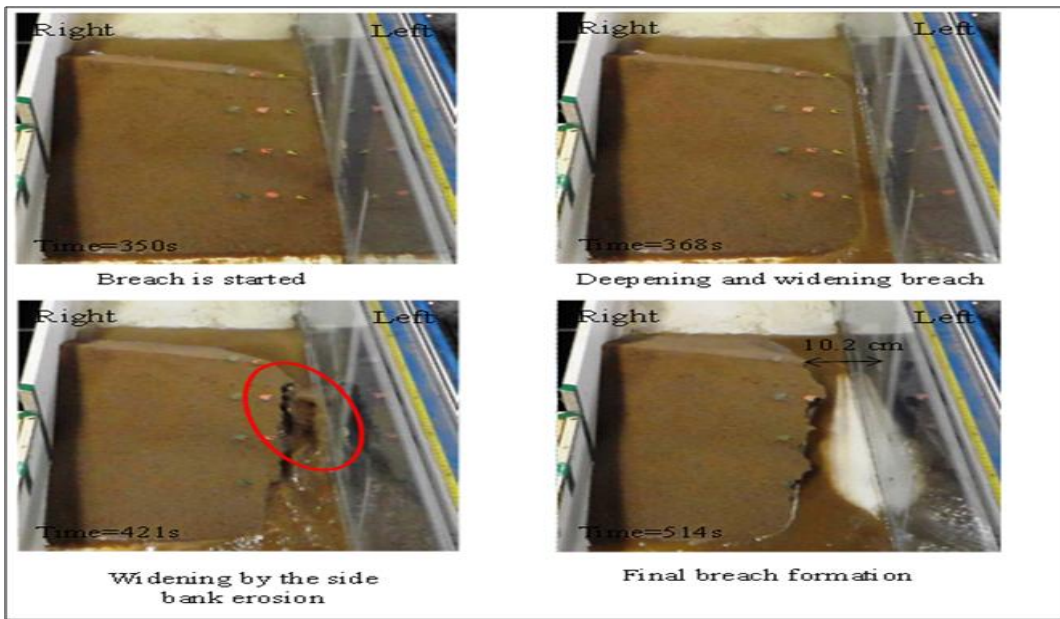


Fig.5 Failure process of landslide dam by overtopping in experiment 1

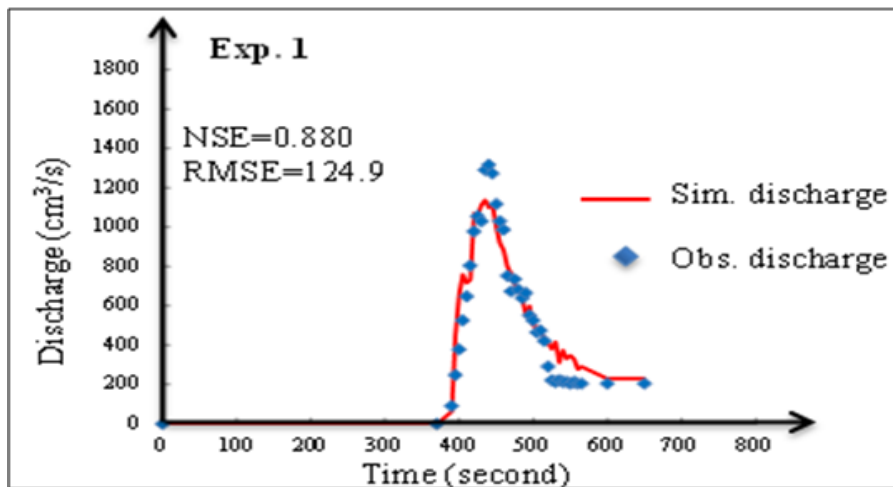


Fig.6 Calibration of ourflow discharge for experiment 1

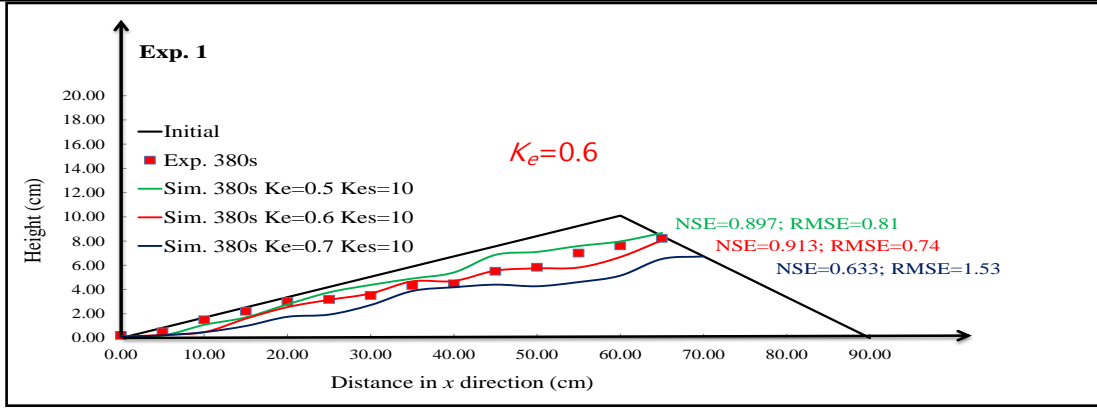


Fig.7 Calibration of bottom erosion velocity, K_e for experiment 1

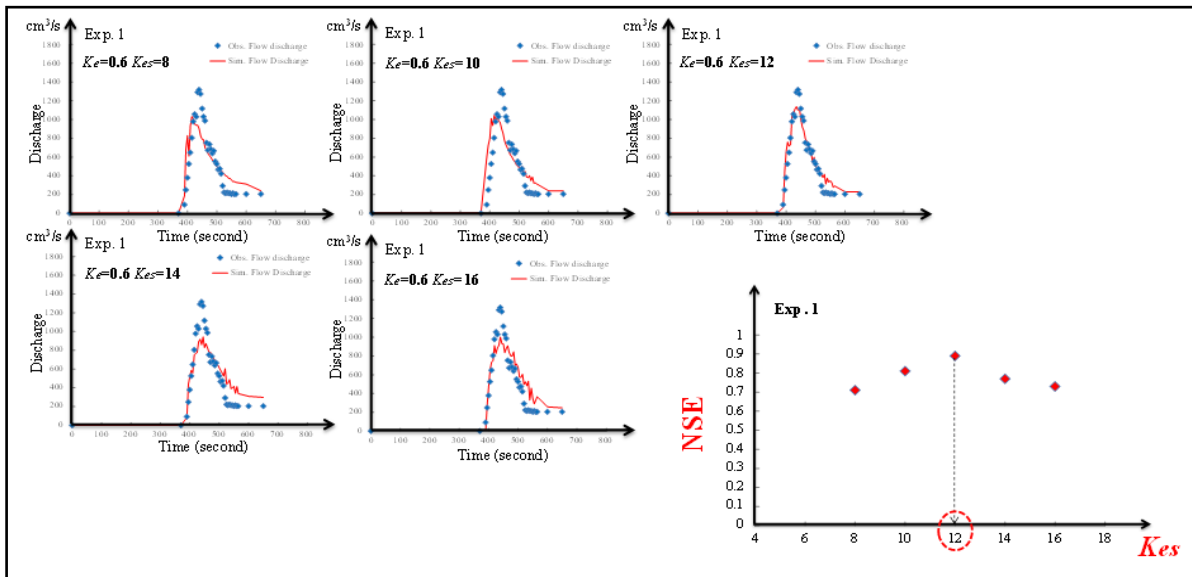


Fig.8 Calibration of side bank erosion velocity, K_{es} for experiment 1

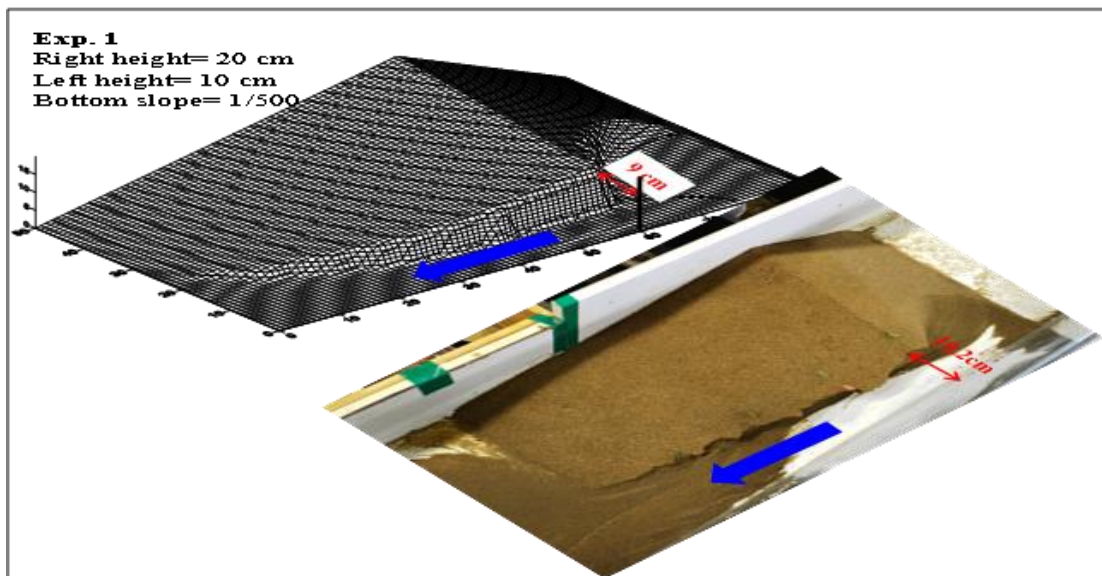


Fig.9 Simulated shape of landslide dam after overtopping failure in experiment 1

Summary and conclusions

This study has investigated the failure process of rainfall induced landslide dam in 3-dimensions through laboratory experiments and numerical approaches. The results indicated that the failure mechanisms of landslide dam by overtopping depend greatly on the bottom and side bank erosion which are mainly driven by bottom erosion velocity, K_e and side bank erosion velocity, K_{es} . Both of these parameters have been calibrated with experimental data obtained from this study for further enhancing the accuracy of the simulation results. The breach process of landslide dam by overtopping, the erosion of longitudinal profile as well as the outflow hydrographs were well simulated by the 2-D surface flow erosion/deposition model proposed in this study. The study also suggested that the water impounded behind the landslide dam would produce a peak discharge which is several times greater than the incoming discharge as overtopping failure of the landslide dam is initiated.

Acknowledgement

This research was supported by a grant (11-TI-C06) from Advanced Water Management Research Program which is funded by Ministry of Land, Infrastructure and Transport of Korean government.

References

- Costa, J.E and Shuster, R.L. 1988. The formation and failure of natural dam. *Geol. Soc. Am. Bull.* 100, pp. 1054-1068.
- Wieczorek, G.F. 1996. Landslide triggering mechanisms, in: *Landslides Investigation and Mitigation*, edited by: Turner, A. K. and Schuster, R. L., special report 247. National Academy Press, Washington D.C.
- Schuster, R. L. 2000. A world wide perspective on landslide dams, in D. Alford and R. L. Schuster (eds.) *Usoi landslide dam and lake Sarez*, ISDR Prevention Series, United Nations, Tajikistan, pp. 19-22.
- Takahashi, T. 1991. Debris flow, monograph series of IAHR. Balkema, pp. 1-165.
- Takahashi, T., Nakagawa, H., Harada, T. and Yamashiki, Y. 1992. Routing debris flows with particle segregation. *Journal Hydraulic Engineering, ASCE*, Vol. 118, No. 11, pp. 1490~1507, DOI: 10.1061/(ASCE)0733-9429(1992)118:11(1490).

*Iron oxide coated activated carbons for arsenate adsorption from groundwater**

Manavanh Muongpak^{1,a}, Sutha Khaodhiar^{2,b*} and Jenyuk Lohwacharin^{3,c*}

Abstract Arsenic is an abundant element that exists in both natural and anthropogenic sources, including groundwater in many parts of the world. Adsorption is one of the best technologies for arsenic removal from water, particularly for a small-scale system. The aim of this study was to investigate the arsenate (As (V)) adsorption onto iron oxide coated activated carbon. The physicochemical properties were characterized by scanning electron microscopy (SEM) with energy dispersive X-ray spectroscopy (EDX), porosity and pore size distribution analysis. Batch experiment was conducted to examine the effects of the equilibrium solution pH, adsorbent dosage, contact time and co-existing ions on arsenate removal. The results indicate that the maximum arsenate adsorption efficiency is achieved 90% in the condition of equilibrium pH 5.5, adsorbent dosage of 5 g/L and contact time of 16 h with the initial arsenate (As (V)) concentration of 1 mg/L. Langmuir and Freundlich models for the arsenate adsorption were used to determine the adsorbent capacity for arsenate removal by iron oxide coated activated carbon. The equilibrium data was described by Langmuir and Freundlich isotherms.

Keywords *Arsenate, Adsorption, Activated carbon, Iron oxide, Groundwater*

Manavanh Muongpak
Department of Environmental Engineering
Chulalongkorn University
Bangkok, Thailand
manavanh.m@student.chula.ac.th

Sutha Khaodhiar
Center of Hazardous Substance Management
Chulalongkorn University
Bangkok, Thailand
Sutha.k@chula.ac.th

Jenyuk Lohwacharin
Department of Urban Engineering
The University of Tokyo
Tokyo, Japan
jenyuk@env.t.u-tokyo.ac.jp

Introduction

Arsenic exists in both natural and anthropogenic sources, including groundwater, and has been recognized as a highly toxic element to all forms of the life and recorded by World Health Organization as the first-priority issue. World Health Organization recommends that the maximum contaminant level (MCL) of 10 µg/L for arsenic in drinking waters (WHO, 2011). Natural sources include the washout and erosion of arsenic containing mineral ores and soil, which probably occurs because of long-term exposure against geochemical changes. Anthropogenic sources include forestry, agricultural application of pesticides, herbicides and fertilizers, and industrial effluents from metallurgy, electronics, mining, glass processing, ceramic, pharmaceuticals, dye and pesticide, wood preservative, petroleum refining and landfill leaching (Smédley and Kinniburgh, 2002; Kim et al., 2002; Budinova et al., 2009). In Laos, arsenic contaminated aquifers exceeding the maximum permissible level of 25 µg/L were found in Champasak province. To remove arsenic, ion exchange, reverse osmosis, chemical coagulation-precipitation, membrane filtration, electrolysis, and adsorption are typically used (George et al., 2006; Pal et al., 2007; Walker et al., 2008; Fogarassy et al., 2009; Guell et al., 2010; Manna et al., 2010; Anirudhan and Jalajamony, 2010). Among these treatment technologies, the chemical precipitation process is suitable for large scale wastewater treatment because of its economical feasibility and simplicity. Ion exchange, reverse osmosis, membrane filtration and electrolysis have disadvantages in terms of maintenance cost and economic viability, thus they have not been widely used. In contrast, adsorption is one of the best technologies for arsenic removal from water due to its ease to operate, no sludge produced, high efficiency, and cost-effectiveness (Jang et al., 2006). The combination of activated carbon and iron oxide have been reported to improve adsorption capacities and mechanical properties, indicating that arsenic adsorption process is becoming to be more effective for arsenic removal (Chen et al., 2007; Jang et al., 2008; Fierro et al., 2009). In this study explores the possibility of iron oxide (FeCl₂) coated activated carbon to eradicate arsenate As(V) in presence of iron which has commonly found in groundwater. The effects of equilibrium pH, contact time, adsorbent dosage and co-

existing ions on arsenate removal were studied and also the optimum kinetics and adsorption isotherm.

Materials and methods

Materials

All chemical, including ferrous chloride ($\text{FeCl}_2 \cdot 4\text{H}_2\text{O}$), sodium arsenate ($\text{HAsNa}_2\text{O}_4 \cdot 7\text{H}_2\text{O}$), ferrous sulphate ($\text{FeSO}_4 \cdot 7\text{H}_2\text{O}$), hydrochloric acid, nitric acid, sodium hydroxide, potassium hydrogen phthalate, borax, potassium dihydrogen phosphate, and sodium bicarbonate were analytical grade. Deionized water (18 $\text{M}\Omega\text{-cm}$) was used in all experiments. As(V) stock solution (100 mg/L) was used to prepare arsenate working solutions by diluting the stock with deionized water. pH adjustment was performed with sodium hydroxide, hydrochloric acid, potassium hydrogen phthalate, borax, potassium dihydrogen phosphate, and sodium bicarbonate. FILTRASORB® 200 granular activated carbon (GAC), is made from select grades of bituminous coal through a process known as re-agglomeration, used in this study. GAC was firstly rinsed with deionized water to remove all impurities, then dried at 105°C overnight and stored in a desiccator. A portion of GAC has been ground by cup mill to generate powdered activated carbon with the effective size of 125-250 μm .

Preparation of iron oxide coated activated carbon

Preparation of iron oxide coated activated carbon used in this study has produced using $\text{FeCl}_2 \cdot 4\text{H}_2\text{O}$ following the methodology by Qigang Chang et al., (2010). Briefly, 30 grams of GAC or PAC was added into a 250-mL glass bottle in contact with 0.5 M ferrous chloride solution and 10% nitric acid, without headspace to avoid ferrous oxidation and precipitation. The bottle was placed on an orbital shaker for 24 hours to ensure saturation and penetration of ferrous ion into GAC and PAC pores. Later, the GAC and PAC were separated from the ferrous solution and washed with deionized water until rinsing water becomes neutral ($\sim\text{pH } 7$). Then, the adsorbents were dried in a convective oven at 105°C for 10h. This step above was repeated three and finally stored in a desiccator for further usage.

Characterization of adsorbents

Specific surface area and total pore volumes of adsorbents were determined from the corresponding N_2 adsorption-desorption isotherm at 77 K using Surface Area Analyzer (Quantachome, Autosorb-1). The surface morphologies of activated carbon before and after coated iron oxide were observed with S-4800 (Hitachi, Japan), a scanning electron microscope (SEM) and analyzed by energy-dispersive X-ray spectroscopy (EDX).

Batch adsorption experiments

Batch adsorption experiments were performed to examine the effects of equilibrium pH, contact time, adsorbent dosage, and co-existing ions on arsenate

adsorption at room temperature ($25 \pm 1^\circ\text{C}$). Arsenate working solution of 1 mg/L was prepared freshly for each experiment in aqueous solution. To determine the effect of pH and contact time on arsenate adsorption, the experiments were performed at various initial pH (2–8) and contact time (15 min–24 h). The initial concentration of 1 mg/L and adsorbent dosage of 5.0 g/L were employed. To determine the effect of adsorbent dosage, and co-existing ions, the experiments were conducted at various adsorbent dosage (1–7 g/L), and co-existing ions (5 mg/L). The experiments were placed in orbital shaker at 200 rpm for approximately 24 hours to ensure the equilibrium was reached. The adsorption kinetic study was performed for arsenate adsorption at equilibrium pH 5.5 with the arsenate initial concentration of 1, 2 and 5 mg/L and 5.0 g/L of adsorbent dosage at room temperature ($24 \pm 1^\circ\text{C}$). After each experiment, the samples were filtered through 0.45 μm membrane filter and analyzed for total arsenic by Inductively Couple Plasma Mass Spectrometry (ICP-MS) at wavelength 193.695 nm in accordance with the USEPA method 200.5. The calibration curve, with a concentration series of 0, 0.001, 0.005, 0.01, 0.05, 0.1, 0.5, 1.0, 3.0 and 5.0 mg/L, was prepared by using arsenic standard solution (1000 mg/L in 7% nitric acid, Ultra Scientific certified). All experiments were repeated thrice and averaged the result has been reported. The adsorption capacity of adsorbents was calculated according to mass balance on arsenate ions express as:

$$q_e = \frac{(C_0 - C_e)V}{M} \quad (1)$$

The removal efficiency (%R) in percentage of the adsorbents were calculated using the following equation:

$$\% \text{Removal} = \frac{C_0 - C_e}{C_0} \cdot 100 \quad (2)$$

where: q_e is the amount of arsenate adsorbed onto unit mass of the adsorbent (mg/g), C_0 and C_e are the initial and equilibrium arsenate concentration in the aqueous solution (mg/L), respectively; V is the volume of solution (L) and M is the mass of adsorbent used (g).

Result and discussion

Characterization of adsorbents

The microstructures of virgin activated carbon and iron oxide coated activated carbons were listed in Table 1. The iron-coated activated carbons show the decrease in the surface area and total pore volume from 765.9 to 721.9 m^2 for GAC, from 768.0 to 561.38 m^2 for PAC and to 0.5363 cc/g for GAC and 0.4312 cc/g for PAC. SEM image and EDX spectrum of pure activated carbons (PAC and GAC) and iron coated activated carbons (Fe-PAC and Fe-GAC) has shown in Figure 1. Comparing the EDX spectrum of activated carbons

(PAC and GAC) before and after coated with iron oxide, the Fe contents of virgin activated carbons (PAC and GAC) and iron oxide activated carbons (Fe-PAC and Fe-GAC) had

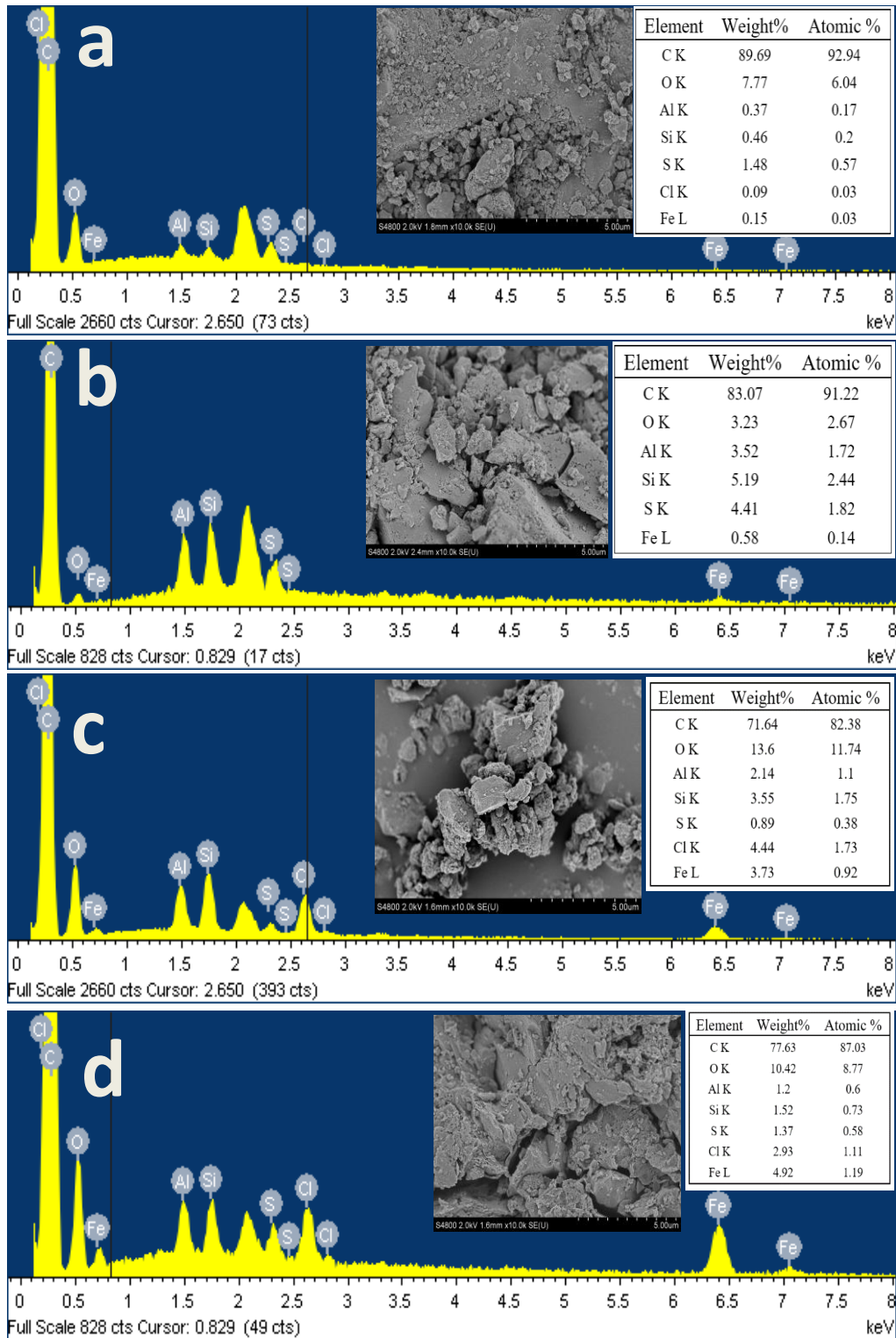


Figure 1. SEM images and EDX spectrum of FILTRASORB® 200 (a: Pure PAC; b: Pure GAC; c: 3.73% iron PAC and d: 4.92% iron GAC)

Table 1 Microstructure of pure activated carbon and iron oxide coated activated carbon

Sample	Multipoint BET (m ² /g)	Total pore volume (cc/g)	Average pore diameter (Å)
PAC	768.06	0.5402	28.13
GAC	765.86	0.5603	29.26
Fe-PAC	561.38	0.4312	30.72
Fe-GAC	721.89	0.5363	29.71

0.15%, 0.58%, 3.73% and 4.92% respectively, indicating successful coating to activated carbon.

Effect of the equilibrium solution pH

The solution pH is an important factor for all water and wastewater treatment systems. Especially in arsenate adsorption in the aqueous phase, because the arsenate species and the surface charge of iron oxide coated activated carbons in aqueous phase depend on pH. Hence, the experiments were performed to investigate the effect of equilibrium pH of the solution to be treated regarding arsenate (As(V)). Therefore, keeping the pH value of the solution at a constant level is needed to investigate the real effect of pH on the arsenate adsorption. Arsenate adsorption on adsorbents was carried out at 7 level of pH at room temperature (25°C ± 1) and 1 mg/L of the arsenate (As(v)) initial concentration. Figure 2 illustrates the percentage of arsenate removal as a function of pH value at pH ranging from 2.0 to 8.0.

It is evident that the arsenate (As(V)) removal strongly depends on the solution pH. Furthermore, it can be noticed that the maximum adsorption capacities of iron oxide coated activated carbon for arsenate removal occurred at pH 2.0-6.0. Arsenate adsorption decreases with increasing pH. The maximum arsenate adsorption capacity was found at lower pHs as observed by several previous studies (Vitela-Rodriguez and Rangel-Mendez,

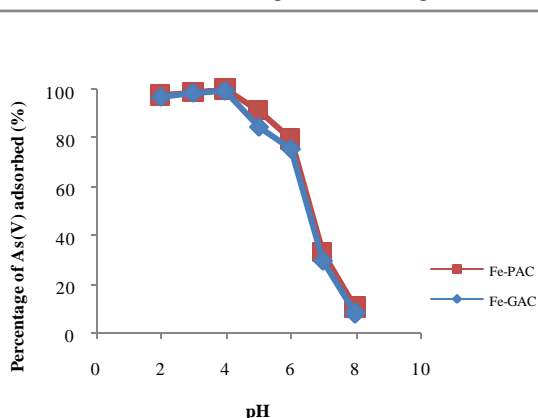


Figure 2 Effect of equilibrium pH on the arsenate adsorption.
 (Experiment conditions employed: initial As(V) concentration 1 mg/L, adsorbent dosage 5.0 g/L, adsorption time 24 hours, shaken speed 200 r/min)

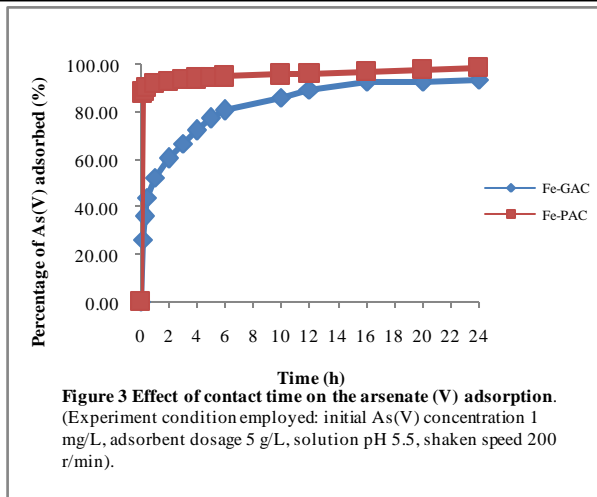


Figure 3 Effect of contact time on the arsenate (V) adsorption.
 (Experiment condition employed: initial As(V) concentration 1 mg/L, adsorbent dosage 5 g/L, solution pH 5.5, shaken speed 200 r/min).

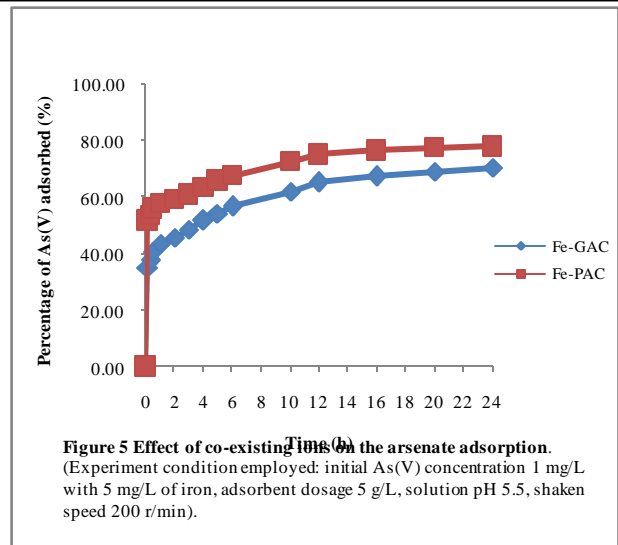
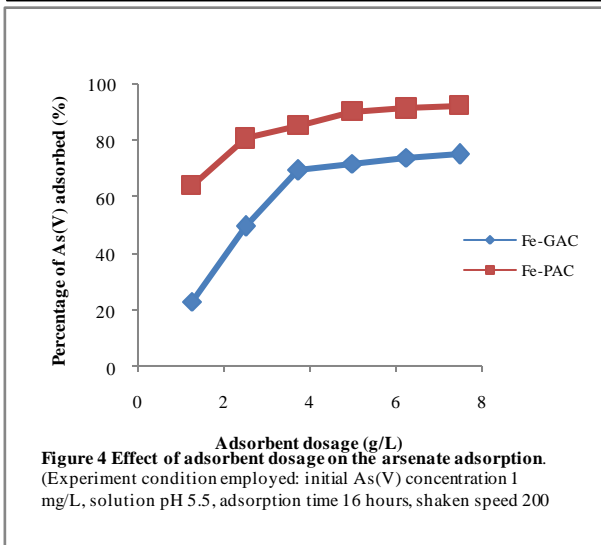
2013; Mondal et al., 2008; Gu et al., 2005; Oliveira et al., 2002). At pH 4.0, adsorption capacities of Fe-PAC and Fe-GAC were 0.178 and 0.176 mg/g, which represented 100 % and 99.64 % arsenate adsorption efficiency, respectively. These results indicated the iron oxide coated activated carbon adsorbents had much higher arsenate adsorption capacities than virgin activated carbon in the literature (Pattanayak et al., 2000). Although the highest removal efficiency had taken place at pH 4.0 (99.64% and 100%), pH 5.5 had selected as an optimum pH condition for further experiments due to is close to pH of real bearing groundwater.

Effect of contact time

Contact time is one of the important factors for batch adsorption process. Figure 3 illustrates the effect of contact time on arsenate adsorption which increases at the initial adsorption phase and continuous increase in low speed until the equilibrium reached. The equilibrium maintained later 16 hours of contact time in the batch experiment. There was no significant change in the arsenate adsorption rates during 16 hours to 24 hours. Based on the result, 16 hours was taken as the contact time in the further adsorption experiment. Normally, the removal rate of adsorbate is rapid at the first stage, but it gradually decreases with contact time until it reaches equilibrium. Since a large number of surface area of adsorbents are available for adsorption at the first stage, and after a period of time in adsorption, the residual surface areas available for arsenate adsorption are hard to be occupied because of repulsive forces among the solute molecules on the bulk and solid phases.

Effect of adsorbent dosage

The effect of adsorbent dosage on arsenate As(V) adsorption had shown in Figure 4. From this figure, the removal efficiency increases with increasing adsorbent dosage. Increasing adsorbent dosage from 1g/L to 5g/L for iron oxide coated activated carbons results in an increase from 23.18% to 71.65% and 63.77% to 90.1% for Fe-GAC and Fe-PAC, respectively. It is proved that the increased adsorbent dosage can raise the arsenate removal percentage for iron oxide coated activated



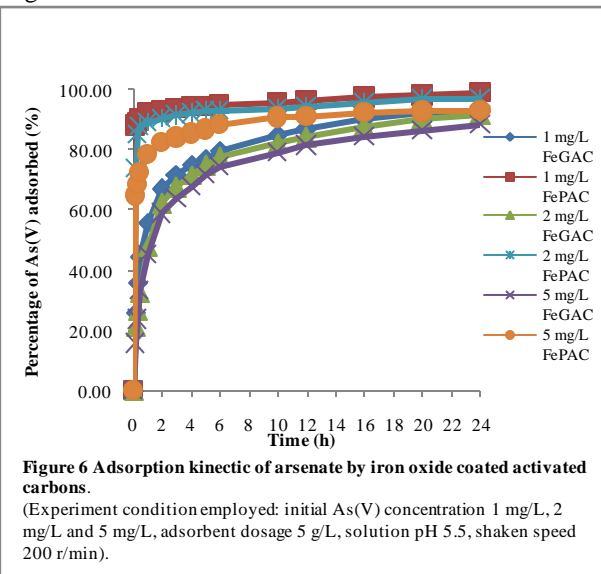
carbons. The additional increase of adsorbent dosage does not cause significant enhancement for arsenate adsorption. Hence, 5 g/L of iron oxide coated activated carbon adsorbent has selected for the next study.

Effect of co-existing ions

Ions such as Fe is usually present in groundwater and can affect in the arsenate adsorption. To examine the effect of co-existing ions on arsenate As(V) adsorption, arsenate liquid solution was interrupted with ferrous sulphate and the arsenate adsorption was determined. At equilibrium pH of 5.5, the effect of co-existing ion on arsenate adsorption showed in Figure 5 that ferrous sulphate caused a lot of reduction in arsenate adsorption. Under the experiment conditions, iron has decreased on arsenate adsorption due to the competition of the ions and arsenate on iron oxide adsorbent pores.

Adsorption kinetics

To obtain the adsorption kinetic of arsenate adsorption onto iron oxide coated activated carbon. 1 mg/L, 2 mg/L and 5 mg/L of the initial concentration had recorded. Figure 6 illustrate that all of three concentration had



reached the equilibrium at 16 hours. For the increasing of time (<16 hours), the adsorption trend appears to be constant. The pseudo-second-order rate equation model has applied to the kinetic data:

$$t/q_t = 1/(k_2 \cdot q_e^2) + t/q_e \quad (3)$$

where: q_t and q_e are the adsorbed amount at time t and equilibrium, respectively. K is the rate constant (Ho and Ofomaja, 2006). The kinetic constant k_2 , can be determined by plotting of t/q_t against t .

The kinetic experiment data are listed in Table 2. The value of the pseudo-second-order rate constant decreased with the increasing of the initial concentration of arsenate.

Adsorption isotherm

The adsorption isotherm indicates how the adsorption molecule distribute between the solid and liquid phase when the adsorption reaches the equilibrium state. The most widely used to describe the experimental data of the adsorption are Langmuir and Freundlich isotherm models. The adsorption isotherm model parameter of iron oxide coated activated carbons at pH 5.5 are shown in Table 3. These isotherms represent the adsorption behavior of arsenate on the different types of iron oxide coated activated carbon for a contact time 24 hours.

Table 2 Kinetic parameters for arsenate adsorption onto iron oxide activated carbons

Adsorbent	C_0 (mg/L)	q_e (mg/g)	K_2 (L/(mg.min))	R^2
Fe-PAC	1	0.187	5.289	0.9998
	2	0.352	2.806	0.9998
	5	0.752	1.310	0.9998
Fe-GAC	1	0.1728	5.493	0.9984
	2	0.3216	2.885	0.9976
	5	0.688	1.347	0.9977

Table 3 The adsorption parameters of Langmuir and Freundlich equation

Adsorbent	Langmuir equation			Freundlich equation		
	q_m (mg/g)	B (L/mg)	R^2	1/n	K_f	R^2
Fe-PAC	0.923	12.44	0.9754	0.4323	1.1721	0.9976
Fe-GAC	1.495	1.545	0.9998	0.7186	1.060	0.9962

Conclusion

Iron oxide coated activated carbons were successfully prepared as an adsorbent material for arsenate removal. However, there is an effect of pH on the arsenate adsorption capacity, which decrease as the pH increases. The co-existing ions present in groundwater, mainly Ferrous compete with arsenate for active sites. Lastly, the performance of iron oxide coated activated carbons were compared to another adsorbent in literature which has higher adsorption capacity. Therefore, they can be an alternative for arsenate removal on continuous and large scale system. The adsorption kinetic illustrated very well by the pseudo-second order rate equation. The arsenate adsorption onto iron oxide activated carbons are fitted with Freundlich models well.

Reference

Anirudhan, T. and S. Jalajamony (2010). "Cellulose-based anion exchanger with tertiary amine functionality for the extraction of arsenic (V) from aqueous media." Journal of environmental management**91**(11): 2201-2207.

Budinova, T., et al. (2009). "Biomass waste-derived activated carbon for the removal of arsenic and manganese ions from aqueous solutions." Applied Surface Science **255**(8): 4650-4657.

Chang, Q., et al. (2010). "Preparation of iron-impregnated granular activated carbon for arsenic removal from drinking water." Journal of hazardous materials**184**(1): 515-522.

Chen, W., et al. (2007). "Arsenic removal by iron-modified activated carbon." Water research **41**(9): 1851-1858.

Fierro, V., et al. (2009). "Arsenic removal by iron-doped activated carbons prepared by ferric chloride forced hydrolysis." Journal of hazardous materials **168**(1): 430-437.

Fogsarassy, E., et al. (2009). "Treatment of high arsenic content wastewater by membrane filtration." Desalination **240**(1): 270-273.

George, C. M., et al. (2006). "Reverse osmosis filter use and high arsenic levels in private well water." Archives of environmental & occupational health **61**(4): 171-175.

Gu, Z., et al. (2005). "Preparation and evaluation of GAC-based iron-containing adsorbents for arsenic removal." Environmental science & technology **39**(10): 3833-3843.

Güell, R., et al. (2010). "Modelling of liquid-liquid extraction and liquid membrane separation of arsenic

species in environmental matrices." Separation and Purification Technology**72**(3): 319-325.

Ho, Y.-S. and A. E. Ofomaja (2006). "Pseudo-second-order model for lead ion sorption from aqueous solutions onto palm kernel fiber." Journal of hazardous materials**129**(1): 137-142.

Jang, M., et al. (2006). "Removal of arsenite and arsenate using hydrous ferric oxide incorporated into naturally occurring porous diatomite." Environmental science & technology**40**(5): 1636-1643.

Jang, M., et al. (2008). "Preloading hydrous ferric oxide into granular activated carbon for arsenic removal." Environmental science & technology**42**(9): 3369-3374.

Kim, M.-J., et al. (2002). "Arsenic species and chemistry in groundwater of southeast Michigan." Environmental Pollution**120**(2): 379-390.

Manna, A. K., et al. (2010). "Removal of arsenic from contaminated groundwater by solar-driven membrane distillation." Environmental Pollution**158**(3): 805-811.

Mondal, P., et al. (2008). "Effects of adsorbent dose, its particle size and initial arsenic concentration on the removal of arsenic, iron and manganese from simulated ground water by Fe³⁺ impregnated activated carbon." Journal of hazardous materials**150**(3): 695-702.

Oliveira, L. C., et al. (2002). "Activated carbon/iron oxide magnetic composites for the adsorption of contaminants in water." Carbon**40**(12): 2177-2183.

Pal, P., et al. (2007). "Removal of Arsenic from Drinking Water by Chemical Precipitation—A Modeling and Simulation Study of the Physical-Chemical Processes." Water environment research**79**(4): 357-366.

Pattanayak, J., et al. (2000). "A parametric evaluation of the removal of As (V) and As (III) by carbon-based adsorbents." Carbon**38**(4): 589-596.

Smedley, P. and D. Kinniburgh (2002). "A review of the source, behaviour and distribution of arsenic in natural waters." Applied geochemistry**17**(5): 517-568.

Vitela-Rodriguez, A. V. and J. R. Rangel-Mendez (2013). "Arsenic removal by modified activated carbons with iron hydro (oxide) nanoparticles." Journal of environmental management**114**: 225-231.

Walker, M., et al. (2008). "Effectiveness of household reverse-osmosis systems in a Western US region with high arsenic in groundwater." Science of the Total Environment**389**(2): 245-252.

SWAT and MODFLOW Modeling of Spatio-Temporal Runoff and Groundwater Recharge Distribution

J. Laonamsai^{1,a} and A. Putthividhya^{2,a*}

Abstract Thailand's changing climate patterns has led to instability and challenges to the people and the nation's economy. Drought caused by irregular rainfall has become a significant issue in Thailand in the most recent years as the central plain has no large water reservoirs of its own and is currently relying on dams in the lower Northern region for water. Effective water management needs to be practiced and conjunctive use of surface water and groundwater is being implemented. Interactions between groundwater and surface water in a basin have significant impacts on water management both at local and regional scales, particularly the spatial patterns of these interactions, as they provide basic knowledge on surface water and groundwater dynamic behavior. This paper aims to explore SWAT model for spatio-temporal surface water simulation and the estimation of groundwater recharge rates throughout Yom river basin during 1999-2012. Sensitivity analysis, calibration, validation, and uncertainty analysis are performed by SWAT-CUP software against streamflow and groundwater level. Due to the semi-distributed features of SWAT and the difficulty of calculating groundwater distributed parameters, recharge values estimated by SWAT are used in a MODFLOW model for groundwater simulation at steady and unsteady states. Although daily time steps are used to calculate groundwater discharge rates along the stream, modeling results are also averaged by month to determine seasonal trends. Results indicate high spatial variability in groundwater discharge. Average annual groundwater discharge is $24.73 \text{ m}^3/\text{s}$, with maximum and minimum rates occurring in September-October and March-April, respectively. Annual average rates increase by approximately $2.03 \text{ m}^3/\text{s}$ per year over the 14-year period, negligible compared with the average annual rate with 71.43% of the stream network experiences an increase in groundwater discharge rate between 1999 and 2012.

Keywords SWAT, MODFLOW, groundwater recharge, runoff, conjunctive use

A. Putthividhya

Assistant Professor : Department of Water Resources
Engineering
Faculty of Engineering, Chulalongkorn University
Bangkok, Thailand
dr.aksara.putthividhya@gmail.com

J. Laonamsai

Graduate Student : Department of Water Resources
Engineering
Faculty of Engineering, Chulalongkorn University
Bangkok, Thailand
teeyoon100@gmail.com

Introduction

Thailand's changing climate patterns has led to instability and challenges to the people and the nation's economy. Drought caused by irregular rainfall has become a significant issue in Thailand in the most recent years as the central plain has no large water reservoirs of its own and is currently relying on dams in the lower Northern region for water. Long periods of droughts are impacting rice and other cash crops production. Water scarcity is a global threat that is estimated to hit Thailand hard and the country is in need to develop a long-term plan to deal with these challenges. A thorough understanding of watershed hydrology is essential for sustainable water management, of particular importance are the interactions of groundwater and surface water. Without proper understanding of the hydrologic components for the planning of water resources, many problems may arise when attempting to establish water resource planning and security, optimize conjunctive use of groundwater and surface water (Sophocleous 2002); and evaluate the sensitivity of stream flows to changing climate or landuse alterations. These problems might eventually lead to complications and inaccurate predictions.

Up till now, hydrologic component analysis in Thailand has concentrated on the management of surface water, while problems related to groundwater have not been managed in a proper manner. Furthermore, the groundwater model frequently used in Thailand was not adequately linked to surface water analysis. The main focus in many previous studies has been primarily on aquifer management. For example, groundwater recharge could not be considered in terms of hydrological processes, which are directly related to precipitation, evapotranspiration, and surface runoff. Groundwater recharge rate was then an output to the groundwater model and had therefore been determined from trial and error during calibration.

Many techniques have been employed to estimate patterns of groundwater/surface water interactions at spatial and temporal scales, including water balance (Krause et al. 2007), Permeameter tests and seepage meters (Avery 1994), electrical resistivity surveys (Nyquist et al. 2008), and tracer

tests (Harvey and Bencala 1993). Typically these previous studies have been undertaken at small spatial scales over a short time period. For assessment at larger spatio-temporal scales, numerical modeling approaches have frequently applied. The best modeling effort should rely on a long-term rainfall runoff simulation that can effectively produce an integrated analysis for both the groundwater and the surface runoff. It is also essential for the model to be able to examine the hydrologic effects while concurrently allowing hydraulic interaction between surface water and groundwater. SWAT model is widely used for long-term runoff and water quality simulations. It was originally developed from the CREAMS (Knisel 1980) and SWRRB (Williams et al. 1985) models with channel routing and groundwater components added for larger watersheds. One of the most essential components of an efficient groundwater model is the accuracy of recharge rates within the input data. The conventional groundwater flow analysis is performed by MODFLOW often overlooks the accuracy of the recharge rates that are required to be calculated into the model. Consequently, there is considerable uncertainty in the simulated groundwater flow results.

To enhance understanding of large-scale groundwater-surface water interactions, and to taken the accuracy of the groundwater recharge component into consideration, this study virtually integrate SWAT and MODFLOW models to explore the spatial patterns of surface water and groundwater discharge to the stream and river network of a relatively large basin as well as estimate the groundwater discharge rate based on the hydrologic analysis from the watershed. Our study area is focused at the Yom river basin located in the North of Thailand with large irrigation serviced fields scattered all over the place, leading to individual private groundwater wells installation to compensate the frequent shortage of surface water. Spatio-temporal surface water simulation and the estimation of groundwater recharge rates are being conducted. Sensitivity analysis, calibration, validation, and uncertainty analysis were performed by SWAT-CUP software against streamflow and groundwater level. Due to the semi-distributed features of SWAT and the difficulty of calculating groundwater distributed parameters, recharge values estimated by SWAT are used in a MODFLOW model for groundwater simulation at steady and unsteady states. Although daily time steps are used to calculate groundwater discharge rates along the stream, modeling results are also averaged by month to determine seasonal trends. The combined use of both surface water and groundwater to meet the total local water demand provides a solution to this insecure situation as known as conjunctive water management (Chun 1964). Factors affecting the degree of interactions of surface water and groundwater include topography, underlying geology, subsurface hydraulic properties, temporal and spatial variation in precipitation, and local groundwater flow patterns (Cey et al. 1998). Determining the surface water-groundwater interactions and groundwater recharge sources is important for the effective management of groundwater resources, especially in drought threatening water resources management, and in the future

conditions under climate uncertainties as well as determination of migration pathways for contaminants (i.e., contaminated shallow aquifer recharges deep groundwater).

Study area

The upper Chao Phraya plain of Thailand shown in Figure 1 covers about 160,000 km² with a population of 4 million people. The main landuse is 63% agriculture, out of which 21% is irrigated, and 24% is devoted for forestry. More than 90,000 groundwater wells exist in the region to serve as primary and secondary source of water supply.

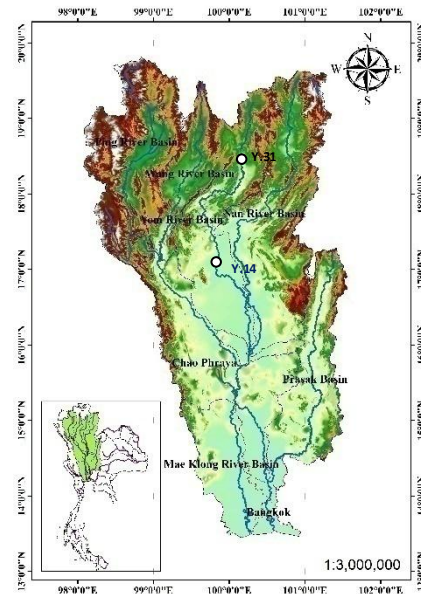


Fig. 1 Study area (Upper Chao Phraya River Basin)

Yom river basin is one of the eight sub-basins, stretching from latitude 15° 50' N to 19° 25' N and from longitude 99° 16' to 100° 40' E with a watershed area of 23,616 km². The basin covers about 16.56% of the Chao Phraya river basin. The climate of the study area belongs to the tropical monsoon type. Terraced mountain mainly characterize the topography of upper Yom basin from Phayao province to Phrae province, and then followed by floodplain area at Sukhothai, Pichit, and parts of Phitsanulok provinces. The main landuse of the basin is predominantly rice cultivation and cattle grazing. Most surface water is utilized for agricultural purposes in rainy season. Domestic and industrial water rely on water supply and groundwater. Agricultural sector also uses groundwater in conjunction with surface water in dry period. Groundwater table decline is spotted in some parts of the irrigated serviced fields due to uncontrolled severe pumping, leading to the critical current and future groundwater accessibility problems for the entire public water users in the system. To understand the use of water resources in this basin, the fundamental characteristics and recharge sources of the groundwater aquifer need to be analyzed.

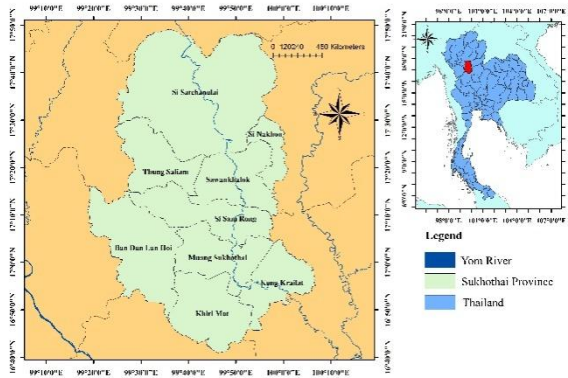


Fig. 2 Study area (Sukhothai Sub-Groundwater Basin)

Hydrogeological Conditions of the Study Area

Chao Phraya river basin is divided by 5 major rivers that flow from North to South, forming a depositional flood plain geological unit with average elevation of 40-60 m above MSL. On the Eastern and Western sides are surrounded by mountains of volcanic rocks. The basin drains directly into the lower basin in the South, though the free discharge is partially obstructed by crystalline rocks. Annual average rainfall of 900-1,450 mm is reported in the study region. The wet season starts from April to September and accounted for 81% of the total precipitation. On the other hand, 19% of the total rainfall occurs in the dry season between October and March. Irrigation water is diverted from Nan River at Naresuan diversion dam. The groundwater aquifer forms the geological basis as a depositional flood plain from North to Southeast with mountains of volcanic rocks surrounded in the West. More than 3,000 groundwater wells are present in this area with several groups of active intensive groundwater extraction. The aquifer system was defined as two-layered aquifer with the thickness of the upper, semi-confining layer varying between 10-70 m and lower confining layer between 100-300 m based on the hydrostratigraphic concepts that relying on the geological conditions of similar hydrogeologic properties and their confining boundaries.

Hydrogeologically, the Chao Phraya river basin is comprised of seven groundwater sub-basins: Chiangmai-Lampoon basin, Lampang basin, Payao basin, Prae basin, Nan basin, upper Chao Phraya basin, and lower Chao Phraya basin. Within these groundwater sub-basins, water is held in either confined or unconfined aquifers. Eight separate confined aquifers are located in the Upper Tertiary to Quaternary strata of the Bangkok area. Groundwater storage and renewable resources have been estimated for each groundwater sub-basin, as shown in Table 1.

Table 1 Groundwater storage and renewable water resources of the sub-basins (UNESCO)

Groundwater Basin	Groundwater Storage (million m ³)	Renewable Water Resources (million m ³)
Chiangmai-Lampoon	485	97
Lampang	295	59
Chiangrai-Prayao	212	42
Prae	160	32
Nan	200	40
Upper Chao Phraya	6,400	1,280
Lower Chao Phraya	6,470	1,294
Total	14,222	2,844

Overview of SWAT and MODFLOW

SWAT was developed by the US Department of Agricultural Research Service to simulate water flow, nutrient mass transport and sediment mass transport at the watershed scale. It is a continuous, basin-scale, distributed-parameter watershed model emphasizing surface processes, dividing the watershed into sub-basins which are then further divided into multiple unique combinations (HRUs) of land use, soil and slope for which detailed water, nutrient and sediment mass balance calculations are performed. These HRUs may or may not be spatially contiguous within a sub-basin.

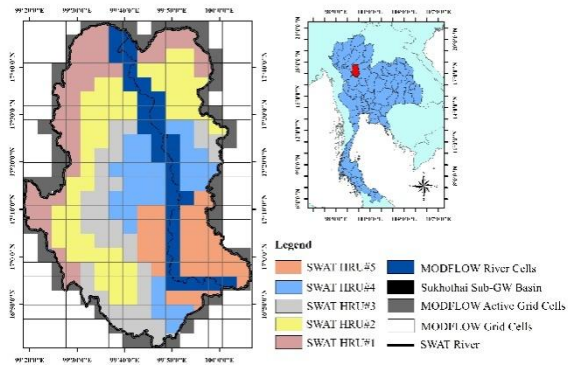


Fig. 3 Schematic demonstrating the SWAT-MODFLOW coupling and spatial interaction from SWAT Hydrologic Response Units (HRUs) to MODFLOW grid cells.

Calculations in SWAT are performed for each HRU and then scaled up to the sub-basin outlet by the percent area of the HRU within the sub-basin. This approach results in the HRUs lacking the spatial relations typically seen in a fully distributed model, but yields a computationally efficient calculation scheme allowing for rapid watershed simulation over long time periods. Additionally, water, nutrient and sediment output from each HRU are routed directly to the sub-basin stream from routing through the stream network. For groundwater-surface water interactions, therefore, system response variables such as groundwater discharge to streams or river seepage to the aquifer are available only at the sub-basin level. Furthermore, indicators of groundwater storage such as water table

elevation are not geographically located. Because of the simplistic representation of subsurface processes, SWAT often performs poorly when applied to watersheds wherein groundwater discharge contributes significantly to streamflow (Perterson and Hamlet 1998; Spruill et al. 2000; Chu and Shirmohammadi 2004; Srivastava et al. 2006; Gassman et al. 2007).

MODFLOW is a three-dimensional, physically based, distributed finite-difference groundwater model for variably saturated subsurface systems. A recent addition to MODFLOW is a Newtonian-based solver algorithm that better satisfies the complex non-linear drying and rewetting of grid cells in unconfined groundwater systems (Niswonger et al., 2011), a problem with previous model versions. Available processes to be simulated in MODFLOW include groundwater recharge, vadose zone percolation (UZFI package) (Niswonger et al. 2006), evapotranspiration, pumping, discharge to subsurface drains and river-aquifer interactions. However, model application is limited to investigating management and climate effects on groundwater and groundwater-surface interactions, as MODFLOW does not simulate surface processes, such as land-atmosphere interactions, infiltration and surface runoff, nutrient cycling and transport, plant growth and the impacts of management practices on agricultural systems.

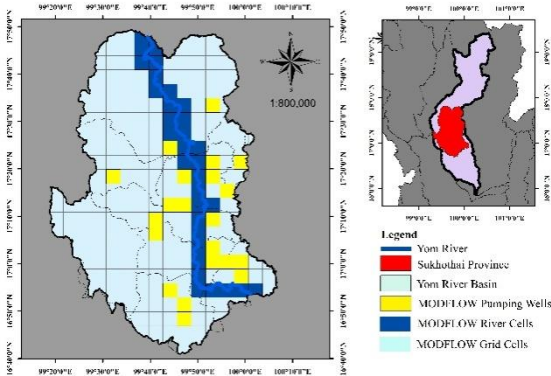


Fig. 4 Modular Groundwater Flow (MODFLOW) grid, showing the stream network, the river cells and the cells in which pumping wells are located.

MODFLOW and SWAT were developed and calibrated separately for Sukhothai Sub-Groundwater basin. Later on, the calibrated SWAT and MODFLOW models developed after this study will be used to investigate the impacts of combined climate change and landuse pattern change on surface runoff and baseflow in the studying area. The original MODFLOW model encompasses the entire Sukhothai Sub-Groundwater basin., an area of approximately 6,956 km². The region was discretized completely into finite difference grid cells with a lateral dimension of 1000 m by 1000 m, aligned in a grid consisting of 200 east-west oriented rows and 100 north-south oriented columns with the aquifer discretized vertically into 2 layers of varying thickness based on the local hydrogeologic units. The simulation period of the model is from 1999 to 2012, but

was only calibrated for period between 2008 and 2012 at station well NT99 and NT92. Shown in Figure 5.

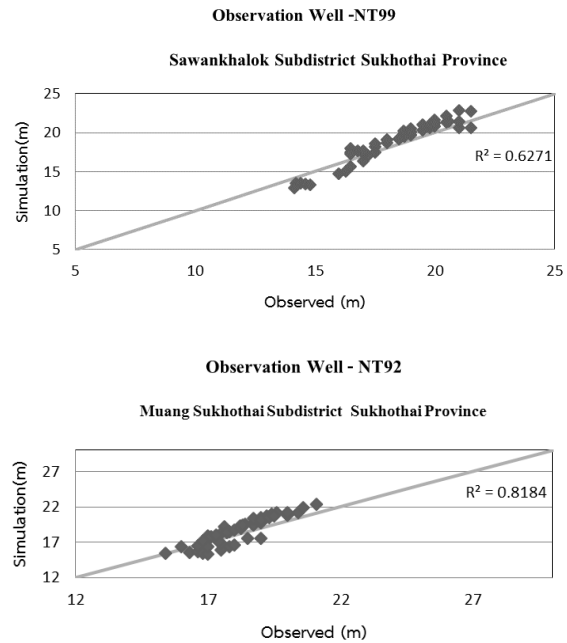


Fig. 5 Observed and SWAT-MODFLOW simulated time series of watertable (m) for Sukhothai Province.

The SWAT model used for Yom river basin included a 30 m National Elevation Dataset raster for land surface topography, a National Hydrography Dataset stream layer to delineate the stream network, a National Land Cover dataset 2006 for land use, and the national soil map provided by Land Development Department (LDD). The model was calibrated and tested during the 2004-2008 period using monthly stream discharge, with automated calibration. Model performance was generally acceptable for monthly stream flow with a Nash Sutcliff of greater than 0.7 in the calibration and validation periods at station Y.31 and Y.14 (basin outlets). The 30 river cells in Yom river basin are illustrated along the stream network in Figure 4.

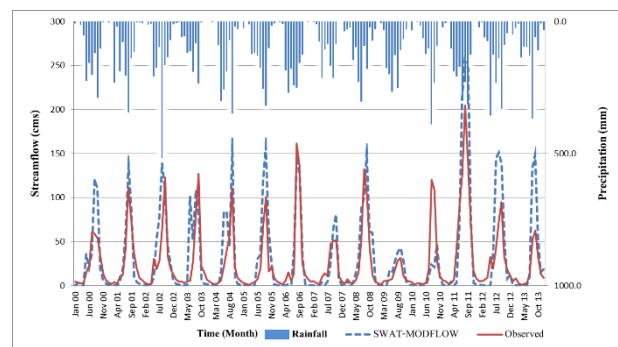


Fig. 6 Observed and SWAT-MODFLOW simulated time series of stream discharge (m³/s²) for The discharge gauge (Y.31) of The Yom River Basin.

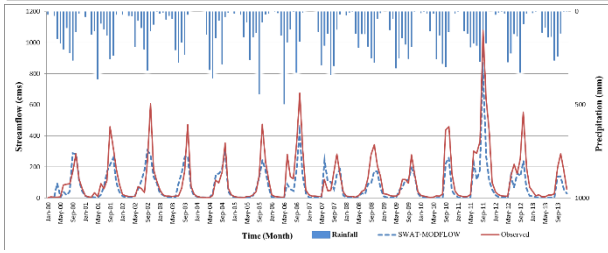


Fig. 7 Observed and SWAT-MODFLOW simulated time series of stream discharge (m^3/s) for The discharge gauge (Y.14) of The Yom River Basin.

Results and discussion

General model results

Annual average recharge (mm) calculated from the daily recharge values in SWAT is shown in Figure 8, demonstrating higher recharge rates in the upland forested areas and the watershed outlet area, with low recharge rates along the main central area of the floodplain.

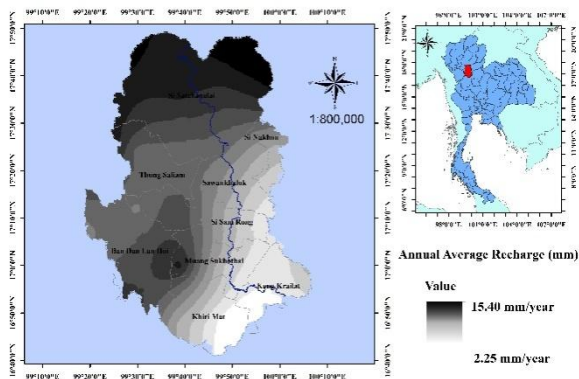


Fig. 8 Spatially-varying annual average recharge (mm) in Sukhothai sub-groundwater basin as simulated by the coupled model

Simulated groundwater hydraulic head in m at the end of the simulation is shown in Figure 9, with the highest water table elevation of 472 m. (MSL) occurring in the mountainous regions of Yom river and low groundwater level of 181 m. (MSL) occurring along the Yom river and tributaries. Overall, simulated groundwater head in the Northwest region of the basin is absolutely higher than the Southeast region.

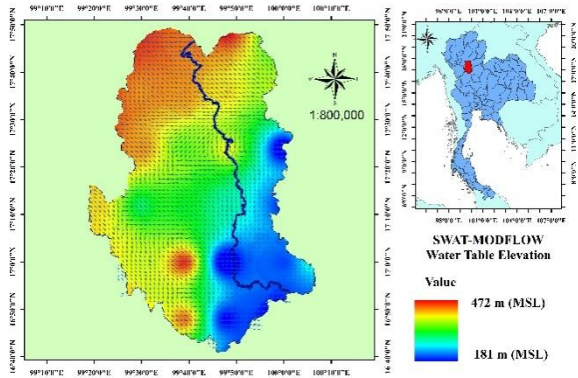


Fig. 9 Cell-wise water table elevation for MODFLOW grid in the Sukhothai sub-groundwater basin at the end of the simulation period (2012)

For streamflow in the main Yom river, observed and simulated stream discharge at gauging stations along the river (see Figure 1 for location) is illustrated in Figure 6 and 7, demonstrating fairly good trend of the model simulation results with the long-term hydrograph. Comparison statistics (Nash-Sutcliff *NSE*; coefficient of determination R^2) between the observed and simulated discharge rates are presented in Table 2. The *NSE* for monthly discharge rates are considerably acceptable as they are greater than 0.5 (Moriyas et al. 2007). A possible contribution to the low fitting statistical parameters is perhaps due to the sparse groundwater data at some observation points.

Table 2 Comparison statistics (*NSE*, R^2) between the observed and simulated hydrograph at stream gauge (Y.31 and Y.14) of the Yom river basin for the SWAT-MODFLOW model

Stream Flow Calibration and Validation at Y.31			
Index	Calibration (2004-2008)	Validation (1999-2003)	Validation (2009-2012)
R2	0.705	0.628	0.695
NSE	0.649	0.599	0.511
Stream Flow Calibration and Validation at Y.14			
Index	Calibration (2004-2008)	Validation (1999-2003)	Validation (2009-2012)
R2	0.716	0.638	0.77
NSE	0.673	0.622	0.695

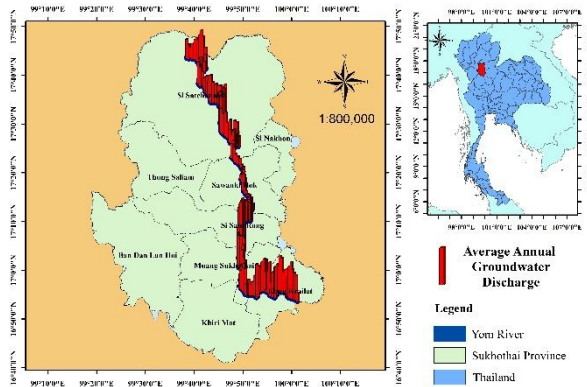


Fig. 10 Simulated Average annual Groundwater discharge (m^3/s) from the aquifer to the stream network. The principal groundwater discharge have between $3.21 \text{ m}^3/\text{s}$ to $35.64 \text{ m}^3/\text{s}$.

Figure 10 shows the average annual groundwater discharge (CMD) for various stations along main Yom river. As seen in the figure, the vast majority of groundwater-surface water interaction is discharge from the aquifer to the stream, which matches previous study using isotope fingerprinting technique.

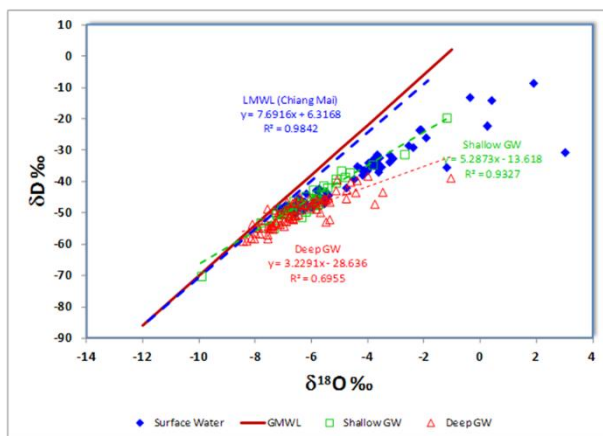


Fig. 11 Plot of δD vs. $\delta^{18}\text{O}$ for groundwater samples in upper Chao Phraya river basin and LMWL (Chiang Mai province). LMWL represents the Local Meteoric Water Line.

Acknowledgement

The authors thank the following for financial support:

- Asahi Glass Foundation for their financial support in academic year 2015
- The Science and Technology Research Partnership for Sustainable Development, JST_JICA, Japan
- The 90th Anniversary of Chulalongkorn University Rachadapisek Sompote Fund

References

- Acheampong, S.Y., and Hess, J.W. (2000) Origin of the Shallow Groundwater System in the Southern Voltaic Sedimentary Basin of Ghana: An Isotopic Approach. *J. Hydrol.* 233: 37-53.
- Andreo, B., Liffián, C., Carasco, F., Jimenez de Cisneros, C., Caballero, F., and Mudry, J. (2004) Influence of Rainfall Quantity on the Isotopic Composition (^{18}O and ^2H) of Water in Mountainous Areas. Application for Groundwater Research in the Yunquera-Nieves Karst Aquifers (S Spain). *Appl. Geochem.* 19: 561-574.
- Blasch, K.W., and Bryson, J.R. (2007) Distinguishing Sources of Groundwater Recharge by Using δD and $d^{18}\text{O}$. *Ground Water*, 45(3), 294-308.
- Cey, EE, Rudolph, DL, Parkin, GW., and Aravana, R. (1998) Quantifying Groundwater Discharge to a Small Perennial Stream in Southern Ontario, Canada. *J. Hydrol.* 210: 21-37.
- Chun, R.Y.D., Mitchell, L.R., and Mido, K.W. (1964) Groundwater Management for the Nation's Future – Optimum Conjunctive Operation of Groundwater Basin. *J. Hydraul. Div.* 90: 79-95.
- Clark, I.D., and Fritz, P. (1997) *Environmental Isotopes in Hydrology*; Lewes Publishers, New York.
- Coleman, M.L., Shepherd, T.J., Duham, J.J., Rouse, J.E., and Moore, G.R. (1982) Reduction of Water with Zinc for Hydrogen Isotope Analysis. *Anal. Chem.* 54: 993-995.
- Craig, H. (1961) Isotopic Variations in Meteoric Waters. *Science*, 133(3465): 1702-1703.
- Criss, R.E. (1999) *Principles of Stable Isotope Distribution*; Oxford University Press, New York.
- Dansgaard, W. (1964) Stable Isotopes in Precipitation. *Tellus*, 16: 436-468.
- Darling, W.G., and Amannsson, H. (1989) Stable Isotopic Aspects of Fluid Flow in the Krafla, Namafjall and Theistareykir Geothermal Systems of Northeast Iceland. *Chem. Geol.*, 76: 197-213.
- Deshpande, R.D., Bhattacharya, S.K., Jani, R.A., and Gupta, S.K. (2003) Distribution of Oxygen and Hydrogen Isotopes in Shallow Groundwaters from Southern India: Influence of a Dual Monsoon System. *J. Hydrol.* 271: 226-239.
- Epstein, S., and Mayeda, T. (1953) Variation of ^{18}O Content of Waters from Natural Sources. *Geochim Cosmochim. Acta*, 4(5): 213-224.
- Friedman, I., Redfield, A.C., Schoen, B., and Harris, J. (1964) The Variation of the Deuterium Content of Natural Waters in the Hydrologic Cycle. *Reviews in Geophysics*, 2: 1-124.
- Fritz, P. (1981) River Waters. In: Cat, J.R. and Gonfiantini, R. (Editors), *Stable Isotopic Hydrology: Deuterium and Oxygen-18 in the Water Cycle*, IAEA (International Atomic Energy Agency) Technical Report Series 210, 177-201.
- Gammons, C.H., Poulson, S.R., Pelliconi, D.A., Reed, P.J., Roesler, A.J., and Petrescu, E.M. (2006) The Hydrogen and Oxygen Isotopic Composition of

- Precipitation, Evaporated Mine Water, and River Water in Montana, USA. *J. Hydrol.*, 328: 319-330.
- Gat, J.R. (1980) The Isotopes of Hydrogen and Oxygen in Precipitation. In: Fritz, P. and Fontes, Jh. (Editors), *Handbook of Environmental Isotope Geochemistry*, pp. 21-47.
- Gat, J.R. (1996) Oxygen and Hydrogen Isotopes in the Hydrologic Cycle. *Annu. Rev. Earth Planet Sci.*, 24: 225-262.
- Gat, J.R. and Tzur, Y. (1967) Modification of the Isotopic Composition of Rainwater by Processes which Occur before Groundwater Recharge. In *Proceedings 2nd IAEA Symposium on Isotopes in Hydrology*. IAEA, Vienna, 49-60.
- Genereux, D.P., and Hooper, R.P. (1998) Streamflow Generation and Isotope Tracing. In: Kendall, C., and McDonnell, J.J. (Editors.), *Isotope Tracers in Catchment Hydrology*, Elsevier, Amsterdam, 319-346.
- Gibson, J.J., Edwards, T.W.D., Birks, S.J., St Amour, N.A., Buhay, W.M., McEachem, P., Wolfe, B.B., and Peters, D.L. (2005) Progress in Isotope Tracer Hydrology in Canada. *Hydrol. Process.*, 19: 303-327.
- Heilweil, V.M., Solomon, D.K., Gingerich, S.B., and Verstraeten, I.M. (2009) Oxygen, Hydrogen, and Helium Isotopes for Investigating Groundwater Systems of the Cape Verde Islands, West Africa. *Hydrogeol. J.*, 17: 1157-1174.
- International Atomic Energy (1983) *Guidebook on Nuclear Techniques in Hydrology*; Vienna, Technical Reports, Series No. 91, p. 439.
- International Atomic Energy Agency/WMO (2001) *Global Network of Isotopes in Precipitation: The GNP Database* <http://isohis.iaea.org>.
- Jacobson, G., Janowski, J., and Abell, R.S. (1991) Groundwater and Surface Water Interactions at Lake George, New South Wales. *J. Australian Geol. Geophys.*, 12: 161-190.
- Kuo, C.H., and Wang, C.H. (2001) Implication of Seawater Intrusion on the Delineation of the hydrologic framework of the shallow Pingtung Plain Aquifer, Western Pacific. *Earth Sci.*, 1(4), 459-471.
- Lee, K.S., Wenner, D.B., and Lee, I. (1999) Using H- and O-Isotopic Data for Estimating the Relative Contributions of Rainy and Dry Season Precipitation to Groundwater: Example from Cheju Island, Korea. *J. Hydrol.*, 222: 65-74.
- Leibundgut, C., Maloszewski, P., and Kiills, C. (2009) *Tracers in Hydrology*; Wiley-Blackwell, Oxford, UK.
- Lu, H.Y., Peng, T.R., Liu, T.K., Wang, C.H., and Huang, C.C. (2006) Study of Stable Isotopes for Highly Deformed Aquifers in the Hsinchu-Miaoli Area, Taiwan. *Environ. Geol.*, 50(7): 885-898.
- Mizota, C., and Kusakabe, M. (1994) Spatial Distribution of δD - $d^{18}O$ in South Korea and East China, *Geochem. J.* 28: 387-410.
- Payne, B.R., and Yurtsever, Y. (1974) Environmental Isotopes as a Hydrogeological Tool in Nicaragua. *Isotope Techniques in Groundwater Hydrology*, International Atomic Energy Agency, Vienna, Austria, pp. 193-201.
- Peng, T.R., Wang, C.H., Huang, C.C., Chen, W.C., Fei, L.Y., and Lai, T.C. (2002) Groundwater Recharge and Salinization in South Chianan Plain: Hydrogen and Oxygen Isotope Evidences. *J. Chin. Soil Water Conserv.*, 33(2): 87-100.
- Sakai H., and Matsubaya, O. (1977) Stable Isotopic Studies of Japanese Geothermal System Geothermics, 5: 97-124.
- Salati, E., Oall'Ollo, A., Matsui, E., and Gat, J.R. (1979) Recycling of Water in the Amazon Basin, an Isotope Study. *Water Resources Research*, 15: 1250-1258.
- Sanford, W.E., and Buapeng, S. (1996) Assessment of Groundwater Flow Model of Bangkok Basin, Thailand, using Carbon-14-Based Ages and Paleohydrology. *Hydrogeol. J.*, 4: 26-40.
- Singh, M., Kumar, S., Kumar, B., Singh, S., and Singh, I.B. (2013) Investigation on the Hydrodynamics of Ganga Alluvial Plain using Environmental Isotopes: A Case Study of the Gomati River Basin, Northern India. *Hydrogeol. J.*, 21: 687-700.
- Space, M.L., Ingramham, N.L., and Hess, J.W. (1991) The Use of Stable Isotopes in Quantifying Groundwater Discharge to a Partially Diverted Creek. *J. Hydrol.*, 129: 175-193.
- Vandenschrick, G., van Wesemael, B., Frot, E., Pulido-Bosch, A., Molina, L., Sievenard, M., and Souchez, R. (2002) Using Stable Isotope Analysis (δD and $\delta^{18}O$) to Characterize the Regional Hydrology of the Sierra de Gador, South East Spain. *J. Hydrol.*, 265: 43-55.
- Yeh, H.F., Lee, C.H., and Hsu, K.C. (2011) Oxygen and Hydrogen Isotopes for the Characteristics of Groundwater Recharge: A Case Study from Chih-Pen Creek Basin, Taiwan. *Environ. Earth Sci.*, 62: 393-402.
- Yin, L., Hou, G., Su, X., Wang, D., Dong, J., Hao, Y., and Wang, X. (2011) Isotopes (δD and $\delta^{18}O$) in Precipitation, Groundwater, and Surface Water in the Ordos Plateau, China: Implications with Respect to Groundwater Recharge and Circulation. *Hydrogeol. J.*, 19: 429-443.
- Yurtsever, Y., and Gat, J.R. (1981) Atmospheric Waters, In: Gat, J.R. and Gonfiantini, R. (Editors), *Stable Isotopic Hydrology: Deuterium and Oxygen-18 in the Water Cycle*, IAEA (International Atomic Energy Agency) Technical Report Series 210, 103-142.

Groundwater Vulnerability and Risk Assessment in Thailand using GIS-Based Modified DRASTIC Approach

AKSARA Putthividhya^{1,a,*} and SASIN Jirasirak^{2,c}

Abstract Groundwater resources in Thailand have become increasingly important due to surface water shortage problem in the dry season, especially in the agricultural-intensive area located in the Chao Phraya river basin. While water supply is a crucial issue, there is also evidence to suggest that the quality of groundwater resources is also under threat as a result of high concentrations of human/economic activities (e.g., industrial, agricultural, and household). Numerous groundwater contaminated sites have been reported from both natural and anthropogenic activities with extent of plume consumption. Therefore, this paper attempts to assess groundwater vulnerability and risk maps on the basis of hydrological and hydrogeological aspects and human impacts. All major hydrological, geological, and hydrogeological factors affecting and controlling groundwater migration, including water depth (D), net recharge (R), aquifer media (A), soil media (S), topography (T), impact of vadose zone (I), and hydraulic conductivity (C), were incorporated into the well-established DRASTIC model in a Geographical Information System (GIS)-based environment. Three different vulnerability zones were determined in the representative basins according to DRASTIC scores low (< 100), medium (100-140), and high (> 140). The linear regression statistical analysis between rainfall-groundwater depth and adjusted hydraulic conductivity (K) will be applied to modify some parameters in the original DRASTIC model. The final original and modified DRASTIC models will be tested using hydrochemical data. The original DRASTIC model provided a conservative estimate of low risk while the advanced DRASTIC one represents an advanced stage of physical correlation between the vulnerability index and contaminant concentration in the representative area.

Keywords *Climate change, Groundwater, Vulnerability, DRASTIC, Groundwater-Surface Water Interactions*

Aksara Putthividhya
Department of Water Resources Engineering
Chulalongkorn University
Bangkok, Thailand
Dr.aksara.putthividhya@gmail.com

Sasin Jirasirak
Department of Water Resources Engineering
Chulalongkorn University
Bangkok, Thailand
Sasin_sk@hotmail.com

Introduction

Groundwater is one of the most valuable natural resources, which supports human health, economic development and ecological diversity [1-3]. It has been recognized as the major and the preferred source of drinking water in rural as well as urban areas and caters up to 80% of the total drinking water requirement and 50% of the agricultural requirement in many parts of Thailand. The occurrence of drought and heavy rainfall are the most important climatic extremes having both short-term and long-term impacts on the groundwater availability. Besides the natural forces creating pressure on water resources, ever-increasing human activities have become the primary drivers of the pressure affecting our planet's water systems.

As rainfall comprises an important component of the hydrologic cycle and is proven as the primary source of recharge for many aquifers, variations of rainfall and groundwater table depth are closely related. However, the correlation may sometimes be imperfect because difference in rainfall intensity and distribution produce different amounts of recharge for the same amount of rainfall. Consequently, the declining groundwater levels in some parts of Thailand require necessary understanding for groundwater dynamics and to be able to qualitatively estimate the temporal and spatial variability of sustainable water resources under urbanization and changing climate.

A very useful tool for analyzing groundwater level fluctuations is the use of statistical tools, which are advantageous for water resources management and can be effectively used to derive the long-term trends of groundwater. Statistical methods for trend analysis vary from simple linear regression to more advanced parametric and non-parametric method. The Geographical Information System (GIS) nowadays additionally plays an important role in the effective management of groundwater resources, as it helps in preparing a scientific geodatabase of the resources and

also facilitates for updating the data. GIS has been put to effective use in many earlier groundwater studies in Thailand and found to be extremely successful.

Several analytical techniques to study the sensitivity of aquifer water levels have been proposed, including crossing theory approach [4], general circulation models [5-7], hydrologic models [4], geostatistics [8], wavelet analysis [9], semi-analytical model [10], cross-correlation analysis [11]. However, the application of statistical analysis techniques to surface water-groundwater response is still very scarce in Thailand.

In this study, statistical analysis of water table data was carried out at the representative areas in Chao-Phraya river basin of Thailand. The study areas were selected because some degradation of the catchment area, indiscriminate groundwater use, and irregular rainfall have been observed, and therefore the current necessity for better planning and management of groundwater resources in the area are mandatory. By conducting multiple linear correlation analysis to study the influence of rainfall, antecedent rainfall, and antecedent groundwater table depth on current groundwater depth at special locations. The influencing variables have been selected based on the measures of multiple linear correlations. The monthly groundwater depth and rainfall data from raingage stations located in the basin for the period of 2007-2008 were collected from the Department of Groundwater Resources (Thailand) and Royal Irrigation Department (RID). Monthly groundwater table depth model at each piezometric station was developed using the rainfall, antecedent rainfall, and antecedent groundwater table depth data under consideration and also the piezometric stations upstream. Multiple correlation analysis was performed to initially test the direct correlation of rainfall vs. groundwater table depth and also to identify the influencing parameters. The performance of the model was verified through selected performance evaluation criteria in terms of several numerical model performance indicators, such as the coefficient of determination (R^2), root mean square error ($RMSE$) and efficiency coefficient (EC) are chosen for the present study. The scattered plots of the observed versus estimated groundwater table depths are selected as a graphical indicator. The relationships proposed may be adopted to predict the groundwater table depths to a reasonable degree of accuracy for better planning and management of groundwater resources of the basin in Thailand.

Materials and Methods

Study area

Pitsanulok and Sukhothai are the 2 focusing areas selected for this study as illustrated in Fig. 1. Pitsanulok

and Sukhothai are located in the upper central plain of Thailand covering approximately 38,000 km² (180 km × 300 km). The main landuse is 63% agricultural, out of which 21% is irrigated and 24% forest. The basin is surrounded in the East and West by volcanic rocks. The average elevation of the basin is 40-60 m above mean sea level. The basin drains into the lower basin in the South where some free discharge is partially obstructed by crystalline rocks. The 900-1,450 mm annual rainfall within the study region is apportioned to 81% in the wet season (April-September) and 19% in the dry season (October-March).

General model development

The monthly groundwater table depth and rainfall data in Pitsanulok and Sukhothai from piezometric and raingage stations were collected for the period of 2007-2008 and employed for model development. Tables 1 and 2 present the rainfall and groundwater table depths at the raingages and monitoring wells, respectively. The groundwater table depth data show that there is no systematic trend with rainfall as the processes are complex exhibiting high degree of both spatial and temporal variability. The model coefficients, however, may be updated to obtain the refined model for better forecasting accuracy.

Arial representative rainfall in each study area was generated using Thiessen polygon technique. The time series monthly rainfall data at representative rainfall station were paired up with monthly groundwater level from piezometric stations located within the same representative Thiessen polygon as illustrated in Fig. 2. Correlations of rainfall and groundwater level were acquired from scattered diagrams of time-series data of rainfall vs. groundwater level for each pairing stations. Rainfall and groundwater level pairs yielded high correlations were further employed in multiple regression analyses.

An association of three or more variables is best investigated by multiple regression and correlation analysis. Since linear equations are easier to treat than nonlinear relations, variables of nonlinear relations for the purpose of development of a multiple regression model. If there are m variables to correlate, including one dependent and $(m-1)$ independent variables, the multiple linear regression model can be generally expressed as:

$$X_1 = b_1 + b_2X_2 + b_3X_3 + \dots + b_iX_i + \dots + b_mX_m \quad (1)$$

b_1 is the intercept and b_i ($i = 2, 3, \dots, m$) are the multiple regression coefficients of the dependent variable X_1 on

Table 1. Monthly rainfall in *mm* at selected raingauge stations in the study area

Raingauge Station	Year	Months											
		Jan	Feb	Mar	Apr	May	Jun	Jul	Aug	Sep	Oct	Nov	Dec
39013	2006	0.0	0.9	1.2	2.6	6.2	6.6	6.6	5.9	9.3	8.3	1.8	0.0
	2007	0.0	1.4	0.2	4.0	11.1	4.1	9.9	4.9	11.3	6.7	0.1	0.1
	2008	0.0	0.2	0.7	1.4	5.2	3.1	4.4	9.2	9.4	6.2	3.4	0.0
39042	2006	0.0	0.0	1.3	4.5	4.5	7.7	10.1	10.7	6.3	5.2	0.2	0.0
	2007	0.2	1.5	0.4	1.0	8.2	5.1	2.3	0.0	7.4	6.7	0.0	0.0
	2008	0.0	0.0	2.7	2.8	3.2	5.2	8.1	6.1	6.8	5.5	0.9	0.0
39062	2006	0.0	0.3	0.0	1.3	6.3	5.0	6.1	9.2	11.5	2.6	0.0	0.0
	2007	0.0	0.5	0.1	3.5	8.7	8.7	4.5	6.6	7.0	5.4	0.4	0.1
	2008	0.0	0.0	0.4	0.0	3.3	2.3	6.8	4.1	8.8	5.1	0.4	0.0
39161	2006	0.0	0.0	0.0	1.1	7.8	6.4	9.2	11.5	14.7	7.7	0.0	0.0
	2007	0.0	0.0	0.0	2.8	12.0	9.3	3.6	7.2	10.2	6.0	0.0	0.0
	2008	0.0	0.3	0.8	2.7	4.1	5.0	4.4	7.3	5.2	4.3	1.2	0.0
59022	2006	0.0	0.0	0.0	5.2	18.5	4.2	1.5	4.0	15.5	3.5	0.1	0.0
	2007	0.1	0.1	0.0	0.4	8.3	4.0	2.5	5.6	8.3	4.3	0.0	0.0
	2008	0.0	0.0	0.0	1.4	3.1	2.2	3.4	2.3	6.6	12.0	4.3	0.0
59032	2006	0.0	0.0	0.0	0.0	0.0	0.0	0.0	0.0	0.0	0.0	0.0	0.0
	2007	0.1	1.4	0.1	0.0	0.0	0.0	0.0	0.0	0.0	0.0	0.0	0.0
	2008	0.0	0.0	2.1	3.6	4.0	5.3	4.4	4.9	5.0	7.6	1.3	0.1
59082	2006	0.0	0.0	0.0	4.3	11.1	3.1	6.3	9.2	18.1	2.8	0.0	0.1
	2007	0.2	1.1	0.5	0.0	10.1	7.7	1.9	7.5	12.3	3.8	0.0	0.0
	2008	0.0	0.0	2.8	2.7	3.4	5.7	3.5	5.7	1.8	6.2	1.0	0.0

Table 2. Monthly groundwater table depth in *m* at piezometric stations

Piezometric Station	Months									
	Jan	Mar	May	Jul	Sep	Nov	Jan	Mar	May	Jul
NT50/1	27.68	27.57	29.34	29.40	28.88	28.22	30.40	26.60	27.31	27.00
NT50/2	31.68	31.73	29.88	30.93	29.98	29.60	30.86	29.98	30.00	30.03
NT48/1	13.56	13.41	27.46	15.58	-	13.93	13.89	28.76	28.79	28.00
NT48/2	37.12	37.00	36.99	37.37	-	37.00	35.69	37.86	37.91	37.65
NT54/1	34.68	34.50	34.74	34.80	34.59	34.50	35.62	31.60	32.00	33.22
NT54/2	31.98	31.88	32.00	31.90	31.87	31.29	31.98	29.37	30.03	30.88
NT53/1	26.91	27.15	26.82	27.10	26.91	26.78	27.68	27.78	28.00	27.92
NT53/2	27.29	27.03	27.02	27.35	27.30	27.04	27.83	24.99	25.12	26.22
NT53/3	38.85	38.97	39.42	39.73	39.59	39.00	39.38	36.30	37.38	37.90
NT93	32.60	32.94	33.00	-	-	32.74	32.22	32.65	32.70	32.78
NT96/1	30.98	27.31	28.20	29.92	29.48	29.15	27.99	28.11	28.19	28.40
NT96/2	30.61	27.00	28.09	29.60	29.03	29.00	27.48	28.20	28.25	28.49
NT96/3	31.35	24.92	28.02	29.43	29.04	28.92	21.98	25.14	26.00	26.18

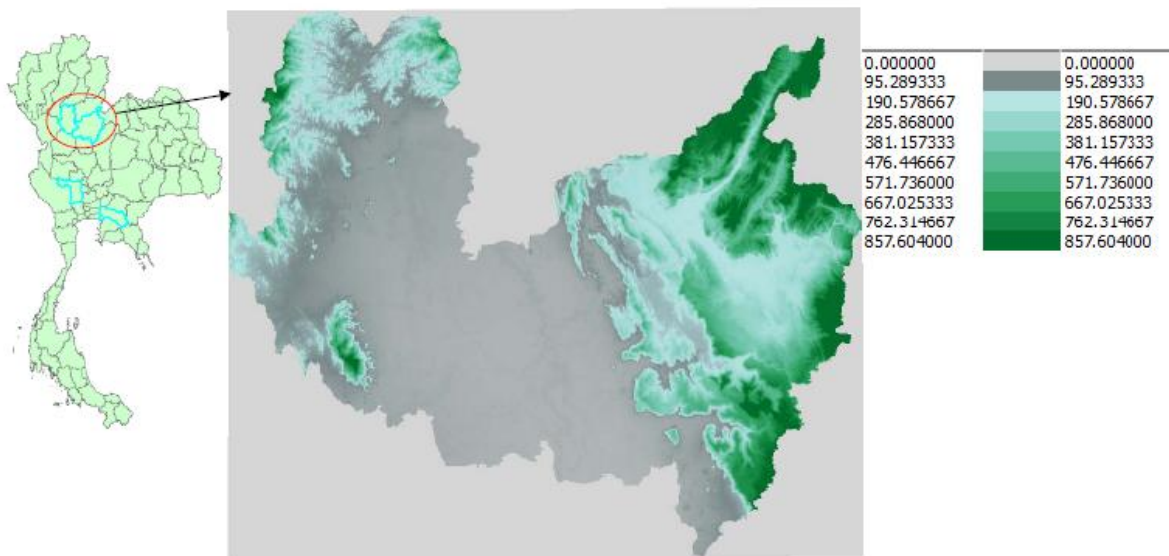


Figure 1 Digital elevation model (DEM) of the study areas in Pitsanulok and Sukhothai provinces

Table 3. Multiple linear correlation of groundwater and rainfall at 13 locations

Piezo metric Station	Multiple Correlation Coefficient	
	R_t	R_{t-1}
NT50/1	0.92	0.73
NT50/2	0.84	0.83
NT48/1	0.62	0.61
NT48/2	0.68	0.05
NT54/1	0.87	0.23
NT54/2	0.70	0.33
NT53/1	0.73	0.84
NT53/2	0.83	0.20
NT53/3	0.95	0.12
NT93	0.87	0.26
NT96/1	0.65	0.19
NT96/2	0.54	0.38
NT96/3	0.83	0.18

Table 4. Regression equations

Piezo metric Station	Regression Equation
NT50/1	$G_t = 0.1224 R_1 + 0.2344 R_2 - 0.1382 R_3 + 0.3183 R_4 + 26.6751$
NT50/2	$G_t = 0.0635 R_1 + 0.1839 R_2 - 0.0077 R_3 + 0.2112 R_4 + 28.2122$
NT48/1	$G_t = 0.0830 R_1 - 0.1548 R_2 - 0.1548 R_3 + 0.1500 R_4 + 26.1034$
NT48/2	$G_t = 0.0672 R_1 - 0.0635 R_2 + 0.0807 R_3 + 0.0899 R_4 + 38.9392$
NT54/1	$G_t = 0.0324 R_1 - 0.0552 R_2 - 0.0088 R_3 + 0.0772 + 34.3177$
NT54/2	$G_t = -0.0623 R_1 + 0.0178 R_2 + 0.1702 R_3 + 0.0477 R_4 + 30.3891$
NT53/1	$G_t = 0.0710 R_1 - 0.0373 R_2 + 0.0188 R_3 - 0.006 R_4 + 26.8748$
NT53/2	$G_t = 0.1944 R_1 - 0.5011 R_2 + 0.3427 R_3 + 0.1805 R_4 + 26.0033$
NT53/3	$G_t = 0.1944 R_1 - 0.5011 R_2 + 0.3427 R_3 + 0.1805 R_4 + 26.0033$
NT93	$G_t = 0.0366 R_1 + 0.3375 R_2 - 0.5377 R_3 + 0.1418 R_4 + 32.4985$
NT96/1	$G_t = 0.0437 R_1 + 0.1119 R_2 + 0.0854 R_3 - 0.0010 R_4 + 27.7827$
NT96/2	$G_t = 0.0494 R_1 + 0.0957 R_2 + 0.0977 R_3 - 0.0387 R_4 + 27.7117$
NT96/3	$G_t = 0.5109 R_1 - 0.0306 R_2 + 0.5765 R_3 - 0.1542 R_4 + 22.9779$

Table 5. Performance evaluation indicators

Piezo metric Station	R^2	EC(%)
NT50/1	0.55	55.13
NT50/2	0.58	57.86
NT48/1	0.81	81.32
NT48/2	0.89	88.65
NT54/1	0.40	39.61
NT54/2	0.48	47.88
NT53/1	0.30	29.51
NT53/2	0.51	50.68
NT53/3	0.49	49.24
NT93	0.64	63.54
NT96/1	0.84	84.46
NT96/2	0.80	80.30
NT96/3	0.94	94.42

the independent variable X_i ($i = 2, 3, \dots, m$) with all other variables kept constant.

Applying the least squares method of the sum of residuals, the m partial differential equations in $b_1, b_2, \dots,$ and b_m yielded m linear equations. The solution of these equations facilitates determination of m parameters.

Linear regression model

In this study, the monthly groundwater table depth model at a piezometric station is developed using the rainfall, antecedent rainfall and antecedent groundwater table depth data of the piezometric stations under consideration and also the piezometric station upstream. The modeling steps briefly include: 1) identification of influencing parameters; 2) development of a model; and 3) performance evaluation of the model developed.

Identification of influencing parameters

The identification of influencing parameters is based on multiple correlation analysis. The values of multiple and partial correlation coefficients indicate the degree of influence of independent variables on the dependent one.

Development of model

The linear regression model in terms of influencing parameters is expressed as a simple linear model as follows:

$$G_t = b_1 + b_2 R_t + b_3 R_{t-1} + b_4 G_{t-1} + b_5 G_{t-1(US1)} + b_6 G_{t-1(US2)} + \dots \quad (2)$$

where G_t is the groundwater depth in m in the t^{th} month; b_1, b_2, \dots are empirical constants; R_t is the rainfall in mm in the t^{th} month; R_{t-1} is the antecedent rainfall in mm; and G_{t-1} is the antecedent groundwater depth also in m at the stations. $G_{t-1(us1)}, G_{t-1(us2)}, \dots$ are the groundwater table depths at the piezometric stations upstream of the piezometric station under consideration.

Performance evaluation criteria

The performance of the model is verified through selected performance evaluation criteria as explained below. Out of several numerical model performance indicators, the coefficient of determination (R^2), root mean square error ($RMSE$) and efficiency coefficient (EC) are chosen for the present study. The scattered plot of the observed versus estimated groundwater table depths is selected as a graphical indicator. Coefficient of determination (R^2) is the square of the correlation coefficient (R) and the correlation coefficient can be expressed as:

$$R = \frac{\sum_{i=1}^n (y_i - \bar{y}) \left(\hat{y}_i - \bar{\hat{y}} \right)}{\left[\sum_{i=1}^n (y_i - \bar{y})^2 \sum_{i=1}^n \left(\hat{y}_i - \bar{\hat{y}} \right)^2 \right]^{1/2}} \times 100 \quad (3)$$

where y_i and \hat{y}_i are the observed and estimated values respectively. \bar{y} and $\bar{\hat{y}}$ are the means of observed and estimated values.

Root mean square error ($RMSE$) yields residual error in terms of the mean square error and can be expressed as:

$$RMSE = \sqrt{\frac{\sum_{i=1}^n (y_i - \hat{y}_i)^2}{n}} \quad (4)$$

where n is the number of observations.

Efficiency coefficient (EC) is used to assess the performance of the models and can be given as :

$$EC = \left(1 - \frac{F}{F_o} \right) \times 100 \quad (5)$$

where $F_o = \sum_{i=1}^n (y_i - \bar{y})^2$ and $F = \sum_{i=1}^n (y_i - \hat{y}_i)^2$

A value of EC greater than 90% generally indicates a very satisfactory model performance while a value in the range 80-90% represents a fairly good one. Values in the range of 60-80% would generally indicate an unsatisfactory model fit.

Results and Discussions

The mean monthly groundwater levels for the representative Thiessen polygons of individual rainfall stations in two study areas are illustrated in Fig. 2 along with the rainfall bar graphs of the corresponding rainfall station. Fig. 2 reveals that the rainfalls in Pitsanulok and Sukhothai are fairly large compared to those at other stations throughout the year. The groundwater levels at those stations are also relatively higher than other stations in the same study area, suggesting that the groundwater levels are influenced by large amounts of rainfall, among other factors.

The results of regression analyses between monthly rainfall and groundwater level data for the period of 2007-2008 are depicted in Table 3 for the total of 13 locations. Apparently, R^2 values for 13 rainfall stations in both Pitsanulok and Sukhothai are greater than 0.5,

indicating that the groundwater levels are influenced by rainfall at some level in all these locations. However, response of groundwater to antecedent rainfall yields relatively poorer correlations ($R^2 < 0.25$; multiple correlation coefficients shown in Table 3) at some stations (such as stations NT48/2, NT54/1, NT53/2, NT53/3, NT96/1, and Nt96/3). The overall correlation between surface water-groundwater pairs suggests the direct response of groundwater to rainfall. Literally speaking, the correlation analyses additionally demonstrate the possible hydraulic connectivity among the study sites or similarity in the response of groundwater among the sites due to hydrological and anthropogenic factors. Further attempts are being investigated to statistically analyze the temporal response of groundwater to rainfall based on monsoon pattern of the study area.

The high multiple correlation coefficients literally indicate that the monthly groundwater table depth at any station can better be correlated with rainfall, antecedent rainfall and groundwater table depths of the station and the upstream stations. Lower correlation coefficients of antecedent rainfall observed at some locations in the studying area may be due to the fact that rainfall perhaps directly recharges to groundwater aquifer underneath quite rapidly or groundwater in the basin may be overexploited at the higher rates than recharging rate during that period.

The linear regression models created in terms of influencing parameters are presented in Table 4. The scattered plots of observed versus estimated groundwater table depths are shown in Fig. 3.

The results of this study have been closely evaluated through R^2 , $RMSE$, and EC as tabulated in Table 5. The higher values of R^2 and EC in majority, combining with the lower values of $RMSE$ indicates that the regression models are fairly good and yield quite satisfactory results in the studying areas. Therefore the regression models developed may be adopted for the reasonable estimation of groundwater table depths at the particular piezometric stations based on rainfall, antecedent rainfall, and antecedent groundwater table depth for effective planning and management of groundwater resources of the basin of interest.

Summary and Conclusions

Since groundwater is one of the most valuable natural resources in Thailand as it serves as the major and the preferred source of drinking water in rural as well as urban areas of the country. Response of the groundwater levels to rainfall was investigated in this study via statistical analyses. Statistical analysis of water table

data is carried out in Sukhothai and Pitsanulok provinces located in Chao-Phraya river basin of Thailand. The study areas are selected because some degradation of the catchment area, indiscriminate groundwater use, and irregular rainfall have been observed. The current necessity for better planning and management of groundwater resources in the area are mandatory.

Necessary data, including rainfall, groundwater level, antecedent rainfall, and antecedent groundwater table depth from the period of 2007-2008 are gratefully provided by the Department of Groundwater Resources (Thailand) and Royal Irrigation Department (RID). Multiple correlation analysis is conducted to initially test the direct correlation of the rainfall vs. groundwater table depth and also to identify the influencing parameters. Linear regression model in terms of influencing parameters is then developed. The performance of the model is verified through selected performance evaluation criteria in terms of several numerical model performance indicators, such as the coefficient of determination (R^2), root mean square error ($RMSE$) and efficient coefficient (EC). The scattered plots of the observed versus estimated groundwater table depths are selected as a graphical indicator.

The results indicate that R^2 values for 13 rainfall stations are higher than 0.5, suggesting that the groundwater levels are influenced by rainfall at some level. On the other hand, some lower correlation coefficients of antecedent rainfall observed at some locations may be due to the fact that the rainfall in the area directly recharge to groundwater aquifer underneath quite rapidly or groundwater in the basin may be overexploited at the higher rates than recharging rate during the period. Similar and dissimilar response of groundwater levels at Sukhothai and Pitsanulok indicated extent of hydraulic connectivity in the aquifer system underlying the observed sites. Such information is particularly important for efficient groundwater management.

Linear regression models created in terms of influencing parameters are proposed with high R^2 and EC and lower $RMSE$. The relationships proposed may be adopted to predict the groundwater table depths to a reasonable degree of accuracy for better planning and management of groundwater resources of the basin in Thailand.

Acknowledgement

The authors wish to acknowledge the time and effort spent in collecting data from RID, TMD, and DGR.

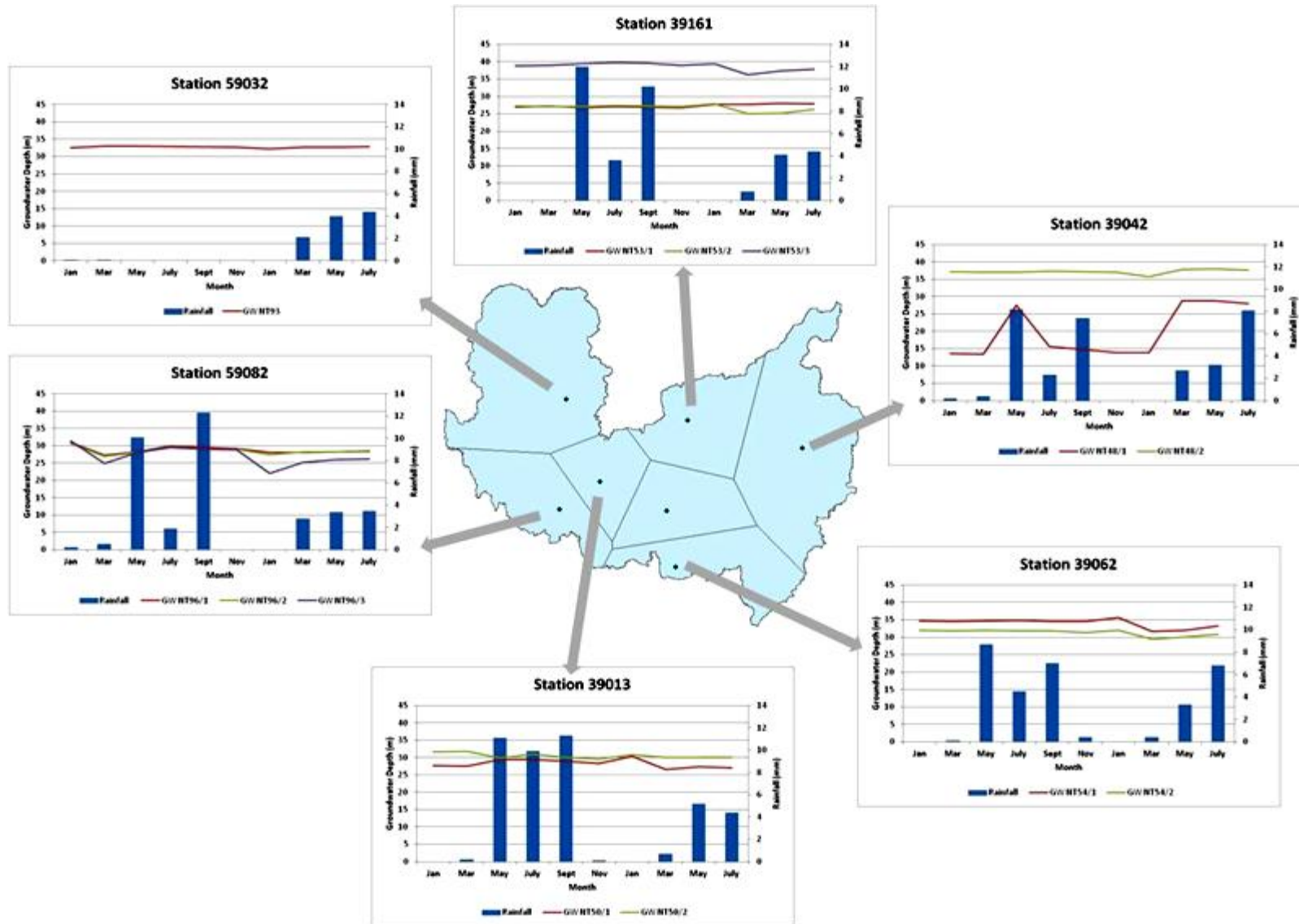


Figure 2 Comparison of observed and estimated groundwater table depths

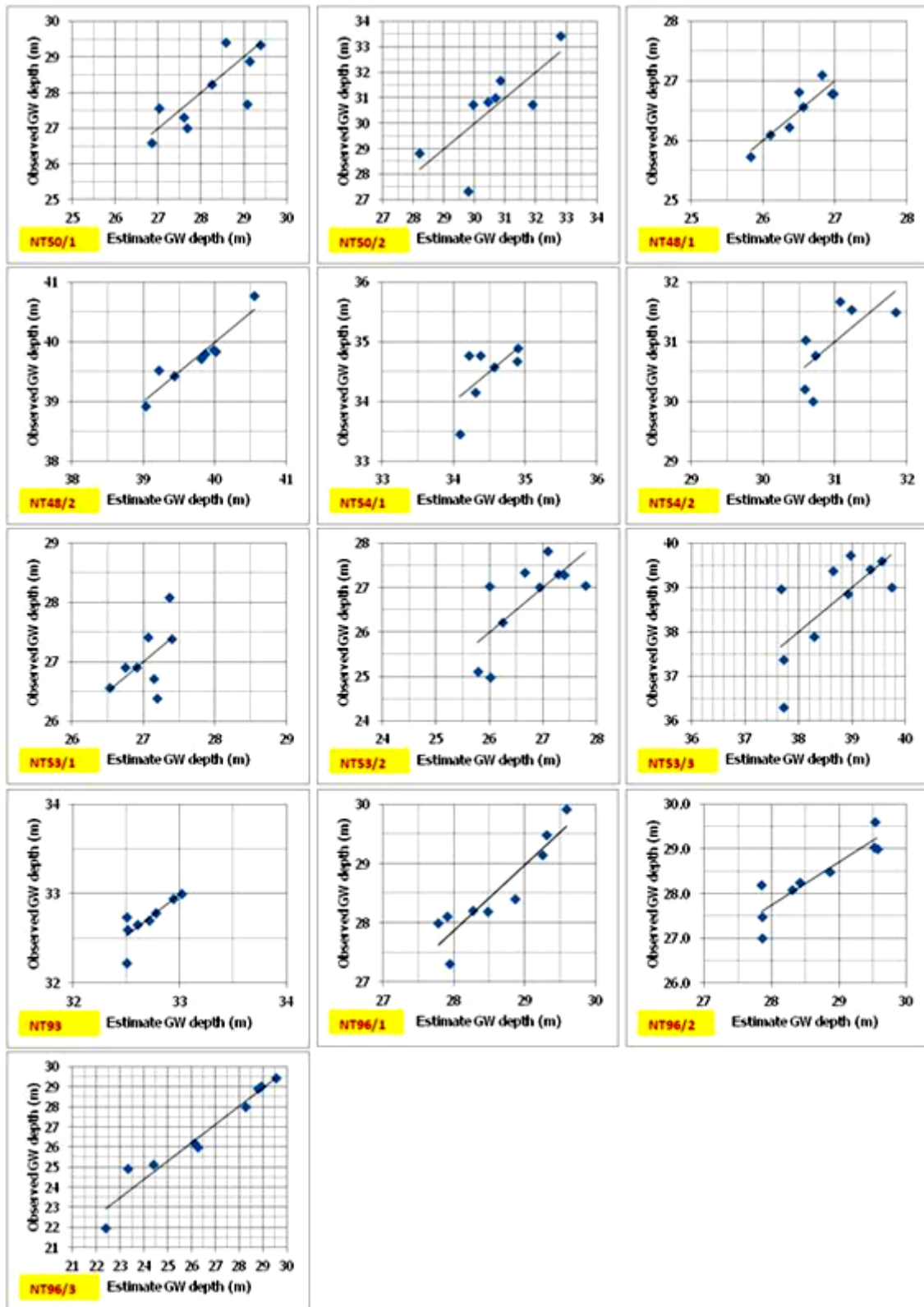


Figure 3 Comparison of observed and estimated groundwater table depths using linear regression model

Also we wish to thank the reviewers for constructive comments in reviewing and improving the manuscript.

References

1. Zekster, I.S., *Groundwater and the Environment: Applications for the Global Community*. Lewis Publishers, Boca Raton, Florida, USA (2000).
2. Humphreys, W.F., Hydrogeology and groundwater ecology: does each inform other?. *Hydrogeology Journal*, 17(1): 5-21 (2009).
3. Steube, C., S. Richter, and C. Griebler, First attempts towards an integrative concept for the ecological assessment of groundwater ecosystems. *Hydrogeology Journal*, 17(1): 23-25 (2009).
4. Eltahir, E.A.B., and P.J.F. Yeh, On the asymmetric response of aquifer water level to floods and droughts in Illinois. *Water Resources Research*, 35(4): 1199-1217 (1999).
5. Loaiciga, H.A., D.R. Maidment, and J.B. Valdes, Climate change impacts in a regional karst aquifer, TX, USA. *Journal of Hydrology*, 227: 173-194 (2000).
6. Allen, D.M., D.C. Mackie, and M. Wei, Groundwater and climate change: a sensitivity analysis for the grand forks aquifer, southern British Columbia, Canada. *Hydrogeology Journal*, 12(3): 270-290 (2004).
7. Gunawardhana, L.N., and S. Kazama, Statistical and numerical analyses of the influencing of climate variability on aquifer water levels and groundwater temperatures: the impacts of climate change on aquifer thermal regimes. *Global and Planetary Change*, 86-87: 66-78 (2012).
8. Moukana, J.A., and K. Koike, Geostatistical model for correlating declining groundwater levels with changes in land cover detected from analyses of satellite images. *Computers and Geosciences*, 34: 1527-1540 (2008).
9. Tremblay, L., M. Larocque, F. Anctil, and C. Riyard, Teleconnections and interannual variability in Canadian groundwater levels. *Journal of Hydrology*, 410(3-4): 178-188 (2011).
10. Park, E., and J.C. Parker, A simple model for water table fluctuations in response to precipitation. *Journal of Hydrology*, 356: 344-349 (2008).
11. Venencio, M.V., and N.O. Garcia, Interannual variability and predictability of water table levels at Santa Fe province (Argentina) within the climate change context. *Journal of Hydrology*, 409(1-2): 62-70 (2011).

Potential Impact and Risk Assessments of Future Climate Conditions on Salinisation in Central Huai Luang River Basin, Northeast, Thailand

Kewaree Pholkern^{1, a}, Phayom Saraphirom^{2, b*}, Wanpen Wirojanagud^{3, c}, and Kriengsak Srisuk^{4, d}

Abstract Potential impact and risk of the future climate conditions on salinity distribution were assessed in order to have the possible future land and groundwater conditions database for the integrated agricultural system planning for the next 10, 20 and 30 years in Huai Luang River Basin. Hydrodynamic of the groundwater and soil salinities were dependent on hydrologic, hydrogeologic, climate and land use conditions. The study area was the most important rice production area of Udon Thani Province, which covered by saline soils around 35%. The assessment was performed by two hydrological models, HELP for recharge estimation, and SEAWAT for groundwater flow and salt transport simulations. After calibration, validation and sensitivity analysis, three scenarios of the projected weather datasets namely, ECHAM5 A1B, WET, and DRY were used to project the movement of waterlogging and salinity area boundaries. The expansion of saline groundwater and waterlogging areas were found for all future climate conditions, especially for the Wet and ECHAM5 A1B. The highly saline area will be reduced, while the medium saline to slightly brackish area will be extending in the next 30 years. The future risk areas were found at the discharge areas around Mueang district and Kut Chap District covering the area about 79.96%, 75.34%, and 73.57% for ECHAM5 A1B, Wet, and Dry scenarios, respectively. Future risk areas will be increased from 2015 around 17%.

Keywords *soil salinity, climate change, groundwater model, Huai Luang River Basin, SEAWAT*

Kewaree Pholkern

Groundwater Resources Research Institute (GWRI), and Department of Environmental Engineering, Faculty of Engineering, Khon Kaen University (KKU), Thailand
Rekaweew@hotmail.com

Phayom Saraphirom

GWRI, and Department of Agricultural Engineering, Faculty of Engineering, KKU, Thailand
Payosa@kku.ac.th*

Wanpen Wirojanagud

Department of Environmental Engineering, Faculty of Engineering, KKU, Thailand
Wanpen@kku.ac.th

Kriengsak Srisuk

GWRI, KKU, Thailand

Kriengsk@kku.ac.th

Introduction

Salt affected soils cover about 36,100 km² of the Northeast Thailand (Arunin, 1996). The salt source for saline groundwater and soils in Northeast Thailand is primarily from rock salt of the Maha Sarakham Formation underlain at variable depths of ground surface. Movement of groundwater and consequently soil water are the main causes of the waterlogging and soil salinization. The major processes of spreading saline groundwater to be saline soil and subsurface water are groundwater flow and evaporation of soil water (Srisuk, 1994); naturally occurring salt affected areas such as these are referred to as primary salinity (Allan, 1994). While the source of the salts is natural, the process of salinization in dryland environment refers to human intervention. It was recognised as early as the 1980s that various human activities were responsible for the spreading of salinisation (Arunin, 1984). The activities include deforestation, construction of reservoirs in areas of shallow saline groundwater, salt making and irrigation (Arunin, 1989 and Yuvaniyama, 2004). This is beginning to dramatically affect natural environment, reduce the viability of agricultural sector (Arunin, 1984 and Beresford et al., 2001). The saline areas that have resulted from human activity are referred to as secondary salinity (Beresford et al., 2001).

The global climate is changing. The result from the Southeast Asia Climate Analyses & Modeling (SEACAM) regional climate modeling experiment shows that the significant changes of the climate in the Northeast region are precipitation and temperature. The projection shows significant increasing trend in average annual rainfall and average annual temperature in the period of 2016-2056 (Chinvanno, 2014). Changes in climatic variables can significantly alter hydrologic cycle and groundwater recharge which control salinity distribution of shallow aquifer systems and thus affect land availability for agriculture (Saraphirom, 2013). The concern is that the higher rainfall may cause this region to have more recharge leading to the extension of the waterlogging and making high potential risk salinisation areas in the future. That is the motivation of this

research study on the specific watershed area that currently encountered with salinity.

Study area

The study area covers an area of 1,529 km² of the southwestern part of Udon Thani Province or central part of Huai Luang River Basin. It covers 3 Districts of Udon Thani Province; Muang Udon Thani, Kut Chap and Nong Wua So. The topographic elevation of the study area varies from 160 to 564 meters above Mean Sea Level (m AMSL) as shown in Fig. 1. The mountainous and hilly terrains bound in the western, southern and northern parts. They are also act as the surface and groundwater divides of the basin. Population of about 448,000 persons is living in this basin or about 29% of Udon Thani Province population (DPA, 2013).

Climate: The study area has a tropical grassland climate or Savanna-Aw with an annual average temperature of 26.7 °C and average relative humidity is 71%. An average annual rainfall, calculated from Udon Thani meteorological station recorded data and 11 rainfall stations during the years of 1984-2013 is 1,437.90 mm/year (TMD, 2014 and RID, 2014). An average evaporation from class A pan measurement is 1,683 mm/year. The annual rainfall is varies from 1,200-1,700 mm and have a trend to increase during period of 1984-2013. The record shows average annual rainfall of 1,191, 1,559 and 1,563 mm/year during 1984-1993, 1994-2003 and 2004-2013, respectively.

Land use and soil salinity: The study area is covered by the agricultural areas, the main land use types are paddy field, field crops (sugarcane and cassava), urban area, water bodies, and forest (Fig. 1). Paddy field occupies along Huai Luang River floodplain and eastern parts of about 40% of the study area. The field crop is grown in the trend of northwest to southwest regions covering an area of about 23%. Forestry area, urban, water bodies covered the area of about 19%, 13% and 5% respectively (LDD, 2013).

Soil group were characterized based on their infiltration rates, parent material and relief. Two groups were classified: lowland soils (slow and moderate infiltration rates) and upland soils (rapid infiltration rates) (Farr et al., 1986). The trajectory of salinity in the area typically commences with deforestation, salt making and replacement with shallow root crop which has led to significant increases in recharge rates, and escalating salinity problems (Arunin, 1984). Soil salinity was classified into five categories as shown in Fig. 2. Moderately to Highest saline soils are the soils that have salt crust occurring on ground surface more than 1-50%, covered the lowland of central and eastern parts of study area. Slightly and non saline soils were found at highland and upland in the western and southern parts of study area. In the slightly and moderately salt affected areas farmers can growth rice, but the plant growth is non-uniform and affected by invasion of salt tolerant weeds (Doberman and Fairhurt, 2000).

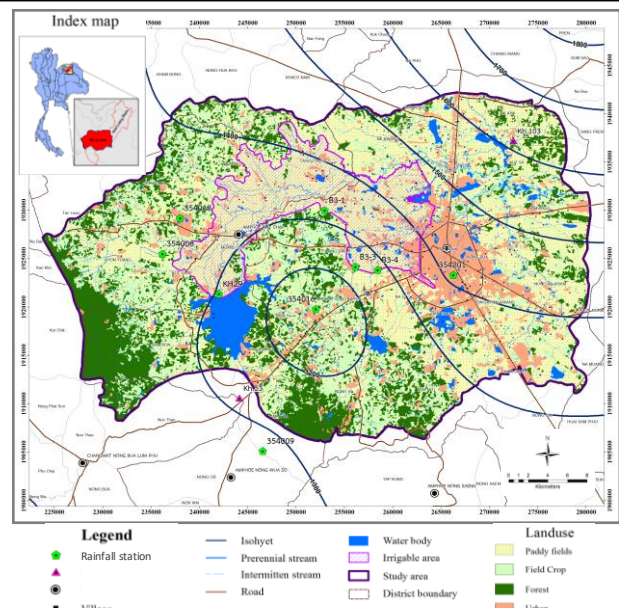


Fig.1 Boundary of study area, isohyets, river and streams, land use and irrigation area

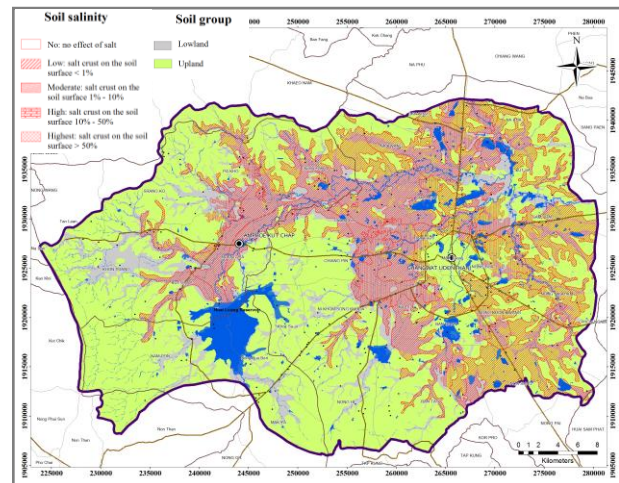


Fig.2 Soil group and soil salinity map (modified from LDD, 2007 and 2006)

Hydrology and Hydrogeology: Hydrological and hydrogeological investigations were conducted during September 2014 to December 2015. Huai Luang dam and Huai Luang River are major water sources for Udon Thani water supply and irrigation systems. Huai Luang River flows from west to east with length, width and depth of 50 km, 50-90 m and 5-7 m, respectively. Two stream gauging stations in Huai Luang River are KH.53 and KH.103. Huai Luang dam is located in the southwestern part of the study area. During the dry season water quality in Huai Luang River and its tributary are mildly brackish with electrical conductivities (EC) of up to 1,500 µS/cm or Total Dissolved Solids (TDS) up to 1,000 mg/l, whereas during the rainy season surface water becomes fresh to slightly brackish. TDS of Groundwater varies between less than 1,000 (fresh) to less than 10,000 (brackish) and greater than 10,000 mg/l (saline). The high TDS or salinity varies with depths and found in the low land at

the central part of study area along Huai Luang River or discharge area. The groundwater type of discharge area that classified based on Deutsch, (1997) is Na-Cl type.

The study area is underlain by sand, clay and gravel of Alluvium and Terrace Deposit units that located along the flood plain of Huai Luang River. Siltstone and sandstone aquifer of the Upper Phu Thok unit was underneath Alluvium unit with the thickness of 30 m, and shale and mudstone deposited with a thickness of 50 to 200 m of the Lower Phu Thok unit is underlain by the rock salt layers of the Maha Sarakham unit. And Khok Kruat unit is found at the toe of the mountain consisting of siltstone, sandstone with a thickness of 430 to 700 m (DMR, 2009; Suwanich, 1986; Cotanont, 2014). According to water level measurements from the year 2014-2015, Fig. 3 shows that regional groundwater flow pattern is replicated to topographic elevation and flow from recharge area to discharge area or from the western and southern to the central regions along the Huai Luang River.

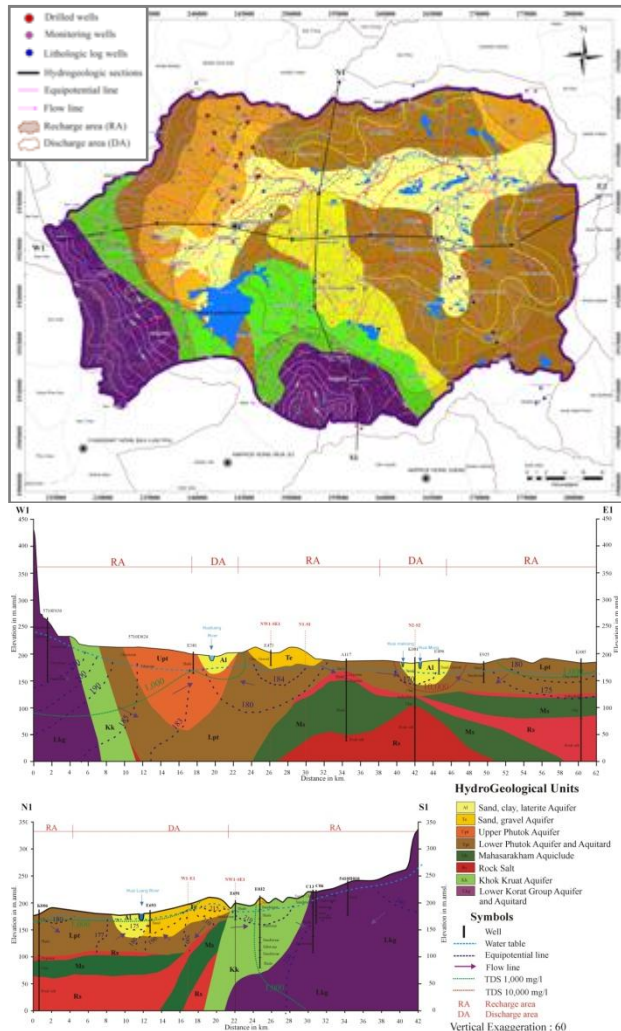


Fig. 3 Hydrogeologic map of the central Huai Luang River Basin

Methodology

Groundwater simulations: Potential impact of climate change on areas affected by waterlogging and shallow saline groundwater was evaluated using the variable density groundwater model, SEAWAT version 4 (Langevin et al., 2008) supported by recharge estimation model HELP3 (Schroeder et al., 1994). Simulation of groundwater flow and salt transport under the projected climate scenarios were carried out using the weather output data of the climate models. Southeast Asia Climate Analyses & Modeling (SEACAM) regional climate modeling experiment provides high resolution (25 km) information on future climate projections for the Southeast Asia region up to the end of this century. This was done by dynamical downscaling of the Met Office HadCM3Q ensemble and the ECHAM5 model using the Met Office PRECIS model (SEACAM et al., 2014). The SEACAM modeling under the 3 scenarios namely ECHAM5A1B (A1B), HadCM3Q10_DRY (DRY) and HadCM3Q11_WET (WET) were used as the input data for recharge estimations. Results from the recharge estimation were assigned into groundwater flow and salt transport model to simulate movement of the saline groundwater boundary (Fig. 4). The impact of future climate change on waterlogging and salinity distribution in the watershed was determined by means of areal distribution of water table depth and saline groundwater boundaries under the results from the prediction simulation results in the next 30 years (2016 - 2046) for each climate scenario.

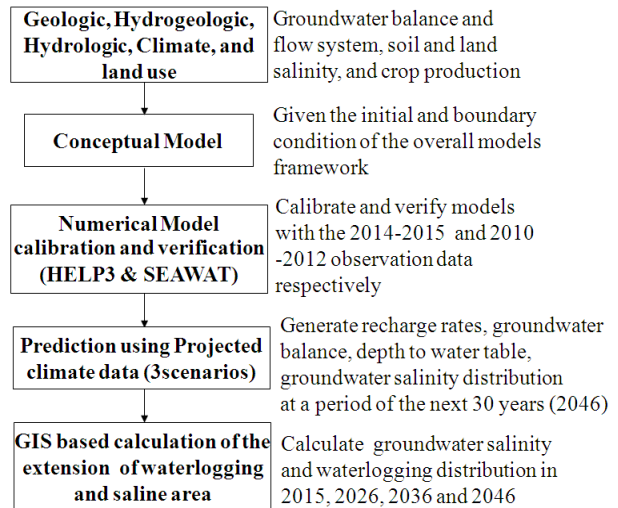


Fig. 4 Procedural diagram representing the modeling approach

Soil salinity risk mapping: In order to develop the soil salinity risk areas under future climate conditions, five criteria were used to analyze in a GIS spatial tool. The criteria included:

(i) shallow saline groundwater area, groundwater salinity that has TDS more than 1,000 mg/l have high potential to be saline soils, the expansion of shallow groundwater salinity area was characterize to 3 level as shows in Table 1,

(ii) waterlogging area, the area where depth of watertable can upward movement to soil surface and cause the accumulation of salt,

(iii) existing salt crust on ground surface, one of salt sources that can be spreading to other area and indicate the potential of salinity distribution,

(iv) irrigation area, this criteria is indicated the sufficiency of water for controlling salinity impact on rice production, which will be reduce the risk from salinity (Doberman and Fairhurt, 2000) and,

(v) soil group, most of the saline soil that found in study area is lowland soil, upland soil were found to be a coarser texture compared to the fine texture of lowland soil, capillary force was low in uplands and high in lowland soils (Saxena, et al., 1971) indicating thereby that lowland soils have higher percentage to move from shallow groundwater to be saline soil.

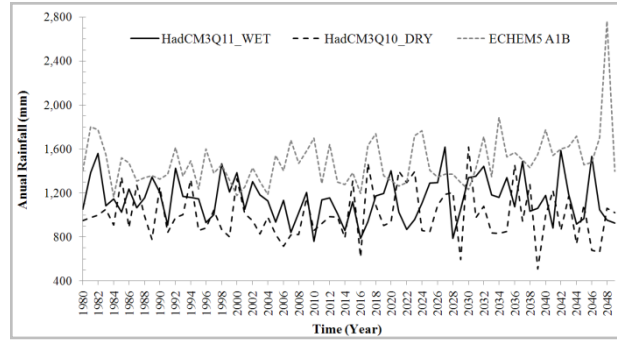
Table 1. Criteria for soil salinity risk map development

Parameter	Parameterscore	Class	Class score
Shallow groundwater salinity	10	TDS <1,000 mg/l	0.3
		1,000-5,000 mg/l	0.8
		>5,000 mg/l	1.0
Water-logging	9	<2 m	1.0
		2-4 m	0.8
		>4 m	0.5
Existing Salt crust	10	Non salt crust	0.3
		salt crust < 1%	0.5
		salt crust 1-10%	0.8
Irrigation area	7	Irrigation area	0.3
		Non Irrigation area	1.0
Soil group	5	Lowland soil	1.0
		Upland soil	0.5

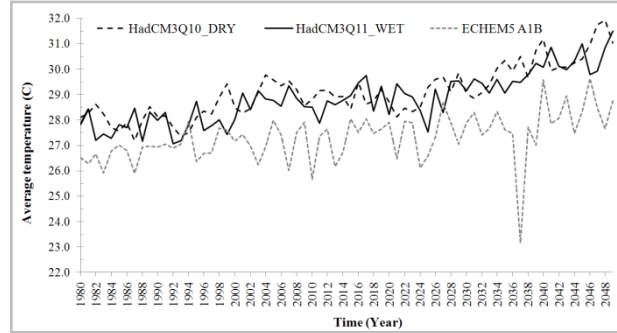
For this purpose different thematic maps were prepared from existing maps and data sets. These data were rating and ranking by using Fuzzy logic. Classification, scoring of the Fuzzy set and weighting of criteria were assigned based on the collected field evidences and detailed field works (Table 1). These criteria were integrated in GIS tool by the Weighted Index Overlay Analysis (WIOA) (Ghayounian et al., 2007)

Results and discussion

Future climate conditions: DRY scenario represented the dryer climate condition. While scenario WET represented wet climate condition. The A1B scenario represented general projected climate condition. The projected average temperature of 3 scenarios has an increasing trend as shown in Fig. 5. The higher temperature of DRY and WET scenarios has a significantly higher than scenario A1B. At the end of the century the temperature is approximately 31.5 °C, which will be significantly impact to the hydrological condition of the river basin.



(a) Annual rainfall



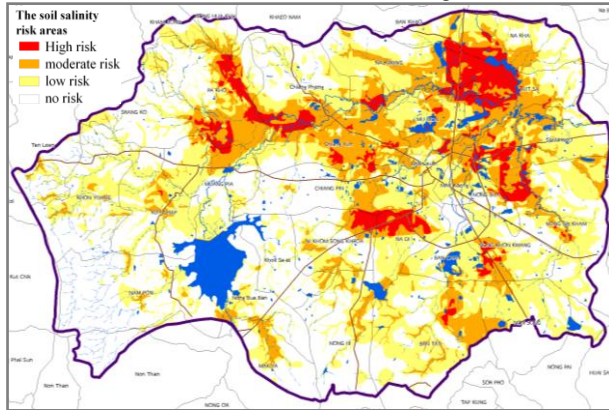
(b) Average annual temperature

Fig. 5 Projected annual rainfall and annual temperature of projected climate scenarios.

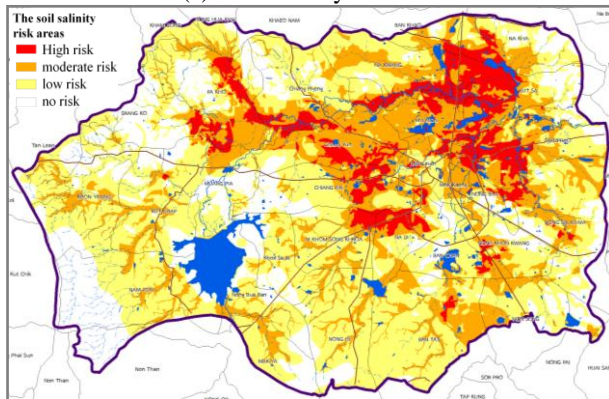
Groundwater salinity: groundwater simulation result indicated that area of shallow saline groundwater (TDS > 1,000 mg/l) that affects the salinity of the top soil increase for all scenarios. At present condition saline shallow groundwater covers an area of 205 km² or 13.8% of the study area and will gradually increase every year until the year of 2046, from WET climate scenario saline shallow groundwater will increase from present condition by 7.7%, while A1B and DRY climate conditions have the lower expansion rate. The waterlogging area (water table <4 m) also increase in all climate scenarios, the highest expansion area was found in A1B scenario. The present condition waterlogging area covers an area of 567 km² or 37.8% of the study area. And will increase about 29.0% in A1B scenario. The groundwater simulation result also show that aquifer water balance of study area have water inflow to aquifer more than water outflow from aquifer about 74.23-139.80 Mm³/year, it mean that the groundwater level have tent to increase every year for all scenarios. The waterlogging and saline groundwater areas occur in the flood plain of Huai Luang River Basin at Muang Pia, Pa Kho, Chiang Yun, Chiang Pin, Mu Mon, Kut Sa, and Sam Prao subdistricts. The extension of the waterlogging and saline groundwater areas will extend to Ban Leum, Nong Bua, Mu Mon and Na Kwang sub districts. The salinity of groundwater and soil were likely to increase in the future because of the increasing in groundwater recharge that will rise up the saline groundwater water table.

The soil salinity risk areas: the salinity risk areas maps of the various climate scenarios were produces for all climate scenarios. The risk areas were classified into 4 classes, namely, high risk, moderate risk, low risk, and no

risk. The risk areas have the highest increasing trend under the A1B scenario. This scenario has the risk area of 918 km² (60%) and in the next 30 years will increase to be 1,219 km² (80%), while the WET and DRY scenarios have the lower expansion of risk area. The risk area occurred in the low land of Huai Luang River floodplain and will be extend to the Chiang Pin, Chiang Yun, Kut Sa, and Sam Prao subdistricts as shown in Fig.6 and Table 2.



(a) Soil salinity risk areas in 2015



(b) Soil salinity risk areas in 2046

Fig. 6 Current and projected soil salinity risk areas in 2046 under A1B scenario

Table 2. The soil salinity risk areas under current and the projected scenarios in 2026 2036 and 2046

Risk area	high risk		moderate risk		low risk		no risk	
	km ²	%	km ²	%	km ²	%	km ²	%
2015	86.81	5.69	280.13	18.37	551.19	36.14	607.51	39.84
HadCM3Q11_WET scenario								
2026	112.59	7.38	318.22	20.87	571.02	37.44	523.77	34.35
2036	124.70	8.18	350.81	23.00	623.45	40.88	426.64	27.98
2046	130.82	8.58	374.26	24.54	643.94	42.23	376.60	24.70
HadCM3Q10_DRY scenario								
2026	112.26	7.36	319.16	20.93	568.75	37.30	525.42	34.45
2036	126.86	8.32	349.20	22.90	604.79	39.66	444.74	29.16
2046	131.23	8.61	372.06	24.40	618.70	40.57	403.63	26.47
ECHM5 A1B scenario								
2026	111.98	7.34	328.20	21.52	588.59	38.60	496.81	32.58
2036	123.49	8.10	363.60	23.84	643.34	42.19	395.19	25.91
2046	131.58	8.63	393.45	25.80	694.44	45.54	306.17	20.08

The salinity risk area (SRA) increased for all climate scenarios. The total SRA of A1B scenario was projected to be highest expansion from 60.2% of current situation to 79.9% in the next 30 years. The results indicated that the higher rainfall climate conditions

(WET and A1B) will give the higher SRA in the future. This is due to the fact that rainfall is the most importance factor controlling the flow and salt transport of the groundwater system. The SRA expansion rate is very high in the first decade and gradually lower in the second and third decades for all scenarios. The dry condition has the lowest expansion rate.

Conclusions and Recommendations

Potential impact and risk of salinity in the Central Huai Luang River Basin was assessed by HELP3 and SEAWAT hydrological models and Weighted Index Overlay Analysis to assess the soil salinity risk areas in the future under 3 climate conditions. Due mainly to higher precipitation the recharge rates in the study area were predicted to increase in the periods of 2016-2046 under WET, DRY and A1B climate conditions. The extensions of shallow saline groundwater areas were found from the model results for all climate scenarios and the same results trend also found in case of waterlogging area. The projected soil salinity risk areas were also found to be increasing in every risk levels for all climate scenarios. The salinity risk area from A1B scenario projection has the highest increasing trend. However, the extension of the soil salinity risk areas can be found for all scenarios.

Due to high uncertainty of the future climate projection, the management adaptation options are recommended to apply in order to find the suitable adaptation options for planning to living in salinity environment and minimize the impact of climate condition and the extension of salt affected areas in the future.

Acknowledgement

This research work was funded by the Thailand Research Fund (TRF). Authors would like to thanks the Groundwater Resources Regional Bureau 10, Udon Thani Province, Department of Groundwater Resources (DGR), Ministry of Natural Resources and Environment and Land Development Regional Office 5, Khon Kaen, Land Development Department (LDD), Ministry of Agriculture and Cooperatives for supporting data. We also grateful to staffs of Thai Royal Irrigation Department (RID) and Thai Meteorological Department (TMD) for sharing water level and weather data as well.

References

- Allan, M.J. (1994). An assessment of secondary dryland salinity in Victoria. CLPR Technical Report No. 14.CNR.
- Arunin, S. (1984). Characteristic and management of salt-affected soils in the northeast of Thailand.
- Arunin, S. (1989). Prevention of saline soil distribution by reforestation. *Journal of Agricultural Sciences*, 22(2), 141-153. (in Thai).
- Arunin, S. (1996). *Saline Soils in Thailand*. Bangkok: Department of Land Development. (in Thai).

- Beresford, Q, Bekle, H, Phillips, H, & Mulcock, J. (2001). *The Salinity Crisis: Landscapes, Communities and Politics*, University of Western Australia Press, Crawley.
- Chinvanno, S. (2014). *Adaptation to climate change and strategic for developing. Projection for building capacity for Adaptation to climate change: case study of in Huai Luang River Basin Thailand*. Southeast Asia START Regional Center. (in Thai).
- Cotanont, T. (2014). *The application of environmental isotopes and Fractured analysis for sustainable groundwater development: A case study of fractured sandstone and siltstone aquifers, Udon Thani Province*. Ph.D. Thesis, Department of Geotechnology, Khon Kaen University, Thailand.
- Department of Mineral Resources (DMR). (2009). *Hydrogeological map of Thailand 1:250,000*. Ministry of Natural Resources and Environment: Bangkok.
- Deutsch, W.J. (1997). *Groundwater Chemistry - Fundamentals and Applications to Contamination*. Lewis Publishers, New York. 221 p
- Dobermann, A., and Fairhurst, T. (2000). *Economics of fertilizer use*. In ‘Rice: Nutrient disorders & nutrient management’. pp. 38-39. Potash & Phosphate Institute, Potash & Phosphate Institute of Canada, and International Rice Research Institute.
- Farr, E. and Henderson, W.C. (1986). *Land Drainage* (Longman handbooks in agriculture). Longman Higher Education.
- Ghayoumian, J., Mohseni, S. M., Feiznia, S., Nouri, B., and Malekian, A. (2007). *Application of GIS Techniques to Determine Areas Most Suitable for Artificial Groundwater Recharge in a Coastal Aquifer in Southern Iran*. *Asian Earth Sciences* 30 (2): 364–74.
- Gumma, M. K., Thenkabail, P. S., Fujii, H., and Namara, R. (2009). *Spatial Models for Selecting the Most Suitable Areas of Rice Cultivation in the Inland Valley Wetlands of Ghana Using Remote Sensing and Geographic Information Systems*. *Journal of Applied Remote Sensing* 3 (June): 1–21.
- Land Development Department (LDD) (2013). *Land Use Map scale: 1:100,000*. Bangkok, Thailand: Land Development Department. Ministry of Agriculture and Cooperatives: Bangkok.
- Land Development Department (LDD). (2006). *Saline Soil Map of Northeast Thailand scale: 1:100,000*. Bangkok, Thailand: Land Development Department. Ministry of Agriculture and Cooperatives: Bangkok.
- Land Development Department (LDD). (2007). *Soil Series Map scale: 1:25,000*. Bangkok, Thailand: Land Development Department. Ministry of Agriculture and Cooperatives: Bangkok.
- Langevin, C.D., Thorne, D.T., Jr., Dausman, A.M., Sukop, M.C., and Guo, Weixing. (2008). *SEAWAT Version 4: A Computer Program for Simulation of Multi-Species Solute and Heat Transport*: U.S. Geological Survey Techniques and Methods Book 6, Chapter A22, 39 p.
- Nag, S. K. (2005). *Application of Lineament Density and Hydrogeomorphology to Delineate Groundwater Potential Zones of Baghmundi Block in Purulia District, West Bengal*. *Journal of the Indian Society of Remote Sensing* 33 (4): 522–9.
- Royal Irrigation Department (RID). (2557). *Rainfall and Steam flow data of Udon Thani Province*. Ministry of Agriculture and Cooperatives: Udon Thani Province.
- Saraf, A. K, and Choudhury, P. R. (1998). *Integrated Remote Sensing and GIS for Groundwater Exploration and Identification of Artificial Recharge Sites*. *International Journal of Remote Sensing* 19 (10): 1825–41.
- Saraphirom, P. (2013). *Impact of Climate Change on Salinity Distribution and Ecohydrological Management: Case Study of Huai Khamrian Subwatershed, NE, Thailand*. PhD Thesis in Environmental Engineering, Khon Kaen University, Thailand.
- Saxena, V.P., Mehrotra, C.L., Srivastava, K.C. (1971). *Physical characteristics of some problem soils of Uttar Pradesh*. Proc. All India Symp. Soil Salinity, Kanpur, 1971, 30-7.
- Schroeder, P. R., Dozier, T.S., Zappi, P. A., McEnroe, B. M., Sjoström, J. W., and Peyton, R. L. (1994). *The Hydrologic Evaluation of Landfill Performance (HELP) Model: Engineering Documentation for Version 3*, EPA/600/R-94/168b, U.S. Environmental Protection Agency Office of Research and Development, Washington, DC.
- Srisuk, K. (1994). *Genetic characteristics of Groundwater Regime in the Khon Kaen Drainage Basin*. Ph. D. Thesis, University of Alberta, Canada.
- Suwanich, P. (1986). *Potash and Rock salt in Thailand*. *Nonmetallic Minerals Bulletin No.2*. Economic Geology Division, Department of Mineral Resources, Bangkok, Thailand.
- Thai Meteorological Department (TMD). (2014). *Weather data of Udon Thani Province*. Ministry of Information and Communication Technology: Bangkok.
- The Southeast Asia Climate Analyses & Modeling (SEACAM), The Centre for Climate Research Singapore of the Meteorological Service Singapore (CCRS-MSS), the Met Office Hadley Centre (MOHC), the region’s National Meteorological & Hydrological Services (NMHSs), and Research Institutes (RIs). (2014). *A Regional Climate Modelling Experiment for Southeast Asia. Using PRECIS Regional Climate Model and selected CMIP3 Global Climate Models*.
- Yuvaniyama, A. (2004). *Manual of saline soils management and reclamation*. Bangkok: Land Development Department.

Impact of decreasing percentage of imperviousness area with flooding in urban area at Sukhumvit, Bangkok, Thailand.

Detchphol Chiwatkulsiri^{1,a,*}, Sutat Weesakul^{2,b} and Ashish Shrestha^{3,c}

Abstract The trend of frequency, intensity and volume of extreme precipitation under climate change has been increased. Urban flooding has become more frequent phenomenon in most of the cities. The climate change could have potentially outsized impact in existing ecological, human system and built systems. Most of the urban drainage systems are designed under stationary climate consideration, as the consequences most of them are running over capacity before their design period. The technologies for the urban drainage have been developed over a long period of time. For example, rainwater harvesting, green roofs, urban green space and pervious pavements. These technologies have multiple benefits alongside with flood mitigation by decreasing of imperviousness area in the urban area. The study, specific to Sukhumvit, Bangkok, aims to analyze the performance of urban drainage under the changing rainfall due to the normal and climate change condition in different percentage of imperviousness. The effect of decreasing imperviousness area is studied with application of 1 dimensional and 2 dimensional modeling approach using tools like Mike Urban and Mike Flood software.

The study shown the flood inundation area and flood inundation duration are reducing due to the effect of decreasing imperviousness in the study area. The two step of decreasing, from 70% (as model calibration) to 60% and 50% investigated that the flood inundation area was reduced as same as the normal and climate change condition. It is confirmed that impervious area have an important impact on runoff. The Flood inundation area and floodinundation duration was reducing compared from present condition with cases of decreasing percentage of imperviousness area.

Keywords *Urban flooding, drainage system, imperviousness area, infiltration*

Detchphol Chiwatkulsiri
Valaya Alongkom Rajabhat University under the Royal Patronage.
Pathumtani, Thailand.
armearm_19@hotmail.com

Introduction

Urbanization is the process of turning green field sites into developments. For example, building in the countryside. Infiltration is rainfall soaking into the ground and eventually ending up in rivers over a period of days. Once the site has been developed and the site is now impermeable so the rainfall becomes surface runoff quickly without soaking into the ground to get to the rivers in hours or even minutes. These make the hydrograph to peak higher and sharper (more water in less time) and flooding occurs.

Climate change is making weather less predictable, rains more uncertain and heavy storm rainfalls more likely. The unpredictability of rainfall can be caused by flooding in urban areas. Urban floods are a great disturbance of daily life in the city. Roads can be blocked, people can't go to work or to schools. The economic damages are high but the number of casualties is usually very limited, because of the nature of the flood. The water slowly rises on the city streets. When the city is on flat terrain the flow speed is low and you can still see people driving through it. The water rises relatively slow and the water level usually does not reach life endangering heights.

In the central part of Bangkok, Sukhumvit area, is a representative of urbanization. Bangkok metropolitan administration (BMA) has department of drainage and sewerage (DDS) working on flood problem in Bangkok. Several studies from DDS have shown that drainage capacity of the existing system is still not perfect enough. In Sukhumvit area has primary drainage system from surrounded canals and the secondary drainage system inside area. Therefore, when the water level in primary drainage system around this area is getting higher, the secondary drainage system will have problem to drain water out.

The study in Sukhumvit area by using modeling tool and analyze the decreasing percentage of imperviousness can show the capability of infiltration effect to the urban area. These can help to reduce impact of floods in the urban area. Moreover, this study will concern only about adaptation of urban drainage system from impact of climate change by applying some of adaptation into the model and find out which one can perform well in the

area and which alternative of adaptation can reduce peak of rainfall more or less.

Study area

In this study, an urban area was selected to apply the urban drainage model using the rainfall forecast results to simulate and predict flood situation. At present, levees with 100-year return period are being constructed along the river to prevent river and tidal flood. The main remaining cause is the heavy rainfall over the city. The drainage system in Bangkok is old and designed for 2 and 5-year return periods, which may not be adequate for stormwater in extreme events. The polder system has been proposed by NEDECO (Netherlands Engineering Consultants) in order to provide adequate pumping capacity for each several areas in the city. At present, there are 15 polders in the primary drainage of Bangkok as summarized by DDS (1996). Each polder has its own drainage, so-called secondary drainage system. Sukhumvit catchment is the one of them. Sukhumvit catchment is very highly urbanized area and one of the central business districts of eastern Bangkok, located in inner part of Bangkok in the right side of Chao Phraya River. It has an area of 24 km² with population density of 8,400 person/km². It is bounded by canals and the Chao Phraya River. Average elevation of the Sukhumvit area is 0.4 to 1.0m above mean sea level (MSL). Maximum levees elevation along klong Sean Seap and klong Tan/Phra Khanong are approximated as 1.2m MSL. This catchment is a flat plain. Although, this area could be prevented from flooding caused by overflow from the Chao Phraya River in 1995 and 1996, stormwater is difficult to be drained out by gravity into existing canals. Pumping stations are necessarily needed as main drainage structures.

Methodology

Hydrologic models - In urban hydrologic models, mathematical equations primarily simulate rainfall loss and runoff routing. The loss equations are responsible for estimating the loss of rainfall due to infiltration and depression storage whilst routing equations transform the effective rainfall to a runoff hydrograph based on catchment characteristics. The loss and routing are simulated at the same time. The general process is to remove the loss from the total rainfall and then simulate the routing process. There are a number of hydrologic modelling approaches such as the time-area method and kinematic wave method (O’Loughlin and Stack 2003; MIKE URBAN 2014). These methods use different theoretical concepts to integrate peak attenuation and travel time of runoff due to the storage action of the catchment and the drainage channels. Time-area method has been widely used in hydrologic research due to its ability to simulate urban catchments compared with other methods. Therefore, the theory of the time area method is discussed in this section. The time-area routing models can simulate the flow at the outlet of a

catchment based on the variation of contributing area with time. The time-area curve can calculate the runoff hydrograph for a simulated catchment and given rainfall event. The peak discharge is the sum of flow contributions from the subdivisions of the catchment defined by time contours, which are lines of equal flow-time to the catchment outlet where the peak discharge is required. The time-area curve is obtained based on the time of concentration which can be defined as the time taken for the flow from the most remote part of the catchment to reach the outlet. The variation of the cumulative time-area curve with distance from the outlet depends on the shape and surface characteristics of the catchment. That means that the time-area curve can be drawn as a concave, convex or linear shape.

Input parameters

Rainfall reduction factor, accounts for water losses caused by e.g. evapo transpiration, imperfect imperviousness, etc. on the contributing area. The value is 0.65 refer to model calibration from Loetluck (2015) in analysis of flooding in klong toei wattana polder, Bangkok using mike flood urban model.

Percentage of impervious area, For modelling approach, sensitivity analysis was found that the impervious area is most effective parameter for model calibration. This parameter affected directly with the water volume and also water level. In this study, the effect of infiltration adapted by decreasing percentage of imperviousness area in study area. The previous calibration and verification model, it set the percentage of impervious surface equal 70% for all sub catchment. Thus, these three cases are created for compare the effect by varied from 70% as a normal condition, 60% for decreasing 10% and 50% for decreasing 20%.

Effect of infiltration and rainfall. Marselek (2000) was found that the low return period and short of rainfall significant to effect of infiltration. In this study, the rainfall events are 2 and 5 years return period with varied duration 30 minute and 1 hour.

Scenarios for this study. There are two groups of scenarios. First group of rainfall is due to existing data and the second is based on climate change IDF curve results that simulated from IPCM4 under SRA1B. In each rainfall duration, the percentage of imperviousness area will be varied from 70% (present condition) to 60% and 50% (increase infiltration by decreasing imperviousness area)

Table 1 Scenarios in case of existing rainfall.

Rainfall duration	Return period (Tr)					
	2			5		
30 minute	70% ex	60% ex	50% ex	70% ex	60% ex	50% ex
1 hour	70% ex	60% ex	50% ex	70% ex	60% ex	50% ex

Table 2 Scenarios in case of climate change rainfall.

Rainfall duration	Return period (Tr)					
	2			5		
30 minute	70% cc	60% cc	50% cc	70% cc	60% cc	50% cc
1 hour	70% cc	60% cc	50% cc	70% cc	60% cc	50% cc

Results and discussion

The results were showed according to the main objective as the effect of increase infiltration by decreasing imperviousness area varied from 70% (present condition) to 60% and 50% in difference scenarios. The results present the performance of the drainage system as well as quantitative evaluation of criteria that represent the hazards associate with the events of floods. In general hazards are categorized based on the flood depth. The implication of climate change through increasing rainfall intensities in urban basin could create the hazard as a consequence of flood in socio-economic environment. The increasing extents of Flood inundation duration connote significant disturbances in socio-economic activities. The following scatter plot diagrams show the hazard in term of depth. Each point is the 2D computation cell where depth is computed. The scatter plots are considered for each return period to compare flood hazard from present to future extents. Some of results in study as shown flood inundation duration and flood inundation level were shown in Figure 1, 2, 3 and 4 below:

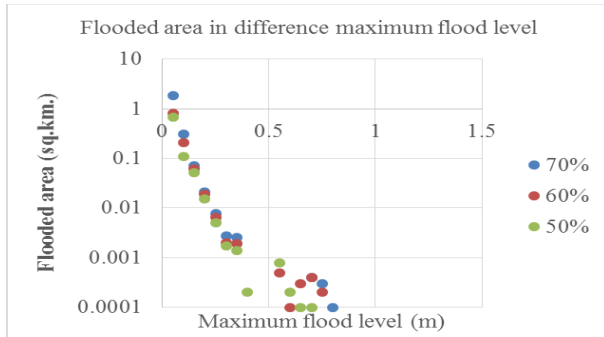


Fig. 1 Flood inundation area in difference of maximum flood level in case of using 2 years return period of existing rainfall with 30 minute duration

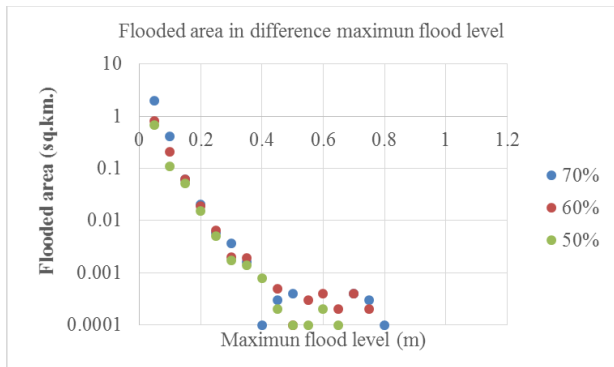


Fig.2 Flood area in difference of maximum flood level in case of using 2 years return period of climate change rainfall with 30 minute duration

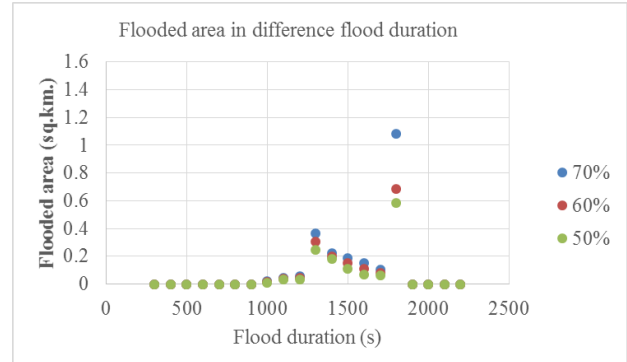


Fig.3 Flood area in difference of flood duration in case of using 2 years return period existing rainfall with 30 minute duration

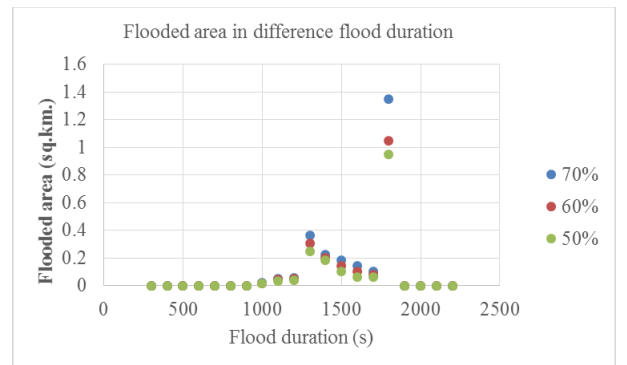


Fig.4 Flood area in difference of flood duration in case of using 2 years return period of climate change rainfall with 30 minute duration

Summary and conclusions

In summary, the flood area from 2D flood computation comparing with difference percentage of imperviousness area in varied of rainfall event.

Table 3 Decreasing percentage of number of flood inundation area in 2D computation (existing)

Rainfall duration	Return period (Tr)					
	2			5		
30 minute	70%	60%	50%	70%	60%	50%
1 hour	70%	60%	50%	70%	60%	50%

Table 4 Decreasing percentage of number of flood inundation area in 2D computation (climate change)

Rainfall duration	Return period (Tr)					
	2			5		
30 minute	70%	60%	50%	70%	60%	50%
1 hour	70%	60%	50%	70%	60%	50%

Impervious area have an important impact on runoff flow. The peak of water level was decreasing compared from present condition with cases of decreasing percentage of imperviousness area. The slope of hydrograph is lower comparing to present condition and Time to peak is longer. As the results of climate change urban drainage system will become inadequate in capacity thus more upgrades and maintenance is necessary in future. The future change in IDF curve under un-stationary climate shall be taken into consideration while selecting the design criteria of rainfall intensity in future.

The flood hazards are generally described in relation to the velocity and depth. The climate change impact on flood hazard arising from pluvial floods showed the resulting hazard as medium hazard in all cases.

In conclusion, impervious area has an important impact on runoff flow. The peak of water level was decreasing compared from present condition with cases of decreasing percentage of imperviousness area. Moreover, time to peak is longer. The suitable percentage of decreasing imperviousness is 10%. It can reduce almost 50% of flooded area comparing to present condition. The percentage of impervious area should be considered for future urban planning. Thus, the impact from pluvial flooding in urban area will be lower than the present condition.

Acknowledgement

The study will not be finished without the meteorological data provided from Department of Drainage and sewerage, BMA. Moreover, this study is partial supported funding from APN project.

References

BMA, s.f. STATISTICAL PROFILE OF BANGKOK METROPOLITAN ADMINISTRATION 2012, s.l.: Bangkok Metropolitan Administration.

Boonya-aroonnet, S., Weesakul, S. & Mark, O., 2001. Modeling of Urban Flooding in Bangkok, s.l.: Global Solutions for Urban Drainage, American Society of Civil Engineers.

Cardona, O. D. & van Aalst, M. K., 2012. Determinants of Risk: Exposure and Vulnerability. En: Managing the Risks of Extreme Events and Disasters to Advance Climate Change Adaptation. Cambridge University Press, Cambridge, UK, and New York, NY, USA: Intergovernmental Panel on Climate Change (IPCC), pp. 65 - 108.

Dassanayake, D., Burzel, A., Kortenhaus, A. & Oumeraci, H., 2010. Framework and Methods for the Evaluation of Intangible Losses and their Integration in Coastal Flood Risk Analysis, s.l.: s.n.

de Man, H. y otros, 2013. Quantitative assessment of infection risk from exposure to waterborne pathogens in urban floodwater, s.l.: Elsevier Ltd.

DHI 1D-2D Modelling, W. & E., 2014. MIKE FLOOD. 1D-2D Modelling User Manual. s.l.:s.n.

DHI Advection/Dispersion Module, W. & E., 2014. MIKE 21 FLOW MODEL. Advection/Dispersion Module User Guide. s.l.:s.n.

DHI Hydrodynamic Module, W. & E., 2014. MIKE 21 FLOW MODEL. Hydrodynamic Module User Guide. s.l.:s.n.

DHI MOUSE, W. & E., 2014. MOUSE. Short introduction and Tutorial. s.l.:s.n.

DHI Pollution Transport, W. & E., 2014. MOUSE. Pollution Transport. Reference Manual. s.l.:s.n.

Few, R., Ahern, M., Matthies, F. & Kovats, S., 2004. Floods, health and climate change: a strategic review, s.l.: Tyndall Centre for Climate Change Research.

Gouldby, B. & Samuels, P., 2005. Language of Risk.. Integrated Flood Risk Analysis and Management Methodologies, p. 47.

Gronewold, A. D., Wolpert, R. L. & Reckhow, K. H., 2008. Modeling the relationship between most probable number (MPN) and colony-forming unit (CFU) estimates of fecal coliform concentration, Durham, NC 27708, USA: Elsevier Ltd.

Hashimoto, M. y otros, 2014. Assessing the relationship between inundation and diarrhoeal cases by flood simulations in low-income communities of Dhaka City, Bangladesh, s.l.: Japan Society of Hydrology and Water Resources.

Hashizume, M. y otros, 2008. Factors determining vulnerability to diarrhoea during and after severe floods in Bangladesh, s.l.: IWA Publishing.

Horton, M. B., 2010. A Guide for Health Impact Assessment, s.l.: California Department of Public Health.

Hunter, P., 2003. Climate change and waterborne and vector-borne disease. Journal of Applied Microbiology, Volumen The Society for Applied Microbiology, p. 37S-46S.

Jonkman, S. N., 2007. Loss of life estimation in flood risk assessment. Theory and applications, s.l.: s.n.

Kazama, S. y otros, 2012. A quantitative risk assessment of waterborne infectious disease in the inundation area



- of a tropical monsoon region, s.l.: Sustainability Science.
- Kelman, I., 2003. Defining Risk. FloodRiskNet Newsletter, p. 3.
- Mark, O. & Hammond, M., 2014. Health Impacts Model. University of Exeter, United Kingdom, CORFU is a Collaborative Project in the FP7 Environment Programme.
- BMA, s.f. STATISTICAL PROFILE OF BANGKOK METROPOLITAN ADMINISTRATION 2012, s.l.: Bangkok Metropolitan Administration.
- Boonya-aroonnet, S., Weesakul, S. & Mark, O., 2001. Modeling of Urban Flooding in Bangkok, s.l.: Global Solutions for Urban Drainage, American Society of Civil Engineers.
- Cardona, O. D. & van Aalst, M. K., 2012. Determinants of Risk: Exposure and Vulnerability. En: Managing the Risks of Extreme Events and Disasters to Advance Climate Change Adaptation. Cambridge University Press, Cambridge, UK, and New York, NY, USA: Intergovernmental Panel on Climate Change (IPCC), pp. 65 - 108.
- Dassanayake, D., Burzel, A., Kortenhaus, A. & Oumeraci, H., 2010. Framework and Methods for the Evaluation of Intangible Losses and their Integration in Coastal Flood Risk Analysis, s.l.: s.n.
- de Man, H. y otros, 2013. Quantitative assessment of infection risk from exposure to waterborne pathogens in urban floodwater, s.l.: Elsevier Ltd.
- DHI 1D-2D Modelling, W. & E., 2014. MIKE FLOOD. 1D-2D Modelling User Manual. s.l.:s.n.
- DHI Advection/Dispersion Module, W. & E., 2014. MIKE 21 FLOW MODEL. Advection/Dispersion Module User Guide. s.l.:s.n.
- DHI Hydrodynamic Module, W. & E., 2014. MIKE 21 FLOW MODEL. Hydrodynamic Module User Guide. s.l.:s.n.
- DHI MOUSE, W. & E., 2014. MOUSE. Short introduction and Tutorial. s.l.:s.n.
- DHI Pollution Transport, W. & E., 2014. MOUSE. Pollution Transport. Reference Manual. s.l.:s.n.
- Few, R., Ahern, M., Matthies, F. & Kovats, S., 2004. Floods, health and climate change: a strategic review, s.l.: Tyndall Centre for Climate Change Research.
- Gouldby, B. & Samuels, P., 2005. Language of Risk.. Integrated Flood Risk Analysis and Management Methodologies, p. 47.
- Gronewold, A. D., Wolpert, R. L. & Reckhow, K. H., 2008. Modeling the relationship between most probable number (MPN) and colony-forming unit (CFU) estimates of fecal coliform concentration, Durham, NC 27708, USA: Elsevier Ltd.
- Hashimoto, M. y otros, 2014. Assessing the relationship between inundation and diarrhoeal cases by flood simulations in low-income communities of Dhaka City, Bangladesh, s.l.: Japan Society of Hydrology and Water Resources.
- Hashizume, M. y otros, 2008. Factors determining vulnerability to diarrhoea during and after severe floods in Bangladesh, s.l.: IWA Publishing.
- Horton, M. B., 2010. A Guide for Health Impact Assessment, s.l.: California Department of Public Health.
- Hunter, P., 2003. Climate change and waterborne and vector-borne disease. Journal of Applied Microbiology, Volumen The Society for Applied Microbiology, p. 37S-46S.
- Jonkman, S. N., 2007. Loss of life estimation in flood risk assessment. Theory and applications, s.l.: s.n.
- Kazama, S. y otros, 2012. A quantitative risk assessment of waterborne infectious disease in the inundation area of a tropical monsoon region, s.l.: Sustainability Science.
- Kelman, I., 2003. Defining Risk. FloodRiskNet Newsletter, p. 3.
- Mark, O. & Hammond, M., 2014. Health Impacts Model. University of Exeter, United Kingdom, CORFU is a Collaborative Project in the FP7 Environment Programme.
- OEHHA, s.f. A Guide to Health Risk Assessment. [En línea]
Available at: <http://www.oehha.ca.gov/>
[Último acceso: 19 03 2015].
- Official Journal of the European Union, 2006. DIRECTIVE 2006/7/EC OF THE EUROPEAN PARLIAMENT AND OF THE COUNCIL of 15 February 2006 concerning the management of bathing water quality and repealing Directive 76/160/EEC. s.l., s.n.
- Parkinson, J. & Mark, O., 2005. Urban Stormwater Management in Developing Countries. London: IWA Publishing.



Price, R. K. & Vojinovic, Z., 2012. Urban Hydroinformatics. London: IWA Publishing.

Sayers, P. y otros, 2003. Risk, Performance and Uncertainty in Flood and Coastal Defence, Ergon House, UK: Defra – Flood Management Division .

Shrestha, A., 2013. IMPACT OF CLIMATE CHANGE ON URBAN FLOODING IN SUKHUMVIT AREA OF BANGKOK, Bangkok, Thailand: M.Sc. Thesis, Asian Institute of Technology .

Sterk, G., ten Veldhuis, J., Clemens, F. & Berends, B., 2008. Microbial risk assessment for urban pluvial flooding, Edinburgh, Scotland, UK: 11th International Conference on Urban Drainage.

Sutat, W., Ole, M., Chayalit, C. & Uraya, W., 2005. Real Time Hydological Information for the people of Thailand, s.l.: s.n.

ten Veldhuis, J., Clemens, F., Sterk, G. & Berends, B., 2010. Microbial risks associated with exposure to pathogens in contaminated urban flood water, Heverlee, Belgium: Elsevier Ltd.

Vojinovic, Z. & Abbott, M. B., 2013. Flood Risk and Social Justice. London: IWA Publishing.

Land Cover/Use Scenario Building and its Impact on Flooding inside the Iligan River Basin

Milano, Alan E., Suson, Peter D., Salcedo, Stephanie Mae B. and Blasco, Jennifer G.

Abstract This study aims to assess the impact on flooding when no proper land use management is done and another is when sound land use management is adopted. Hence, two (2) land cover/use scenarios were created. The two scenarios were the Projected Land Cover and the Desired Land Use. The two scenarios were created from a previous study whereby the impact on the two scenarios on runoff behavior was determined. The output of that study was then used as an input to determine the impact of flooding in terms of extent and depth/level. The results shows that the effect on flooding by Projected Land Cover shows more areas have been flooded with more areas inundated with higher flood depth level as compared to the Desired Land Use scenario in the five (5) Rainfall Return Period which is the 5 years, 10 years, 25 years, 50 years and 100 years. The reason behind this is because the Projected Land Cover has higher runoff values as against the Desired Land Use scenario considering that runoff is the source for flood waters.

The difference in runoff values between the two land cover/land use scenarios is attributed to forest vegetation. In particular, the Desired Land Use scenario has more forest vegetation cover and it has better forest cover quality than the projected land cover scenario. Such condition helps improve soil infiltration and thus reduces runoff. In addition the presence of agroforestry in the Desired Land Use scenario which is non-existent for the Projected Land Cover scenario also contributes to lower runoff in the Desired Land Use scenario. That is because Agroforestry land use is also known to improve soil infiltration. The study shows when land cover conditions are left by itself without any intervention, the impact of flood disaster is magnified. The study also proves the important role in adopting proper land use management in mitigating flood hazard as represented by the Desired Land Use scenario.

Keywords *flooding depth and extent, runoff, projected land cover, desired land use*

Introduction

The Iligan River Basin is located in Northern Mindanao, Philippines with coordinates at 8°08’0”N to 8°12’30”N Latitude and 124°12’30”E to 124°17’30”E Longitude (Figure 1). The downstream of the basin is Iligan City; a highly urbanized city. In December 17, 2011 Tropical Storm Washi struck the city. An updated assessment shows that 1,278 died, 28,730 families displaced, 35 out of the 44 villages were affected and initial structural damage assessment was about USD 81.4 Million^[1]. It is because of that fateful event that spurred an interest in studying the flooding behavior of the basins and/or watersheds traversing Iligan City (Figure 1).

This study aims to determine what happens to runoff after some given time in the absence of any intervening land use management and compare it when sound land use management is adopted. In that light, two (2) scenarios were created. One is the Projected Land Cover in 2026 and the other scenario is the Desired Land Use. The two scenarios were created from a previous study of ours whereby the impact on the two scenarios on runoff behavior was determined.

The Authors are connected to the LiDAR1 Project, College of Engineering, MSU-Iligan Institute of Technology, Philippines. It is sponsored by DOST-PCIEERD.

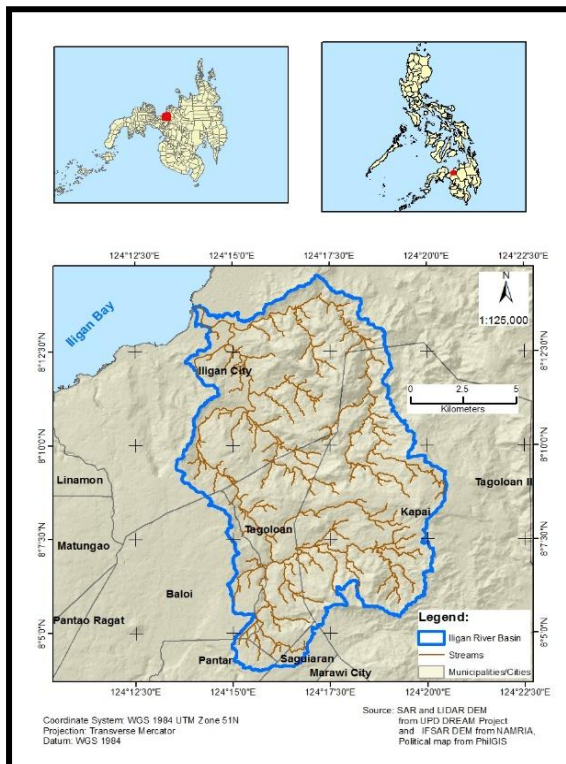


Figure 1. Location Map of the Study Area

Methodology

The output on the impact of the Projected Land Cover and the Desired Land Use to runoff in the previous study was used as an input to determine the impact of the aforementioned land cover scenarios to flooding. The software that was used to determine flooding was the Hydrologic Engineering Center's- River Analysis System (HEC-RAS) 2D model and a GIS extension application called HEC-Geo-RAS. The LiDAR-DTM (Light Detection and Ranging-Digital Terrain Model) bathymetrically burned geospatial raster dataset was as the input for the software processing of the flood.

The flood parameters that were determined was flood depth/level and extent for the different rainfall return periods in particular the 5 year, 10 year, 25 year, 50 year and 100 year. There were three flood depth or level that were determined, this was low, medium and high with corresponding values in range namely: 0-0.5 m, 0.5-1.5 m and >1.5 m. The study area involves the whole Iligan River Basin. Geometric data was prepared in HECRAS by manually delineating the 2D area and generating a 50x50 mesh. Unsteady flow was simulated for 5,10,25,50 and 100yr RRP in 10min flow data interval with an EG Slope of 1 and a min. Flow of 27 m³/s. Animation and visualization was done in RAS Mapper which is also capable in exporting flood map results in files readable to GIS.

Results and discussion

Annexes 1a to 5b shows the flood hazard map of the Projected Land Cover and the Desired Land Use for the rainfall return period of years 5, 10, 25, 50 and 100. Flood depth or level is lower in the Desired Land Use than the Projected Land Cover and this is much pronounced at higher flood level or depth in all of the rainfall return period events (Table 1). Likewise, the total extent of flooding is much lower in the Desired Land Use than the Projected Land Cover (Table 1).

The reason for a lower flood depth and extent for the Desired Land Use than the Projected Land Cover is because based on our previous study the Projected Land Cover has higher runoff values in terms of discharge volume, peak discharge and Lag Time as against the Desired Land Use scenario. This is in view of the fact that runoff is the major source for flood waters (Figures 2-4). The difference in runoff values between the two land cover/land use scenarios is attributed to forest vegetation.

In particular, the Desired Land Use scenario has more forest vegetation cover and it has better forest cover quality than the projected land cover scenario as represented by the Forest Protection land use (Figure 5). Such condition helps improve soil infiltration and thus reduces runoff. In addition the presence of agroforestry in the Desired Land Use scenario which is non-existent for the Projected Land Cover scenario also contributes to lower runoff in the Desired Land Use scenario. That is because Agroforestry land use is also known to improve soil infiltration due to its soil and water conservation function.

Table 1. Extent of Flood Level at Nth Year Rainfall Return Period

Rainfall Return Period	Classification	FLOOD EXTENT AREA (Hectare)	
		Projected Land Cover	Desired Landuse
5-YEAR	Low	55.29	26.31
	Medium	102.35	51.45
	High	473.86	151.72
	TOTAL	631.50	229.48
10-YEAR	Low	73.59	56.26
	Medium	149.49	103.89
	High	713.93	457.75
	TOTAL	937.01	617.90
25-YEAR	Low	79.71	64.57
	Medium	152.48	119.89
	High	831.14	537.01
	TOTAL	1063.33	721.47
50-YEAR	Low	70.81	70.70
	Medium	151.06	133.96
	High	1001.36	585.27
	TOTAL	1223.23	789.93
100-YEAR	Low	79.84	73.68
	Medium	163.79	140.70
	High	981.45	624.10
	TOTAL	1225.08	838.48

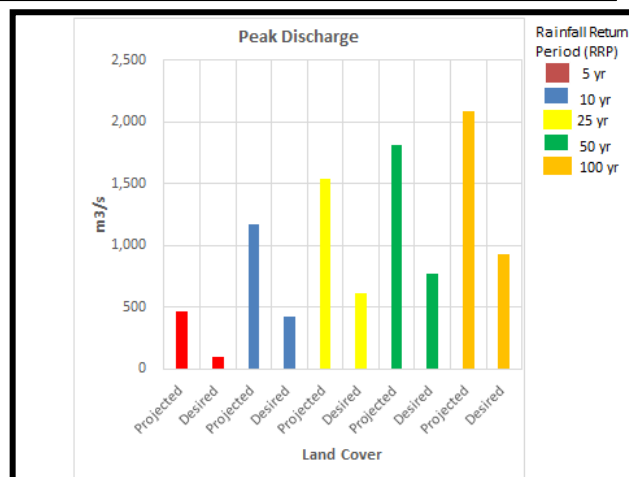


Figure 3. Peak Discharge Comparison

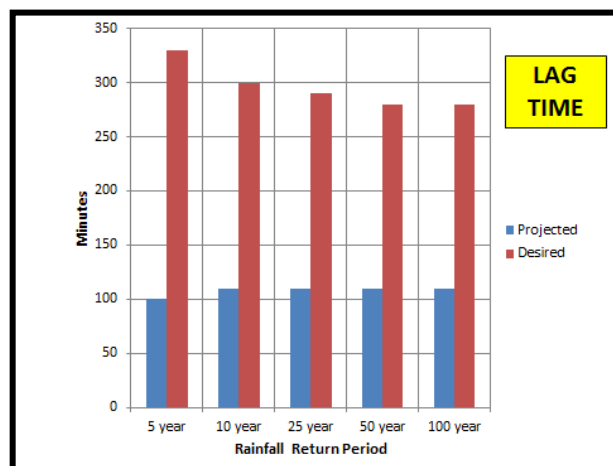


Figure 4. Lag Time Comparison

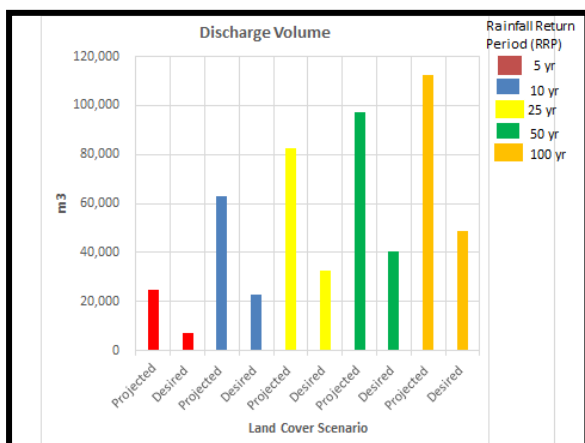


Figure 2. Discharge Volume Comparison

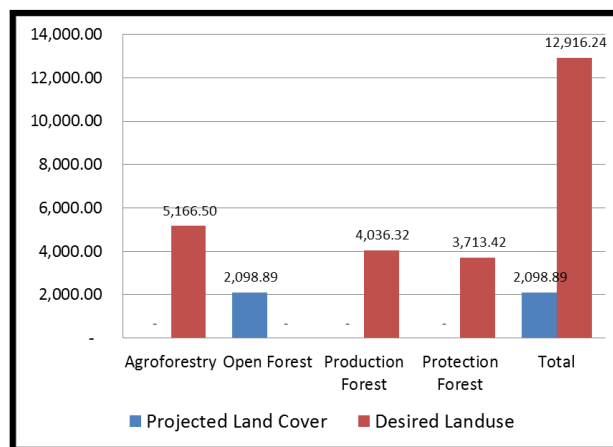


Figure 5. Forest Type and Total Land Cover

Summary and Conclusion

The study shows when land cover conditions are left by itself without any intervention as represented by the Projected Land Cover scenario, the impact of flood disaster in terms of higher flood level extent and the total extent of flooding is more likely to be magnified due to higher runoff. The study also shows that flood disaster can be mitigated if the Desired Land Use scenario will be adopted as one of the course of action in flood disaster risk reduction management since it has lower runoff. Hence this study lends credence the significant role of adopting sound land use management in mitigating flood hazard.

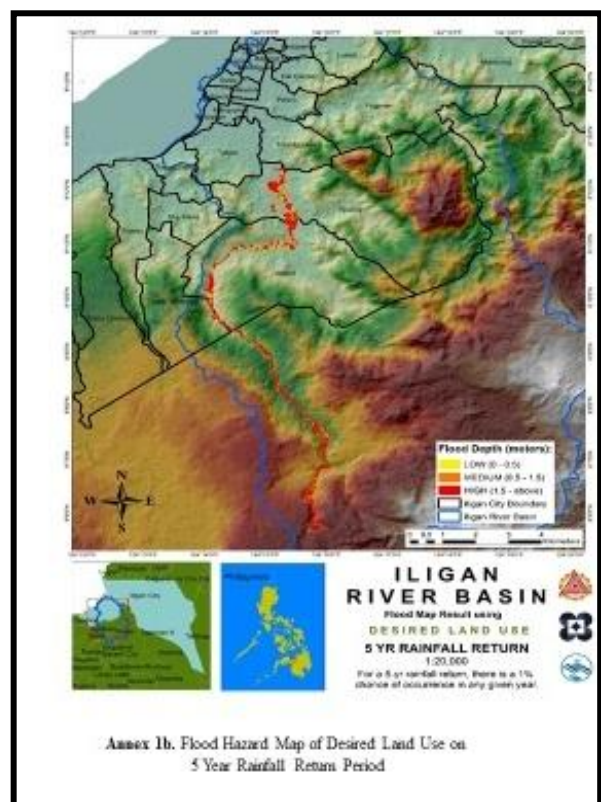
Acknowledgement

We are very grateful for the help and support given to us by DOST – PCIEERD, UP-Diliman LiDAR Team, and MSU- Iligan Institute of Technology, Philippines in making this study a success.

References

- [1] Iligan City Disaster Risk Reduction Management Council, 2013. Final Report on Typhoon Sendong (Washi), Iligan City, Philippines.
- [2] Milano, Alan E., Suson, Peter D., Salcedo, Stephanie Mae B., Blasco, Jennifer G. and Ignacio, Teresa T. Unpublished. Land Cover/Use Scenario Building and its Impact on Runoff Process inside the Iligan River Basin
- [3] Taylor, Matthew, Mulbolland, Murray and Thomburrow, Danny, “Infiltration Characteristics of Soils Under Forestry and Agriculture in the Upper Waikato Catchment”, 12 September 2008, <http://www.waikatoregion.govt.nz/PageFiles/13347/Tr0918.pdf>.
- [4] Noordwijk, Meine Van and Verbist, Bruno, “Overstory # 104-Soil and Water Conservation”, <http://www.agroforestry.net/the-overstory/165-overstory-104-soil-and-water-conservation>

Annexes





Annex 2b. Flood Hazard Map of Desired Land Use on 10 Year Rainfall Return Period



Annex 3a. Flood Hazard Map of Projected Land Cover on 25 Year Rainfall Return Period



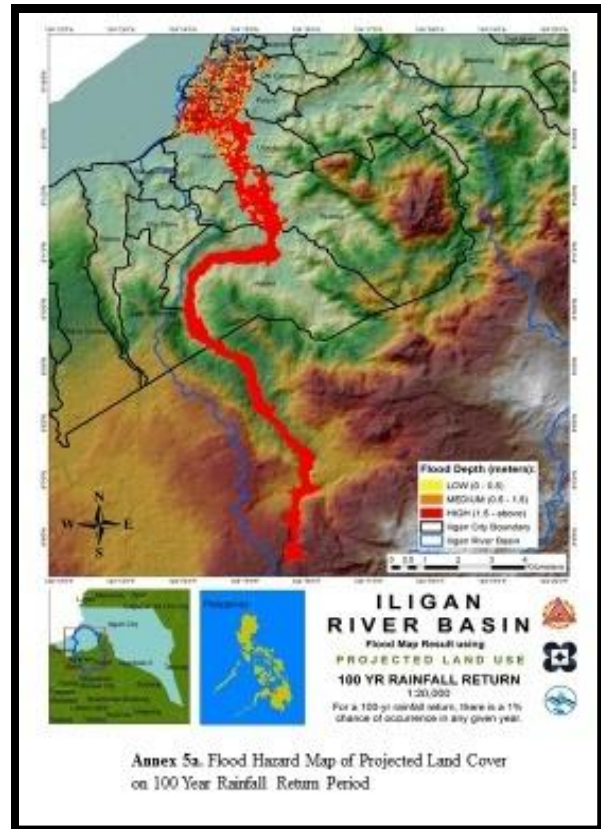
Annex 2a. Flood Hazard Map of Projected Land Cover on 10 Year Rainfall Return Period



Annex 3b. Flood Hazard Map of Desired Land Use on 25 Year Rainfall Return Period



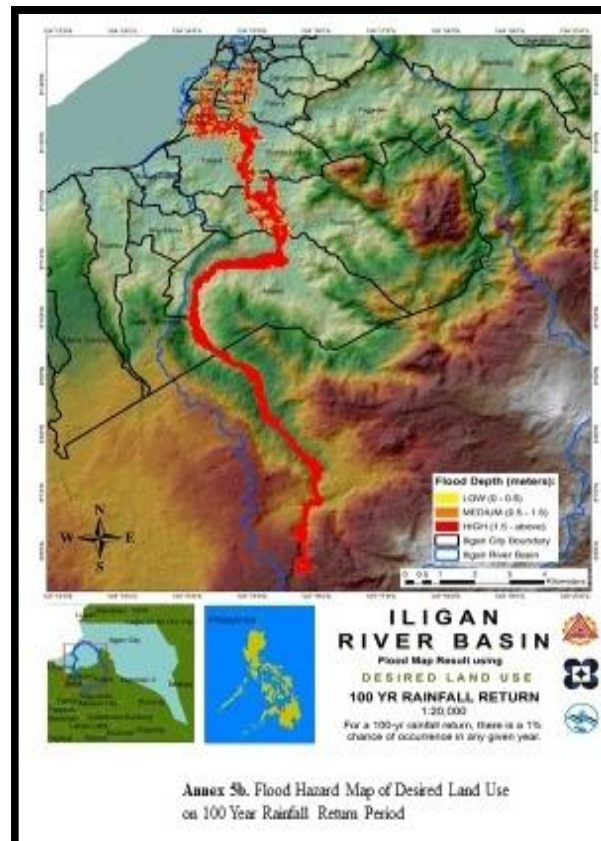
Annex 4a. Flood Hazard Map of Projected Land Cover on 50 Year Rainfall Return Period



Annex 5a. Flood Hazard Map of Projected Land Cover on 100 Year Rainfall Return Period



Annex 4b. Flood Hazard Map of Desired Land Use on 50 Year Rainfall Return Period



Annex 5b. Flood Hazard Map of Desired Land Use on 100 Year Rainfall Return Period

Input-Output Analysis of Water Deficits in Nan River Basin, Thailand

Pavisorn Chuenchum^{1,a}, Pongsak Suttinon^{2,b*} and Piyatida Ruangrassamee^{3,c}

Abstract Increasing demand of water resources along with high variabilities of precipitation pose a challenge in managing water resources under physical and economic constraints. An integrated hydro-economic accounting allows tracking of sectoral water consumption and assessing economic value of water resources. This study applies Input-Output Table for analysis of sectoral water deficits in Nan River Basin, Thailand. Nan River Basin is one of the most important tributaries of the Chao Phraya River in Thailand. It contributes about 25 to 40 percent of annual flows in the Lower Chao Phraya River Basin. Regional Input-Output Table was developed based on the National Input-Output Table. Water supply was calculated from runoff stations of basin using water balance. Water demand for domestic, agricultural, manufacturing, and service sectors were estimated using available secondary database. The calculation of sectoral water deficits, and Regional Input-Output Table was based on data from 2010. The results showed that economic loss of water deficits from the input-output analysis was comparable with the reported figures. In addition, economic loss from cross-sectoral analysis was found to be about sixty percent higher than that from analysis of each sector separately.

Keywords *Water deficits, Input-Output Table, Economic loss, Nan River Basin*

Pavisorn Chuenchum, M. Eng.
Research Assistant
Department of Water Resources Engineering
Faculty of Engineering, Chulalongkorn University
Bangkok, Thailand
E-mail: pavisornchuenchum@gmail.com

Pongsak Suttinon, D. Eng.
Lecturer, Department of Water Resources Engineering
Faculty of Engineering, Chulalongkorn University
Bangkok, Thailand
E-mail: pongsak.su@chula.ac.th
*Corresponding author

Piyatida Ruangrassamee, Ph.D.
Lecturer, Department of Water Resources Engineering
Faculty of Engineering, Chulalongkorn University
Bangkok, Thailand
E-mail: piyatida.h@chula.ac.th

Introduction

Droughts is weather-related phenomena that can cause severe social and economic impacts around the world. The Chao Phraya River Basin is a major economic hub of Thailand for agriculture, manufacturing and service sectors. During 2012 to 2016 the amount of water supplies in the four main reservoirs of the basin, namely Bhumibhol, Sirikit, Kwaenoibumrunngdan, and Pasakcholasitreservoirs, had been inadequate for all sectors. Meanwhile, water demands of all sectors tend to increase following social and economic development. Increasing demand of water resources along with high variabilities of precipitation pose a challenge in managing water resources under physical and economic constraints. Nan River Basin, a tributary of Chao Phraya River, had been affected by droughts and its damage was estimated approximately 1,000 Million Baht (DDPM, 2010), especially in agricultural sector. The objective of this study is to estimate economic loss of water deficits using Nan River Basin as a case study. Water supply was calculated from runoff stations of the basin. Water demand for domestic, agricultural, manufacturing, and service sectors were estimated using available secondary database. Economic value of water and economic loss from water deficits were calculated based on Regional Input-Output Model, which is transformed from National Input-Output Table year 2010. The estimated economic loss can help provide information for policymaker in water resources management and water allocation to achieve effective water resources management and respond to the economic growth of the country.

Study area

Nan River Basin is in the northern part of Thailand. It is one of the sub-basins in greater Chao Phraya River Basin. The total area of the basin is 34,682 km², traversing 11 provinces including Kamphaengphet, Phayao, Phrae, Nan, Loei, Sukhothai, Uttaradit, Phitsanulok, Phichit, Phetchabun and Nakhonsawan. It stretches from latitude 15° 42' N to 18° 37' N and from longitude 99° 51' E to 101° 21' E as shown in Fig 1. It contributes about 25 to 40 percent of flows of Chao Phraya River. The mean annual precipitation and mean annual runoff are approximately 1,267 mm and 11,955 MCM, respectively. The average economic growth of

Gross Domestic Product (GDP) of Nan River Basin is about 2.53% from three sectors, which are agriculture (5.6%), manufacturing (0.6%) and service (1.6%) (Suttinon, 2015). Most areas of upper basin are mountain and forest thus it is not suitable for cultivation. The area of lower basin is alluvial plains, which is suitable for agriculture. Land use map of Nan River Basin is shown in Fig 1. Nan River Basin has a large storage reservoir for water resources management and allocation, namely Sirikit Dam. The amount of water in the reservoir at the end of rainy season is taken into account for water allocation during dry season for Lower Chao Phraya River Basin.

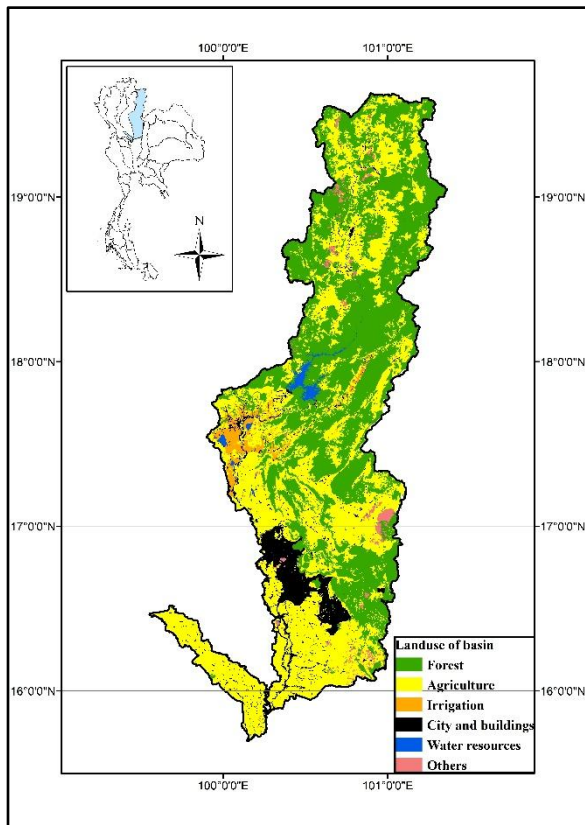


Fig. 1. Land use of Nan River Basin

Methodology

This study consists of six parts: calculation of water supply, estimation of water demands, calculation Regional Input-Output Model from GDP of basin, estimation of economic value of water, and analysis of water deficits and economic loss. Water supply can be estimated from runoff stations using water balance approach. Water demand is calculated from criteria of each sector, such as water demand in agricultural sector is calculated from crop water demand (ET_{crop}) based on crop coefficient (K_c) and reference crop evapotranspiration (E_{T0}). Regional Input-Output Model of Nan River Basin is calculated from GDP of three economic sectors, namely agriculture, manufacturing and service sectors. Economic value of water of each sector is calculated by using the Regional

Input-Output Model hybridized with water demand. Then, economic value of water is evaluated and compared between three sectors for policy guidelines. The methodological framework of this study is shown in Fig 2.

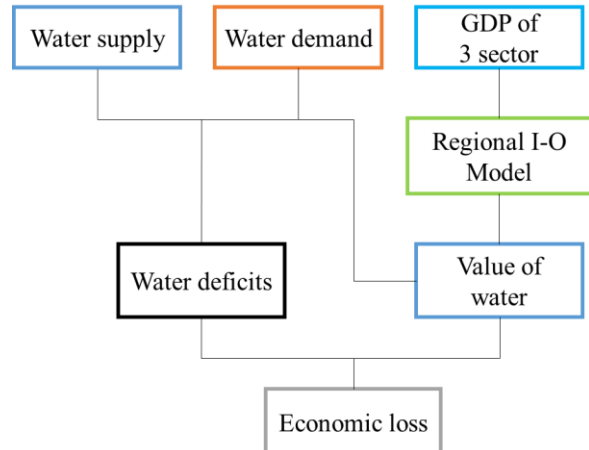


Fig. 2 The methodologies framework

Water supply of Nan River Basin

Water supply (WS) used for calculation of water deficits in this study is based on data of year 2010. It is calculated from water balance between runoff stations in Nan River Basin. In this study, Nan River Basin is divided into two parts, upper and lower basins. The amount of water supply can be estimated from four runoff stations, namely N.64, Inflow Station of Sirikit reservoir, N.12A and N.5A as shown in Fig. 3.

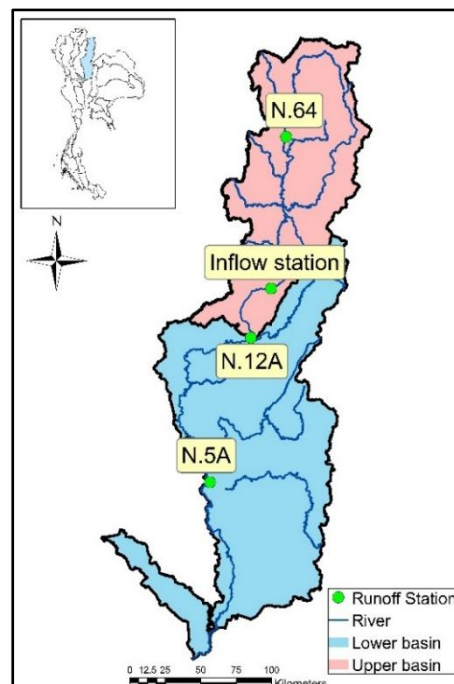


Fig.3 The runoff stations used in this study

The calculation of water supply is considered from the water balance approach as shown in Fig 4. The net water or water supply is calculated from the outflow minus the inflow. The water balance is expressed as the equation, $\Delta S = O - I + P + L$, but precipitation and lateral flow are lumped. If the outflow is greater than the inflow, there may be lateral flow and rainfall into a region. The water supply of the Upper Nan River Basin is calculated from runoff station N.64 and Inflow of Sirikit Dam, and the water supply of the Lower Nan River Basin is calculated from runoff stations N.12A and N.5A.

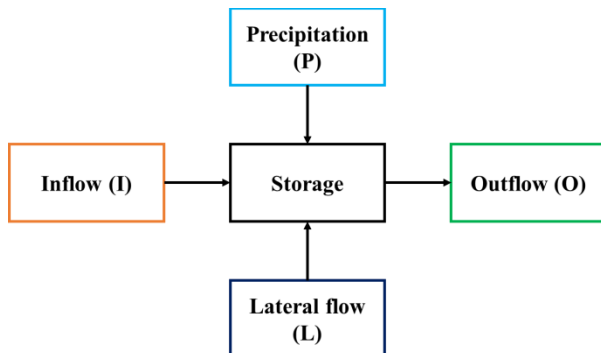


Fig.4 The calculation of water supply

Water Demand of Nan River Basin

Water demand (WD) used in this study is based on data of year 2010 because the Regional Input-Output Model of Nan River Basin is calculated by using the National Input-Output Table year 2010. The calculation of water demand for the three economic sectors is as follows:

1. Water demand of agricultural sector

The calculation of water demand of agriculture is calculated by using crop water demand approach as shown in Equation (1).

$$ET_{crop} = K_c \times ET_o(1)$$

$$WD \text{ of agriculture} = ET_{crop} \times \text{crop area} \quad (2)$$

Where ET_{crop} is crop water demand (mm/day), K_c is crop coefficient and ET_o is reference crop evapotranspiration (mm/day). The Royal Irrigation Department (RID) provided the crop coefficient (K_c) for 40 different crops, and monthly reference crop evapotranspiration (ET_o) in each province. The monthly ET_o are calculated by using Penman Monteith method. The total crop water demand is calculated from ET_{crop} multiplied with crop area and summed over a year as shown in Equation (2).

2. Water demand of manufacturing sector

The calculation of water demand of manufacturing can be calculated by using horsepower from manufacturing plants in the basin. The horsepower is

multiplied with coefficient of water demand for each type of manufacturing plant (CU WRSRU, 2005) as shown in Equation (3).

$$WD \text{ of manufacturing} = \text{Horsepower} \times (\text{Coefficient} \times \text{Correction factor}) \quad (3)$$

The coefficient of water demand based on type of manufacturing plant is based on the data of year 2005. Thus, it needs to be adjusted to reflect water demand of year 2010. The correction factor is used in the adjustment and is calculated from total water demand of manufacturing year 2010 per total water demand of manufacturing year 2005, which is found to be 0.31.

3. Water demand of service sector

Water demand of service sector includes household, tourism and service business etc. The calculation of water demand on service is complicated, for service sector consists of variety sectors. Water demand of service sector is categorized into two groups, namely household and service and tourism as shown in Equation (4).

$$WD \text{ of service} = \text{Household} + \text{Service and tourism} \quad (4)$$

Water demand of household can be calculated from household water usage (L_{pcd} , liters per capita per day) multiplied with population. The data are obtained from the Department of Provincial Administration of the Ministry of Interior. For service and tourism, it consists of education, tourism and health sectors. The data of water usage for service and tourism can be obtained from the National Statistical Office.

Regional Input-Output Model of Nan River Basin

Regional Input-Output Model is a tool for assessing economic value of water in the basin. GDPs and National Input-Output Table year 2010 are needed in creating Regional Input-Output Model of Nan River Basin. National Input-Output Table are transformed to the Regional Input-Output Model by using RAS method (Miller et al. 2009). The methodology requires finding GDP of the three sectors, which include agriculture, manufacturing, and service. The calculation of GDP in Nan River Basin for each sector is as follows:

1. GDP of agricultural sector

GDP of agricultural sector (A) is calculated from the land use data in 2009 from the Land Development Department based on land use for different crop types. The information of yields and the monetary values for each crop type are obtained from the Office of Agricultural Economics and the Department of Internal Trade, respectively. The crop area is multiplied with the yield of crop and the monetary values in each crop type. Results of the calculation are selling price of each crop,

which are the sum of cost and profit. GDP is a profit or value added in Input-Output Table; thus, selling price is deducted by cost of each crop. Summation of the profit from every crop type is the GDP of agricultural sector. Costs of each of crop type are obtained from the National Input-Output Table (NESDB, 2010).

2. GDP of manufacturing sector

GDP of manufacturing sector (M) can be calculated from an economic model from macroeconomics, the Cobb-Douglas Production Function as shown in Equation (5).

$$Q = aK^bL^c \quad (5)$$

Where Q is GDP of manufacturing sector (Baht), K and L are the capital input and labor input, respectively and constants a, b, and c are the total factor productivity, the output elasticity of capital and of labor respectively. The constants a, b, and c are estimated by multiple linear regression of manufacturing data in provinces (Chuenchum, 2005). GDP of manufacturing sector is calculated from number of industries, capital and labor in the basin. The manufacturing data are obtained from the Department of Industrial Works.

3. GDP of service sector

GDP of service sector (S) is calculated based on Gross Province Product (GPP) from 11 provinces in the Nan River Basin. The GPP is further distributed to district level by weighting ratio of number of population of district level to number of population of provincial level.

Economic value of water in Nan River Basin

Economic value of water is value of water in generating monetary value (Baht) per one cubic meter (m³) of water. Economic value of water is different for each sector. The economic value of water can be obtained from Regional Input-Output Model of Nan River Basin by dividing the total economic input value (Total Input, TI) with the water demand for each sector of Nan River Basin. The calculation of economic value of water is shown in Equation (6).

$$\text{Value of Water} = \frac{\text{Total Input}}{\text{Water Demand}} \quad (6)$$

Where Value of Water is the economic value of water in generating monetary value, Total Input is the sum of total inter-transaction (IT) and value added (VA) or GDP for each sector, Water Demand is water use of each sector.

Economic losses from water deficits

The economic losses from water deficits can be estimated as direct loss and indirect loss by using two methodologies. The direct loss is calculated based on the economic value of water of each sector and the indirect loss is calculated based on the cross-sectoral economic value of water.

1. Direct economic loss

The first methodology considers the economic losses from value of water in each sector but not considering cross-sectoral loss yet. The first methodology involves multiplying value of water with the amount of water deficit in each region of the river basin to obtain the monetary value of economic loss from water deficits of each sector as shown in Equation (7).

$$\text{Economic loss} = \text{Water deficits} \times \text{Value of water} \quad (7)$$

2. Indirect economic loss

The second methodology considers the economic losses across sectors. In fact, the economic losses of one sector will affect another sector through supply chain in economic system. The indirect losses can be calculated from value of water in each sector and Regional Input-Output Model of Nan River Basin using the *Leontief inverse matrix* (Miller et al. 2009) as shown in Equation (8).

$$X = (I-A)^{-1}F \quad (8)$$

Where X is the economic losses across sectors, I is a 3×3 identity matrix, A is a 3×3 matrix whose vertical entries are quotients of contribution from intermediate sectors and the Total Input (TI) of each sector and F is the Final demand (FD) of the product that considers losses only in individual sector as obtained in the first methodology. The multiplication of the inverse matrix (I-A)⁻¹ with F allows X to be computed as economic losses involving all sectors.

Results and discussion

Water demand of Nan River Basin

The total water demand in the Nan River Basin in 2010 for agriculture, manufacturing, and service are 32,058 MCM, 3.75 MCM and 161.7 MCM, respectively. The water demands of Lower Nan River Basin are higher than the water demands of Upper Nan River Basin. The Lower Nan River Basin includes Uttaradit, Phitsanulok, Pijitand Nakhonsawan provinces. This area consists of large agricultural area including irrigated and rainfed rice fields and other cash crops such as sugar cane and maize and there are several populated urban areas.

Regional Input-Output Model of Nan River Basin

Regional Input-Output Model of the Nan River Basin is transformed from the National Input-Output Table year 2010 and the GDP of the basin using RAS method. The result is shown in Table 1.

Table. 1 Regional Input-Output Model (2010) of Nan River Basin

	A	M	S	SUM IT	SUM FD	SUM TO	GDP
A	18,073	24,647	17,039	59,760	10,014	69,773	43,412
M	5,448	20,070	33,308	58,826	11,849	70,675	17,704
S	2,843	8,257	85,528	96,627	210,120	306,748	170,867
SUM IT	26,361	52,971	135,881	(Unit: Million Baht)			
SUM VA	43,412	17,704	170,867				
SUM TI	69,773	70,675	306,748				

*A: agriculture, M: manufacturing and S: service sectors
 **IT: Inter-Transaction, FD: Final Demand, TI: Total Input and TO: Total Output

The GDP of the basin is approximately 231,983 million Baht in 2010. The service sector has highest GDP of the basin because Phitsanulok province is the center of logistics, education and tourism in north of Thailand, and has highest population in the basin. The GDP of agricultural sector ranks second because most Lower Nan River Basin area is agricultural area, which is mostly rice area, and Upper Nan River Basin area is grown corn, orange and longan. The price of orchard products is higher than the price of rice, such as one kilogram (kg) of longan is 30 baht, but one kilogram of rice is 8 baht. The GDP of manufacturing sector ranks third in the basin because there is no industrial estate in Nan River Basin. Most manufacturing plants are agricultural processing industries and agricultural equipment repairing.

Economic value of water in Nan River Basin

From the calculation of water demand and Regional Input-Output Model of Nan River Basin, the economic value of water in the Nan River Basin can be calculated. Table 2 shows the economic value of water in each sector for two regions of the basin. The economic value of water is calculated from Equation (6). It is considered from Total Input (sum of cost and profit in each sector) and sectoral water demand. In Nan River Basin, the manufacturing sector has the highest economic value of water for both regions. This sector uses the less water, and it generates high GDP in driving economic growth compare with other sectors. The second economic value of water is the service sector. The monetary value of service sector includes hotel business, tourism, transportations and hospital business. The service sector uses water less than the agricultural sector, and it can generate higher monetary value. Conversely, the agricultural sector has the highest water demand in the

basin, but it generates less GDP. For instance, the average water demand of rice crop is 1,200 m³ per rai (1 rai = 1,600 m²), and the average price of rice per ton is 8,000 baht. The economic values of water in the Upper of the basin for the three sectors are 182, 271,829, and 9,240 Baht, respectively. Those of the Lower of the basin are 3, 21,417, and 2,387 Baht, respectively. However, this study does not imply that priority should be given based on the economic value of water. The purpose of this study aims to quantify economic value of water explicitly so it can be used as a tool for economic loss estimation within and across sectors.

Table. 2 Water demand and Economic value of water

Basin	Water demand (MCM)			Economic value of water (Baht)		
	A	M	S	A	M	S
Upper	383.5	0.26	33.2	182	271,829	9,240
Lower	31,674	3.3	128.5	3	21,417	2,387

*A = Agriculture sector, M = Manufacturing sector and S = Service sector

Analysis of water deficits in Nan River Basin

From the calculation of the water demand and water supply of two regions in Nan River Basin, namely the Upper Nan River Basin and Lower Nan River Basin, the Upper Nan River Basin had lower water demands for all sectors comparing to the Lower region. The average total water demands in the Upper region were approximately 34.7 MCM, and there was only water deficit in agricultural sector. It was found that this region had the water deficits of approximately 181.2 MCM. Fig. 5 shows monthly water demand and supply in the Upper Nan River Basin and water deficits in agricultural sector during March to July and October.

The Lower Nan River Basin had higher water demands. The average total water demands were approximately 2,650.5 MCM, and this region had extreme water deficits in agricultural sector. This is because the Lower Nan River Basin has large amount of agricultural area, especially rice fields in Uttradit, Phitsanulok, Pijit and Nakhonsawan provinces. Fig 6 shows water deficits of agricultural sector throughout the year. It was found that this region had the water deficits of approximately 27,776.4 MCM. Comparing to the Upper region, water demand of Lower region is much higher.

The deficit volume of water is obtained from calculation of monthly deficit between water demand and water supply. The total water deficits of two regions of the basin are approximately 27,957.6 MCM.

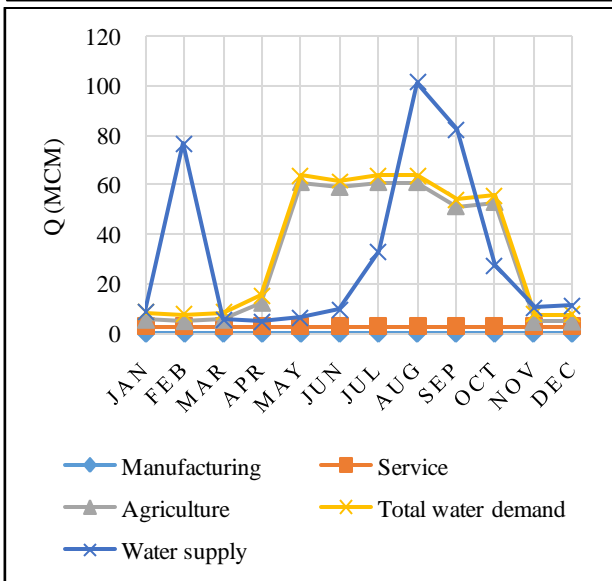


Fig. 5 Analysis of monthly water demand and supply in the Upper Nan River Basin

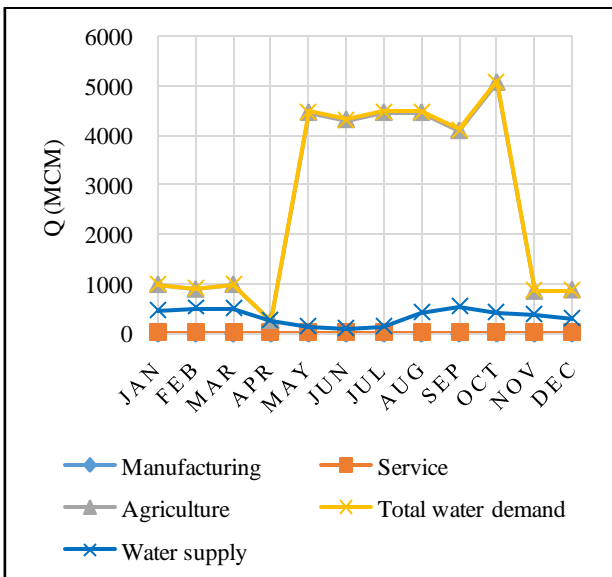


Fig. 6 Analysis of monthly water demand and supply in the Lower Nan River Basin

Economic losses from water deficits

Based on Thailand’s water allocation policy among three sectors (agriculture, manufacturing, and service), the first priority is service sector and domestic use, the second priority is manufacturing sector and the third priority is agricultural sector. The calculation of economic losses is assessed based on these priorities. The direct and indirect economic losses from water deficits of Nan River Basin are calculated and shown in Table 3 and 4. Since there were only water deficits in agricultural sector for both regions, the direct economic losses only occur in agricultural sector. The direct assessment quantifies the economic losses in individual sector, and the indirect or cross-sectoral assessment quantifies the economic losses that affect across sectors.

Table. 3 Direct loss from water deficits

Sectors	Upper basin (Million Baht)	Lower basin (Million Baht)
Agriculture	39,978	55,553
Manufacturing	N/A	N/A
Service	N/A	N/A

Table. 4 Indirect loss from water deficits

Sectors	Upper basin (Million Baht)	Lower basin (Million Baht)
Agriculture	47,472	79,967
Manufacturing	5,724	9,642
Service	3,609	6,080
Total damages	56,805	95,688

From the assessment of economic losses from water deficits in the Nan River Basin, it was found that the direct and indirect losses were approximately 95,531 and 152,493 million baht, respectively. The indirect losses were about sixty percent higher than the direct losses. From the water deficit analysis, water deficiency only occurred in the agricultural sector. Cross-sectoral economic losses between agricultural sector and manufacturing and service were 15,366 and 9,689 million baht, which accounted for sixteen percent of the indirect losses. The direct economic losses of water deficits in year 2010 of the Nan River Basin (95,531 million baht) estimated from this study were comparable to the figures reported by Department of Disaster Prevention and Mitigation (approximately 115,000 million baht). It is to emphasize that the results from this study aim to explicitly and quantitatively demonstrate economic value of water in each sector and its economic losses from water deficits based on relation within its own sector and inter-relation across sectors. This study does not take into account social impacts of water deficits. Thus, it by no means implies water allocation policy to be based on the calculated economic value of water but it can be used as a tool for economic loss estimation within and across sectors. Additionally, the procedures implemented in this study can be used as a guideline for increasing economic value of water as water demands are increasing and water supply is subjected to higher variability. As value of water is a function of Total Input and Water Demand, to increase value of water measures to increase total input and decrease water demand should be implemented simultaneously.

Conclusions

This study demonstrates the application of hydrologic analysis coupled with economic analysis to assess economic losses from water deficits using Nan River Basin and data from 2010 as a case study. Economic value of water can be calculated using Regional Input-Output Model and water demand. The Regional Input-

Output Model can be created from the National Input-Output Table and GDP of the basin for each sector of interest. The methodology used in this study not only allows assessment of direct economic losses in individual sector but also assessment of indirect losses across sectors. The results of studies show that GDPs from Nan River Basin in agricultural, manufacturing, and service sectors were 43,412, 17,704, and 170,867 million Baht, respectively. The water demand in these sectors was 32,058, 3.56 and 161.7 MCM. The economic value of water for the Upper Nan River Basin for the three sectors was 182, 271,829, and 9,240 Baht; whereas those of the Lower Nan River Basin were 3, 21,417, and 2,387 Baht. In 2010, water deficit only occurred in the agricultural sector with the water deficiency of 27,957.6 MCM. The direct economic loss is 95,531 million Baht, and the indirect loss is 152,493 million Baht. The indirect losses were about sixty percent higher than the direct losses. The direct economic losses of water deficits in year 2010 of the Nan River Basin estimated from this study were comparable to the figures reported by Department of Disaster Prevention and Mitigation. It is to emphasize that the results from this study aim to explicitly and quantitatively demonstrate economic value of water in each sector and its economic losses from water deficits based on relation within its own sector and inter-relation across sectors. This study does not take into account social impacts of water deficits. Thus, it by no means implies water allocation policy to be based on the calculated economic value of water but the analysis demonstrated can be used as a tool for economic loss estimation within and across sectors. Additionally, the procedures implemented in this study can be used as a guideline for increasing economic value of water as water demands are increasing and water supply is subjected to higher variability. As value of water is a function of Total Input and Water Demand, to increase value of water measures to increase total input and decrease water demand should be implemented simultaneously.

Acknowledgement

The authors would like to express sincere gratitude to government agencies of Thailand for data used in this research, namely, Department of Industrial works (DIW), Department of Internal Trade (DIT), Department of Provincial Administration (DPA), Land Development Department (LDD), Office of The National Economic and Social Development Board (NESDB), National Statistical Office (NSO), Office of Agricultural Economics (OAE), Office of Water Management and Hydrology (OWMH), Royal Irrigation Department (RID) and Water Institute for Sustainability (WIS). We also would like to express our gratitude to Chulalongkorn University Water Resources System

Research Unit (CU_WRSRU) for their support and data used in this study.

References

- Chuenchum, N. (2005). Theory of Economics and Analysis. Thammasat University, Bangkok, Thailand.
- Chuenchum, P., Suttinon, P. and Ruangrassamee, P. (2015). Impact of Changing Climate on Inflows into Sirikit Dam. The 21st National Convention on Civil Engineering (NCCE21), Songkla, Thailand.
- DDPM (Department of Disaster Prevention and Mitigation). (2010). Disaster Statistics of Thailand, Ministry of Interior, Bangkok, Thailand.
- Koontanakulvong, S., Suksri, C., Kitpaisalsakul, T., Santithamnon, P., Putthividhya, A., Hoisungwan, P., Gupta, A.D., NASU, S. (2005). Effectiveness Aspect of Surface Water Management and Impact on Groundwater, Water Resources System Unit Chulalongkorn University, Thailand Research Fund (TRF), Bangkok, Thailand.
- Koontanakulvong, S., Suksri, C., Kitpaisalsakul, T., Santithamnon, P., Putthividhya, A., Hoisungwan, P., Gupta, A.D., NASU, S. (2011). Water Resources Study for Strategic Water Management in Nan Basin Phase 1, Water Resources System Unit Chulalongkorn University, Thailand Research Fund (TRF), Bangkok, Thailand.
- Koontanakulvong, C., Kitpaisalsakul, Ruangrassamee, P., Suttinon, P., Visessri, S., NASU, S. (2015). Water Resources Study for Strategic Water Management in Nan Basin Phase 3, Water Resources System Unit Chulalongkorn University, Thailand Research Fund (TRF), Bangkok, Thailand.
- Miller, R. E. and Blair, P.D., (2009). Input-Output Analysis Foundations and Extensions 2nd Edition. University of Pennsylvania, Pennsylvania, USA.
- NESDB (Office of The National Economic and Social Development Board), (2010). Gross Domestic Product and Input-Output Table of Thailand. Prime Minister's Office, Bangkok, Thailand.
- Suttinon, P., Nasu, S., Bongochetsakul, N., Uemoto, K. and Ihara T. (2014). Hybrid water input-output model for regional management. Society for Social Management Systems Internet Journal.

Reviewers

Full name	Organization	Country
Assoc.Prof.Amnat Chidthaisong	King Mongkut's University of Technology Thonburi	Thailand
Prof. KS Cheng	Taiwan	Taiwan
Assoc.Prof.Dr.Bancha Kwanyuen	Kasetsart Uuniversity	Thailand
Dr. Yutthana Talaluxmana	Kasetsart Uuniversity	Thailand
Prof. Yutaka Matsuno	Kindai University	Japan
Dr. Kimihito Nakamura	Kyoto University	Japan
Dr. Andrew Whitaker	Niigata University	Japan
Dr. Shinji Fukuda	Tokyo University of Agriculture and Technology	Japan
Dr. Takanori Nagano	Kobe University	Japan
Dr. WT Feng	Taiwan	Taiwan
Assoc.Prof.Dr.Sucharit Koontanakulvong	Chulalongkorn University	Thailand
Dr. Supattra Visessri	Chulalongkorn University	Thailand
Dr. Pongsak Suttinon	Chulalongkorn University	Thailand
Dr. P Lin	Taiwan	Taiwan
Assoc.Prof.Dr.Sangam Shrestha	Asian Institute of Technology	Thailand
Asst.Prof.Dr.Nguyen Hoang Duc	Asian Institute of Technology	Thailand
Assoc.Prof.Dr.Avishek Datta	Asian Institute of Technology	Thailand
Asst.Prof.Dr.Sarawut Ninsawat	Asian Institute of Technology	Thailand
Prof. Tachikawa Yasuto	Kyoto University	Japan
Assoc.Prof.,Dr. Yutaka Ichikawa	Kyoto University	Japan
Assoc.Prof.,Dr. Kenji Tanaka	Kyoto University	Japan
Assoc.Prof.,Dr. Takahiro Sayama	Kyoto University	Japan
Prof. Koike Toshio	International Centre for Water Hazard and Risk Management	Japan
Prof. Kwansue Jung	Korea Water Resources Association	Korea
Prof. Tae-woong Kim	Hanyang University	Korea
Prof. Juheon Lee	Joongbu University	Korea
Prof. Giha Lee	Kyongpook National University	Korea
Prof. Chang-lae Jang	Korea National University of Transport	Korea
Prof. Hyunuk An	Chungnam National University	Korea
Wansik Yu	Chungnam National University	Korea
Prof. Wei-Cheng Lo	National Cheng Kung University	Taiwan
Prof. Jian-Ping Suen	National Cheng Kung University	Taiwan
Dr. Meng-Hsuan Wu	National Cheng Kung University	Taiwan
Dr. Oranuj	Department of Groundwater Resources	Thailand
Dr. Piyatida Ruangrassamee	Chulalongkorn University	Thailand
Dr. Anurak Sriariyawat	Chulalongkorn University	Thailand
Assoc.Prof.Dr. Tuantan Kitpaisalsakul	Chulalongkorn University	Thailand
Asst.Prof.Dr. Aksara Putthividhya	Chulalongkorn University	Thailand



Supported by



Sponsored by

